

Bahman Zohuri

Directed- Energy Beam Weapons



Springer

Directed-Energy Beam Weapons



Bahman Zohuri

Directed-Energy Beam Weapons

 Springer

Bahman Zohuri
Galaxy Advanced Engineering, Inc.
Albuquerque, NM, USA

ISBN 978-3-030-20793-9 ISBN 978-3-030-20794-6 (eBook)
<https://doi.org/10.1007/978-3-030-20794-6>

© Springer Nature Switzerland AG 2019

This work is subject to copyright. All rights are reserved by the Publisher, whether the whole or part of the material is concerned, specifically the rights of translation, reprinting, reuse of illustrations, recitation, broadcasting, reproduction on microfilms or in any other physical way, and transmission or information storage and retrieval, electronic adaptation, computer software, or by similar or dissimilar methodology now known or hereafter developed.

The use of general descriptive names, registered names, trademarks, service marks, etc. in this publication does not imply, even in the absence of a specific statement, that such names are exempt from the relevant protective laws and regulations and therefore free for general use.

The publisher, the authors, and the editors are safe to assume that the advice and information in this book are believed to be true and accurate at the date of publication. Neither the publisher nor the authors or the editors give a warranty, express or implied, with respect to the material contained herein or for any errors or omissions that may have been made. The publisher remains neutral with regard to jurisdictional claims in published maps and institutional affiliations.

This Springer imprint is published by the registered company Springer Nature Switzerland AG
The registered company address is: Gewerbestrasse 11, 6330 Cham, Switzerland

This book is dedicated to my son, Sasha

Preface

As we have seen in past decades, the directed-energy weapons (DEWs) are pushing toward a different direction and taking a new approach as directed-energy beam weapon (DEBWs), which is the dawn of new age defenses. This book focuses on new class of weapons that, as we stated, are known as directed-energy beam weapons, which not only have focused on high-energy laser (HEL) but have described particle-beam weapons (PBWs) as well as kinetic energy weapons (KEWs).

This book also contains two new chapters: high-power microwave (HPM) as weapon of new approach to directed beam weapons and a new high-energy wave known as scalar longitudinal wave (SLW) which has a new potential as weapon of directed energy.

The only difference between these two beam weapons and high-power or high-energy lasers is that these types of directed-energy weapons do not suffer from the deficiency of thermal blooming seen in high-energy laser beams when such laser beam travels through atmosphere, in particular when they propagate as either ground-based laser (GBL) or airborne laser (ABR) systems.

Last one decade or so has also seen emergence of a new class of weapons known as directed-energy weapons (DEWs), leading to enhanced global interest from scientists and engineers in DEW development. Lasers, high-power microwaves, and high-energy particle beams have been exploited for DEW development. These weapons, with the exception of particle-beam weapons (PBWs) and laser-induced plasma channel (LIPC) weapons, generate streams of electromagnetic energy that can be precisely directed over long distances to disable or destroy intended targets.

Laser is no longer confined to premises of prominent research centers like Bell Laboratories and Hughes Research Laboratories and major academic institutes like Columbia University, USA, as it was in its early stages of development and evolution. In the last five decades, after Theodore Maiman demonstrated the first laser in May 1960 at Hughes Research Laboratories, there has been an explosive growth in industrial, medical, scientific, and military applications of lasers. Application areas continue to grow with every passing day.

Lasers have been used in various military applications since the early days of development that followed their invention. There has been large-scale proliferation of lasers and optronic devices and systems for applications like range finding, target designation, target acquisition and tracking, precision-guided munitions, and so on during the 1970s and the 1980s.

These devices continue to improve in performance and find increased acceptance and usage in contemporary battlefield weaponry. Technological advances in optics, optoelectronics, and electronics leading to more rugged, reliable, compact, and efficient laser devices are largely responsible for making these indispensables in modern warfare.

Last one decade or so has also seen emergence of a new class of weapons known as directed energy weapons (DEWs) leading to enhanced global interest from scientists and engineers in DEW development. Lasers, high-power microwaves and high-energy particle beams have been exploited for DEW development. These weapons, with the exception of Particle Beam Weapons (PBWs) and Laser-Induced Plasma Channel (LIPC) weapons, generate streams of electromagnetic energy that can be precisely directed over long distances to disable or destroy intended targets.

Although scalar longitudinal wave (SLW) phenomenon is nothing new since Tesla introduced such wave more than a century ago, a lot of attention has been paid to this particular generation of wave in recent years, where it can be derived easily from the more complete equation of Maxwell using vector calculus and shows one more term added to Maxwell-Ampere equation, as illustrated in the new chapter of this book under the title of "All About Wave Equations."

High-power electromagnetic pulse (HPEP) is covered under the chapter with the title of "High Power Microwave" presented by Dr. Carlo Kopp.

High-power electromagnetic pulse generation techniques and high-power microwave technology have matured to the point where practical E-bombs (electromagnetic bombs) are becoming technically feasible, with new applications in both strategic and tactical information warfare. The development of conventional E-bomb devices allows their use in nonnuclear confrontations. This paper discusses aspects of the technology base and weapon delivery techniques and proposes a doctrinal foundation for the use of such devices in warhead and bomb applications.

High-power microwave (HPM) sources have been under investigation for several years as potential weapons for a variety of combat, sabotage, and terrorist applications. Due to classification restrictions, details of this work are relatively unknown outside the military community and its contractors. A key point to recognize is the insidious nature of high-power microwave (HPM). Due to the gigahertz-band frequencies (4 to 20 GHz) involved, HPM has the capability to penetrate not only radio front ends but also the most minute shielding penetrations throughout the equipment. At sufficiently high levels, as discussed, the potential exists for significant damage to devices and circuits. For these reasons, HPM should be of interest to the broad spectrum of EMC practitioners.

The chapter under the title of "Particle Beam Weapons" is presented by Dr. Richard M. Roberds. Although much has been written on the high-energy laser (HEL), this category of directed-energy weapon appears to be well understood

by members of the defense community. Laser weapons have been under active development for 20 years and easily constitute the most advanced of the directed-energy devices.

In contrast, the particle-beam weapon (PBW) has been the “sleeping” among directed-energy weapons until very recently. Enshrouded in secrecy, it began as a project sponsored by the Advanced Research Projects Agency (now called Defense Advanced Research Projects Agency better known as DARPA) as early as 1958, 2 years before the first scientific laser demonstration in 1960. Code-named Seesaw, the project was designed to study the possible use of particle beams for ballistic missile defense. Today while its development lags that of the high-energy laser, the particle-beam weapon is viewed by some military technicians as the follow-on weapon to the laser, because of its higher potential lethality.

Generally speaking, this book will provide a holistic approach to new-generation Star Wars weapon system for the readers who would like to extend their knowledge beyond just high-energy laser (HEL) as directed-energy weapon as it was introduced by this author in a similar book published by Springer in 2016.

Albuquerque, NM, USA
2016

B. Zohuri

Acknowledgment

I am indebted to the many people who aided, encouraged, and supported me beyond my expectations. Some are not around to see the results of their encouragement in the production of this book, yet I hope they know of my deepest appreciations. I especially want to thank my friend Bill Kemp, to whom I am deeply indebted, who has continuously given his support without hesitation. He has always kept me going in the right direction.

Above all, I offer very special thanks to my late mother and father and to my children, in particular my son, Sasha. They have provided constant interest and encouragement, without which this book would not have been written. Their patience with my many absences from home and long hours in front of the computer to prepare the manuscript are especially appreciated.

About This Document

This section describes the document's purpose, scope, and audience; lists documents that provide additional, related information; and provides definitions of terms.

Purpose

The purpose of this document is to describe dimensional analysis, similarity, and modeling methods.

Contents

1	Introduction to Directed Energy Weapon	1
1.1	Introduction	1
1.2	Directed Energy Weapons (DEWs)	3
1.3	Directed Energy Weapons (DEWs) Versus Kinetic Energy Weapons (KEWs)	4
1.4	Types of Directed Energy Weapons (DEWs)	5
1.5	Beam Weapons Almost Ready for Battle at Speed of Light and Electron	17
1.5.1	Ripe for Transformation?	18
1.5.2	Niche for New Technology	18
1.5.3	Unknown Unknowns	19
1.5.4	Relay Mirrors	20
1.5.5	History Lesson	20
1.6	Space Warfare, a New Age of Military Weaponry	21
1.6.1	History	21
1.7	Earth Orbital Space Is a Militarily and Theoretical Space Weaponry	26
1.7.1	Ballistic Warfare	27
1.7.2	Electronic Warfare	31
1.7.3	Kinetic Bombardment	33
1.7.4	Directed Energy Weapons	35
1.7.5	Airborne-Based Laser (ABL)	39
1.7.6	Space-Based Laser (SBL)	40
1.7.7	Ground-Based Laser (GBL)	42
1.8	Practical Considerations	43
1.9	Space Debris	45
1.10	Possible Warfare Over Space	45
1.11	The Three Major Phases of Effective Missile Defense Systems	46
1.12	Combatting Ballistic Missile Threats	52
	References	53

2 All About Wave Equations 55

2.1 Introduction 55

2.2 The Classical Wave Equation and Separation of Variables 58

2.3 Standing Waves 64

2.4 Seiche Wave 66

2.4.1 Lake Seiche 67

2.4.2 Sea and Bay Seiche 69

2.5 Underwater or Internal Waves 70

2.6 Maxwell’s Equations and Electromagnetic Waves 70

2.7 Scalar and Vector Potentials 78

2.8 Gauge Transformations, Lorentz Gauge,
and Coulomb Gauge 81

2.9 Infrastructure, Characteristic, Derivation, and Properties
of Scalar Waves 84

2.9.1 Derivation of the Scalar Waves 93

2.9.2 Wave Energy 131

2.9.3 The Particles or Charge Field Expression 133

2.9.4 Particle Energy 136

2.9.5 Velocity 138

2.9.6 The Magnetic Field 142

2.9.7 The Scalar Field 146

2.9.8 Scalar Fields, from Classical Electromagnetism
to Quantum Mechanics 150

2.9.9 Our Body Works with Scalar Waves 182

2.9.10 Scalar Wave Superweapon Conspiracy Theory 187

2.9.11 Deployment of Superweapon Scalar Wave Drive
by Interferometer Paradigm 194

2.10 The Quantum Waves 212

2.11 The X-Waves 218

2.12 The Nonlinear X-Waves 224

2.13 The Bessel’s Waves 225

2.14 Generalized Solution to Wave Equation 227

References 234

3 Laser Beam Energy as Weapon 239

3.1 Introduction 239

3.2 Possible Targets 240

3.3 Energy Level at the Target 240

3.4 Absorption and Scattering 242

3.5 Atmospheric Structure with Altitude 244

3.6 The Major Laser Weapon Concepts 245

3.7 Small-Scale Weapons Using Lab-Type Lasers 247

3.8 High-Energy Lasers as Weapons 247

- 3.9 High-Energy Laser (HEL) Safety Program 248
 - 3.9.1 Airborne Laser (YAL-1A) 249
 - 3.9.2 Tactical High-Energy Laser for Air Defense 254
- 3.10 Lasers for Air Defense 255
 - 3.10.1 Target Acquisition for Combat Operations 258
 - 3.10.2 Overview 258
 - 3.10.3 Description 258
- 3.11 Target-Background Discrimination for Surveillance 261
 - 3.11.1 Overview 261
 - 3.11.2 Description 262
- References 268
- 4 High-Power Microwave Energy as Weapon 269**
 - 4.1 Introduction 269
 - 4.2 High-Power Microwave 271
 - 4.3 E-Bomb 271
 - 4.4 The Electromagnetic Pulse Effect (EMP) 272
 - 4.5 The Technology Base for Conventional Electromagnetic Bombs 273
 - 4.5.1 Explosively Pumped Flux Compression Generators 273
 - 4.5.2 Explosive and Propellant-Driven Magnetohydrodynamic (MHD) Generators 277
 - 4.5.3 High-Power Microwave Sources: The Vircator 277
 - 4.6 The Lethality of Electromagnetic Warheads 279
 - 4.6.1 Coupling Modes 279
 - 4.6.2 Maximizing Electromagnetic Bomb Lethality 282
 - 4.7 Targeting Electromagnetic Bombs 284
 - 4.8 The Delivery of Conventional Electromagnetic Bombs 287
 - 4.9 Defense Against Electromagnetic Bombs 290
 - 4.10 Limitations of Electromagnetic Bombs 292
 - 4.11 The Proliferation of Electromagnetic Bombs 293
 - 4.12 A Doctrine for the Use of Conventional Electromagnetic Bombs 294
 - 4.12.1 Electronic Combat Operations Using Electromagnetic Bombs 295
 - 4.12.2 Strategic Air Attack Operations Using Electromagnetic Bombs 297
 - 4.12.3 Offensive Counter Air (OCA) Operations Using Electromagnetic Bombs 301
 - 4.12.4 Maritime Air Operations Using Electromagnetic Bombs 302
 - 4.12.5 Battlefield Air Interdiction Operations Using Electromagnetic Bombs 302

4.12.6 Defensive Counter Air, Air Defense Operation,
and Electromagnetic Warhead 303

4.12.7 A Strategy of Graduated Response 303

4.13 Conclusions 305

Breakdown in Air Produced by High-Power Microwaves 306

References 307

5 Particle Beam Energy as Weapon 309

5.1 Introduction 309

5.2 What Is a Particle Beam Weapon? 310

5.3 Particle Beam Description 312

5.4 Types of Particle Beam Weapons 313

5.5 Development Areas for PBWs 314

5.6 Lethality of Particle Beam Weapon 314

5.7 Propagation of the Beam 316

5.8 Fire Control/Pointing and Tracking Technology 318

5.9 Accelerator Technology 318

5.10 Power Supply Technology 320

References 321

6 Scalar Wave Energy as Weapon 323

6.1 Introduction 323

6.2 Transverse and Longitudinal Wave Descriptions 324

6.2.1 Transverse Waves 325

6.2.2 Longitudinal Waves 326

6.2.3 Pressure Waves and More Details 332

6.2.4 What Are Scalar Longitudinal Waves 338

6.2.5 Scalar Longitudinal Wave Applications 339

6.3 Description of $\vec{B}^{(3)}$ Field 352

6.4 Scalar Wave Description 354

6.5 Longitudinal Potential Waves 358

6.6 Transmitters and Receiver for Longitudinal Waves 361

6.6.1 Scalar Communication System 365

6.7 Scalar Wave Experiments 366

6.7.1 Tesla Radiation 366

6.7.2 Vortex Model 368

6.7.3 Experiment 372

6.8 Summary 373

References 374

7 Millimeter-Wave Energy as Weapon 377

7.1 Introduction 377

7.2 Active Denial System 379

7.3 Military Applications 380

7.4 Current Configuration 387

7.5 Effects and Critical Issues 388

 7.5.1 Human Effects 390

 7.5.2 Possible Long-Term Effects 390

7.6 Technogym Demonstration 391

7.7 Emerging Technogym Configuration 391

7.8 Active Denial System II 392

7.9 Concepts for Use 392

7.10 Controversy 394

Reference 396

Appendix A: Microwave Breakdown in Gases 397

References 423

Index 425

About the Author

Bahman Zohuri currently works for Galaxy Advanced Engineering, Inc., a consulting firm that he started in 1991 when he left both the semiconductor and defense industries after many years of working as a chief scientist. After graduating from the University of Illinois in the field of physics and applied mathematics, he then went to the University of New Mexico, where he studied nuclear engineering and mechanical engineering. He joined Westinghouse Electric Corporation, where he performed thermal hydraulic analysis and studied natural circulation in an inherent shutdown, heat removal system (ISHRS) in the core of a liquid metal fast breeder reactor (LMFBR) as a secondary fully inherent shutdown system for secondary loop heat exchange. All these designs were used in nuclear safety and reliability engineering for a self-actuated shutdown system. He designed a mercury heat pipe and electromagnetic pumps for large pool concepts of a LMFBR for heat rejection purposes for this reactor around 1978, when he received a patent for it. He was subsequently transferred to the defense division of Westinghouse, where he oversaw dynamic analysis and methods of launching and controlling MX missiles from canisters. The results were applied to MX launch seal performance and muzzle blast phenomena analysis (i.e., missile vibration and hydrodynamic shock formation). Dr. Zohuri was also involved in analytical calculations and computations in the study of nonlinear ion waves in rarefying plasma. The results were applied to the propagation of the so-called soliton waves and the resulting charge collector traces in the rarefaction characterization of the corona of laser-irradiated target pellets. As part of his graduate research work at Argonne National Laboratory, he performed computations and programming of multi-exchange integrals in surface physics and solid-state physics. He earned various patents in areas such as diffusion processes and diffusion furnace design while working as a senior process engineer at various semiconductor companies, such as Intel Corp., Varian Medical Systems, and National Semiconductor Corporation. He later joined Lockheed Martin Missile and Aerospace Corporation as senior chief scientist and oversaw research and development (R&D) and

the study of the vulnerability, survivability, and both radiation and laser hardening of different components of the Strategic Defense Initiative, known as Star Wars.

This included payloads (i.e., IR sensor) for the Defense Support Program, the Boost Surveillance and Tracking System, and Space Surveillance and Tracking Satellite against laser and nuclear threats. While at Lockheed Martin, he also performed analyses of laser beam characteristics and nuclear radiation interactions with materials, transient radiation effects in electronics, electromagnetic pulses, system-generated electromagnetic pulses, single-event upset, blast, thermo-mechanical, hardness assurance, maintenance, and device technology.

He spent several years as a consultant at Galaxy Advanced Engineering serving Sandia National Laboratories, where he supported the development of operational hazard assessments for the Air Force Safety Center in collaboration with other researchers and third parties. Ultimately, the results were included in Air Force Instructions issued specifically for directed-energy weapons operational safety. He completed the first version of a comprehensive library of detailed laser tools for airborne lasers, advanced tactical lasers, tactical high-energy lasers, and mobile/tactical high-energy lasers, for example.

He also oversaw SDI computer programs, in connection with Battle Management C³I and artificial intelligence, and autonomous systems. He is the author of several publications and holds several patents, such as for a laser-activated radioactive decay and results of a through-bulkhead initiator. He has published the following works: *Heat Pipe Design and Technology: A Practical Approach* (CRC Press); *Dimensional Analysis and Self-Similarity Methods for Engineers and Scientists* (Springer); *High Energy Laser (HEL): Tomorrow's Weapon in Directed Energy Weapons*, Volume I and Volume II (Trafford Publishing Company); and recently the book on the subject *Directed Energy Weapons and Physics of High Energy Laser* with Springer. He has other books with Springer Publishing Company, such as *Thermodynamics in Nuclear Power Plant Systems* (Springer) and *Thermal-Hydraulic Analysis of Nuclear Reactors* (Springer).

Chapter 1

Introduction to Directed Energy Weapon



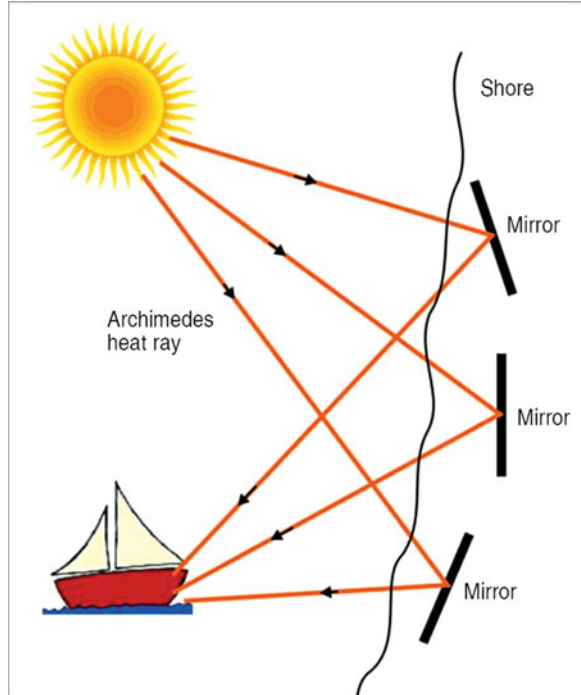
This chapter focuses on new class of weapons known as directed energy weapons (DEWs) along with the exception of particle beam weapon (PBW) and laser-induced plasma channel (LIPC) weapons that generate a stream of electromagnetic energy that can be precisely directed over long distance to disable or destroy intended targets.

1.1 Introduction

It has been known since prehistory that sunlight can make absorbing surface hot, and in Greek antiquity it was known that concentrated sunlight, having traversed spherical water-filled flasks or convex pieces of glass, could kindle fires. Archimedes proposed to concentrate the sun's rays by means of reflecting the harbor of Syracuse. He hoped to ignite the ropes, sails, and spars of the vessels of enemy's fleet. See Fig. 1.1.

The power flux density of the sun in zenith on the earth's surface is about 0.13 W/cm^2 that leads to the solar furnaces with temperatures near $3000 \text{ }^\circ\text{C}$. If the irradiated area is large enough, lateral heat conduction may be ignored. The radiative loss of a black-body surface is given by Stefan–Boltzmann's law. If the irradiated area is large enough, lateral heat conduction may be ignored. The power flux density, σT^4 , corresponds to 1 kW/cm^2 at $T = 3644 \text{ K}$. Convective cooling by airflow over a 3000 K surface at Mach number unity is only a few hundred W/cm^2 . At pressures prevailing at booster burnout altitudes, $80\text{--}160 \text{ km}$, convective cooling is completely negligible. From the foregoing, it is clear that the temperature of most materials may be raised above the melting temperature T_m and the vaporization temperature T_v for CW laser flux densities in the range of $1\text{--}100 \text{ kW/cm}^2$. In the early days of laser history, in 1961, when the pulsed ruby laser was the most powerful available, it was established that a focused ruby laser pulse of about 1 J energy could punch a hole in a razor blade. Two very simple cases serve to establish the order of magnitude of

Fig. 1.1 Archimedes death ray concept



fluxes and fluencies on target required for lethality. Most analyses that we have showed so far are applicable for the CW laser type as well.

Laser is no longer confined to premises of prominent research centers like Bell Laboratories, Hughes Research Laboratories, and major academic institutes like Columbia University, USA, as it was in its early stages of development and evolution. In the last five decades, after Theodore Maiman demonstrated the first laser in May 1960 at Hughes Research Laboratories, there has been explosive growth in industrial, medical, scientific, and military applications of lasers. Application areas are continuing to grow with every passing day.

Lasers have been used in various military applications since the early days of development that followed their invention. There has been large-scale proliferation of lasers and optronic devices and systems for applications like range finding, target designation, target acquisition and tracking, and precision-guided munitions during 1970s and 1980s.

These devices continue to improve in performance and find increased acceptance and usage in contemporary battlefield weaponry. Technological advances in optics, optoelectronics, and electronics leading to more rugged, reliable, compact, and efficient laser devices are largely responsible for making these indispensables in modern warfare.

Last one decade or so has also seen emergence of a new class of weapons known as directed energy weapons (DEWs) leading to enhanced global interest from

scientists and engineers in DEW development. Lasers, high-power microwaves, and high-energy particle beams have been exploited for DEW development. These weapons, with the exception of particle beam weapons (PBWs) and laser-induced plasma channel (LIPC) weapons, generate streams of electromagnetic energy that can be precisely directed over long distances to disable or destroy intended targets.

After decades of research and development, directed energy weapons (DEWs) are now becoming an operational reality. This has been possible due to their unique characteristics that potentially enable new concepts of military operation and also because there has been considerable progress over the past two decades in developing relevant technologies such as power sources, beam-control concepts, and pointing and tracking techniques. For these applications, lethal energy from a high-power laser or a source of high-power microwaves or high-energy particle beam is delivered to the targets for causing either neutralization of electro-optic sensors onboard the target platform or structural damage to the target itself.

1.2 Directed Energy Weapons (DEWs)

A directed energy weapon (DEW) system, with the exception of LIPC weapons, primarily uses directed energy in the form of concentrated beam of electromagnetic energy, or atomic or subatomic particles in the targeted direction to cause intended damage to the enemy's equipment, facilities, and personnel. Intended damage could be lethal or nonlethal.

Ever since H.G. Wells published *War of the Worlds* in 1898, directed energy weapons (DEWs) have been a recurring theme in science fiction literature. Idea of a death ray, which can instantly destroy or burn a target at a distance, in fact, dates back to a belief that Archimedes used a burning glass to set afire Roman ships during the siege of Syracuse in 212 B.C. Although many images of the death ray depict Archimedes with a parabolic mirror, use of a set of individual flat mirrors appropriately positioned seemed to be a more practical implementation of the concept as illustrated in Fig. 1.1.

Though the story has long been dismissed as a myth, interest generated by it has led to a number of experiments being conducted to verify the technical feasibility of such an event. Experiments conducted by Comte de Buffon and Dr. Ioannis Sakkas, and more recently by students of Massachusetts Institute of Technology (MIT), USA, have established the feasibility of such an occurrence. See Fig. 1.2.

Buffon assembled 168 mirrors, 20.3 cm \times 25.4 cm (8 in. \times 10 in.) each, adjusted to produce the smallest image 45.7 m (150 ft) away. The array turned out to be a formidable weapon. With this elaborate setup, he performed several experiments. He demonstrated igniting a creosoted plank at 20.1 m (66 ft) distance using only 40 mirrors. 128 mirrors could ignite a pine plank instantly and, in another experiment, 45 mirrors melted 2.7 kg (six pounds) of tin at 6.1 m (20 ft).



Fig. 1.2 Technical feasibility of death ray, an MIT experiment

In another effort, Dr. Sakkas lined up nearly 60 Greek sailors, each holding an oblong mirror tipped to catch the sun's rays, and directed these at a wooden ship 48.7 m (160 ft) away. The ship caught fire at once.

As recently as 2009, MIT students carried out an experiment with 11.7 sqm (127 sqft) mirrors focusing solar radiation on to a boat 30.5 m (100 ft) away, causing a sustained flame and confirming technical feasibility of what Archimedes might have achieved with his death ray (see Fig. 1.2).

1.3 Directed Energy Weapons (DEWs) Versus Kinetic Energy Weapons (KEWs)

At the most fundamental level, directed energy weapons (DEWs) share the concept of delivering a large amount of stored energy from the weapon to the target to produce structural and incendiary damage effects. Kinetic energy weapons (KEWs) deliver this effect at subsonic or supersonic speeds while directed energy weapons (DEWs) do so at the speed of light.

Both kinetic energy weapons (KEWs) and directed energy weapons (DEWs) need to address two fundamental issues. The first major concern is related to travel or propagation through the atmosphere and hitting the target. In the case of KEWs, it is getting the projectile to successfully travel through the atmosphere and hit the target.

In the case of directed energy weapons (DEWs), it is the propagation of high-energy beams such as high-power electromagnetic radiation or high-energy particle beams through the atmosphere and directing these to hit the target.

The second major concern is to produce sufficient damage to the intended target. This is where interaction of high energy with matter comes into play. This implies that having a high-power laser or a HPM emitter alone does not make a directed energy weapon (DEW).

Three important constituents of directed energy weapons (DEW) therefore are the high-energy sources influencing operational range, target-tracking and beam-pointing technology determining probability of target hit, and interaction of high-energy beams with matter that determines lethality.

1.4 Types of Directed Energy Weapons (DEWs)

Four major categories of DEWs are:

1. Particle beam weapons (PBWs)
2. High-power microwave (HPM)-based DEWs
3. High-energy laser (HEL)-based DEWs
4. Laser-induced plasma channel (LIPC) weapons

However, this author is suggesting the fifth category that is known as scalar longitudinal wave (SLW) [1] and refer to Chap. 7 of this book for more details.

A PBW uses a high-energy beam of atomic or subatomic particles to inflict intended damage to the target by disrupting its atomic and/or molecular structure. It is the least mature of the four directed energy weapon (DEW) technologies and receives by far the least amount of research effort. It is not a true DEW. Unlike high-energy laser weapons and high-power microwaves that direct electromagnetic energy towards the target, it delivers kinetic energy into the target's atomic structure and is only a hard-kill weapon. See Figs. 1.3 and 1.4.

A microwave-based directed energy weapon (DEW) system is designed to produce the equivalent of electromagnetic interference to damage enemy's electronics systems. Due to concerns regarding unintended side effects on the host platform, it is usually preferred to put such weapons only on unmanned combat air vehicles. Also, under consideration is the use of high-power microwaves as a weapon to attack underground and deeply buried targets that are resistant to high explosives.

At the core of the laser-based DEW is a high-power laser that has enough power in the case of continuous wave laser, or sufficient pulse energy in the case of pulsed laser, to inflict physical damage to the target. Though the lasers intended for already established applications such as range finding, target designation for munition guidance, and more will continue to improve as newer technologies evolve and develop, it is the use of lasers as weapon that is going to rewrite the military balance in the next 15–20 years.



Fig. 1.3 Concept of space-based PBW in science fiction



Fig. 1.4 Another concept of space-based PBW

Another conceptual aspect of space-based particle beam weapon (PBW) is depicted in Fig. 1.4.

Introduction of laser-based directed energy weapons (DEWs) is set to dramatically alter the war-fighting capabilities of nations by making possible execution of missions that would be extremely complex, if not impossible, to realize with conventional KEWs. These include ground-based laser systems for disabling low earth orbit satellites and destroying missiles, airborne laser systems for destroying

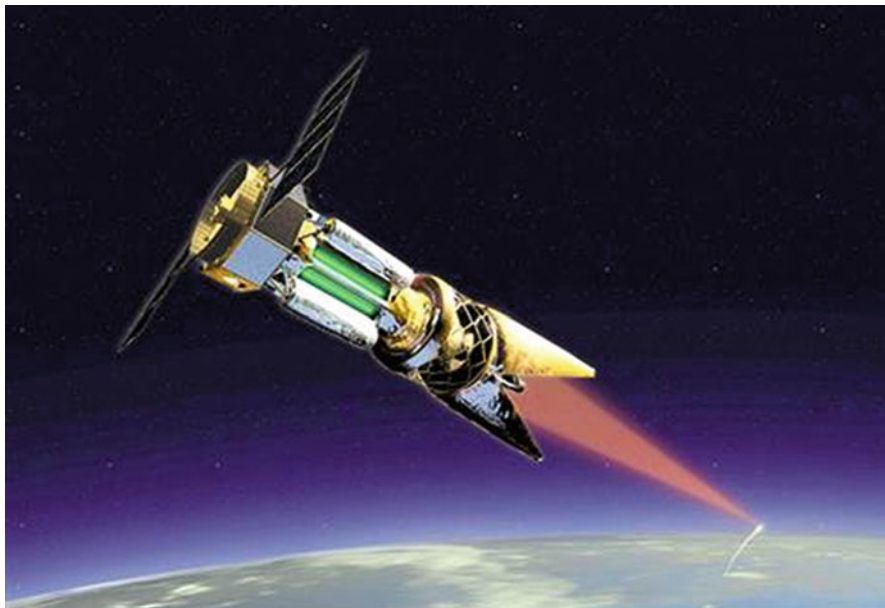


Fig. 1.5 Space-based laser (SBL)

ballistic missiles, and space-based laser systems for neutralizing theater and intercontinental ballistic missiles.

A large number of experiments with laser-based directed energy weapons (DEWs) to demonstrate these or similar capabilities have been carried out in different parts of the world. Realizability of these weapons has been established beyond doubt, and these weapons have been projected by strategists as the weapons of the twenty-first century. See Fig. 1.5, where a laser fires from space towards earth in this artistic rendering.

The Air Force Research Laboratory's Directed Energy Directorate is conducting research in a wide variety of laser weapon technologies

Laser-induced plasma channel (LIPC) weapons are hybrid weapons that use a laser to ionize a path of molecules to the target, via which an electric charge can be delivered into the target to cause damaging effects. These can be used to destroy anything that conducts electricity better than the air or ground surrounding it. This works as follows:

- A high-intensity train of picosecond laser pulses is used to create a powerful electromagnetic pulse around itself that strips electrons from air molecules, thereby creating a plasma channel through the air. Since the air is composed of neutral particles that act as insulators, LIPC is relatively a good conductor. A high-voltage current discharge is sent down this conducting filament to the target rather than arcing unpredictably through the air—a phenomenon similar to lightning that finds its way from clouds to ground via the path of least resistance.

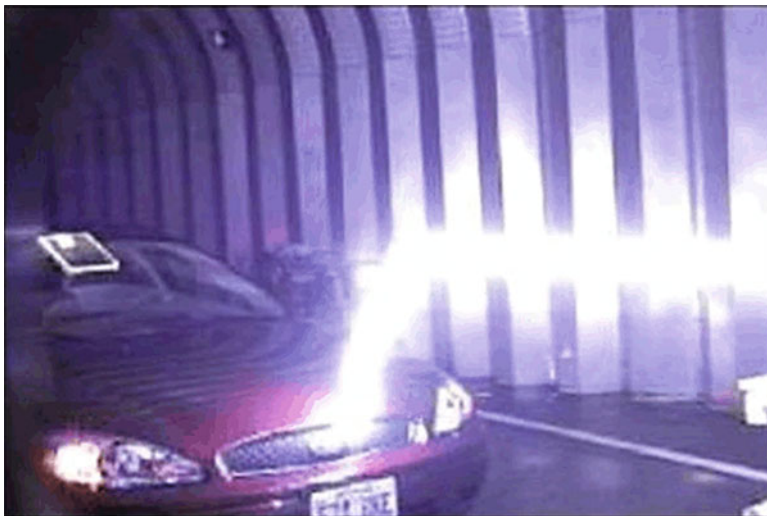


Fig. 1.6 Car meets lightening weapon

An electro-laser is a type of electroshock weapon that is also a directed energy weapon. It uses lasers to form an electrically conductive laser-induced plasma channel (LIPC). A fraction of a second later, a powerful electric current is sent down this plasma channel and delivered to the target, thus functioning overall as a large-scale, high-energy, long-distance version of the Taser electroshock gun.

Alternating current is sent through a series of step-up transformers, increasing the voltage and decreasing the current. The final voltage may be between 108 and 109 V. This current is fed into the plasma channel created by the laser beam.

Over at Picatinny Arsenal, the research and development facility and proving ground for the US Army's weaponry, engineers are developing a device that shoots lightning bolts along a laser beam to annihilate its target. That's right: lightning bolts shot down laser beams. This story could easily end right here and still be the coolest thing we've written today, but for the scientifically curious we'll continue. See Fig. 1.6.

As it can be observed in Fig. 1.6, the LIPC weapon is capable of emitting "huge" power as the researchers on this type of directed energy weapon are claiming.

The laser-induced plasma channel (LIPC) is designed to hit targets that conduct electricity better than the air or ground that surrounds them.

The weapon went through extensive testing in January 2012.

George Fischer, lead scientist on the project, said: "We never got tired of the lightning bolts zapping our simulated targets."

Details of the weapon were released on the US Army's website.

Mr. Fischer explained how the usually unpredictable lightning bolts can be controlled.

“If a laser puts out a pulse with modest energy, but the time is incredibly tiny, the power can be huge,” Mr. Fischer said.

“During the duration of the laser pulse, it can be putting out more power than a large city needs, but the pulse only lasts for two-trillionths of a second.” This is a 50 billion watts energy, which means as Mr. Fischer says the air could be manipulated to “act like lens.” He claims that they use an ultrashort-pulse laser of modest energy to make a laser beam so intense that it focuses on itself in air and stays focused in a filament.”

A laser-induced plasma channel (LIPC) is formed by the following process:

- A laser emits a laser beam into the air.
- The laser beam rapidly heats and ionizes surrounding gases to form plasma.
- The plasma forms an electrically conductive plasma channel.

Because a laser-induced plasma channel relies on ionization, gas must exist between the electro-laser weapon and its target. If a laser beam is intense enough, its electromagnetic field is strong enough to rip electrons off of air molecules, or whatever gas happens to be in between, creating plasma. Similar to lightning, the rapid heating also creates a sonic boom.

Methods of the usage of this weapon are summarized as below:

- To kill or incapacitate a living target through electric shock.
- To seriously damage, disable, or destroy any electric or electronic devices in the target.
- As electro-lasers and natural lightning both use plasma channels to conduct electric current, an electro-laser can set up a light-induced plasma channel for uses such as to study lightning.
- During a thunderstorm, to make lightning discharge at a safe time and place, as with a lightning conductor [2].
- Directing atmospheric lightning to a terrestrial collection station for the purpose of electrical power generation.
- As a weapon, to make a thunderhead deliver a precise lightning strike onto a target from an aircraft; in this case, the aircraft and laser can be compared to a triggered spark gap, in that the relatively minor amount of initial input from the laser allows a large amount of energy to flow between the cloud and the ground.

Because of the plasma channel, an electro-laser may cause an accident if there is a thunderstorm (or other electricity sources such as overhead powerlines). (See Taser for more information—principles of operation, controversies, etc.)

An electro-laser is not presently practical for wireless energy transfer due to danger and low efficiency.

Of these four categories mentioned above, high-energy laser weapons have the greatest potential in the near term to become worthy of a potent weapon system. However, evidences are presented by certain researchers that scalar longitudinal wave (SLW) has been in use by countries such as previous Soviet Union (USSR) since early 1980, through a photo that was taken by the US high-resolution reconnaissance satellite KH-11 as depicted in Fig. 1.7 [1].

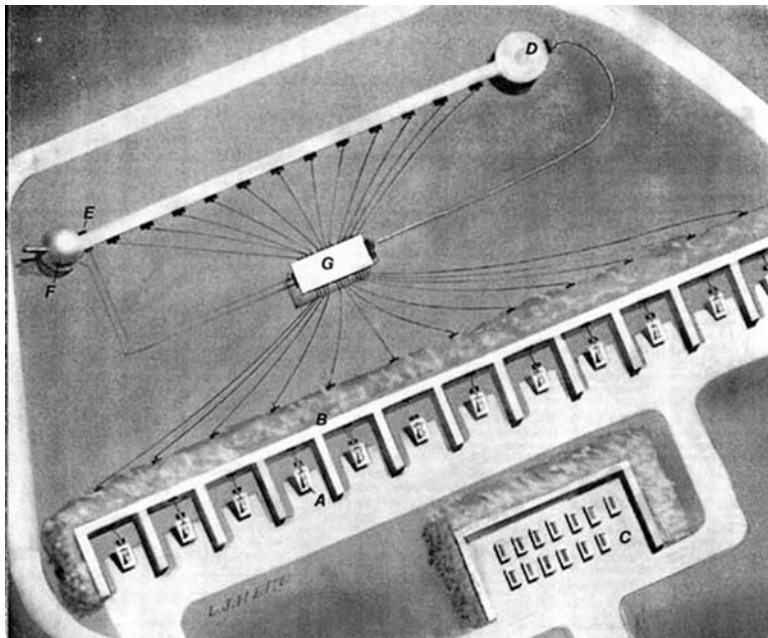


Fig. 1.7 Aviation Week & Space Technology July 28, 1980, Page 48 (the photo is taken by the US high-resolution reconnaissance satellite KH-11)

According to Tom Bearden [3], a department of defense scientist, the scalar interferometer is a powerful superweapon that the Soviet Union used for years to modify weather in the rest of the world [7]. It taps the quantum vacuum energy, using a method discovered by T. Henry Moray in the 1920s [8]. It may have brought down the Columbia spacecraft [9, 10]. However, some conspiracy theorists believe that Bearden is an agent of disinformation on this topic, and thus we leave this matter to the reader to make their own conclusions and be able to follow up their own finding and this author does not claim that any of these matters are true or false. However, in the 1930s Tesla announced other bizarre and terrible weapons: a death ray, a weapon to destroy hundreds or even thousands of aircraft at hundreds of miles range, and his ultimate weapon to end all war—the Tesla shield, which nothing could penetrate. However, by this time no one any longer paid any real attention to the forgotten great genius. Tesla died in 1943 without ever revealing the secret of these great weapons and inventions. Tesla called this superweapon as scalar potential howitzer or death ray as artistically depicted in Fig. 1.8 and later it was demonstrated by Soviets in their Sary Shagan Missile Range during pick of Strategic Defense Initiative (SDI) time period and mentioned it during SALT treaty negotiation.

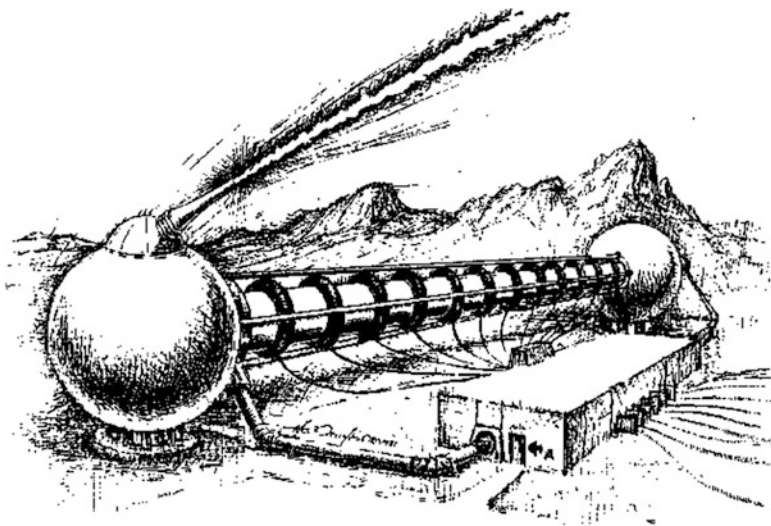


Fig. 1.8 Scalar potential interferometer (multimode Tesla weapon)

Bearden claims that in 1981 the Soviet Union has long since discovered and weaponized the Tesla scalar wave effects. Here we only have time to detail the most powerful of these frightening Tesla weapons—which Brezhnev undoubtedly was referring to in 1975 when the Soviet side at the SALT talks suddenly suggested limiting the development of new weapons “more frightening than the mind of man had imagined.” One of these weapons is the Tesla howitzer recently completed at the Sary Shagan, a ballistic missile range near the Sino-Soviet border in Southern Russia, according to high-level US officials and presently considered to be either a high-energy laser or a particle beam weapon (see *Aviation Week & Space Technology*, July 28, 1980, p. 48, for an artistic conception).

As Fig. 1.7 illustrates, the Sary Shagan howitzer has four modes of operation.

He also claims that the Sary Shagan howitzer actually is a huge Tesla scalar interferometer with four modes of operation. One continuous mode is the Tesla shield, which places a thin, impenetrable hemispherical shell of energy over a large defended area. The 2-dimensional shell is created by interfering two Fourier-expansion, 2-dimensional scalar hemispherical patterns in space so they pair-couple into a dome-like shell of intense, ordinary electromagnetic energy. The air molecules and atoms in the shell are totally ionized and thus highly excited, giving off intense, glowing light. Anything physical which hits the shell receives an enormous discharge of electrical energy and is instantly vaporized—it goes pfft! like a bug hitting one of the electrical bug killers now so much in vogue. See Fig. 1.9.

Bearden goes on further to say that if several of these hemispherical shells are concentrically stacked, even the gamma radiation and EMP from a high-altitude nuclear explosion above the stack cannot penetrate all the shells due to repetitive absorption and reradiation and scattering in the layered plasmas.

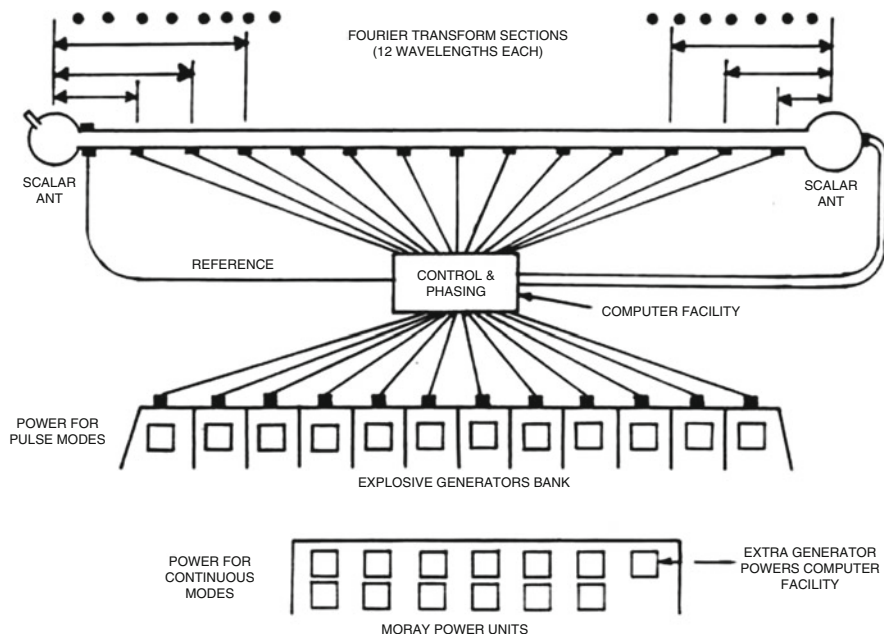


Fig. 1.9 Tesla weapons at Sary Shagan

In the continuous shield mode, the Tesla interferometer is fed by a bank of Moray free energy generators, so that enormous energy is available in the shield. A diagram of the Sary Shagan-type Tesla howitzer is shown in Fig. 1.9. Hal Crawford's fine drawing of the interferometer end of the Tesla howitzer is shown in Fig. 1.8. Hal's exceptional rendition of the Tesla shield produced by the howitzer is shown in Figs. 1.10 and 1.11 as well.

In the pulse mode, a single intense 2-dimensional scalar phi-field pulse form is fired, using two truncated Fourier transforms, each involving several frequencies, to provide the proper 2-dimensional shape (Fig. 1.12). This is why two scalar antennas separated by a baseline are required. After a time delay calculated for the particular target, a second and faster pulse form of the same shape is fired from the interferometer antennas. The second pulse overtakes the first, catching it over the target zone and pair-coupling with it to instantly form a violent EMP of ordinary vector (Hertzian) electromagnetic energy. There is thus no vector transmission loss between the howitzer and the burst. Further, the coupling time is extremely short, and the energy will appear sharply in an "electromagnetic pulse (EMP)" strikingly similar to the two-pulsed EMP of a nuclear weapon.

This type of weapon is what actually caused the mysterious flashes off the southwest coast of Africa, picked up in 1979 and 1980 by Vela satellites. The second flash, e.g., was in the infrared only, with no visible spectrum. Nuclear flashes do not do that, and neither does super-lightning, meteorite strikes, meteors, etc. In addition, one of the scientists at the Arecibo Ionospheric Observatory observed a gravitational

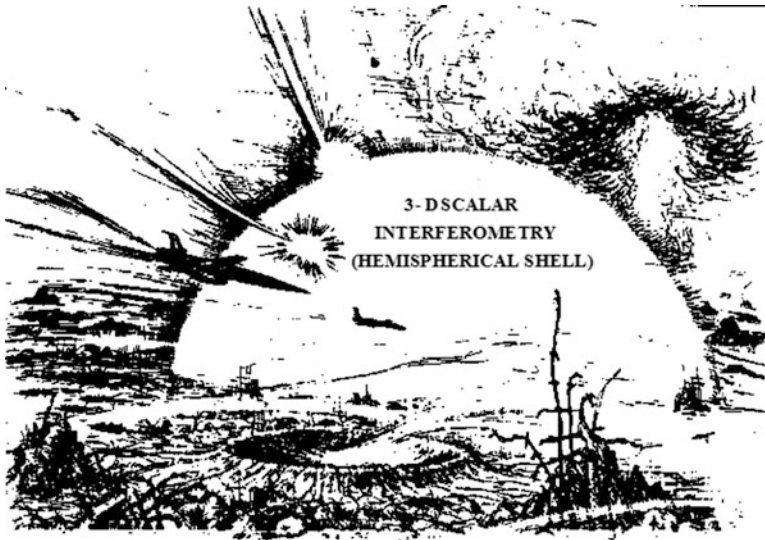


Fig. 1.10 The Tesla shield

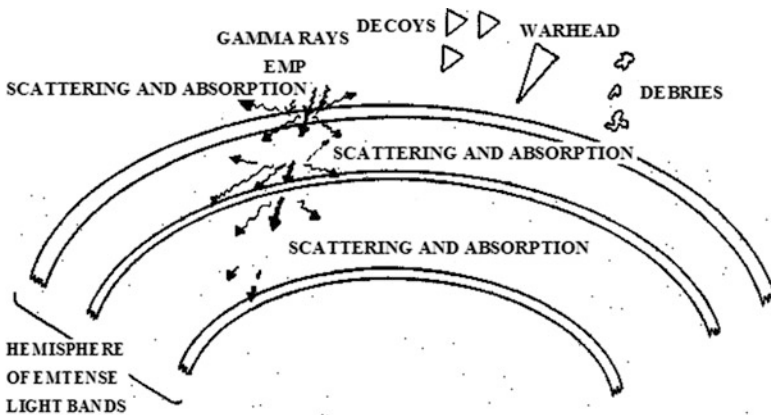
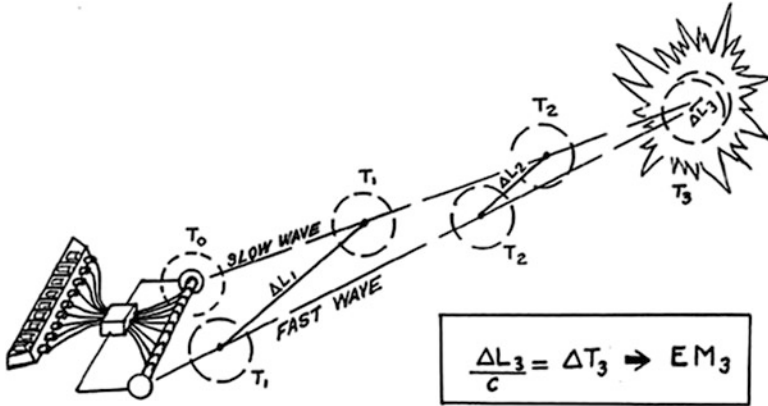


Fig. 1.11 Tesla terminal area defense system

wave disturbance—signature of the truncated Fourier pattern and the time-squeezing effect of the Tesla potential wave—traveling towards the vicinity of the explosion.

The pulse mode may be fed from either Moray generators or—if the Moray generators have suffered their anomalous “all fail” malfunction—ordinary explosive generators. Thus, the Tesla howitzer can always function in the pulse mode, but it will be limited in power if the Moray generators fail.

In the continuous mode, two continuous scalar waves are emitted—one faster than the other—and they pair-couple into vector energy at the region where they



TESLA HOWITZER
(SCALAR INTERFEROMETER)

Fig. 1.12 Conceptual nuclear flash theory

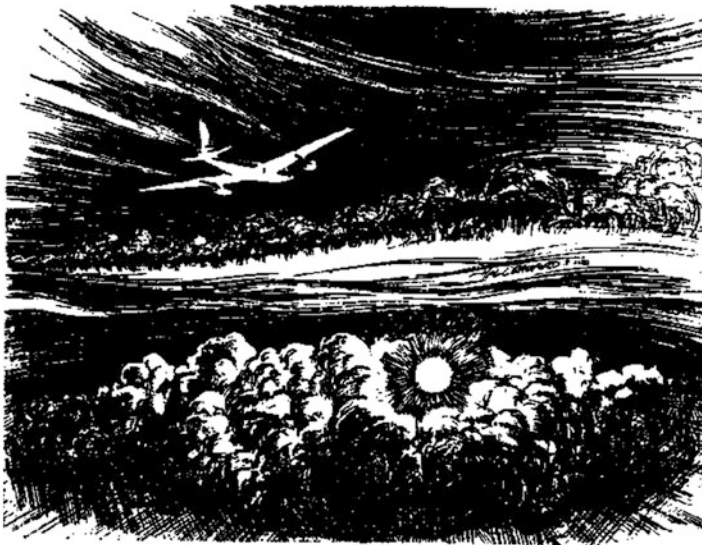


Fig. 1.13 Continuous Tesla fireball

approach an in-phase condition. In this mode, the energy in the distant “ball” or geometric region would appear continuously and be sustained—and this is Tesla’s secret of wireless transmission of energy at a distance without any losses. It is also the secret of a “continuous fireball” weapon capable of destroying hundreds of aircraft or missiles at a distance. This mode of operation is shown in Fig. 1.13.

Fig. 1.14 Artistic illustration of Tesla EMP globe



The volume of the Tesla fireball can be vastly expanded to yield a globe which will not vaporize physical vehicles but will deliver an EMP to them to dud their electronics. An artistic test of this mode is shown in Fig. 1.14.

If the Moray generators fail anomalously, then a continuous mode limited in power and range could conceivably be sustained by powering the interferometer from more conventional power sources such as advanced magnetohydrodynamic generators.

Typical strategic ABM uses of Tesla weapons are shown in Fig. 1.15. In addition, of course, smaller Tesla howitzer systems for anti-tactical ballistic missile defense of tactical troops and installations could be constituted of more conventional field missile systems using paired or triplet radars, of conventional external appearance, in a scalar interferometer mode.

Bearden also suggests that with Moray generators¹ as power sources and multiple-deployed reentry vehicles with scalar antennas and transmitters, ICBM reentry systems now can become long-range “blasters” of the target areas, from thousands of kilometers distance (Fig. 1.16). Literally, “Star Wars” is liberated by the Tesla technology. And in air attack, jammers and ECM aircraft now become “Tesla blasters.” With the Tesla technology, emitters become primary fighting components of stunning power.

¹<http://www.cheniere.org/books/excalibur/moray.htm>

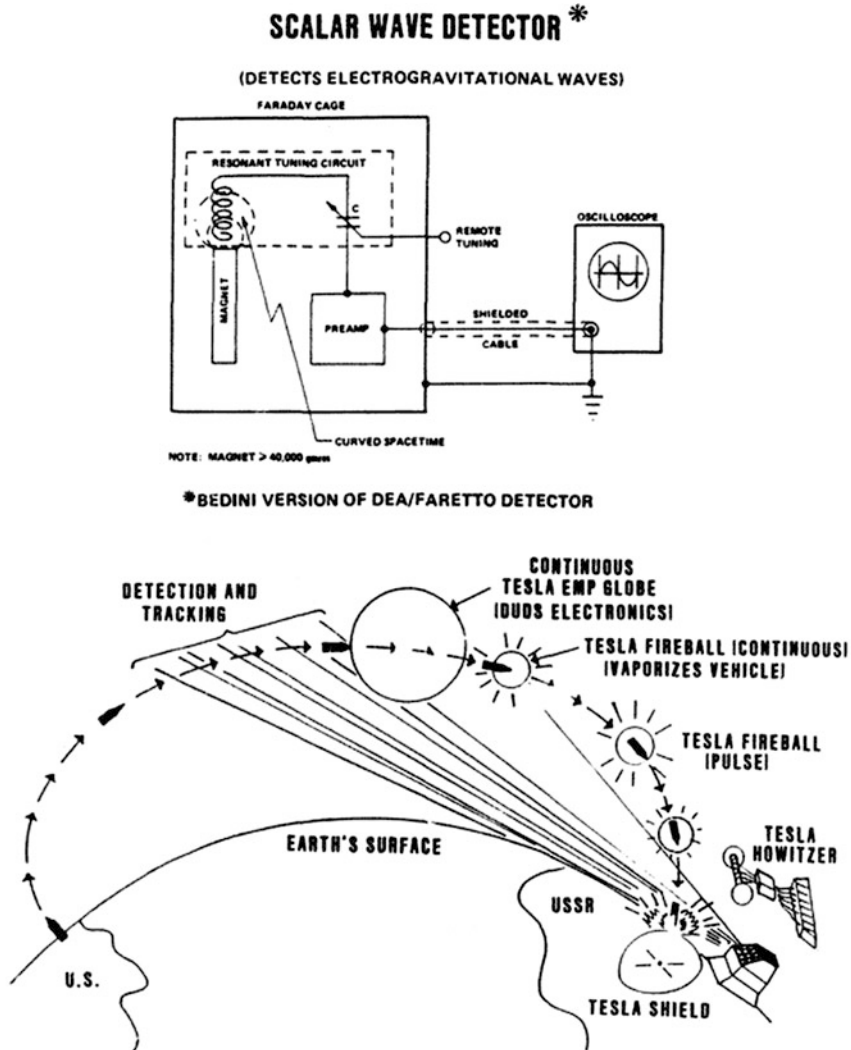
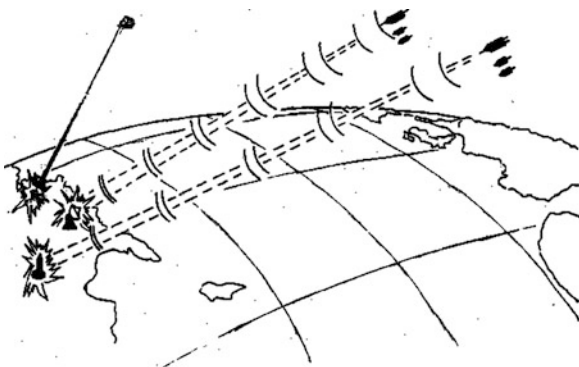


Fig. 1.15 Antistatic conceptual Tesla ABM defenses

The potential peaceful implications of Tesla waves are also enormous. By utilizing the “time squeeze” effect, one can get antigravity, materialization and dematerialization, transmutation, and mind-boggling medical benefits. One can also get subluminal and superluminal communication, see through the earth and through the ocean, etc. The new view of phi field also provides a unified field theory, higher orders of reality, and a new super-relativity, which need to be investigated and tested as well.

Fig. 1.16 Moray/Tesla technology



1.5 Beam Weapons Almost Ready for Battle at Speed of Light and Electron

There is a new breed of weaponry fast approaching—and at the speed of light, no less. They are labeled “directed energy weapons,” and they may well signal a revolution in military hardware—perhaps more so than the atomic bomb.

Directed energy weapons take the form of lasers, high-powered microwaves, and particle beams. Their adoption for ground, air, sea, and space warfare depends not only on using the electromagnetic spectrum, but also upon favorable political and budgetary wavelengths.

That is the outlook of J. Douglas Beason, author of the recently published book “The E-Bomb: How America’s New Directed Energy Weapons Will Change the Way Wars Will Be Fought in the Future.” Beason previously served on the White House staff working for the president’s science adviser under both the Bush and Clinton administrations.

After more than two decades of research, the United States is on the verge of deploying a new generation of weapons that discharge beams of energy, such as the airborne laser and the active denial system, as well as the tactical high-energy laser (THEL) [4].

“History has shown that, without investment in high technology, fighting the next war will be done using the ‘last war’ type of technique,” Beason told [Space.com](#). Putting money into basic and long-range research is critical, Beason said, adding: “You can’t always schedule breakthroughs.”

A leading expert in directed energy research for 26 years, Beason is also director of threat reduction here at the Los Alamos National Laboratory. However, he noted that he was expressing his own views rather than the policy of the laboratory, the Defense Department, or the Energy Department.



Fig. 1.17 An Airborne Laser system onboard of an aircraft

1.5.1 Ripe for Transformation?

Though considerable work has been done in lasers, high-power microwaves, and other directed energy technologies, weaponization is still an ongoing process.

For example, work is continuing in the military's Airborne Laser program. It utilizes a megawatt-class, high-energy chemical oxygen iodine laser toted skyward aboard a modified Boeing 747-400 aircraft. Purpose of the program is to enable the detection, tracking, and destruction of ballistic missiles in the boost phase, or powered part of their flight. See Fig. 1.17, where an artist's conception shows a reddish beam emanating from an Airborne Laser system, with another beam being used against missiles in the background. In reality, the beam itself might be invisible.

Similarly, testing of the US Army's tactical high-energy laser in White Sands, NM, has shown the ability of heating high-flying rocket warheads, blasting them with enough energy to make them self-detonate. THEL uses a high-energy, deuterium fluoride chemical laser. A mobile THEL also demonstrated the ability to kill multiple mortar rounds.

Then there's active denial technology—a nonlethal way to use millimeter-wave electromagnetic energy to stop, deter, and turn back an advancing adversary. This technology, supported by the US Marines, uses a beam of millimeter waves to heat a foe's skin, causing severe pain without damage, and making the adversary flee the scene.

Beason also pointed to new exciting research areas underway at the Los Alamos National Laboratory: free-electron laser work with the Navy and a new type of directed energy that operates in the terahertz region.

1.5.2 Niche for New Technology

While progress in directed energy is appreciable, Beason sees two up-front problems in moving the technology forward. One issue has to do with “convincing the

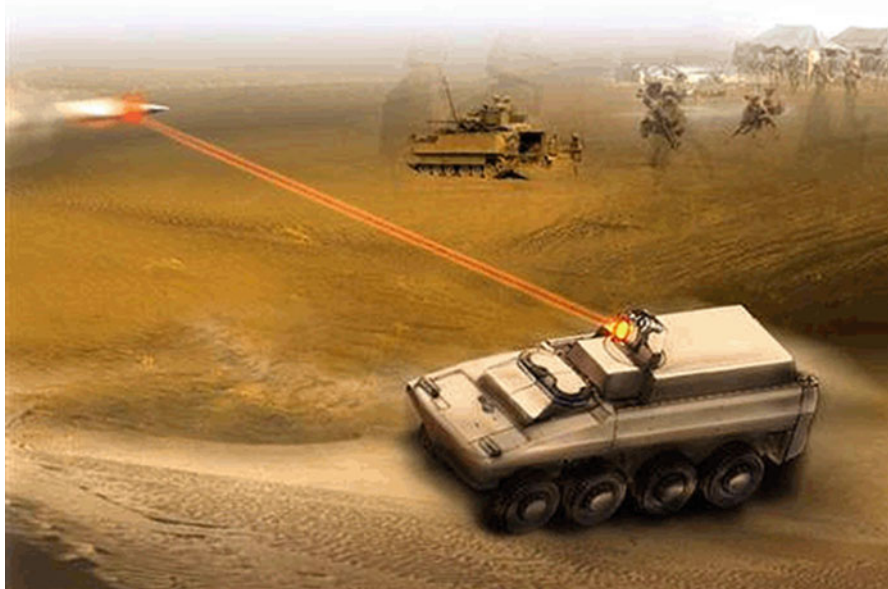


Fig. 1.18 Illustration of a future army combat systems

warfighter that there's a niche for this new type of weapon," and the other relates to making sure that these new systems are not viewed as a panacea to solve all problems. "They are only another tool," he said.

Looming even larger is the role of those who acquire new weapons. "The U.S. could put ourselves in a very disastrous position if we allow our acquisition officials to be non-technically competent," Beason explained.

Over the decades, Beason said that the field of directed energy has had its share of "snake-oil salesmen," as well as those advocates who overpromised. "It wasn't ready for prime time."

At present, directed energy systems "are barely limping along with enough money just to prove that they can work," Beason pointed out. Meanwhile, huge slugs of money are being put into legacy-type systems to keep them going.

"It's a matter of priority," Beason said. The time is now to identify high-payoff, directed energy projects for the smallest amounts of money, he said. See Fig. 1.18, where it shows a conceptual look at putting a solid-state laser on an armored ground combat vehicle for potential use in the US military's Future Combat Systems program.

1.5.3 Unknown Unknowns

In Beason's view, active denial technology, the Airborne Laser program, and the THEL project, as well as supporting technologies such as relay mirrors, are all works in progress that give reason for added support and priority funding.

“I truly believe that as the Airborne Laser goes, so goes the rest of the nation’s directed-energy programs. Right now, it’s working on the margin. I believe that there are still ‘unknown unknowns’ out there that are going to occur in science and technology. We think we have the physics defined. We think we have the engineering defined. But something always goes wrong . . . and we’re working too close at the margin,” Beason said.

Stepwise demonstration programs that spotlight directed energy weapon systems are needed, Beason noted. Such in-the-field displays could show off greater beam distance-to-target runs, mobility of hardware, ease of operation, battlefield utility, and other attributes.

Directed energy technologies can offer a range of applications, from botching up an enemy’s electronics to performing “dial-up” destructive strikes at the speed of light with little or no collateral damage.

Beason said that he has a blue-sky idea of his own, which he tags “the voice from heaven.” By tuning the resonance of a laser onto earth’s ionosphere, you can create audible frequencies. Like some boom box in the sky, the laser-produced voice could bellow from above down to the target below: “Put down your weapons.”

1.5.4 Relay Mirrors

Regarding the use of directed energy space weapons, Beason advised that “we’ll eventually see it.”

However, present-day systems are far too messy. Most high-powered chemical lasers—in the megawatt class—require onboard fuels and oxidizers to crank out the amount of energy useful for strategic applications. Stability of such a laser system rooted in space is also wanting.

On the other hand, Beason said that he expected to see the rise of more efficient lasers—especially solid-state laser systems. “What breakthroughs are needed . . . I’m not sure. Eventually, I think it’s going to happen, but it is going to be a generation after the battlefield lasers.”

Shooting beams “through space” is another matter, Beason quickly added. Space-based relay mirrors—even high-altitude airships equipped with relay mirrors—can direct ground-based or air-based laser beams nearly around the world, he said.

“So, you’re using space . . . exploiting it. But you are going through space to attack anywhere on Earth,” Beason said.

1.5.5 History Lesson

Late last year, speaking before the Heritage Foundation in Washington, Beason told his audience that laser energy, power sources and beam control, as well as knowledge about how laser beams interact with earth’s atmosphere are quite mature technologies that are ready for the shift into front-line warfare status.

“The good news is that directed energy exists. Directed energy is being tested, and within a few years directed energy is going to be deployed upon the battlefield,” Beason reported. “But the bad news is that acquisition policies right now in this nation are one more gear toward evolutionary practices rather than revolutionary practices.”

“Visionaries win wars . . . and not bureaucrats. We’ve seen this through history,” Beason observed.

1.6 Space Warfare, a New Age of Military Weaponry

Space warfare is a combat that takes place in outer space. The scope of space warfare therefore includes ground-to-space warfare, such as attacking satellites from the earth, as well as space-to-space warfare, such as satellites attacking satellites.

In the early 1960s the US military produced a film called *Space and National Security* which depicted space warfare.²

From 1985 to 2002 there was a United States Space Command, which in 2002 merged with the United States Strategic Command, leaving Air Force Space Command as the primary American military space force. The Russian Space Force, established on August 10, 1992, which became an independent section of the Russian military on June 1, 2001, was replaced by the Russian Aerospace Defense Forces starting December 1, 2011, but was reestablished as a component of the Russian Aerospace Forces on August 1, 2015.

Only a few incidents of space warfare have occurred in world history, and all involved training missions, as opposed to actions against real opposing forces. In 1985 a USAF pilot in an F-15 (see Fig. 1.19) successfully shot down the P78-1, an American research satellite, in a 345-mile (555 km) orbit.

As it is observed in Fig. 1.19, a USAF F-15 Eagle launching an ASM-135 ASAT (anti-satellite) missile in 1985.

In 2007 China used a missile system to destroy one of its obsolete satellites (see 2007 Chinese anti-satellite missile test), and in 2008 the United States similarly destroyed its malfunctioning satellite USA-193. As of 2018 there have been no human casualties resulting from conflict in space.

International treaties are in place that regulate conflicts in space and limit the installation of space weapon systems, especially nuclear weapons.

1.6.1 History

Early efforts to conduct space warfare were directed at space-to-space warfare, as ground-to-space systems were considered to be too slow and too isolated by earth's atmosphere and gravity to be effective at the time.

²PBS Nova Program “Astrospies,” Broadcast February 12, 2008.

Fig. 1.19 A USAF F-15 Eagle launching an ASM-135 ASAT



P78-1 Satellite



(continued)

P78-1 or Solwind was a US satellite launched aboard an Atlas F rocket from Vandenberg Air Force Base in California on February 24, 1979. The satellite operated until it was destroyed in orbit on September 13, 1985, to test the ASM-135 ASAT anti-satellite missile.

The satellite's Orbiting Solar Observatory (OSO) platform included a solar-oriented sail and a rotating wheel section. Ball Aerospace was the primary contractor for design and construction and provided the attitude control and determination computer programs.³ The P78-1 carried a gamma-ray spectrometer, a white-light coronagraph, an extreme-ultraviolet imager, an X-ray spectrometer, a high-latitude particle spectrometer, an aerosol monitor, and an X-ray monitor. The X-ray monitor, designated NRL-608 or XMON, was a collaboration between the Naval Research Laboratory and Los Alamos National Laboratory. The white-light coronagraph and the ultraviolet imager were combined in a single package, designated NRL-401 or SOLWIND, which was built by the Naval Research Laboratory. The coronagraph was the flight spare of the white-light coronagraph on the OSO-7 satellite. The ultraviolet imager used a CCD imager, one of the first uses of a CCD in space.

By 1985, the satellite's batteries were degrading. This caused more and more frequent "undervoltage cutoffs," a condition where the satellite detected a low main bus voltage and automatically shut down all non-vital systems. In addition, the last of the three tape recorders failed in the spring of 1985, so data collection could only occur while the spacecraft was in contact with a ground station [1]. A normal contact lasted only about 15 min, so this was a serious impediment. Special arrangements could be made to string several contacts together. As a result of these failures, an ever-increasing amount of time and network resources were spent reconfiguring the satellite for normal operation. Data collection from the few remaining payloads was severely limited. Because of the additional burden on the Air Force Satellite Control Network (e.g., extra support and antenna time at the tracking stations), discussions were already underway to terminate the mission.

This led to the satellite being chosen as a test target for an ASM-135 ASAT anti-satellite missile. The mission was extended for several weeks solely to support the test. During this final phase, the satellite was often allowed to remain in the undervoltage condition for several days at a time.

(continued)

³Space Test Program P78-1 at Ball Aerospace.

On September 13, 1985, the satellite was destroyed in orbit at 2043 UTC at 35°N 126°W with an altitude of 525 km (326 mi) [4] by an ASM-135 ASAT launched from a US Air Force F-15 Eagle fighter aircraft. The test resulted in 285 cataloged pieces of orbital debris. One piece of debris remained in orbit to at least May 2004,⁴ but had deorbited by 2008 [4].

The test outraged some scientists because although five of P78-1's instruments had failed at the time of the test, two instruments remained in operation, and the satellite was what one solar physicist called "the backbone" of coronal research through the last 7 years.

The history of active space warfare development goes back to the 1960s when the Soviet Union began the Almaz project, a project designed to give them the ability to do on-orbit inspections of satellites and destroy them if needed. Similar planning in the United States took the form of the Blue Gemini project, which consisted of modified Gemini capsules that would be able to deploy weapons and perform surveillance.

One early test of electronic space warfare, the so-called Starfish Prime test, took place in 1962, when the United States exploded a ground-launched nuclear weapon in space to test the effects of an electromagnetic pulse. The result was a deactivation of many then-orbiting satellites, both American and Soviet. The deleterious and unfocused effects of the EMP test led to the banning of nuclear weapons in space in the Outer Space Treaty of 1967.

1.6.1.1 1970s–1980s

Through the 1970s, the Soviet Union continued their project and test-fired a cannon to test space station defense. This was considered too dangerous to do with a crew on board, however, so the test was conducted after the crew had returned to earth.

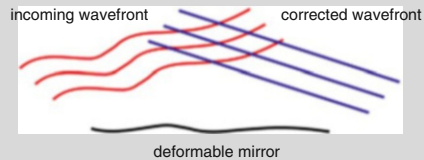
Space warfare strongly influenced the final design of the United States Space Shuttle. The distinctive delta wing shape was needed if the shuttle were to launch a military payload towards the Soviet Union and perform an immediate deorbit after one rotation to avoid being shot down [5].

Both the Soviets and the United States developed anti-satellite weaponry designed to shoot down satellites. While early efforts paralleled other space-to-

⁴Satellite Shoot Down: How It Will Work (February 19 2008), Space.com. Accessed 21 Feb 2008.

space warfare concepts, the United States was able in the 1980s to develop ground-to-space laser anti-satellite weapons. None of these systems are known to be active today; however, a less powerful civilian version of the ground-to-space laser system is commonly used in the astronomical technique of adaptive optics.

Adaptive Optics



Adaptive optics (AO) is a technology used to improve the performance of optical systems by reducing the effect of incoming wave-front distortions by deforming a mirror in order to compensate for the distortion. It is used in astronomical telescopes and laser communication systems to remove the effects of atmospheric distortion, in microscopy, optical fabrication, and retinal imaging systems to reduce optical aberrations.

1.6.1.2 2000s

The People's Republic of China successfully tested (see 2007 Chinese anti-satellite missile test) a ballistic missile-launched anti-satellite weapon on January 11, 2007. This resulted in harsh criticism from the United States, Britain, and Japan.

The United States developed an interceptor missile, the SM-3, testing it by hitting ballistic test targets while they were in space. On February 21, 2008, the United States used a SM-3 (Fig. 1.20) missile to destroy a spy satellite, USA-193, while it was 247 km (133 nautical miles) above the Pacific Ocean (see footnote 4).^{5,6,7}

Japan fields the US-made SM-3 missile, and there have been plans to base the land-based version in Romania and Vietnam

⁵Navy Hits Satellite with Heat-Seeking Missile (February 21, 2008), Space.com. Accessed 21 Feb 2008.

⁶DoD Succeeds in Intercepting Non-Functioning Satellite (Release No. 0139-08) (Press release) (February 20, 2008). US Department of Defense. Accessed 20 Feb 2008.

⁷Navy Succeeds in Intercepting Non-Functioning Satellite (Release NNS080220-19) (Press release) (February 20, 2008). US Navy. Accessed 20 Feb 2008



Fig. 1.20 A SM-3 missile is launched from a US ship to intercept a failing spy satellite

1.7 Earth Orbital Space Is a Militarily and Theoretical Space Weaponry

Earth orbital space is a militarily and economically critical arena to the United States, and it became a battleground in 1944, when the first operational Nazi German V-2 weapons briefly exited the earth's atmosphere on their way to raining destruction on London [6].

Although space has never actually been forcibly contested, this initial period of coincidental inability and unwillingness to fight over space is coming to an end. A growing number of states are developing the means with which not merely to access and exploit space but to conduct space warfare as well. The time has arrived to address the issue of warfare in space, driving the need for a conceptual framework with which to approach the defense of US space assets and related military and economic security. A theory of warfare in space must first be derived before any sort of space-combat preparations can begin. With such a framework, increased clarity regarding the nature, mechanics, and goals of war in space can then be applied to the process of designing weapon systems as well as planning, deploying, training, and conducting space-combat operations.

Carl von Clausewitz, one of the great military writers of history, defined the purpose of a theory.

“The first business of every theory is to clear up conceptions and ideas which have been jumbled together, and, we may say, entangled and confused; and only when a right understanding is established as to names and conceptions, can we hope to progress with clearness and facility, and be certain that author and reader will always see things from the same point of view” [7].

The first step in generating the requirements for a conceptual framework for war in space is to consider the essential elements of warfighting in general. As Clausewitz writes, “War therefore is an act of violence to compel our opponent to fulfill our will” [8].

This holds true regardless of the medium, for the motivations driving a nation to resort to armed violence, to war, will hold for that nation regardless of the route by which war is pursued.

There are a number of essential underlying elements for any effective warfighting strategy. These elements must maximize the warfighter’s chances of success while at the same time avoiding defeat. They must take into account the warfighter’s strengths and weaknesses while exploiting the enemy’s weaknesses and avoiding his strengths. The elements must seek and exploit advantages by any means and of any kind. They must take into account the types and ranges of actions available in the medium under consideration or embarkation. They must also use deception and misdirection.

As part of space weaponry, the following categories do apply as part of elements of space warfare that are listed in each subsection below.

1.7.1 Ballistic Warfare

In the late 1970s and through the 1980s the Soviet Union and the United States theorized, designed, and in some cases tested a variety of weaponry designed for warfare in outer space. Space warfare was seen primarily as an extension of nuclear warfare, and so many theoretical systems were based around the destruction or defense of ground- and sea-based missiles. Space-based missiles were not attempted due to the Outer Space Treaty, which banned the use, testing, or storage of nuclear weapons outside the earth's atmosphere. When the United States gained “interest in utilizing space-based lasers for ballistic missile defense,” two facts emerged, one being that the ballistic missiles are fragile and two chemical lasers project missile killing energy (3000 km). This meant that lasers could be put into space to intercept a ballistic missile as it can be launched from even ballistic submarine such as Trident missile (see Fig. 1.21) [9].

Figure 1.21 is an illustration of Vanguard class ballistic missile submarine, which is launching a Trident missile.

Fig. 1.21 A Trident missile launched from a royal navy



Ballistic Missile Submarine



A ballistic missile submarine is a submarine capable of deploying submarine-launched ballistic missiles (SLBMs) with nuclear warheads. The US Navy's hull classification symbols for ballistic missile submarines are SSB and SSBN—the SS denotes submarine (or submersible ship), the B denotes ballistic missile, and the N denotes that the submarine is nuclear powered.

Note: A ballistic missile follows a ballistic trajectory to deliver one or more warheads on a predetermined target as it is illustrated in Fig. 1.22. These weapons

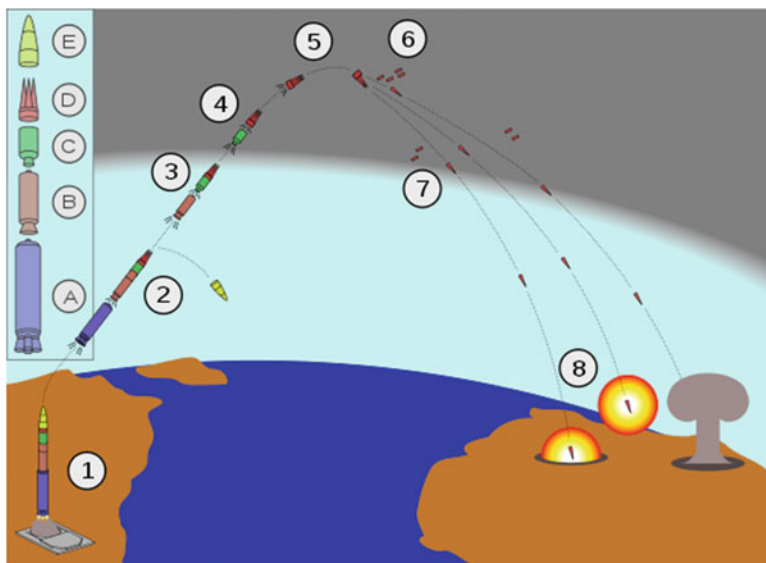


Fig. 1.22 Launch sequence of a Minuteman III MIRV

are only guided during relatively brief periods of flight—most of their trajectory is unpowered, being governed by gravity and air resistance if in the atmosphere.

Figure 1.22 is an illustration of sequential launch of Minuteman III, a multiple independently targetable reentry vehicle (MIRV).

Multiple Independently Targetable Reentry Vehicle



A multiple independently targetable reentry vehicle (MIRV) is a missile payload containing several warheads, each capable of being aimed to hit a different target. The concept is almost invariably associated with intercontinental ballistic missiles carrying thermonuclear warheads, even if not strictly being limited to them.

Ballistic warfare systems proposed ranged from measures as simple as ground- and space-based anti-missiles to rail guns, space-based lasers, orbital mines, and

similar weaponry. Deployment of these systems was seriously considered in the mid-1980s under the banner of the Strategic Defense Initiative (SDI) announced by Ronald Reagan in 1983, using the term “evil empire” to describe the Soviets (hence the popular nickname “Star Wars”) [11]. If the Cold War had continued, many of these systems could potentially have seen deployment: the United States developed working rail guns, and a laser that could destroy missiles at range, though the power requirements, range, and firing cycles of both were impractical. Weapons like the space-based laser were rejected, not just by the government, but by universities, moral thinkers, and religious people because it would have increased the waging of the arms race and questioned the United States’ role in the Cold War [12].

Rail Gun



A rail gun is a device that uses electromagnetic force to launch high-velocity projectiles, by means of a sliding armature that is accelerated along a pair of conductive rails. It is typically constructed as a weapon, and the projectile normally does not contain explosives, relying on the projectile’s high speed to inflict damage.

Note: A laser is a device that emits light through a process of optical amplification based on the stimulated emission of electromagnetic radiation. The term “laser” originated as an acronym for “light amplification by stimulated emission of radiation.” See Fig. 1.23.

Strategic Defense Initiative



(continued)

Fig. 1.23 Illumination of laser beam in action

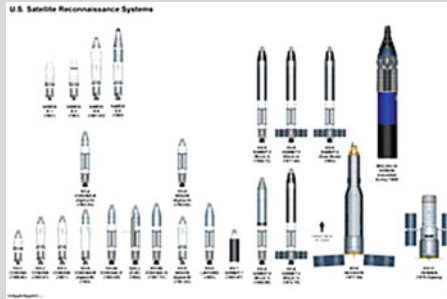


The Strategic Defense Initiative (SDI) was a proposed missile defense system intended to protect the United States from attack by ballistic strategic nuclear weapons (intercontinental ballistic missiles and submarine-launched ballistic missiles). The concept was first announced publicly by President Ronald Reagan on 23 March 1983.

1.7.2 Electronic Warfare

With the end of the Cold War and continued development of satellite and electronics technology, attention was focused on space as a supporting theater for conventional warfare. Currently, military operations in space primarily concern either the vast tactical advantages of satellite-based surveillance, communications, and positioning systems or mechanisms used to deprive an opponent of said tactical advantages.

Reconnaissance Satellite



A reconnaissance satellite (commonly, although unofficially, referred to as a spy satellite) is an earth observation satellite or communications satellite deployed for military or intelligence applications. The first-generation type (i.e., Corona and Zenit) took photographs, and then ejected canisters of photographic film which would descend to earth.

Communications Satellite



A communications satellite is an artificial satellite that relays and amplifies radio telecommunications signals via a transponder; it creates a communication channel between a source transmitter and a receiver at different locations on earth. Communications satellites are used for television, telephone, radio, Internet, and military applications.

Accordingly, most spaceborne proposals which would traditionally be considered “weapons” (a communications or reconnaissance satellite may be useful in warfare but isn’t generally classified as a weapon) are designed to jam, sabotage, and outright destroy enemy satellites, and conversely to protect friendly satellites against such attacks. To this end, the United States (and presumably other countries) is researching groups of small, highly mobile satellites called “microsats” (about the size of a refrigerator) and “picosats” (approximately 1 cubic foot (~27 L) in volume) nimble enough to maneuver around and interact with other orbiting objects to repair, sabotage, hijack, or simply collide with them.

Global Positioning System



The global positioning system (GPS), originally Navstar GPS, is a satellite-based radio-navigation system owned by the US Government and operated by the US Air Force. It is a global navigation satellite system that provides geolocation and time information to a GPS receiver anywhere on or near the earth where there is an unobstructed line of sight to four or more GPS satellites.

1.7.3 Kinetic Bombardment

Another theorized use involves the extension of conventional weaponry into orbit for deployment against ground targets. Though international treaties ban the deployment of nuclear missiles outside the atmosphere, other categories of weapons are largely unregulated. Traditional ground-based weapons are generally not useful in orbital environments, and few if any would survive reentry even if they were, but as early as the 1950s the United States has toyed with kinetic bombardment, i.e., orbiting magazines of nonexplosive projectiles to be dropped onto hardened targets from low earth orbit.

Atmospheric Entry



Atmospheric entry is the movement of an object from outer space into and through the gases of an atmosphere of a planet, dwarf planet, or natural

(continued)

satellite. There are two main types of atmospheric entry: uncontrolled entry, such as the entry of astronomical objects, space debris, or bolides, and controlled entry (or reentry) of a spacecraft capable of being navigated or following a predetermined.

A kinetic bombardment or a kinetic orbital strike is the hypothetical act of attacking a planetary surface with an inert projectile, where the destructive force comes from the kinetic energy of the projectile impacting at very high speeds. The concept originated during the Cold War.

Low Earth Orbit



A low earth orbit (LEO) is defined by Space-Track.org as an earth-centered orbit with at least 11.25 periods per day (an orbital period of 128 min or less) and an eccentricity less than 0.25. Most of the man-made objects in space are in LEO orbits.

Kinetic weapons have always been widespread in conventional warfare—bullets, arrows, swords, clubs, etc.—but the energy a projectile would gain while falling from orbit would make such a weapon rival all but the most powerful explosives. A direct hit would presumably destroy all but the most hardened targets without the need for nuclear weapons.

Such a system would involve a “spotter” satellite, which would identify targets from orbit with high-power sensors, and a nearby “magazine” satellite to deorbit a long, needlelike tungsten dart onto it with a small rocket motor or just dropping a very big rock from orbit (such as an asteroid). This would be more useful against a larger but less hardened target (such as a city). Though a common device in science fiction, there is no publicly available evidence that any such systems have actually been deployed by any nation.

Another antiballistic defense system is the US Army Terminal High Altitude Area Defense (THAAD), Fig. 1.24, formerly Theater High Altitude Area Defense, which is an American antiballistic missile defense system designed to shoot down short-



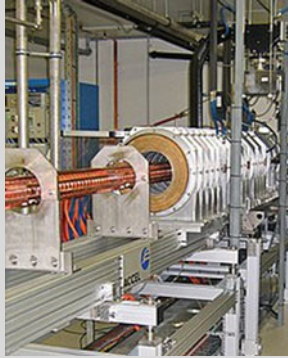
Fig. 1.24 US army THAAD launcher

medium-, and intermediate-range ballistic missiles in their terminal phase (descent or reentry) by intercepting with a hit-to-kill approach. THAAD was developed after the experience of Iraq's Scud missile attacks during the Gulf War in 1991.

1.7.4 Directed Energy Weapons

Weapon systems that fall under this category include lasers, linear particle accelerators or particle-beam-based weaponry, microwaves, and plasma-based weaponry. Particle beams involve the acceleration of charged or neutral particles in a stream towards a target at extremely high velocities, the impact of which creates a reaction causing immense damage. Most of these weapons are theoretical or impractical to implement currently, aside from lasers which are starting to be used in terrestrial warfare. That said, directed energy weapons are more practical and more effective in a vacuum (i.e., space) than in the earth's atmosphere, as in the atmosphere the particles of air interfere with and disperse the directed energy.

Linear Particle Accelerator



A linear particle accelerator is a type of particle accelerator that accelerates charged subatomic particles or ions to a high speed by subjecting them to a series of oscillating electric potentials along a linear beamline. The principles for such machines were proposed by Gustav Ising in 1924, while the first machine that worked was constructed by Rolf Widerøe in 1928 at the RWTH Aachen University. Linacs have many applications: they generate X-rays and high-energy electrons for medicinal purposes in radiation therapy, serve as particle injectors for higher energy accelerators, and are used directly to achieve the highest kinetic energy for light particles for particle physics.

Particle Beam Weapon

A particle beam weapon uses a high-energy beam of atomic or subatomic particles to damage the target by disrupting its atomic and/or molecular structure. A particle beam weapon is a type of directed energy weapon, which directs energy in a particular and focused direction using particles with miniscule mass. Some particle beam weapons have potential practical applications, e.g., as an antiballistic missile defense system for the United States and its cancelled Strategic Defense Initiative. The vast majority, however, are science fiction and are among the most common weapon types of the genre. They have been known by myriad names: phasers, particle accelerator guns, ion cannons, proton beams, lightning rays, ray guns, etc.

High-power microwave (HPM) past few years is also drawing a lot of attention as a kind of directed energy beam weapon as well.

Microwave



Microwaves are a form of electromagnetic radiation with wavelengths ranging from about 1 m to 1 mm, with frequencies between 300 MHz (1 m) and 300 GHz (1 mm). Different sources define different frequency ranges as microwaves; the above broad definition includes both UHF and EHF (millimeter wave) bands.

A more common definition in radio engineering is the range between 1 and 100 GHz (wavelengths between 0.3 m and 3 mm) [2]. In all cases, microwaves include the entire SHF band (3–30 GHz, or 10–1 cm) at minimum. Frequencies in the microwave range are often referred to by their IEEE radar band designations, S, C, X, Ku, K, or Ka band, or by similar NATO or EU designations.

Plasma-Based Weapon

When discussing weapons in science fiction, a plasma weapon is a type of ray gun that fires a stream, bolt(s), pulse, or toroid of plasma (i.e., very hot, very energetic excited matter).

The primary damage mechanism of these fictional weapons is usually thermal transfer; it typically causes serious burns, and often immediate death of living creatures, and melts or evaporates other materials. In certain fiction, plasma weapons may also have a significant kinetic energy component, that is to say, the ionized material is projected with sufficient momentum to cause some secondary impact damage in addition to causing high thermal damage. In some fictions, like Star Wars, plasma is highly effective against mechanical targets such as droids. The ionized gas disrupts their systems.

(continued)

Particle Beam

A particle beam is a stream of charged or neutral particles, in many cases moving at near the speed of light. There is a difference between the creation and control of charged particle beams and neutral particle beams, as only the first type can be manipulated to a sufficient extent by devices based on electromagnetism.

Nazi Germany had a project for such a weapon, considered a wunderwaffe, the sun gun, which would have been an orbital concave mirror able to concentrate the sun's energy on a ground target.

Wunderwaffe



Wunderwaffe is German for “miracle weapon” and was a term assigned during World War II by the Nazi Germany propaganda ministry to some revolutionary “superweapons.” Most of these weapons however remained prototypes, which either never reached the combat theater or, if they did, were too late or in too insignificant numbers to have a military effect.

The V-weapons, which were developed earlier and saw considerable deployment, especially against London and Antwerp, trace back to the same pool of highly inventive armament concepts. Therefore, they are also included here.

As the war situation worsened for Germany from 1942, claims about the development of revolutionary new weapons which could turn the tide became an increasingly prominent part of the propaganda directed at Germans by their government.



Fig. 1.25 Airborne laser (ABL) antiballistic missile weapon system

1.7.5 Airborne-Based Laser (ABL)

The Boeing YAL-1 Airborne Laser Testbed (formerly Airborne Laser) weapon system as illustrated in Fig. 1.25 was a megawatt-class chemical oxygen iodine laser (COIL) mounted inside a modified Boeing 747-400F. It was primarily designed as a missile defense system to destroy tactical ballistic missiles (TBMs) while in boost phase. The aircraft was designated YAL-1A in 2004 by the US Department of Defense.

The Boeing YAL-1 Airborne Laser Testbed (formerly Airborne Laser) weapon system was a megawatt-class chemical oxygen iodine laser (COIL) mounted inside a modified Boeing 747-400F. It was primarily designed as a missile defense system to destroy tactical ballistic missiles (TBMs) while in boost phase. The aircraft was designated YAL-1A in 2004 by the US Department of Defense.⁸

The YAL-1 with a low-power laser was test-fired in flight at an airborne target in 2007.⁹ A high-energy laser was used to intercept a test target in January 2010,¹⁰ and in the following month successfully destroyed two test missiles [13]. Funding for the program was cut in 2010 and the program was canceled in December 2011.¹¹ It made its final flight on February 14, 2012, to Davis–Monthan Air Force Base in Tucson, Arizona, to be kept in storage at the “Boneyard” by the 309th Aerospace

⁸DoD 4120.15-L, Model Designation of Military Aerospace Vehicles (PDF). US Department of Defense. May 12, 2004.

⁹Airborne Laser returns for more testing. Air Force. Archived from the original on March 8, 2007.

¹⁰Archived January 28, 2010, at the Wayback Machine.

¹¹Boeing YAL-1 Airborne Laser impacted by Pentagon spending priorities. Flight Image of the Day. Archived from the original on October 20, 2013.

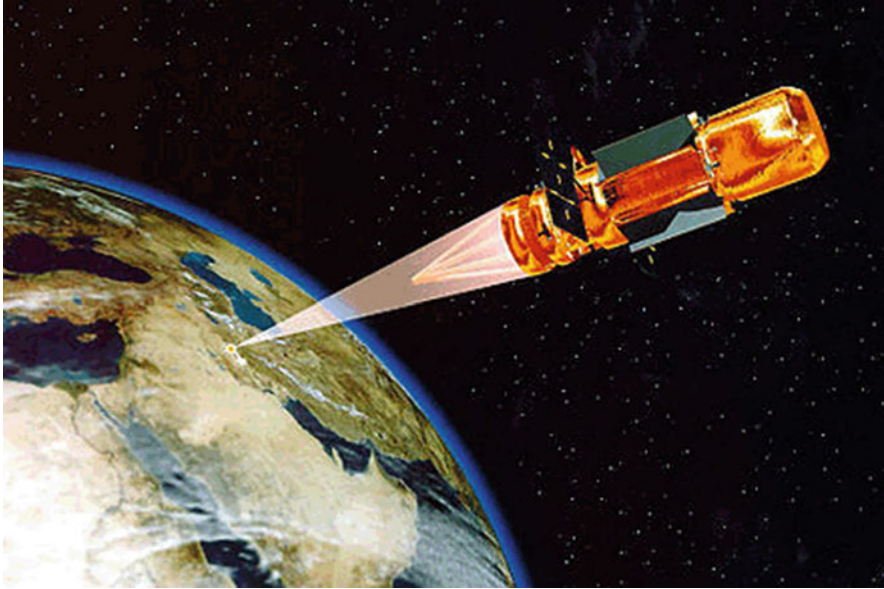


Fig. 1.26 Artistic illustration of space-based laser system

Maintenance and Regeneration Group. It was ultimately scrapped in September 2014 after all usable parts were removed.

1.7.6 Space-Based Laser (SBL)

Figure 1.26 is an artistic illustration of light amplification by the stimulated emission of radiation (LASER) pump energy into molecules, creating an electronic state that releases energy in the form of photons. The photons pass by other molecules, spreading energy, making more photons. To make an actual laser, a beam has to pass through mass quantities of laser medium by bouncing back and forth between mirrors placed at opposing ends. Then the light beam exits through one of the mirrors which is more transparent than the other. Making a functional laser requires the electrons to not only reach their excited state but also be reliant on the time it takes for them to get excited, and also the time for the energy created to reach new electrons. The efficiency of the laser relies on the amount of heat that exits. In terms of lasers, the power of the laser far outweighs the chemical efficiency. Of course, the trajectory of the laser matters as well as its ability to hit the target it is aimed at, but when lasers are placed in space diffraction can cause interference [14].

“Waiting until an adversary is in midcourse [phase of flight] is giving the adversary a free pass to launch,” Michael Griffin, the undersecretary of defense for research and engineering, told reporters during a media roundtable at the Space and Missile Defense Symposium.

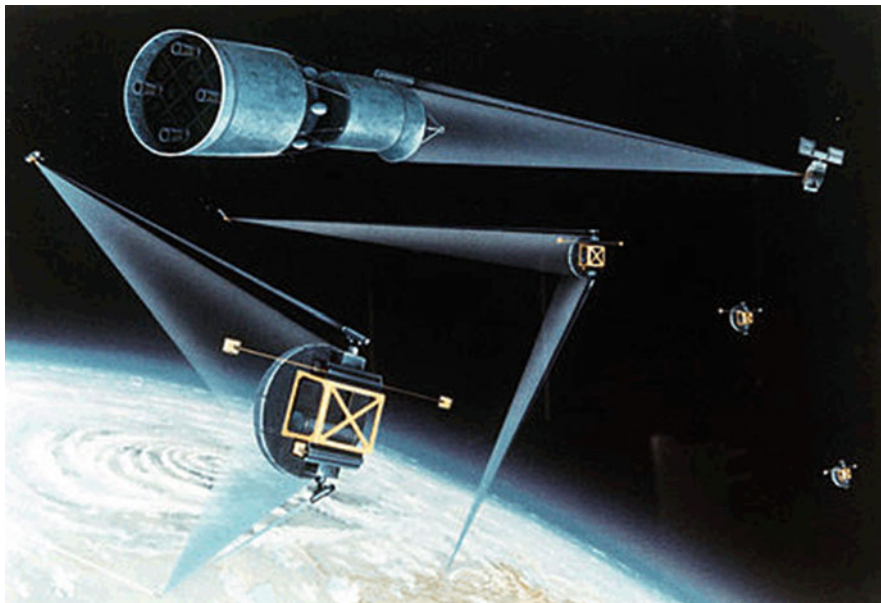


Fig. 1.27 Space laser system

Aug 14, 2018—Space-based laser weapons could ultimately take out missile threats in boost phase. Congress says that Pentagon must come up with boost-phase missile defense plan next year. DoD Presses On In Pursuit of Laser Weapons. Coming in 2021: A laser weapon for fighter jets.

1.7.6.1 Lethality of Space Lasers

As illustrated in Fig. 1.27 an artistic of space lasers requires mirrors in the system to direct their beams to achieve impact, but if not done correctly major damage can affect the skin. However, if the laser or lasers do make impact,

“a 10 m mirror with a HF laser beam would yield a 0.32 micro-radian divergence angle and create a laser spot 1.3 m in diameter at a range of 4000 m. The distribution of the 20 MW over the laser spot would create an energy flux of 1.5 kilowatts per square centimeter (kW/cm^2). The laser spot would need to dwell on the target for 6.6 s to create the nominal lethal fluence of 10 kilojoules per square centimeter (kJ/cm^2)”

meaning that the laser would essentially blow holes into missiles they are aimed at, as long as the laser mirrors are aimed correctly, and the heated molecules exit the beam quickly. Other factors of impact would be the type of laser itself, the amount of exposure, what the laser is attempting to hit (the target), environmental factors, and the ability of the target to either absorb or reflect the laser beam itself [15]. So what happens when a target is hit? Since this is a topic of space-based lasers it's safe to assume that the target is in the atmosphere so

“a beam with an intensity of around 10 million watts per square centimeter would cause the air immediately in front of the target to ionize, which would create a layer of plasma as the beam hits the surface. The plasma would absorb the energy of the laser beam and grow extremely hot (around 6000 °C). The plasma would distribute this energy in two ways, by emitting ultraviolet radiation and by expanding explosively. These mechanisms could increase the extent of the beam energy attached to the target to approximately 30% and reduce the amount of energy the laser would have to produce.”

When a laser is placed on the ground there are many more chances for obscurity in terms of a laser beam having to travel through the atmosphere as well as a much farther length of travel for the beam to hit the target. Other issues that can cause the laser beam to not be efficient is a state called thermal blooming when the laser heats up the air around it which can cause diffusion because of the heat and sparking, and simply decreasing the beam size by increasing the mirror size could fight against thermal blooming. The atmosphere can also cause absorption, scattering, turbulence, and sparking to the beam, even simply bending the beam so the target isn't accurate [16].

1.7.6.2 Characteristics of Space-Based Laser

Directed energy weapons might be put on satellites in earth orbit, but the altitude of the satellite would depend on what the laser is supposed to be targeting and where. The height of the satellite, the capacity of the laser, and the hardness of the missiles determine the optimum placement so that the positioning of the satellite allows for targeting the furthest boosting missile but is not far enough out that the beam misses any of its targets. “When the Soviet Union was considered to be the main threat, polar orbits were chosen since they provided good coverage of the northern latitudes,” even though there were no ballistic missiles deployed there. Equipment in the satellite improves the performance of surveillance, acquisition, and tracking, as well as damage assessment, and management functions. A ballistic missile booster may be required as well to be able to locate the missiles [17].

1.7.7 Ground-Based Laser (GBL)

As it is illustrated in Fig. 1.28, a second major alternative to destroying theater ballistic missiles with laser weapons is to place the laser on the ground and relay the beam to the missile with large mirrors in space.

The distinct advantage of this architecture is that the high-energy laser is kept on the ground, which eliminates the need to fit a laser platform onto an existing launch vehicle and the need to refuel the laser weapon's chemicals in space.

In addition, the complex and maintenance-intensive equipment, i.e., the laser, fuels, and pumping systems, are left on the ground. If problems develop with the ground laser systems, the equipment is readily accessible without the need for

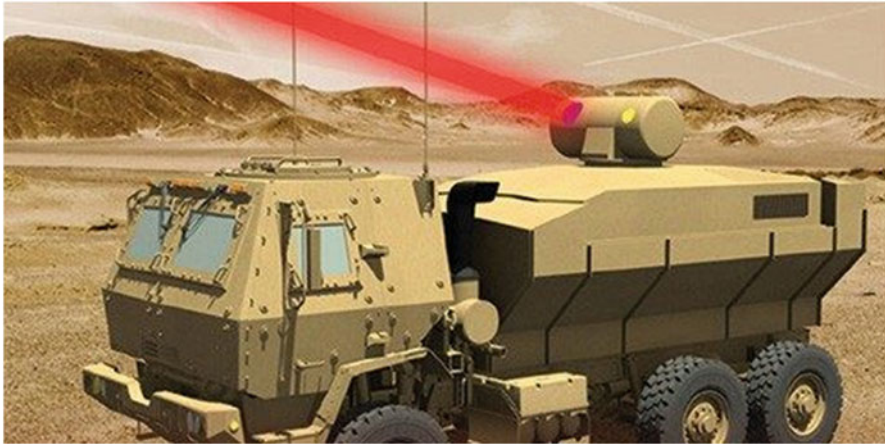


Fig. 1.28 A ground-based laser system

planning, funding, and recovering satellites from orbit. A further benefit is that the ground laser and beam director are not as constrained by diameter, weight, or volume as is the case for a space platform that must fit within a launch vehicle.

Unlike the space-based laser architecture, the ground-based laser system concept utilizes large optical systems in space to pass the laser beam from a ground laser to the ballistic missile. However, as with the space-based laser, the ground-based laser concept evolved during the Strategic Defense Initiative era but received far less emphasis than the space-based laser system given the technological challenges involved with this architecture. The earlier cited Strategic Defense Initiative-type scenario for the ground-based laser system suggested that the system would be required to kill 40 missiles per second, if the Soviets attacked with 2000 simultaneously launched ICBMs. This scenario drove the architecture requirements for at least 150 ground telescopes and 50 powerful ground lasers. Since then the threat has changed dramatically and so have the technologies. This section presents an architecture that is based on this reduced threat and an evaluation of the technological feasibility, maturity, and cost of this operational concept.

1.8 Practical Considerations

Space warfare is likely to be conducted at far greater distances and speeds than terrestrial combat. The vast distances involved pose difficult challenges for targeting and tracking, as even light requires a few seconds to traverse ranges measured in hundreds of thousands of kilometers. For example, if attempting to fire upon a target at the distance of the Moon from the earth, the image one sees reflects the position of the target slightly more than a second earlier. Thus, even a laser would need approximately 1.28 s, meaning a laser-based weapon system would need to lead a

target's apparent position by $1.28 \times 2 = 2.56$ s. A projectile from a rail gun recently tested by the US Navy would take over 18 h to cross that distance, assuming that it would travel in a straight line at a constant velocity of 5.8 km/s along its entire trajectory.

Three factors conspire to make engaging targets in space very difficult. First, the vast distances involved mean that an error of even a fraction of a degree in the firing solution could result in a miss by thousands of kilometers. Second, space travel involves tremendous speeds by terrestrial standards—a geostationary satellite moves at a speed of 3.07 km/s whereas objects in low earth orbit can move at up to 8 km/s. Third, though distances are large, targets remain relatively small. The International Space Station, currently the largest artificial object in earth orbit, measures slightly over 100 m at its largest span. Other satellites can be orders of magnitude smaller; for example Quickbird measures a mere 3.04 m. External ballistics for stationary terrestrial targets is enormously complicated—some of the earliest analog computers were used to calculate firing solutions for naval artillery, as the problems were already beyond manual solutions in any reasonable time—and the issues in targeting objects in space make a difficult problem even harder. Additionally, though not a problem for orbital kinetic weapons, any directed energy weapon would require large amounts of electricity. So far, the most practical batteries are lithium batteries, and the most practical method of generating electricity in space is through photovoltaic modules, which are currently only up to 30% efficient,¹² and fuel cells, which have limited fuel. Current technology might not be practical for powering effective lasers, particle beams, and rail guns in space. In the context of the Strategic Defense Initiative, the Lawrence Livermore National Laboratory in the United States worked on a project for expandable space-based X-ray lasers powered by a nuclear explosion, Project Excalibur, a project canceled in 1992 for lack of results [18].

Regardless of one's reasons for going to war, at present those reasons are not likely to suggest major targets located in space. Most of the main theories which attempt to explain human proclivity for warfare—psychological, sociological, demographic, economic, political, or otherwise—would not indicate space as a likely location of conflict until a significant population is engaged in large-scale activity there. Until then, space warfare is likely to take a supporting role to conventional, terrestrial warfare.

Aside from applications such as communications, reconnaissance, global positioning satellite (GPS), and the like, which would be difficult or impossible without satellites, there do not appear to be any major advantages to basing weapon systems in space. The main reason is simply cost. Space warfare that involves humans being deployed in space to fight each other is not currently practical because of the difficulty and cost of sustaining human life in space, especially over long periods of time.

Additionally, there are few things that could be accomplished by space warfare that any nation wealthy enough to finance them cannot accomplish far more cheaply

¹²“photovoltaics.” Spectrolab. Spectrolab, Inc. (2009). Accessed 4 April 2014.

through conventional means. Raising any significant mass beyond earth's gravity will always require a large amount of energy, and the cost increases with mass. For example, though kinetic bombardment potentially offers the ability to strike any target anywhere in the world within minutes, both the United States and Russia, possibly the only nations with the resources and facilities necessary to implement such a system, have sufficiently long-range supersonic bombers that the same target could already be destroyed in a matter of hours at a mere fraction of the cost.

General William L. Shelton has said that in order to protect against attacks, Space Situational Awareness is much more important than additional hardening or armoring of satellites.¹³ The Air Force Space Command has indicated that their defensive focus will be on “Disaggregated Space Architectures.”¹⁴

1.9 Space Debris

Anti-satellite attacks, especially ones involving kinetic kill vehicles, can contribute to the formation of space debris which can remain in orbit for many years and could interfere with future space activity or in a worst case trigger a Kessler syndrome [19]. In January 2007 China demonstrated a satellite knockout whose detonation alone caused more than 40,000 new chunks of debris with a diameter larger than 1 cm and a sudden increase in the total amount of debris in orbit.¹⁵ The PRC is reported to be developing “soft-kill” techniques such as jamming, and vision kills that do not generate much debris [20].

1.10 Possible Warfare Over Space

Most of the world’s communications systems rely heavily on the presence of satellites in orbit around earth. Protecting these assets might seriously motivate nations dependent upon them to consider deploying more space-based weaponry, especially in conflicts involving advanced countries with access to space.

Since 2017, the US Air Force has run an annual military exercise called “Space Flag” at Peterson Air Force Base, which involves a red team simulating attacks on US satellites [21].

¹³Future of USAF Space Command. Archived 2012-10-02 at the Wayback Machine. Defense News, 30 September 2012.

¹⁴The Future of our Space Architecture.

¹⁵Problem Weltraumschrott: Die kosmische Müllkippe—SPIEGEL ONLINE—Wissenschaft. Spiegel Online. Accessed 22 April 2017.

1.11 The Three Major Phases of Effective Missile Defense Systems

Ballistic Missile Defense (BMD), Ground-Based Midcourse Defense (GMD), Missile Defense Agency (MDA), Inter-Continental Ballistic Missile (ICBM), Advanced Air Defense (AAD) system, Terminal High Altitude Area Defense (THAAD), Aegis . . . are all terms that you have likely heard in recent news reports about ongoing threats of missile launches from North Korea. What would happen if a nuclear missile was launched at the United States? How would the United States respond to such a threat? These questions and more will soon be answered for you! You're also going to learn the three key phases that every ballistic missile goes through during the process of saving us from a terrible outcome.

Luckily the United States has been preparing for such a threat with a collection of complex systems that are part of our Ballistic Missile Defense (BMD) system. These systems are comprised of satellite sensors, ground- and maritime-based RADARs, and interceptor missiles.

Figure 1.29 depicts the primary roles of selected BMDS elements against a missile threat, which is listed below as three stages that are known as three key

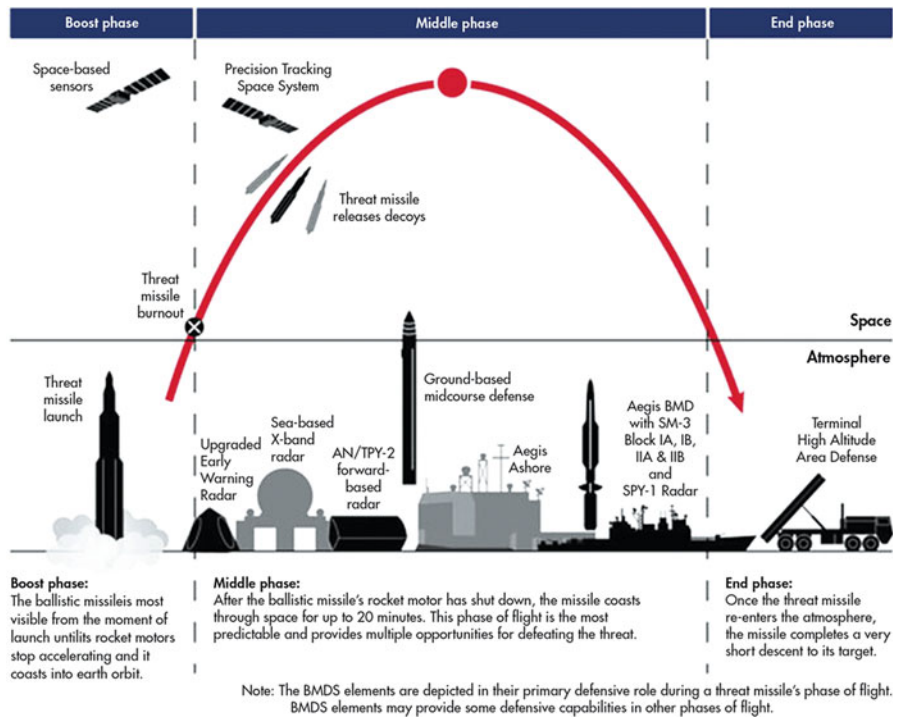


Fig. 1.29 depicts the primary roles of selected BMDS elements against a missile threat

phases where Ballistic Missile Defense must address these three major phases of a missile threat:

1. Boost

The BMD system tracks the missile threat through all three phases of flight. Satellite infrared sensors monitor known launch areas for missile launch heat signatures. Once a launch is detected by a satellite, the missile tracking is transferred to forward-deployed RADAR systems. These systems are responsible for calculating the initial missile trajectory. The boost phase is when the missile is most visible to the BMD system.

The boost phase includes the initial missile launch into space and lasts until the rocket engines have completed firing. The midcourse phase begins after rocket booster separation from the warhead and continues as the warhead travels through space, ending once the warhead begins reentry into the earth's atmosphere. The terminal phase is when the warhead hurtles towards the designated target during earth reentry.

2. Midcourse

The BMD system then transitions from boost phase to midcourse phase warhead tracking using ground-, sea-, and maritime-based RADARs. The warhead trajectory is monitored and broadcasted to the entire BMD network. The midcourse phase is the longest portion of the missile flight profile.

Midcourse tracking systems include the Raytheon TPY-2, Lockheed Martin Aegis Ashore, Lockheed Martin Long Range Discrimination RADAR (LRDR), Raytheon Air and Missile Defense RADAR (AMDR), and Lockheed Martin Aegis SPY-1 RADARs. Here's a great video example of how the Raytheon TPY-2 RADAR works for early detection.

3. Terminal/End

The BMD system transitions to close-in warhead tracking as the warhead enters the terminal phase. The warhead gains speed as it enters the earth's atmosphere and approaches its final target. Missile accuracy is defined in terms of circular error probability (CEP), which is the area where there is a 50% chance of the missile striking. The CEP can grow through the entire missile flight phase depending on missile system performance at various stages of flight.

Some midcourse tracking systems can be used for terminal tracking of warheads. The Lockheed Martin Terminal High Altitude Area Defense (THAAD) RADAR is a terminal tracking system designed to track close-in threats. The United States recently deployed THAAD systems to South Korea, and THAAD systems are currently deployed in Guam protecting US civilian and military assets in the region.

Ballistic Missile Defense (BMD)



The Aegis Ballistic Missile Defense System is a US Department of Defense Missile Defense Agency program developed to provide missile defense against short- to intermediate-range ballistic missiles. It is part of the US national missile defense strategy.

Ground-Based Midcourse Defense (GMD)



Ground-Based Midcourse Defense (GMD) is the United States' antiballistic missile system for intercepting incoming warheads in space, during the mid-course phase of ballistic trajectory flight. It is a major component of the American missile defense strategy to counter ballistic missiles, including intercontinental ballistic missiles (ICBMs) carrying nuclear, chemical, biological, or conventional warheads. The system is deployed in military bases in the states of Alaska and California, and comprises 44 interceptors and spans 15 time zones with sensors on land, at sea, and in orbit.

GMD is administered by the US Missile Defense Agency (MDA), while the operational control and execution are provided by the US Army, and support functions are provided by the US Air Force. Previously known as National Missile Defense (NMD), the name was changed in 2002 to differentiate it from other US missile defense programs, such as space-based and sea-based intercept programs, or defense targeting the boost phase and reentry flight phases [3]. The program was projected to have cost \$40 billion by 2017. That year,

(continued)

the MDA scheduled its first intercept test in 3 years in the wake of North Korea's accelerated long-range missile testing program.

Missile Defense Agency (MDA)



The Missile Defense Agency (MDA) has its origins in the Strategic Defense Initiative (SDI) which was established in 1983 by Ronald Reagan which was headed by Lt. General James Alan Abrahamson. Under the Strategic Defense Initiative's Innovative Sciences and Technology Office headed by physicist and engineer Dr. James Ionson, the investment was predominantly made in basic research at national laboratories, universities, and industry. These programs have continued to be key sources of funding for top research scientists in the fields of high-energy physics, supercomputing/computation, advanced materials, and many other critical science and engineering disciplines—funding which indirectly supports other research work by top scientists, and which was most politically viable to fund within the military budget of the US environment (see footnote 4). It was renamed the Ballistic Missile Defense Organization in 1993, and then renamed the Missile Defense Agency in 2002. The current commander is US Air Force Lt. Gen. Samuel A. Greaves.

Rapid changes in the strategic environment due to the rapid dissolution of the Soviet Union led, in 1993, to Bill Clinton focusing on theater ballistic missiles and similar threats and renaming it the Ballistic Missile Defense Organization (BMDO). With another change to a more global focus made by George W. Bush, in 2003 the organization became the Missile Defense Agency.

The Missile Defense Agency is partially or wholly responsible for the development of several Ballistic Missile Defense (BMD) systems, including the Patriot PAC-3, Aegis BMD, THAAD, and the Ground-Based Midcourse Defense system. They also led the development of numerous other projects, including the Multiple Kill Vehicle and the newer Multi-Object Kill Vehicle, the Kinetic Energy Interceptor, and the Airborne Laser. As the inheritor of the SDI and BMDO work, the MDA continues to fund fundamental research in high-energy physics, supercomputing/computation, advanced materials, and many other science and engineering disciplines.

(continued)

Intercontinental Ballistic Missile (ICBM)



An intercontinental ballistic missile (ICBM) is a guided ballistic missile with a minimum range of 5500 km (3400 mi) [1] primarily designed for nuclear weapon delivery (delivering one or more thermonuclear warheads). Similarly, conventional, chemical, and biological weapons can also be delivered with varying effectiveness but have never been deployed on ICBMs. Most modern designs support multiple independently targetable reentry vehicles (MIRVs), allowing a single missile to carry several warheads, each of which can strike a different target.

Early ICBMs had limited precision, which made them suitable for use only against the largest targets, such as cities. They were seen as a “safe” basing option, one that would keep the deterrent force close to home where it would be difficult to attack. Attacks against military targets (especially hardened ones) still demanded the use of a more precise, manned bomber. Second- and third-generation designs (such as the LGM-118 Peacekeeper) dramatically improved accuracy to the point where even the smallest point targets can be successfully attacked.

ICBMs are differentiated by having greater range and speed than other ballistic missiles: intermediate-range ballistic missiles (IRBMs), medium-range ballistic missiles (MRBMs), short-range ballistic missiles (SRBMs), and tactical ballistic missiles (TBMs). Short and medium-range ballistic missiles are known collectively as theater ballistic missiles.

Advanced Air Defense (AAD)



(continued)

The Indian Ballistic Missile Defense Program is an initiative to develop and deploy a multilayered ballistic missile defense system to protect from ballistic missile attacks.

Introduced in light of the ballistic missile threat from mainly Pakistan, it is a double-tiered system consisting of two land- and sea-based interceptor missiles, namely the Prithvi Air Defense (PAD) missile for high-altitude interception and the Advanced Air Defense (AAD) Missile for lower altitude interception. The two-tiered shield should be able to intercept any incoming missile launched from 5000 km away (see footnote 1). The system also includes an overlapping network of early warning and tracking radars, as well as command and control posts.

The PAD was tested in November 2006, followed by the AAD in December 2007. With the test of the PAD missile, India became the fourth country to have successfully developed an anti-ballistic missile system, after the United States, Russia, and Israel (see footnote 2). The system has undergone several tests, but it is yet to be officially commissioned.

Terminal High Altitude Area Defense (THAAD)



Terminal High Altitude Area Defense (THAAD), formerly Theater High Altitude Area Defense, is an American antiballistic missile defense system designed to shoot down short-, medium-, and intermediate-range ballistic missiles in their terminal phase (descent or reentry) by intercepting with a hit-to-kill approach.

Missile defense can take place either inside (endoatmospheric) or outside (exoatmospheric) the earth's atmosphere. The trajectory of most ballistic missiles takes them inside and outside the earth's atmosphere, and they can be intercepted in either place. There are advantages and disadvantages to either intercept technique.

Some missiles such as THAAD can intercept both inside and outside the earth's atmosphere, giving two intercept opportunities.

The United States has four options for addressing missile threats in the midcourse and terminal phase. Defeating a ballistic missile threat is akin to shooting a bullet travelling at 15,000 miles per hour with another bullet. Typically, decoys are released along with the warhead to confuse the tracking RADAR or interceptor

systems. Warheads can also use infrared countermeasures. These tactics used by adversaries make the job of the BMD even more complicated.

1.12 Combatting Ballistic Missile Threats

The most reliable defense against ballistic missile attack is the United States' Aegis Ballistic Defense (Fig. 1.30). The Aegis RADAR is manufactured by Lockheed Martin and integrated with the broader Command and Control and weapon systems aboard Aegis Class destroyers. The Aegis system is also available in land-based systems. The Aegis system is designed to combat short- and medium-range ballistic missiles through the use of RADAR tracking and interceptor launch. The Aegis system has an approximately 80% intercept success rate.

The Ground-Based Midcourse Defense (GMD) system can be utilized during the midcourse phase of flight. The GMD system tracks initial and projected trajectory of the missile with RADAR data and then launches interceptor missiles from locations in Alaska or California. These interceptor missiles reach space and collide with the warhead. The GMD system has approximately a 50% success rate during operational testing.

The Terminal High Altitude Area Defense (THAAD) system is used to combat missile threats in the terminal phase. The THAAD system consists of a RADAR,



Fig. 1.30 Aegis class destroyer USS Hopper (DDG-70) is shown launching a Standard Missile (SM) 3 Block IA in July 2009

interceptors, launchers, and a fire control system that is truck deployable. The THAAD system is designed to combat short- and medium-range ballistic missiles. The THAAD is the newest BMD system in the US arsenal and currently has a 100% success rate during flight testing.

The Patriot Advanced Capability-3 (PAC-3) system is the final BMD system in that arsenal. The PAC-3 is used to combat missile threats in the terminal phase. You may be familiar with the original Patriot missile system used during the first Persian Gulf War. The Patriot system is the most mature BMD system in the arsenal. The PAC-3 system is designed to combat short- and medium-range ballistic missiles. The PAC-3 can also intercept missiles at lower altitudes than the THAAD systems.

Let us hope that we never have to make use of this technology. However, as you can see, the United States has put in a great amount of thought and effort into keeping us safe if a threat does approach. Thank you engineering and radars! Consider learning how to find and eliminate phase noise in RADAR and communication systems.

References

1. B. Zohuri, *Scalar Wave Driven Energy Applications* (Springer Publishing Company, 2018).
2. B. Forestier, A. Houard, I. Revel, M. Durand, Y.B. André, B. Prade, A. Jarnac, J. Carbonnel, M. Le Nevé, J.C. de Miscault, B. Esmiller, D. Chapuis, A. Mysyrowicz, Triggering, guiding and deviation of long air spark discharges with femtosecond laser filament. *AIP Adv.* **2**(1), 012151 (2012). <https://doi.org/10.1063/1.3690961>
3. T.E. Bearden, *Solutions to Tesla's Secrets and the Soviet Tesla Weapons* (Tesla Book Company, Millbrae, CA, 1981)
4. B. Zohuri, *Directed Energy Weapons: Physics of High Energy Lasers (HEL)* (Springer Publishing Company, 2016)
5. A.C. Draper, M.L. Buck, W.H. Goesch, A delta shuttle orbiter. *Astronautics Aeronautics* **9**, 26–35 (1971)
6. L. Wood, *Ballistic Missile Defense In An Ideal World* (The George C. Marshall Institute, Washington, DC, 2005)
7. Carl von Clausewitz, *On War* (Dummlers Verlag, 1832), Book II, Chapter 1
8. B.H. Liddell-Hart, *Strategy*, 2nd edn. (Meridian Books, New York, 1991), pp. 334–337
9. Staff, Sun Tzu the art of war site on modern strategy and leadership, sonshi.com, 2006, Chapter 1
10. M. Mowthorpe, *The Militarization and Weaponization of Space* (Lexington Books, Lanham, MD, 2004), pp. 140–141. ISBN: 0-7391-0712-5
11. D. Hoffman, *The Dead Hand* (Double Day, New York, NY, 2009), p. 71. ISBN: 978-0-385-52437-7
12. P. Bracken, *The Second Nuclear Age* (Times Books, Henry Holt and Company, LLC, New York, NY, 2012), pp. 37–38. ISBN: 978-0-8050-9430-5
13. Jim Wolf. U.S. successfully tests airborne laser on missile. (February 12, 2010). reuters.com
14. M. Mowthorpe, *The Militarization and Weaponization of Space* (Lexington Books, New York, NY, 2004), pp. 141–142. ISBN: 0-7391-0712-5
15. M. Mowthorpe, *The Militarization and Weaponization of Space* (Lexington Books, New York, NY, 2004), pp. 142–144. ISBN: 0-7391-0712-5
16. M. Mowthorpe, *The Militarization and Weaponization of Space* (Lexington Books, New York, NY, 2004), pp. 145–146. ISBN: 0-7391-0712-5

17. M. Mowthorpe, *The Militarization and Weaponization of Space* (Lexington Books, New York, NY, 2004), p. 147. ISBN: 0-7391-0712-5
18. Michael Gordon. 'Star Wars' X-Ray Laser Weapon Dies as Its Final Test Is Canceled. The New York Times (20 July 1992)
19. Craig Covault. China's Asat Test Will Intensify U.S.-Chinese Faceoff in Space. Aviation Week. Archived from the original on 27 January 2007 (2007). Retrieved 21 Jan 2007
20. John Grady, U.S. Dependence on Space Assets Could be a Liability in a Conflict with China. usni.org. U.S. Naval Institute (2014). Accessed 29 Jan 2014
21. Tom Risen, U.S. Air Force to expand Space Flag satellite war game, American Institute of Aeronautics and Astronautics (2018)

Chapter 2

All About Wave Equations



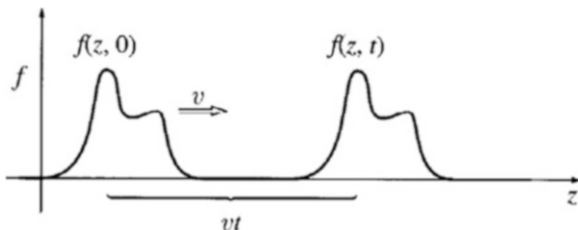
The fundamental definition of the terminology that is known to us as *wave* consists of a series of examples of different situations, which we are referring to as waves. However, the one feature that is a common denominator for the type of waves is that they propagate in one or other directions, and they create some kind of “disturbance” in their path of their propagations; for example in case of water waves, we observe the elevation of water surface and in case of sound wave we experience pressure variations in its path of traveling, with a velocity characteristic of the medium the wave goes through. However, for us to be able to describe a wave we need a more definitive of describing the wave with the use of mathematics, and primarily the concept of partial differential equation-type scenarios, which goes beyond the level of most of any basic textbook. Thus, in this chapter we try to establish first of all what the wave is in general, and secondly describe each form or shape that these waves are produced both from classical and relativistic mechanics, as well as electrodynamics point of views. This approach allows us to identify mechanical wave, electromagnetic waves, and finally the quantum mechanical waves as well. Within each of these categories then we can establish types of wave and classify them such as soliton wave, scalar wave, plasma wave, and shock waves.

2.1 Introduction

To put the wave definition in perspective, we say that a wave is a *disturbance of a continuity medium that propagates with a fixed shape at constant velocity*. However, in the presence of absorption, the wave will diminish in size as it moves, and the following circumstances do apply:

1. If the medium is dispersive, then different frequencies travel at different speeds.
2. In two or dimensions, as the wave spreads out, its amplitude will decrease.
3. Of course, the *standing waves* do not propagate at all.

Fig. 2.1 Illustration of moving wave of constant shape and constant speed



We take a constant shape of wave traveling to the right of the page at constant speed v as it is illustrated in Fig. 2.1, where the wave is drawn at two different times, once at time $t = 0$, and again at some later time t , and then each point on the wave it simply shifts to the right of the page by an amount which is vt .

Let us say that the wave demonstrated in Fig. 2.1 is generated by shaking one end of rope and suppose the function $f(z, t)$ represents the displacement of the rope at the point z at time t . If we assume that the initial shape of the rope is $g(z) \equiv f(z, 0)$, then the displacement at point z at the later time t is the same as the displacement at a distance vt to the left at $(z - vt)$, back at time $t = 0$; therefore, mathematically we can write the following relationship for the wave displacement function as

$$f(z, t) = f(z - vt, 0) = g(z - vt) \quad (2.1)$$

Equation (2.1) represents the general form of wave equation and it captures the wave function mathematically, for a wave in motion. This equation also tells us that the function $f(z, t)$ might have depended on variables z and t in only very special combination such as $(z - vt)$, where function of $f(z, t)$ represents a wave of fixed shape traveling in the z -direction at constant speed of v .

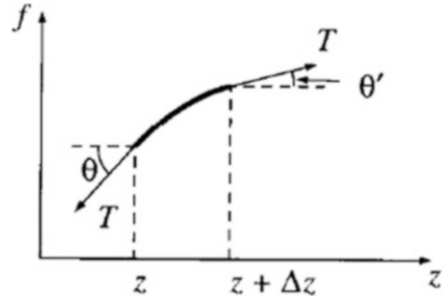
For example, if A and b are constants with the appropriate units, we can write the following relations as

$$\begin{cases} f_1(z, t) = Ae^{-b(z-vt)^2} \\ f_2(z, t) = A \sin [b(z - vt)] \\ f_3(z, t) = \frac{A}{b(z - vt)^2 + 1} \end{cases} \quad (2.2)$$

Sets of equations that are given in Eq. (2.2) all are representations of the wave function in one form or the other. However, the following functions are not representation of a wave function:

$$\begin{cases} f_4(z, t) = Ae^{-b(bz)^2} \\ f_5(z, t) = A \sin (bz) \cos (bvt)^3 \end{cases} \quad (2.3)$$

Fig. 2.2 A rope with tension T



Using Fig. 2.2 and the second law of Newton in classical mechanics for the rope tension of T , we can write that

$$\Delta F = T \sin \theta' - T \sin \theta \tag{2.4}$$

For small angle of θ and θ' , we can reform Eq. (2.4) by replacing sine with tangent of these angles as

$$\begin{aligned} \Delta F &= T(\tan \theta' - \tan \theta) \\ &= T\left(\left.\frac{\partial f}{\partial Z}\right|_{z+\Delta z} - \left.\frac{\partial f}{\partial Z}\right|_z\right) \\ &= T\left(\frac{\partial^2 f}{\partial Z^2}\right)\Delta Z \end{aligned} \tag{2.5}$$

If the mass of rope per unit length is designated by symbol μ , then the Newton's second law says that

$$\Delta F = \mu(\Delta z)\frac{\partial^2 f}{\partial t^2} \tag{2.6}$$

Comparing Eq. (2.5) with Eq. (2.6) would provide us the following result as

$$\begin{aligned} \mu(\Delta Z)\frac{\partial^2 f}{\partial t^2} &= T\left(\frac{\partial^2 f}{\partial Z^2}\right)\Delta Z \\ \frac{\partial^2 f}{\partial Z^2} &= \frac{\mu}{T}\frac{\partial^2 f}{\partial t^2} \end{aligned} \tag{2.7}$$

Evidently, small disturbance on the rope satisfies the following differential equation as

$$\frac{\partial^2 f}{\partial z^2} = \frac{1}{v}\frac{\partial^2 f}{\partial t^2} \tag{2.8}$$

Now, comparing Eq. (2.8) with Eq. (2.7), we conclude that

$$\left\{ \begin{array}{l} \frac{1}{v^2} = \frac{\mu}{T} \\ v^2 = \frac{T}{\mu} \end{array} \right. \Rightarrow \boxed{v = \sqrt{\frac{T}{\mu}}} \quad (2.9)$$

where in Eq. (2.9), the symbol v represents the speed of propagation for the wave on the rope, and this equation is known as *classical wave equation*.

This type of wave is not the only kind that we know; there are other types of waves, which we will describe in the following sections throughout this chapter, as we progress through.

2.2 The Classical Wave Equation and Separation of Variables

In the previous section Eq. (2.9) was developed as a general form of classical wave equation and here in this section we are in quest of a general solution to be able to solve not only Eq. (2.8), which is in one-dimensional space but eventually in all the appropriate coordinate systems known to us. Obviously, the easiest one is Cartesian coordinate and one-dimensional problem of string such as a piano or violin string that is stretched tightly, and its ends fastened to supports at $x = 0$ and $x = L$. When the string is vibrating, its vertical displacement u is always very small and the slope $\partial u / \partial x$ of the string at any point is far away from its stretched equilibrium position. In fact, we do not distinguish between the length of the string and the distance between the supports, although it is clear that the string must stretch a little as it vibrates out of its equilibrium position.

Under these assumptions, the displacement u satisfies the one-dimensional classical wave equation and can be written as

$$\frac{\partial^2 u}{\partial x^2} = \frac{1}{v^2} \frac{\partial^2 u}{\partial t^2} \quad (2.10)$$

In Eq. (2.10), the following definitions would apply:

u = is displacement.

v = is wave velocity and depends on the tension and the linear density of the string as it was described by Eq. (2.9).

Now the question is how do we solve this second-order, linear, partial differential equation that is given in Eq. (2.10)?

The most important technique we can use is the separation of variables by trying the approach like the following form of general solution as the combination of two separate independent function of $X(x)$ and $T(t)$ as

$$u(x, t) = X(x)T(t) \tag{2.11}$$

By plugging in Eq. (2.11) into Eq. (2.10), we get the following form of separation of variables:

$$\frac{\partial^2}{\partial x^2} \left[\begin{array}{c} X(x) \\ \text{not operated on} \\ \underbrace{T(t)}_{\text{by } \frac{\partial}{\partial x}} \end{array} \right] = \frac{1}{v^2} \frac{\partial^2}{\partial t^2} \left[\begin{array}{c} X(x) \\ \text{not operated on} \\ \underbrace{T(t)}_{\text{by } \frac{\partial}{\partial t}} \end{array} \right] \tag{2.12}$$

Multiplying Eq. (2.12) on the left by $\frac{1}{X(x)T(t)}$, we get the following form of equation:

$$\underbrace{\frac{1}{X(x)} \frac{\partial^2 X(x)}{\partial x^2}}_{\text{only } x} = \frac{1}{v^2} \underbrace{\frac{1}{T(t)} \frac{\partial^2 T}{\partial t^2}}_{\text{only } t} \tag{2.13}$$

In Eq. (2.13), as it can be seen that x and t are independent variables. This equation can only be valid if both sides are equal to a constant K . This is called the *separation constant*.

$$\begin{cases} \frac{1}{X} \frac{d^2 X}{dx^2} = K \\ \frac{1}{v^2 T} \frac{d^2 T}{dt^2} = K \end{cases} \tag{2.14}$$

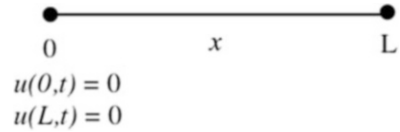
Note that we have *total* not *partial* derivatives: linear, second-order, and ordinary differential equation.

The general solutions of two sets of Eq. (2.14) have the form of solutions as

$$\begin{cases} K > 0 \\ K < 0 \end{cases} \begin{cases} e^{+kx}, e^{-kx} \\ \sin(kx), \cos(kx) \end{cases} \text{ if we let } \begin{cases} K = k^2 \\ K = -k^2 \end{cases} \tag{2.15}$$

We always have two linearly independent solutions for second-order partial differential equation:

Fig. 2.3 Illustration of the boundary conditions



$$\begin{cases} K > 0 \\ K < 0 \end{cases} \text{ general solution is either } \begin{cases} X(x) = Ae^{kx} + Be^{-kx} \\ X(x) = C \sin(kx) + D \cos(kx) \end{cases} \quad (2.16)$$

Also, for $T(t)$ equation part of Eq. (2.14), we have

$$\frac{d^2 T}{dt^2} = v^2 K T \quad (2.17)$$

We now look at our boundary conditions that we stated at the bringing of this problem as depicted in Fig. 2.3:

For $K > 0$, try to satisfy boundary conditions; thus we can write

$$\begin{aligned} X(0) = Ae^0 + Be^{-0} &= 0 \\ A + B = 0 \quad A &= -B \end{aligned} \quad (2.18a)$$

and

$$\begin{aligned} X(L) = 0 &= Ae^{kL} + Be^{-kL} = A(e^{kL} - e^{-kL}) \\ e^{kL} - e^{-kL} &\text{ can never be } 0 \\ A = 0 \quad u(x,t) &= 0 \end{aligned} \quad (2.18b)$$

So, solution of Eqs. (2.18a) and (2.18b) does not look good for the given boundary condition. What about the case when $K < 0$ solution?

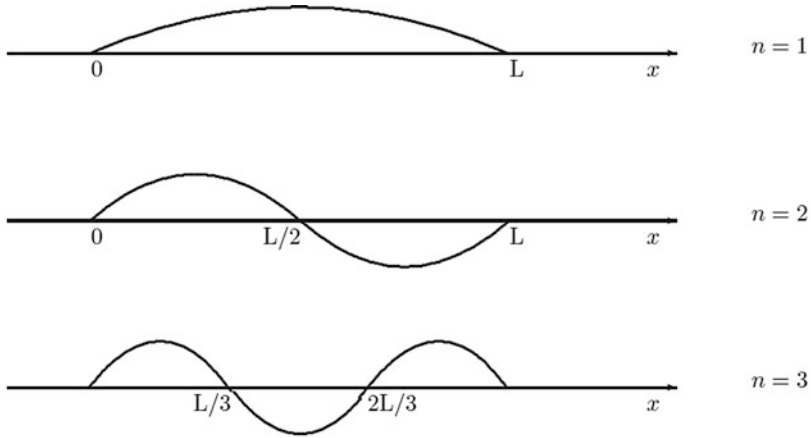
$$\begin{aligned} X(0) = C \sin(0) + D \cos(0) &= 0 \\ D = 0 \end{aligned} \quad (2.19a)$$

and

$$\begin{aligned} X(L) = C \sin(kL) + 0 &= 0 \\ kL = n\pi \quad n = 0, 1, 2, \dots \end{aligned} \quad (2.19b)$$

where we can say that

$$k_n = \frac{n\pi}{L} \quad n = 0, 1, 2, \dots \quad (2.19c)$$



-
- # nodes is $n - 1$
 - nodes are equally spaced at $x = L/n, \lambda_n = 2(L/n)$.
 - all lobes are the same, except for alternating sign

Fig. 2.4 Depiction of quantization solutions

Are the “quantization” term and pictures in Fig. 2.4 drawn without looking at the equation or using a computer to plot them for this quantization?

Now, we look at $T(t)$ equation for $K < 0$; then we get the following result:

$$\begin{cases} T(t) = E \sin(vk_n t) + F \cos(vk_n t) \\ \omega_n \equiv vk_n \\ T(t) = E \sin(\omega_n t) + F_n \cos(\omega_n t) \end{cases} \quad (2.20)$$

Normal modes are

$$u_n(x, t) = \left[A_n \sin\left(\frac{n\pi}{L}x\right) \right] (E_n \sin(\omega_n t) + F_n \cos(\omega_n t)) \quad (2.21)$$

The time-dependent factor of the n th normal mode can be rewritten in “frequency, phase” form as

$$E'_n \cos[\omega_n t + \phi_n] \quad (2.22)$$

The next step is to consider the $t = 0$ pluck of the system. This pluck is expressed as a linear combination of the normal modes:

$$u(x, t) = \sum_{n=1}^{\infty} (A_n E'_n) \sin\left(\frac{n\pi}{L}x\right) \cos(\omega_n t + \phi_n) \quad (2.23)$$

There is a further simplification based on the trigonometric formula:

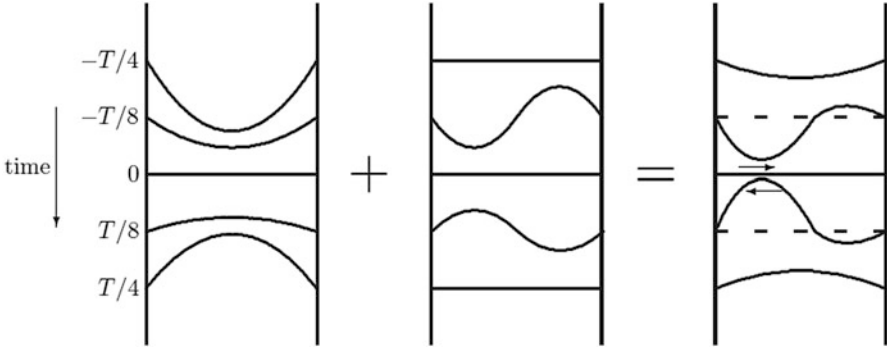


Fig. 2.5 Illustration of time steps for $T/8$

$$\sin(A) \cos(B) = \frac{1}{2} [\sin(A + B) + \sin(A - B)] \tag{2.24}$$

which enables us to write Eq. (2.23) as

$$u(x, t) = \sum_{n=1}^{\infty} \left[\frac{A_n E'_n}{2} \right] \left\{ \sin\left(\frac{n\pi}{L}x + \omega_n t + \phi_n\right) + \sin\left(\frac{n\pi}{L}x - \omega_n t - \phi_n\right) \right\} \tag{2.25}$$

From Eq. (2.25), we can now write the following conclusions:

- A single normal mode is a standing wave: no left-right motion, no “breathing.”
- A superposition of two or more normal modes with different values of n gives more complicated motion. For two normal modes, where one is even- n and the other is odd- n , the time-evolving wave packet will exhibit left-right motion. For two normal modes where both are odd or both are even, the wave packet motion will be “breathing” rather than left-right motion.

Here is a crude time-lapse move of a superposition of the $n = 1$ and $n = 2$ (fundamental and first overtone) modes.

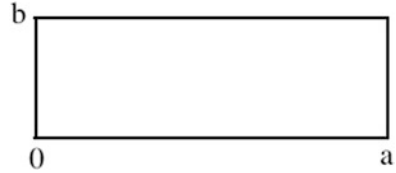
The period of the fundamental is $T = 2\pi/\omega$. We are going to consider time step of $T/8$ as depicted in Fig. 2.5.

As it can be seen in Fig. 2.5, the time-lapse move of the sum of two normal modes can be viewed as moving to left at $t = -T/4$, close to the left turning point at $t = -T/8$, at the left turning point but at $t = 0$, moving to the right at $t = +T/8$. It will reach the right turning point but at $t = T/2$.

In quantum mechanics you will see wave packets that exhibit motion, breathing, dephasing, and rephrasing. The “center of the wave packet” will follow a trajectory that obeys Newton’s laws of motion.

If we generalize from waves on a string to waves on a rectangular drum head, such as in Fig. 2.6, then the separation of variable solution to the wave equation will have the form of

Fig. 2.6 A drum head



$$u(x, y, t) = X(x)Y(y)T(t) \tag{2.26}$$

There will be two separation constants, and we will find that the normal mode frequencies are

$$\omega_{nm} = v\pi \left[\frac{n^2}{a^2} + \frac{m^2}{b^2} \right]^{1/2} \tag{2.27}$$

This is a more complicated quantization rule than for waves on a string, and it should be evident to an informed listener that these waves are on a rectangular drum head with edge lengths a and b .

Some important conclusions we can draw as part of the above discussion: The underlying unity of the e^{kx} , e^{-kx} , $\sin(kx)$, and $\cos(kx)$ solution to the following form of linear ordinary differential equation is

$$\frac{d^2y}{dx^2} = k^2y \tag{2.28}$$

If we want to solve Eq. (2.16), take a step back and look at the two simplest second-order ordinary differential equations:

$$\frac{d^2y}{dx^2} = +k^2y \rightarrow y(x) = Ae^{kx} + Be^{-kx} \tag{2.29a}$$

and

$$\frac{d^2y}{dx^2} = -k^2y \rightarrow y(x) = C \sin(kx) + D \cos(kx) \tag{2.29b}$$

The solutions to these two equations are more similar than they look at first glance.

Euler’s formula provides that

$$e^{+i\theta} = \cos \theta + i \sin \theta \tag{2.30a}$$

or

$$\begin{cases} \frac{1}{2}(e^{i\theta} + e^{-i\theta}) = \cos \theta \\ \frac{1}{2}(e^{-i\theta} - e^{i\theta}) = \sin \theta \end{cases} \quad (2.30b)$$

So, we can express the solution of the second differential equation in (complex) exponential form to bring out its similarity to the solution of the first differential equation:

$$\begin{aligned} y(x) &= C \sin(kx) + D \cos(kx) \\ &= \frac{i}{2}C(e^{-ikx} - e^{ikx}) + \frac{1}{2}D(e^{ikx} + e^{-ikx}) \end{aligned} \quad (2.31a)$$

Rearranging Eq. (2.40) will yield as

$$y(x) = \frac{1}{2}(D - iC)e^{ikx} + \frac{1}{2}(D + iC)e^{-ikx} \quad (2.31b)$$

The $\sin\theta$, $\cos\theta$, $e^{i\theta}$, and $e^{-i\theta}$ forms are two sides of the same coin. Insight. Convenience. What do we notice? *The general solution to a second-order differential equation consists of the sum of two linearly independent functions, each multiplied by an unknown constant.*

2.3 Standing Waves

Standing wave, also called stationary wave, is a combination of two waves moving in opposite directions, each having the same amplitude and frequency. The phenomenon is the result of interference, that is, when waves are superimposed, their energies are either added together or cancelled out. In the case of waves moving in the same direction, interference produces a traveling wave; for oppositely moving waves, interference produces an oscillating wave fixed in space. A vibrating rope tied at one end will produce a standing wave, as shown in the figure; the wave train (line B), after arriving at the fixed end of the rope, will be reflected back and superimposed on itself as another train of waves (line C) in the same plane. Because of interference between the two waves, the resultant amplitude (R) of the two waves will be the sum of their individual amplitudes. Part I of the figure shows the wave trains B and C coinciding, so that standing wave R has twice their amplitude. In part II, $1/8$ period later, B and C have each shifted $1/8$ wavelength. Part III represents the case $1/8$ period still later, when the amplitudes of the component waves B and C are oppositely directed. At all times there are positions (N) along the rope, called nodes, at which there is no movement at all; there the two wave trains are always in opposition. On either side of a node is a vibrating antinode (A). The antinodes

alternate in the direction of displacement so that the rope at any instant resembles a graph of the mathematical function called the sine, as represented by line R. Both longitudinal (e.g., sound) waves and transverse (e.g., water) waves can form standing waves [1] (Figs. 2.7 and 2.8).

Fig. 2.7 Location of fixed nodes in a standing wave

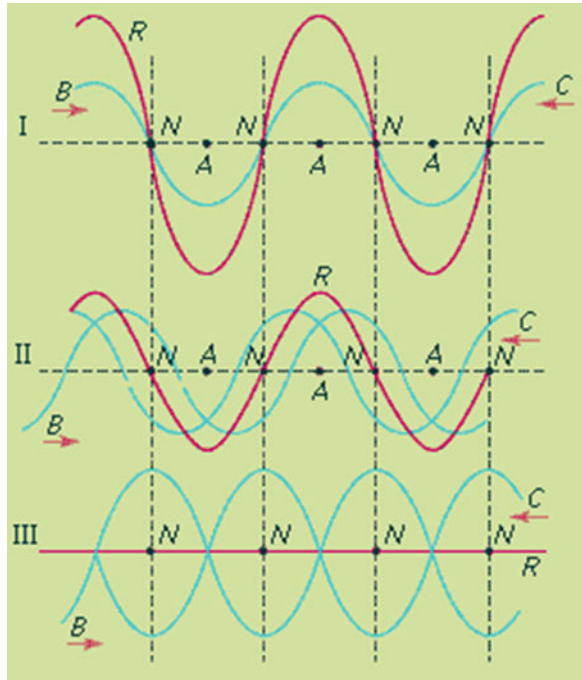
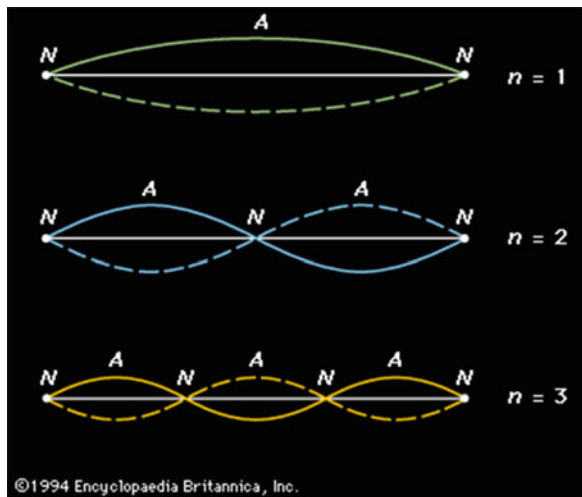


Fig. 2.8 The first three harmonic standing waves in a stretched string. Nodes (N) and antinodes (A) are marked. The harmonic number (n) for each standing wave is given on the right (see text)



©1994 Encyclopaedia Britannica, Inc.

2.4 Seiche Wave

A seiche is a standing wave in an enclosed or a partially enclosed body of water. Seiches and seiche-related phenomena have been observed on lakes, reservoirs, swimming pools, bays, harbors, and seas. The key requirement for formation of a seiche is that the body of water be at least partially bounded, allowing the formation of the standing wave [2].

The term was promoted by the Swiss hydrologist François-Alphonse Forel in 1890, who was the first to make scientific observations of the effect in Lake Geneva, Switzerland [3]. The word originates in a Swiss French dialect word that means “to sway back and forth,” which had apparently long been used in the region to describe oscillations in alpine lakes.

Seiche, rhythmic oscillation of water in a lake, or a partially enclosed coastal inlet such as a bay, gulf, or harbor: A seiche may last from a few minutes to several hours or for as long as 2 days. The phenomenon was first observed and studied in Lake Geneva (Lac Léman), Switzerland, in the eighteenth century.

Seiches may be induced by local changes in atmospheric pressure. They also may be initiated by the motions of earthquakes and by tsunamis, in the case of coastal inlets. Seismic surface waves from the Alaska earthquake of 1964, for example, triggered seiche surges in Texas in the southwestern United States when they passed through the area. Studies of seiche behavior have shown that once the surface of the water is disturbed, gravity seeks to restore the horizontal surface, and simple vertical harmonic motion ensues. The impulse travels the length of the basin at a velocity dependent on the water depth and is reflected back from the basin’s end, generating interference. Repeated reflections generate standing waves with one or more nodes, or points, that experience no vertical motion. The length of the lake is an exact multiple of the distance between nodes.

Seiches may disturb shipping by generating strong reversible currents at the entrances to harbors or by causing moored vessels to oscillate against their mooring cables and break free. Seiches also may drown unwarned persons on piers and shores.

Seiches are often imperceptible to the naked eye, and observers in boats on the surface may not notice that a seiche is occurring due to the extremely long wavelengths.

The effect is caused by resonances in a body of water that has been disturbed by one or more factors, most often meteorological effects (wind and atmospheric pressure variations), seismic activity, or tsunamis [4]. Gravity always seeks to restore the horizontal surface of a body of liquid water, as this represents the configuration in which the water is in hydrostatic equilibrium.

Vertical harmonic motion results, producing an impulse that travels the length of the basin at a velocity that depends on the depth of the water. The impulse is reflected back from the end of the basin, generating interference. The frequency of the oscillation is determined by the size of the basin, its depth and contours, and the water temperature.

The longest natural period of a seiche is the period associated with the fundamental resonance for the body of water—corresponding to the longest standing wave. For a surface seiche in an enclosed rectangular body of water this can be estimated using Merian’s formula: as given below [5, 6]:

$$T = \frac{2L}{\sqrt{gh}} \quad (2.32)$$

where T is the longest natural period, L is the length, h is the average depth of the body of water, and g is the acceleration of gravity.

Higher order harmonics are also observed. The period of the second harmonic will be half the natural period, the period of the third harmonic will be a third of the natural period, and so forth.

2.4.1 Lake Seiche

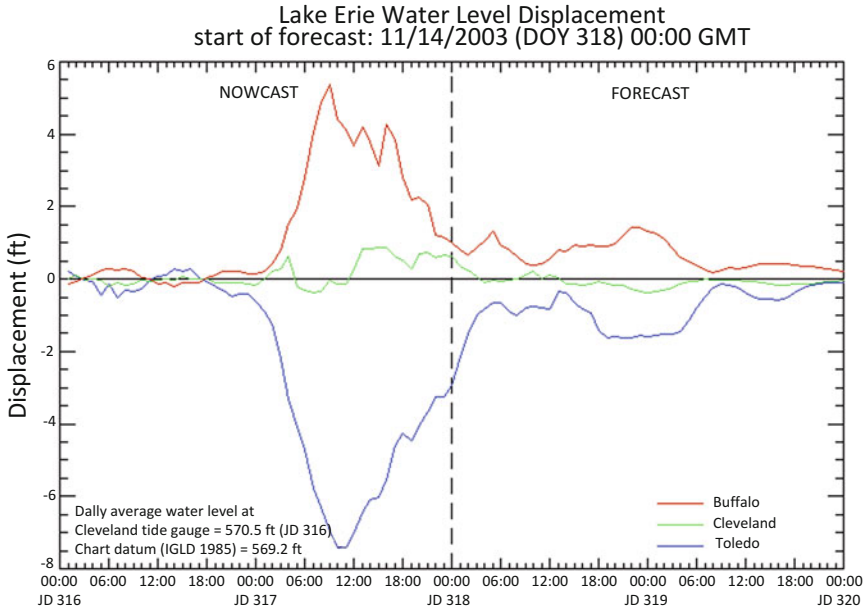
Low rhythmic seiches are almost always present on larger lakes. They are usually unnoticeable among the common wave patterns, except during periods of unusual calm. Harbors, bays, and estuaries are often prone to small seiches with amplitudes of a few centimeters and periods of a few minutes.

Among other lakes well known for their regular seiches is New Zealand’s Lake Wakatipu, which varies its surface height at Queenstown by 20 cm in a 27-min cycle. Seiches can also form in semi-enclosed seas; the North Sea often experiences a lengthwise seiche with a period of about 36 h.

The National Weather Service issues low water advisories for portions of the Great Lakes when seiches of 2 ft or greater are likely to occur [7]. Lake Erie is particularly prone to wind-caused seiches because of its shallowness and its elongation on a northeast-southwest axis, which frequently matches the direction of prevailing winds and therefore maximizes the fetch of those winds. These can lead to extreme seiches of up to 5 m (16 ft) between the ends of the lake. See Fig. 2.9.

The effect is similar to a storm surge like that caused by hurricanes along ocean coasts, but the seiche effect can cause oscillation back and forth across the lake for some time. In 1954, Hurricane Hazel piled up water along the northwestern Lake Ontario shoreline near Toronto, causing extensive flooding, and established a seiche that subsequently caused flooding along the south shore.

Lake seiches can occur very quickly: on July 13, 1995, a large seiche on Lake Superior caused the water level to fall and then rise again by 3 ft (1 m) within 15 min, leaving some boats hanging from the docks on their mooring lines when the water retreated. The same storm system that caused the 1995 seiche on Lake Superior produced a similar effect in Lake Huron, in which the water level at Port Huron changed by 6 ft (1.8 m) over 2 h. On Lake Michigan, eight fishermen were swept away from piers at Montrose and North Avenue Beaches and drowned when a 10-ft (3.0 m) seiche hit the Chicago waterfront on June 26, 1954.



NOAA Great Lakes Coastal Forecasting System
Great Lakes Environmental Research Laboratory
National Weather Service

Fig. 2.9 Lake Erie water-level displacement

Lakes in seismically active areas, such as Lake Tahoe in California/Nevada, are significantly at risk from seiches. Geological evidence indicates that the shores of Lake Tahoe may have been hit by seiches and tsunamis as much as 10 m (32.8 ft) high in prehistoric times, and local researchers have called for the risk to be factored into emergency plans for the region.

Earthquake-generated seiches can be observed thousands of miles away from the epicenter of a quake. Swimming pools are especially prone to seiches caused by earthquakes, as the ground tremors often match the resonant frequencies of small bodies of water. The 1994 Northridge earthquake in California caused swimming pools to overflow across southern California. The massive Good Friday earthquake that hit Alaska in 1964 caused seiches in swimming pools as far away as Puerto Rico. The earthquake that hit Lisbon, Portugal, in 1755 caused seiches 2000 miles (3000 km) away in Loch Lomond, Loch Long, Loch Katrine, and Loch Ness in Scotland and in canals in Sweden. The 2004 Indian Ocean earthquake caused seiches in standing water bodies in many Indian states as well as in Bangladesh, Nepal, and northern Thailand. Seiches were again observed in Uttar Pradesh, Tamil Nadu, and West Bengal in India as well as in many locations in Bangladesh during the 2005 Kashmir earthquake.

The 1950 Chayu-Upper Assam earthquake is known to have generated seiches as far away as Norway and southern England. Other earthquakes in the Indian

subcontinent known to have generated seiches include the 1803 Kumaon-Barahat, 1819 Allah Bund, 1842 Central Bengal, 1905 Kangra, 1930 Dhubri, 1934 Nepal-Bihar, 2001 Bhuj, 2005 Nias, and 2005 Teresa Island earthquakes. The February 27, 2010, Chile earthquake produced a seiche on Lake Pontchartrain, Louisiana, with a height of around 0.5 ft. The 2010 Sierra El Mayor earthquake produced large seiches that quickly became an Internet phenomenon.

Seiches up to at least 1.8 m (6 ft) were observed in Sognefjorden, Norway, during the 2011 Tōhoku earthquake.

2.4.2 Sea and Bay Seiche

Seiches have been observed in seas such as the Adriatic Sea and the Baltic Sea. This results in the flooding of Venice and St. Petersburg, respectively, as both cities are constructed on former marshland. In St. Petersburg, seiche-induced flooding is common along the Neva River in the autumn. The seiche is driven by a low-pressure region in the North Atlantic moving onshore, giving rise to cyclonic lows on the Baltic Sea. The low pressure of the cyclone draws greater-than-normal quantities of water into the virtually land-locked Baltic. As the cyclone continues inland, long, low-frequency seiche waves with wavelengths up to several hundred kilometers are established in the Baltic. When the waves reach the narrow and shallow Neva Bay, they become much higher—ultimately flooding the Neva embankments [8]. Similar phenomena are observed in Venice, resulting in the MOSE Project [9], a system of 79 mobile barriers designed to protect the three entrances to the Venetian Lagoon. MOSE (MODulo Sperimentale Elettromeccanico, *Experimental Electromechanical Module*) is a project intended to protect the city of Venice, Italy, and the Venetian Lagoon from flooding.

Seiches can also be induced by tsunamis, a wave train (series of waves) generated in a body of water by a pulsating or abrupt disturbance that vertically displaces the water column. On occasion, tsunamis can produce seiches as a result of local geographic peculiarities. For instance, the tsunami that hit Hawaii in 1946 had a 15-min interval between wave fronts. The natural resonant period of Hilo Bay is about 30 min. That meant that every second wave was in phase with the motion of Hilo Bay, creating a seiche in the bay. As a result, Hilo suffered worse damage than any other place in Hawaii, with the tsunami/seiche reaching a height of 26 ft along the Hilo Bayfront, killing 96 people in the city alone. Seiche waves may continue for several days after a tsunami.

Tide-generated internal solitary waves (solitons) can excite coastal seiches at the following locations: Magueyes Island in Puerto Rico, Puerto Princesa in Palawan Island, Trincomalee Bay in Sri Lanka, and the Bay of Fundy in eastern Canada, where seiches cause some of the highest recorded tidal fluctuations in the world. A dynamical mechanism exists for the generation of coastal seiches by deep-sea internal waves. These waves can generate a sufficient current at the shelf break to excite coastal seiches.

2.5 Underwater or Internal Waves

Although the bulk of the technical literature addresses surface seiches, which are readily observed, seiches are also observed beneath the lake surface acting along the thermocline in constrained bodies of water. The thermocline is the boundary between colder lower layer (hypolimnion) and warmer upper layer (epilimnion). See Fig. 2.10.

In analogy with the Merian formula, the expected period of the internal wave can be expressed as

$$T = \frac{2L}{c} \quad (2.33)$$

with

$$c^2 = g \left(\frac{\rho_2 - \rho_1}{\rho_2} \right) \left(\frac{h_1 h_2}{h_1 + h_2} \right) \quad (2.34)$$

where T is the natural period, L is the length of the water body, while h_1 and h_2 are the average thicknesses of the two layers separated by stratification (e.g., epilimnion and hypolimnion), and finally ρ_1 and ρ_2 are the densities of these two same layers and g is the acceleration of gravity force.

2.6 Maxwell's Equations and Electromagnetic Waves

As we have discussed in previous chapters, the principles of guiding and propagation of electromagnetic energy in its widely different applications and regimes may differ in detail from one application to another; however, they all are governed by one of the equations that we know as Maxwell's equations, which are based on experimental observations and provide the foundations of *all* electromagnetic phenomena and their applications. Many of the underlying concepts starting in early nineteenth century were developed by earlier scientists, especially Michael Faraday, who was a visual and physical thinker, but not enough of a mathematician to express his ideas in a complete and self-consistent form to provide a theoretical framework.

However, Maxwell started putting Faraday's ideas into strict perspective of mathematical form and thus established a theory that predicted the existence of electromagnetic waves. Based on Maxwell's ideas and his development of his famous equations that were established in Chap. 2 and Eqs. (2.31a), (2.31b), (2.32), (2.33), and (2.34), now we can establish the electromagnetic waves.

One of the important aspects of Maxwell's equations is the equations for electromagnetic wave propagation in a linear medium that we have analyzed in Chap. 4.

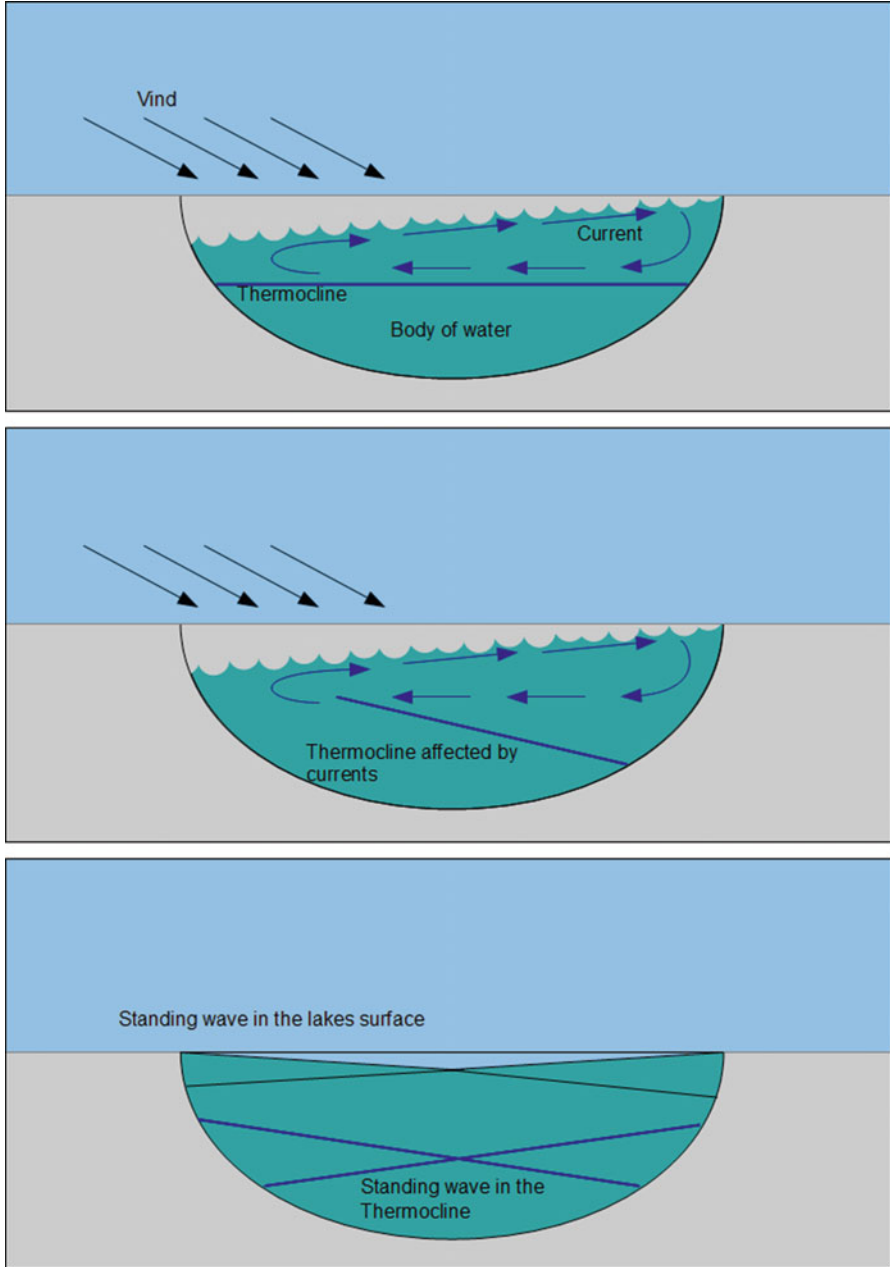


Fig. 2.10 Illustration of the initiation of surface and subsurface thermocline seiches

However, we need to establish the wave equation for electromagnetic field \vec{H} by taking the curl of Eq. (2.34) as follows:

$$\begin{cases} \vec{\nabla} \times \vec{H} = \vec{J} + \frac{\partial \vec{D}}{\partial t} \\ \vec{\nabla} \times \vec{\nabla} \times \vec{H} = \vec{\nabla} \times \vec{J} + \vec{\nabla} \times \frac{\partial \vec{D}}{\partial t} \end{cases} \quad (2.35)$$

Putting $\vec{D} = \epsilon \vec{E}$ and $\vec{J} = g \vec{E}$ in a linear medium, and assuming that g and ϵ are constants, using the second equation of Eq. (2.35), we obtain the following result:

$$\vec{\nabla} \times \vec{\nabla} \times \vec{H} = g \vec{\nabla} \times \vec{E} + \epsilon \frac{\partial}{\partial t} (\vec{\nabla} \times \vec{E}) \quad (2.36)$$

In Eq. (2.36), if electric field \vec{E} is a well-behaved function, as we assume to be the case, then the order of time and space differentiation can be interchanged. Equation (2.31a) and (2.31b) can now be used to eliminate $\vec{\nabla} \times \vec{E}$ from Eq. (2.45); thus, it yields

$$\vec{\nabla} \times \vec{\nabla} \times \vec{H} = g\mu \frac{\partial \vec{H}}{\partial t} + \epsilon\mu \frac{\partial^2 \vec{H}}{\partial t^2} \quad (2.37)$$

where $\vec{B} = \mu \vec{H}$ with μ as a constant has been used. The following vector identity from Table 1.1 can be used:

$$\vec{\nabla} \times \vec{\nabla} \times \vec{F} = \vec{\nabla} (\vec{\nabla} \cdot \vec{F}) - \nabla^2 \vec{F} \quad (2.38)$$

Therefore, Eq. (2.37) can be reformed as

$$\vec{\nabla} (\vec{\nabla} \cdot \vec{H}) - \nabla^2 \vec{H} = -g\mu \frac{\partial \vec{H}}{\partial t} - \epsilon\mu \frac{\partial^2 \vec{H}}{\partial t^2} \quad (2.39)$$

Since μ is a constant, then from $\vec{B} = \mu \vec{H}$ relation, we can write that

$$\vec{\nabla} \cdot \vec{H} = \frac{1}{\mu} (\vec{\nabla} \cdot \vec{B}) = 0 \quad (2.40)$$

Consequently, the first term on the left-hand side of Eq. (2.39) vanishes. The final wave equation, then, is equal to

$$\nabla^2 \vec{H} - \varepsilon\mu \frac{\partial^2 \vec{H}}{\partial t^2} - g\mu \frac{\partial \vec{H}}{\partial t} = 0 \quad (2.41)$$

The vector \vec{E} satisfies the same wave equation, as readily seen by first taking the curl of Eqs. (2.31a) and (2.31b) as

$$\vec{\nabla} \times \vec{\nabla} \times \vec{E} = -\vec{\nabla} \times \frac{\partial \vec{B}}{\partial t} \quad (2.42)$$

Using Eq. (2.34) to eliminate the magnetic field and treating g , μ , and ε as constants, Eq. (2.42) yields

$$\vec{\nabla} \times \vec{\nabla} \times \vec{E} = -g\mu \frac{\partial \vec{E}}{\partial t} - \varepsilon\mu \frac{\partial^2 \vec{E}}{\partial t^2} \quad (2.43)$$

Applying the vector identity of Eq. (2.38), again, and restricting the application of equation to a charge-free medium so that $\vec{\nabla} \cdot \vec{D} = 0$ give

$$\nabla^2 \vec{E} - \varepsilon\mu \frac{\partial^2 \vec{E}}{\partial t^2} - g\mu \frac{\partial \vec{E}}{\partial t} = 0 \quad (2.44)$$

The wave equations derived above govern the electromagnetic field in a homogeneous, linear medium in which the charge density is zero, whether this medium is conducting or nonconducting. However, it is not enough that these equations be satisfied; Maxwell's equations must also be satisfied. It is clear that Eqs. (2.41) and (2.44) are a necessary consequence of Maxwell's equation, but the converse is not true [10].

There are many methods available to solve the wave equations, but special care must be taken to obtain a useful solution for Maxwell's equations; however one method that works very well for monochromatic waves is to obtain a solution for vector electric field \vec{E} . The curl of \vec{E} (i.e., $\vec{\nabla} \times \vec{E}$) then gives the time deviation of magnetic field \vec{B} , which for monochromatic waves is sufficiently simply related to \vec{B} , so that \vec{B} can be easily found.

Monochromatic waves may be described as waves that are characterized by a single frequency. The methods of complex variable analysis afford a convenient way of treating such waves and the time dependency of the vector field \vec{E} is taken to be as $e^{-i\omega t}$, so that

$$\vec{E}(\vec{r}, t) = \vec{E}(\vec{r})e^{-i\omega t} \quad (2.45)$$

Note that the physical electric field is obtained by taking the real part of Eq. (2.54), which is the convenient mathematical description in terms of complex variables to the physical quantities by taking either the real or the imaginary part of the complex quantity. Furthermore $\vec{E}(\vec{r})$ is in general complex, so that the actual electric field is proportional to $\cos(\omega t + \phi)$, where ϕ is the phase of $\vec{E}(\vec{r})$. Using Eq. (2.45) in Eq. (2.44) provides the following result:

$$e^{-i\omega t} (\nabla^2 \vec{E} + \omega^2 \epsilon \mu \vec{E} + i\omega g \mu \vec{E}) = 0 \quad (2.46)$$

In Eq. (2.46), the common factor $e^{-i\omega t}$ for governing the spatial variation of the electric field can be dropped out. Now, we put our effort behind solving Eq. (2.46) in various spatial cases of interest to determine the spatial variation of the electromagnetic field. This is treated in Chap. 4 and in a simple form of possibility we assume that the “medium” is empty space, so that $g = 0$, $\epsilon = \epsilon_0$, and $\mu = \mu_0$ (see Chaps. 1 and 2). Furthermore, we suppose that $\vec{E}(\vec{r})$ varies in only one-dimensional form in z -direction, and it is independent of x and y coordinates. Then, Eq. (2.46) becomes

$$\frac{d^2 \vec{E}(z)}{dz^2} - \left(\frac{\omega}{c}\right)^2 \vec{E}(z) = 0 \quad (2.47)$$

where we have the following relation:

$$\epsilon_0 \mu_0 = \frac{1}{c^2} \quad (2.48)$$

So, the solution to Eq. (2.47) is given by

$$\vec{E}(z) = \vec{E}_0 e^{\pm ikz} \quad (2.49)$$

where \vec{E}_0 is a constant vector, providing that

$$k = \frac{\omega}{c} \quad (2.50)$$

Substituting the $\vec{E}(\vec{r})$ into Eq. (2.45), we get the full solution as

$$\vec{E}(\vec{r}, t) = \vec{E}_0 e^{-i(\omega t \mp kz)} \quad (2.51)$$

or taking the real part of Eq. (2.60), we get

$$\vec{E}(\vec{r}, t) = \vec{E}_0 \cos(\omega t \mp \kappa z) \quad (2.52a)$$

with Eq. (2.50) as an equivalent form as

$$\vec{E}(\vec{r}, t) = \vec{E}_0 \cos \omega(t \mp z/c) \quad (2.52b)$$

The final form of Eq. (2.52b) is the representation of a sinusoidal wave traveling to the right or left in the z -direction, depending on whether the minus or plus sign is applied. The velocity of propagation of the wave is speed of light c and if light is a form of electromagnetic radiation, then Maxwell's equations *predict* that $c = 1/\sqrt{\epsilon_0\mu_0} = 2.9979 \times 10^8$ m/s is the velocity of light in vacuum. The form in Eq. (2.61) shows that the wave frequency is $f = \omega/2\pi$ and the wavelength is $\lambda = 2\pi/k$. Thus, Eq. (2.50) is the familiar result for a wave as

$$\lambda f = c \quad (2.53)$$

In a nonconducting, nonmagnetic dielectric, we still maintain that $g = 0$ and $\mu = \mu_0$, but now $\epsilon = \epsilon_0\kappa$. The preceding derivation will carry through just the same, except that now Eq. (2.50) becomes

$$k = \sqrt{K}(\omega/c) \quad (2.54)$$

Now, if we define $n = \sqrt{K}$, we see that the results are the same in vacuum, except that the velocity of wave propagation is now c/n instead of just c and the quantity n is the *index of refraction* of the dielectric medium and for vacuum $n = 1$. The value of 1 for n accounts for refractive effects in transparent materials, as it is seen in the below discussion here.

If the medium is conducting, then $g > 0$; thus, the third term in Eq. (2.46) must be retained. When g is small the result will be merely that the wave is damped [10]. By small g , we mean that the third term of Eq. (2.46) is small compared with the second term, which led to the wave solution, or

$$\begin{aligned} \omega g \mu &\ll \omega^2 \epsilon \mu \\ g &\ll \omega \epsilon \end{aligned} \quad (2.55)$$

In the other extreme, when $g \gg \omega \epsilon$, we may neglect the second term of Eq. (2.46). Again, restricting attention to the one-dimensional case, we get the following wave equation:

$$\frac{d^2 \vec{E}(z)}{dz^2} + i\omega g \mu \vec{E}(z) = 0 \quad (2.56)$$

We can make the coefficient of $\vec{E}(z)$ real if we assume that $\alpha = i\omega$ is real or, in other words, that the frequency is imaginary. Then, if

$$k = \sqrt{\alpha g \mu} \quad (2.57)$$

The spatial dependence $\vec{E}(\vec{r})$ of the solution is just the same as before. The difference is that the time dependence Eq. (2.54) becomes

$$\vec{E}(\vec{r}, t) = \vec{E}(\vec{r}) e^{-\alpha t} \quad (2.58)$$

That is, the field simply decays exponentially with time, instead of oscillating in a wavelike manner. The transition between the decaying and the wave behavior occurs when

$$|\omega| = |\alpha| \cong \left| \frac{g}{\epsilon} \right| = \frac{1}{t_c} \quad (2.59)$$

where t_c is the relaxation time of the material of medium. Note that we repeat that caution is needed when this condition is applied to a metal, since g/ϵ is itself strongly dependent on ω .

Now tracing the derivation of Eq. (2.46) back to Maxwell's equations in sets of Eqs. (2.31a), (2.31b), (2.32), (2.33), and (2.34), we notice that the second term, or $\partial^2 \vec{E}(\vec{r}, t) / \partial t^2$ in Eq. (2.44), derives from the displacement current $\partial \vec{D} / \partial t$ in Eq. (2.34), whereas the third term, or $\partial \vec{D}(\vec{r}, t) / \partial t$ in Eq. (2.44), derives from the transport current density \vec{J} in Eq. (2.34). Thus, the very existence of electromagnetic wave propagation depends on Maxwell's introduction of the displacement current. Without it, only exponential decay of the fields could occur.

Based on our discussion so far, we can claim that the electromagnetic plane waves are transverse and in vacuum we can write the general form of the wave in z -direction as

$$\left\{ \begin{array}{l} \vec{\nabla} \cdot \vec{E} = 4\pi\rho \Rightarrow \rho = 0 \text{ in vacuum} \\ \vec{\nabla} \cdot \vec{E} = 0 \quad \vec{\nabla} \cdot \vec{E} = \frac{\partial E_z(z, t)}{\partial z} = 0 \end{array} \right. \quad (2.60)$$

Equation (2.60) says that E_z is independent of z . That E_z is also independent of time t can be seen by considering Maxwell's "displacement current," Eq. (2.32). Thus,

$$\frac{\partial \vec{E}}{\partial t} = c^2 \vec{\nabla} \times \vec{B} \quad (2.61)$$

Take the z component of Eq. (2.61). The right-hand side involves $\partial B_y/\partial x$ and $\partial B_x/\partial y$, both of which are zero. Thus, $\partial E_z/\partial t$ is zero. We conclude that E_z is a constant. For simplicity, we take the constant to be zero; similarly, the fact that we have from Eq. (2.33) $\vec{\nabla} \cdot \vec{B} = 0$ tells us that $B_z(z, t)$ has no z dependence. That is, also no time dependence is seen by considering the z component of Faraday's law, Eqs. (2.31a) and (2.31b), which gives $\partial B_z/\partial t$ to be zero. Although there may be some steady magnetic fields due to big steady currents somewhere, they have no space or time dependence and are not of present interest to us. We therefore take B_z to be zero by using the superposition principle.

Traveling harmonic wave was established by Eq. (2.61) and assume that the x component of electric E_x is given by the following relation:

$$E_x = A \cos(\omega t - kz) \quad (2.62)$$

Then, by coupling of E_x and B_y , we have the following sets of equations:

$$\frac{\partial E_x}{\partial t} = -c^2 \frac{\partial B_y}{\partial z} \quad \frac{\partial B_y}{\partial t} = -\frac{\partial E_x}{\partial z} \quad (2.63)$$

Similarly

$$\frac{\partial E_y}{\partial t} = c^2 \frac{\partial B_x}{\partial z} \quad \frac{\partial B_x}{\partial t} = \frac{\partial E_y}{\partial z} \quad (2.64)$$

Then by using Eq. (2.50), Eq. (2.63) becomes

$$\begin{aligned} \frac{\partial B_y}{\partial z} &= \frac{1}{c^2} \frac{\partial E_x}{\partial t} \\ &= \frac{\omega}{c^2} \frac{\partial E_x}{\partial t} = \frac{1}{c} \frac{\partial E_x}{\partial t} \end{aligned} \quad (2.65)$$

$$\begin{aligned} \frac{\partial B_y}{\partial t} &= -\frac{\partial E_x}{\partial z} \\ &= -kA \sin(\omega t - kz) \\ &= -\frac{1}{c} \frac{\partial E_x}{\partial t} \end{aligned} \quad (2.66)$$

According to Eqs. (2.65) and (2.66), the variation of B_y with respect to z and t is the same as that of E_x . Thus, we see that in a traveling harmonic plane wave propagation in the $+z$ -direction B_y and E_x are equal, aside from uninteresting additive constant, which we "superpose to zero."

If we consider a harmonic traveling wave propagating in the $-z$ -direction, we find that B_y is the negative of E_x , as you can easily see by replacing k with $-k$ in the above equations. Both directions of propagation are included in the summarizing equations as below:

$$\text{Traveling waves : } \begin{cases} |\vec{E}(z, t)| = |\vec{B}(z, t)| \\ \vec{E} \cdot \vec{B} = 0 \\ \hat{E} \times \hat{B} = \hat{v} \end{cases} \quad (2.67)$$

Standing harmonic wave then comes to play assuming that E_x is given by

$$E_x(z, t) = A \cos \omega t \cos kz \quad (2.68)$$

Then, we can show that

$$B_y(z, t) = A \sin \omega t \sin kz = E_x \left(z - \frac{1}{4}\lambda, t - \frac{1}{4}T \right) \quad (2.69)$$

From Eqs. (2.68) and (2.69), we see that in an electromagnetic standing plane wave in vacuum \vec{E} and \vec{B} are perpendicular to one another and to unit vector \hat{z} have the same amplitude, and are 90 degrees out of phase both in space and in time.

This behavior is similar to that of the pressure and velocity in a standing sound wave or that of the transverse tension and velocity in a standing wave on a string or rope as we described early in Sect. 2.3.

2.7 Scalar and Vector Potentials

As we have learned so far, Maxwell's equations consist of a set of coupled first-order partial differential equation relating the various components of electric and magnetic fields as below:

$$\begin{cases} \vec{\nabla} \times \vec{H} = \frac{4\pi}{c} \vec{J} + \frac{1}{c} \frac{\partial \vec{D}}{\partial t} & \vec{\nabla} \cdot \vec{D} = 4\pi\rho \\ \vec{\nabla} \times \vec{E} + \frac{1}{c} \frac{\partial \vec{B}}{\partial t} = 0 & \vec{\nabla} \cdot \vec{B} = 0 \end{cases} \quad (2.70)$$

Given that in linear media $\vec{D} = \epsilon \vec{E}$ and $\vec{B} = \mu_0 \vec{H}$, different format of set of Eq. (2.70) can be written as

$$\left\{ \begin{array}{ll} \text{(i)} \quad \vec{\nabla} \cdot \vec{E} = \frac{1}{\epsilon_0} \rho & \text{(iii)} \quad \vec{\nabla} \times \vec{E} = -\frac{\partial \vec{B}}{\partial t} \\ \text{(ii)} \quad \vec{\nabla} \cdot \vec{B} = 0 & \text{(iv)} \quad \vec{\nabla} \times \vec{B} = \mu_0 \vec{J} + \mu_0 \epsilon_0 \frac{\partial \vec{E}}{\partial t} \end{array} \right. \quad (2.71)$$

Given that $\rho(\vec{r}, t)$ and $\vec{J}(\vec{r}, t)$, what are the fields $\vec{E}(\vec{r}, t)$ and $\vec{B}(\vec{r}, t)$? In the static case, in case of time-independent Maxwell's equation configuration, as we saw in Chap. 1 of this book, Coulomb's law and the Biot-Savart law provide the answer.

However, what we are looking for, then, is the generalization of those laws to time-dependent Maxwell's equation configuration, as we discussed in Chap. 1 of this book.

These sets of equations can be solved as they stand in simple situations, but it is often convenient to introduce potentials, obtaining a small number of second-order equations, while satisfying some of Maxwell's equations identically. We are already familiar with the concept in electrostatics and magnetostatics, where we used the scalar potential ϕ and vector potential \vec{A} .

In electrostatics $\vec{\nabla} \times \vec{E} = 0$ allows us to write \vec{E} as the gradient of a scalar potential as $\vec{E} = -\vec{\nabla}\phi$; however in electrodynamics this is no longer possible, because the curl of \vec{E} is nonzero (i.e., $\vec{\nabla} \times \vec{E} \neq 0$). But \vec{B} remains divergence and that is $\vec{\nabla} \cdot \vec{B} = 0$ still holds, so we can define \vec{B} in terms of a vector potential as in magnetostatics as

$$\vec{B} = \vec{\nabla} \times \vec{A} \quad (2.72)$$

Putting Eq. (2.72) into Faraday's law of (iii) in Eq. (2.71) will yield the following result:

$$\vec{\nabla} \times \vec{E} = -\frac{\partial}{\partial t} (\vec{\nabla} \times \vec{A}) \quad (2.73a)$$

or

$$\vec{\nabla} \times \left(\vec{E} + \frac{1}{c} \frac{\partial \vec{A}}{\partial t} \right) = 0 \quad (2.73b)$$

This means that the quantity with vanishing curl in Eq. (2.73b) can be written as the gradient of some scalar function, namely, a scalar potential ϕ as

$$\begin{cases} \vec{E} + \frac{1}{c} \frac{\partial \vec{A}}{\partial t} = -\vec{\nabla} \phi \\ \vec{E} = -\vec{\nabla} \phi - \frac{1}{c} \frac{\partial \vec{A}}{\partial t} \end{cases} \quad (2.74)$$

The definition of \vec{B} and \vec{E} in terms of the potentials \vec{A} and ϕ according to Eqs. (2.72) and (2.74) satisfies identically the two homogeneous Maxwell's equations. The dynamic behavior of \vec{A} and ϕ will be determined by the two homogeneous equations in Eq. (2.71).

At this point it is convenient to restrict our considerations to the microscopic form of Maxwell's equations. Then the inhomogeneous Eq. (2.71) can be written in terms of the both vector and scalar potentials \vec{A} and ϕ accordingly as

$$\nabla^2 \phi + \frac{1}{c} \frac{\partial}{\partial t} (\vec{\nabla} \cdot \vec{A}) = -4\pi\rho \quad (2.75)$$

and

$$\nabla^2 \vec{A} - \frac{1}{c^2} \frac{\partial^2 \vec{A}}{\partial t^2} - \vec{\nabla} \left(\vec{\nabla} \cdot \vec{A} + \frac{1}{c} \frac{\partial \phi}{\partial t} \right) = -\frac{4\pi}{c} \vec{J} \quad (2.76)$$

We have now reduced the set of four Maxwell's equations to two equations, but they are still coupled equations. The uncoupling can be accomplished by exploiting the arbitrariness involved in the definition of the potentials \vec{A} and ϕ . Since \vec{B} is defined through Eq. (2.81) in terms of \vec{A} , the vector potential is arbitrary to the extent that the gradient of some scalar function Λ can be added. Thus, magnetic intensity \vec{B} is left unchanged by the transformation such as [11]

$$\vec{A} \rightarrow \vec{A}' = \vec{A} + \vec{\nabla} \Lambda \quad (2.77)$$

In order that the electric field \vec{E} in Eq. (2.74) to stay unchanged as well, the scalar potential ϕ must be simultaneously transformed as [11]

$$\phi \rightarrow \phi' = \phi - \frac{1}{c} \frac{\partial \Lambda}{\partial t} \quad (2.78)$$

The freedom implied by Eqs. (2.77) and (2.78) means that we can choose a set of potentials \vec{A} and ϕ such that

$$\vec{\nabla} \cdot \vec{A} + \frac{1}{c} \frac{\partial \phi}{\partial t} = 0 \quad (2.79)$$

Equation (2.79) will uncouple the pair of Eqs. (2.75) and (2.76) and leave two inhomogeneous wave equations, one for scalar potential ϕ and one for vector potential \vec{A} as follows:

$$\nabla^2 \phi - \frac{1}{c^2} \frac{\partial^2 \phi}{\partial t^2} = -4\pi\rho \quad (2.80)$$

and

$$\nabla^2 \vec{A} - \frac{1}{c^2} \frac{\partial^2 \vec{A}}{\partial t^2} = -\frac{4\pi}{c} \vec{J} \quad (2.81)$$

Equations (2.80) and (2.81), plus Eq. (2.79), form a set of equations equivalent in all respects to Maxwell's equations.

2.8 Gauge Transformations, Lorentz Gauge, and Coulomb Gauge

In this section, we refer to Jackson [11] and describe each of these topics in conjunction with scalar and vector potentials of previous section of this chapter.

The transformation of Eqs. (2.71) and (2.78) is called a *gauge transformation*, and the invariance of the fields under such transformations is called *gauge invariance*. The relation given by Eq. (2.79) between \vec{A} and ϕ is called *Lorentz condition*. To see that potentials can always be found to satisfy the Lorentz condition, suppose that the potentials \vec{A} and ϕ that satisfy Eqs. (2.75) and (2.76) do not satisfy Eq. (2.79). Then let us make a gauge transformation to potentials \vec{A}' and ϕ' thus, and demand that \vec{A}' and ϕ' satisfy the Lorentz condition:

$$\vec{\nabla} \cdot \vec{A}' + \frac{1}{c} \frac{\partial \phi'}{\partial t} = 0 = \vec{\nabla} \cdot \vec{A} + \frac{1}{c} \frac{\partial \phi}{\partial t} + \nabla^2 \Lambda - \frac{1}{c^2} \frac{\partial^2 \Lambda}{\partial t^2} \quad (2.82)$$

Thus, provided a gauge function Λ can be found to satisfy the following:

$$\nabla^2 \Lambda - \frac{1}{c^2} \frac{\partial^2 \Lambda}{\partial t^2} = -\left(\vec{\nabla} \cdot \vec{A} + \frac{1}{c} \frac{\partial \phi}{\partial t} \right) \quad (2.83)$$

The potentials \vec{A}' and ϕ' will satisfy the Lorentz condition and the wave Eqs. (2.80) and (2.81).

Even for potentials, which satisfy the Lorentz condition Eq. (2.79), there is arbitrariness. Evidently the *restricted gauge transformation* is

$$\begin{cases} \vec{A} \rightarrow \vec{A} + \vec{\nabla} \Lambda \\ \phi \rightarrow \phi + \frac{1}{c} \frac{\partial \Lambda}{\partial t} \end{cases} \quad (2.84)$$

where

$$\nabla^2 \Lambda - \frac{1}{c^2} \frac{\partial^2 \Lambda}{\partial t^2} = 0 \quad (2.85)$$

preserves the Lorentz condition, provided that \vec{A} and ϕ satisfy it initially. All potentials in this restricted class are said to belong to the *Lorentz gauge*. The Lorentz gauge is commonly used, first because it leads to the wave Eqs. (2.80) and (2.81), which is independent of the coordinate system chosen and so fits naturally into the considerations of special relativity. See Chaps. 2 and 6 of this book.

Another useful gauge for the potentials is the so-called *Coulomb, radiation, or transverse gauge*. This is the gauge in which we have

$$\vec{\nabla} \cdot \vec{A} = 0 \quad (2.86)$$

From Eq. (2.80), we see that the scalar potential satisfies the Poisson equation (see Eq. 2.87) as

$$\nabla^2 \phi = -4\pi\rho \quad (2.87)$$

with solution as

$$\phi(\vec{x}, t) = \int \frac{\rho(\vec{x}', t)}{|\vec{x} - \vec{x}'|} d^3\vec{x}' \quad (2.88)$$

The scalar potential is just *instantaneous* Coulomb potential due to the charge density $\rho(\vec{x}, t)$ using Cartesian coordinate notation. This is the origin of the name “Coulomb gauge.”

The vector potential satisfies the inhomogeneous wave equation as

$$\nabla^2 \vec{A} - \frac{1}{c^2} \frac{\partial^2 \vec{A}}{\partial t^2} = -\frac{4\pi}{c} \vec{J} + \frac{1}{c} \nabla \left(\frac{\partial \phi}{\partial t} \right) \quad (2.89)$$

The term involving the scalar potential can, in principle, be calculated from Eq. (2.88). Since it involves the gradient operator it is a term that is *irrotational*, that is, has vanishing curl. This suggests that it may cancel a corresponding piece of

the current density. The current density or any vector field can be written as the sum of two terms as

$$\vec{J} = \vec{J}_l + \vec{J}_t \quad (2.90)$$

where \vec{J}_l is called the *longitudinal current* or *irrotational current* and has $\vec{\nabla} \times \vec{J}_l = 0$, while \vec{J}_t is called the *transverse current* or *solenoidal current* and has $\vec{\nabla} \cdot \vec{J}_t = 0$. Substituting from the vector identity of Table 1.1, we get the following:

$$\vec{\nabla} \times (\vec{\nabla} \times \vec{J}) = \vec{\nabla} (\vec{\nabla} \cdot \vec{J}) - \nabla^2 \vec{J} \quad (2.91)$$

Together with $\nabla^2 \left(\frac{1}{|\vec{x} - \vec{x}'|} \right) = -4\pi\delta(\vec{x} - \vec{x}')$ as per definition Dirac-delta function in Chap. 1, Sect. 1.8.3, it can be shown that \vec{J}_l and \vec{J}_t can be constructed explicitly from \vec{J} as follows:

$$\vec{J}_l = -\frac{1}{4\pi} \int \frac{\vec{\nabla}' \cdot \vec{J}}{|\vec{x} - \vec{x}'|} d^3\vec{x}' \quad (2.92)$$

and

$$\vec{J}_t = \frac{1}{4\pi} \vec{\nabla} \times \vec{\nabla} \times \int \frac{\vec{J}}{|\vec{x} - \vec{x}'|} d^3\vec{x}' \quad (2.93)$$

With the help of the continuity equation and Eq. (2.93), it is seen that

$$\vec{\nabla} \left(\frac{\partial \phi}{\partial t} \right) = 4\pi \vec{J}_t \quad (2.94)$$

Therefore, the source for the wave equation for \vec{A} can be expressed entirely in terms of the transverse current, Eq. (2.93), as

$$\nabla^2 \vec{A} - \frac{1}{c^2} \frac{\partial^2 \vec{A}}{\partial t^2} = -\frac{4\pi}{c} \vec{J}_t \quad (2.95)$$

This, of course, is the origin of the name “transverse gauge.” The name “radiation gauge” stems from the fact that transverse radiation fields are given by the vector potential alone, the instantaneous Coulomb potential contributing only to the near

fields. This gauge is particularly useful in quantum electrodynamics. A quantum-mechanical description of photons necessitates quantization of only the vector potential.

The Coulomb or transverse gauge is often used when *no sources* are present. Then, $\phi = 0$, and \vec{A} satisfies the homogeneous wave equation. The fields are given by

$$\begin{cases} \vec{E} = -\frac{1}{c} \frac{\partial \vec{A}}{\partial t} \\ \vec{B} = \vec{\nabla} \times \vec{A} \end{cases} \quad (2.96)$$

In passing we note a peculiarity of the Coulomb gauge. It is well known that electromagnetic disturbances propagate with finite speed. Yet Eq. (2.97) indicates that the scalar potential “propagates” instantaneously everywhere in space. The vector potential, on the other hand, satisfies the wave Eq. (2.99), with its implied finite speed of propagation c . At first glance it is puzzling to see how this obviously unphysical behavior is avoided. A preliminary remark is that it is the fields, not the potentials, that concern us. A further observation is that the *transverse* current Eq. (2.93) extends over all space, even if \vec{J} is localized [12].

2.9 Infrastructure, Characteristic, Derivation, and Properties of Scalar Waves

More details of this interest subject of this section and naturally this book are provided in Chap. 6 of this book; however, the scalar wave also is a member of wave family that we are talking about in this chapter; thus we need to bring it up as part of wave family here.

Starting from Faraday’s discovery—instead of the formulation of the law of induction according to Maxwell—an extended field theory is derived, which goes beyond the Maxwell theory with the description of potential vortices (noise vortices) and their propagation as a scalar wave but contains the Maxwell theory as a special case. The new field theory with that doesn’t collide with the textbook opinion, but extends it in an essential point with the discovery and addition of the potential vortices.

Also, the theory of objectivity, which follows from the discovery, is compared in the form of a summary with the subjective and the relativistic point of view and the consequences for variable velocity of propagation of the scalar waves, formed from potential vortices, are discussed.

From Maxwell’s field equations only, the well-known transverse or Hertzian can be derived, whereas the calculation of longitudinal scalar waves (LSW) gives zero as a result. This is a flaw of the field theory, since scalar waves exist for all particle waves, like plasma waves, as photon or neutrino. Starting from Faraday’s discovery,

instead of the formulation of the law of induction according to Maxwell, an extended field theory is derived, which goes beyond the Maxwell theory with the description of potential vortices such as noise vortices and their propagation as a scalar wave but contains the Maxwell theory as a special case. With that the extension is allowed and does not contradict textbook physics.

It was a transverse wave, for which the electric and the magnetic field pointers oscillate perpendicular to the direction of propagation. This can be seen as the reason that the velocity of propagation is showing itself field independent and constant. It is the speed of light c .

With that Hertz had experimentally proven the properties of this wave, previously calculated in a theoretical way by Maxwell, and at the same time proven the correctness of the Maxwellian field theory. The scientists in Europe were just saying to each other “well done!” as completely other words came across from a private research laboratory in New York: “Heinrich Hertz is mistaken, it by no means is a transverse wave but a longitudinal wave!”

Besides the mathematical calculation of scalar waves this section of the book contains a voluminous material collection concerning the information technical use of scalar waves, infrastructure, derivation, and properties of such wave. If the useful signal and usually interfering noise signal change their places, a separate modulation of frequency and wavelength makes a parallel image transmission possible. If it concerns questions of the environmental compatibility for the sake of humanity such as bio-resonance among others or to harm humanity as for example electro-smog or even the high-energy weapon application of Star Wars also known as Strategic Defense Initiative (SDI) [13].

With regard to the environmental compatibility a decentralized electrical energy technology should be required, which manages without overhead powerlines, without combustion and without radioactive waste. The liberalization of the energy markets will not on any account solve our energy problem, but only accelerate the way into the dead end.

A useful energy source could be represented by space quanta, which hit upon the earth from the sun or from space. They however only are revealed to the measurement technician, if they interact. It will be shown that the particles oscillate and an interaction or collection with the goal of the energy technical use only is possible in the case of resonance.

Since these space quanta as oscillating particles have almost no charge and mass averaged over time, they have the ability of penetration proven for neutrinos. In the case of the particle radiation discovered 100 years ago by Tesla, it obviously concerns neutrinos. We proceed from the assumption that in the future decentral neutrino converters will solve the current energy problem. Numerous concepts from nature and engineering, like on the one hand lightning or photosynthesis and on the other hand the rail gun or the Tesla converter, are instanced and can be discussed.

Giving all the above scenario, we start our discussion of scalar wave subject in this section and this chapter by asking ourselves what is a “scalar wave” exactly. Scalar wave (hereafter SW) is just another name for a “longitudinal” wave. The term

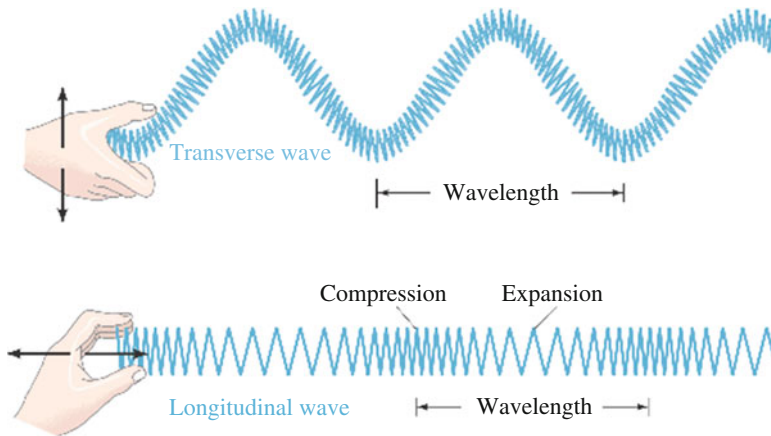


Fig. 2.11 Illustration of transverse versus longitudinal wave

“scalar” is sometimes used instead because the hypothetical source of these waves is thought to be a “scalar field” of some kind similar to the Higgs field for example.

There is nothing particularly controversial about longitudinal waves (hereafter LW) in general as illustrated in Fig. 2.11. They are a ubiquitous and well-acknowledged phenomenon in nature. Sound waves traveling through the atmosphere (or underwater) are longitudinal, as are plasma waves propagating through space also known as Birkeland currents. Longitudinal waves moving through the earth’s interior are known as “telluric currents.” They can all be thought of as pressure waves of sorts.

In modern-day electrodynamics (both classical and quantum), electromagnetic waves (EMW) traveling in “free space” (such as photons in the “vacuum”) are generally considered to be TW. But this was not always the case. When the preeminent mathematician James Clerk Maxwell first modeled and formalized his unified theory of electromagnetism in the late nineteenth century neither the EM SW/LW nor the EM TW had been experimentally proven, but he had postulated and calculated the existence of both.

After Heinrich Hertz demonstrated experimentally the existence of transverse radio waves in 1887, theoreticians (such as Heaviside, Gibbs, and others) went about revising Maxwell’s original equations (who was now deceased and could not object). They wrote out the SW/LW component from the original equations because they felt that the mathematical framework and theory should be made to agree only with experiment. Obviously, the simplified equations worked—they helped make the AC/DC electrical age engineerable. But at what expense?

Soon after Hertz’s claim of discovering Maxwell’s transverse EM waves Tesla visited him and personally demonstrated the experimental error to him. Hertz agreed with Tesla and had planned to withdraw his claim, but varying agendas intervened and set the stage for a major rift in the “accepted” theories that soon became

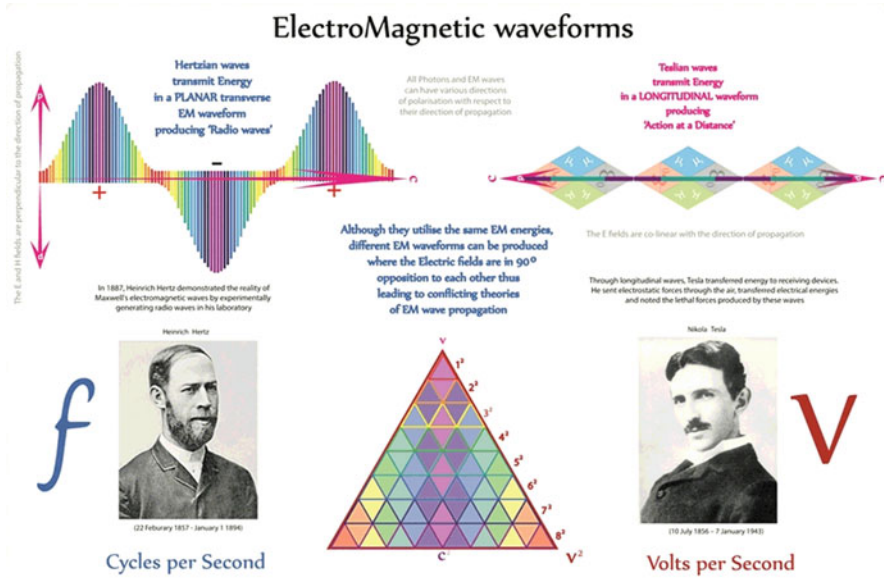


Fig. 2.12 Electromagnetic wave (EMW)

transformed into the fundamental “laws” of the electric science that have held sway in industry and the halts of academia to the present day. See Fig. 2.12.

Then in the 1889 Nikola Tesla (a prolific experimental physicist and inventor of AC) threw a proverbial wrench in the works when he discovered experimental proof for the elusive electric scalar wave. This seemed to suggest that SW/LW, opposed to transverse wave (TW), could propagate as pure electric waves or as pure magnetic waves. Tesla also believed that these waves carried a hitherto-unknown form of excess energy he referred to as “radiant.” This intriguing and unexpected result was said to have been verified by Lord Kelvin and others soon after. See Figs. 2.13 and 2.14.

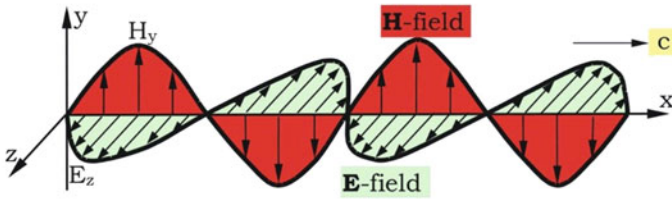
However, instead of merging their experimental results into a unified proof for Maxwell’s original equations, Tesla, Hertz, and others decided to bicker and squabble over who was more correct. In actuality, they both derived correct results. But because humans (even “rational” scientists) are fallible and prone to fits of vanity and self-aggrandizement, each side insisted dogmatically that they were right, and the other side was wrong.

The issue was allegedly settled after the dawn of the twentieth century when:

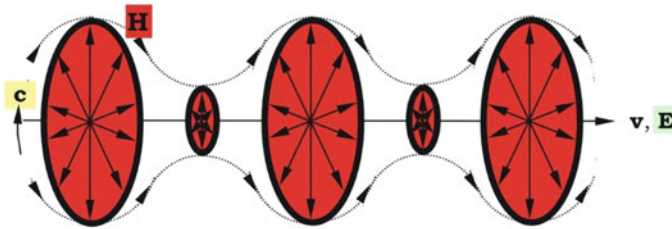
- (A) The concept of the mechanical (passive/viscous) ether was purportedly disproven by Michelson-Morley and replaced by Einstein’s relativistic space-time manifold.
- (B) Detection of SW/LWs proved much more difficult than initially thought (mostly due to the wave’s subtle densities, fluctuating frequencies, and orthogonal directional flow). As a result, the truncation of Maxwell’s equations was upheld.

The different waveforms

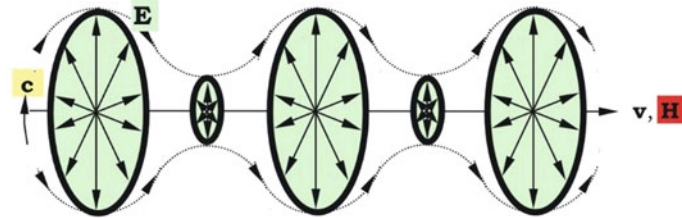
1. *H. Hertz*: electromagnetic wave (transverse)



2. *Nikola Tesla*: electric wave (longitudinal)



3. magnetic wave (longitudinal)



The three basic types according to the wave equation
(electric, magnetic and electromagnetic wave)

Fig. 2.13 Illustration of different waveforms

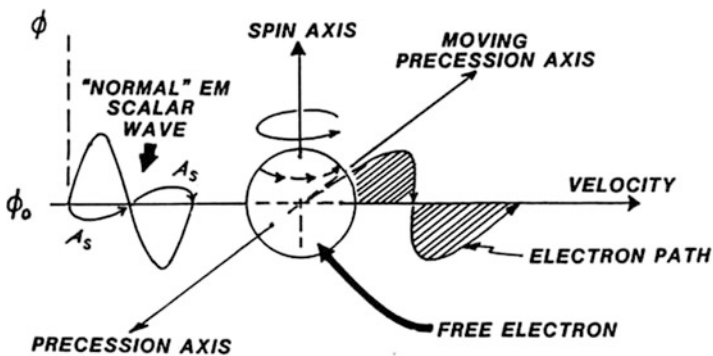


Fig. 2.14 Illustration of electron path and normal EM scalar wave



Fig. 2.15 Imaginary hyperspace

SW/LWs in free space however are quite real. Beside Tesla, empirical work carried out by electrical engineers such as Eric Dollard, Konstantin Meyl, Thomas Imlauer, and Jean-Louis Naudin (to name only some) has clearly demonstrated their existence experimentally. These waves seem able to exceed the speed of light, pass through EM shielding also known as Faraday cages, and produce over-unity (more energy out than in) effects. They seem to propagate in a yet-unacknowledged counter-spatial dimension also known as hyperspace, pre-space, false vacuum, aether, implicit order, etc. See Fig. 2.15.

Because the concept of an all-pervasive material ether was discarded by most scientists, the thought of vortex-like electric and/or magnetic waves existing in free space, without the support of a viscous medium, was thought to be impossible. However later experiments carried out by Dayton Miller, Paul Sagnac, E.W. Silvertooth, and others have contradicted the findings of Michelson and Morley. More recently Italian mathematician-physicist Daniele Funaro, American physicist-systems theorist Paul LaViolette, and British physicist Harold Aspden have all conceived of (and mathematically formulated) models for a free-space ether that is dynamic, fluctuating, and self-organizing, and allows for the formation and propagation of SW/LW.

A harmonic set of bidirectional longitudinal EM wave pairs in 2.space is depicted in Fig. 2.16. Unseen here is the time-polarized EM wave in the time domain, which reacts with the source charge to produce the 2.space bi-wave potential.

The potential as observed or detected is a harmonic set of bidirectional longitudinal wave in 2.space. That is, this potential is the “effect” of transduction of an incoming time-polarized EM wave interacting with the source charge.

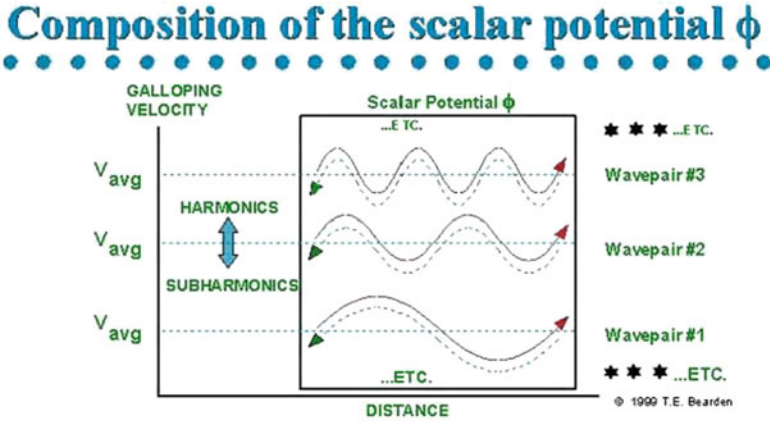


Fig. 2.16 A harmonic set of bidirectional longitudinal EM wave pairs in 2.space

Fig. 2.17 Shape of a Möbius supercoil

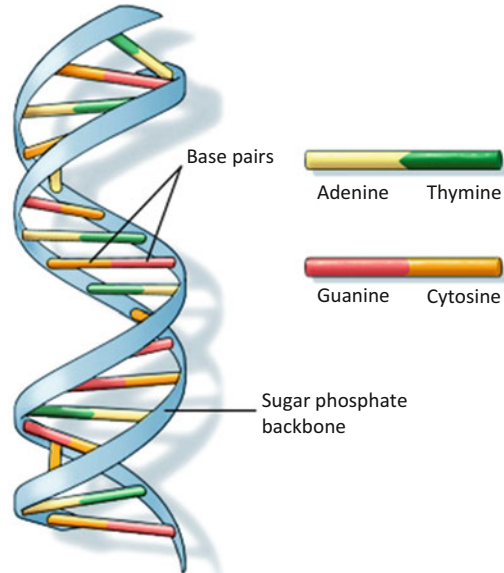


Therefore, defining the characteristic of scalar wave, we can express that the *scalar waves* are produced when two electromagnetic waves of the same frequency are exactly out of phase (opposite to each other) and the amplitudes subtract and cancel or destroy each other. The result is not exactly an annihilation of magnetic fields but a transformation of energy back into a *scalar wave*. This scalar field has reverted back to a vacuum state of potentiality. Scalar waves can be created by wrapping electrical wires around a figure eight in the shape of a Möbius coil as illustrated in Fig. 2.17. When an electric current flows through the wires in opposite directions, the opposing electromagnetic fields from the two wires cancel each other and create a scalar wave.

An example of what we just stated above within our day-to-day life is the DNA antenna in our body and cells. “The DNA antenna in our cells’ energy production centers (Mitochondria) assumes the shape of what is called a super-coil. Supercoil DNA look like a series of Möbius coils. These Möbius supercoil DNA are hypothetically able to generate scalar waves. Most cells in the body contain thousands of these Möbius supercoils, which are generating scalar waves throughout the cell and throughout the body.”

The standard definition of scalar waves is that they are created by a pair of identical waves (usually called the wave and its anti-wave) that are in phase spatially (space), but out of phase temporally (time). That is, to say, the two waves are

Fig. 2.18 Illustration of DNA structure



U.S. National Library of Medicine

physically identical, but 180 degrees out of phase in terms of time. They even look different—like an infinitely projected Möbius pattern on axis.

The DNA antenna in our cell energy production centers (mitochondria) assumes the shape of what is called a supercoil. Supercoil DNA looks like a series of Möbius coils. These Möbius supercoil DNAs are (science will not verify this, so for now it is hypothetical) able to generate scalar waves. Most cells in the body contain thousands of these Möbius supercoils, which are generating scalar waves throughout the cell and throughout the body. Scalar energy can regenerate and repair itself indefinitely. This also has important implications for the body DNA synthesis. See Fig. 2.18.

Mitochondrial DNA is only a small portion of the DNA in a cell; most of the DNA can be found in the cell nucleus. In most species on earth, including human beings, **mitochondrial DNA** is inherited solely from the mother. Mitochondria have their own genetic material, and the mechanism to manufacture their own RNAs and new proteins. This process is called protein biosynthesis. Protein biosynthesis refers to the process whereby biological cells generate new sets of proteins. See Fig. 2.19.

A scalar wave is also called a standing wave (see Sect. 3.3); it is a pattern of moving energy that stays in one place. We generally think of waves as moving through space as well as vibrating “up and down” but a scalar wave is stationary or standing. Scalar waves are used by the controllers to generate interference or feedback systems or to stimulate the nervous system of bodies to repeatedly loop in a certain manner—well if you can visualize the kind of waveform described you can probably imagine.

In the water resonance, the DNA sends a longitudinal wave that propagates in the direction of the magnetic field vector. The computed frequencies from the structure

Fig. 2.19 Image of mitochondria



of the DNA agree with those of the biophoton radiation as predicted. The optimization of efficiency by minimizing the conduction losses leads to the double-helix structure of DNA. The vortex model of the magnetic scalar wave not only covers many observed structures within the nucleus from perfect, but also introduces the hyperboloid channels in the matrix, if two cells communicate with each other.

Physical results revealed in 1990 form the basis of the essential component of a potential vortex scalar wave. The need for an extended field theory approach has been known since 2009 by the discovery of magnetic monopoles. For the first time this provides the opportunity to explain the physical basis of life not only from the biological discipline of science understanding. Nature covers the whole spectrum of known scientific fields of research for the first time this interdisciplinary understanding is explaining such complex relationships.

Decisive are the characteristics of the potential vortex. With its concentration effect, it provides a miniaturization down to a few nanometers, which allows the outrageously high information density in the nucleus for the first time.

Here for the first time magnetic scalar wave theory explains dual-based pair-stored information of the genetic code and a process of converting into an electrical modulation to, say, “piggyback” information transfer from the cell nucleus to another cell. At the receiving end the reverse process takes place in writing a chemical structure physically. The energy required to power the chemical process comes from the scalar wave itself. As an example of such piggyback scenario, we can observe the carrier wave piggybacking in Scientific Consciousness Interface Operation (SCIO) technology.

Figure 2.20 is an illustration such technology; when we set our radio or TV to a wave length such as 103.5, we get the wave of the radio station. The music and voice are superimposed onto the master wavelength in a piggyback function known as a

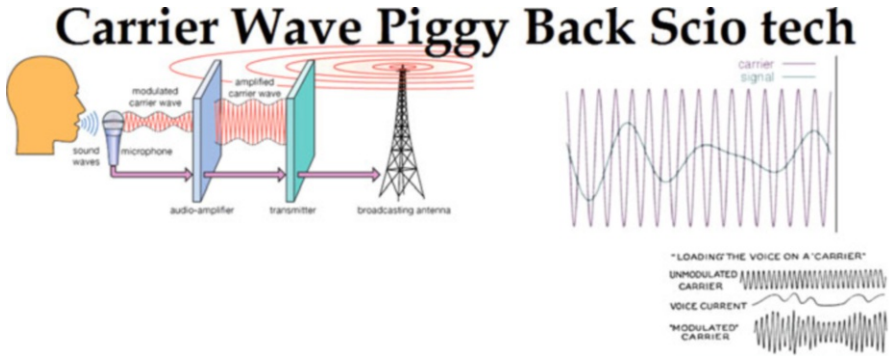


Fig. 2.20 Demonstration of carrier wave piggyback SCIO technology

carrier wave. Therefore, when we make a master signal from the SCIO/Educator we can superimpose a piggyback signal onto the carrier wave.

2.9.1 Derivation of the Scalar Waves

Imagine a three-dimensional space that is continuous. This space is governed by a flow of time that is uniform and constant for every point in the space. This space contains no matter and no particles of any kind. The space is at absolute rest, and furthermore it defines an absolute rest, where there exists no concept of velocity for a body exists. This space allows for the existence of three fields. There are two vector fields, with the electric field being \vec{E} and the magnetic field being \vec{B} as they are viewed classically through sets of Maxwell's equations. There is also a third field which is a scalar field that we call it the *scalar magnetic field* or just *scalar field* for short and designated by the symbol of β . These fields are related by the following equations:

$$\vec{\nabla} \cdot \vec{E} = \frac{\partial \beta}{\partial t} \tag{2.97}$$

$$\vec{\nabla} \times \vec{E} = -\frac{\partial \vec{B}}{\partial t} \tag{2.98}$$

$$\vec{\nabla} \cdot \vec{B} = 0 \tag{2.99}$$

$$\vec{\nabla} \times \vec{B} + \nabla \beta = \frac{1}{c^2} \frac{\partial \vec{E}}{\partial t} \tag{2.100}$$

where c is the speed of light and we call these four equations the *field equations*. Note that if $\beta = 0$, then the above four equations postulate the Maxwell's equations in free space and their energy content. See the next sets of equation below for further details.

Note that the difference between scalar field and scalar vector simply can be expressed as that, in general, any scalar is a quantity (number) without direction, like speed and temperature, while the vector has quantity and direction, like velocity, acceleration, and force. The field is a physical entity which occupies certain domain where its effect appears; for example the gravitational field is a vector field, the electromagnetic field is a vector field, while Higgs field is scalar; it is everywhere, around us, with no specific direction, and also gauge field is a scalar field. Any vector has direction in addition to the quantity, while any scalar is quantity without specific direction.

Mathematically, a scalar field on a region U is a real or complex-valued function or distribution on U . The region U may be set in some Euclidean space, Minkowski space, or more generally a subset of a manifold, and it is typical in mathematics to impose further conditions on the field, such that it be continuous or often continuously differentiable to some order. A scalar field is a tensor field of order zero, and the term "scalar field" may be used to distinguish a function of this kind with a more general tensor field, density, or differential form.

Physically, a scalar field is additionally distinguished by having units of measurement associated with it. In this context, a scalar field should also be independent of the coordinate system used to describe the physical system—that is, any two observers using the same units must agree on the numerical value of a scalar field at any given point of physical space. Scalar fields are contrasted with other physical quantities such as vector fields, which associate a vector to every point of a region, as well as tensor fields and spinor fields. More subtly, scalar fields are often contrasted with pseudo-scalar fields.

So, put it in simple form, we express the following:

1. **Scalar Field:** If at every point in a region a scalar function has a defined value, the region is called a scalar field.

Example: Temperature distribution in a rod

2. **Vector Field:** If at every point in a region a vector function has a defined value, the region is called a vector field.

Example: Velocity field of a flowing fluid

Now back to our discussion about the field equation, the field equations do not tell us what the fields are, but only how they interact. These three fields could exist alone in a region of space or simultaneously in any combination of magnitudes and directions, if they would not violate the above Eqs. (2.97) through (2.100).

Besides these relations, there is a dynamic content which can be conveniently expressed by the energy of each of the field. These are given by

$$\xi_E = \frac{\varepsilon}{2} \int E^2 d\tau \quad (2.101)$$

$$\xi_B = \frac{1}{2\mu} \int B^2 d\tau \quad (2.102)$$

$$\xi_\beta = \frac{1}{2\mu} \int \beta^2 d\tau \quad (2.103)$$

τ is the volume element, ε is the permittivity, and μ is the permeability of free space and we will call these three Eqs. (2.101) through (2.103) the *energy equations*.

These seven Eqs. (2.97) through (2.103) and the static particle-less space constitute the postulates of *stationary field theory* and that is the reason for saying if $\beta = 0$; these postulates are Maxwell's equations in free space and their energy content as it can be found in any textbook on the subject such as Jackson [11] or Griffiths [18]. Also, the nature of the space that these fields occupy is consistent with the classical view of electromagnetic.

Now the question is why we need to postulate stationary field in our theory of static particle-less space and it is called stationary field theory. To answer this question, we start by decoupling the four field equations of (2.97) through (2.100) to obtain equations related independently to each field and we can easily see that each field is a wave equation. This means that typically, given the presence of any of the fields, the fields would essentially work in tandem to propagate themselves through the space at the speed of light [19].

At this stage we are interested in the properties of the space itself where we derived our four sets of equations that we called *field equations*, and have not yet added anything to the space to produce the fields. Imagine that you have a large pan filled with water and the water is just standing motionless sitting in the pan, so it seems undisturbed, so the water just sits there in the pan. We know that if we touch the water let say in the center of water in the pan, it would produce waves. This is because water has certain properties, which are conducive to the production of waves.

We know that the wave in space travels at the speed of light and it is experimentally proven as well as being verified theoretically by Maxwell and others. However, the question here from particularly modern physics point of view is "velocity relative to what." There are no particles or matter in this space that we assumed at the beginning by which any wave velocity would be measured. In other words, any velocity in the space is absolute, just like as any wave velocity of water in our pan is based on the frame of reference of the pan wall holding the water and not the motion of the figure touching it, provided a constraint that the water is not flowing around in the pan. Thus, there is no reason to consider that different regions of space itself would have some kind of associated velocity, like water flowing around the pan, and Maxwell's equations contain nothing that would suggest the idea. Therefore, another property of the space is that it is stationary, and thus the name *stationary field theory*.

Many scientists take such a contradiction as an acknowledged fact because there is no way to measure any sort of absolute velocity experimentally; that is, most are designed to measure absolute velocity and experiments fail to do so. Furthermore, the strict and pervasive employment of absolute velocity here, which we are describing, would conflict with experiments if we perform them.

Many scientists will take such contradiction as an accepting fact since there exists no way to measure any sort of absolute velocity experimentally that is designed to measure such absolute velocity and experiment fails to do so. Furthermore, the strict and pervasive employment of absolute velocity here that we are describing would be in conflict with experiments if we perform one.

So, while the field equations described by sets of four Eqs. (2.93) through (2.100) show the relationship between the three fields, one needs some initial conditions to set up an applicable problem; in other words, we should imagine that some fields exist and then from these conditions the equations will tell us what will happen. In order to get a better understanding of this idea and the situation we are in and what would happen it will be useful to decouple the equations. The decoupling of these field equations will take place in the following manner:

Firstly, we take the curl of Eq. (2.98) as follows:

$$\begin{aligned}\vec{\nabla} \times (\vec{\nabla} \times \vec{E}) &= -\nabla \times \frac{\partial \vec{B}}{\partial t} \\ \nabla \times \frac{\partial \vec{B}}{\partial t} &= -\vec{\nabla} \times (\vec{\nabla} \times \vec{E})\end{aligned}\tag{2.104}$$

Next, we take the gradient of Eq. (2.97) as

$$\begin{aligned}\vec{\nabla} (\vec{\nabla} \cdot \vec{E}) &= \vec{\nabla} \left(\frac{\partial \beta}{\partial t} \right) \\ \vec{\nabla} \left(\frac{\partial \beta}{\partial t} \right) &= \vec{\nabla} (\vec{\nabla} \cdot \vec{E})\end{aligned}\tag{2.105}$$

Then, we take the time derivative of Eq. (2.100) as

$$\begin{aligned}\frac{\partial}{\partial t} (\vec{\nabla} \times \vec{B} + \nabla \beta) &= \frac{\partial}{\partial t} \left(\frac{1}{c^2} \frac{\partial \vec{E}}{\partial t} \right) \\ \vec{\nabla} \times \frac{\partial \vec{B}}{\partial t} + \vec{\nabla} \left(\frac{\partial \beta}{\partial t} \right) &= \frac{1}{c^2} \frac{\partial^2 \vec{E}}{\partial t^2} \\ \vec{\nabla} \left(\frac{\partial \beta}{\partial t} \right) + \vec{\nabla} \times \frac{\partial \vec{B}}{\partial t} &= \frac{1}{c^2} \frac{\partial^2 \vec{E}}{\partial t^2}\end{aligned}\tag{2.106}$$

Now, we can take the results in Eqs. (2.104) and (2.105) and substitute them into final form of Eq. (2.106), which then yields the following form:

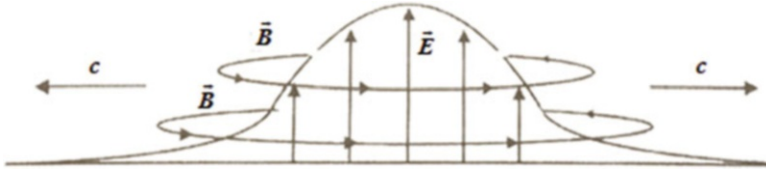


Fig. 2.21 Electromagnetic wave propagation depiction

$$\vec{\nabla} (\vec{\nabla} \cdot \vec{E}) - \vec{\nabla} \times (\vec{\nabla} \times \vec{E}) = \frac{1}{c^2} \frac{\partial^2 \vec{E}}{\partial t^2} \tag{2.107}$$

By using the vector identity $\vec{\nabla} \times (\vec{\nabla} \times \vec{F}) = \vec{\nabla} (\vec{\nabla} \cdot \vec{F}) - \nabla^2 \vec{F}$ in Table 1.1, then Eq. (2.107) ends up in a final form as

$$\nabla^2 \vec{E} = \frac{1}{c^2} \frac{\partial^2 \vec{E}}{\partial t^2} \tag{2.108}$$

Equation (2.108) indicates that electric field can propagate as a wave through the space of interest while appearing identical to classical electromagnetism type wave and being not a solenoidal type.

This wave equation has also a longitudinal component made possible by the scalar field. Therefore, if the initial conditions are that some electric vector field exists, then the electric field will propagate at the speed of light. From a localized initial field, the wave will spread out in all directions. For a somewhat artificial example, we consider a localized electric field where the field vector is always in the same direction as shown in Fig. 2.21.

As it is seen in Fig. 2.21, the electric field at the center will propagate outward along with the magnetic field.

Secondly, we take the curl of Eq. (2.100), and thus we have

$$\vec{\nabla} \times (\vec{\nabla} \times \vec{B}) + \vec{\nabla} \times (\vec{\nabla} \beta) = \frac{1}{c^2} \vec{\nabla} \times \frac{\partial \vec{E}}{\partial t} \tag{2.109}$$

Then we take the time derivative of Eq. (2.98), so we have

$$\vec{\nabla} \times \frac{\partial \vec{E}}{\partial t} = -\frac{\partial^2 \vec{B}}{\partial t^2} \tag{2.110}$$

We can then substitute Eq. (2.110) into Eq. (2.109), which yields

$$\vec{\nabla} \times (\vec{\nabla} \times \vec{B}) = \frac{1}{c^2} \frac{\partial^2 \vec{B}}{\partial t^2} \tag{2.111}$$

Using the vector identity $\vec{\nabla} \times (\vec{\nabla} \times \vec{F}) = \vec{\nabla} (\vec{\nabla} \cdot \vec{F}) - \nabla^2 \vec{F}$ from Table 1.1 again,

$$\vec{\nabla} (\vec{\nabla} \cdot \vec{B}) - \nabla^2 \vec{B} = \frac{1}{c^2} \frac{\partial^2 \vec{B}}{\partial t^2} \quad (2.112)$$

And with divergence of the magnetic field being zero we have

$$\nabla^2 \vec{B} = \frac{1}{c^2} \frac{\partial^2 \vec{B}}{\partial t^2} \quad (2.113)$$

Equation (2.113) shows that the magnetic field propagates along the electric field. The magnetic propagation is only solenoidal and tracks the solenoidal propagation of the electric field.

Thirdly, we take the divergence of Eq. (2.100), so we have

$$\vec{\nabla} \cdot (\vec{\nabla} \times \vec{B}) + \vec{\nabla} \cdot (\vec{\nabla} \beta) = \frac{1}{c^2} \vec{\nabla} \cdot \frac{\partial \vec{E}}{\partial t} \quad (2.114)$$

Using the vector identity $\vec{\nabla} \cdot (\vec{\nabla} \times \vec{F}) = 0$ from Table 1.1, we can see that the first term on left-hand side of Eq. (2.114) is zero, and then we are left with the following result:

$$\nabla^2 \beta = \frac{1}{c^2} \nabla \cdot \frac{\partial \vec{E}}{\partial t} \quad (2.115)$$

Then taking the time derivative of Eq. (2.97), we obtain

$$\vec{\nabla} \cdot \frac{\partial \vec{E}}{\partial t} = \frac{\partial^2 \beta}{\partial t^2} \quad (2.116)$$

We can then substitute Eq. (2.116) into Eq. (2.115) to yield the following result:

$$\nabla^2 \beta = \frac{1}{c^2} \frac{\partial^2 \beta}{\partial t^2} \quad (2.117)$$

Equation (2.117) indicates that the scalar field propagates along with the electric field tracks as the *longitudinal propagation* of the electric field as shown in Eqs. (2.108) and Equation (2.113) and finally Eq. (2.115) and they will be called the **wave equations**.

Note that the scalar field only exists when the electric field has divergence. If there is no divergence, the electric field has only solenoidal propagation. These three

Eqs. (2.108), (2.113), and (2.115) then revert to typical electromagnetic wave propagation in free space as they can be derived from Maxwell’s equations. See Chap. 1 of this book.

The scalar field propagates as a wave along the other fields as well. In other words, the electric field propagates through space, where the magnetic field propagates along the supporting propagation of the electric field that is perpendicular to the direction of propagation in a solenoidal wave condition and the scalar field propagates along with the electric field that is longitudinal to the direction of propagation which we know by now as **longitudinal wave**.

This longitudinal propagation might seem to immediately defy observations, but it actually does not occur in electromagnetic radiation for complicated reasons that need to be explained, which is done by Enslie [19] and is given in the next section of this chapter as well. Nonetheless, scalar propagation does exist in a limited form and shape or context.

Further analysis of Eq. (2.108) will provide us some mathematical reasoning and shed some light over the proof of scalar wave.

Taking apart Eq. (2.108) of the Laplace operator according to rules of vector identity analysis of Table 1.1 to be $\nabla^2 \vec{F} = \nabla (\nabla \cdot \vec{F}) - \nabla \times \nabla \times \vec{F}$, the result is what we show in the following form with more detailed breakdown:

$$\underbrace{\nabla^2 \vec{E}}_{\text{Wave}} = \underbrace{\nabla (\nabla \cdot \vec{E})}_{\text{Longitudinal}} - \underbrace{\nabla \times (\nabla \times \vec{E})}_{\text{Transverse}} \tag{2.118}$$

We can compare Eq. (2.118) to solution of Maxwell’s field equations with the following interpretation:

Hertzian Wave = Transverse Wave

I. Solution of Maxwell’s field equations with no source, and then Eq. (2.118) reduces to

$$\nabla \cdot \vec{E} = 0 \quad \text{and} \quad -\nabla \times \nabla \times \vec{E} = \frac{1}{c^2} \frac{\partial^2 \vec{E}}{\partial t^2} \tag{2.119}$$

II. Transverse Wave:

Field pointers oscillate crosswise to the direction of propagation. The propagation occurs with the speed of light c .

The claim we have had is that

Tesla Radiation = Longitudinal Wave

III. Special case: Irrotationally

$$\vec{\nabla} \times \vec{E} = 0 \quad \text{and} \quad \vec{\nabla} (\vec{\nabla} \cdot \vec{E}) = \frac{1}{c^2} \left(\frac{\partial^2 \vec{E}}{\partial t^2} \right) \quad (2.120)$$

IV. Longitudinal Wave, Shock Wave, Standing Wave

File pointer oscillates in the direction of propagation. Velocity of propagation is variable.

By taking apart the wave equation, one plunges into the adventure of an entirely new field theory, it first of, all should be traced and analyzed, what the latest textbooks say about scalar wave which there are non-exists so far except few notes here and there by different researchers and scientist.

We introduced scalar and vector potentials so far. There the constant of dielectricity κ is written in complex variable, although it is physically seen and concerns a material constant, only to be able to calculate with this trick artificially a loss angle, which should indicate the losses occurring in a dielectric, where in reality it concerns vortex losses. Of course, one can explain the dielectric losses of a capacitor or the heating in a microwave oven entirely without vortex physics with such a label fraud, but it should be clear to anyone that in a complex constant lies buried an inner contradiction, which is incompatible with physical concepts.

We are used to such auxiliary descriptions so much that the majority of today's physicists tend to attribute physical reality to this mathematical nonsense. As pragmatists they put themselves on the standpoint if with that experimental results can be described, then such an auxiliary description cannot be so wrong after all. Doing so the circumstance is forgotten that here the ground of pure science is abandoned and is replaced by creeds.

We find everything we need so far, in the wave equation, as it can be found in all classical textbook, including the wave equation (2.108). Behind this formulation two completely different kinds of waves are hiding, because the usage of Laplace operator consists of two parts according to the rules of vector analysis given by Table 1.1 and we demonstrated them above; thus, again we can write

$$\underbrace{\vec{\nabla} (\vec{\nabla} \cdot \vec{E})}_{\text{Longitudinal}} - \underbrace{\vec{\nabla} \times (\vec{\nabla} \times \vec{E})}_{\text{Transverse}} = \underbrace{\nabla^2 \vec{E}}_{\text{Wave}} \quad (2.121)$$

We should discuss two special cases:

If we put the left part in Eq. (2.121) to zero ($\vec{\nabla} \cdot \vec{E} = 0$) which is tantamount to no sources of the field then the well-known radio wave remains, which is also called Hertzian wave, after Heinrich Hertz, as said, had experimentally detected it in Karlsruhe 1888 and that is written in the form of Eq. (2.121), again as

$$\vec{\nabla} \cdot \vec{E} = 0 \quad \text{and} \quad -\vec{\nabla} \times \vec{\nabla} \times \vec{E} = \frac{1}{c^2} \frac{\partial^2 \vec{E}}{\partial t^2} \quad (\text{Special Case}) \quad (2.122)$$

This equation concerns the transverse wave, described by Maxwell, for which the field pointers oscillate crosswise to the direction of propagation. The propagation again occurs with the speed of light c , so much concerning the state of the art of technology.

But as we see, in the mathematical formulation of the wave equation is hiding, yes, even more than only the generally known electromagnetic wave. The no sources approach is a neglect, which is valid only under certain prerequisites!

The other thing we mentioned is the Tesla claim and mathematical reasoning behind the scalar wave and that is

Tesla Radiation = Longitudinal Wave

$$\vec{\nabla} \times \vec{E} = 0 \quad \text{and} \quad \vec{\nabla} (\vec{\nabla} \cdot \vec{E}) = \frac{1}{c^2} \left(\frac{\partial^2 \vec{E}}{\partial t^2} \right) \quad (2.123)$$

And in condition of special case, we can write that

Source field, because $\vec{\nabla} \cdot \vec{E} \neq 0$, then

Source = Charge Carriers (Plasma Waves)

Source = Vortex Structure

Then, we take an approach, where $\vec{\nabla} \cdot \vec{E} \neq 0$ is scalar wave, which gives us the indication that \vec{E} field vector can be derived from a scalar potential ϕ via its gradient, as we have said all along and that is

$$\vec{E} = -\vec{\nabla} \phi \quad (2.124)$$

and

$$\vec{\nabla} \cdot \vec{E} = -\vec{\nabla} \cdot \vec{\nabla} \phi = \nabla^2 \phi \quad (2.125)$$

Insert Eq. (2.123) into Eq. (2.121), and then we obtain **homogeneous scalar wave equation** as

$$\nabla^2 \phi = \frac{1}{c^2} \left(\frac{\partial^2 \phi}{\partial t^2} \right) \quad (2.126)$$

which is analogous to Eq. (2.117) above.

For the case of an additional space charge density, where we need to consider ρ_{electric} in the matter, then we can write

$$\text{div } \vec{D} = \rho_{\text{electric}} \tag{2.127}$$

where \vec{D} is called the electric “displacement”. See Eq. ((1.115)) as well.

In this case we get *inhomogeneous scalar wave equation*, which is nothing more than plasma wave and that is

$$\nabla^2 \phi = \frac{1}{c^2} \left(\frac{\partial^2 \phi}{\partial t^2} \right) - \frac{\rho_{\text{electric}}}{\epsilon} \tag{2.128}$$

where ϵ is the permittivity of materials.

One solution to plasma wave of Eq. (2.128) is Langmuir waves, where $\omega^2 = c^2 k^2 + \omega_{\text{plasma}}^2$. In this relationship ω is the frequency of oscillation (i.e., Longmuir oscillation) that is propagating and ω_{plasma} is the frequency of plasma, while k is the wave number and c is the speed of light. See reference by Zohuri [20].

Equation (2.128) is the derivation of the plasma wave as an example of the existence of scalar wave in the wave equation. The solution of Eq. (2.128) describes dispersion relation of plasma wave 20, which is longitudinal wave movements + Langmuir oscillation of the electron density.

Nikola Tesla explains the difference between his scalar wave radiation and the Hertzian wave and it is depicted in Figs. 2.22 and 2.23 here.

In Fig. 2.23, we see the ground waves, which follow the curvature of the earth and radio waves reflected at the ionosphere. This figure also indicates that the interference and fading with which the radio amateur is fighting are a result of the differently fast-arriving wave parts and doing so the scalar wave part tunnels as straight line right through earth as shown in Fig. 2.23.

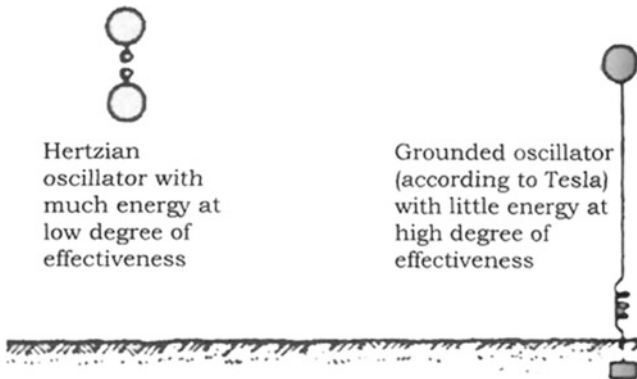


Fig. 2.22 Comparison between Hertzian and scalar wave per Tesla

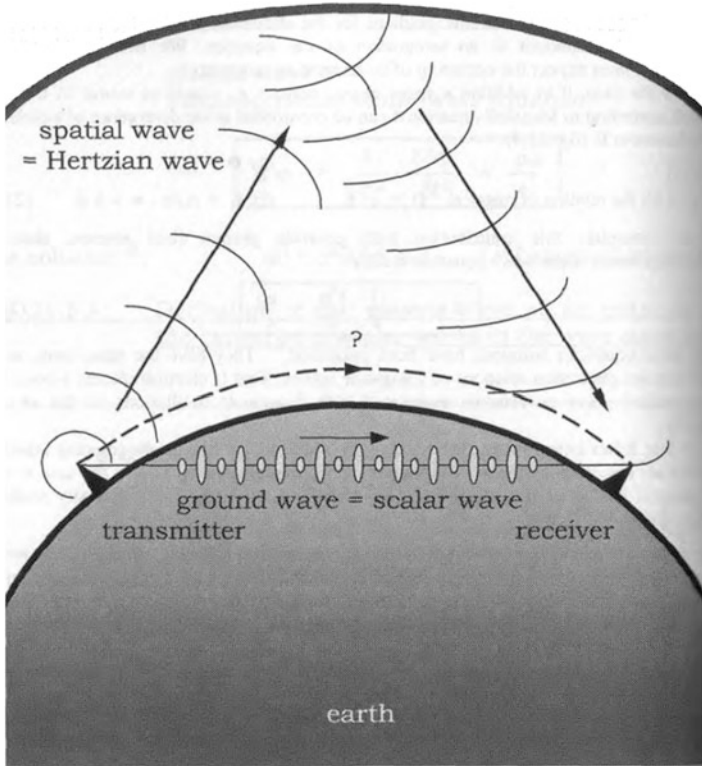


Fig. 2.23 Hertzian wave vs. scalar wave

Driving the plasma wave can be done without formation of the gradient in order to obtain homogeneous equation which is tantamount to an integration of the equation. Thus, under certain conditions, we must expect the occurring of an integration constant.

This is the case if in addition a space charge density occurs as source of the field, which according to Maxwell equation (1.115) can be considered as the divergence of a dielectric displacement \vec{D} in respect of the material relation such as

$$\begin{aligned}
 \vec{D} &= \epsilon \vec{E} \\
 \vec{\nabla} \cdot \vec{D} &= \rho_{\text{electric}} \\
 \vec{\nabla} \cdot \vec{E} &= \frac{\rho_{\text{electric}}}{\epsilon} = -\nabla^2 \phi
 \end{aligned}
 \tag{2.129}$$

If we complete these contributions with possible present field source, then the inhomogeneous scalar wave equation yields as we illustrated in Eq. (2.128), and solution for this wave has been established by many plasma physicists. They have

the same form, as the well-known dispersion relations of Langmuir waves. That is electron plasma waves and thus longitudinal wave movements associated with Langmuir oscillations of the electron density.

With that it has been proven that scalar waves and longitudinally propagating standing waves are described by the wave equation and are contained in it. This in any case is valid in general just as in the special case of a plasma wave, as mathematically could be derived here.

From our above discussion and derivation of plasma waves as in Eq. (2.128), we can easily see that the scalar waves by all means are nothing new and their existence was known to us both theoretically and experimentally.

One important scenario that can be taken away from all these is that for wave absorption means nothing, however transverse waves in the case of a disturbance rolling up to vortices in measurement of localized wave and vortices for standing wave, localized vortex and broadband antenna for electromagnetic compatibility (EMC) measurements as shown in Fig. 2.24.

As far as decoupling of the wave parts is concerned, the set of difficulties of ground waves makes clear the coupling of longitudinal and transverse waves as two aspects or parts of a wave. As the corresponding Eq. (2.112), mathematically taken apart into Eq. (2.125) dictates, does every transmitter emit both parts.

In this case from other areas of applications of these waves, for instance from flow dynamics point of view, or for body sound it is generally known that both wave parts exist and in addition occur jointly. In the case of a propagation through the earth, like for an earthquake, both parts are received and utilized. Because their propagation is differently fast, the faster oscillations arrive first and that are the longitudinal ones. From the time delay with which the transverse waves arrive at the measurement station, the distance to the epicenter of the quake is determined by means of the different velocity of propagation. For geophysicists this tool is part of everyday knowledge. See Fig. 2.25.

As we can see, it is obvious that the electromagnetic wave is not just purely transverse and sound wave purely longitudinal wave either. It is true that a transverse sound wave does not get too far in air, for which reason sound as a rule is considered as a purely longitudinal wave by neglecting this part, but such a neglect may not be carried out in general; it must be checked if it is legitimate from case to case and an error consideration should be carried out.

Further examples for the coupling of the wave parts are furnished by the latest tunnel experiments. Here so-called pure transverse waves are sent into a tunnel, through which they do not fit through at all. The Maxwell theory then dictates that behind the tunnel no signal should be measurable. But a signal is being measured, which in the tunnel in addition was faster than allowed.

So, this should tell us about the thoughts of the phase velocities of an EMW, which is not present at all, before instantaneous tunneling, during which the clocks should stop. The wave equation, however, supplies the only possible answer; that is, the tunnel filters out the SW parts and lets it to pass from them only if they are sufficiently small and correspondingly fast [13].

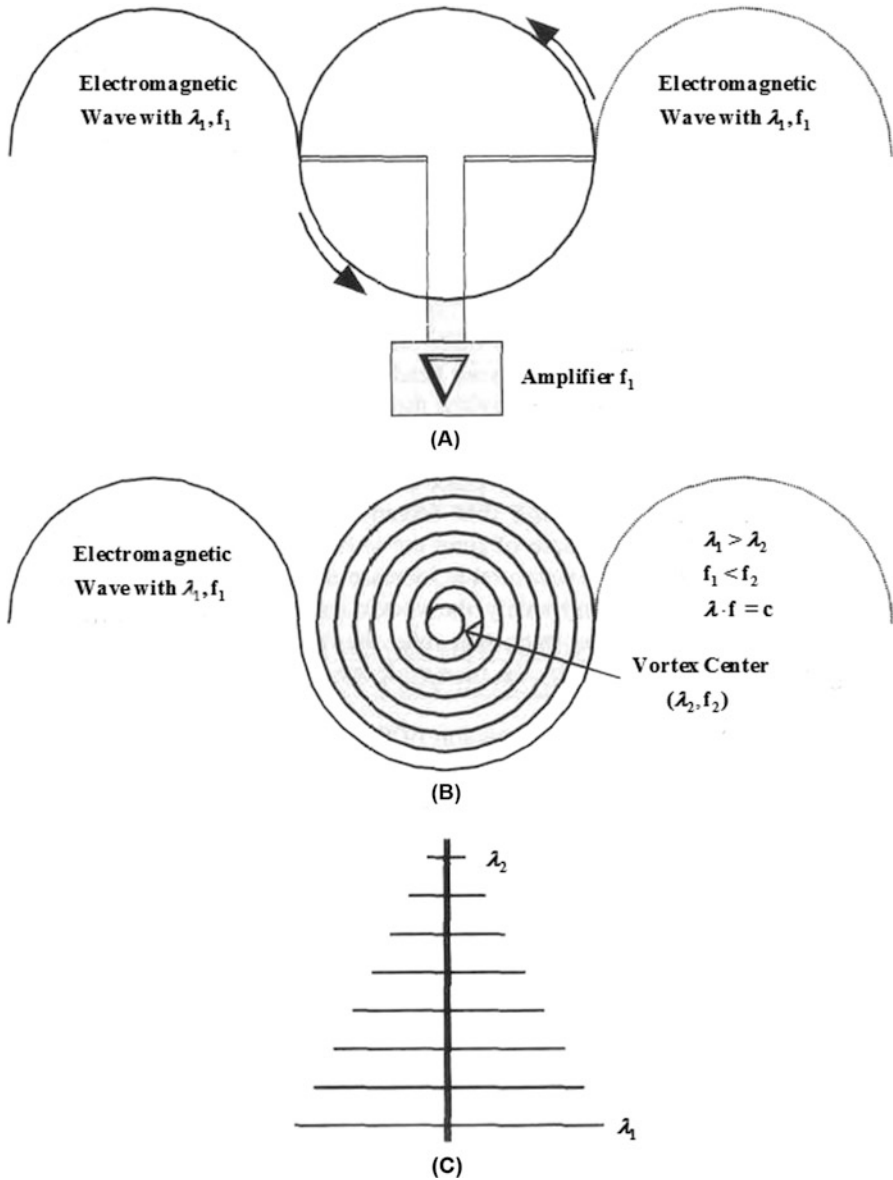
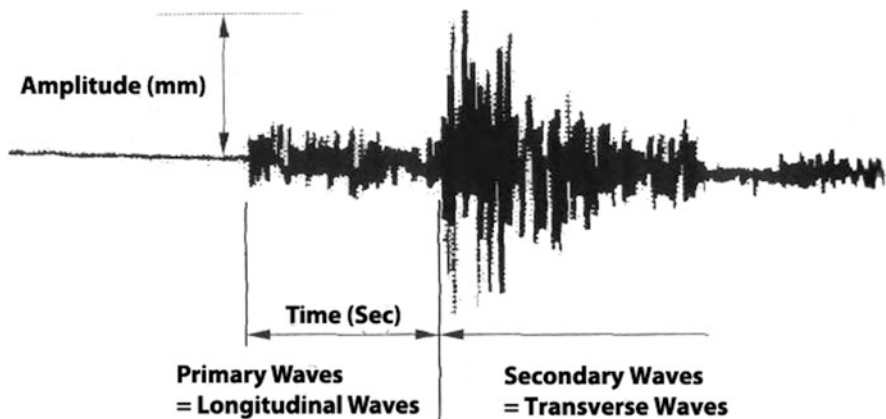
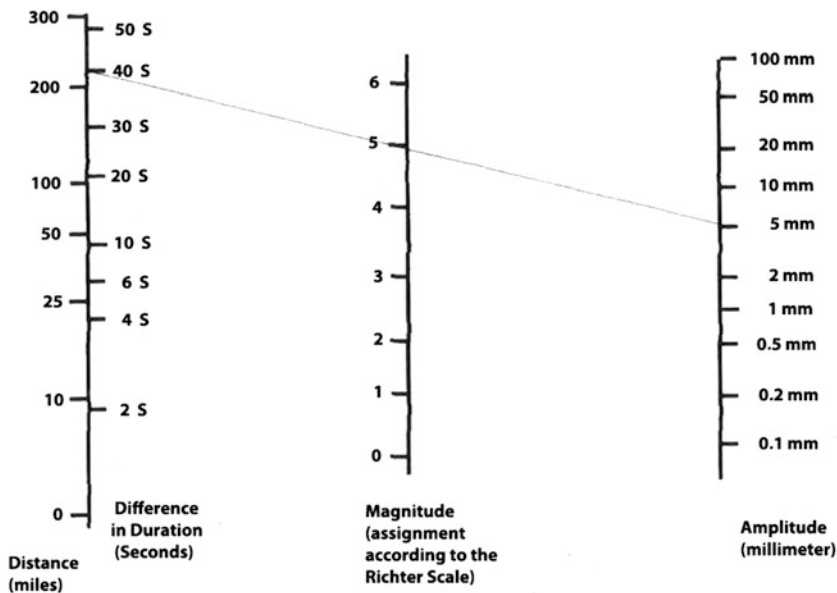


Fig. 2.24 Measurement of localized waves and vortices. (a) Standing wave. (b) Standing wave. (c) Broadband antenna for EMC measurements



(A)



(B)

Fig. 2.25 Illustration of earthquake waves and magnitude. (a) Longitudinal and transverse earthquake waves. (b) Analysis according to Richter scale (e.g., 40-s duration between S-wave and P-wave for 5 mm amplitude means an earthquake of strength 5 in a distance, of 220 miles)

2.9.1.1 Near-Field Difficulties

Sets of difficulties that we face in the near field can also be discussed as follows. In high-frequency technology it is distinguished between the near field and the far field. Both have fundamentally other properties [13].

Heinrich Hertz did experiment in the short-wave range at wavelengths of some meters. From today's viewpoint his work would rather be assigned the far field. As a professor in Karlsruhe he had shown that his, the electromagnetic, wave propagates like a light wave and can be refracted and reflected in the same way. It is a transverse wave for which the field pointers of the electric and the magnetic field oscillate perpendicular to each other and both again perpendicular to the direction of propagation. It hence would be obvious, if in the case of the Hertzian wave it would concern the far field. Besides the propagation with the speed of light also being the characteristic there occurs no phase shift between \vec{E} -field and \vec{H} -field [13].

For the approach of vortex and closed-loop field structures derivations for the near field are known. Doing so it must be emphasized that the structures do not follow from the field equations according to Maxwell, but the calculations are based on assumed rotation symmetrical structures. The Maxwell theory by no means is capable of such a structure shaping by principle. The calculation provides an important result that in the proximity of the emitting antenna a phase shift exists between the pointers of the \vec{E} -field and the \vec{H} -field. The antenna current and the H-field coupled with it lag the E-field of the oscillating dipole charges for 90° (see Fig. 2.26). These charges form a longitudinal standing wave of the antenna rod or antenna dipole. For this reason, also, the fields produced by high-frequency currents at first have the properties of a longitudinal wave in the proximity of the antenna.

These two fields, namely, \vec{E} -field and the \vec{H} -field, are completely different in the proximity. The proximity concerns distances to the transmitter of less than the wavelength divided by 2π . Nikola Tesla has broadcasted in the range of long waves around 100 kHz, in which case the wavelength already is several meters. For the experiments concerning the resonance of the earth he has operated his transmitter in Colorado Springs at frequencies down to 6 Hz. Doing so the whole earth moves into the proximity of his transmitter. We probably have to proceed from the assumption that the Tesla radiation primarily concerns the proximity, which also is called the radiant range of the transmitting antenna.

The near field already is used in practice in anti-theft devices, as they are installed in the entrance area of stores. The customer walks through the scalar wave transmitters. If the coupling coil has not been removed at the cash point, then a signal from the alarm system sounds. The coils work purely passive; that is, they are supplied with electric energy per scalar wave and stimulated to oscillate for their part. Then the effect back on the transmitter is being utilized. Even if the principle is functioning, people still should be warned not to use a technology, which has not been understood completely. Then not-explained catastrophes are inevitable.

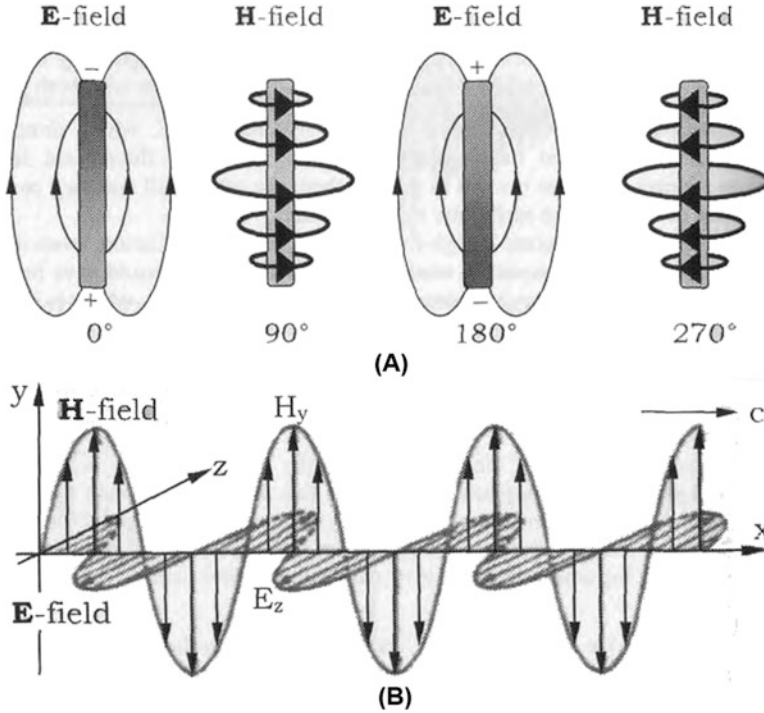


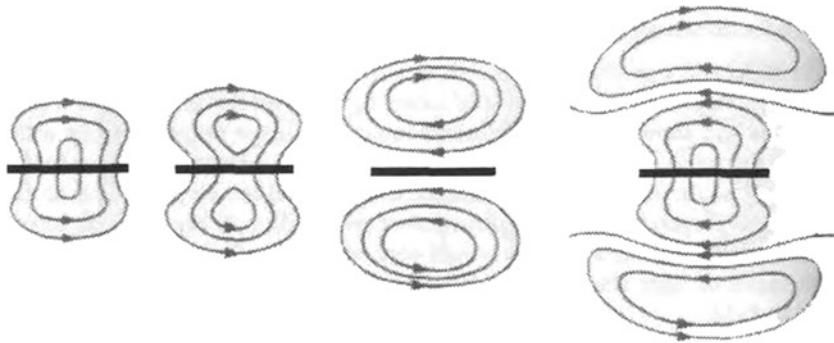
Fig. 2.26 The antenna current of oscillating dipole charges. (a) The fields of the oscillating dipole antenna. (b) The planar electromagnetic wave in the proximity

2.9.1.2 Far-Field Transition

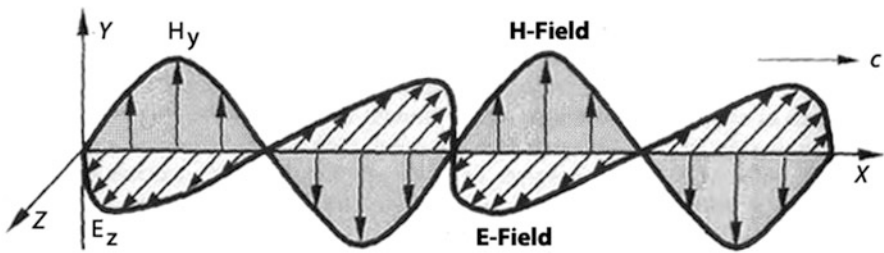
We talked about transition in near field above and now we discuss the transition in far field as well. In sufficient distance to the transmitting antenna as far field the transverse electromagnetic wave results (see Fig. 2.27b). It is distinguished by nonoccurrence of a phase shift between \vec{E} - and \vec{H} -field anymore. Every change of the electric alternating field is followed immediately and at the same time by a change of the magnetic alternating field and vice versa [13].

In the proximity however, the phase shift amounts to 90°. Somewhere and somehow between the causing antenna current and the far field a conversion from a longitudinal into a transverse wave occurs. How should one imagine the transition?

The coming off of a wave from a dipole is represented according to Fig. 2.27a. The fields come off the antenna, the explanation reads. If we consider the structure of the fields coming off then we see field vortices, which run around a point, which we can call the vortex center. Such field structures naturally are capable of forming standing waves and carrying an impulse. We will understand the scalar wave field in general and the near field in special only with suitable vortex physics and with a field



(A) The Coming off, of the Electric Field Lines from a Dipole



(B) The Planar Electric Wave in the Far Zone

Fig. 2.27 (a) The forming vortex structures found a longitudinal electric wave carrying impulse and (b) electromagnetic wave (transverse)

theory extended for corresponding vortices we also will be able to calculate it. Postulates cannot replace field physics! [13].

Be that as it may, the vortex, after having left the antenna, for bigger getting distance at some time seems to unroll to propagate further as an electromagnetic wave. There takes place a transition from longitudinal to transverse, or spoken figuratively from vortex to wave. How complete this conversion takes place, how big the respective wave parts are afterwards, on the one hand depends on the structure and the dimensions of the antenna. Information is given by the measurable degree of effectiveness of the antenna.

The vortex structures on the other hand are the stable, the smaller and faster they are. If they are as fast as the light or even faster, then they become stable elementary particles, for instance neutrinos. Slower vortex structures however are predominantly instable. They preferably unwind to waves. Vortex and wave prove to be two possible and under certain conditions even stable field configurations.

Let us emphasize: A Hertzian dipole doesn't emit Hertzian waves! An antenna as near field without exception emits vortices, which only at the transition to the far field unwind to electromagnetic waves. A Hertzian wave just as little can be received with a dipole antenna! At the receiver the conditions are reversed. Here the wave is

rolling up to a vortex, which usually is called and conceived as a standing wave. Only this field vortex causes an antenna current in the rod, which the receiver afterwards amplifies and utilizes.

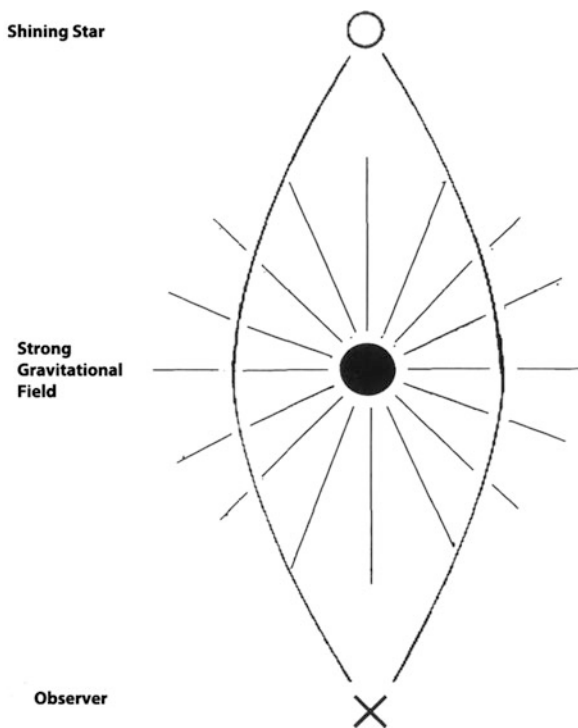
The mostly unknown or not-understood near-field properties prove to be the key to the understanding of the wave equation and of the method of functioning of transmitting and receiving antenna. The question asked is how one should imagine the rolling up of waves to vortices and vice versa the unrolling. How could a useful vortex mode look like?

2.9.1.3 Scalar Wave Model

The light, as electromagnetic wave, in the presence of a heavy mass or of strong fields is bent towards the field source (see Fig. 2.28).

The wave normally propagating in a straight line thus can be diverted. The square of the speed of light further is inversely proportional to the permeability and dielectricity, or in short in the presence of matter it is more or less strongly slowed down. If this slowing down of the wave occurs one-sidedly, then a bending of the path can be expected as well. At the end of the antenna a reflection and a going back of the wave can occur, which at the other end again hits itself. Now the wave has

Fig. 2.28 Diversion of the light by a strong gravitation field



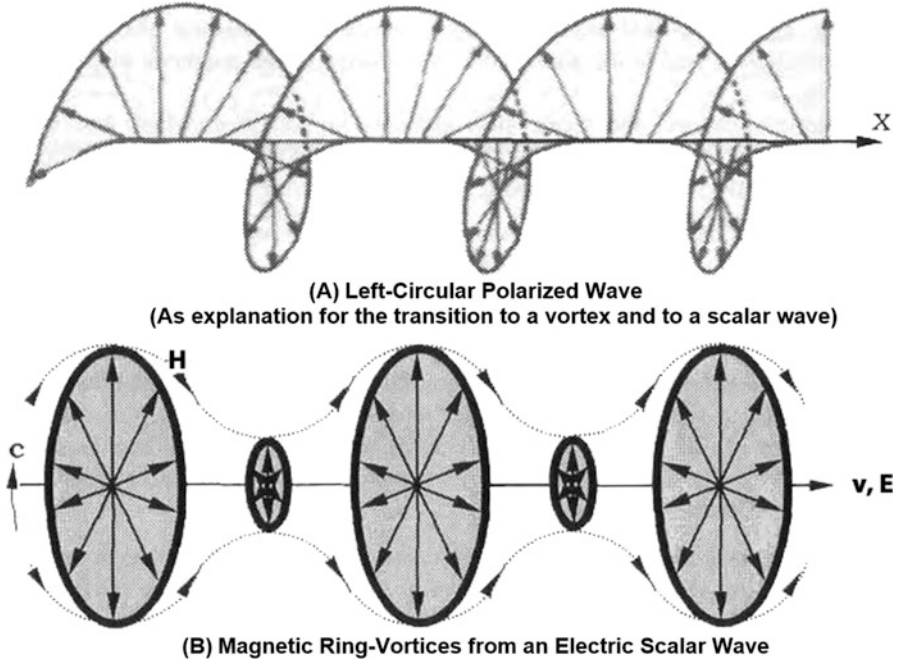


Fig. 2.29 (a) Circular polarized wave (transverse) and (b) electric wave (longitudinal)

found a closed-loop structure, which can be called vortex. Figures 2.29b and 2.30a show the two possible structures.

In most technical textbooks the vortex with the properties of a “standing wave” is described, such as near field and standing wave that are two examples that can be seen; however their description mathematically does not go through much of the details of scalar wave properties, without having a good attention towards vortex physics description and to have a better understanding of a pure scalar wave transmission according to Nikola Tesla and properties of this wave type. With vortex concept of an extended field physics a new horizon can be opened.

Note the following details in respect to Fig. 2.29:

Vortex and Wave = Two Stable Field Configuration

Electromagnetic Wave = Transverse Wave Propagation in a Straight Line

---Ring Like Vortex = Transverse Wave Running in Circles

---Vortex Velocity = Speed of Light c

Change of Structure = If the Field is Disturbed without Expense of Energy

If we pay further attention to Figs. 2.29b and 2.30a, they reveal that, in both cases, electromagnetic waves are represented, where it propagates with the speed of light, with the exception that the wave does not go forward in a straight line, but instead runs around in circles.

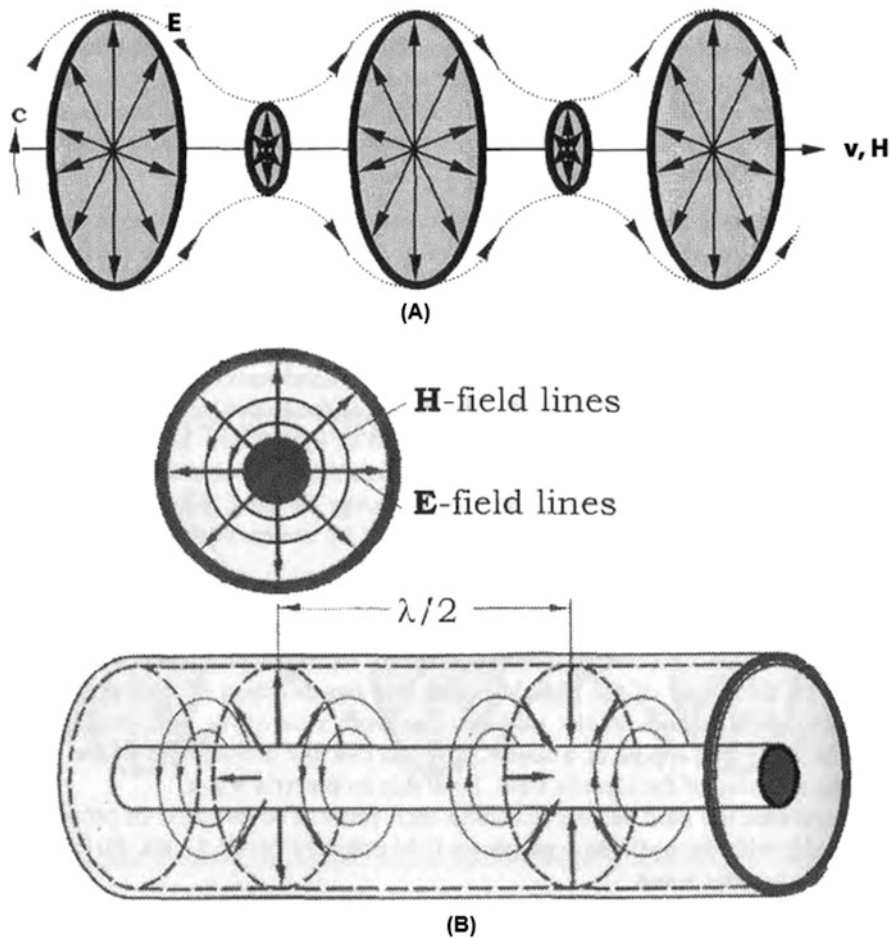


Fig. 2.30 (a) Magnetic wave (longitudinal) and (b) wave propagation in a coaxial cable

Furthermore, the wave is transverse, simply because the field pointers of the \vec{E} -field and the \vec{H} -field are oscillating perpendicular to speed of light c direction, so by virtue of the orbit the speed of light c now does become the vortex velocity, as well as the wave and the vortex turn out to be two possible and stable field configurations.

For the transition from one to the other no energy is used; it is only a question of structure. The vortex structure thus stabilizes itself by means of the field dependency of the speed of light.

Under the circumstance that the vortex direction of the ringlike vortex is determined, and the field pointers further are standing perpendicular to it, as well as perpendicular to each other, there result two theoretical formation forms for the

scalar wave. In the first case (Fig. 2.29b), the vector of the H-field points to the direction of the vortex center and that of the E-field axially to the outside. The vortex however will propagate in this direction in space and appear as a scalar wave, so that the propagation of the wave takes place in the direction of the electric field. We call this an electric wave.

In the second case the field vectors exchange their place. The direction of propagation this time coincides with the oscillating magnetic field pointer (Fig. 2.30a), for which reason we speak of a magnetic wave.

The vortex picture of the rolled-up wave already fits very well, because the propagation of a wave direction of its field pointer characterizes a longitudinal wave, because all measurement results are perfectly covered by the vortex model. It even is clear that no energy has to be utilized for the conversion, since merely the structure has changed. If it becomes a vortex the wave just doesn't run in a straight line anymore but in circles, to wrap around either the magnetic field vector (Fig. 2.29b) or the electric field vector (Fig. 2.30a).

2.9.1.4 Double-Frequent Oscillation of Size

Due to the fact that a longitudinal wave propagates in the direction of the field, the field pointer also will oscillate with the velocity of propagation v . This hence isn't constant at all; it can significantly differ from that of the light and can take arbitrary values. According to the theory of objectivity the field oscillating with it determines its momentary size of

$$E, H \sim \frac{1}{v} \quad (2.130)$$

The velocity of propagation v of the scalar wave thus oscillates double-frequently and with opposite phase to the corresponding field. A detailed description would mean that if the field strives for its maximum value, the velocity v of the wave reaches its smallest value.

In the field minimum the scalar wave vice versa accelerates to its maximum value. For longitudinal waves therefore only an averaged velocity of propagation is given and measured, as this for instance is usual for the sound wave, and this can vary very strong as is well known (body sound compared to air sound, etc.).

The two dual-field vectors of \vec{E} and \vec{H} , the one in the direction of propagation and the one standing perpendicular to it, occur jointly. Both oscillate with the same frequency and both form the ringlike vortex in the respective direction. As a result, the ringlike vortex also oscillates in its diameter double-frequently and with opposite phase to the corresponding field (Figs. 2.29b and 2.30a).

This circumstance owes the ringlike vortex its property to tunnel. No Faraday cage is able to stop it, as could be demonstrated in experiments. Therefore the ground wave runs only through the earth and not along the curvature of the earth. A further

example is the coaxial cable (Fig. 2.30b). Also, this acts as a long tunnel and so it isn't further astonishing that the electric field lines have the same orientation, as for a magnetic scalar wave. As a practical consequence in this place it should be warned of open cable ends, wave guides, or horn radiators with regard to uncontrolled emitted scalar waves!

At present time, we see a lot of discussion about if the cable network runs there is possibility of distribution and impact of it on for example airline radio traffic.

The original opening for cable frequencies actually are reserved for the airline radio traffic, based on the erroneous assumption that conflicts are unthinkable. But then the planes were disturbed in their communication. As the cause TV cables made out, which hadn't been closed according to the rules with a resistor, as it by, all means can occur on building sites and during renovation works.

On the other hand, it is being argued with the small current, which flows through the coaxial cable, and the large distance to the planes also is cited. According to that it actually cannot concern Hertzian waves. It presumably is scalar waves, which escape from the open cable ends and which are collected by a receiver in the plane. It indeed is very little field energy, but because it again is being collected and bundled, the scalar wave is able to exceed the part of the radio wave by far just at large distances and to cause problems.

For such examples from practice the scalar wave theory is fully taking effect.

2.9.1.5 Electric and Magnetic Scalar Wave

Per our discussion so far, on the wave propagation, there are three possible and stable states as illustrated in Fig. 2.31 and they are listed as follows:

1. The transverse electromagnetic wave according to Heinrich Hertz (Fig. 2.31a)
2. The longitudinal electric wave according to Nikola Tesla (Fig. 2.31b)
3. A longitudinal magnetic wave (Fig. 2.31c), which is not connected yet with a name of a discoverer

The last one is a pure product of my theoretical derivation. The question asked is which practical meaning the magnetic wave could have.

It is formed by individual electric field vortices, which were discovered by Meyl [13] and called potential vortices in 1990. He did proceed from the assumption that the youngest of the three waves will play the by far biggest role in the future, because its properties are unattainable, both with regard to the energy technical and the information technical use.

One example for each should support this good research at the level of a doctorate thesis.

The experiments concerning the electric wave according to Nikola Tesla, wherein he worked with electrically charged spheres, don't show a particularly high power. Magnetic converters, per the experiences of my laboratory activities, are superior to an electrostatic converter as a collector for free energy by far. That even can be

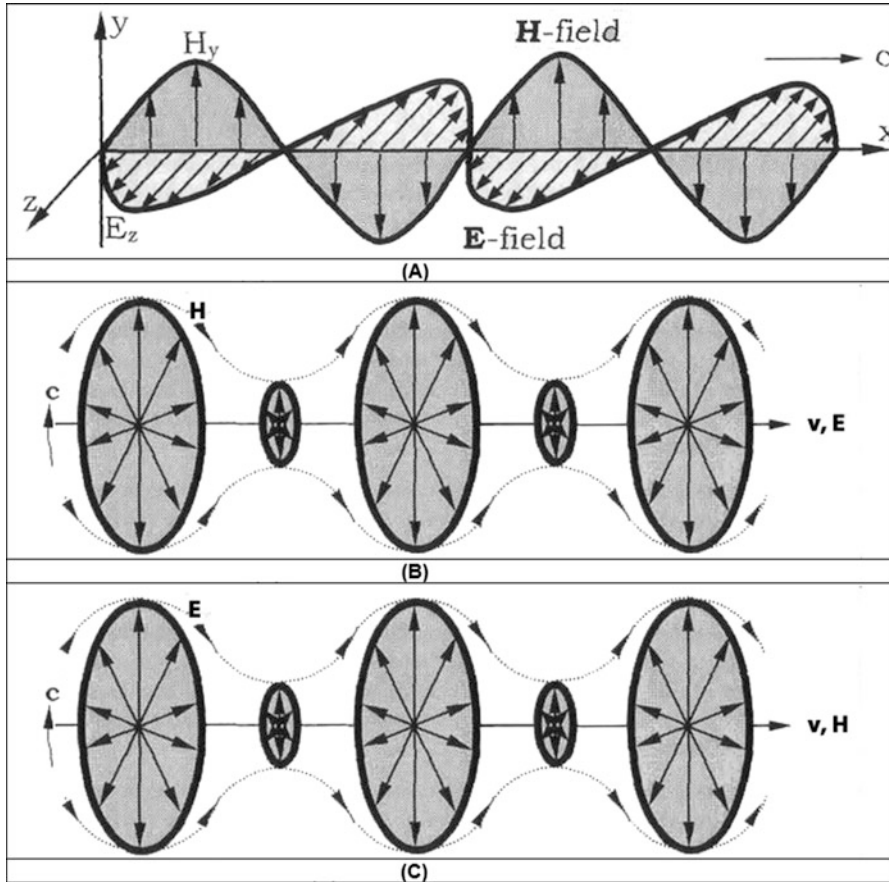


Fig. 2.31 The three basic types of wave according to the wave equations (electric, magnetic, and electromagnetic waves).
 (a) H. Hertz: electromagnetic wave (transverse). (b) Nikola Tesla: electric wave (longitudinal). (c) Magnetic wave (longitudinal)

expected, because a magnetic engine is much smaller than an electrostatic engine of the same power as is well known.

At a congress of medicines was given a talk on the basic regulation of the cells, on the communication of the cells with each other. Professor Heine in his decades of research work has found out that the cells for the purpose of communication build up channels for instance in the connective tissue, which after having conducted the information again collapse. Interestingly the channels have a hyperboloid structure, for which no conclusive explanation exists.

The structure of the data channels however is identical with the one of a magnetic scalar wave, as shown in Fig. 2.31c. Through a channel formed such, which functions like a tunnel or a dissimilarly formed waveguide, only one very particular scalar wave can run through.

Waves with different frequencies or wavelengths don't fit through the hyperboloid formed tunnel at all in the first place. Through that the information transmission obtains an extremely high degree of safety for interference.

To the biologist here a completely new view at the function of a cell and the basic regulation of the whole organism is opening. The information tunnel temporarily forms more or less a vacuum, through which only potential vortices can be conducted, and that without any losses—simply perfect! From this example it is becoming clear that nature is working with scalar waves, namely with magnetic waves.

One other point should be recorded: The mentioned tunnel experiments, in which speed faster than light is being measured with most different devices, impressively confirm the presence of scalar waves. But if scalar waves exist which are faster than light and other ones, which are slower, then it is almost obvious that such ones will also exist, which propagate exactly with the speed of light. These then will have all the properties of the light and won't differ from the corresponding electromagnetic wave in the observable result. As scalar wave it however is formed by vortex configurations, which unambiguously have particle nature. Nothing would be more obvious than to equate these quantum structures with the photons.

2.9.1.6 Scalar Wave Properties

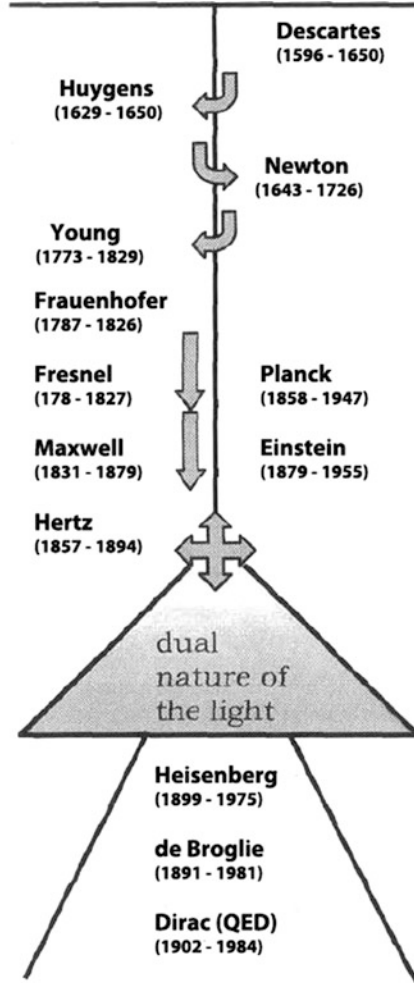
Famous physicists and scientists of high caliber had come together, and they were concerned about the question if the light quanta hypothesis is a wave or particle or even has both properties simultaneously?

For both variants experimental proof was present, the discussion became inflamed, and the things boiled over. Finally, they were as smart as before, as Werner Heisenberg presented his ideas concerning the uncertainty principle. This compromise, on which one eventually came to an agreement, with good cause may be called the worst in the history of physics. It dictates me what I shall see and how exact we may look. With it the contradiction should be overcome that the light contrary to every causality should be wave and particle at the same time. See Fig. 2.32.

Such fixings have not only a funny but also a tragic side. Since it was authorities, which have approved the compromise and the whole community of science has confidence in the statements of its authorities, which immediately and unfiltered is entered in all textbooks.

At the meeting it simply and solely concerned the wave equation and only that could have supplied the correct and only possible answer: It falls apart into two parts and this explains why the light one time appears as an electromagnetic wave and the next time as a vortex particle, which is called photon. The conversion can take place at any time spontaneously and without putting on energy, so that depending on the used measuring technique the particle appears as wave or as particle, but of course never as both at the same time!

**Seen Strictly Casual
i.e. Physically in the
Period between
1600 and 1900**



**Turning away from
classical physics:
(removing of the
principle of
cause and effect)**

Fig. 2.32 The view of some physicists concerning the nature of the light as wave or as particle

Looking back, one can say that the funny thing about the situation was that all discussed about the wave and its properties known at that time, and that all should know the wave equation. An equation as is well known says more than a thousand words and one look would have sufficed entirely to answer the controversial question once and for all. It would have saved us a lot.

Concerning the measure of light, the uncertainty principle with the interpretation of Heisenberg, i.e., the light is wave and particle at the same time, is incompatible with the wave equation. Heisenberg puts an equal sign, wherein the wave equation in reality is present in addition to both wave parts. Fortunately, in mathematics there is no need of speculating that a derivation is right or wrong. Nothing is changed to that even if all physicists of the world should go in the wrong direction following the

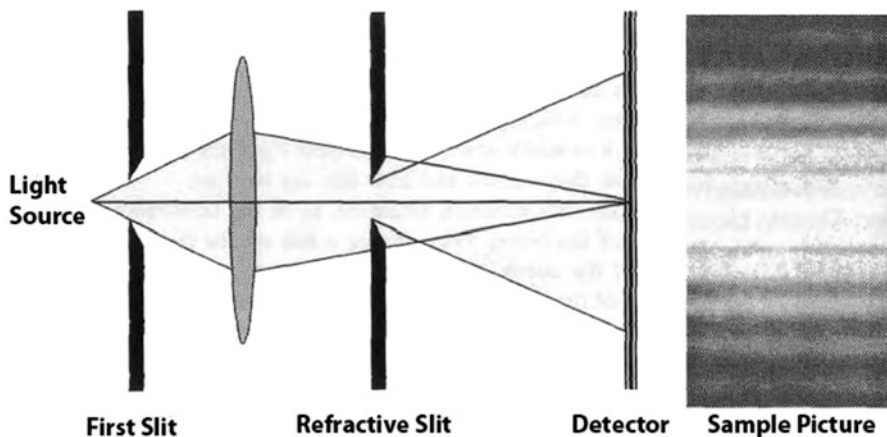


Fig. 2.33 Depiction of light form interference at the slit

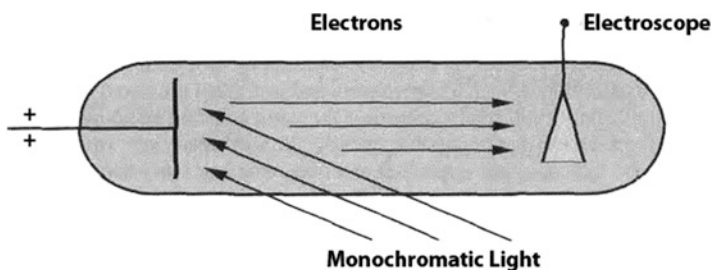


Fig. 2.34 The photoelectric effect

prevailing opinion. The wave equation exerts an influence on the interpretation of the light experiments, on the one hand the ones concerning the interference and refraction of the light, where electromagnetic waves are becoming visible (Fig. 2.33), and on the other hand the photoelectric effect, as proof of light quanta (Fig. 2.34).

Already the wave theory of Huygens requires interference patterns of light rays, as they for instance are observed behind a slit, and demonstrate with that the wave nature. If on that occasion the particle nature is lost, if thus the photons present before the slit cannot be detected behind the slit anymore, then plain and simple the measuring method, thus the slit is to blame for that. The vortices have unrolled themselves at the slit to waves.

Corresponding experiments have also been carried out with matter. At the Massachusetts Institute of Technology whole sodium atoms were converted into waves. At the detector pure interference patterns were observed, which go as evidence for the successful dematerialization. But the vortex physicists show still more: they reveal that atoms merely are waves rolled up to spherical vortices, which at any time and spontaneously can again unroll to waves at a lattice.

In Fig. 2.33 light strips are formed, where the waves oscillate in phases, dark stripes, where they oscillate out of phase.

The common interpretation, i.e., the wave nature is detectable behind a slit, must have been present in the same form already before the slit is untenable and in the end wrong, as it is clear from the experiment with the sodium atoms.

The photoelectric effect, which on the other hand shows the quantum nature of the light, has been discovered by Heinrich Hertz, further investigated by Lenard, and finally rendered more precisely by Robert Millikan in 1916 (Fig. 2.34b). It bases on the circumstance that light of higher frequency, thus blue light, has more energy than red light of lower frequency. But if electrons are knocked out a metal plate by light then occurs by the waves rolling up to vortices. Now indeed photons are at work, which are detected with an electroscope indirectly.

In the same way a photon ray in a bubble chamber can be photographed. But also, here the measuring method is responsible for what is being observed.

A good example is the human eye, the rods and cones of which merely can pick up potential vortices and pass them on to the nerves as so-called reaction potentials. Incident waves can only be detected, if they first have rolled up to vortices in the corpus vitreum of the eye, which is a transparent jellylike substance filling the interior of the eyeball behind the lens; it is composed of a delicate network (vitreous stroma) enclosing in its meshes a watery fluid (vitreous humor). Synonym. For us seeing, it does not play a role of how many percent vortices and waves the light is consisting.

Behind a sheet of glass for instance a larger vortex part can be expected and still the light has the same brightness as without sheet; the sheet of glass is perceived as transparent. We nevertheless must assume that light with a large wave part has another quality, then such light behind glass or artificial light with a large part of photons.

2.9.1.7 Comparison of the Parts of Tesla and Hertz

Rule that is established for light from quantum physics perspective is that it always is formed as photon, even at the surface of the sun. If at the end the sun radiation waves arrive on the earth, then the vortices sometime on the way to us from such wave radiation must have unrolled to waves.

Photon radiation after all is a scalar wave radiation, which generally is predominant in the near field of the source of radiation. There is no reason why the light should act in another way than the wave radiated by a radio transmitter, which as well forms vortices in the near-field area, as we already have discussed. For different interpretations of wave properties of one and the same physical phenomenon there is no place in a unified theory.

If we want to take under consideration the comparison of the parts of Tesla and Hertz as indicated in Table 2.1, then it is not an individual case that an experimental setup is responsible for what is being measured and observed. A parallel case to the experiments concerning the nature of the light is the one that is concerning the wave

Table 2.1 The two parts of wave equation

$\nabla^2 \vec{E} = \nabla(\nabla \cdot \vec{E}) - \nabla \times \nabla \times \vec{E} = \frac{1}{c^2} \left(\frac{\partial^2 \vec{E}}{\partial t^2} \right) \text{ Equation (2.125)}$	
<p>Nikola Tesla • Scalar Wave = (Electric or Magnetic) Longitudinal Wave</p>	<p>Heinrich Hertz • Electromagnetic Wave = Transverse Wave</p>
<p>Form (each time for velocity of propagation v):</p> <ul style="list-style-type: none"> • ($v > c$): Neutrino radiation, morphogenetic fields, . . . • ($v = c$): Photons • ($v < c$): Plasma wave, thermal vortices, biophotons, earth radiation, . . . • ($v = 0$): Noise 	<p>Form (each time for frequency):</p> <ul style="list-style-type: none"> • Cosmic radiation • X-rays • Light • UV radiation • Microwave • Radio waves • VLF, ULF, . . .

propagation. Hertz has received and utilized the transverse part and Tesla the longitudinal part and either one claimed that only he is right. There does not exist another equation, which has been and is being ignored and misunderstood so thoroughly as the wave equation.

Table 2.1 shows in a survey the two parts of the wave equation in the assignment to the terms and forms, where the right-hand side is the electromagnetic wave descriptions according to Heinrich Hertz and left-hand side is the scalar wave described by Nikola Tesla. The terms on the one hand are transverse wave and on the other hand longitudinal wave relating to the kind of wave propagation.

If the field pointers oscillate crossways to the direction of propagation, then as a consequence the velocity of propagation is decoupled from the oscillating fields. The result in all cases is the speed of light, and from what we know is constant value.

It is usual to make a list for increasing frequency, starting from the longest waves (extremely low frequency (ELF) and very low frequency (VLF)) over the radio waves (long frequency (LW), medium wave (MW), short wave (SW), ultrahigh frequency (UHF)), the TV channels (VHF, UHF), the microwaves, the infrared radiation, the light, and the X-rays up to the cosmic radiation.

It really is interesting that it concerns one and the same phenomenon despite the different forms! As long as Maxwell only had published a theory for the light, in the world of science of 24 years long at first nothing at all happened. Only Heinrich Hertz with his short-wave experiments opened the eyes. Now all suddenly started at the same time to research into various phenomena on the frequency scale, from Madame Curie over Conrad Roentgen up to Nikola Tesla, who primarily researched the area of long waves.

With regard to the scalar wave so far there are not many corresponding and collective documentations or textbooks one can identify, except reference such as Meyl [13] or few papers here and there that are published by different scientists and physicists, so far. The immense area is new ground scientifically, which is awaiting to be explored systematically. Thus, what we need to try is to make a contribution by

rebuilding a scalar wave transmission line according to the plans that were proposed by Tesla.

2.9.1.8 Noise, a Scalar Wave Phenomenon

Longitudinal waves can take arbitrary velocities between zero and infinity, because they propagate in the direction of an oscillating field pointer and as a consequence of that their velocity of propagation oscillates as well and by no means is constant. It does make sense to list the forms of scalar waves according to their respective velocity of propagation (see Table 2.1, left column).

If we start with a localized vortex, a wave rolls up, which further contracts. Doing so the wavelength gets smaller and smaller, whereas the frequency increases. An even frequency mixture distributed over a broad frequency band is observed. This phenomenon is called noise (see Fig. 2.35). But besides the localized noise, noise vortices can also be on the way with a certain velocity as a scalar wave, e.g., for the radio noise. In this case they show the typical properties of a standing wave with nodes and antinodes.

Also, the earth radiation is said to have standing wave nature, which can be interpreted as slowed-down neutrino radiation. If it is slowed down on the way through the earth, then the neutrino properties are changing, as this was measured in the Kamiokande detector in Japan recently. Unfortunately, the proof occurs only indirectly, because there still don't exist measuring devices for scalar waves. We'll talk about this problem area later and are content with the clue that already within living memory the standing wave property has been used to find water and deposits of ores and still is used today (see Fig. 2.36).

If we continue our considerations concerning the forms of scalar waves, as they are listed in Table 2.1, the scalar waves, which are slower on the way than the light, are joined by the plasma waves. This is confirmed by measurements and calculations.

For thermal vortices, as they have been investigated by Max Planck and for biophotons, as they can be detected in living cells by colleague Popp, the velocity of propagation, however, is unknown. It was not and still has not being measured at all, now more than ever. The research scientists have confidence in the assumption that all waves go with the speed of light, but that is a big mistake.

For all wave kinds there at least exists also one vortex variant; for radio waves for instance it is the radio noise, which propagates with a velocity different from c . The velocity is the product of frequency and wavelength:

$$v = f \cdot \lambda \quad (2.131)$$

From the three variables v , f , and λ at least two must be measured, if one has a suspicion that it could concern scalar waves. At this place most errors are made in the laboratories. Countless experiments concerning the biological compatibility, medical therapy methods, and similar experiments must be repeated, because as a rule

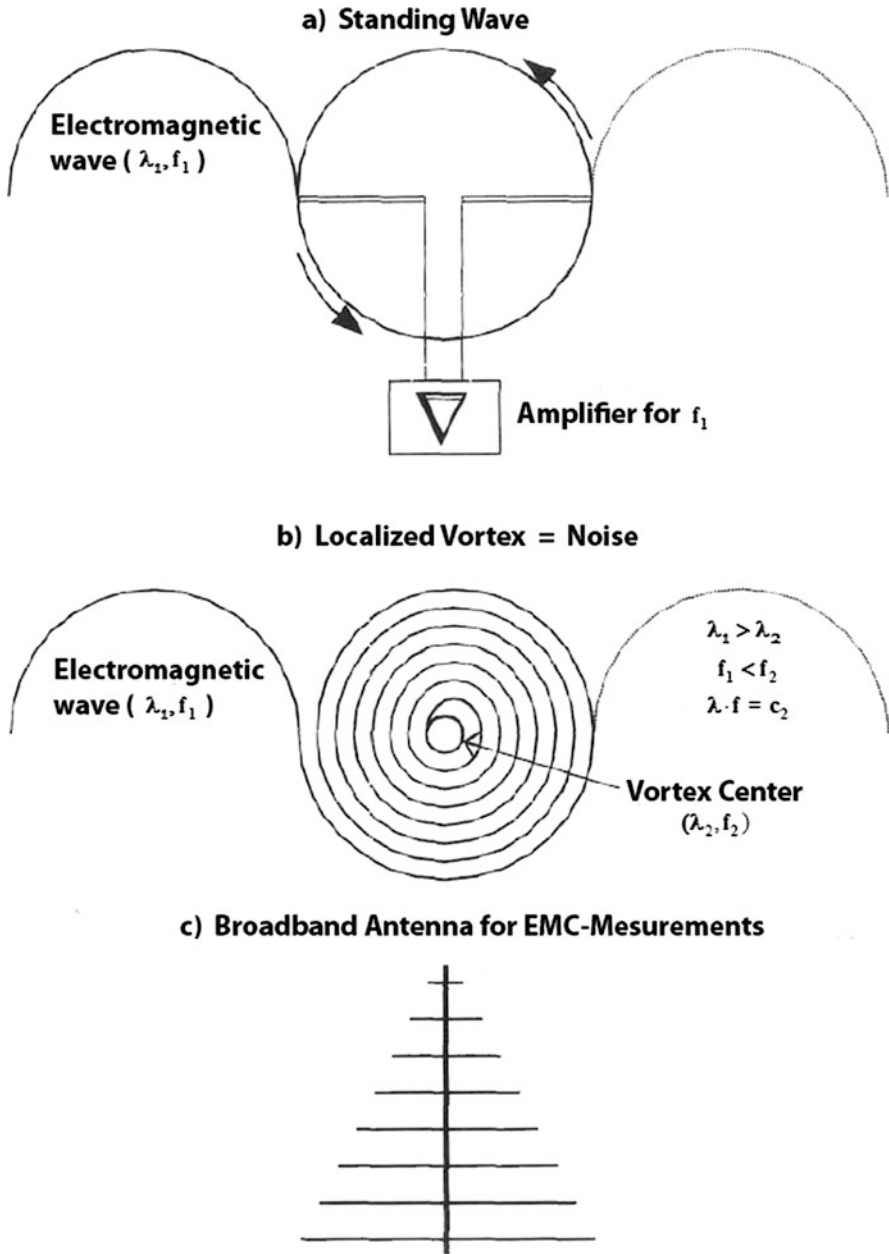


Fig. 2.35 Measurement of localized waves and vortices

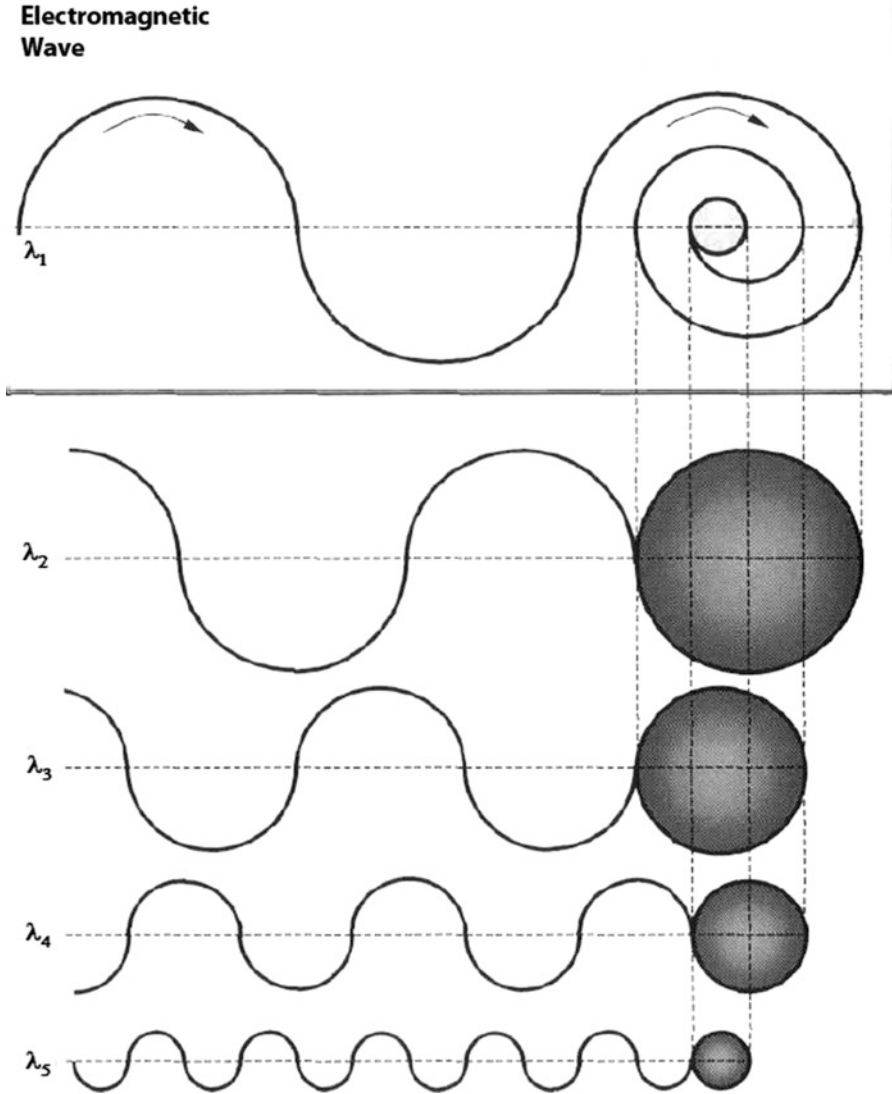


Fig. 2.36 The wave rolling up to a vortex

only the frequency is being measured and it has been omitted to at least check the wavelength or the velocity of the wave. Countless research scientists must put up with this accusation.

Much too blind the scientists, who now again may start from the very beginning with their work, have had confidence in the predominance of the speed of light.

2.9.1.9 Neutrino Radiation

From historical point of view, Tesla was the first person to discover the neutrino radiation and in the New York Times February 6, 1932, Page 16 Column 8 issue, he writes that he has discovered and investigated the phenomenon of the cosmic radiation, long before others started their research.

He claims and says that “According to my theory a radioactive body is only a target, which constantly is being bombarded by infinitely small balls (neutrinos), which are projected from all parts of the universe. If this, at present unknown, cosmic radiation could be interrupted completely, then no radioactivity would exist any longer. I made some progress regarding the solution of the mystery, until I in the year 1898 attained mathematical and experimental evidence, that the sun and similar celestial bodies emit energy-rich radiation, which consist of inconceivable small particles and have velocities, which are considerable *faster than the speed of light*. The ability of penetration of this radiation is so large, that it penetrates thousands of kilometers of solid matter, without their velocity being reduced noticeably.”

It must be admired how Tesla guided by experimental observations and a reliable instinct comes to the correct result. He, merely with the conclusion that because of the missing interaction the neutrinos have to be inconceivably small, is not quite right. Their size rather depends on the velocity, because the overfast neutrinos are being length contracted stronger. Tesla however hit the nail exactly on the head, when he on the occasion of the press conference for his 81st birthday declared that the radioactivity is a clear proof of the existing of an outer radiation of cosmic origin. “If Radium could be shielded against this radiation in an effective way, “Tesla wrote in an essay of 1934, “then it would not be radioactive anymore.” At this occasion he contradicted Albert Einstein, without thereby pronouncing the name, and was indignant at the wrong working method of the scientists.

However, as part of neutrino radiation, the neutrino scientists make the error of proceeding from the assumption that their particles are on the way with a speed somewhat less than the speed of light c .

This contradicts the observation according to which black holes should represent strong sources of neutrinos, which are black only for the reason that no particle radiation is able to escape them, which is on the way with c or even slower. If a black hole does hurl neutrino radiation into space, then that must be considerably faster than c , as normal neutrino scientists still by no means can imagine it today [13].

But the neutrino radiation can be detected only after it has been slowed down to a value, which is smaller than c . If the slowing down occurs slightly asymmetrical, then therefore a mean of the mass different from zero appears. The “measurement” of such a rest mass, as it at present is propagated and celebrated, is a classical measurement error! As long as a neutrino on the way to us still is faster than the light, the mean of its mass is generally zero. The effective value of the mass of a neutrino is however considerable. Only it is able to give account for the sought-for dark matter, as far as it must exist in the today supposed form anyway (see Fig. 2.37) [13].

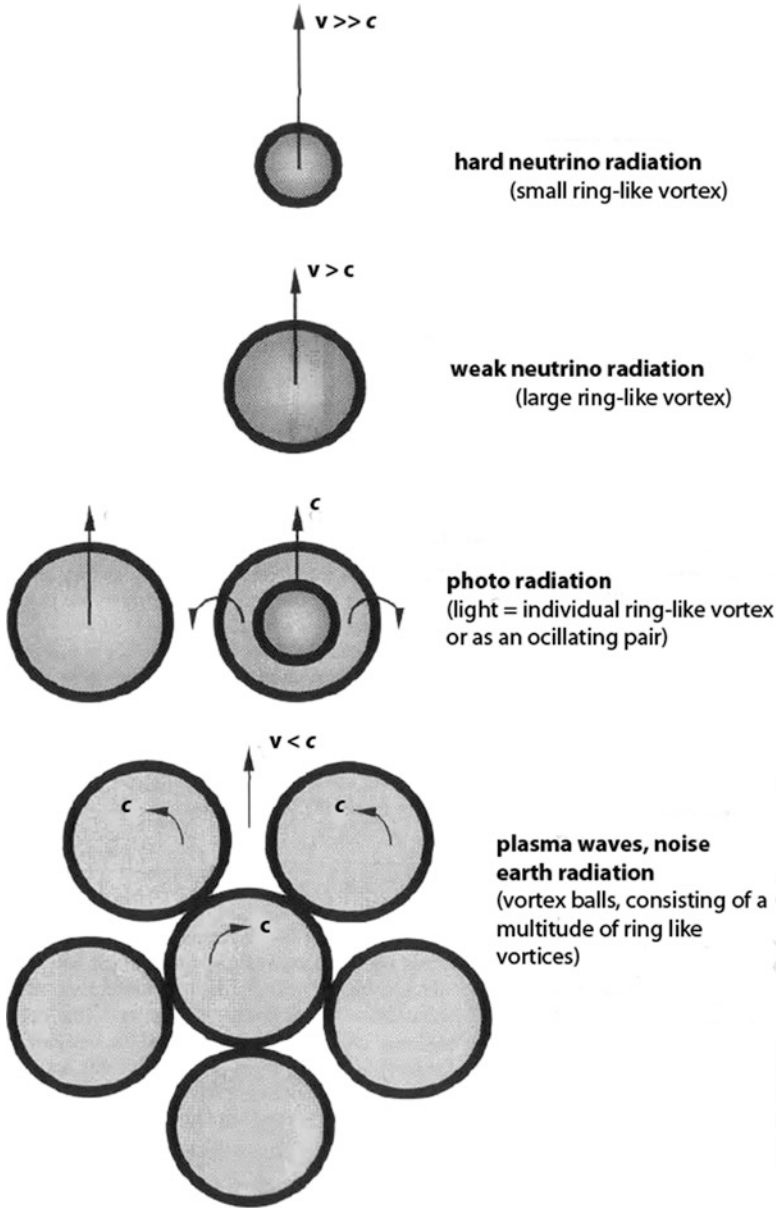


Fig. 2.37 The ringlike vortex model of scalar waves

The Tesla radiation, that the discoverer Nikola Tesla already in own experiments had found out, is faster than speed of light as it was described earlier at the beginning of this section. Since this Tesla radiation according to the description is identical with the neutrino radiation, it forms a subset.

We will call the neutrino radiation as a form of scalar waves, which are faster than the speed of light c . This stretches from the weak radiation at low frequencies up to the hard neutrino radiation of cosmic origin. But the hardness of the radiation not only does increase with the frequency, but it also in particular increases with the velocity.

The neutrino radiation first of all is carrying energy. On top of this basic wave radiation in addition information can be modulated. Doing so extremely complex modulation variants are offering. Of this kind we must imagine thoughts, as being complex modulated vortices, which can propagate as scalar wave in space. Rupert Sheldrake calls this vortex field a morphogenetic field. At this place merely is pointed at his very interesting research results.

Thoughts can be standing in space, in the form of localized noise, but they can also move with speeds faster than light. According to that a communication with intelligent beings from other star systems by all means would not be a Utopia anymore.

Every fast neutrino forms an individual ringlike vortex (see Fig. 2.38).

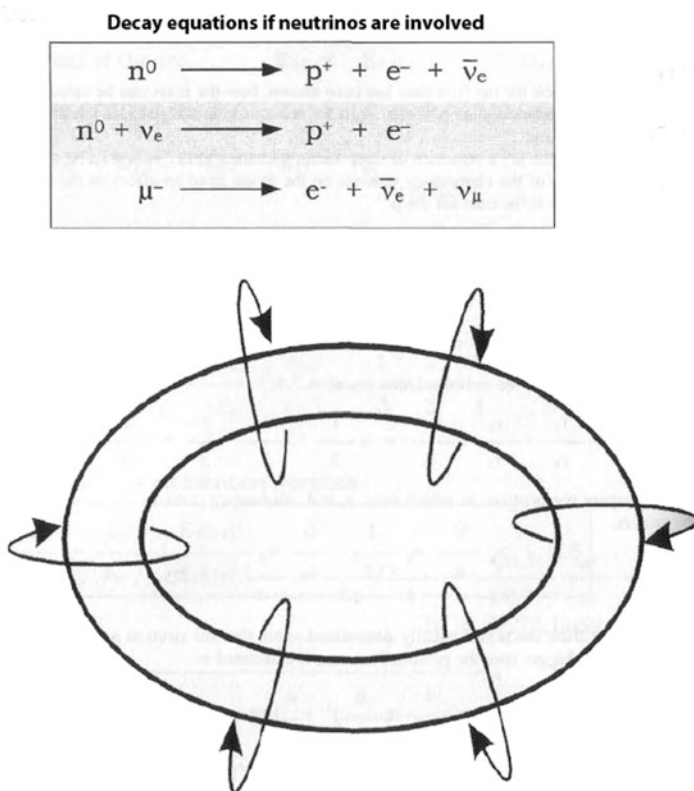


Fig. 2.38 The electron-neutrino as a ringlike vortex

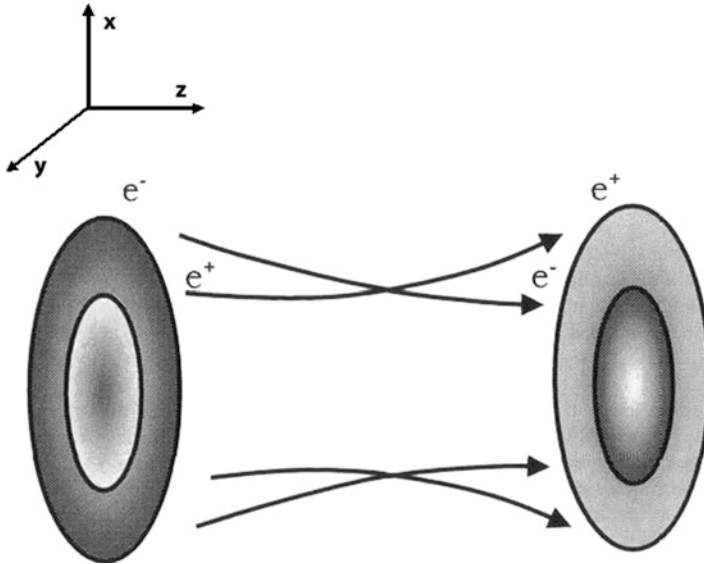


Fig. 2.39 The photon as oscillating electron-positron pair

The slower the scalar wave is, the more dependent the vortices become. The photon already can consist of two ringlike vortices (Fig. 2.39), whereas plasma waves and other slow scalar waves can form from a multitude of individual vortices, which are rotating around each other, to form vortex balls and vortex streets. From this circumstance already results very different scalar wave behavior in the different areas of the velocity of propagation.

This trend for small velocities can as well be observed towards lower frequencies. For a certain wavelength the frequency after all (according to Eq. (2.135)) is proportional to the velocity of propagation v .

Keep in your mind that the vortex principle is self-similar [21]. This means that the properties of an individual vortex also for the collection of numerous vortices again appear and can be observed in a similar manner. That's why a vortex ball behaves entirely similar as an individual isolated vortex.

The same concentration effect, that keeps the vortex together, shows its effect for the vortex ball and keeps it together as well.

Something corresponding holds for a basic property of potential vortices, being of a completely different nature. It is the property to bind matter in the vortex and carry it away with the vortex. Well known are the vortex rings that skillful cigarette smokers can blow in the air. Of course, also nonsmokers can produce these air eddies with their mouth, but these remain invisible. Solely by the property of the vortex ring to bind the smoke it becomes visible to the human eye.

If the potential vortex transports something out, then it should rather be a dielectric material, such as water preferably. Therefore, if in the environmental air we are surrounded by potential vortices that we can detect for instance as noise, then they

are capable with their “phenomenon of transport,” to pick up water and to keep it in the vortex. In this way the atmospheric humidity is explicable as the ability of the air particles to bind comparatively heavy water molecules. If the vortex falls apart then it inevitably releases the water particles and it rains. This is merely a charming alternative for the classical representation without claim to completeness [13].

2.9.1.10 Parallel Instead of Seral Image Transmission

We continue with our considerations concerning the special properties of scalar waves, represented in the left column, and compare these with the well-known behavior of electromagnetic waves in the right column (Table 2.1 is now followed by Fig. 2.40). If we again take up the possibilities for modulation and the

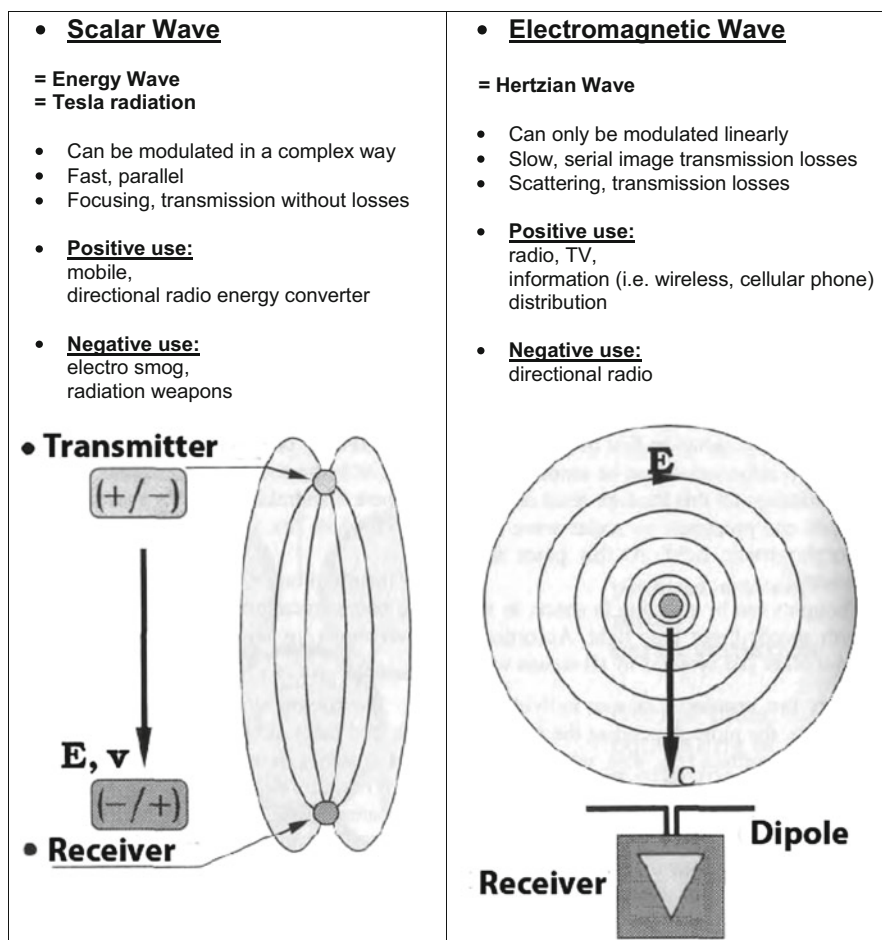


Fig. 2.40 Comparison of scalar wave and radio wave properties

transmission of information, then it becomes very clear from the comparison that we today work with a technology, which is the true master more or less, but which is everything else but optimum.

For the Hertzian wave the velocity of propagation is constant and meanwhile the frequency and therefore the wavelength are being modulated at the same time. However, that strongly limits the information transmission. An image for instance must be transmitted serially from one point after another as well line after line. The serial image transmission takes place very slowly, for which reason the velocity of the personal computers (PCs) permanently must be increased, so that the amount of data can be managed accordingly.

With the clock frequency on the other hand also the losses increase, so that in the end the CPU cooler limits the efficiency of modern PCs. Something our engineers obviously do wrong, as a comparison with the human brain clarifies. Our brain works without a fan. For it a clock frequency of 10 Hertz is sufficient. It needs neither megahertz nor gigahertz frequencies and despite that it is considerably more efficient.

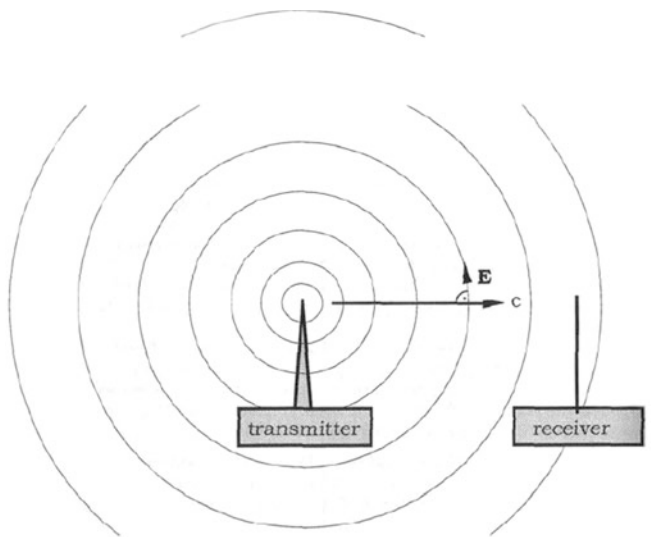
Nature only works with the best technology. The second best technology, as it is to put, to use in our machines in the evolution wouldn't have had the slightest chance of surviving. The strategies to optimize the nature are merciless in a free economy that goes completely different. There the "bunglers" are joining together with the companies dominating the market, buying up the innovative ideas without further ado, to let them disappear in the drawer, so that they can bungle further in the way they did until now. It after all have been the lousy products which have made them the companies they are today. The ego of power is incompatible with the interests of nature [13].

Nature works with scalar waves and their velocity of propagation is arbitrary. Wavelength and frequency now can be modulated, and information can be recorded separately. In this manner a whole dimension is gained to modulate, and the image transmission can take place in parallel, which means considerably faster, safer, and more reliable. As anyone of us knows by own experience, assembling the image takes place all at once, and the memory of past images takes place ad hoc. Nature is indescribable more efficient than technology with the scalar wave technique (see Fig. 2.41).

Take the right-hand side of Fig. 2.40, with the properties of the Hertzian wave. In the opinion of Nikola Tesla, it is a gigantic waste of energy. The broadcasting power is scattered in all directions and the transmission losses are enormous. At the receiver virtually, no power arrives anymore. To receive a radio signal the antenna power has to be amplified immensely. It is a wave which can be used only as radio wave, and thus as a wave with which arbitrarily many participants should be reached [13].

2.9.1.11 Research of Scalar Wave

Scalar waves are still an unexplored area, scientific new ground as it was. Individual research scientists already have selectively ventured forward in this area and have



Tesla radiation (radiations) = scalar wave, longitudinal wave propagation:

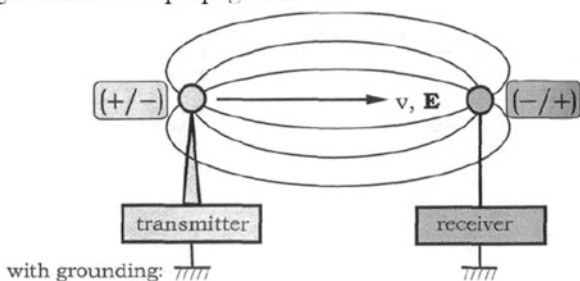


Fig. 2.41 Comparison of radio waves according to hertz and electric scalar waves according to Tesla

described properties of the scalar wave investigated by them in their special research area mostly in measurement technical manner. But as a rule of thumb, they lack the physical relation, as it is derived in this book for the first time. If we don't proceed from individual measurements, but from the wave equation and the mathematical physical derivation of scalar waves, then we have the great chance to understand as something belonging together on the one hand noise, photons, neutrinos, and lots of other known phenomena as well as on the other hand still unknown phenomena, which are called para-scientific.

We should remember that we without theory of Maxwell and the representation in a frequency band today still would not know that the radio waves (LW, MW, KW, UHF), the microwaves (μW), the infrared thermal radiation (IR), the light, and the

X-rays concern just the same phenomenon. The graphic representation of both waves in one diagram in this place is extremely helpful.

2.9.2 Wave Energy

In this section, we describe the fields or actually the space itself that contains energy and as the fields propagate through the space energy also propagates through the space. The space remains stationary, just like the water in the pan as we described the situation before, but the energy can travel through the space. This is the same as waves in any material where the material itself does not move with wave, but the energy is transmitted to a new location, very similar to situation if we tap the stationary water in the pan at the center of water surface and we see wave creation that travels in all direction through the interior of pan wall. The derivation below gives us the exact quantities involved in this process.

So, since the fields contain energy, this energy is transported when the waves propagate. It will be useful to derive an expression for this process.

First multiply Eq. (2.98) by $-\vec{B}$ to obtain

$$-\vec{B} \cdot \vec{\nabla} \times \vec{E} = \vec{B} \cdot \left(\frac{\partial \vec{B}}{\partial t} \right) \quad (2.132)$$

Then, multiply Eq. (2.132) by $1/\mu$ and bring the magnetic field into time derivative using a product rule; then we obtain the following result:

$$-\frac{1}{\mu} (\vec{B} \cdot \vec{\nabla} \times \vec{E}) = \frac{1}{2\mu} \left(\frac{\partial}{\partial t} B^2 \right) \quad (2.133)$$

Notice that the right-hand side of Eq. (2.133) is now representing the time derivative of the energy density of the magnetic field.

Now we multiply Eq. (2.100) by \vec{E} so we obtain the following result:

$$\vec{E} \cdot \vec{\nabla} \times \vec{B} + \vec{E} \cdot \vec{\nabla} \beta = \frac{1}{c^2} \vec{E} \cdot \frac{\partial \vec{E}}{\partial t} \quad (2.134)$$

Multiply Eq. (2.134) by $1/\mu$ and bring the electric field into the time derivative using a product rule; it yields the following:

$$\frac{1}{\mu} \vec{E} \cdot \vec{\nabla} \times \vec{B} + \frac{1}{\mu} \vec{E} \cdot \vec{\nabla} \beta = \frac{\epsilon}{2} \left(\frac{\partial}{\partial t} E^2 \right) \quad (2.135)$$

Equation (2.135) gives the time change in the electric field energy density as well.

We then multiply Eq. (2.97) by β , so we get

$$\beta(\vec{\nabla} \cdot \vec{E}) = \beta\left(\frac{\partial}{\partial t}\beta\right) \quad (2.136)$$

Now multiply Eq. (2.136) by $1/\mu$ to obtain the following form:

$$\frac{1}{\mu}\beta(\vec{\nabla} \cdot \vec{E}) = \frac{1}{2\mu}\left(\frac{\partial}{\partial t}\beta^2\right) \quad (2.137)$$

Now, we can add all the energy densities together to get the following conclusion:

$$\begin{aligned} & \frac{\partial}{\partial t}\left(\frac{\epsilon}{2}E^2 + \frac{1}{2\mu}B^2 + \frac{1}{2\mu}\beta^2\right) \\ &= \frac{1}{\mu}\left\{(\vec{E} \cdot \vec{\nabla} \times \vec{B} - \vec{B} \cdot \vec{\nabla} \times \vec{E}) + \vec{E} \cdot \vec{\nabla} \beta + \beta \vec{\nabla} \cdot \vec{E}\right\} \end{aligned} \quad (2.138)$$

Using the vector quantity $\vec{\nabla} \cdot (\varphi \vec{F}) = (\vec{\nabla} \varphi) \cdot \vec{F} + \varphi \vec{\nabla} \cdot \vec{F}$ from Table 1.1 on the third term on the left-hand side of Eq. (2.138) yields

$$\begin{aligned} & \frac{\partial}{\partial t}\left(\frac{\epsilon}{2}E^2 + \frac{1}{2\mu}B^2 + \frac{1}{2\mu}\beta^2\right) \\ &= \frac{1}{\mu}\left\{(\vec{E} \cdot \vec{\nabla} \times \vec{B} - \vec{B} \cdot \vec{\nabla} \times \vec{E}) + \vec{\nabla} \cdot (\beta \vec{E})\right\} \end{aligned} \quad (2.139)$$

Using the vector quantity $\vec{\nabla} \cdot (\vec{F} \times \vec{G}) = \vec{G} \cdot (\vec{\nabla} \times \vec{F}) - \vec{F} \cdot (\vec{\nabla} \times \vec{G})$ from Table 1.1 on the first term and second term on the left-hand side of Eq. (2.143) yields the following result:

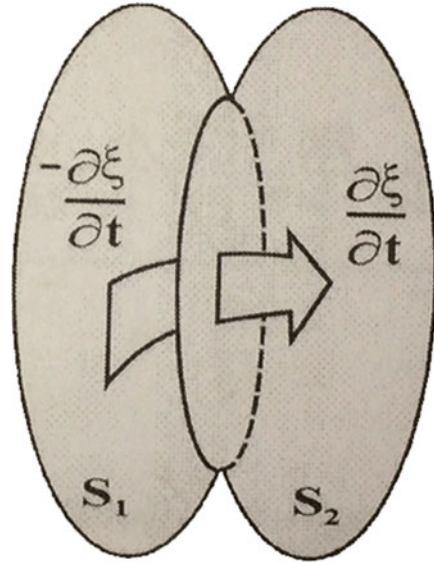
$$\frac{\partial}{\partial t}\left(\frac{\epsilon}{2}E^2 + \frac{1}{2\mu}B^2 + \frac{1}{2\mu}\beta^2\right) = \frac{1}{\mu}\vec{\nabla} \cdot (\vec{B} \times \vec{E} + \beta \vec{E}) \quad (2.140)$$

Then, integrating both sides over a volume, we have

$$\begin{aligned} & \frac{\partial}{\partial t}\left(\frac{\epsilon}{2}\int E^2 d\tau + \frac{1}{2\mu}\int B^2 d\tau + \frac{1}{2\mu}\int \beta^2 d\tau\right) \\ &= \frac{1}{\mu}\int \vec{\nabla} \cdot (\vec{B} \times \vec{E} + \beta \vec{E}) d\tau \end{aligned} \quad (2.141)$$

Finally, using the divergence theorem on the right-hand side and using Eqs. (2.101) through (2.103) result in

Fig. 2.42 Energy flow between two regions



$$\frac{\partial}{\partial t} (\xi_E + \xi_B + \xi_\beta) = \frac{1}{\mu} \oint_S (\vec{B} \times \vec{E} + \beta \vec{E}) \cdot d\vec{s} \tag{2.142}$$

Equation (2.142) is representing what we call the **energy continuity equation**. This shows that the fields as they are on a particular closed surface indicate how the energy in the surrounded volume is changing. This is a statement that energy is conserved as the fields propagate because as the energy decreases for example in the enclosed region, the energy “flows” through the surface to the exterior region whose energy will increase by the same amount as the decrease of energy in the enclosed region.

Imagine two regions as illustrated in Fig. 2.42, with two surfaces S_1 and S_2 where the two surfaces intersect giving them a mutual area. If the energy flow is confined to this area, then the right-hand side of Eq. (2.142) is of the same magnitude for both regions, but the sign is reversed.

Therefore, the change in energy is reversed and the sum of the energy in both regions remains constant. Notice that if $\beta = 0$, the energy of the scalar field will be zero and Eq. (2.142) reverts to Poynting’s vector or theorem as we presented in Eq. (2.86).

2.9.3 The Particles or Charge Field Expression

If we start with an electric field of specific form as an initial condition, it will not propagate at all and it will just sit there at absolute rest. This is an analogous to our

example of water inside the pan where one could be touching the surface and instead of generating a wave an indentation appears in the wave and just sits there without moving, even after taking the figure away. In reality, due to the wave properties of the water, this is not actually possible; however, the wave properties of space are different due to the vector nature of the fields, which allows such possibility. This is not just an imaginary suggestion, yet it is a proof which comes directly from the equations that define the wave behavior of empty space.

Therefore, it is possible for there to exist an electric field which being governed by these equations would not propagate. The answer to such postulate is yes. All we have to do is set the time derivative of the wave Eq. (2.108) to zero. Thus, Eq. (2.108) reduces to the Laplacian form of electric field as

$$\nabla^2 \vec{E} = 0 \quad (2.143)$$

The electric field that satisfies Eq. (2.143) will not propagate as one can see, but yet remains at absolute rest. To begin we will not solve it in complete generality. We will just find a solution as we have done in Chap. 1 of this book. Again, we can try with an approach, if there exists a solution when there exists only a radial electric field. Using the spherical coordinate from Appendix E and setting $E_\theta = 0$ and $E_\phi = 0$ yield

$$\begin{aligned} \frac{\partial^2 E_r}{\partial r^2} + \frac{2}{r} \frac{\partial E_r}{\partial r} \\ + \frac{1}{r^2} \frac{\partial^2 E_r}{\partial \theta^2} + \frac{\coth \theta}{r^2} \frac{\partial E_r}{\partial \phi^2} \\ + \frac{1}{r^2 \sin^2 \theta} \frac{\partial^2 E_r}{\partial \phi^2} - \frac{2}{r^2} E_r = 0 \end{aligned} \quad (2.144)$$

$$\frac{2}{r^2} \frac{\partial E_r}{\partial \theta} = 0 \quad (2.145)$$

$$\frac{2}{r^2 \sin \theta} \frac{\partial E_r}{\partial \phi} = 0 \quad (2.146)$$

Substituting Eqs. (2.146) and (2.145) into Eq. (2.144) will yield

$$\frac{\partial^2 E_r}{\partial r^2} + \frac{2}{r} \frac{\partial E_r}{\partial r} - \frac{2}{r^2} E_r = 0 \quad (2.147)$$

The result in Eq. (2.147) is a second-order differential equation that is dependent only on variable r and thus if we multiply both sides of this equation by variable r^2 we obtain a new form of Eq. (2.147) as

$$r^2 \frac{\partial^2 E_r}{\partial r^2} + 2r \frac{\partial E_r}{\partial r} - 2E_r = 0 \quad (2.148)$$

Equation (2.148) is a Euler equation which can be solved by assuming a solution which is some power of r ; thus, we can write

$$\begin{cases} E_r = r^a \\ \frac{\partial E_r}{\partial r} = ar^{a-1} \\ \frac{\partial^2 E_r}{\partial r^2} = a(a-1)r^{a-2} \end{cases} \quad (2.149)$$

Substituting Eq. (2.149) into Eq. (2.148) for each appropriate term, we obtain the following result which is the auxiliary form of Eq. (2.148):

$$a(a-1)r^a + 2ar^a - 2r^a = 0 \quad (2.150)$$

We can divide Eq. (2.150) by r^a which can then provide us with the characteristic form of Eq. (2.150) as a quadric equation:

$$a(a-1) + 2a - 2 = 0 \quad (2.151)$$

Solving for a will provide two different answers as should be expected, and thus we have

$$\begin{cases} a = 1 \\ a = -2 \end{cases} \quad (2.152)$$

Equation (2.150) will give us two different power-type solutions to Eq. (2.148) to form the solution. The solution thus will be

$$E_r = k_1 r + \frac{k_2}{r^2} \quad (2.153)$$

As we can observe Eq. (2.153) has two terms; the first is invalid at infinity, and the second is invalid at the center of the radial field. This suggests that we should use the two different solutions in the different region of space that while being piecewise continuous still covers the whole space. We will designate an internal field (i.e., E_i) and an external (i.e., E_e) field such that

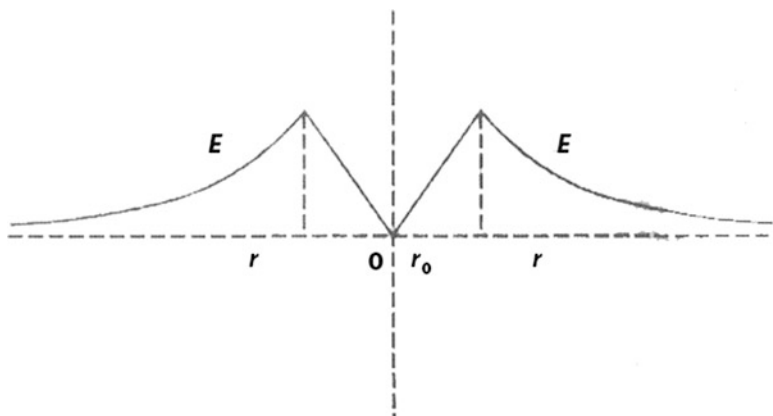


Fig. 2.43 Magnitude of a charge field

$$\vec{E}_e = \frac{k\hat{r}}{r^2} \quad (2.154)$$

and

$$E_i = \frac{kr\hat{r}}{r_0^3} \quad (2.155)$$

Thus, which solution is used is dependent on whether considering the region within r_0 or outside of r_0 . We have set it up so that at the boundary the fields match and they then both relate to the same constant of integration k . The field then along a line bisecting the center would have an intensity as illustrated in Fig. 2.43.

From now on we will call this stationary field a **charge field** for reason that is cleared in the next two following sections.

It is interesting that while typically electric fields will propagate at the speed of light and spread out in all direction, the electric field is of a certain form, and it does not behave this way.

In this case here, it does not propagate at all.

As we continue, we will find out other special and interesting electric fields that propagate in special ways. To designate these cases in general we will use the term **constrained propagation**.

2.9.4 Particle Energy

Thus far, we have seen that by Maxwell's equations there is energy in the spec itself. If this is not the scenario, then the waves could not transmit through the so-called void of space. As modern physics indicates, there is mass involved in energy. One

can use this postulate to determine what is sometimes called the classical radius of the electron. By calculating the energy in the charge field as we discussed, which would be similar to the field created by an electron, one can calculate a mass.

Since the mass of the electron is known, as we sum up the energy, starting at infinite distance and approaching its center, we come to a distance, where the energy in the electric field matches the mass of the electron and then we are done at this stage, since all the energy is accounted for. If there were something else inside this radius the energy would no longer balance, and this actually is an argument against the existence of a material body in the space. We also in previous section demonstrated that a physical particle cannot exist at all, and it is important to point out that the idea that all particles must be wave pulses is *not* a postulate of this theory and we know that these postulates are simply classical electromagnetism point of view.

Thus, the charge field has energy as described by Eq. (2.101) and assuming the external field as

$$E_e = \frac{q_e}{4\pi\epsilon r^2} \quad (2.156)$$

By substituting Eq. (2.156) into Eq. (2.101), we have

$$\xi_e = \frac{\epsilon}{2} \int \left(\frac{q_e}{4\pi\epsilon r^2} \right)^2 d\tau \quad (2.157)$$

Performing the integration over Eq. (2.157), we obtain

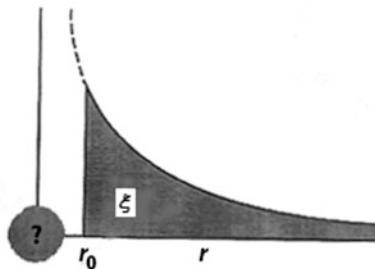
$$\begin{aligned} \xi_e &= \frac{\epsilon}{2} \int_{r_0}^{\infty} \left(\frac{q_e}{4\pi\epsilon r^2} \right)^2 4\pi r^2 dr \\ \xi_e &= \frac{q_e^2}{8\pi\epsilon} \int_{r_0}^{\infty} \frac{dr}{r^2} \\ \xi_e &= \frac{q_e^2}{8\pi\epsilon} \left. \frac{-1}{r} \right|_{r=r_0}^{\infty} \\ \xi_e &= \frac{q_e^2}{8\pi\epsilon r_0} \end{aligned} \quad (2.158)$$

The final result of Eq. (2.158) is the energy of the external field of particle. As mentioned, we can easily find that this energy represents a mass. If we have the mass of the particle, then we can determine the radius of this particle in the final step of Eq. (2.158).

However, this imposes an interesting problem for if we consider some particle like an electron, all the mass would be accounted for by the time the summation reaches this radius as shown and depicted in Fig. 2.44.

This situation might tell us that there could be nothing inside the radius or the energy could no longer balance. This is typically called the classical radius of the

Fig. 2.44 Energy in the electric field of a particle



electron and is well known as it appears in textbook like the one by Jackson [22] on pages 681 and 790, which refers to it as the classical diameter versus radius.

This supports the concept of stationary field theory, where everything is based on the field with no separate object existing in the space. More details on this discussion can be found in the book by Ensle [19] and readers should refer to it, if there is any interest on their part.

2.9.5 Velocity

So, for what we have done one may notice that our charge field is at absolute rest; of course, charges are not all stationary and sitting around at absolute rest. They are all moving at various velocities and none of these velocities is the speed of light, being the speed that the wave properties of space tell us they should be going. Furthermore, typically electromagnetic waves spread out. They do not move like a wave pulse in a single direction. Thus, we come to perhaps the most significant derivation that the book of Ensle [19] shows by deriving the *particle equation*, which when solved tells us what form of electric is needed. Details of such derivation are beyond the scope of this chapter, and we just write the final answers and refer readers to the reference [19] for further information.

The final form of the particle equation is written as

$$\nabla^2 \vec{E} - \frac{1}{c^2} (\vec{v} \cdot \vec{\nabla}) (\vec{v} \cdot \vec{\nabla}) \vec{E} = 0 \quad (2.159)$$

The reason that Eq. (2.159) is called particle equation is because the electric field that satisfies this equation will propagate as a coherent pulse in a single direction behaving kinematically as a particle in a vacuum.

As it turns out this is not an easy equation to deal with; however if we consider the space external to the charge, where the divergence is zero, we can do some vector calculus manipulation in such a way as to find a set of solution, not in a general form though, but one working solution. See Ensle [19] for details. Using spherical coordinate system and assuming the following relation for a particle of spherical shape, we can find a separable partial differential equation as result; thus we have

$$\begin{aligned}\vec{E} &= E\hat{r} \\ \vec{v} &= v \cos \theta \hat{r} - v \sin \theta \hat{\theta}\end{aligned}\quad (2.160)$$

Thus, we find

$$\vec{v} \cdot \vec{E} = v \cos \theta E \quad (2.161)$$

and

$$\vec{v} (\vec{v} \cdot \vec{E}) = v^2 \cos^2 \theta E \hat{r} - v^2 \sin \theta \cos \theta E \hat{\theta} \quad (2.162)$$

Thus, the final form of Eq. (2.159) reduces to a separable partial differential equation with two variables r and θ as

$$\frac{v^2}{c^2} E - \frac{v^2}{c^2} r \frac{\partial E}{\partial r} - \frac{\left(1 - \frac{v^2}{c^2} \sin^2 \theta\right)}{\sin \theta \cos \theta} \frac{\partial E}{\partial \theta} = 0 \quad (2.163)$$

Assuming $E = R\Theta$ where R is only dependent on r and Θ is only dependent on θ and using the separation method by substituting $E = R\Theta$ into Eq. (2.163) as well as doing the proper algebra manipulation, we obtain the following:

$$\frac{v^2}{c^2} - \frac{v^2}{c^2} \frac{r}{R} \frac{\partial R}{\partial r} - \frac{\left(1 - \frac{v^2}{c^2} \sin^2 \theta\right)}{\sin \theta \cos \theta} \frac{1}{\Theta} \frac{\partial \Theta}{\partial \theta} = 0 \quad (2.164)$$

The form of Eq. (2.164) suggests two possible forms by separation of variables methodology of using λ as separation constant which could be anything and will be as follows:

$$\frac{v^2}{c^2} - \frac{v^2}{c^2} \frac{r}{R} \frac{\partial R}{\partial r} = \lambda \quad (2.165)$$

and

$$\frac{\left(1 - \frac{v^2}{c^2} \sin^2 \theta\right)}{\sin \theta \cos \theta} \frac{1}{\Theta} \frac{\partial \Theta}{\partial \theta} = -\lambda \quad (2.166)$$

The two differential Eqs. (2.165) and (2.166) could be rearranged to the new form as below:

$$\frac{v^2}{c^2} r \frac{\partial R}{\partial r} + \left(\frac{v^2}{c^2} - \lambda \right) R = 0 \quad (2.167)$$

$$-\frac{\left(1 - \frac{v^2 \sin^2 \theta}{c^2} \right)}{\sin \theta \cos \theta} \frac{\partial \Theta}{\partial \theta} + \lambda \Theta = 0 \quad (2.168)$$

The solution to both Eqs. (2.167) and (2.168) for their characteristic parts is given as follows [19]:

$$R = kr^{(1-\lambda\frac{c^2}{v^2})} \quad (2.169)$$

However, more analysis of Eq. (2.169) tells us that the radial field has to fall off by the power of -2 (i.e., $1/r^2$ as it is demonstrated at the end of Sect. 2.9.7 of this chapter). This is because the divergence of the electric field must be zero. Therefore, the radial solution becomes

$$R = \frac{k}{r^2} \quad (2.170)$$

and the separation constant is given by

$$\lambda = 3\frac{v^2}{c^2} \quad (2.171)$$

Now if also consider the characteristic solution of Eq. (2.168), with some mathematical manipulation we get the following result:

$$\Theta = \frac{k}{\left(1 - \frac{v^2}{c^2} \sin^2 \theta \right)^{3/2}} \quad (2.172)$$

where k is the constant of integration in solution process of both Eqs. (2.167) and (2.168) as well.

Now if we take both results in Eqs. (2.170) and (2.172) and plug them into relationship of $E = R\Theta$, we obtain the final solution for Eq. (2.163), as

$$\vec{E} = \frac{k \hat{r}}{r^2 \left(1 - \frac{v^2}{c^2} \sin^2 \theta \right)^{3/2}} \quad (2.173)$$

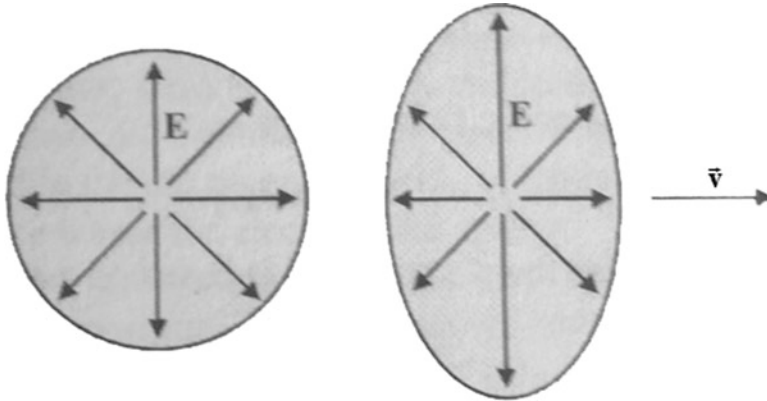


Fig. 2.45 Electric field of a charge field at rest and moving with velocity \vec{v}

We can easily show that Eq. (2.173) is the final solution of Eq. (2.163) by plugging it back into original wave in Eq. (2.163). If this is done, the wave equation will show a coherent propagation in one direction at the velocity of \vec{v} . This means that the particle equation was the correct method to determine the field and that a correct solution was found for the particle equation.

Notice that the electric field retains its cylindrical symmetry but becomes asymmetric on the longitudinal axis as in the following diagram as Fig. 2.45 and the case of scalar wave will create the vortex shape depicted in Fig. 2.31.

From Fig. 2.45, we see that the image on left side of this figure is the representation of the electric field at rest, while the image on the right side of it shows the field when the charge field is propagation at velocity \vec{v} .

Note that the transverse field is increased and actually the longitudinal field is decreased as the constant of integration k itself is dependent on velocity. To determine the value of constant of integration is not an easy task; however Enslie [19] shows that this constant with its dependency on the velocity \vec{v} is calculated as follows:

$$k = \frac{q_e}{4\pi\epsilon} \sqrt{1 - \frac{v^2}{c^2}} \tag{2.174}$$

Therefore, the electric field Eq. (2.171) for a moving charge will yield as a final form as

$$\vec{E} = \frac{q_e}{4\pi\epsilon} \frac{\sqrt{1 - \frac{v^2}{c^2}}}{r^2 \left(1 - \frac{v^2}{c^2} \sin^2 \theta\right)^{3/2}} \hat{r} \tag{2.175}$$

Note that the electric field transverses to its velocity ($\theta = \pi/2$) and thus it is given by

$$E_T = \frac{q_e}{4\pi\epsilon r^2} \frac{1}{\left(1 - \frac{v^2}{c^2}\right)} \quad (2.176)$$

and it increases with velocity, while the field longitudinal to its velocity ($\theta = 0$) is

$$E_L = \frac{q_e}{4\pi\epsilon r^2} \left(1 - \frac{v^2}{c^2}\right) \quad (2.177)$$

So, it decreases with velocity.

The velocity being discussed here is absolute. It is a wave velocity in a continuum that itself defines absolute rest.

Equation (2.173) of the field represents a type of constrained propagation, which emulates a particle.

2.9.6 The Magnetic Field

Thus far, we have not stated as a postulate that moving charge produces a magnetic field as it is done in Maxwell's equations. In fact, we began without any charge at all, stationary or moving. Thus, at this time all we know is that a changing electric field causes a magnetic field. Imagine that a charge field is approaching a point in space. As it approaches, the electric field at that point increases; therefore, the changing electric field produces a magnetic field. It then becomes a simple matter of how much the electric field changes at a stationary point in relation to the velocity that the charge approaches the point.

We then get a relation of the velocity of the charge field, the electric field at a certain point, and the resulting magnetic field at the same point. This gives the expected amount. Therefore, the result is not really anything new, but it is interesting the way in which we have found it.

From the postulates, the magnetic field is created when the electric field changes over time. However, this time change can also be caused by the coherent propagation of the charge. Thus, given that the charge fields are ready-made and can move at some velocity, it is convenient to know how this velocity produces a magnetic field. Since we are interested in the field outside of the charge we can say that

$$\begin{cases} \vec{\nabla} \cdot \vec{E} = 0 \\ \beta = 0 \end{cases} \quad (2.178)$$

We can replace the time derivative of Eq. (2.100) with the motion operator, and thus we have the following relationship:

$$\vec{\nabla} \times \vec{B} = -\frac{1}{c^2} (\vec{v} \cdot \vec{\nabla}) \vec{E} \quad (2.179)$$

Using vector quantity $\vec{\nabla} \times (\vec{F} \times \vec{G}) = (\vec{\nabla} \cdot \vec{G}) \vec{F} - (\vec{\nabla} \cdot \vec{F}) \vec{G} + (\vec{G} \cdot \vec{\nabla}) \vec{F} - (\vec{F} \cdot \vec{\nabla}) \vec{G}$ from Table 1.1 will result in

$$\vec{\nabla} \times \vec{B} = -\frac{1}{c^2} (\nabla \times (\vec{v} \times \vec{E})) \quad (2.180)$$

Consider the case where the electric field is based on a signal charge field for an elementary charge; then we have

$$\vec{E} = \frac{q_e \hat{r}}{4\pi\epsilon r^2} \quad (2.181)$$

Substituting Eq. (2.181) into Eq. (2.180) yields

$$\begin{cases} \vec{\nabla} \times \vec{B} = -\frac{1}{c^2} \left((\vec{v} \times \frac{q_e \hat{r}}{4\pi r^2}) \right) \\ \vec{\nabla} \times \vec{B} = -\frac{1}{c^2} \vec{\nabla} \times \left((\vec{v}) \times \frac{q_e \hat{r}}{4\pi\epsilon r^2} \right) \end{cases} \quad (2.182)$$

There is not enough information to solve for the magnetic field unless we also know the divergence of the field, but we do, so that is not a problem; however, we still do not know the complete vector field on the right-hand side of Eq. (2.182) unless we know its divergence. Now in the special condition where both sides have a divergence of zero, the equivalence of the curl of the two vector fields leads to the vector field being equivalent, plus a constant of integration. So, first we must verify that the vector field of the right-hand side of Eq. (2.182) has zero divergence. That is

$$\vec{\nabla} \cdot \left(\vec{v} \times \frac{q_e \hat{r}}{4\pi\epsilon r^2} \right) = 0 \quad (2.183)$$

Using a vector quantity $\vec{\nabla} \cdot (\vec{F} \times \vec{G}) = \vec{F} \cdot (\vec{\nabla} \times \vec{G})$ from Table 1.1, we obtain the following:

$$-\vec{v} \cdot \left(\vec{\nabla} \times \frac{q_e \hat{r}}{4\pi\epsilon r^2} \right) = 0 \quad (2.184)$$

Thus, from a relation in $\vec{\nabla} \cdot (\vec{\nabla} \times \vec{F}) = 0$, we can see that the divergence is zero. Therefore, Eq. (2.182) leads to the following result:

$$\vec{B}_e = \frac{1}{c^2} \left(\vec{v} \times \frac{q_e \hat{r}}{4\pi\epsilon r^2} \right) + k \quad (2.185)$$

where k is a constant and note that when $v = 0$, the magnetic field is zero, so the constant is zero.

Therefore, we can write

$$\vec{B}_e = \frac{1}{c^2} \left(\vec{v} \times \frac{q_e \hat{r}}{4\pi\epsilon r^2} \right) \quad (2.186)$$

However, there is a problem with Eq. (2.186). We assumed that the electric field remained the same regardless of its velocity. This is not true as we have seen in Chap. 1 of this book.

This relationship in Eq. (2.186) is useful for velocities much less than the velocity of light but becomes more inaccurate as the velocity increases. However, if we simply replace the charge field with the electric field, the magnetic field now relates directly to the electric field and as it changes with velocity, the magnetic field tracks the change. Thus, we have simply the following equation:

$$\vec{B} = \frac{1}{c^2} (\vec{v} \times \vec{E}) \quad (2.187)$$

Equation (2.165) is valid at all velocities. Notice that it corresponds directly to the electric field as it exists at the point in space where the magnetic field is created. However, the magnetic field is in some way independent of the electric field; so if the magnetic field is created by an electric field somewhere in space and in another region, the electric field is canceled out by another electric field; it would be possible for the magnetic field, which is not being canceled out, to extend into a space where the electric field is zero [19].

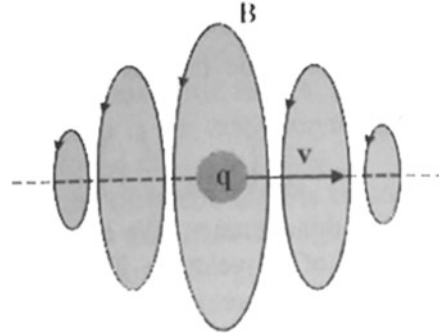
We now know how a moving elementary charge produces a magnetic field. Then by superposition it can be applied to any collection of charges in motion. This again gives the expected result, which was defined as Biot-Savart law as we have seen in Chap. 1 of this book.

Given the magnetic field from a moving charge as we found in Eq. (2.186), we obtain the new following form:

$$\vec{B}_e = \frac{\mu}{4\pi} \left(q_e \vec{v} \times \frac{\hat{r}}{r^2} \right) \quad (2.188)$$

Equation (2.166) would be the magnetic field of moving change as it is depicted in Fig. 2.46.

Fig. 2.46 Magnetic field of a charge in motion



Because of superposition, we can sum any number of charge fields, which could be treated as a charge density spread out over a volume, and thus

$$\vec{B} = \frac{\mu}{4\pi} \int \rho \vec{v} \times \frac{\vec{r} - \vec{r}_0}{|\vec{r} - \vec{r}_0|^3} d\tau \tag{2.189}$$

where r_0 is the position vector of the charge element. We will define the **current density** such that

$$\vec{J} \equiv \rho \vec{v} \tag{2.190}$$

So, we can write that

$$\vec{B} = \frac{\mu}{4\pi} \int \vec{J} \times \frac{\vec{r} - \vec{r}_0}{|\vec{r} - \vec{r}_0|^3} d\tau \tag{2.191}$$

which again is just the Biot-Savart law as before. If one imagines an infinity thin line of charge density, Eq. (2.169) becomes

$$\vec{B} = \frac{\mu}{4\pi} \int \vec{I} \times \frac{\hat{r}}{r^2} dl = \frac{\mu I}{4\pi} \int d\vec{l} \times \frac{\hat{r}}{r^2} \tag{2.192}$$

Finally, notice that if we take the time derivative of the charge density Eq. (2.190), we can finally obtain the following relationship:

$$\frac{\partial \rho}{\partial t} = - \vec{v} \cdot \vec{\nabla} \rho \tag{2.193}$$

Or with vector identity given in Table 1.1 we convert Eq. (2.193) to the following form:

$$\frac{\partial \rho}{\partial t} = - \vec{\nabla} \cdot \vec{v} \rho \quad (2.194)$$

Utilizing Eq. (2.168) equality, Eq. (2.172) provides a different form as

$$\frac{\partial \rho}{\partial t} = - \vec{\nabla} \cdot \vec{J} \quad (2.195)$$

Equation (2.195) is typically called the **continuity equation**. Furthermore, if we consider the charge, we have

$$\frac{\partial q}{\partial t} = - \int \vec{\nabla} \cdot \vec{J} \, d\tau \quad (2.196)$$

And by the divergence theorem, Eq. (2.196) forms a different format as

$$\frac{\partial q}{\partial t} = - \oint_S \vec{J} \cdot d\vec{s} \quad (2.197)$$

This equation is called the **charge continuity equation**, which states that charge is conserved as it moves from one location to another. It is analogous to the energy continuity Eq. (2.142).

2.9.7 The Scalar Field

Now to get back to our electrodynamic study of charge field in an electric field, we look at the case where when charge field approaches a point, the change in the electric field at the point also causes a scalar field. However, this situation only occurs when the electric field has a divergence. In this case, we treat the charge field as a point charge to simplify calculations, but it is still useful since by superposition it can be generally applied. Even though the non-divergent electric field does not contribute to the situation, by continuity rule the scalar field extends into the non-divergent region. The way the scalar field extends into the non-divergent electric field makes it possible to relate the scalar field directly to the non-divergent electric field as we could do for magnetic field, but they are not directly linked [19].

It is just a correspondence, though it could be useful in practical calculations. The field is most positive in front of the moving charge and most negative behind the charge motion. On the plane bisecting the charge perpendicular to its motion, the scalar field is zero. This is opposite in a sense to the magnetic field as the magnetic field is strongest on the perpendicular plane, but directly in front or behind the magnetic field is zero.

To continue with this matter, we now like magnetic field, determine that the scalar magnetic field in relative to the velocity of a charge field will be derived by taking the divergence of Eq. (2.100) to obtain the following:

$$\begin{cases} \vec{\nabla} \times \vec{B} + \vec{\nabla} \beta = \frac{1}{c^2} \left(\frac{\partial \vec{E}}{\partial t} \right) \\ \vec{\nabla} \cdot (\vec{\nabla} \times \vec{B}) + \vec{\nabla} \cdot (\vec{\nabla} \beta) = \frac{1}{c^2} \left(\vec{\nabla} \cdot \frac{\partial \vec{E}}{\partial t} \right) \end{cases} \quad (2.198)$$

Using Table 1.1, we can see that the divergence of a curl is zero, and thus Eq. (2.198) reduces to the following form:

$$\nabla^2 \beta = \frac{1}{c^2} \left(\vec{\nabla} \cdot \frac{\partial \vec{E}}{\partial t} \right) \quad (2.199)$$

or

$$\nabla^2 \beta = \frac{1}{c^2} \frac{\partial}{\partial t} (\vec{\nabla} \cdot \vec{E}) \quad (2.200)$$

Now let us do this for a charge field using the interior field where the divergence is not zero and use the relation of ρ/ϵ to signify it. It then becomes

$$\nabla^2 \beta_e = -\mu \vec{v} \cdot \nabla \rho_e \quad (2.201)$$

Using the vector identity $\vec{\nabla} \cdot (\varphi \vec{F}) = (\vec{\nabla} \varphi) \cdot \vec{F} + \varphi \vec{\nabla} \cdot \vec{F}$ from Table 1.1, Eq. (2.201) yields

$$\nabla^2 \beta_e = -\mu \vec{\nabla} \cdot \vec{v} \rho_e \quad (2.202)$$

Equation (2.202) looks like the Poisson equation and thus has the solution such as

$$\beta_e = \frac{\mu}{4\pi} \int \left[\frac{\vec{\nabla} \cdot \vec{v} \rho_e}{|\vec{r} - \vec{r}_0|} \right] d\tau \quad (2.203)$$

If we use same vector quantity as above again, we can break Eq. (2.203) into two parts as

$$\beta_e = \frac{\mu}{4\pi} \int \vec{\nabla} \cdot \frac{\vec{v} \rho_e}{|\vec{r} - \vec{r}_0|} d\tau - \frac{\mu}{4\pi} \int \vec{v} \rho_e \cdot \vec{\nabla} \left(\frac{1}{|\vec{r} - \vec{r}_0|} \right) d\tau \quad (2.204)$$

Applying divergence theorem Eq. (1.61) to the first term integral in Eq. (2.204), we obtain the following:

$$\beta_e = \frac{\mu}{4\pi} \oint_S \frac{\vec{v} \rho_e}{|\vec{r} - \vec{r}_0|} d\vec{s} - \frac{\mu}{4\pi} \int \vec{v} \rho_e \cdot \vec{\nabla} \left(\frac{1}{|\vec{r} - \vec{r}_0|} \right) d\tau \quad (2.205)$$

Notice that the velocity direction is the direction of the velocity and the velocity into closed surface is the same as the velocity out of the closed surface; thus, we have

$$\frac{\mu}{4\pi} \oint_S \frac{\vec{v} \rho_e}{|\vec{r} - \vec{r}_0|} \vec{v} \cdot d\vec{s} = 0 \quad (2.206)$$

Therefore, Eq. (2.206) reduces to the following form:

$$\beta_e = \frac{\mu}{4\pi} \int \vec{v} \rho_e \cdot \vec{\nabla} \left(\frac{1}{|\vec{r} - \vec{r}_0|} \right) d\tau \quad (2.207)$$

Resolving the gradient within integral of Eq. (2.207) yields the following:

$$\beta_e = \frac{\mu}{4\pi} \int \frac{\vec{v} \rho_e |\vec{r} - \vec{r}_0|}{|r - r_0|^3} d\tau \quad (2.208)$$

Then finishing of the integration of Eq. (2.208) for a point charge, we obtain

$$\beta_e = \frac{\mu q_e}{4\pi} \frac{\vec{v} \cdot \hat{r}}{r^2} \quad (2.209)$$

Equation (2.209) gives us the scalar field of a moving charge; however, it suffers from the same defect as the magnetic field has [19].

This relation is useful for velocities much less than the velocity of light but becomes more inaccurate as the velocity increases. However, if we simply replace the charge field with the electric field, the magnetic field now relates directly to the electric field and as it changes with velocity the scalar field tracks the charge. Thus, we can simply have the following relationship:

$$\beta_e = \frac{1}{c^2} (\vec{v} \cdot \vec{E}) \tag{2.210}$$

Equation (2.210) is valid at all velocities and note that we can relate the scalar field to the electric field like we have done it for magnetic field. However, unlike the magnetic field, the scalar field has no direct connection to the electric field, where the divergence is zero. While the scalar field extends into the non-divergent region, it does not exist unless the electric field has divergence somewhere. Nonetheless, this Eq. (2.210) in relation to the electric field can be employed provided that the electric field in question is related to a charge field and as we said in case of the magnetic field the scalar field has a certain independence and if the electric field is canceled out somewhere the scalar field can exist even where the electric field is zero [19].

Like with the magnetic field we use superposition to relate it to current density where it is then analogous to the Biot-Savart law. However, there are significant differences in this relationship. If there is a closed loop or current, no scalar field is generated. The current has to be open and at the points where the charge accumulates a scalar field is generated.

Given the scalar field from a moving charge as it is shown in Eq. (2.209), we have

$$\beta_e = \frac{\mu}{4\pi} \left(q_e \vec{v} \cdot \frac{\hat{r}}{r^2} \right) \tag{2.211}$$

This equation is the indication of scalar magnetic field of a moving charge as depicted in Fig. 2.47.

Because of superposition, we can sum any number of charge fields, which could be treated as a charge density spread out over a volume; thus

$$\beta = \frac{\mu}{4\pi} \int \rho \vec{v} \cdot \left(\frac{\vec{r} - \vec{r}_0}{|r - r_0|^3} \right) d\tau \tag{2.212}$$

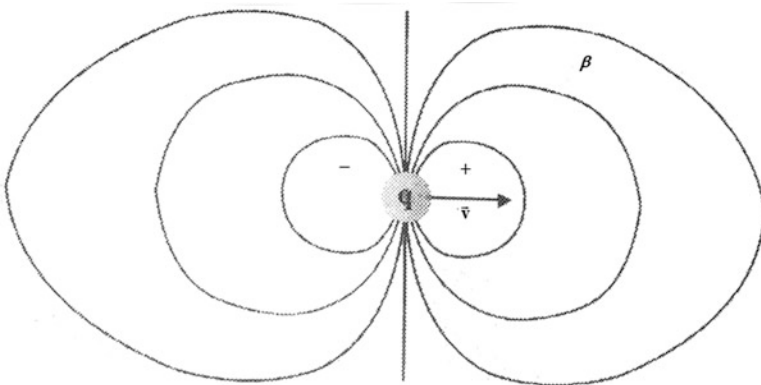


Fig. 2.47 Scalar magnetic field of a charge in motion

Using our definition for current density as before (i.e., $\vec{J} = \rho \vec{v}$), Eq. (2.146) becomes

$$\beta = \frac{\mu}{4\pi} \int \vec{J} \cdot \left(\frac{\vec{r} - \vec{r}_0}{|\vec{r} - \vec{r}_0|^3} \right) d\tau \quad (2.213)$$

If one imagines an infinitely thin line of charge density Eq. (2.213) results in

$$\beta = \frac{\mu}{4\pi} \int \vec{I} \cdot \frac{\hat{r}}{r^2} dl = \frac{\mu I}{4\pi} \int \frac{\hat{r}}{r^2} \cdot d\vec{l} \quad (2.214)$$

where I is the current. Notice that the integrand can be viewed as a potential and we can then apply the gradient theorem; thus

$$\beta = -\frac{\mu I}{4\pi} \int \nabla \left(\frac{1}{r} \right) \cdot d\vec{l} = -\frac{\mu I}{4\pi} \left(\frac{1}{r_2} - \frac{1}{r_1} \right) \quad (2.215)$$

The scalar field exists, when the current is discontinuous. If the current is in a loop, no scalar field is created since $r_1 = r_2$. It should be noted though that microscopically the scalar field exists for each charge field that is propagating, but this is not observed at any point external to the current.

Note that for a $1/r$ field the energy is infinite, but the scalar field is always created as two opposite poles; that is, it is a dipole and the distant field falls off as $1/r^2$.

2.9.8 *Scalar Fields, from Classical Electromagnetism to Quantum Mechanics*

As we have learned so far, in classical electrodynamics, the vector and scalar potentials conveniently were introduced by utilizing Maxwell's equations as an aid for calculating these fields and from there we managed to analyze them in the quantum electrodynamics via Lagrangian and Hamiltonian aspect of gauge theory and its invariance postulation. See Chap. 5 of this book for more details. However, it is a known fact that in order to obtain a classical canonical formalism the potentials are needed. Nevertheless, the fundamental equation of motion can always be described directly in terms of the fields alone.

However, in the quantum mechanics, the canonical formalism is necessary, and as a result the potentials cannot be eliminated from the basic equations. Nevertheless, these equations, as well as the physical quantities, are all gauge invariant, so that it may seem that even in quantum mechanics the potentials themselves have no independent significance [23].

For us to be able to take these fields, in particular, the *scalar field* and its prediction from *classical electromagnetism* and interaction from *quantum mechanics*, we assume that readers have met the principle of least action (see Chap. 5 of this book as well) in *classical mechanics*, and the related concepts of the *Lagrangian*, the *Hamiltonian*, and finally the *Euler-Lagrange* equations.

In this section, we briefly examine them from special relativistic point of view and leave the details for Chap. 5 of this book, so we begin with the summary of the classical results both as reminder and the to introduce the notation we need for the subject of this section in hand.

Judicially, in classical mechanics, the classical Lagrangian mechanics is branching off from Newton's law of force and acceleration as well as momentum as

$$\vec{f} = m \vec{a} = m \frac{d\vec{v}}{dt} = \frac{d(m\vec{v})}{dt} = \frac{d\vec{p}}{dt} \quad (2.216)$$

with which we can write Eq. (2.216) in a new form as

$$-\nabla \vec{V} = m \frac{d\vec{x}}{dt} \quad (2.217)$$

The basic idea of Lagrangian mechanics is to replace this vector treatment by a treatment based on a scalar quantity called the Lagrangian, which allows vector equations to be extracted by taking derivatives just as $\nabla \vec{V}$ is a vector extracted from the potential energy V . This approach proves to be more flexible and it simplifies many problems in classical mechanics.

At any given instant of time, the state of a physical system is described by a set of n variables q_i called *coordinates*, and their time derivatives \dot{q}_i called *velocities*. For example, these could be the positions and velocities of a set of particles making up the system.

Define a function \mathcal{L} called the *Lagrangian*, given by

$$\mathcal{L} = T - V \quad (2.218)$$

In Eq. (2.218), T and V are the kinetic energy and potential energies of the system, respectively. The Lagrangian is therefore a function of the positions and velocities, and it can be a function of time. This is indicated by the notation $\mathcal{L} = \mathcal{L}(\{q_i\}, \{\dot{q}_i\}, t)$, which we abbreviate to $\mathcal{L} = \mathcal{L}(q, \dot{q}, t)$. For particle motion with no external time-dependent fields, the Lagrangian has no explicit dependence on time. The phrase “no explicit dependence on time” means that it has no dependence on time over and above that which is already implied by the fact that q and \dot{q} may depend on time. For example, a single particle undergoing simple harmonic motion has the Lagrangian $\mathcal{L} = (1/2)m(\dot{x}^2 - \omega^2 x^2)$. An example motion of the particle is $x = x_0 \sin(\omega t)$, and for this motion the Lagrangian can also be written as

$(m\omega^2 x_0^2/2) \cos 2\omega t$, which is a function of time. However, the latter form hides the dependence on x and \dot{x} , which is what we are mainly interested in, and furthermore in general the Lagrangian cannot be deduced from the motion, but the motion can be deduced from the Lagrangian when the latter is written as a function of coordinates and velocities.

For this reason, the variables $\{q, \dot{q}_i\}$ are said to be the “natural” or “proper” variables of \mathcal{L} . A similar issue arises in the treatment of functions of state in thermodynamics as well.

The time integral of the Lagrangian along a path $q(t)$ is called the *action* S and written as

$$S[q(t)] = \int_{q_1, t_1}^{q_2, t_2} \mathcal{L}(q, \dot{q}, t) dt \quad (2.219)$$

The *principle of least action* states that the path followed by the system is the one that gives an extreme value either maximum or minimum of S with respect to small changes in the path. The title “Least” action comes from the fact that in practice a minimum is more usual than a maximum. The path is to be taken between given starting and finishing “properties” q_1, q_2 at time t_1, t_2 [24].

To find the extremum of S we need to ask for a zero derivative with respect to changes in all the variables describing the path. The calculus of variation may be used to show that the conclusion is that action S reaches an extremum for the path satisfying.

We are now at the point that we can establish and define the ***Euler-Lagrange equations*** as

$$\frac{d}{dt} \left(\frac{\partial \mathcal{L}}{\partial \dot{q}_i} \right) = \frac{\partial \mathcal{L}}{\partial q_i} \quad (2.220)$$

The physical interpretation of Eq. (2.320) is found by discovering its implications. The end result of such a study is summarized as follows:

$$\underbrace{\frac{d}{dt}}_{\text{(Rate of change of)}} \quad \underbrace{\left(\frac{\partial \mathcal{L}}{\partial \dot{q}_i} \right)}_{\text{('Momentum')}} = \underbrace{\left(\frac{\partial \mathcal{L}}{\partial q_i} \right)}_{\text{('Force')}} \quad (2.221)$$

The “force” here is called a *generalized force*, and the “momentum” is called *canonical momentum*, defined by

$$\tilde{p}_i \equiv \left(\frac{\partial \mathcal{L}}{\partial \dot{q}_i} \right) \quad (2.222)$$

In the simplest cases such as motion of a free particle, or a particle subject to conservative forces, the canonical momentum may be equal to a familiar momentum such as linear momentum or angular momentum, but this does not have to happen. A counterexample occurs for the motion of a particle in a magnitude field.

The Hamiltonian of a system is defined as

$$\mathcal{H}(q, \tilde{p}, t) \equiv \left(\sum_i^n \tilde{p}_i \dot{q}_i \right) - \mathcal{L}(q, \dot{q}_i, t) \quad (2.223)$$

In Eq. (2.223), \dot{q}_i are to be written as functions of the q_i and \tilde{p}_i , so that the result is a function of coordinates and canonical momentum as the natural variables of the Hamiltonian. For conservative forces, one finds that the sum in Eq. (2.223) evaluates to twice the kinetic energy, and then the final form of Hamiltonian can be written as

$$\mathcal{H} = T + V \quad (2.224)$$

This equation is clearly the total energy of the system.

The Euler-Lagrange equation will yield Hamilton's canonical equation as

$$\begin{cases} \frac{dq_i}{dt} = \frac{\partial \mathcal{H}}{\partial \tilde{p}_i} \\ \frac{d\tilde{p}_i}{dt} = -\frac{\partial \mathcal{H}}{\partial q_i} \end{cases} \quad (2.225)$$

Thus, the Hamiltonian with the canonical equations offers an alternative to the Lagrangian with Euler-Lagrange equations.

Now that we have built and refreshed our knowledge of classical mechanics and motion of particles based on Lagrangian and Hamiltonian definition, we can go back to the stream of our original goal for this section on the topic of significance of electromagnetic potentials in quantum theory and scalar fields as well as their prediction from classical electromagnetism and interpretation from quantum mechanics.

If we begin our discussion with a charged particle inside a "Faraday cage" connected to an external generator as it was suggested by Aharonov, Y. and D. Bohm (1959) [23], which causes the potential on the gage to alternate in time, such condition adds to the Hamiltonian of the particle, a term $V(x, t)$, which is, for the region inside the gage, a function of time only. In the nonrelativistic limit and if we assume this situation almost everywhere, then we have for the region inside the gage

$$\mathcal{H} = \mathcal{H}_0 + V(t) \quad (2.226)$$

In Eq. (2.226), the quantity \mathcal{H}_0 is the Hamiltonian, when the generator is not functioning, and $V(t) = \exp \phi(t)$. If $\psi_0(x, t)$ is a solution of the Hamiltonian, \mathcal{H}_0 , then the solution for \mathcal{H} is

$$\begin{aligned}\psi &= \psi_0 e^{-iS/\hbar} \\ S &= \int V(t) dt\end{aligned}\tag{2.227}$$

which follows from

$$i\hbar \frac{\partial \psi}{\partial t} = \left(i\hbar \frac{\partial \psi_0}{\partial t} + \psi_0 \frac{\partial S}{\partial t} \right) e^{-iS/\hbar} = [\mathcal{H}_0 + V(t)]\psi = H\psi\tag{2.238}$$

This new solution differs from the old one just by a phase factor and it corresponds to no change in physical result.

Building the analysis based on Eq. (2.238), Aharonov, Y. and D. Bohm (1959) [23] show that, from relativistic considerations, it can be seen that the covariance of their analysis concludes a demand of a similar result involving the vector potential \vec{A} .

As we have learned so far, a scalar can be defined non-rigorously as a point with magnitude but no direction in contrast to a vector, which is defined as a point with both magnitude and direction.

As we said previously, Hertzian waves, which consist of oscillating transverse electric and magnetic fields, are vector waves and therefore cannot be the scalar waves, which Tesla has used. The other types of fields, which show promise in describing scalar fields, are the potential fields and in the paper written by Aharonov, Y. and D. Bohm (1959) [23], these authors described a subtle effect arising from potential fields, when both the electric and magnetic fields were absent. A short account of these two authors' published paper presents a phenomenon that today we know as Aharonov-Bohm effect and will follow as below.

2.9.8.1 The Aharonov-Bohm Effect

In a region with electric and magnetic fields \vec{E} and \vec{B} , classical physics predicts that a particle of charge q will encounter a force \vec{F} that we have introduced as Lorentz force in Chap. 1 of this book and we wrote it as

$$\vec{F} = q \vec{E} + \frac{q}{c} (\vec{v} \times \vec{B})\tag{2.229}$$

where c is the speed of light and \vec{v} is the particle velocity. If the \vec{E} - and \vec{B} -fields are radiation fields with time varying, then the energy flow Poynting's vector is written as

$$\vec{S} = \frac{1}{2} \frac{c}{4\pi} (\vec{E} \times \vec{B})\tag{2.230}$$

If both the both fields, namely electric and magnetic fields, are zero, then it could be that all forces are zero and all energy flows are zero accordingly. Thus, no physical consequences can be observed if the \vec{E} - and \vec{B} -fields are zero.

Quantum mechanics requires the use of potential fields rather than the \vec{E} and \vec{B} force fields. The *vector potential*, \vec{A} , and the *scalar potential*, ϕ , are related to the \vec{E} and \vec{B} via Eqs. (2.81) and (2.83) as before, and they are repeated here again as

$$\vec{E} = -\nabla\phi - \frac{1}{c} \frac{\partial \vec{A}}{\partial t} \quad (2.231)$$

and

$$\vec{B} = \nabla \times \vec{A} \quad (2.232)$$

We assume here again that the use of ϕ and \vec{A} is equivalent to the use of \vec{E} - and \vec{B} -fields, and Eq. (2.229) was created based on the kinematical state of charged particle of interest with velocity \vec{v} depending on the Lorentz force \vec{F} , where the electromagnetic continuum is described in classical physics by the local values of both electric field \vec{E} and magnetic field \vec{B} strengths, which are given by Eqs. (2.231) (2.81) and (2.232) (2.83).

Bear in your mind that the distribution of electromagnetic potentials is not uniquely determined by the distribution of the field strengths, as a change in the gauge of the potentials such as

$$\phi' = \phi - \frac{1}{c} \frac{\partial f}{\partial t} \quad (2.233a)$$

and

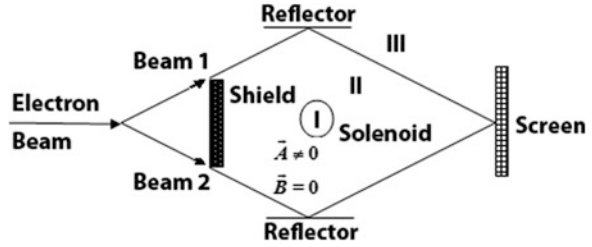
$$\vec{A}' = \vec{A} + \nabla f \quad (2.233b)$$

Leave the field strengths unaffected, for an arbitrary gauge function f of space and time. Therefore, in classical electromagnetism, the potentials are considered as mathematical entities, without physical significance.

However, Aharonov, Y. and D. Bohm (1959) [23] in their paper showed that the potential fields ϕ and \vec{A} can result in physical consequences when \vec{E} - and \vec{B} -fields are zero.

The quantum mechanical Schrödinger's equation for an electron in an electromagnetic field is given by the following form:

Fig. 2.48 Setup for Aharonov-Bohm interface with time-independent experiment



$$\frac{1}{2m} \left[\frac{\hbar}{c} \nabla - \frac{q}{c} \vec{A} \right] \Psi(x, t) + q\phi \Psi(x, t) = \vec{E} \Psi(x, t) \quad (2.234)$$

In Eq. (2.234), $\Psi(x, t)$ is the electron wave function. Aharonov and Bohm [23] suggested an experiment where an electron beam was split into two beams enclosed in tightly wound long solenoid, under special case, where only a path in space was considered, i.e., $t = \text{constant}$. The experiment is depicted in Fig. 2.48.

The beams are recombined at a screen and their interference pattern is observed. If neither magnetic field \vec{B} nor vector potential field \vec{A} is present as shown in Fig. 2.48, and the path length is the same, then the electrons will interface constructively, because their phases were the same in the initial beam. Now the solenoid is turned on and a magnetic flux exits inside the solenoid. However, since it is a long and highly wounded solenoid, there exists no magnetic flux in *Region II*. At the same time a vector potential field will be in form as the following equation exists in *Region II* as

$$\vec{A} = (A_r, A_\theta, A_z) = (0, 2N\pi a^2 / cr, 0) \quad (2.235)$$

In this equation

- i = the current.
- N = the number of turns per unit length.
- a = the radius of the solenoid.
- r = the distance from solenoid axis.

It can be seen from Eq. (2.232) that indeed magnetic field \vec{B} is zero (i.e., $\vec{B} = 0$), and thus we can write

$$\vec{B} = \vec{\nabla} \times \vec{A} = 0 \quad (2.236)$$

Considering Eq. (2.236), we are encountering a situation, where $\vec{B} = 0$ but on the other hand $\vec{A} \neq 0$. So, the question is that does this have any physical consequences? However, the solution to Schrödinger's equation for an electron-traversing path of the *Beam 1* in Fig. 2.48 is

$$\Psi = \Psi_0 \exp \left[\frac{iq}{\hbar c} \int_{X_1} \vec{A} \cdot d\vec{l} \right] \quad (2.237)$$

where Ψ_0 is the free particle solution and the integral measure of the summation of \vec{A} along the path of travel X_1 . The combined solution for an electron path 1 and another electron path 2 designed as X_2 will provide a new form of solution for the Schrödinger's equation as [23]

$$\begin{aligned} \Psi = \Psi_1 + \Psi_2 = \Psi_0 \exp \left[\frac{iq}{\hbar c} \int_{X_1} \vec{A} \cdot d\vec{l} \right] \\ + \Psi_0 \exp \left[\frac{iq}{\hbar c} \int_{X_2} \vec{A} \cdot d\vec{l} \right] \end{aligned} \quad (2.238)$$

What is observed is the probability density as shown here:

$$\Psi^* \Psi = 2|\Psi_0|^2 \exp \left[\frac{iq}{\hbar c} \oint \vec{A} \cdot d\vec{l} \right] \quad (2.239)$$

where the integral denotes the summation of \vec{A} along the closed loop path 1 plus path 2 and Ψ^* is the conjugate of wave function Ψ . The remarkable property is that the observable $\Psi^* \Psi$ varies with \vec{A} even though no \vec{B} -field interacts with the electrons! Thus, Aharonov and Bohm [23] theoretically predicated electron phase shifts, when no force fields are present. Many experiments have been performed, which confirmed the existence of this effect as it can be seen from Eqs. (2.232), (2.234), and (2.235).

2.9.8.2 The Existence of Potential and Scalar Fields and Waves

The above-described experimental setup used locally generated potential fields and the electron beams enclosed a magnetic flux. In fact, the phase integral is equal to the enclosed magnetic flux as

$$\oint \vec{A} \cdot d\vec{l} = \phi_B \quad (2.240)$$

These are severe and serious limitations. If potential fields have any correspondence to scalar fields, then they should exist independently of enclosed fluxes and can originate from nonlocal sources.

In fact, electromagnetic theory does predict the existence of potential waves traveling at the speed of light. If we substitute Eqs. (2.231) and (2.232) into all four Maxwell's Eqs. (2.80) and using charge e for electron in place of charge q , then they yield the following form of sets of equations:

$$\begin{aligned}
\vec{\nabla} \cdot \vec{E} &= 4\pi e \\
\vec{\nabla} \cdot \vec{B} &= 0 \\
\vec{\nabla} \times \vec{B} &= \frac{4\pi}{c} \vec{J} + \frac{1}{c} \frac{\partial \vec{E}}{\partial t} \\
\vec{\nabla} \times \vec{E} &= -\frac{1}{c} \frac{\partial \vec{B}}{\partial t}
\end{aligned} \tag{2.241}$$

And using the Lorentz gauge condition, we obtain (see Sect. 3.8 as well as Eq. (2.89))

$$\vec{\nabla} \cdot \vec{A} + \frac{1}{c} \frac{\partial \phi}{\partial t} = 0 \tag{2.242}$$

and assuming we are far away from sources, we arrive with two potential wave equations as before and then they are (see Sect. 3.8 as well as Eq. (2.90))

$$\nabla^2 \phi - \frac{1}{c^2} \frac{\partial^2 \phi}{\partial t^2} = 0 \tag{2.243}$$

$$\nabla^2 \vec{A} - \frac{1}{c^2} \frac{\partial^2 \vec{A}}{\partial t^2} = 0 \tag{2.244}$$

The important question is now whether the \vec{A} and ϕ waves need to be always in association with \vec{B} and \vec{E} waves. For the static or quasi-static case (the Aharonov-Bohm effect) we see that \vec{A} can decouple from \vec{B} . For the time varying case it is more complicated because if we initially have [34]

$$\vec{B} = \vec{\nabla} \times \vec{A}(t) = 0 \tag{2.245}$$

then

$$\vec{E} = -\nabla \phi - \frac{1}{c} \frac{\partial \vec{A}(t)}{\partial t} \tag{2.246}$$

\vec{E} is not necessarily zero. \vec{E} not equal to zero automatically generates a \vec{B} and thus \vec{A} will be forced to couple with \vec{B} .

However, if our generating source forces \vec{B} to be zero at all times, then we automatically insure that $\vec{E} = 0$ for all times because

$$E_0 = cB_0 \tag{2.247}$$

where B_0 and E_0 are the magnitude of the \vec{B} and \vec{E} fields. $\vec{E} = 0$ means that from Eq. (2.251), we can obtain the following result:

$$-\nabla\phi - \frac{1}{c} \frac{\partial \vec{A}}{\partial t} = 0 \quad (2.248)$$

Equation (2.248) can always be satisfied with a scalar super-potential field, χ , in Weber unit as

$$\vec{A} = \vec{\nabla} \chi \quad (2.249)$$

and

$$\phi = -\frac{1}{c} \frac{\partial \chi}{\partial t} \quad (2.250)$$

If Eqs. (2.249) and (2.250) are substituted into Eq. (2.240), the yield would be

$$\nabla^2 \chi - \frac{1}{c^2} \frac{\partial^2 \chi}{\partial t^2} = 0 \quad (2.251)$$

which is a wave equation for χ . Thus, we have predicted the existence of scalar waves, and this is what we are looking for:

Scalar Super-Potential

The scalar super-potential is the substrate of physicality, the ether permeating and underlying the universe, from which all matter and force fields derive [1]:

Super-potential \rightarrow Potential \rightarrow Force field

It is a scalar field, meaning each point in that field has one value associated with it. This value is the degree of magnetic flux at that point, whose unit is the Weber. This is not the magnetic force field we all know, composed of vectors whose units are Wb/m [2], but a magnetic *flux* field of scalar values whose unit of measure is simply Wb.

The scalar super-potential symbol is defined by Greek letter Chi as χ . The scalar super-potential may be written as $\chi = \chi(x, y, z, t)$, an equation assigning a flux value to each coordinate in space-time.

By itself, the absolute flux value has no direct physical significance in terms of measurable forces; however it is closely associated with the quantum phase θ of a wave function as follows:

(continued)

$$\chi = \frac{h}{q}\theta \quad (\text{I})$$

where

q = electric charge

h = Planck's constant

So, its effects are limited to the quantum domain and determine the degree of intersection and interaction between different probable realities. However, certain distortions in its distribution do give rise to measurable forces.

If we expand upon magnetic vector potential \vec{A} , then we can express that the magnetic vector potential \vec{A} is the gradient of the scalar super-potential, meaning the flux must change over some distance to comprise a vector potential and it can be written as

$$\vec{A}(x, y, z, t) = \nabla\chi \quad (\text{II})$$

The absolute value of flux or super-potential does not figure into this, just as altitude above sea level does not figure into the measurement of "inclination" of a hillside:

$$\nabla\chi = \nabla(\chi + \chi_0) \quad (\text{III})$$

While certain perturbations of the vector potential give rise to certain force fields, by itself \vec{A} has no physical significance in terms of measurable forces, but because it is made of super-potential it alters the quantum phase θ of charged particles per the Aharonov-Bohm effect:

$$\chi = \int \vec{A} \cdot d\vec{l} \quad (\text{IV})$$

$$\theta = \frac{q}{h} \int \vec{A} \cdot d\vec{l} \quad (\text{V})$$

James Maxwell also considered \vec{A} as the primary field in electrodynamics and likened it to electromagnetic momentum.

Super-Potential of Magnetic Field

In order to define this matter, we ask the question of what is the underlying scalar super-potential of $\vec{A} = \hat{\phi}/s$ where s is the element of surface area. The

(continued)

answer is that the gradient of the super-potential gives rise to the vector potential \vec{A} as defined by (VI) below:

$$\nabla\chi = \frac{1}{s}\hat{\phi} \quad (\text{VI})$$

By comparing this to the definition of gradient in cylindrical coordinates, we have the following relation:

$$\begin{cases} \frac{1}{s} = \frac{1}{s} \frac{\partial\chi}{\partial\phi} \\ \chi = \frac{s}{s} \end{cases} \quad (\text{VII})$$

Outside the origin surrounded by element surface, where $s \neq 0$, the results in (VII) will simplify to $\chi = \phi$, while at the origin the flux can be analyzed as being equal to 2π ; thus we can write

$$\chi = \begin{cases} 2\pi & s = 0 \\ \phi & s \neq 0 \end{cases} \quad (\text{VIII})$$

So, this is the fundamental super-potential field of an irrotational vector potential, which has a singularity at the central axis of rotation that produces a nonzero \vec{B} at the origin. Since \vec{B} is zero everywhere else, χ is allowed to have a gradient everywhere else besides the origin.

But what does this mean? The χ -field is a corkscrew of infinite width that winds around the z -axis. The infinite width is not a problem; it simply means that phenomena that depend on the path around the flux do not depend on the distance from it.

One example is the Aharonov-Bohm effect, where an electron traveling around a long thin solenoid picks up a phase factor that depends on the magnetic flux inside the solenoid, but not distance from it. If this solenoid were bent into a closed toroid so that all flux was absolutely confined inside, the effect would still exist.

Another example is a loop of wire wound around a ferromagnetic rod in which there is a changing magnetic field. The electromotive force induced by the changing magnetic flux is independent of the diameter of the loop. If the flux were completely confined inside a toroidal core, it would still produce the same electromotive force.

That is because the electron is not actually experiencing the flux itself, but rather the corkscrew super-potential surrounding the flux lines.

(continued)

A changing flux creates a changing gradient in the super-potential, and an electron in that path will be pumped along the gradient. Stated another way, a changing gradient generates an electric field, which places a force on the electron as expected.

1. **Website: scalarphysics.com, A Brief Introduction to Scalar Field by: Thomas Minderle Version 0.2, May 23, 2014**

Here the scalar waves replace the potential waves, when the physical \vec{E} - and \vec{B} -fields are zero.

The scalar fields are more primitive than the potential fields in that the latter are derived from the former. If we assume that χ varies harmonically with time then we can state that

$$\vec{A} = i \vec{K} \chi \quad (2.252)$$

In Eq. (2.252), \vec{K} is the representation of the wave vector pointing in the direction of travel. It is seen from the above equation that the wave of \vec{A} , in the absence of electric and magnetic fields, is purely longitudinal in that the \vec{A} vector points in the direction of travel. It has been generally assumed by physicists that longitudinal modes of motion can only be supported in a plasma, but now it is seen that pure potential fields can also support longitudinal waves as well.

We substituted Eq. (2.249) into Eq. (2.237), and then the result was

$$\Psi = \Psi_0 \exp \left[\frac{iq}{\hbar c} \chi \right] \quad (2.253)$$

However, for two interfering electrons

$$\Psi^* \Psi = |\Psi_1|^2 + |\Psi_2|^2 + 2|\Psi_1||\Psi_2| \exp \left[\frac{iq}{\hbar c} (\chi_1 - \chi_2) \right] \quad (2.254)$$

and the exponential phase factor may be directly observed.

Consider the radiation from an oscillating dipole. The vector potential field is given by

$$A \sim \frac{\sin [\omega(t - r/c)]}{r} \quad (2.255)$$

In the radiation zone where $r \gg \lambda$ we can write that

$$E \sim \frac{\cos [\omega(t - r/c)]}{r} \quad (2.256)$$

and

$$B \sim \frac{\cos [\omega(t - r/c)]}{r} \quad (2.257)$$

The energy received at the receiving antenna will be

$$S \sim E \times B \propto \frac{1}{r^2} \quad (2.258)$$

The scalar phase parameter, χ , also appears to have a $1/r$ dependence and is written as

$$\chi \sim \frac{\cos [\omega(t - r/c)]}{r} \quad (2.259)$$

Thus, we see that in detecting a scalar field such as χ -field a $1/r$ drop in intensity will be observed, while in detecting radio waves a $1/r^2$ drop in intensity will be observed. It is also interesting that \vec{A} -fields, when decoupled from electric field \vec{E} and magnetic field \vec{B} of Maxwell's equations, become χ scalar fields, which penetrate all objects because there will be no energy transfer to objects, when \vec{E} and \vec{B} are zero. However, if \vec{A} interacts slightly with highly nonlinear media if \vec{A} has a weak coupling with \vec{B} and \vec{E} , then it is possible that \vec{A} can be rotated enough such that

$$\vec{B} = \vec{\nabla} \times \vec{A} \neq 0 \quad (2.260)$$

In such situations, scalar fields may be detected using highly nonlinear or metastable systems.

2.9.8.3 Scalar Field Generators

A simple \vec{A} -field generator consists of a toroid coil such as the one demonstrated in Fig. 2.49, the \vec{B} -field flux is enclosed inside the coil, and only \vec{A} -fields exist outside. At extreme low frequency (ELF) this setup can generate strong \vec{A} -fields.

However, at radio frequencies, \vec{E} - and \vec{B} -fields will be generated outside as well. A true scalar generator is shown in Fig. 2.50.

Fig. 2.49 Toroid \vec{A} -field generator [34]

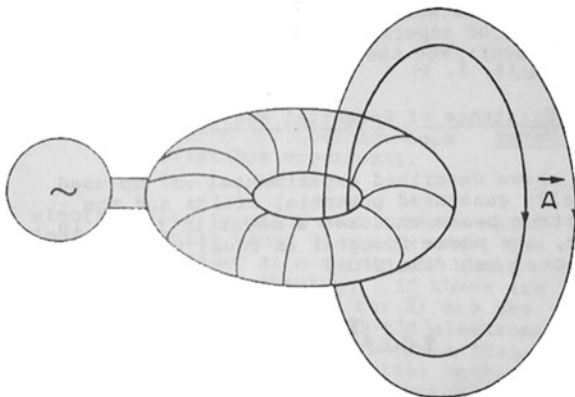


Fig. 2.50 Möbius scalar generator [34]

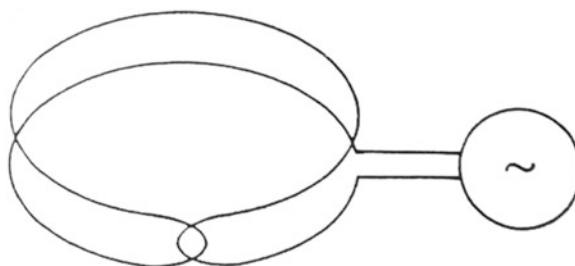


Fig. 2.51 Toroidal Möbius coil configuration



A finished Möbius coil should look like something like the image that is shown in Fig. 2.51. This coil is composed of a series of quadrifocal cable with a 45-degree helical twist; the cable is then wound with a toroidal winding pattern.

The first wrap of the cable serves as the core around which to wind the toroid. Realistically, it will seldom be a perfect 45 degrees if wound by hand. Angles between say 38 and 45 seem to work well enough but the closer to 45 the better.

Möbius coil merely consists of a loop in Fig. 8 as illustrated in Fig. 2.17 configuration with a double twist at the neck and fold over itself. This configuration insures that nearly all electromagnetic fields and potential fields are cancelled.

However, the scalar field need not be zero. The scalar field measures the phase of the current and an electron at the beginning of the loop will have a different phase than at the end of the loop due to lattice scattering. Thus, there should be an average phase difference between the top loop and the bottom loop. The scalar fields will reflect this average phase difference.

Internet search shows that such a device has been developed and certain properties of scalar fields have been qualitatively confirmed as in Eq. (2.241). The generated fields appear to penetrate everything and seemed to have a $1/r$ dependence as we talked and discussed about here in this section and at the end of Sect. 2.9.7.

Another feature of the device operating near the earth's Schumann resonance frequencies (about 7–10 Hz) was that it has a calming effect on humans and animals. See Sects. 2.9.9, 2.13, and 2.14 in this book as well.

2.9.8.4 The Detection of Scalar Fields

Biological organisms and gas tubes serve as highly nonlinear media, and for this reason they can serve as scalar field detectors. However, the efficiency may be rather low. For high-efficiency detection, an electron interference device should be used. The setup can be as shown in an illustration, in Fig. 2.48. It is the understanding of this author that this setup can measure fields from Region III as well as from Region II as again depicted and noted in Fig. 2.48. For a local source closer to beam 1, this beam will be phase shifted more than beam 2. Hence, interference effects will be observed on the screen if the source intensity changes.

2.9.8.5 Power Transmission and the Extension to Nuclear Fields

Tesla's claims for wireless power transmission [25] at his time and Bearden's qualitative theory [26] for this process can now be examined in light of the above-described scalar fields.

The wireless transference of power requires ultimately the conversion of scalar waves into the usual electromagnetic waves. Bearden [26] claimed that this conversion may be accomplished through the interference of two scalar waves at the target location. Maxwell's equations and gauge conditions are linear equations. The superposition of two scalar fields, which depend on linear equations at least to the first order, can only yield more scalar fields and not the usual electromagnetic fields. Hence it can be concluded that the predicated scalar waves cannot be used for power transmission.

The electromagnetic field is just one of the four fundamental fields known to science. The others are the nucleonic (weak), strong, and gravitational fields. The nucleonic field represents the next level of mathematical complexity in comparison

with the electromagnetic field. The nucleonic field transforms under rotation as a tensor, represented by a 2×2 matrix (the special unitary (SU(2)) group). This field is inherently nonlinear. It can be speculated that two forceless nucleonic fields can interact to produce energy fields at a distance. The forceless nucleonic fields may be found through a procedure analogous to the procedure for finding the scalar fields.

Note: In mathematics, the special unitary group of degree n , denoted SU(n), is the Lie group of $n \times n$ unitary matrices with determinant 1. The group operation is that of matrix multiplication. The special unitary group is a subgroup of the unitary group U(n), consisting of all $n \times n$ unitary matrices, which is itself a subgroup of the general linear group GL(n , C). More general unitary matrices may have complex determinants with absolute value 1, rather than real 1 in the special case.

First, the potential fields are generalized using space-time notations and can be written as

$$A^\mu = (\phi, \vec{A}) \quad \mu = 0,1,2,3 \quad (2.261)$$

Equations (2.243) and (2.244) are now combined into the field strength tensor and can be written as

$$f^{\mu\nu} = \partial^\mu A^\nu - \partial^\nu A^\mu \quad (2.262)$$

where ∂^μ and ∂^ν partials are shorthand for partial derivatives. Equation (2.262) describes the forceless \vec{A} -field from which the scalar field was derived. Similarly, the field strength tensor for the nucleonic field may be obtained via 2.237 and set to zero. Thus, we can write

$$F^{\mu\nu} = \partial^\mu W^\nu - \partial^\nu W^\mu + gW^\mu \times W^\nu = 0 \quad (2.263)$$

where W^μ is the nucleonic field and g a coupling strength parameter. The solution for (2.263) is being studied by the author but it is also encouraged that other interested investigators pursue and share interesting solutions for this equation.

The original description of the nucleonic field by Yang and Mills [27] predicted massless exchange particles (called vector bosons) between two nucleons such as a proton and a neutron. These massless particles, in analogy with photons, have long range and thus can be used for power transmission. However, the standard unified field theory, U(1) \times SO(2) \times SO(3), uses the Higgs mechanism to introduce mass to the vector bosons and consequently their range becomes too short for power transmission. Hence, the original Yang-Mills fields are the best candidates for the Tesla/Bearden scalar fields for wireless power transmission

2.9.8.6 The Conclusion

In this section, certain claims for the existence of non-Hertzian waves were examined in light of classical electromagnetism and quantum mechanics. In the process,

the existence of scalar fields and waves was predicted. These are fields with long range and great penetrating power. The associated potential waves are longitudinal waves in contrast to the familiar transverse electromagnetic waves. The scalar waves cannot be detected directly because they do not impart energy and momentum to matter. On the other hand, they impart phase shifts to matter and they may be detected through interference means. Because of their elusive nature they may also be called scalar vacuum waves. The underlying scalar field is already known to physicists in the context of quantum field theory and is known as the scalar gauge field. It is gratifying that in this period of research other researchers reported the observation of fields which behaved qualitatively similar to the predicted scalar fields. The extension of the forceless field concept to the nucleonic field should yield higher order fields with even more interesting properties than the scalar fields. This matter is being under investigation.

2.9.8.7 Scalar Interactions

Up to now we have considered only the coupling of particles to the electromagnetic field. This interaction distinguishes particles from antiparticles. There is another type of interaction which plays an important role in elementary particle physics, and that is a scalar interaction which treats particles and antiparticles alike. Suppose that nonrelativistically we have a potential energy $S(\vec{r}, t)$ that is the same for particles and antiparticles. The Schrödinger equation (see Appendix B of this book as well) with this potential is given as

$$i\hbar \frac{\partial \Psi(\vec{r}, t)}{\partial t} = \left[-\frac{\hbar^2 \nabla^2}{2m} + S(\vec{r}, t) \right] \Psi(\vec{r}, t) \quad (2.264)$$

We would like to be able to include such a potential in the relativistic wave equation.

One possible way, which as we shall see is a relativistic generalization of Eq. (2.264), is the following. Suppose that $S(\vec{r}, t)$ is a real scalar function; that is, its value at a given space-time point is the same in all Lorentz frames. Then if we add $2mS(\vec{r}, t)$ onto m^2c^2 in the Klein-Gordon equation Eq. (B.70) of Appendix B of this book, we obtain the following relation:

$$\left(\frac{i\hbar}{c^2} \frac{\partial}{\partial t} \right)^2 \Psi(\vec{r}, t) = \left(\frac{\hbar}{i} \nabla \right)^2 \Psi(\vec{r}, t) + m^2c^2 \Psi(\vec{r}, t) \quad (2.265)$$

Equation (2.265) is Klein-Gordon equation that is derived in Appendix B of this book; thus adding the term $2mS(\vec{r}, t)$ onto m^2c^2 would yield

$$-\frac{\hbar^2}{c^2} \frac{\partial^2}{\partial t^2} \Psi(\vec{r}, t) = \left[-\hbar^2 \nabla^2 + m^2 c^2 + 2mS(\vec{r}, t) \right] \Psi(\vec{r}, t) \quad (2.266)$$

We find that $\Psi(\vec{r}, t)$ is still a *scalar* under a Lorentz transformation.

Equation (2.266) is the wave equation corresponding to a modified energy momentum relation; thus we can write the following mathematical relationship using similar approach as Einstein's theory of general relativity of energy (i.e., $E = mc^2$) and momentum (i.e., $p = mc$) or final version of relativistic energy using the Lorentz factor $\gamma = [1 + (p/mc)]^{1/2}$; then the energy equation from relativistic point of view will be (see Appendix of this book as well)

$$E = mc^2 \sqrt{1 + \left(\frac{p}{mc}\right)^2} \quad (2.267)$$

Or by adding the term of $2mS(\vec{r}, t)$ for relativistic condition, we obtain

$$E^2 = c^2 p^2 + m^2 c^4 + 2mS(\vec{r}, t) \quad (2.268)$$

In the nonrelativistic limit, Eq. (2.268) reduces to

$$E = mc^2 + S(\vec{r}, t) + \frac{p^2}{2m} \quad (2.269)$$

Since $S(\vec{r}, t)$ is real, both wave function $\Psi(\vec{r}, t)$ and its conjugate $\Psi^*(\vec{r}, t)$ are solution of Eq. (2.266); thus antiparticles behave the same in the potential energy $S(\vec{r}, t)$ as what it takes place for the particles.

If $S(\vec{r}, t)$ is independent of time and is just the function of position \vec{r} (i.e., $S = S(\vec{r})$) then Klein-Gordon Eq. (2.264) is no longer in transient mode and for stationary states becomes

$$\frac{E^2 - m^2 c^4}{2mc^2} \Psi(\vec{r}) = \left[-\frac{\hbar^2 \nabla^2}{2m} + S(\vec{r}) \right] \Psi(\vec{r}) \quad (2.270)$$

Equation 2.270 is the relativistic generalization of the Schrödinger equation in the potential energy $S(\vec{r})$, since in the nonrelativistic limit $E \approx mc^2$ and thus we can write the following equation:

$$\frac{E^2 - m^2 c^4}{2mc^2} = \frac{(E - mc^2)(E + mc^2)}{2mc^2} \approx E - mc^2 \quad (2.271)$$

The fact that Eq. (2.270) depends only on E^2 means that if E is an eigenvalue, so is $-E$. There is a symmetry between positive and negative energy solutions because the scalar potential S does not distinguish particles and antiparticles.

Solving Eq. (2.270) is equivalent to solving the nonrelativistic equation as

$$E' \Psi(\vec{r}) = \left[-\frac{\hbar^2 \nabla^2}{2m} + S(\vec{r}) \right] \Psi(\vec{r}) \quad (2.272)$$

The eigenvalues of this equation are related obviously to those of Eq. (2.270) by the following relation:

$$E^2 = c^2 p^2 + m^2 c^4 E' \quad (2.273)$$

In order that E^2 be positive, only the eigenvalues of Eq. (2.272) satisfy

$$E' > -\frac{1}{2}(mc^2) \quad (2.274)$$

corresponding to physical solution of the relativistic Eq. (2.270).

2.9.8.8 Quantum Gauge Invariance

We begin with a brief review of gauge invariance in quantum mechanics. The classical Hamiltonian, \mathcal{H} , describing the motion of a charged particle in the presence of vector potential $\vec{\phi}$, and scalar potential \vec{A} , is given by

$$\mathcal{H} = \frac{1}{2m} \left[\vec{p} - \frac{q}{c} \vec{A} \right]^2 + qc \quad (2.275)$$

where:

m is the particle mass.

\vec{p} is the dynamical momentum of the particle.

q is the particle charge.

c is the speed of light.

From this we obtain the Schrödinger equation (i.e., nonrelativistic and neglecting spin) in the usual way by the substitutions of the following terms, and we have

$$\begin{aligned} \mathcal{H} &\rightarrow i\hbar \frac{\partial}{\partial t} \\ \vec{p} &\rightarrow i\hbar \vec{\nabla} \end{aligned} \quad (2.276)$$

Thus, we can write Eq. (2.275) in the following form:

$$\frac{\hbar}{i} \frac{\partial \Psi(\vec{r}, t)}{\partial t} = \frac{1}{2m} \left[\frac{\hbar}{i} \vec{\nabla} - \frac{q}{c} \vec{A} \right] \left[\frac{\hbar}{i} \vec{\nabla} - \frac{q}{c} \vec{A} \right] \Psi(\vec{r}, t) + q\phi \Psi(\vec{r}, t) \quad (2.277)$$

where

\hbar is Planck's constant/ 2π (i.e., $\hbar = h/2\pi$).

$\Psi(\vec{r}, t)$ is the wave function.

$\vec{\nabla}$ is del or nabla operator (i.e., $\partial/\partial x$, $\partial/\partial y$, $\partial/\partial z$).

By convention the Schrödinger equation is expressed in the Coulomb gauge with $\vec{\nabla} \cdot \vec{A} = 0$.

The quantum mechanical transformation that preserves the gauge invariance of the Schrödinger equation is a simple extension of classical gauge invariance. Thus, if

$$\vec{E} = -\nabla\phi - \frac{1}{c} \frac{\partial \vec{A}}{\partial t} \quad (2.278)$$

and

$$\vec{B} = \vec{\nabla} \times \vec{A} \quad (2.279)$$

where again

\vec{E} is the electric field

\vec{B} is the magnetic field

and if x is any scalar, then the substitutions of the following terms would leave \vec{E} and \vec{B} invariant; those terms are

$$\vec{A}' = \vec{A} - c\nabla x \quad (2.280a)$$

$$\phi' = \phi + \frac{\partial x}{\partial t} \quad (2.280b)$$

In quantum mechanics the additional transformation of the wavefunction by minimal substitution (Gates [29]) is required. This is given by the following equation:

$$\Psi' = e^{-ix} \Psi \quad (2.281)$$

The invariance of the Schrödinger equation is shown as follows:

Since

$$\frac{\partial}{\partial x} \Psi' = \frac{\partial}{\partial x} e^{ix} \Psi = e^{-ix} \frac{\partial \Psi}{\partial x} - i \frac{\partial x}{\partial x} \Psi e^{-ix} \quad (2.282)$$

or

$$i\hbar \nabla (e^{-ix} \Psi) = e^{-ix} (-i\hbar \nabla - \hbar \nabla_x) \Psi \quad (2.283)$$

$$\left(i\hbar \nabla - \frac{q}{c} \vec{A} \right) e^{-ix} \Psi = e^{-ix} \left(-i\hbar \nabla - \hbar \nabla_x - \frac{q}{c} \vec{A} \right) \Psi \quad (2.284)$$

Performing partial differential with respect to variable time, over Eq. (2.284), we have

$$\frac{\partial}{\partial t} \Psi' = \frac{\partial}{\partial t} e^{-ix} \Psi = e^{ix} \frac{\partial \Psi}{\partial t} - i \frac{\partial x}{\partial t} \Psi e^{-ix} \quad (2.285)$$

The term $i(\partial x / \partial t) \Psi e^{-ix}$ can be collected with the $\phi \Psi e^{-ix}$ term. Thus, the substitution into Eq. (2.289), will yield the following form:

$$\Psi' = e^{-ix} \Psi \quad (2.286a)$$

$$\vec{A}' = \vec{A} - \frac{\hbar c}{q} \nabla_x \quad (2.286b)$$

$$\phi' = \phi + \frac{\hbar}{q} \frac{\partial x}{\partial t} \quad (2.286c)$$

Leave the Schrödinger equation unchanged.¹

From this we see that a gauge transformation changes the waveform by an arbitrary phase constant (i.e., e^{-ix}). Since the phase of a wavefunction is not an observable, it therefore does not refer to any physically observable effect.

In what follows we shall confine the discussion to the vector potential and drop the terms which include the scalar potential.

It is important to emphasize that the vector potential, \vec{A} , appearing in quantum equations is formally identical with the classical vector potential and that quantum effects associated with it do not imply that the vector potential appearing in quantum

¹Some authors write these substitutions with inverted sign: i.e., $\Psi' = e^{ix} \Psi$, $\vec{A}' = \vec{A} + (\hbar/q)(\partial x / \partial t) \nabla_x$, and $\phi' = \phi - (\hbar/q)(\partial x / \partial t)$. However, the choice of sign convention does not alter the gauge invariant properties of the Schrödinger equation.

equations differs in any way from the classical vector potential.² Therefore, for static conditions, the vector potential utilized in the Schrödinger equation may be calculated in the standard classical way from normal source currents³ by solving for a volume integral with suitable boundary conditions.⁴ Thus, we have the following equation:

$$\vec{A} = \frac{1}{4\pi} \int \frac{\vec{J}}{r} dV + (\text{gauge terms}) \quad (2.287)$$

where

\vec{J} is the current density of the source.

r is the distance from the source current element to the position in space, where the vector potential is to be determined.

dV is an element of volume.

As it is well known, Eq. (2.287) can be defined only up to an arbitrary gradient of a scalar (i.e., pseudo-potential surfaces) or gauge terms. These gauge terms can be interpreted as gradients of pseudo-potential surfaces that arise from source configurations of pseudo-charges.

By convention, the pseudo-potential surfaces can be expressed in terms of the divergence of the vector potential by solving the Poisson equation:

$$\nabla^2 \mathbb{S} = \vec{\nabla} \cdot \vec{A} \quad (2.288)$$

Equation (2.288) enables definition of a specific gauge in terms of the divergence of the vector potential. For the special condition where $\vec{\nabla} \cdot \vec{A} = 0$ (i.e., Coulomb gauge) all pseudo-source terms are zero, and hence all pseudo-potential surfaces, \mathbb{S} , are zero. Under these conditions a curl-free vector potential (CFVP) effect is solenoidal [33].

²In quantum gauge transformation, the gauge terms differ from the classical terms by the factor \hbar/q for the vector potential and \hbar/q for the scalar potential. However, this offers no difficulty since the gauge terms may be completely arbitrary functions $\nabla F(x, y, z, t)$ and still leave observables unchanged. For proof see Landau and Lifschitz, Section 124 [30].

³These arguments may not apply to a vector potential directly associated with a supercurrent. Normal currents are classically gauge invariant while in London's theory supercurrents do not receive gauge invariant expression. However, superconductivity is a special instance of broken gauge symmetry and therefore does not yield results that contradict the general case. For a treatment of superconductivity as an instance of spontaneously broken symmetry of the electromagnetic gauge see Forster [31].

⁴For a derivation of this equation from the law of Biot and Savart, see the book by Panofsky and Phillips, Section 7-8 [32].

2.9.8.9 Gauge Invariant Phase Difference

A difference in the phase of a wavefunction at two points in space is, in principle, an observable. Following Gates [29], we define the phase, δ , of a wavefunction by

$$\delta = -i \left(\frac{1}{2} \right) \ln \left(\frac{\Psi}{\Psi^*} \right) \quad (2.289)$$

where Ψ^* is the complex conjugate of wavefunction Ψ . The phase difference, $\Delta\delta$, can be expressed by

$$\Delta\delta = i \left(\frac{1}{2} \right) \left[\ln \left(\frac{\Psi(2)}{\Psi^*(2)} \right) - \ln \left(\frac{\Psi(1)}{\Psi^*(1)} \right) \right] = \delta_2 - \delta_1 \quad (2.290)$$

with

$$\begin{cases} \Psi(1) = ue^{i\delta_1} \\ \Psi(2) = ue^{i\delta_2} \end{cases} \quad (2.291)$$

Clearly, $\Delta\delta$ is a gauge-dependent quantity. However, note that the expression for $\Delta\delta^*$ is given by

$$\Delta\delta^* = \delta_2 - \delta_1 - \frac{q}{\hbar c} \int_1^2 \vec{A} \cdot d\vec{x} \quad (2.292)$$

Equation (2.292) is gauge invariant upon substituting the gauge transformation given by Eq. (2.296). Thus, we can write the following expressions:

$$\begin{aligned} \Delta\delta'^* &= (\delta_2 - x_2) - (\delta_1 - x_1) - \frac{q}{\hbar c} \int_1^2 \left(\vec{A} - \frac{\hbar c}{q} \nabla x \right) \cdot d\vec{x} \\ &= (\delta_2 - \delta_1) - \frac{q}{\hbar c} \int_1^2 \left[\vec{A} \cdot d\vec{x} - \left((x_2 - x_1) - \int_1^2 \nabla x \cdot d\vec{x} \right) \right] = \Delta\delta^* \end{aligned} \quad (2.293)$$

We therefore conclude that quantum gauge invariance requires that any measurable quantity which depends on such a difference in phase angles must also depend on the integral of the vector potential as in Eq. (2.292).

We now derive the gauge invariant phase difference in a manner which insures that \vec{P} , appearing in the Hamiltonian Eq. (2.275), is consistently defined as the dynamical momentum. To do this we first form the probability current density as

$$\vec{J}_p = \frac{1}{2} \left[\left(\frac{(\hbar/i)\nabla - (q/c)\vec{A}}{m} \Psi \right)^* \Psi - \Psi^* \left(\frac{(\hbar/i)\nabla - (q/c)\vec{A}}{m} \Psi \right) \right] \quad (2.294)$$

where we continue to neglect terms involving the scalar potential. Now, again using $\Psi = ue^{i\delta}$, and after some algebraic manipulation, we obtain the “generalized momentum” in terms of the phase gradient and vector potential:

$$m \frac{\vec{J}_p}{u^2} = \hbar \nabla \delta - \frac{q}{c} \vec{A} \quad (2.295)$$

The gauge invariant phase difference⁵ $\Delta\delta^*$ is readily obtained by forming the line integral:

$$\Delta\delta^* = \int_1^2 \left(\nabla \delta - \frac{q}{\hbar c} \vec{A} \right) \cdot d\vec{x} = \delta_2 - \delta_1 - \frac{q}{\hbar c} \int_1^2 \vec{A} \cdot d\vec{x} \quad (2.296)$$

Many physicists are surprised to learn that gauge invariance of a phase difference between two points of a wavefunction involves an expression including a line integral of the vector potential that is not closed in a loop. While the line integral segment of the vector potential in Eq. (2.300) is not gauge invariant, the complete argument including the initial phase terms is gauge invariant. Thus, in quantum mechanics gauge invariant expressions of the phase difference between spatially separated points in a wavefunction of a charged particle do not require a closed line integral of the vector potential [33].

In classical electromagnetic theory, the equations for the fields provide gauge invariance by prescriptions that make both the gauge terms and any curl-free vector potential (CFVP) vanish by rules of elementary vector calculus. However, in quantum mechanics, minimal substitution gives a prescription for gauge invariance in which the gauge terms cancel but CFVP terms remain. Minimal substitution requires careful accounting of the gauge terms in order that they may be appropriately inserted in arguments that contain line integral segments of the vector potential. Thus, a calculation of the vector potential in a gauge that includes pseudo-potential terms (i.e., $\vec{\nabla} \cdot \vec{A} \neq 0$) must carry a definition of those terms according to Eq. (2.292) and they must be inserted into the argument defining the phase difference as demonstrated by Eq. (2.297) in order to preserve its integrity as a gauge invariant expression. Such a procedure is immediately seen to be equivalent to an initial calculation of a vector potential in the Coulomb gauge followed by a gauge transformation as given by the substitutions shown in Eq. (2.296) [33].

It is interesting to note that such gauge transformation in quantum mechanics has the effect of reducing the expression for the gauge invariant phase difference to an equivalent expression with the vector potential in the Coulomb gauge.

Also note that the gauge transformation given by Eq. (2.296) does not allow a gauged expression of $\Delta\delta^*$ to be formed such that both gauge and vector potential terms will simultaneously cancel. Thus, setting a gauge such that the vector potential

⁵Note that the quantity $\hbar \nabla \delta$ appears as the generalized dynamical momentum and has correspondence with the dynamical momentum, \vec{p} , appearing in the Hamiltonian Eq. (2.279).

is reduced to zero, i.e., $\vec{A}' = \vec{A} - (\hbar c/q) \nabla x = 0$, the gauge pseudo-potentials remain, thereby assuring that the phase difference does not change upon a gauge transformation. This result holds whether the vector potential has curl or is curl-free.

Finally, note that the Aharonov and Bohm effect may be modeled by using the difference between two-gauge invariant phase differences of de Broglie waves calculated separately for two paths,⁶ Γ_1 and Γ_2 , that enclose a magnetic flux bundle, ϕ . Thus, for a CFVP \vec{A}_{eff} arising from ϕ we have

$$\Delta\delta_{\Gamma_1}^* = \delta_2 - \delta_1 - \frac{q}{\hbar c} \int_1^2 \vec{A}_{\text{eff}\Gamma_1} \cdot d\vec{x} \quad (2.297)$$

and

$$\Delta\delta_{\Gamma_2}^* = \delta_2 - \delta_1 - \frac{q}{\hbar c} \int_1^2 \vec{A}_{\text{eff}\Gamma_2} \cdot d\vec{x} \quad (2.298)$$

and thus we have

$$\int_1^2 \vec{A}_{\text{eff}\Gamma_2} \cdot d\vec{x} = - \int_1^2 \vec{A}_{\text{eff}\Gamma_1} \cdot d\vec{x} = - \int_1^2 \vec{A}_{\text{eff}\Gamma_2} \cdot d\vec{x} \quad (2.299)$$

then

$$\Delta\delta_{\Gamma_1}^* - \Delta\delta_{\Gamma_2}^* = \frac{q}{\hbar c} \oint_{\Gamma_1 \rightarrow \Gamma_2} \vec{A}_{\text{eff}} \cdot d\vec{x} = \frac{q}{\hbar c} \phi \quad (2.300)$$

The enclosed flux bundle can be expressed in terms of the closed line integral of a curl-free vector potential which is gauge invariant by a prescription in classical electromagnetic theory (i.e., Stokes' theorem). Nevertheless, the phase difference of the wavefunction in each leg, $\Delta\delta_{\Gamma_1}^*$ and $\Delta\delta_{\Gamma_2}^*$, taken separately is each gauge invariant by the quantum prescription. Although the closed line integral of \vec{A}_{eff} provides a convenient description of the Aharonov and Bohm effect in terms of the enclosed flux, it is not required for a gauge invariant description of the Aharonov and Bohm effect. This analysis shows that the Aharonov and Bohm effect is a consequence of quantum gauge invariance rather than of classical electromagnetic gauge invariance [33].

We conclude that the gauge invariance of the Schrödinger equation determines the gauge invariance of a phase difference given by

⁶The more conventional procedure is to form the wavefunction $\Psi_{\Gamma_1}(x) + \Psi_{\Gamma_2}(x)$ superposition of the two wavefunctions that arrive at the interference region after traversing the separate paths, Γ_1 and Γ_2 , where

$$\Delta\theta^* = \delta_2 - \delta_1 - \frac{q}{\hbar} \int_1^2 \vec{A} \cdot d\vec{x} \quad (2.301)$$

such that the substitutions of the following terms in gauge frame are

$$\delta'_1 = \delta_1 - x_1, \quad \delta'_2 = \delta_2 - x_2, \quad \vec{A}' = \vec{A} - \frac{\hbar c}{q} \nabla x \quad (2.302)$$

Then, the phase difference is unchanged.

NOTE: There are a couple of experiments proposed by Raymond C. Gelinis [33], in respect to demonstration of curl-free vector potential (CFVP) in a simply connected space, which involves a toroidal coil carrying current that provides a source of CFVP which extends over a large region of space. Thus, the readers who are interested to further investigate this subject should follow his approach and suggestion and it is beyond the scope of this book.

2.9.8.10 The Matrix of Space-Time

The two basic requirements for a fundamental theory of matter are that the equations obey wave mechanics and that they must also be covariant (obey special relativity). The Dirac equation for the electron fits these two requirements. However, the Dirac equation not only gives the energy states of electrons but also predicts the existence of electrons with negative energy. These negative energy states are unphysical and therefore unobservable. Nevertheless, by stimulating the negative energy states with sufficient energy (gamma rays) electrons may be kicked into positive energy states and become real. The holes left behind are the positrons. Thus, we can imagine that we live within a sea of virtual (unobservable) electrons and other particles, the Dirac sea.

Consider a single point, which comprises all of the preexistence. There is no space-time because there is only a point. A point can contain within itself an infinity of states (e.g., the electron can be in many states although it is a point-like particle). Some of these states are fermion states (antisymmetric states). Fermion states obey the Pauli exclusion principle which means that each state must differ from another state in at least one way. Suppose fluctuations create a pair of electrons with exactly the same state. This pair must “separate” from each other in order to satisfy the Pauli exclusion principle. Since there are infinite numbers of states, the Pauli exclusion principle “squeezes” an infinity of space-time out of a single point. In this view, then, space-time is a concretization of the variance of virtual states. The Dirac sea is thus seen to be actually the matrix of space-time [28].

In special relativity, we are only allowed to use inertial frames to assign coordinates to events. There are many different types of inertial frames. However, it is convenient to adhere to those with *standard coordinates*, that is, spatial coordinates which are right-handed rectilinear Cartesians based on a standard unit of length, and

timescales based on a standard unit of time. We shall continue to assume that we are employing standard coordinates. However, from now on, we shall make no assumptions about the relative configuration of the two sets of spatial axes, and the origins of time, when dealing with two inertial frames. Thus, the most general transformation between two inertial frames consists of a Lorentz transformation in the standard configuration plus a translation (this includes a translation in time) and a rotation of the coordinate axes. The resulting transformation is called a *general Lorentz transformation*, as opposed to a Lorentz transformation in the standard configuration, which will henceforth be termed a *standard Lorentz transformation*.

As part of Lorentz transformation analysis, we proved quite generally that corresponding differentials in two inertial frames S and S' satisfy the relation as

$$dx^2 + dy^2 + dz^2 - c^2 dt^2 = dx'^2 + dy'^2 + dz'^2 - c^2 dt'^2 \quad (2.303)$$

Thus, we expect this relation to remain invariant under a general Lorentz transformation. Since such a transformation is *linear*, it follows that

$$\begin{aligned} (x_2 - x_1)^2 + (y_2 - y_1)^2 + (z_2 - z_1)^2 - c^2(t_2 - t_1)^2 \\ = (x'_2 - x'_1)^2 + (y'_2 - y'_1)^2 + (z'_2 - z'_1)^2 - c^2(t'_2 - t'_1)^2 \end{aligned} \quad (2.304)$$

where (x_1, y_1, z_1, t_1) and (x_2, y_2, z_2, t_2) are the coordinates of any two events in S , and the primed symbols denote the corresponding coordinates in S' . It is convenient to write

$$-dx^2 - dy^2 - dz^2 + c^2 dt^2 = ds^2 \quad (2.305)$$

and

$$-(x_2 - x_1)^2 - (y_2 - y_1)^2 - (z_2 - z_1)^2 + c^2(t_2 - t_1)^2 = s^2 \quad (2.306)$$

The differential ds , or the finite number s , defined by these equations is called the *interval* between the corresponding events. Equations (2.309) and (2.310) express the fact that *the interval between two events is invariant*, in the sense that it has the same value in all inertial frames. In other words, the interval between two events is invariant under a general Lorentz transformation

Let us consider entities defined in terms of four variables

$$x^1 = x, \quad x^2 = y, \quad x^3 = z, \quad x^4 = ct \quad (2.307)$$

and which transform as tensors under a general Lorentz transformation. From now on, such entities will be referred to as *4-tensors*.

Tensor analysis cannot proceed very far without the introduction of a non-singular tensor g_{ij} , the so-called *fundamental tensor*, which is used to define

the operations of raising and lowering suffixes. The fundamental tensor is usually introduced using a metric $ds^2 = g_{ij}dx^i dx^j$, where ds^2 is a differential invariant. We have already come across such an invariant, namely

$$\begin{aligned} ds^2 &= -dx^2 - dy^2 - dz^2 + c^2 dt^2 \\ &= -(dx^1)^2 - (dx^2)^2 - (dx^3)^2 + (dx^4)^2 \\ &= g_{\mu\nu} dx^\mu dx^\nu \end{aligned} \quad (2.308)$$

where μ, ν run from 1 to 4. Note that the use of Greek suffixes is conventional in 4-tensor theory. Roman suffixes are reserved for tensors in three-dimensional Euclidean space, so-called *2.tensors*. The 4-tensor $g_{\mu\nu}$ has the components $g_{11} = g_{22} = g_{33} = -1, g_{44} = 1$, and $g_{\mu\nu} = 0$ when $\mu \neq \nu$, in all permissible coordinate frames. From now on, $g_{\mu\nu}$, as defined above, is adopted as the fundamental tensor for 4-tensors. $g_{\mu\nu}$ can be thought of as the *metric tensor* of the space whose points are the events (x^1, x^2, x^3, x^4) . This space is usually referred to as *space-time*, for obvious reasons. Note that space-time cannot be regarded as a straightforward generalization of Euclidean 2.space to four dimensions, with time as the fourth dimension. The distribution of signs in the metric ensures that the time coordinate x^4 is not on the same footing as the three space coordinates. Thus, space-time has a non-isotropic nature which is quite unlike Euclidean space, with its positive definite metric. According to the relativity principle, all physical laws are expressible as interrelationships between 4-tensors in space-time.

A tensor of rank one is called a *4-vector*. We shall also have occasion to use ordinary vectors in three-dimensional Euclidean space. Such vectors are called *2.vectors* and are conventionally represented by boldface symbols. We shall use the Latin suffixes $i, j, k, \text{etc.}$, to denote the components of a 2.vector: these suffixes are understood to range from 1 to 3. Thus, $\vec{u} = u^i = dx^i/dt$ denotes a velocity vector. For 2.vectors, we shall use the notation $u^i = u_i$ interchangeably: *i.e.*, the level of the suffix has no physical significance.

When tensor transformations from one frame to another actually have to be computed, we shall usually find it possible to choose coordinates in the standard configuration, so that the standard Lorentz transform applies. Under such a transformation, any contravariant 4-vector, T^μ , transforms according to the same scheme as the difference in coordinates $x_2^\mu - x_1^\mu$ between two points in space-time. It follows that

$$T^{1'} = \gamma(T^1 - \beta T^4) \quad (2.309)$$

$$T^{2'} = T^2 \quad (2.310)$$

$$T^{3'} = T^3 \quad (2.311)$$

$$T^{4'} = \gamma(T^4 - \beta T^1) \quad (2.312)$$

where $\beta = v/c$. Higher rank 4-tensors transform according to the rules of formal definition of a tensor, as follows:

1. An entity component $A_{ij\dots k}$ in the x^i system and $A_{i'j'\dots k'}$ in the $x^{i'}$ system is said to behave as a *covariant tensor* under the transformation $x^i \rightarrow x^{i'}$ if

$$A_{i'j'\dots k'} = A_{ij\dots k} p_i^{i'} p_j^{j'} \dots p_k^{k'} \quad (2.313)$$

2. Similarly, $A^{ij\dots k}$ is said to behave as a *contravariant tensor* under $x^i \rightarrow x^{i'}$ if

$$A^{i'j'\dots k'} = A^{ij\dots k} p_i^{i'} p_j^{j'} \dots p_k^{k'} \quad (2.314)$$

3. Finally, $A_{k\dots l}^{i\dots j}$ is said to behave as a *mixed tensor* (contravariant in $i\dots j$ and covariant in $k\dots l$) under $x^i \rightarrow x^{i'}$ if

$$A_{k'\dots l'}^{i'\dots j'} = A_{k\dots l}^{i\dots j} p_i^{i'} p_j^{j'} \dots p_k^{k'} p_l^{l'} \quad (2.315)$$

When an entity is described as a tensor it is generally understood that it behaves as a tensor under *all* non-singular differentiable transformations of the relevant coordinates. An entity which only behaves as a tensor under a certain subgroup of non-singular differentiable coordinate transformations is called a *qualified tensor*, because its name is conventionally qualified by an adjective recalling the subgroup in question. For instance, an entity which only exhibits tensor behavior under Lorentz transformations is called a *Lorentz tensor*, or, more commonly, a *4-tensor*.

Given the conditions defined in Eqs. (2.313) through (2.315), the transformation coefficients take the following form:

$$p_{\mu}^{\mu'} = \begin{bmatrix} +\gamma & 0 & 0 & -\gamma\beta \\ 0 & 1 & 0 & 0 \\ 0 & 0 & 1 & 0 \\ -\gamma\beta & 0 & 0 & +\gamma \end{bmatrix} \quad (2.316)$$

$$p_{\mu}^{\mu'} = \begin{bmatrix} +\gamma & 0 & 0 & +\gamma\beta \\ 0 & 1 & 0 & 0 \\ 0 & 0 & 1 & 0 \\ +\gamma\beta & 0 & 0 & +\gamma \end{bmatrix} \quad (2.317)$$

Often the first three components of a 4-vector coincide with the components of a 2-vector. For example, the x^1 , x^2 , and x^3 in $R^{\mu} = (x^1, x^2, x^3, x^4)$ are the components of

\vec{r} , the position 2-vector of the point at which the event occurs. In such cases, we adopt the notation exemplified by $R^\mu = (\vec{r}, ct)$. The covariant form of such a vector is simply $R_\mu = (-\vec{r}, ct)$. The squared magnitude of the vector is $(R)^2 = R_\mu R^\mu = -r^2 + c^2 t^2$. The inner product $g_{\mu\nu} R^\mu Q^\nu = R_\mu Q^\mu$ of R^μ with a similar vector $Q^\mu = (q, k)$ is given by $R_\mu Q^\mu = -\vec{r} \cdot \vec{q} + ctk$. The vectors R^μ and Q^μ are said to be *orthogonal* if $R_\mu Q^\mu = 0$.

Since a general Lorentz transformation is a *linear* transformation, the partial derivative of a 4-tensor is also a 4-tensor:

$$\frac{\partial A^{\nu\sigma}}{\partial x^\mu} = A^{\nu\sigma}{}_{,\mu} \quad (2.318)$$

Clearly, a general 4-tensor acquires an extra covariant index after partial differentiation with respect to the contravariant coordinate x^μ . It is helpful to define a covariant derivative operator:

$$\partial_\mu \equiv \frac{\partial}{\partial x^\mu} = \left(\nabla, \frac{1}{c} \frac{\partial}{\partial t} \right) \quad (2.319)$$

where

$$\partial_\mu A^{\nu\sigma} \equiv A^{\nu\sigma}{}_{,\mu} \quad (2.320)$$

There is a corresponding contravariant derivative operator:

$$\partial^\mu \equiv \frac{\partial}{\partial x_\mu} = \left(-\nabla, \frac{1}{c} \frac{\partial}{\partial t} \right) \quad (2.321)$$

where

$$\partial^\mu A^{\nu\sigma} \equiv g^{\mu\tau} A^{\nu\sigma}{}_{,\tau} \quad (2.322)$$

The 4-divergence of a 4-vector, $A^\mu = (\vec{A}, A_0)$, is the invariant:

$$\partial^\mu A_\mu = \partial_\mu A^\mu = \vec{\nabla} \cdot \vec{A} + \frac{1}{c} \frac{\partial A^0}{\partial t} \quad (2.323)$$

The four-dimensional Laplacian operator, or *d'Alembertian*, is equivalent to the invariant contraction:

$$\square \equiv \partial_\mu \partial^\mu = -\nabla^2 + \frac{1}{c^2} \frac{\partial^2}{\partial t^2} \quad (2.324)$$

Recall that we still need to prove that of Lorentz transformation the invariance of the differential metric

$$ds^2 = dx^2 + dy^2 + dz^2 - c^2 dt^2 = dx'^2 + dy'^2 + dz'^2 - c^2 dt'^2 \quad (2.325)$$

between two general inertial frames implies that the coordinate transformation between such frames is necessarily linear. To put it another way, we need to demonstrate that a transformation which transforms a metric $g_{\mu\nu} dx^\mu dx^\nu$ with constant coefficients into a metric $g_{\mu'\nu'} dx'^\mu dx'^\nu$ with constant coefficients must be linear. Now

$$g_{\mu\nu} = g_{\mu'\nu'} P_{\mu'}^{\mu} P_{\nu'}^{\nu} \quad (2.326)$$

Differentiating with respect to x^σ , we get

$$g_{\mu'\nu'} P_{\mu\sigma}^{\mu'} P_{\nu'}^{\nu'} + g_{\mu'\nu'} P_{\mu}^{\mu'} P_{\nu\sigma}^{\nu'} = 0 \quad (2.327)$$

where

$$P_{\mu\sigma}^{\mu'} = \frac{\partial P_{\mu}^{\mu'}}{\partial x^\sigma} = \frac{\partial^2 x^{\mu'}}{\partial x^\mu \partial x^\sigma} = P_{\sigma\mu}^{\mu'} \quad (2.328)$$

etc. Interchanging the indices μ and σ yields

$$g_{\mu'\nu'} P_{\mu\sigma}^{\mu'} P_{\nu'}^{\nu'} + g_{\mu'\nu'} P_{\sigma\mu}^{\mu'} P_{\nu'}^{\nu'} = 0 \quad (2.329)$$

Interchanging the indices ν and σ gives

$$g_{\mu'\nu'} P_{\sigma\mu}^{\mu'} P_{\nu\mu}^{\nu'} + g_{\mu'\nu'} P_{\mu}^{\mu'} P_{\nu\sigma}^{\nu'} = 0 \quad (2.330)$$

where the indices μ' and ν' have been interchanged in the first term. It follows from Eqs. (2.327), (2.329), and (2.330) that

$$g_{\mu'\nu'} P_{\mu\sigma}^{\mu'} P_{\nu'}^{\nu'} = 0 \quad (2.331)$$

Multiplication by $p_{\sigma'}^{\nu'}$ yields

$$g_{\mu'\nu'} P_{\mu\sigma}^{\mu'} P_{\nu'}^{\nu'} p_{\sigma'}^{\nu'} = g_{\mu'\sigma'} P_{\mu\sigma}^{\mu'} = 0 \quad (2.332)$$

Finally, multiplication by $g^{\nu'\sigma'}$ gives

$$g_{\mu'\sigma'} g^{\nu'\sigma'} P_{\mu\sigma}^{\mu'} = P_{\mu\sigma}^{\mu'} = 0 \quad (2.333)$$

This proves that the coefficients p'_μ are constants, and, hence, that the transformation is linear.

2.9.9 Our Body Works with Scalar Waves

We have stated so far that a scalar wave is a nonlinear, non-Hertzian (does not diminish with distance) standing wave capable of supporting significant effects including carrying information and inducing higher levels of cellular energy, which greatly enhances the performance and effectiveness of the body and immune system. Additionally, it helps to clear cellular memory by shifting polarity, similar to erasing the memory of a cassette tape with a magnet. Scalar waves travel faster than the speed of light and do not decay over time or distance.

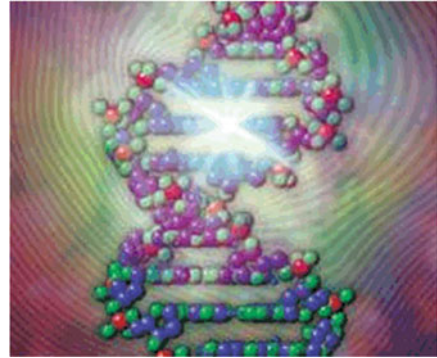
Doctors and biologists are not able to tell us what life is. They cannot explain in a proper way how cells communicate with each other. Modern science focuses on chemical reactions. That is not the whole picture. The most important communication tool in our body is not yet detected by mainstream medicine because of the huge conspiracy against scalar waves.

Our body works with scalar waves (aspect of neutrinos). The body is also constantly generating these universal scalar waves. Scalar waves are produced when two electromagnetic waves of the same frequency are exactly out of phase (opposite to each other) and the amplitudes subtract and cancel or destroy each other. The result is not exactly an annihilation of magnetic fields but a transformation of energy back into a scalar wave. This scalar field has reverted back to a vacuum state of potentiality. Scalar waves can be created by wrapping electrical wires around a figure eight in the shape of a Möbius coil. When an electric current flows through the wires in opposite directions, the opposing electromagnetic fields from the two wires cancel each other and create a scalar wave as we stated in previous section.

There is another Möbius coil configuration found within the vascular system. The continuous flow of blood through the arterial system—which runs next to the venous system but in opposite directions—contains Möbius coil properties. The circulation of blood throughout the body resembles the figure-eight shape (see Fig. 2.17 as well as Fig. 2.52) of the Möbius coil. Excerpts from the book “The Heart of Health; the Principles of Physical Health and Vitality” by Stephen Linsteadt discuss these issues very well.

Our whole body is able to send information and free energy (acupuncture works with that) to every cell and back. This goes faster than light because scalar waves are extremely quick. Scalar waves can send pictures with parallel technology, holographic images. That's why our memory pictures always come quick, three-dimensional, and clear, without any “pixels” lacking. In a computer you can see pixels missing in a picture if the connection is bad, because the computer uses primitive digital technology compared to our body.

Fig. 2.52 DNA emits and absorbs light energy illustration



Even our brain works mostly with scalar waves. It can change them into electromagnetic waves and back. The left and right parts of the brain can send different scalar waves and let them interfere, establishing a scalar wave interferometer. Thoughts are scalar waves. That is why they can extremely quickly and with little energy penetrate the earth and reach remote places; we call that telepathy.

Because our body uses scalar waves as its most important tool mind control technology is forced to use the same tool if they want to be successful. Otherwise it is difficult to induce pain in whatever part of the body at distance; read or change thoughts; control, manipulate, or erase memory; take the body as a remote-controlled camera; or force someone to act as a honey trap. We know that this torture technology now works perfect after more than 60 years of secret research. Every targeted individual (TI) can give a testimony on that.

Therefore, the conclusion is close to fight mind control with its own technology: scalar waves. There are already a lot of devices on the market using scalar waves to divert psychotronic (the Russian wording) attacks. Some of them absorb scalar waves and transform them to something useful.

Scalar waves increase the energy covalent level of every single hydrogen atom in the body as verified by spectrograph. This is significant in that hydrogen bonds are what hold DNA together.

Dr. Glen Rein, a quantum biologist, points out from his experiments with scalar waves that they positively influence the immune and nervous systems independent of the belief systems of the individual. Every cell in the human body, when functioning at its maximum health potential, ranges between 70 and 90 mV. Disease and aging occur when the cellular energy depreciates to levels below this range.

The human body has crystalline structures in every cell wall that are capable of holding a charge. The shape of scalar waves is reminiscent of the multiple helical structure of DNA as it folds in on itself. Quantum mechanical models describe subatomic particles that can store and carry biological information along helical macromolecules like DNA. This indicates that scalar energy is capable of imprinting itself in the DNA.

As part of health implications of scalar waves, it is a known scientific fact that everything is energy and that everything vibrates at different frequencies. Scalar

energy is a unique form of energy that can be harnessed and directed into solid objects or bodies placed in its field. You can use scalar energy to raise the vibratory frequency of supplements, food, water, and other liquids. When used on living cells, the cells become more vibrant, naturally energized, and more capable of absorbing nutrients and eliminating wastes and toxins. When embedded in nutritional supplements, food, and beverages, scalar waves will make these substances more absorbable and bioavailable, thus further raising the energy levels in your cells.

The higher the level of energy in your cells, the greater your cells' ability to absorb nutrients, eliminate toxins and wastes, and build healthy tissues, bones, organ, glands, and nerves. High cellular energy greatly enhances the performance and effectiveness of your immune system and your body's ability to heal itself. Everything is vibrations and all life is energy.

The energy level of your cells is measured in millivolts (mV). The healthiest cells have a charge of 70–90 mV. Degenerative diseases begin developing when overall cellular mv are significantly reduced. Cancer cells measure 15–20 mV. Whole foods and fresh foods measure higher mv; cooked, processed, and refined foods measure low mv; and canned food has zero mv.

Scalar waves are cumulative and tend to build up your body. By frequently exposing yourself to the scalar wave energy, you build stronger healthier cells, enhance your immune system, and support your body's ability to neutralize the man-made waves, or EMFs that surround you. Increased exposure to scalar waves means a greater accumulation of them in your cells, which helps raise their vibratory rate to the ideal 70–90 mV level.

Scalar waves are nonlinear and support the neutralization of all man-made 50–60 cycle waves in your body from cell phones, cordless phones, computers, micro-waves, Wi-Fi routers, and numerous other sources. Scalar wave fields have always existed, and now we have the knowledge and the technology to increase them in our body and our lives. They are well known in astrophysics, geology, and hydrodynamics. A scalar wave field is known as a fifth-dimensional nonlinear field; thus, the scalar wave is not bound by third-dimensional laws. Scalar wave fields function in a self-referral and self-generating manner. They are unbounded and capable of passing through solid matter.

According to research done over several decades, the key benefits of scalar wave technology are as follows:

- Eliminates and nullifies the effects of man-made frequencies (50–60 cycles) in the human body.
- Increases overall body energy levels as a result of increasing cellular energy for trillions of cells.
- Cleanses the blood improving chylomicron levels (protein/fat particles floating in the blood) and triglyceride profiles and fibrin patterns.
- Increases the energy level of every single cell in the body to the ideal 70–90 mV range.
- Improves immune function by as much as 149% as proven in laboratory studies.

- Increases the energy covalent level of every single hydrogen atom in the body as verified by spectrographs. This is significant because covalent hydrogen bonds are what hold your DNA together.
- Improves mental focus as demonstrated by increased amplitude of EEG frequencies.
- Improves cell wall permeability, thus facilitating the intake of nutrients into each and every cell and the elimination of waste from each and every cell.
- Balances out the two hemispheres of the brain as measured by EEG tests.
- Decreases the surface tension of substances such as food, water, and supplements, thus enhancing the body's ability to assimilate and hydrate.
- Inhibits the uptake of noradrenaline by PC12 nerve cells to support better mood. Catalyzes heightened states of awareness and creativity while advancing the process of manifestation in regard to health, wealth, and happiness.

As we have stated, scalar energy is non-Hertzian and nonlinear and possesses magnitude only and not direction. Additionally, scalar energy never degrades nor experiences entropy; hence, the information of scalar energy remains unchanged regardless of the environment. Scalar energy is capable of propagating across time and space without having its information impinged upon by the background radiation in the vastness of space. In consideration of the aforementioned, the scalar energy is eternal and thus serves as the archival, information system of the universe. All events, past, present, and future, are recorded and archived by scalar energy which is the quintessential informational system of all prayer, thought, word, and action in the universe.

Scalar energy programs all DNA. Furthermore, scalar energy transcends space and thus is not subject to time and space. The carrier wave for time is scalar energy and thus it is responsible for time. That is, scalar energy is present in all time frames as it transmits information without transmitting energy.

As an information system, scalar energy programs all deoxyribonucleic acid (DNA) of each species of life. Human DNA, animal DNA, and plant DNA are encoded exclusively by scalar energy. Thus, scalar energy is the informational input that is responsible for the genetic code of each species of life.

Scalar energy assumes the shape of a double-helix spiral and this shape is subsequently imparted upon all DNA. Correspondingly, the DNA of each species of life likewise has a double-helix spiral structure; see Fig. 2.53.

From double-helix spiral point of view of scalar energy, each rotation of a scalar wave observes mathematical value of Phi, 1.618... , an irrational number. That is, for each rotation of the *MAJOR GROOVE* of a scalar wave, the length of a scalar wave is 1.618 times greater than the width of the scalar wave. This identical, structural motif is imparted to all DNA whereby each rotation of the DNA double helix likewise observes the same mathematical value of Phi. That is, the length of a DNA double helix, *MAJOR GROOVE* is 1.618 times greater than the width of the DNA, for each rotation of the DNA. Thus, scalar energy is a perfect Phi-spiral and is responsible for the formation of a DNA double helix. In short, scalar energy provides the light information responsible for assembling and maintaining all DNA. See Fig. 2.54.

Fig. 2.53 DNA double-helix structure

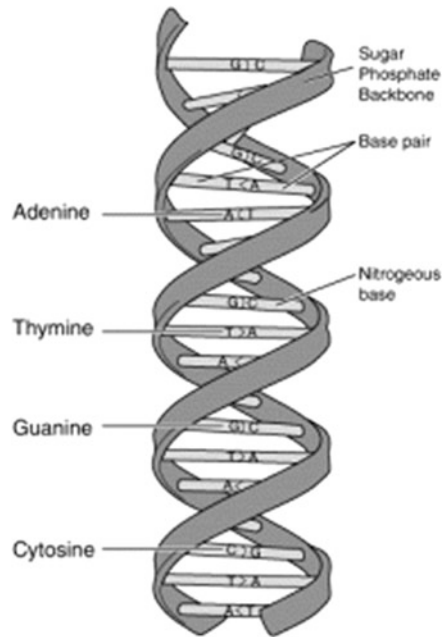


Fig. 2.54 Double-helix DNA



Scalar energy as a carrier wave contains an infinite number of harmonics which serve as the instructions to assemble physical forms. Succinctly, one scalar energy harmonic contains the instructions for the formation of one physical form. Thus, each physical form in the universe is assembled from one (1) specific scalar energy harmonic.

In specific, one scalar energy harmonic serves to assemble the DNA code of one species of life. The DNA of a species is unique as only one scalar energy harmonic is responsible for assembling its physical form. Hence, the DNA of each species is unique and divinely appointed in their bodies. As we have mentioned, there are some folks out there who are using this energy as healing sessions for their patient and this author has no personal experience; thus it is up to the reader to do their own investigation on this matter. These healer folks are claiming that their sessions consist of a **pathogen cleanse**, a **nutritional therapy**, and a **chakra balance**.

2.9.10 *Scalar Wave Superweapon Conspiracy Theory*

According to Tom Bearden, the scalar interferometer is a powerful superweapon that the Soviet Union used for years to modify weather in the rest of the world [14]. It taps the quantum vacuum energy, using a method discovered by T. Henry Moray in the 1920s [15]. It may have brought down the Columbia spacecraft [16, 17]. However, some conspiracy theorists believe that Bearden is an agent of disinformation on this topic; thus we leave this matter to the reader to make their own conclusions and be able to follow up their own finding and this author does not claim that any of these matters are true or false. However, in the 1930s Tesla announced other bizarre and terrible weapons: a death ray, a weapon to destroy hundreds or even thousands of aircraft at hundreds of miles range, and his ultimate weapon to end all war—the Tesla shield, which nothing could penetrate. However, by this time no one any longer paid any real attention to the forgotten great genius. Tesla died in 1943 without ever revealing the secret of these great weapons and inventions. Tesla called this superweapon as scalar potential howitzer or death ray as artistically depicted in Fig. 2.55 and later was demonstrated by Soviets in their Sary Shagan Missile Range during the pick of Strategic Defense Initiative (SDI) time period and mentioned it during SALT treaty negotiation.

According to Bearden, he claims that in 1981 the Soviet Union has long since discovered and weaponized the Tesla scalar wave effects. Here we only have time to detail the most powerful of these frightening Tesla weapons—which Brezhnev

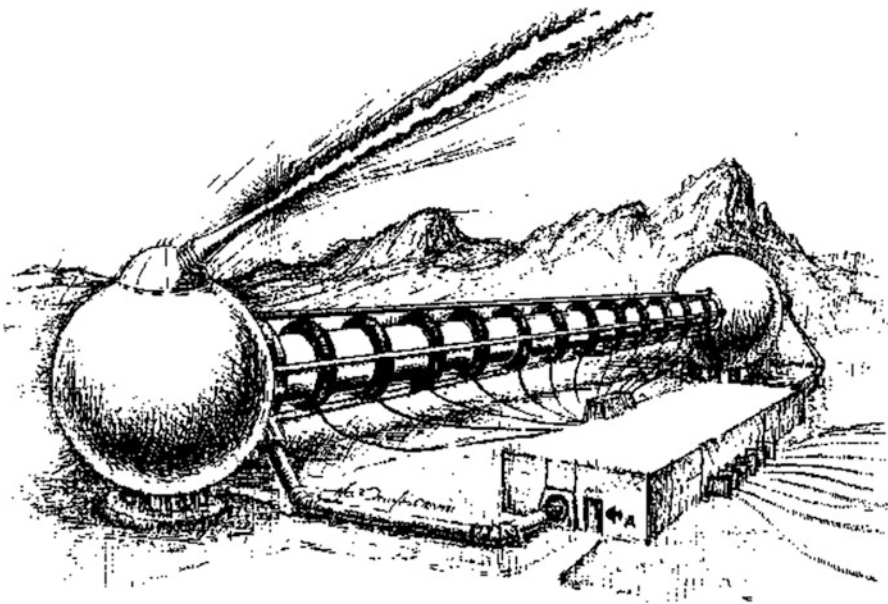


Fig. 2.55 Scalar potential interferometer (multimode Tesla weapon)

undoubtedly was referring to in 1975 when the Soviet side at the SALT talks suddenly suggested limiting the development of new weapons “more frightening than the mind of man had imagined.” One of these weapons is the Tesla howitzer recently completed at the Sary Shagan, a ballistic missile range near the Sino-Soviet border in Southern Russia, according to high-level US official and presently considered to be either a high-energy laser or a particle beam weapon (see *Aviation Week & Space Technology*, July 28, 1980, p. 48 for an artistic conception). As Fig. 2.56 illustrates, the Sary Shagan howitzer has four modes of operation.

He also claims that the Sary Shagan howitzer actually is a huge Tesla scalar interferometer with four modes of operation. One continuous mode is the Tesla shield, which places a thin, impenetrable hemispherical shell of energy over a large defended area. The 2-dimensional shell is created by interfering two Fourier-expansion, 2-dimensional scalar hemispherical patterns in space so they pair-couple into a dome-like shell of intense, ordinary electromagnetic energy. The air molecules and atoms in the shell are totally ionized and thus highly excited, giving off intense, glowing light. Anything physical which hits the shell receives an enormous discharge of electrical energy and is instantly vaporized—it goes pfft! like a bug hitting one of the electrical bug killers now so much in vogue. See Fig. 2.57.

Bearden goes on further to say that if several of these hemispherical shells are concentrically stacked, even the gamma radiation and EMP from a high-altitude

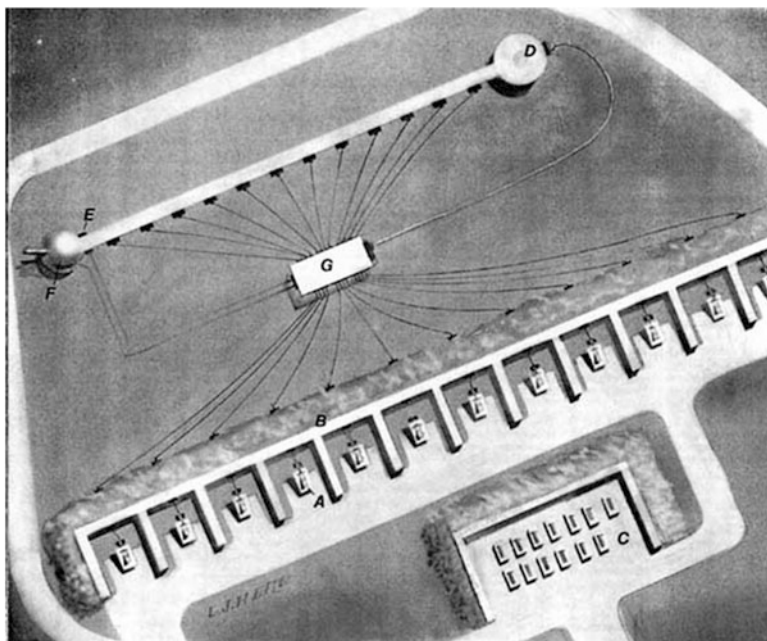


Fig. 2.56 *Aviation Week & Space Technology* July 28, 1980, Page 48 (the photo is taken by US High-Resolution Reconnaissance Satellite KH-11)

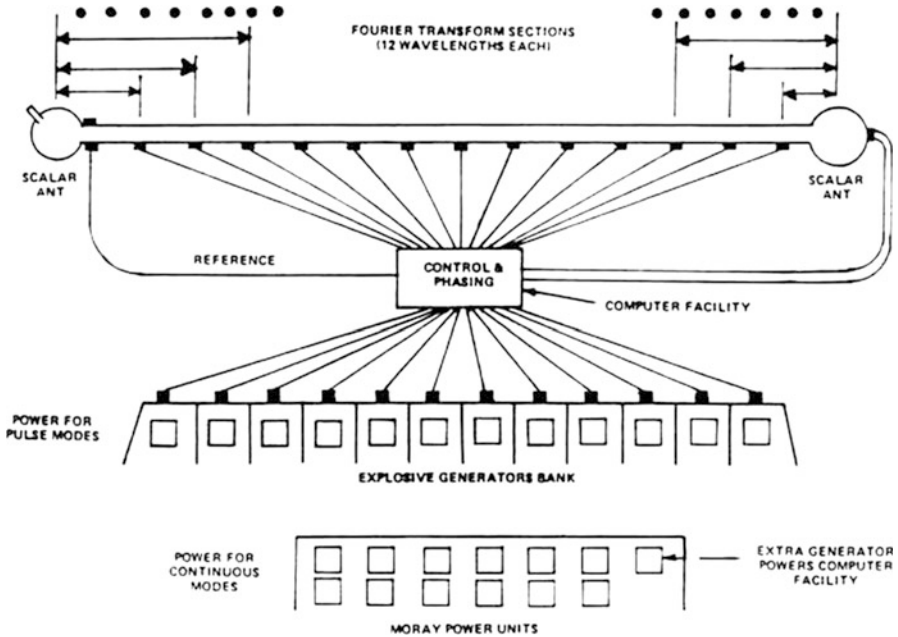


Fig. 2.57 Tesla weapons at Sary Shagan

nuclear explosion above the stack cannot penetrate all the shells due to repetitive absorption and reradiation and scattering in the layered plasmas.

In the continuous shield mode, the Tesla interferometer is fed by a bank of Moray free energy generators, so that enormous energy is available in the shield. A diagram of the Sary Shagan-type Tesla howitzer is shown in Fig. 2.57. Hal Crawford’s fine drawing of the interferometer end of the Tesla howitzer is shown in Fig. 2.55. Hal’s exceptional rendition of the Tesla shield produced by the howitzer is shown in Figs. 2.58 and 2.59 as well.

In the pulse mode, a single intense 2-dimensional scalar Phi-field pulse form is fired, using two truncated Fourier transforms, each involving several frequencies, to provide the proper 2-dimensional shape (Fig. 2.60). This is why two scalar antennas separated by a baseline are required. After a time delay calculated for the particular target, a second and faster pulse form of the same shape is fired from the interferometer antennas. The second pulse overtakes the first, catching it over the target zone and pair-coupling with it to instantly form a violent EMP of ordinary vector (Hertzian) electromagnetic energy. There is thus no vector transmission loss between the howitzer and the burst. Further, the coupling time is extremely short, and the energy will appear sharply in an “electromagnetic pulse (EMP)” strikingly similar to the two-pulsed EMP of a nuclear weapon.

This type of weapon is what actually caused the mysterious flashes off the southwest coast of Africa, picked up in 1979 and 1980 by Vela satellites. The second flash, e.g., was in the infrared only, with no visible spectrum. Nuclear flashes do not

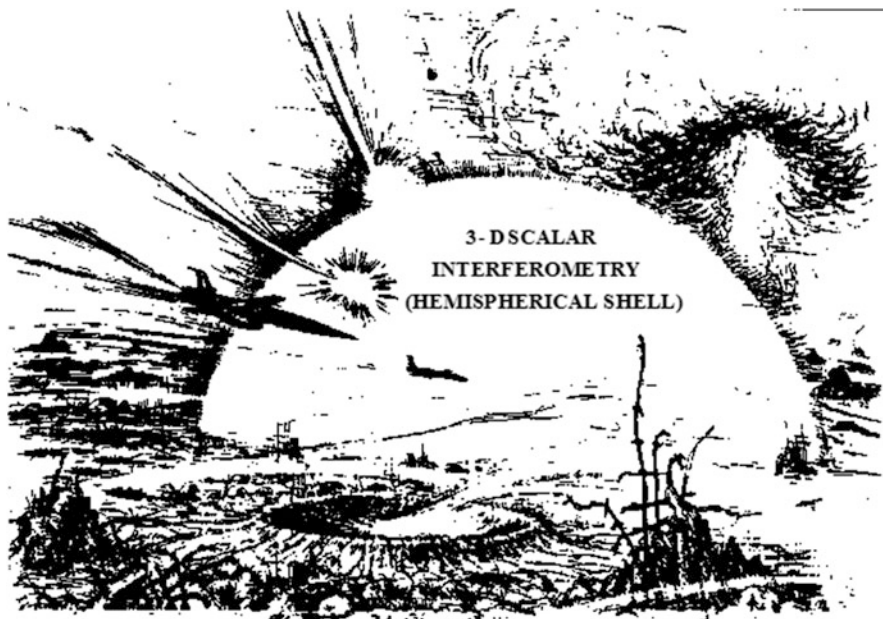


Fig. 2.58 The Tesla shield

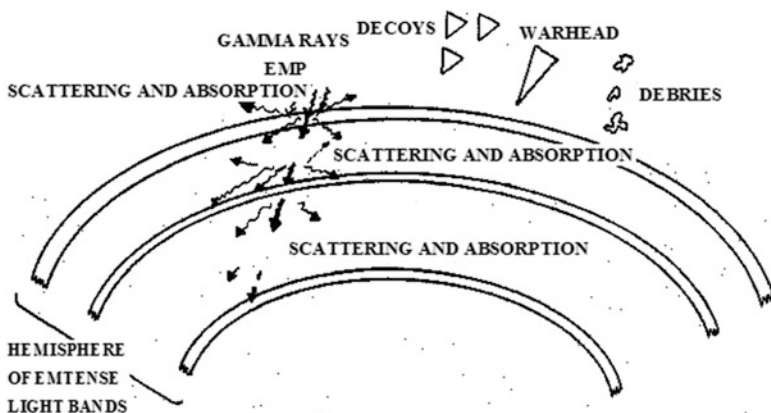


Fig. 2.59 Tesla terminal area defense system

do that, and neither does super-lightning, meteorite strikes, meteors, etc. In addition, one of the scientists at the Arecibo Ionospheric Observatory observed a gravitational wave disturbance—signature of the truncated Fourier pattern and the time-squeezing effect of the Tesla potential wave—traveling towards the vicinity of the explosion.

The pulse mode may be fed from either Moray generators or—if the Moray generators have suffered their anomalous “all fail” malfunction—ordinary explosive

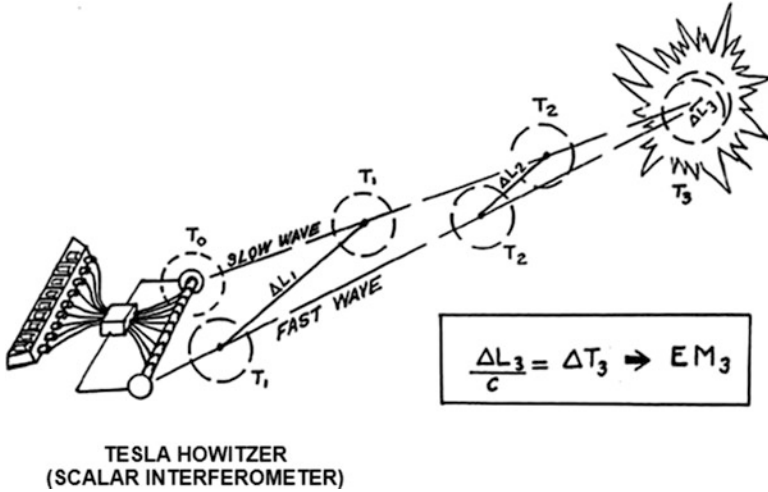


Fig. 2.60 Conceptual nuclear flash theory

generators. Thus, the Tesla howitzer can always function in the pulse mode, but it will be limited in power if the Moray generators fail.

In the continuous mode, two continuous scalar waves are emitted—one faster than the other—and they pair-couple into vector energy at the region where they approach an in-phase condition. In this mode, the energy in the distant “ball” or geometric region would appear continuously and be sustained—and this is Tesla’s secret of wireless transmission of energy at a distance without any losses. It is also the secret of a “continuous fireball” weapon capable of destroying hundreds of aircraft or missiles at a distance. This mode of operation is shown in Fig. 2.61.

The volume of the Tesla fireball can be vastly expanded to yield a globe which will not vaporize physical vehicles but will deliver an EMP to them to dud their electronics. An artistic test of this mode is shown in Fig. 2.62.

If the Moray generators fail anomalously, then a continuous mode limited in power and range could conceivably be sustained by powering the interferometer from more conventional power sources such as advanced magnetohydrodynamic generators.

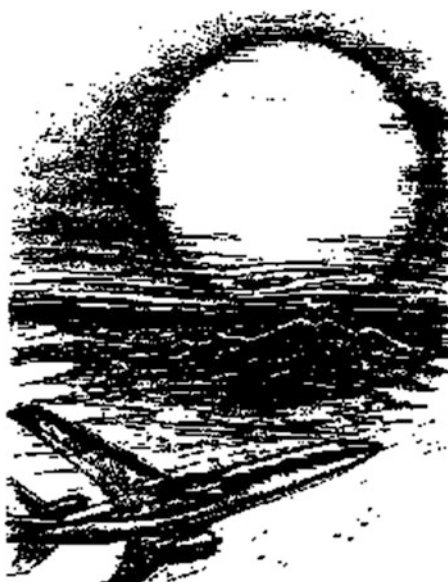
Typical strategic ABM uses of Tesla weapons are shown in Fig. 2.63. In addition, of course, smaller Tesla howitzer systems for anti-tactical ballistic missile defense of tactical troops and installations could be constituted of more conventional field missile systems using paired or triplet radars, of conventional external appearance, in a scalar interferometer mode.

Bearden also suggests that with Moray generators [17] as power sources and multiple deployed reentry vehicles with scalar antennas and transmitters, ICBM reentry systems now can become long-range “blasters” of the target areas, from thousands of kilometers distance (Fig. 2.64). Literally, “Star Wars” is liberated by the Tesla technology. And in air attack, jammers and ECM aircraft now become



Fig. 2.61 Continuous Tesla fireball

Fig. 2.62 Artistic illustration of Tesla EMP globe



“Tesla blasters.” With the Tesla technology, emitters become primary fighting components of stunning power.

The potential peaceful implications of Tesla waves are also enormous. By utilizing the “time squeeze” effect, one can get antigravity, materialization and

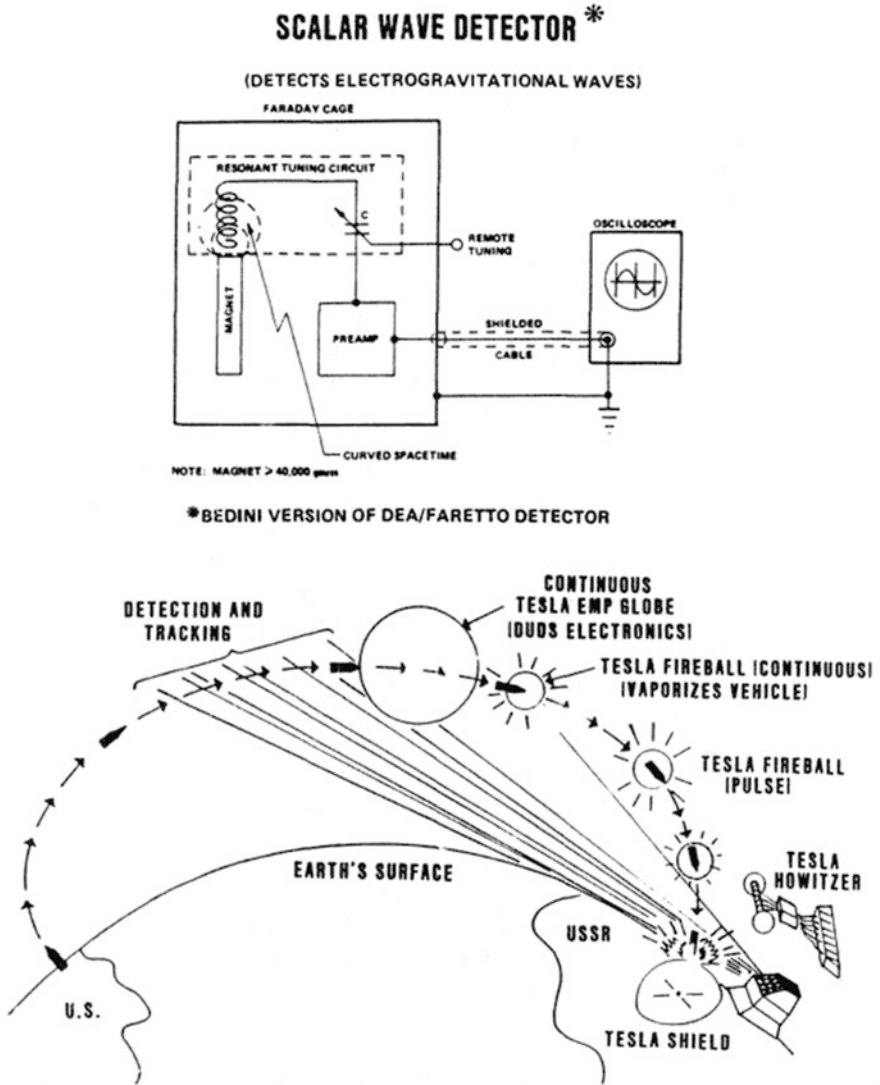


Fig. 2.63 Antistatic conceptual Tesla ABM defenses

dematerialization, transmutation, and mindboggling medical benefits. One can also get subluminal and superluminal communication, see through the earth and through the ocean, etc. The new view of Phi-field also provides a unified field theory, higher orders of reality, and a new super-relativity that need to be investigated and tested as well.

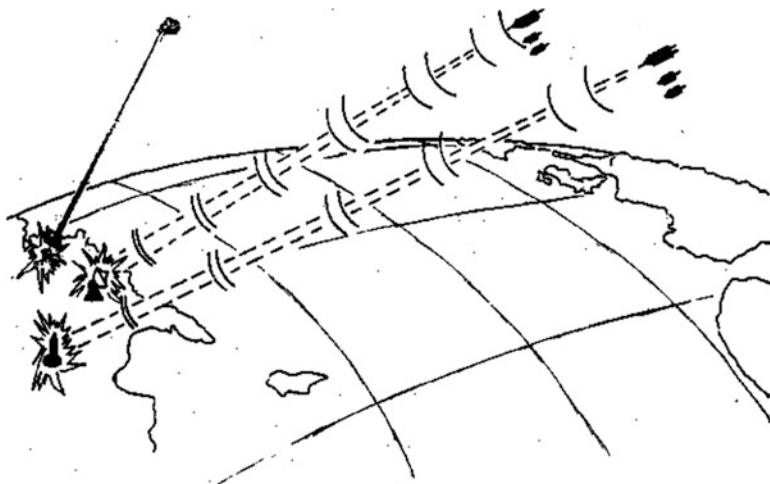


Fig. 2.64 Moray/Tesla technology

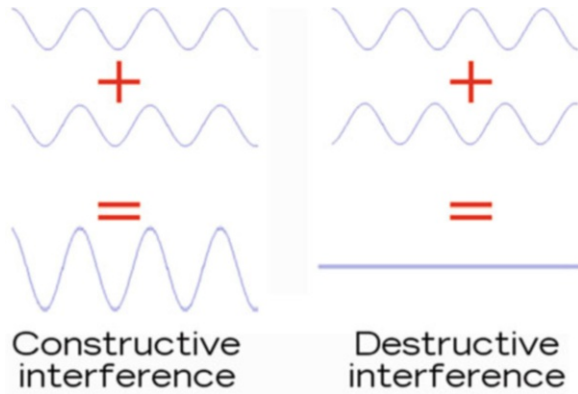
2.9.11 *Deployment of Superweapon Scalar Wave Drive by Interferometer Paradigm*

Considering scalar wave (SW) or sometimes called longitudinal scalar wave (LSW) as one of the superweapons of directed energy, and to overcome the controversy of such phenomena (i.e., SW or LSW), use of a high-energy weapon is the possible deployment of interferometer concept that is known to physicists and scientist for a while. However, before we take this approach, we need to have some understanding of what is interference and as a result interferometers as well as how do interferometers work?

To understand interferometry, you need to understand **interference**. In everyday life, interference simply means getting in the way or meddling, but in physics it has a much more specific meaning. Interference is what happens when two waves carrying energy meet up and overlap. The energy they carry gets mixed up together so, instead of two waves, you get a third wave whose shape and size depend on the patterns of the original two waves. When waves combine like this, the process is called **superposition**.

If you have ever sat making waves in a bathtub, you'll have seen interference and superposition in action. If you push your hand back and forth, you can send waves of energy out from the center of the water to the walls of the tub. When the waves get to the walls, they bounce back off the hard surface more or less unchanged in size but with their velocity reversed. Each wave reflects off the tub just as if you'd kicked a rubber ball at the wall. Once the waves come back to where your hand is, you can make them much bigger by moving your hand in step with them. In effect, you create new waves that add themselves to the original ones and increase the size of their peaks (amplitude).

Fig. 2.65 Illustration of two types of interferences



There are two types of interference waves as described here and depicted in Fig. 2.65:

1. **Constructive interference** means combining two or more waves to get a third wave that's bigger. The new wave has the same wavelength and frequency but more amplitude (higher peaks).
2. **Destructive interference** means waves subtracting and canceling out. The peaks in one wave are canceled by the troughs in the other.

When waves add together to make bigger waves, scientists call it **constructive interference**. If you move your hands in a different way, you can create waves that are out of step with your original waves. When these new waves add to the originals, they subtract energy from them and make them smaller. This is what scientists call **destructive interference**.

Analysis of Fig. 2.65 indicates that interferometer is nothing more than being just a phase. The extent to which one wave is in step with another is known as its phase. If two identical waves are "in phase," it means that their peaks align so, if we add them together, we get a new wave that's twice as big but otherwise exactly the same as the original waves. Similarly, if two waves are completely out of phase (in what we call antiphase), the peaks of one exactly coincide with the troughs of the other so adding the waves together gives you nothing at all. In between these two extremes are all sorts of other possibilities where one wave is partly in phase with the other. Adding two waves like this creates a third wave that has an unusual rising and falling pattern of peaks and troughs. Shine a wave like this onto a screen and you get a characteristic pattern of light and dark areas called interference fringes. This pattern is what you study and measure with an interferometer.

Thus, interferometer is an instrument that uses the interference patterns formed by waves (usually light, radio, or sound waves) to measure certain characteristics of the waves themselves or of materials that reflect, refract, or transmit the waves. Interferometers can also be used to make precise measurements of distance. Interference patterns are produced when two identical series of waves are brought together.

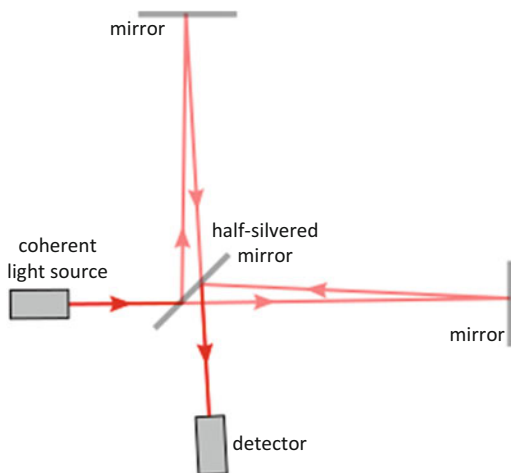
Optical interferometers can be used as spectrometers for determining wavelengths of light and for studying fine details in the lines of a spectrum. Optical interferometers are also used in measuring lengths of objects in terms of wavelengths of light, providing great precision, and in checking the surfaces of lenses and mirrors for imperfections. In astronomy, optical interferometers make it possible to determine the diameter of large, relatively nearby stars and the separation of very close double stars. Radio interferometers are used in astronomy for mapping celestial sources of radio waves. Acoustic, or sound, interferometers are used for measuring the speed and absorption of sound waves in liquids and gases.

In Fig. 2.66, the two light rays with a common source combine at the half-silvered mirror to reach the detector. They may either interfere constructively (strengthening in intensity) if their light waves arrive in phase or interfere destructively (weakening in intensity) if they arrive out of phase, depending on the exact distances between the three mirrors.

Interferometry is a family of techniques in which waves, usually electromagnetic waves, are superimposed causing the phenomenon of interference in order to extract information. Interferometry is an important investigative technique in the fields of astronomy, fiber optics, engineering metrology, optical metrology, oceanography, seismology, spectroscopy (and its applications to chemistry), quantum mechanics, nuclear and particle physics, plasma physics, remote sensing, biomolecular interactions, surface profiling, microfluidics, mechanical stress/strain measurement, velocimetry, and optometry.

Interferometers are widely used in science and industry for the measurement of small displacements, refractive index changes, and surface irregularities. In an interferometer, light from a single source is split into two beams that travel in different optical paths, and then combined again to produce interference. The resulting interference fringes give information about the difference in optical path length. In analytical science, interferometers are used to measure lengths and shape

Fig. 2.66 The light path through a Michelson interferometer



of optical components with nanometer precision; they are the highest precision length measuring existing instruments. In Fourier transform spectroscopy they are used to analyze light containing features of absorption or emission associated with a substance or mixture. An astronomical interferometer consists of two or more separate telescopes that combine their signals, offering a resolution equivalent to that of a telescope of diameter equal to the largest separation between its individual elements.

Furthermore, the way interferometers do work is as follows.

An interferometer is really a precise scientific instrument designed to measure things with extraordinary accuracy. The basic idea of interferometry involves taking a beam of light (or another type of electromagnetic radiation) and splitting it into two equal halves using what's called a beam splitter (also called a half-transparent mirror or half-mirror). This is simply a piece of glass whose surface is very thinly coated with silver. If you shine light at it, half the light passes straight through and half of it reflects back—so the beam splitter is like a cross between an ordinary piece of glass and a mirror. One of the beams (known as the reference beam) shines onto a mirror and from there to a screen, camera, or other detector. The other beam shines at or through something you want to measure, onto a second mirror, back through the beam splitter, and onto the same screen. This second beam travels an extra distance (or in some other slightly different way) to the first beam, so it gets slightly out of step (out of phase).

Artwork of how a basic Michelson interferometer works is again depicted in Fig. 2.67.

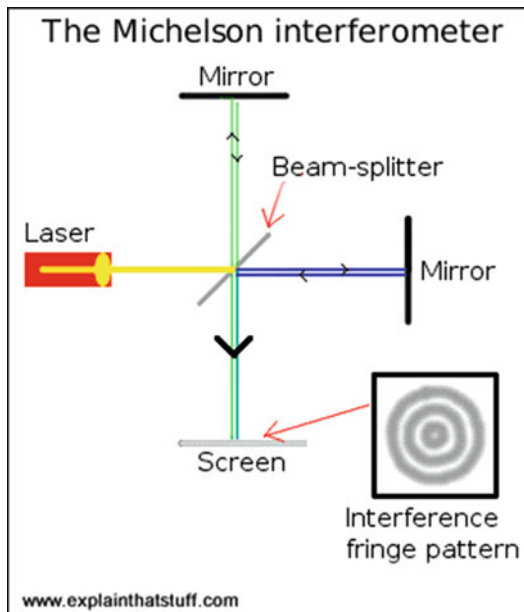
If we take the green beam to be the reference beam, we'd subject the blue beam to some sort of change we wanted to measure. The interferometer combines the two beams and the interference fringes that appear on the screen are a visual representation of the difference between them.

When the two light beams meet up at the screen, they overlap and interfere, and the phase difference between them creates a pattern of light and dark areas (in other words, a set of **interference fringes**). The light areas are places where the two beams have added together (constructively) and become brighter; the dark areas are places where the beams have subtracted from one another (destructively). The exact pattern of interference depends on the different way or the extra distance that one of the beams has traveled. By inspecting and measuring the fringes, you can calculate this with great accuracy—and that gives you an exact measurement of whatever it is you're trying to find.

Instead of the interference fringes falling on a simple screen, often they're directed into a camera to produce a permanent image called an **interferogram**. In another arrangement, the interferogram is made by a detector (like the charge-coupled device (CCD) image sensor used in older digital cameras) that converts the pattern of fluctuating optical interference fringes into an electrical signal that can be very easily analyzed with a computer.

As part of enhancing our knowledge further about interferometer we need to know what are the different types of interferometers and which one is more

Fig. 2.67 Artwork of a basic Michelson interferometer



appropriate for deployment of our application and which one drives scalar wave or per se longitudinal scalar wave.

Interferometers became popular towards the end of the nineteenth century and there are several different kinds, each based roughly on the principle we've outlined above and named for the scientist who perfected it. Six common types are the Michelson, Fabry-Perot, Fizeau, Mach-Zehnder, Sagnac, and Twyman-Green interferometers and they are all described as follows:

- The **Michelson interferometer** (named for Albert Michelson, 1853–1931) is probably best known for the part it played in the famous Michelson-Morley experiment in 1881. That was when Michelson and his colleague Edward Morley (1838–1923) disproved the existence of a mysterious invisible fluid called “the ether” that physicists had believed filled empty space. The Michelson-Morley experiment was an important stepping stone towards Albert Einstein’s theory of relativity.
- The **Fabry-Perot interferometer** (invented in 1897 by Charles Fabry, 1867–1945, and Alfred Perot, 1863–1925), also known as an etalon, evolved from the Michelson interferometer. It makes clearer and sharper fringes that are easier to see and measure.
- The **Fizeau interferometer** (named for French physicist Hippolyte Fizeau, 1819–1896) is another variation and is generally easier to use than a Fabry-Perot. It’s widely used for making optical and engineering measurements.
- The **Mach-Zehnder interferometer** (invented by German Ludwig Mach and Swiss man Ludwig Zehnder) uses two beam splitters instead of one and produces

two output beams, which can be analyzed separately. It's widely used in fluid dynamics and aerodynamics—the fields for which it was originally developed.

- The **Sagnac interferometer** (named for Georges Sagnac, a French physicist) splits light into two beams that travel in opposite directions around a closed loop or ring (hence its alternative name, the ring interferometer). It's widely used in navigational equipment, such as ring-laser gyroscopes (optical versions of gyroscopes that use laser beams instead of spinning wheels).
- The **Twyman-Green interferometer** (developed by Frank Twyman and Arthur Green in 1916) is a modified Michelson mainly used for testing optical devices.

Most modern interferometers use laser light because it is more regular and precise than ordinary light and produces **coherent** beams (in which all the light waves travel in phase), as it is shown schematically in Fig. 2.68. The pioneers of interferometry didn't have access to lasers (which weren't developed until the mid-twentieth century) so they had to use beams of light passed through slits and lenses instead.

As Fig. 2.68 indicates, *most interferometers pass their beams through the open air, but local temperature and pressure variations can sometimes be a source of error. If that matters, one option is to use a fiber-optic interferometer like this. A laser (red, 12) shoots its beam through lenses (gray, 16a/b) into a pair of fiber-optic cables. One of them (blue, 18) becomes the reference beam, bouncing its light straight onto a screen (orange, 22). The other (green, 20) allows its beam to reflect off something that's being measured (such as a vibrating surface) into a third cable (green, 30). The reference and reflected beams meet up and interfere on the screen in the usual way.* Artwork from US Patent 4,380,394: Fiber optic interferometer by David Stowe, Gould Inc., April 19, 1983, courtesy of US Patent and Trademark Office.

Another concern we should have in order to deploy the concept of interferometers is that how accurate they can be.

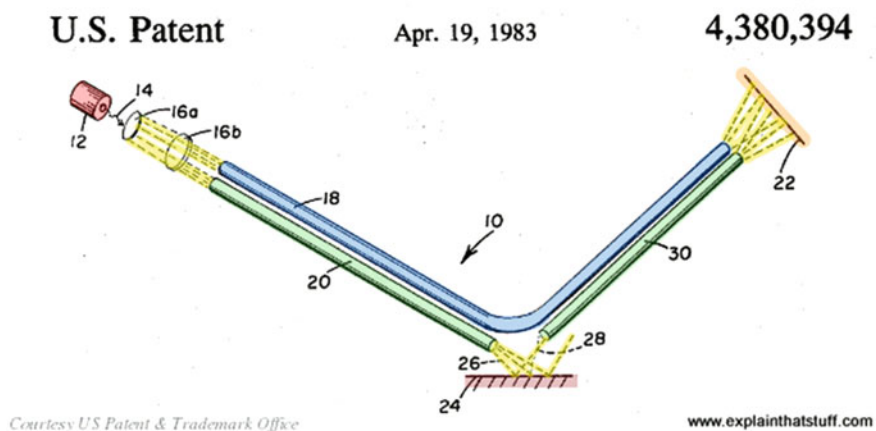


Fig. 2.68 Artwork: Fiber-optic interferometry

A state-of-the-art interferometer can measure distances to within 1 nm, but like any other kind of measurement it's subject to errors. The biggest source of error is likely to come from changes in the wavelength of the laser light, which depends on the refractive index of the material through which it's traveling. The temperature, pressure, humidity, and concentration of different gases in the air all change its refractive index, altering the wavelength of the laser light passing through it and potentially introducing measurement errors. Fortunately, good interferometers can compensate for this. Some have separate lasers that measure the air's refractive index, while others measure air temperature, pressure, and humidity and calculate the effect on the refractive index indirectly; either way, measurements can be corrected, and the overall error is reduced to perhaps one or two parts per million.

The common application of interferometers is depicted in Fig. 2.69, and is widely used in all kinds of scientific and engineering applications for making accurate measurements. By scanning interferometers over objects, you can also make very precise maps of surfaces.

These 3D topographical maps showing long valley in California that are illustrated in Fig. 2.69 were made from the Space Shuttle using a technique called *radar interferometry*, in which beams of microwaves are reflected off earth's contours and then recombined. Photo courtesy of NASA Jet Propulsion Laboratory (NASA-JPL).

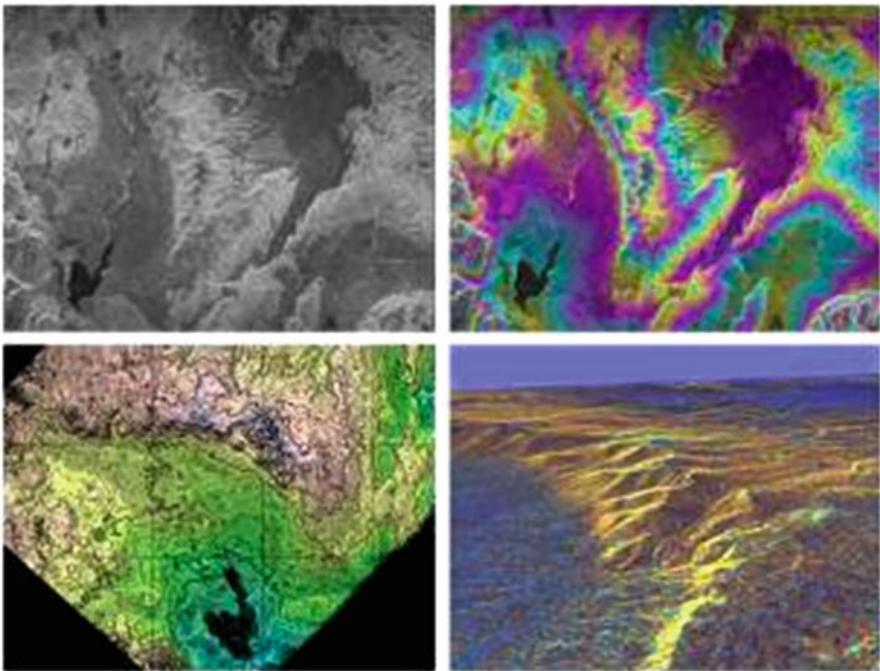


Fig. 2.69 Interferometry in action

By “accurate” and “precise,” I really do mean accurate and precise! The interference fringes that an optical (light-based) interferometer produces are made by light waves traveling fractionally out of step. Since the wavelength of visible light is in the hundreds of nanometers, interferometers can theoretically measure lengths a couple of hundred times smaller than a human hair! In practice, everyday laboratory constraints sometimes make that kind of accuracy hard to achieve. Albert Michelson, for example, found that his ether-detecting apparatus was affected by traffic movements about a third of a kilometer away!

Astronomers also use interferometers to combine signals from telescopes, so they work in the same way as larger and much more powerful instruments that can penetrate deeper into space. Some of these interferometers work with light waves; others use radio waves similar to light waves but with much longer wavelengths and lower frequencies. See Fig. 2.70.

Astronomers have linked the two 10 m (32 ft) optical telescopes in these domes on Mauna Kea, Hawaii, to make what is effectively a single, much more powerful telescope. Photo courtesy of NASA Jet Propulsion Laboratory (NASA-JPL).

An astronomical interferometer achieves high-resolution observations using the technique of aperture synthesis, mixing signals from a cluster of comparatively small telescopes rather than a single very expensive monolithic telescope.

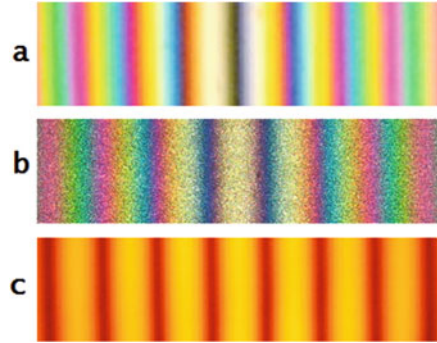
Note that the use of white light will result in a pattern of colored fringes as illustrated in Fig. 2.71. The central fringe representing equal path length may be light or dark depending on the number of phase inversions experienced by the two beams as they traverse the optical system. (See Michelson interferometer for a discussion of this in optics textbook or Internet.)

In Fig. 2.71, we observe (a) white light fringes where the two beams differ in the number of phase inversions; (b) white light fringes where the two beams have

Fig. 2.70 The Keck interferometer photo



Fig. 2.71 Colored and monochromatic fringes in a Michelson interferometer



experienced the same number of phase inversions; and (c) fringe pattern using monochromatic light (sodium D lines).

Early radio telescope interferometers used a single baseline for measurement. Later astronomical interferometers, such as the very large array (VLA) illustrated in Fig. 2.72, used arrays of telescopes arranged in a pattern on the ground. A limited number of baselines will result in insufficient coverage. This was alleviated by using the rotation of the earth to rotate the array relative to the sky. Thus, a single baseline could measure information in multiple orientations by taking repeated measurements, a technique called *earth-rotation synthesis*. Baselines thousands of kilometers long were achieved using very long baseline interferometry.

Astronomical optical interferometry has had to overcome a number of technical issues not shared by radio telescope interferometry. The short wavelengths of light necessitate extreme precision and stability of construction. For example, spatial resolution of 1 milliarcsecond requires $0.5 \mu\text{m}$ stability in a 100 m baseline. Optical interferometric measurements require high-sensitivity, low-noise detectors that did not become available until the late 1990s. Astronomical “seeing,” the turbulence that causes stars to twinkle, introduces rapid, random phase changes in the incoming light, requiring kilohertz data collection rates to be faster than the rate of turbulence. Figure 2.73 shows the picture of ALMA, which is an astronomical interferometer located in Chajnantor Plateau.

Despite these technical difficulties, roughly a dozen astronomical optical interferometers are now in operation offering resolutions down to the fractional milliarcsecond range. This linked video shows a movie assembled from aperture synthesis images of the Beta Lyrae system, a binary star system approximately 960 light-years (290 parsecs) away in the constellation Lyra, as observed by the CHARA array with the MIRC instrument. The brighter component is the primary star, or the mass donor. The fainter component is the thick disk surrounding the secondary star, or the mass gainer. The two components are separated by 1 milliarcsecond. Tidal distortions of the mass donor and the mass gainer are both clearly visible.

Microwave technology plays a more important role in modern industrial sensing applications. Pushed by the significant progress in monolithic microwave integrated



Fig. 2.72 Very large array (VLA) interferometer



Fig. 2.73 ALMA interferometer

circuit technology over the past decades, complex sensing systems operating in the microwave and even millimeter-wave range are available for reasonable costs combined with exquisite performance. In the context of industrial sensing, this stimulates new approaches for metrology based on microwave technology. An old

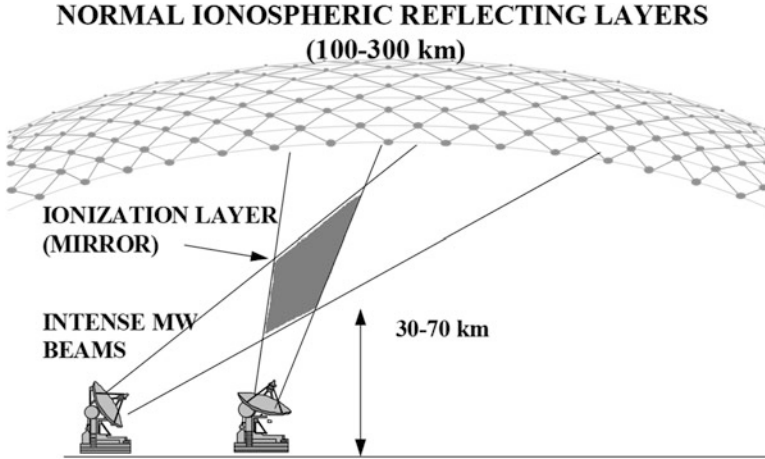


Fig. 2.74 Crossed-beam approach for generating an artificial ionospheric mirror

measurement principle nearly forgotten over the years has recently gained more and more attention in both academia and industry. Both industry and manufacturing technology are experiencing a revolution these days. The demand for products with a high degree of individuality leading to a huge variety of configurations is increasing more and more.

As it is illustrated in Fig. 2.74, as another application of interferometry, a very-high-frequency and microwave interferometric and phase amplitude noise measurement technique allows close-to-the-carrier measurements of both phase and amplitude noise, improving the instrument noise floor by 10–25 dB as compared to the traditional method based on a saturated mixer.

As part of electromagnetic (EM) wave development and their types, we should consider an extremely interesting property of EM waves that propagate in homogeneous waveguides. This will lead to the concept of “modes” and their classification as:

1. **Transverse electric and magnetic (TEM):** The transverse electromagnetic wave cannot be propagated within a waveguide but is included for completeness. It is the mode that is commonly used within coaxial and open-wire feeders. The TEM wave is characterized by the fact that both the electric vector \vec{E} and the magnetic vector \vec{H} are perpendicular to the direction of propagation.
2. **Transverse electric (TE):** This waveguide mode is dependent upon the transverse electric waves, also sometimes called H waves, characterized by the fact that the electric vector \vec{E} is always perpendicular to the direction of propagation.
3. **Transverse magnetic (TM):** Transverse magnetic waves, also called E waves, are characterized by the fact that the magnetic vector \vec{H} is always perpendicular to the direction of propagation.

Figure 2.74 is an artistic schematic of earth ionosphere of transverse electric (TE) in a localized wave (LW) scenario, where the earth and ionosphere can be used to launch TE waveguide modes, thus providing a way to send LWs beyond the line of sight around the globe.

An array of antennas in the MW range can ionize particles in the atmosphere and heat up the ionosphere causing it to change shape affecting weather. This was shown by the High Frequency Active Auroral Research Program (HAARP) technology.

The High Frequency Active Auroral Research Program (HAARP) was initiated as an ionospheric research program jointly funded by the US Air Force, the US Navy, the University of Alaska Fairbanks, and the Defense Advanced Research Projects Agency (DARPA). It was designed and built by BAE Advanced Technologies (BAEAT). Its original purpose was to analyze the ionosphere and investigate the potential for developing ionospheric enhancement technology for radio communications and surveillance. As a university-owned facility HAARP is a high-power, high-frequency transmitter used for the study of the ionosphere.

The most prominent instrument at HAARP is the Ionospheric Research Instrument (IRI), a high-power radio-frequency transmitter facility operating in the high-frequency (HF) band. The IRI is used to temporarily excite a limited area of the ionosphere. Other instruments, such as a very-high-frequency (VHF) and an ultrahigh-frequency (UHF) radar, a fluxgate magnetometer, a digitonide (an ionospheric sounding device), and an induction magnetometer, are used to study the physical processes that occur in the excited region.

HAARP is a target of conspiracy theorists, who claim that it is capable of “weaponizing” weather. Commentators and scientists say that advocates of this theory are uninformed, as claims made fall well outside the abilities of the facility, if not the scope of natural science.

Creation of an artificial uniform ionosphere was first proposed by Soviet researcher A. V. Gurevich in the mid-1970s. An artificial ionospheric mirror (AIM) would serve as a precise mirror for electromagnetic radiation of a selected frequency or a range of frequencies. It would thereby be useful for both pinpoint control of friendly communications and interception of enemy transmissions. By causing a variation in the ionosphere’s particles, the image on the ground causes earth currents and high enough magnetic variations to harm or destroy grid systems.

This concept has been described in detail by Paul A. Kossey et al. in a paper entitled “Artificial Ionospheric Mirrors (AIM)” [43]. The authors describe how one could precisely control the location and height of the region of artificially produced ionization using crossed microwave (MW) beams, which produce atmospheric breakdown (ionization) of neutral species. The implications of such control are enormous: one would no longer be subject to the vagaries of the natural ionosphere but would instead have direct control of the propagation environment. Ideally, the AIM could be rapidly created and then would be maintained only for a brief operational period. A schematic depicting the crossed-beam approach for generation of an AIM is shown in Fig. 2.74.

An AIM could theoretically reflect radio waves with frequencies up to 2 GHz, which is nearly two orders of magnitude higher than those waves reflected by the

natural ionosphere. The MW radiator power requirements for such a system are roughly an order of magnitude greater than 1992 state-of-the-art systems; however, by 2025 such a power capability is expected to be easily achievable.

However, “The capability of influencing the weather even on a small scale could change it from a force degrader to a force multiplier.”

In 1977, the UN General Assembly adopted a resolution prohibiting the hostile use of environmental modification techniques.

Besides providing pinpoint communication control and potential interception capability, this technology would also provide communication capability at specified frequencies, as desired. Figure 4.2 shows how a ground-based radiator might generate a series of AIMs, each of which would be tailored to reflect a selected transmission frequency. Such an arrangement would greatly expand the available bandwidth for communications and also eliminate the problem of interference and cross talk (by allowing one to use the requisite power level).

The first huge scalar potential interferometers [35–37] of strategic range and power (Fig. 2.75) were deployed by the Soviets in 1963, and one was used to kill the USS Thresher nuclear attack submarine (Fig. 2.76),⁷ leaving clearly recognizable signatures [38].

As part of deployment and immediate use of scalar interferometers, Fig. 2.75 shows artistic schematic of such a setup.

Since 1963, the Russians have had the equivalent of more than seven additional Manhattan Projects (using the Russian 5-year program instead of the 4-year Man-

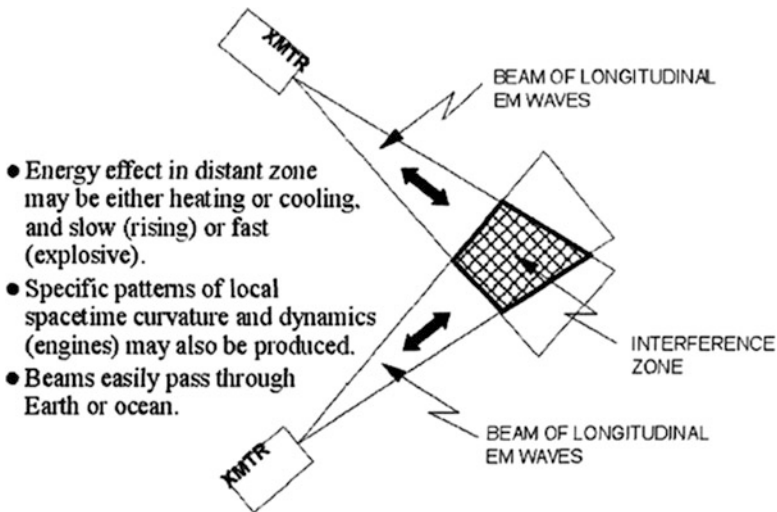


Fig. 2.75 Scalar (longitudinal EM wave) interferometer

⁷This is a claim by T.E. Bearden [38] at the end of this chapter.

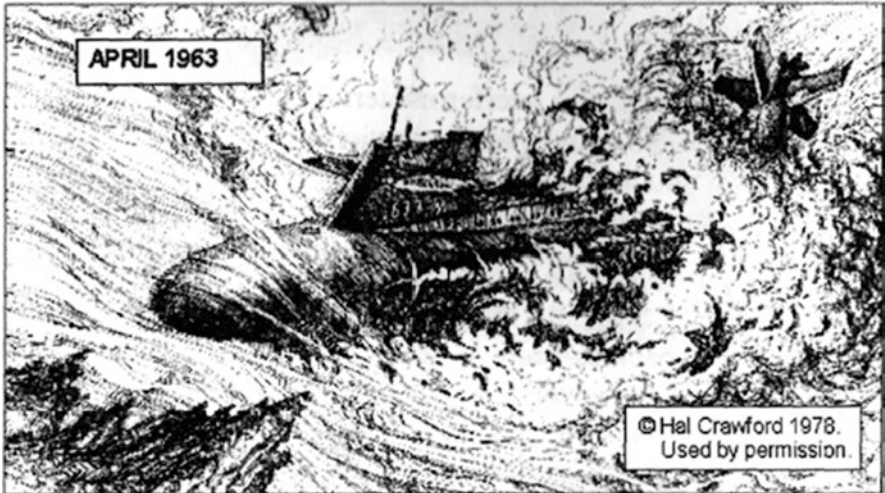


Fig. 2.76 Kill of the USS Thresher. With her controls jammed, the hull of the doomed submarine implodes when she reaches crush depth

hattan Project), back-to-back, in the development of energetics weaponry. The energetics weapons have never been given to the regular Russian forces. Instead, all research, production, siting, manning, and employment are by the KGB and still under ruthless KGB control by die-hard communist factions.

As part of Aharonov-Bohm effect one can conclude that even in the absence of electrical field \vec{E} and magnetic field \vec{B} , the potentials cause real effects to occur in the field-free regions. Using this principle, beams of pure potential without vector force fields (i.e., without electrical field \vec{E} and magnetic field \vec{B}) may be deliberately produced and intersected at a distance to cause effects in the interference zone, in contradiction to classical mechanics. These effects are in fact required by quantum mechanics.

Essentially, energy may be produced directly at the distance interference site or extracted from it, without energy transmission through space.

Implications for weapons built on these concepts are given by the US intelligent community scientist during the period of SDI (Star Wars) activities within the United States and Soviet Union of the time, and several types of such scalar electromagnetic weapons were discussed. One of the claims by these folks, particularly among US scientists, is that evidence of massive Soviet weaponization of these effects for nearly three decades and of Soviet scalar electromagnetic weapon testing on a global scale exists in the open literature.

With the advent of Maxwell's equations and more completeness of Ampere-Maxwell's equation as well as decoupling of such equation, which was demonstrated in our previous sections of this chapter as well as previous chapter in this book,

electricity and magnetism were combined into an elegant electromagnetic theory, and these equations then served as the basis for the development of modern theory of quantum-electrodynamic (QED). Gradually potentials were relegated to a position of inferior importance, and they even came to be regarded as purely mathematical convenience by most scientists.

However, with the advent of Aharonov and Bohm's seminal paper [23], it became crystal clear that potentials are in fact real entities, and they can directly affect and control charged particle systems even in a region where all the fields and hence the forces on the particles have vanished. While this of course is completely contrary to the conclusions of classical mechanics, it follows inescapably from quantum mechanics.

With Chambers's [39] direct experimental proof of the predicted Aharonov-Bohm effects in 1960, [23], this new viewpoint was firmly established for quantum mechanics (QM) and quantum electromagnetic (QE) in general. Same effect even was demonstrating, even affects the gauge theories [40], requiring the concept of non-integrable phase factors and global formulation of gauge fields. Thus, increasingly it is the potentials that are the primary physical entities, and the fields are of secondary, derived importance in modern quantum electrodynamics (QED).

However, the full weapon implications of the Aharonov-Bohm discovery have not yet penetrated the minds and consciousnesses of Western physicists, academia, weapon engineers, and scientists of Star Wars (SDI). Indeed, an extended treatment of such implications has not even been addressed at least not in the open literatures.

Thus, this may be to some degree understandable, since it required almost 30 years for physicists to realize the primary actuality of the potentials in the first place, as the Nobel Prize winner Richard Feynman [40, 41] stated succinctly: "It is interesting that something like this can be around for thirty years but, because of certain prejudices of what is and is not significant, continues to be ignored."

Slowly, the overwhelming importance of the scalar electromagnetic indicated by Aharonov and Bohm [23] has been recognized and noted by Western world weapon analysts, and work to investigate and apply this rich new region of quantum electrodynamics is now most certainly warranted by showing that longitudinal scalar wave indeed can be used as a superweapon of directed energy (DE), which possibly is more effective than the other directed energy weapons (DEWs). Thus, it is imperative that an effort of the highest priority be mounted as soon as possible, for our very own survivability and be considered as part of our National Security Policy, where we are threatened by such tremendous energy from scalar electromagnetic weapons that are evidently already in the hands of the Soviet Union of the past and Russia of today as well as our other adversaries such as China and North Korea maybe. Given this matter as a fact of its existence in Russian new age weapon arsenal, we have absolutely no countermeasure and no defense system whatsoever against such measure and threat.

2.9.11.1 Wireless Transmission of Energy at a Distance Driven by Interferometry

To illustrate one remarkable though typical implication of this new breakthrough area, we may point out that, by changing the potentials while keeping the force field zero [23], one can directly produce energy at a distance as if it were transported through space in the normal fashion and traditional way that occurs as such. Indeed, it may even be possible to utilize pure potential waves to “transport” the energy at any velocity—not limited by the speed of light and will not dissipate at the constraint of $1/r^2$ limit yet maybe at the rate of $1/r$. In some cases a potential, for example, electrostatic scalar potential (ESP), can be regarded as having infinite velocity, simply appearing “everywhere at once” [42].

Furthermore, the electrostatic scalar potential, for example, may be regarded as a sort of “locked-in stress energy” of vacuum, as can any other vacuum potential. Changing the potential in a region or at a point changes the amount of “locked-in” or “enfolded” vacuum energy available or stored in that region or at that point. Yet simply changing the potential at that point or in that region need not involve any local expenditure of work there; the work may be expended elsewhere, and the results realized at a distant region by a change in that region’s potential, according to the Aharonov-Bohm effect [23].

In the remote region, charged particles are imbedded in vacuum potential by their virtual particle charge flux, and in the induced potential gradients the imbedded particles move, producing electrical and magnetic forces and fields and performing work.

This is somewhat analogous to “putting energy in here at point A” and “extracting it out there at point B) without any travel or losses in between—Nikola Tesla’s old “wireless transmission of energy at a distance without losses” idea. Note that quantum mechanically, we may take the view that this is a very special class of macroscopic “energy tunneling” phenomena, as illustrated in Aharonov and Bohm’s original paper [23].

Essentially energy is put into the system at the locations, where the scalar potentials are produced, and is recovered at the distant interference zone where particle effects are produced. See Fig. 2.77 as well as Fig. 2.75 from the interferometry point of view. See also Figs. 2.79 and 2.80.

To pursue the above single example, depicted in Fig. 2.77, and to further show its implications, we point out that in theory one may deliberately make a beam containing zero electric and magnetic fields, simply by properly phase-locking together two or more beams of oscillating ordinary \vec{E} and \vec{B} electrical energy, all at the same frequency. In the perfect hypothetical case, for example, two single-frequency beams phase-locked together with 180 degrees apart would create such a zero-field or scalar beam as depicted in Fig. 2.78.

Fig. 2.77 Illustration vector energy zone produced by two scalar transmitters' drive by interferometry

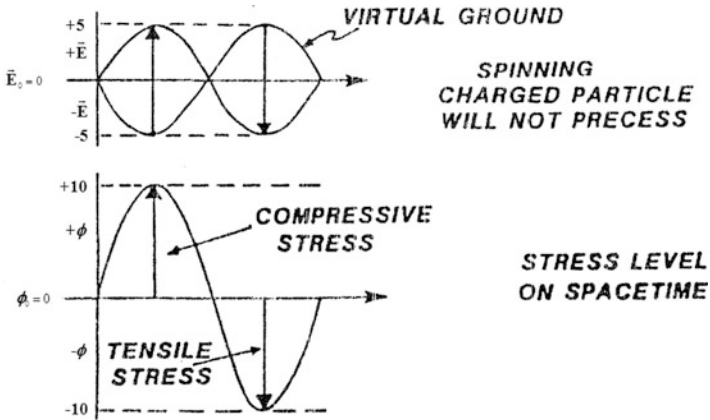
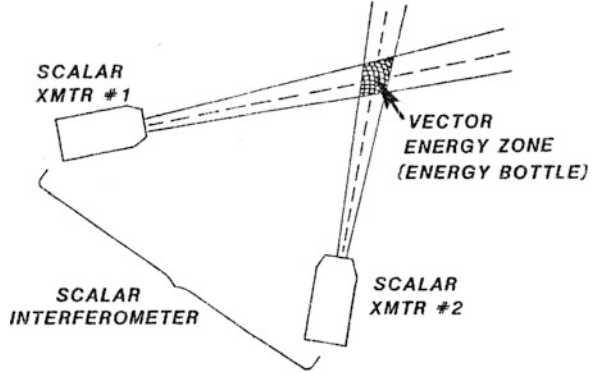


Fig. 2.78 Zero-field or scalar wave beam

In the real bandwidths, how much zero-field beam is obtained at the center of the bandwidth would depend on the sharpness “Q” of each beam.

To purify the beam, it could first be transmitted through a ground Faraday cage or shield, which would remove most of the orthodox \vec{E} - and \vec{B} -field components not properly zeroed out. By successive Faraday “stripping” of the beam, a scalar beam as pure as desired can be obtained. See Fig. 2.55 (Figs. 2.79 and 2.80).

Figure 2.81 is an artistic drawing of scalar potential interferometry between the two sets of bidirectional longitudinal electromagnetic (EM) wave-pair functions producing all EM force field and waves.

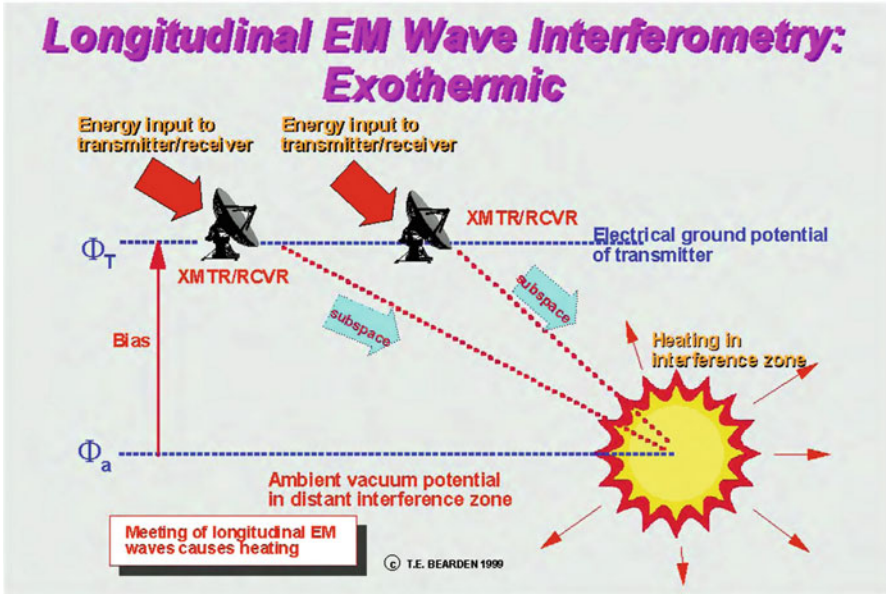


Fig. 2.79 Exothermic longitudinal scalar wave interferometry-1 (using HAARP to create explosive steam pockets underground)

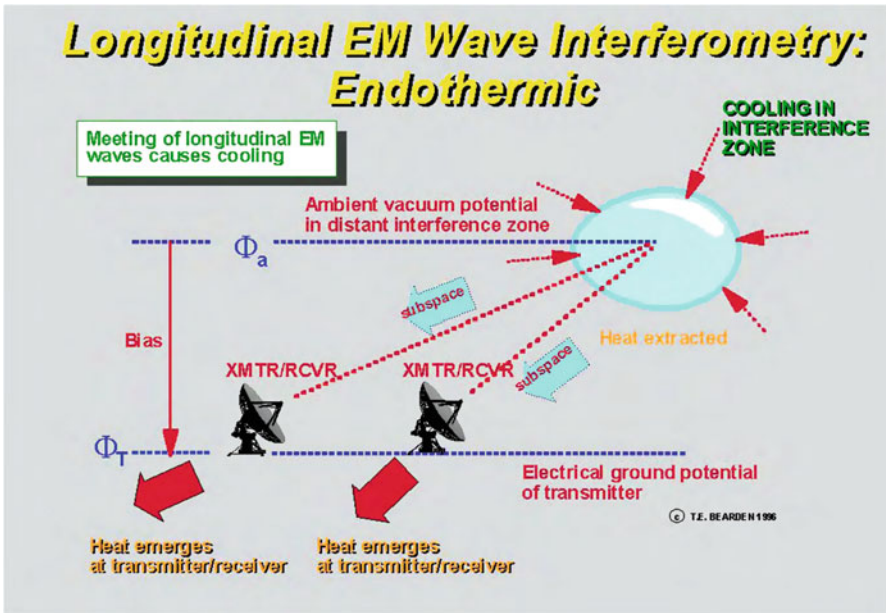


Fig. 2.80 Exothermic longitudinal scalar wave interferometry-1

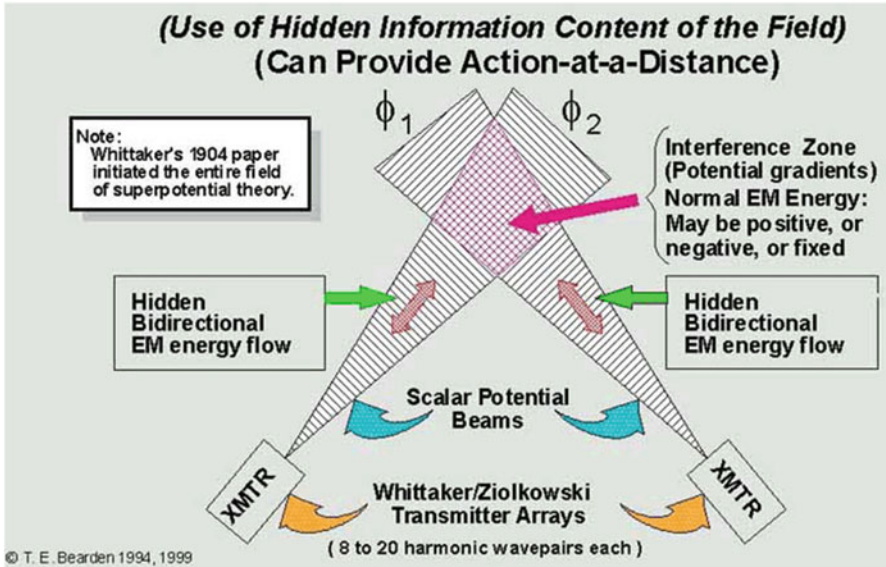


Fig. 2.81 Scalar potential interferometry

2.10 The Quantum Waves

So far, we have defined three principal types of waves as

1. Mechanical wave
2. Electromagnetic wave
3. Quantum wave

Although mechanical waves may be the most obvious in every day of our life, electromagnetic waves may be the most useful to our technological society, where a case can be built that quantum waves are the most fundamental within the paradigm of all things in the universe generating patterns of energy resulting from their motion; thus every bit of matter in the universe behaves like a wave under certain circumstances.

Quantum wave theory is a model of nature that grew in response to several questions:

- What, exactly, is gravity?
- How are charge and gravity related?
- What gives rise to the fundamental unit of energy?
- And especially, what *is* space?

Our attempt to answer these questions evolved into conversations that continued for more than a decade. *Quantum wave theory* is an artwork, a prose poem, that is the result of that collaboration. The theory attempts to unify energy, mass, and force as

Fig. 2.82 The universe as we see



manifestations of a single entity. We refer to that entity as space that is argued by Amy Robinson and John Holland [44].

According to Einstein, space becomes curved by large bodies, such as stars and planets. The results of that curvature are that the earth and planets orbit the sun, our moon orbits the earth, and things on earth “fall” down (towards the center of the earth). But gravity here at home is not acting on us from under our feet; rather, it surrounds us. We are not so much “pulled” down by earth’s gravity as “pushed” down by curved space (Fig. 2.82).

What happens between the sun and planets, and the earth and moon, tells us something not only about the relationships among those large bodies, but about space, as well. Part of Einstein’s genius was his ability to see the sun, planets, *and space* as a unified system, rather than separate, independent phenomena.

Space has been described in various ways throughout the history of physics and cosmology including particulate aether, empty vacuum, Higgs field or Higgs ocean, and space “atoms.”

Quantum wave theory proposes a new model of space. The theory describes space as a continuous, quantized, flexible “field,” nowhere divided or divisible, but capable of discrete motions of compression and rebound.

Space comprises tiny regions able to act independently of the space that surrounds them, although there are no actual boundaries between them. QWT refers to these fundamental units of space as “space quanta.”

Space quanta are tiny, flexible regions of space whose dynamics include compression and rebound. When energized, a quantum of space compresses and deforms along the path of least resistance. The path of least resistance is determined by the origin of a force, its magnitude, and the state of surrounding space.

One quantum of space is the amount of space that will compress in response to the fundamental unit of energy, which is described by Planck’s constant.

Schrödinger’s equation is generalized to a space–time four-manifold, using standard concepts from differential geometry and operator replacement. This fourth-order equation, which reduces and specializes to the Klein–Gordon equation

in the flat space limit, can also be obtained from a variational principle, and must be solved in tandem with the Einstein field equations with suitable stress energy. The propagator, for large momenta, varies like $1/p^4$. A further attractive feature is that no external currents or stress energies need to be imposed: these arise naturally. A generalization to fields with arbitrary spin is proposed. Solving the equation would lead to a determination of the mass, just as energies are found in solving Schrödinger's equation. Flat-space plane wave solutions consist of the superposition of two independent waves, which can be interpreted as propagating strings [45].

Wave and particle characteristics have very different behaviors in the way in which they occupy space, the way they travel through opening, and the way they interact with other particles or waves.

All particles spin, or rotate, and oscillate (tip back and forth about a point of equilibrium). Imagine a ball, under water, spinning as it tips back and forth. The ball's spin disturbs the surrounding water in a circular path, while its oscillation generates alternating wave densities and rarities as it tips back and forth. These combined motions create a disturbance in the surrounding water that translates outward as a distinct, wavy pattern of crests and troughs. That pattern is determined by the size of the ball, its speed of rotation, and the rate and extent of oscillation.

Both the particles themselves, and the traveling wave patterns they generate, are the result of the traveling waves from which they formed.

Traveling waves generated by complementary particles form new particles when they intersect. Each wave carries a portion of the particle's "instructions" for forming a new particle. Particle motion is the "genetic code" of matter.

Every particle is a record of those waves from which it formed, the places from which they came, and the particles from which they were generated.

Superposition, wave function collapse, and uncertainty principle in quantum physics show real and imaginary components of quantum wave functions for free particles and confined particles.

As it can be seen from Fig. 2.83, according to quantum mechanics, all particles in the universe are described by what we refer to as a wave function Ψ . Properties such as position and momentum do not have defined values until they are observed.

However, a particle exists in a well-defined amount of space, if you could pause time at some instant during a particle motion in space. This property means particle is "localized," since the particle is in a particular location at a given time. Wave, on the other hand, exists over an extended region of space.

The probability of the particle being at a particular position is given by the square of the amplitude of the wave function at that location.

As it was described before, a harmonic function such as $\sin(kx - \omega t)$ exists over all values of x , from $-\infty$ to $+\infty$, with no way to distinguish one cycle from another. Thus, a single frequency wave is inherently non-localized; it exists everywhere.

The difference is illustrated in Fig. 2.84, which shows a particle represented in time, where a "snapshot" of the particle and wave is depicted. At the instant of the snapshot, all observers can agree that the particle exists at positions $x = -1$ and $y = 4$. But, where is the wave at the instant?

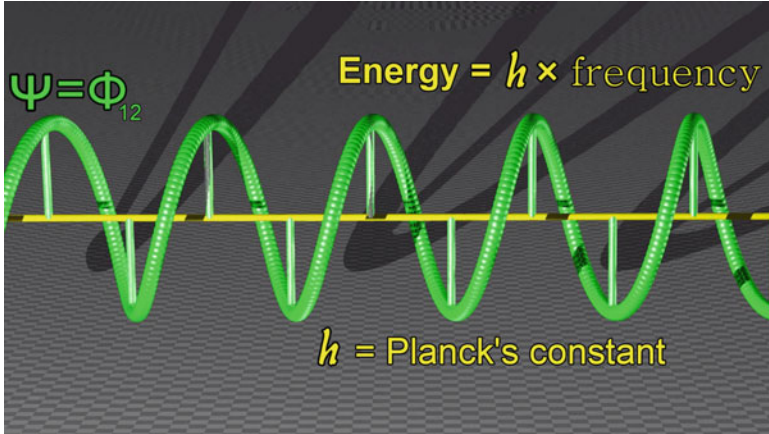


Fig. 2.83 Wave function depiction

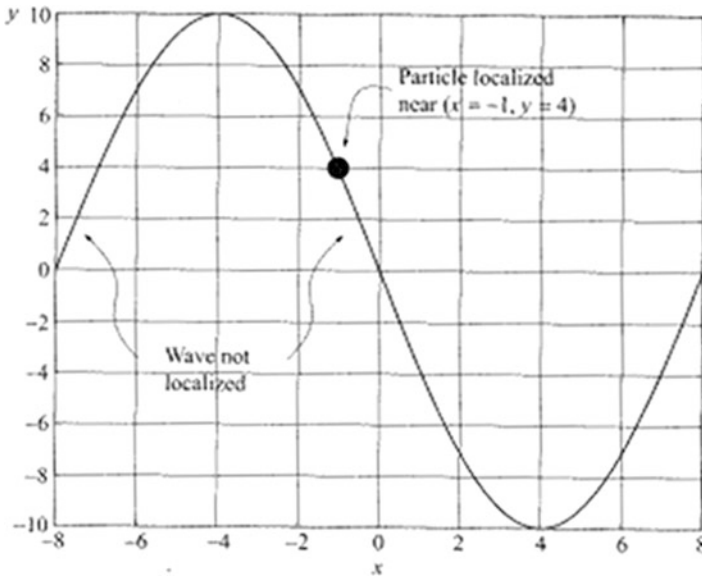


Fig. 2.84 A non-localized wave and a localized particle

The wave exists at $x = -8$, $x = 0$, $x = +8$, and all other values of x , including locations not shown to the left and right of the graph and in between the x values listed in Fig. 2.84.

Any given peak, trough, or zero-crossing of the wave exists at a specific location at certain time, but every cycle looks exactly like other cycle, and the wave itself consists of all its position. Hence, the wave is non-localized.

We have touched up Schrödinger's equation and general relativity briefly here and more details can be found in Appendix B of this book. Now we need to briefly show results of derivation of the field equation [45].

The free-space Schrödinger's equation reads as

$$i\hbar \frac{\partial \Psi}{\partial t} = -\frac{\hbar^2}{2m} \nabla^2 \Psi \quad (2.334)$$

Equation (2.334) should also hold in a frame, which is comoving or nearly comoving with the particle. The idea then is to transform this equation into coordinates that are adapted to the particle's world line. Vuille [45] shows that the first step in the derivation is to reinsert the mass energy, m , which has essentially been scaled out of the traditional equation as

$$i\hbar \frac{\partial \Psi}{\partial t} = -\frac{\hbar^2}{2m} \nabla^2 \Psi + m^2 \Psi \quad (2.335)$$

From Eq. (2.335), Vuille [45] shows that Schrödinger's equation can be generalized to the equivalent equation on a four-manifold by using standard differential geometry and operator replacements and if it is developed the equations describe a scalar field on a curved space-time. The derivation of Eq. (2.339), however, made no demands on the mathematical nature of the wave Ψ . This being the case, the general spinor equation might be written as

$$\nabla^{AA'} \nabla^{BB'} \nabla_{AA'} \nabla_{BB'} \Psi^{D_1 \dots D_n} + \frac{m^2 c^2}{\hbar^2} \nabla^{AA'} \nabla_{AA'} \Psi^{D_1 \dots D_n} = 0 \quad (2.336)$$

We encourage the readers to refer to Vuille's [45] paper for more details on Eqs. (2.30a) and (2.30b) and its derivation step by step.

Related to this section it is worth to show some overall calculation and analysis of Edmond T. Whittaker [46] as part of "*relativity and electromagnetic theory*" where he shows that when any number of electrons are moving in any manner, the functions which define the resulting electrodynamics field, namely, the three components of dielectric displacement in the aether and the three components of the magnetic force at every point of the field, can be expressed in terms of the derivatives of two scalar potential functions.

There some approach and expressed by others in terms of a scalar potential function and a vector potential function, which are equivalent to *four* scalar potential functions. See Chap. 5 of this book as well. However, Whittaker [46] suggests that these two scalar potential functions are explicitly evaluated in terms of the charges and coordinates of the electrons. It is then shown that from these results the general functional form of an electrodynamic disturbance due to electrons can be derived.

He also goes on to extend his work with other activities related to presentation of the electromagnetic entity in vacuo that ends up with his result of calculation

extended to the production of transverse fields and energy by scalar interferometry as well. In this, he shows that transverse field and energy can be produced in vacuo by the interferometry of two beams prepared in such a way that the only component present in each beam is the physical time-like potential, proportional directly to the magnetic flux $(\partial F/\partial t) = i(\partial G/\partial t)$ under conditions of circular polarization in both beams. This indicates when interference occurs; this condition no longer holds, and transverse field and energy appear through the interference of the two beams. It can also be shown that energy is conserved in this process.

Whittaker's first paper on theoretical physics excluding dynamics that was published in 1904 [46] shows that any electric field can be specified in terms of derivatives of *two* real scalar wave functions, F and G , by means of the formula as part of the six components of the dielectric displacement and the magnetic force that can be expressed in terms of the derivatives of these two scalar potentials that are defined by the equations

$$F(x, y, z, t) = \sum \frac{e}{4\pi} \sinh^{-1} \left\{ \frac{\bar{z}' - z}{[(x' - x)^2 + (y' - y)^2]} \right\} \quad (2.337)$$

$$G(x, y, z, t) = \sum \frac{e}{4\pi} \tan^{-1} \left\{ \frac{\bar{y}' - y}{\bar{x}' - x} \right\} \quad (2.338)$$

In these two above equations, the summation is taken over all the electrons in the field and the new form of Maxwell's equation in terms of \vec{E} - and \vec{H} -fields as well as force can be written as

$$\begin{aligned} \vec{E} &= \vec{\nabla} \times \vec{\nabla} \times \vec{F} + \nabla \times \left(\frac{\vec{G}}{c} \right) \\ \vec{H} &= \vec{\nabla} \times \left(\frac{\vec{F}}{c} \right) - \vec{\nabla} \times \vec{\nabla} \times \vec{G} \\ \vec{F} &= (0, 0, F), \quad \vec{G} = (0, 0, G) \end{aligned} \quad (2.339)$$

Thus, the usual specification in terms of the Maxwellian scalar potential ϕ and vector potential \vec{A} is equivalent to *four* real functions connected by the relation $\frac{\partial \phi}{\partial t} + c \vec{\nabla} \cdot \vec{A} = 0$.

These two scalar wavefunctions were evaluated in terms of the charges and coordinates of the electrons generating the field.

It can also without any difficulties be shown that if any number of electrons whose total charge is zero are moving in any manner so as to retain always in the

vicinity of a given point (i.e., to be in *stationary* motion), then the electromagnetic field is generated as a result as the type given by

$$F = \frac{1}{r} f\left(t - \frac{r}{c}\right) \quad G = 0 \quad (2.340)$$

where r is the distance from the point and f is an arbitrary function, or, more generally, of a field of this type superposed on fields of the same type, but related to the axes of y and x in the same as this is related to the axis of z . This is perhaps of some interest in connection with the view advocated by some physicists that the atoms of the chemical elements consist of sets of electrons, whose total charge is zero, in stationary motion.

2.11 The X-Waves

In order to have a better description of the X-waves, we need to have some basic underrating of waves or beams behavior, which among them is superluminal phenomenon.

A superluminal phenomenon is a frame of reference traveling with a speed greater than the speed of light c . There is a putative class of particles dubbed tachyons which are able to travel faster than light. Faster-than-light phenomena violate the usual understanding of the “flow” of time, a state of affairs which is known as the causality problem and also called the “Shalimar Treaty.”

It should be noted that while Einstein’s theory of special relativity prevents (real) mass, energy, or information from traveling faster than the speed of light c [47–50], there is nothing preventing “apparent” motion faster than c (or, in fact, with negative speeds, implying arrival at a destination before leaving the origin). For example, the phase velocity and group velocity of a wave may exceed the speed of light, but in such cases no energy or information actually travels faster than c . Experiments showing group velocities greater than c include that of Wang et al. [51], who produced a laser pulse in atomic cesium gas with a group velocity of $(-310 \pm 5)c$. In each case, they observed superluminal phenomenon.

It turns out that all relativistic wave equations possess infinity families of formal solutions with arbitrary speeds ranging from zero to infinity, called undistorted progressive waves (UPWs) by Rodrigues and Lu [52]. However, like the arbitrary-speed plane wave solutions, UPWs have infinite energy and therefore cannot be produced in the physical world. However, approximations to these waves with finite energy, called finite aperture approximations (FAA), can be produced and observed experimentally [53]. Among the infinite family of exact superluminal solutions of the homogeneous wave equation and Maxwell equations are waves known as X-waves. X-waves do not violate special relativity because all superluminal X-waves have wave fronts that travel with the speed parameter c (the speed of light) that appears in the corresponding wave equation. The superluminal motion of

the peak is therefore a transitory phenomenon similar to the reshaping phenomenon that occurs (under very special conditions) for waves in dispersive media with absorption or gain and which is in this case responsible for superluminal (or even negative) group velocities [53].

Several authors have published theories claiming that the speed-of-light barrier imposed by relativity is illusionary. While these “theories” continue to be rejected by the physics community as ill-informed speculation, their proponents continue to promulgate them in rather obscure journals. An example of this kind is the [Smarandache hypothesis](#) [54], which states that there is no such thing as a speed limit in the [universe](#) [54]. Similarly Shan [69, 70] has concluded that the superluminal communication must exist in the [universe](#) and that they do not result in the casual loop paradox.

The existence of nondiffractive also known to us as localized pulses was long predicted by many scientists [55–58], as well as more recent articles [59, 60]. Note that the so-called *localized waves* (LW), known also as non-diffracting waves, are indeed able to resist diffraction for a long distance in free space. Such solutions to the wave equations and, in particular, to the Maxwell equations under weak hypotheses were theoretically predicted long time ago [55–57, 67] (cf. also Recami et al. [58]). In summary, localized waves are a type of waves that focus energy at a point in space which can be generated with acoustic, microwave, particle, and light energy.

The non-diffracting solutions to the wave equations (scalar, vectorial, spinorial, etc.) are in fashion, both in theory and in experiment since a couple of decades. Rather well known are the ones with luminal or superluminal peak velocity.

Like the so-called X-shaped waves, which are supersonic in acoustics [66], and superluminal in electromagnetism (see [57]; see also [65] and [68]).

In 1983, Brittingham [61] set forth a luminal ($v = c$) solution to the wave equation (more particularly to Maxwell’s equations), which travels rigidly (i.e., without diffraction). The solution proposed [61] possessed infinite energy, however, and once more the problem arose of overcoming such a problem. A way out was first obtained by Sezginer [62], who showed how to construct finite-energy luminal pulses, which, however, do not propagate without distortion for an infinite distance, but, as expected, travel with constant speed and approximately without deformation for a certain (long) depth of field: much longer, in this case, too, than that of ordinary pulses such as the Gaussian pulses [63].

However, at the beginning of the 1990s, Lu et al. [65, 66] constructed, both mathematically and experimentally, new solutions to the wave equation in free space: namely, an X-shaped localized pulse, with the form predicted by the so-called extended special relativity [57, 64]; for the connection between what Lu et al. [65, 66] called *X-waves* and extended relativity, see for example [58].

An X-shaped wave that is a localized superluminal pulse is illustrated in Fig. 2.85. It is an X-wave, possessing the velocity $v > c$, and the figure illustrates the fact that if its vertex or central spot is located at point P_1 and at the time t_0 , it will reach position P_2 at time $t + \tau$, where $\tau = (lP_2 - P_1)/v < (lP_2 - P_1)/c$. This is different from the illusory “scissor effect,” *even if the feeding energy, coming from*

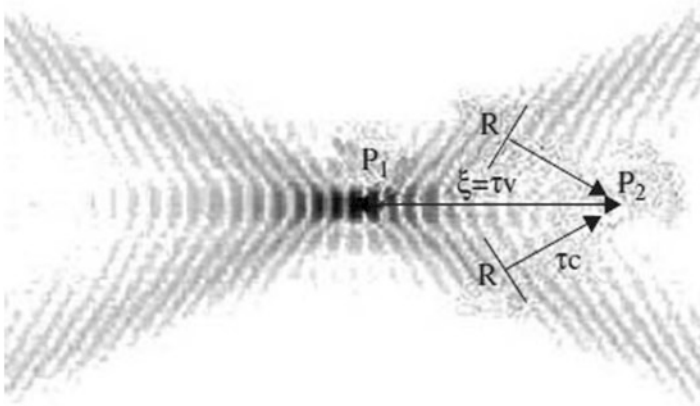


Fig. 2.85 An X-shaped wave [63]

the regions R , has traveled with the ordinary speed c (which is the speed of light in the electromagnetic case, the sound speed in acoustics, etc.).

In Fig. 2.85, we illustrate the fact that if its vertex or central spot is located at point P_1 at the time t_1 , it will reach position P_2 at time $t + \tau$, where $\tau = (l_{P_2} - P_1/v) < (l_{P_2} - P_1/c)$.

Such X-shaped waves resulted in interesting and flexible localized solutions, even if their velocity V is supersonic or superluminal ($v > c$), and have been studied in several papers. Actually, when the phase velocity does not depend on the frequency, it is known that such a phase velocity becomes the group velocity! Remembering how a superposition of Bessel beams is generated (e.g., by a discrete or continuous set of annular slits or transducers), it is clear that the energy forming the X-waves coming from those rings travels at the ordinary speed c of plane waves in the medium considered [71–74]. (Here, c , representing the velocity of the plane waves in the medium, is the speed of sound in the acoustic case, the speed of light in the electromagnetic case, and so on.) Nevertheless, the peak of the X-shaped waves is faster than c . Figure 2.86 is the representation of different configurations of all different waves, with demonstration of their energy locally.

It is possible to generate (in addition to the “classic” X-wave produced by Lu et al. in 1992) [65] infinite sets of new X-shaped waves, with their energy concentrated more and more in a spot corresponding to the vertex region [75]. It may therefore appear rather intriguing that such a spot (even if no violation of special relativity is obviously implied: all the results come from Maxwell’s equations or from the wave equations [76, 77]) travels superluminally when the waves are electromagnetic. We shall call all the X-shaped waves *superluminal* even when, for example, the waves are acoustic.

Furthermore, the word *beam* refers to a monochromatic solution to the considered wave equation, with a transverse localization of its field. However, our considerations, of course, hold for any wave equation such as vectorial, spinorial, and scalar in particular, for the acoustic case too.

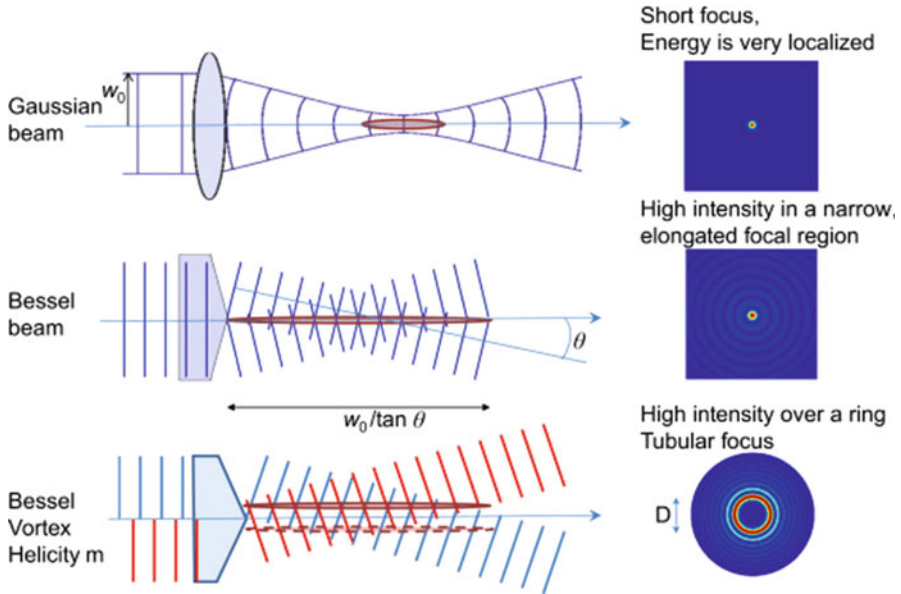


Fig. 2.86 Propagation and configuration of different waves

Additionally, in optical physics, the most common type of optical beam is the Gaussian one, whose transverse behavior is described by a Gaussian function. But all the common beams suffer a diffraction, which spoils the transverse shape of their field, widening it gradually during propagation. As an example, the transverse width of a Gaussian beam doubles when it travels a distance $z_{\text{dif}} = \sqrt{3}\pi\Delta\rho_0^2/\lambda_0$, where $\Delta\rho_0$ is the beam initial width and λ_0 is its wavelength. One can verify that a Gaussian beam with an initial transverse aperture of the order of its wavelength will already double its width after having traveled along a few wavelengths.

It was generally believed that the only wave devoid of diffraction was the plane wave, which does not suffer any transverse changes. Some authors had shown that it is not actually the only one. For instance, in 1941 Stratton [67] obtained a monochromatic solution to the wave equation whose transverse shape was concentrated in the vicinity of its propagation axis and represented by a Bessel function. Such a solution, now called a Bessel beam, was not subject to diffraction since no change in its transverse shape took place with time.

Figure 2.87 illustrates the shape and difference between, for example, Gaussian and Bessel beams.

Mathematically each of these beams can be defined as

$$S(k_\rho, \omega) = 2a^2 e^{-a^2 k_\rho^2} \delta(\omega - \omega_0) \quad \text{Gaussian Beam} \quad (2.341)$$

and

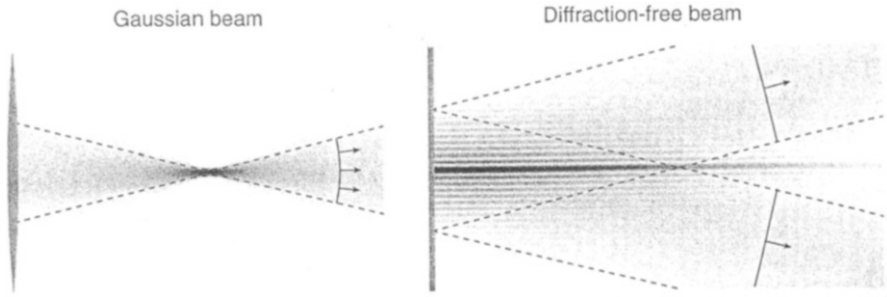


Fig. 2.87 Gaussian vs. Bessel beams

$$S(k_\rho, \omega) = \frac{\delta[k_\rho - (\omega/c) \sin \theta]}{k_\rho} \delta(\omega - \omega_0) \quad \text{Bessel Beam} \quad (2.342)$$

When we compare these two beams from the point of view of diffraction and dispersion, we can state the following:

Diffraction and dispersion are known since long to be the phenomena limiting the applications of (optical, for instance) beams or pulses.

Diffraction is always present, affecting any waves that propagate in 2- or 3-dimensional unbounded media, even when homogeneous. Pulses and beams are constituted by waves traveling along different directions, which produces a gradual spatial broadening. This effect is really a limiting factor whenever a pulse is needed which maintains its transverse localization, like in free-space communications, image forming, optical lithography, and electromagnetic tweezers.

Dispersion on the other hand acts on pulses propagating in material media, causing mainly a temporal broadening: an effect known to be due to the variation of the refraction index with the frequency, so that each spectral component of the pulse possesses a different phase velocity. This entails a gradual temporal widening, which constitutes a limiting factor when a pulse is needed which maintains its time width, like in communication systems.

As we have emphasized, it is important, therefore, to develop techniques able to reduce those phenomena. The so-called localized waves (LW), known also as non-diffracting waves, are indeed able to resist diffraction for a long distance in free space. Such solutions to the wave equations (and in particular to Maxwell equations, under weak hypotheses) were theoretically predicted long time ago.

Based on difference behavior between diffraction and dispersion in Table 2.2, Bessel beams are able to resist these effects which make them useful! For more details on definition of Bessel beam see Sect. 2.13 of this chapter.

In summary, among the infinite family of exact superluminal solutions of Maxwell equations are waves known as X-waves [52]. Scalar X-waves have been measured experimentally by Lu and Greenleaf [65], and subsequently by Lu, who showed that the peak of a finite aperture approximation to an acoustical X-wave can

Table 2.2 Comparison between diffraction and dispersion

Diffraction	Dispersion
<ul style="list-style-type: none"> • Diffraction is a gradual spatial broadening • This is a limiting factor in that it affects the transverse localization 	<ul style="list-style-type: none"> • This effect creates temporal broadening • It is a variation in the refraction index with frequency

travel with speed greater than the sound speed parameter appearing in the homogeneous wave equation [52].

Rodrigues and Lu [52] also performed several simulations for the propagation of X-waves, showing that their peaks can move with superluminal speed, an effect subsequently verified by Saari and Reivelt [78].

These results do not violate special relativity because all the produced superluminal X-waves have wave fronts that travel with the speed parameter c (the speed of light) that appears in the corresponding wave equation. The superluminal motion of the peak is therefore a transitory phenomenon similar to the reshaping phenomenon that occurs (under very special conditions) for waves in dispersive media with absorption or gain and which is in this case responsible for superluminal (or even negative) group velocities [53].

In physics, **X-waves** are localized solutions of the wave equation that travel at a constant velocity in a given direction. X-waves can be sound, electromagnetic, or gravitational waves. They are built as a non-monochromatic superposition of Bessel beams. Ideal X-waves carry infinite energy, but finite-energy realizations have been observed in various frameworks. Electromagnetic X-waves travel faster than the speed of light, and X-wave pulses can have superluminal phase and group velocity [79].

In optics, X-wave solutions have been reported within a quantum mechanical formulation [80].

As a final claim for summary of this section, we can say that one novel family of generalized non-diffracting waves are X-waves and they are exact non-diffracting solutions of the isotropic/homogenous scalar wave equation and are a generalization of some of the previously known non-diffracting waves such as the plane wave, Durnin’s beams, and non-diffracting portion of the Axicon beam equation in addition to an infinity of new beams. One subset of the new non-diffracting waves have X-like shapes that are termed “X-waves.” These non-diffracting X-waves can be almost exactly realized over a finite depth of field with finite apertures and by either broadband or band-limited radiators. With a 25 mm diameter planar radiator, a zeroth-order broadband X-wave will have about 2.5 mm lateral and 0.17 mm axial -6-dB beam widths with a -6-dB depth of field of about 171 mm. The phase of the X-waves changes smoothly with time across the aperture of the radiator; therefore, X-waves can be realized with physical devices. A zeroth-order band-limited X-wave was produced and measured in water by our 10 elements, 50 mm diameter, 2.5 MHz PZT ceramic/polymer composite *Jo* Bessel non-diffracting annular array transducer with -6-dB lateral and axial beam widths of about 4.7 mm and 0.65 mm, respectively, over a -6-dB depth of field of about 358 mm.

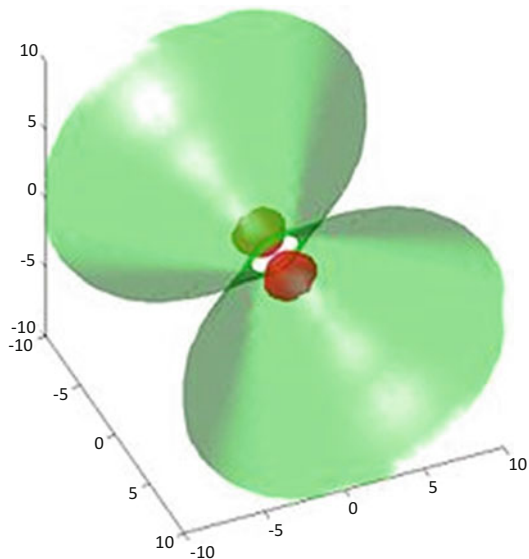
2.12 The Nonlinear X-Waves

As we stated before, in physics, a nonlinear X-wave (NLX) is a multidimensional wave that can travel without distortion. At variance with X-waves, a nonlinear X-wave does exist in the presence of nonlinearity, and in many cases it self-generates from a Gaussian (in any direction) wave packet. The distinctive feature of an NLX is its “biconical” shape (see figure) which appears as an “X” in any section plane containing the wave peak and the direction of propagation. So far, nonlinear X-waves have been only observed in nonlinear optics experiments and have been predicted to occur in a variety of nonlinear media including Bose-Einstein condensates. Figure 2.88 is an illustration of a nonlinear X-wave schematic view.

However, note that what we mean by a localized solution for these non-diffraction waves are as follows: Anything local is a part of the entire space. If the function goes through a portion of the space, and you solve it on some smaller domain, your solution is local. This is seen classically in optimization problems which are not global. They rather give local solutions, which potentially are not global optimum. A global optimum covers the entire domain.

There are other types of such ocean waves, traveling water waves, traveling harmonic waves, as well as energy density and flux in traveling wave that are discussed extensively in other textbooks and one reference that we recommend is the book by Crawford, where we encourage readers to refer themselves to it, and those details are beyond the scope of this book [81].

Fig. 2.88 Nonlinear X-wave schematic view



2.13 The Bessel's Waves

As we did mention above, non-diffracting wave (NDW), known also as localized wave, is, indeed, able to resist diffraction for a long distance (see Table 2.2). Today, NDWs are analyzed and well established both theoretically and experimentally, and have very important and innovative applications not only in vacuum, but also in material both linear and nonlinear and recently in meta-materials media also it is showing resistance to dispersion, and thus they can travel a long distance. Their potential applications are being exploded and explored as well as implemented extensively in military and medical industries, with very surprising and mesmerizing results, in fields such as acoustics, microwaves, and optics, and they are also very promising in mechanical engineering, geophysics [63], and even elementary particle physics [82] and gravitational wave as well.

One interesting acoustic application has been already obtained in high-resolution ultrasound scanning of moving organs in the human body, due to the unique behavior of NDWs that are suitable superpositions of Bessel beams. Furthermore, worth noticing is that peculiar superposition of Bessel beams can be used to obtain “static” NDW field, with high transverse localization, and whose longitudinal intensity pattern can assume a desired shape within a chosen interval of the propagation axis (i.e., $0 \leq z \leq L$); thus such waves with a *static* envelope are called frozen waves (FW) in terms of continuous Bessel beam superpositions. These FWs promise to have very important applications, even in the field of medicine and tumor curing [83].

Figure 2.89 is a presentation of continuous wave (CW) Bessel beam as part of its acoustic application in water, where it was measured for a frequency of 2.5 MHz.

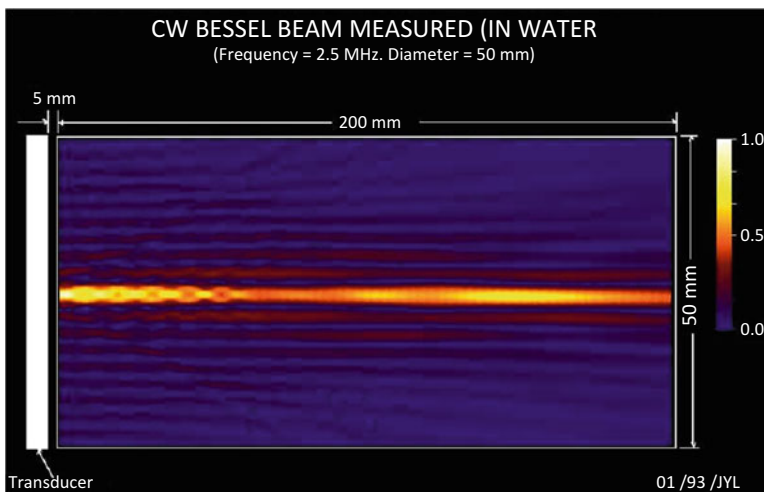


Fig. 2.89 Illustration of continuous wave Bessel beam in water

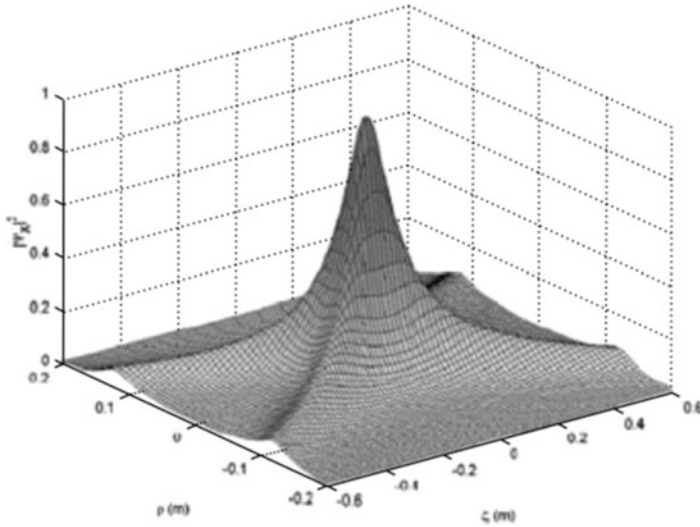


Fig. 2.90 3D plot of the real part of the ordinary X-wave

It is worth to mention that in consideration of Bessel beam application a Bessel beam can travel, approximately without deformation, a distance 28 times larger than a Gaussian beam.

Actually, Lu et al. managed to introduce classic X-wave for acoustics [65, 66], and then later on after having mathematically and experimentally constructed their “classic” acoustic X-wave they did start applying them to ultrasonic scanning, directly obtaining very-high-quality 3D images, and as such they produced images such as in Fig. 2.90 here that depicts the real part of an ordinary X-wave with velocity $v = (1.1)c$ and with $a = 3m$, where a is a positive constant as part of Heaviside step function for the wave equation solution of X-wave that is described in Sect. 2.14 of the chapter.

In this figure ρ is the distance from axis, while ξ is equal to $z - vt$ (i.e., $\xi = z - vt$). Note that X-waves are the superposition of Bessel beams and they are plane waves, where the transverse components of the wave are no longer planar, but rather to make up the surface of two cones whose apexes touch as it is shown in Fig. 2.91 here.

In Fig. 2.91, all the X-waves (truncated or not) must have a leading cone in addition to the rear cone; such a leading cone will have a role even for the peak stability. Long ago, this was also predicted, in a sense, by nonrestricted special relativity. One should not forget, in fact, that all wave equations, and not only Maxwell’s, have an intrinsic relativistic structure.

Note: The localization in space of the wave can be changed along z , which means a soliton-like wave of energy can be accelerated towards a target. If there are particles within this soliton it could act as an electromagnetic/kinetic.

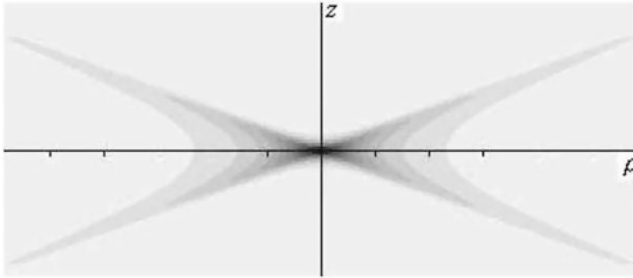


Fig. 2.91 All the X-waves

General solution of Bessel beam function in cylindrical coordinate (see Sect. 2.14 of this book for more details) for localized solution of the wave can be found as

$$\Psi(\rho, z, t) = J_0\left(\frac{\omega_0}{c}\rho \sin(\theta)\right) \exp\left[i\frac{\omega_0}{c}\cos(\theta)\left(z - \frac{c}{\cos(\theta)}t\right)\right] \tag{2.343}$$

As Eq. (2.347) indicates, this beam possesses phase velocity $v_{ph} = c/\cos(\theta)$, and field transverse shape represented by a Bessel function $J_0(\cdot \cdot \cdot)$, so that its field is concentrated in the surroundings of the propagation axis z ; also the reason why this beam is called Bessel beam is because the solution form in Eq. (2.347) involves a Bessel function of zero kind such as $J_0(\cdot \cdot \cdot)$.

2.14 Generalized Solution to Wave Equation

To confine ourselves to electromagnetism, we can consider the present-day studies on electromagnetic tweezers, optical or acoustic scalpels, optical guiding of atoms or charged or neutral corpuscles, optical lithography, optical or acoustic images, communications in free space, remote optical alignment, optical acceleration of charged corpuscles, and so on and so forth.

One of the things that would be interested to touch upon here is a little more detailed introduction to the general solution of a differential equation known as homogeneous wave equation, which is a simple form of wave equation, yet so important in acoustics, electromagnetism (i.e., microwave, optics, . . .), geophysics, and even, as we said, gravitational waves and elementary particle physics.

A monochromatic solution was obtained by Stratton [67] for the wave equation whose transverse shape was concentrated near its propagation axis and represented by a Bessel function. This can be partially justified since Bessel beam was associated with an infinite power flux [as much as the plane waves, incidentally], it being not square-integrable in the transverse direction. An interesting problem, therefore, was that of investigating what would happen to the ideal Bessel beam solution when truncated by a finite transverse aperture.

To continue with our solution to wave equation in a generalized matter, we take under consideration a general form of solution for wave function $\psi(x, y, z, t)$ that can be written in Cartesian coordinate as

$$\left(\frac{\partial^2}{\partial x^2} + \frac{\partial^2}{\partial y^2} + \frac{\partial^2}{\partial z^2} - \frac{1}{c^2} \frac{\partial^2}{\partial t^2} \right) \psi(x, y, z, t) = 0 \quad (2.344a)$$

or

$$\square \psi(x, y, z, t) = 0 \quad (2.344b)$$

where $\square \equiv \nabla^2 - \frac{1}{c^2} \frac{\partial^2}{\partial t^2}$ is known as *d'Alembert operator*.

Now let us write Eqs. (2.344a) and (2.344b) in cylindrical form of coordinate with components of ρ , φ , and z ; thus we seek a solution in this coordinate and for the sake of simplicity we confine our solution to axially symmetric solutions as $\psi(\rho, z, t)$, so we do not have any dependency on angle φ and thus we have a mathematical relation as

$$\left(\frac{\partial^2}{\partial \rho^2} + \frac{1}{\rho} \frac{\partial}{\partial \rho} + \frac{\partial^2}{\partial z^2} - \frac{1}{c^2} \frac{\partial^2}{\partial t^2} \right) \psi(\rho, z, t) = 0 \quad (2.345)$$

In free space, solution $\psi(\rho, z, t)$ can be written in terms of a Bessel-Fourier transform with reference to the variable ρ , and two Fourier transforms with reference to variables z and t , as follows:

$$\psi(\rho, z, t) = \int_0^\infty \int_{-\infty}^{+\infty} \int_{-\infty}^{+\infty} k_\rho J_0(k_\rho \rho) e^{ik_z z} e^{-i\omega t} \bar{\psi}(k_\rho, k_z, \omega) dk_\rho dk_z d\omega \quad (2.346)$$

where $J_0(k_\rho, \rho)$ is an ordinary zero-order Bessel function and $\bar{\psi}(k_\rho, k_z, \omega)$ is the transform of $\psi(\rho, z, t)$. Substituting Eq. (2.346) into Eq. (2.345), one obtains that the relation among ω , k_ρ , and k_z is given by the following form:

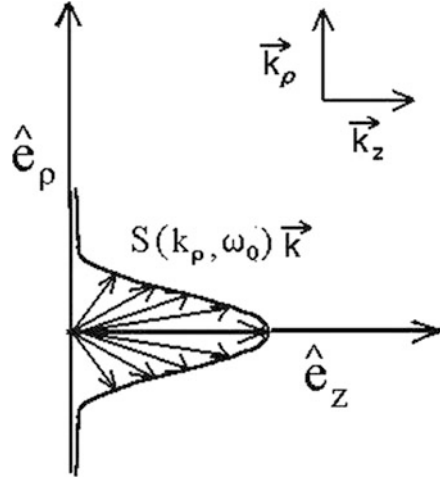
$$\frac{\omega^2}{c^2} = k_\rho^2 + k_z^2 \quad (2.347)$$

Equation (2.347) has to be satisfied. In this way, by using the condition given by Eq. (2.347) in Eq. (2.346), any solution to the wave Eq. (2.349) can be written as

$$\psi(\rho, z, t) = \int_0^{\omega/c} \int_{-\infty}^{+\infty} k_\rho J_0(k_\rho \rho) e^{i\sqrt{\omega^2/c^2 - k_\rho^2} z} e^{-i\omega t} S(k_\rho, \omega) dk_\rho d\omega \quad (2.348)$$

where $S(k_\rho, \omega)$ is the chosen spectral function.

Fig. 2.92 Visual interpretation of the integral solution of Eq. (2.348) [84]



The general integral of Eq. (2.348) yields for instance the **non-localized** Gaussian beams and pulses, to which we shall refer for illustrating the differences of the localized wave with respect to them [84].

A very common non-localized *beam* is the Gaussian beam correspond to the spectrum as [85]

$$S(k_\rho, \omega) = 2a^2 e^{-a^2 k_\rho^2} \delta(\omega - \omega_0) \tag{2.349}$$

In Eq. (2.349), a is a positive constant, which can be shown to depend on the transverse aperture of the initial pulse [84].

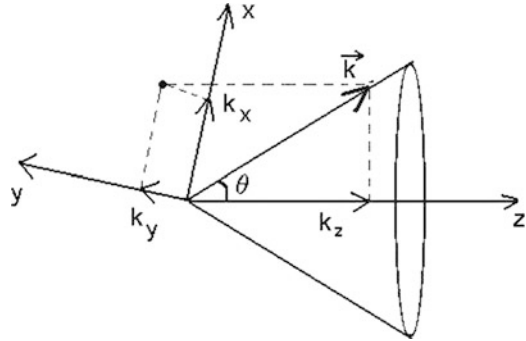
Figure 2.92 illustrates the interpretation of the integral solution of (2.348), with spectral function given in (2.349), as a superposition of plane waves. Namely, from Fig. 2.91 one can easily realize that this case corresponds to plane waves propagating in all directions always with $\vec{k}_z \geq 0$, the most intense ones being those directed along positive z . Notice that in the plane wave case \vec{k}_z is the longitudinal component of the wave vector, $\vec{k} = \vec{k}_\rho + \vec{k}_z$, where $\vec{k}_\rho = k_x + k_y$.

Again, note that Fig. 2.92 is a visual interpretation of the integral solution Eq. (2.348), with the spectrum provided by Eq. (2.348), in terms of a superposition of plane waves.

By substituting Eq. (2.349) into Eq. (2.348) and adopting the paraxial approximation, one meets the Gaussian beam wave equation as

$$\psi_{\text{gauss}}(\rho, z, t) = \frac{2a^2 \exp\left(\frac{-\rho^2}{4(a^2 + iz/2k_0)}\right)}{2(a^2 + iz/2k_0)} e^{ik_0(z-ct)} \tag{2.350}$$

Fig. 2.93 The axially symmetric Bessel beam [84]



where $k_0 = \omega_0/c$. We can verify that such a beam, which suffers transverse diffraction, doubles its initial width $\Delta\rho_0 = 2a$ after having traveled the distance $z_{dif} = \sqrt{3}k_0\Delta\rho_0^2/2$, called diffraction length. The more concentrated a Gaussian beam happens to be, the more rapidly it gets spoiled [84].

It is noticeable as well that the most common non-localized pulse is the Gaussian pulse, which is not deviated from Eq. (2.352) by using the spectrum defined by Zamboni-Rached et al. [86] as

$$S(k_\rho, \omega) = \frac{2ba^2}{\sqrt{\pi}} e^{-a^2k_\rho^2} e^{-b^2(\omega-\omega_0)^2} \tag{2.351}$$

Now, by substituting Eq. (2.351) into Eq. (2.348), and utilizing once more the paraxial approximation, one gets Gaussian pulse as [84]

$$\psi(\rho, z, t) = \frac{a^2 \exp\left(\frac{-\rho^2}{4(a^2 + iz/2k_0)}\right) \exp\left(\frac{-(z - ct)^2}{4c^2b^2}\right)}{a^2 + iz/2k_0} \tag{2.352}$$

endowed with speed c and temporal width $\Delta t = 2b$, and suffering a progressive enlargement of its transverse width, so that its initial value gets doubled already at position $z_{dif} = \sqrt{3}k_0\Delta\rho_0^2/2$, with $\Delta\rho_0 = 2a$.

It is noteworthy to say that the axially symmetric Bessel beam is created by the superposition of plane waves whose vectors lay on the surface of a cone having the propagation axis as its symmetry axis and angle equal to θ that is the ‘‘Axicon angle’’ as illustrated in Fig. 2.93 [84].

Considering Eq. (2.343), it indicates to us that the Bessel beam keeps its transverse shape, which is therefore invariant, while propagation with central ‘‘spot’’ is given as

$$\Delta\rho = \frac{2.405c}{(\omega \sin \theta)} \tag{2.353}$$

Now if we extend our attention to scalar function such as $\Phi(\vec{r}, t)$ for our discussion in the conquest of generalized solution to wave equation, then we consider an N -dimensional isotopic/homogeneous wave equation [89]:

$$\left[\sum_{j=1}^N \frac{\partial^2}{\partial x_j^2} - \frac{1}{c^2} \frac{\partial^2}{\partial t^2} \right] \Phi(\vec{r}, t) = 0 \tag{2.354}$$

where $x_j(j = 1, 2, \dots, N)$ represents rectangular coordinates in an N -dimensional space, $N \geq 1$ is an integer, $\Phi(\vec{r}, t)$ is a scalar function (sound pressure, velocity potential, or Hertz potential in electromagnetics) of spatial variables, $\vec{r} = (x_1, x_2, \dots, x_N)$, and time, t , c , is the speed of sound in a medium or the speed of light in vacuum [87, 88].

In 2-dimensional (i.e., 3D) space, we can utilize the *d'Alembert* operator $\square \equiv \nabla^2 - \frac{1}{c^2} \frac{\partial^2}{\partial t^2}$ and apply it to Eq. (2.354), to write the following forms of the equation:

$$\left(\nabla^2 - \frac{1}{c^2} \frac{\partial^2}{\partial t^2} \right) \Phi(\vec{r}, t) = 0 \tag{2.355a}$$

and

$$\square \Phi(\vec{r}, t) \tag{2.355b}$$

In Eq. (2.359) the symbol of ∇^2 is *Laplace* operator, while in Eq. (2.359) the symbol of \square , as we said, is the *d'Alembert* operator.

In cylindrical coordinate, the wave equation is given by

$$\left[\frac{1}{r} \frac{\partial}{\partial r} \left(r \frac{\partial}{\partial r} \right) + \frac{1}{r^2} \frac{\partial^2}{\partial \varphi^2} + \frac{\partial^2}{\partial z^2} - \frac{1}{c^2} \frac{\partial^2}{\partial t^2} \right] \Phi(\vec{r}, t) = 0 \tag{2.356}$$

where $r = \sqrt{x^2 + y^2}$, using Fig. 2.94, is the radial distance; $\varphi = \tan^{-1}(y/x)$ is the polar angle; and z is the axial axis.

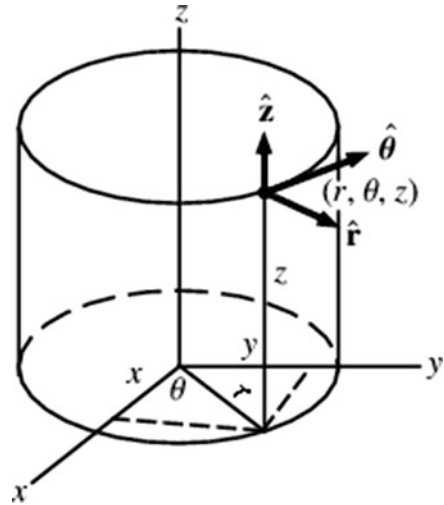
One generalized solution to the N -dimensional wave equation in Eqs. (2.355a) and (2.355b) is given by [65, 88, 89] the following equation [89]:

$$\Phi(x_1, x_2, \dots, x_N, t) = f(s) \tag{2.357}$$

where

$$s = \sum_{j=1}^{N-1} D_j x_j + D_N(x_N \pm c_1 t) \quad N \geq 1 \tag{2.358}$$

Fig. 2.94 Schematic of cylindrical coordinate in 3D



In Eq. (2.358), the parameter D_j are complex coefficients, and in Eq. (2.357), $f(s)$ is any well-behaved complex function of s and c_1 is given by [89]

$$c_1 = c \sqrt{1 + \sum_{j=1}^{N-1} D_j^2 / D_N^2} \tag{2.359}$$

If c_1 is real, $f(s)$ and its linear superposition represent limited diffraction solutions to the N -dimensional wave equation (see Eqs. (2.355a) and (2.355b)).

For example, if $N = 3$, $x_1 = x$, $x_2 = y$, $x_3 = z$, $D_1 = \alpha_0(k, \zeta) \cos \theta$, $D_2 = \alpha_0(k, \zeta) \sin \theta$, and $D_3 = b(k, \zeta)$, with cylindrical coordinates, one obtains families of solutions to Eq. (2.356) [65, 88, 89]:

$$\Phi_\zeta(s) = \int_0^\infty T(k) \left[\frac{1}{2\pi} \int_{-\pi}^{+\pi} A(\theta) f(s) d\theta \right] dk \tag{2.360}$$

and

$$\Phi_K(s) = \int_{-\pi}^{+\pi} D(\zeta) \left[\frac{1}{2\pi} \int_{-\pi}^{+\pi} A(\theta) f(s) d\theta \right] d\zeta \tag{2.361}$$

where

$$s = \alpha_0(k, \zeta) r \cos(\phi - \theta) + b(k, \zeta) [z \pm c_1(k, \zeta) t] \tag{2.362}$$

and where

$$c_1(k, \zeta) = c\sqrt{1 + [\alpha_0(k, \zeta)/b(k, \zeta)]^2} \quad (2.363)$$

and $\alpha_0(k, \zeta)$, $b(k, \zeta)$, $A(\theta)$, $T(k)$, and $D(\zeta)$ are well-behaved functions, and θ , k , and ζ are free parameters. If $c_1(k, \zeta)$ is real, and is not a function of k and ζ , respectively, $\Phi_\zeta(s)$ and $\Phi_K(s)$ are families of limited diffraction solutions to the wave equation (see Eq. (2.356))[89].

The following function is also a family of limited diffraction solution to the wave equation [65, 88, 89], which represents waves that can propagate to an infinite distance without changing their wave shape at the speed of c :

$$\Phi_L(r, \varphi, z - ct) = \Phi_1(r, \rho)\Phi_2(z - ct) \quad (2.364)$$

where $\Phi_2(z - ct)$ is any well-behaved function of $z - ct$ and $\Phi_1(r, \rho)$ is a solution to the transverse Laplace equation:

$$\left[\frac{1}{r} \frac{\partial}{\partial r} \left(r \frac{\partial}{\partial r} \right) + \frac{1}{r^2} \frac{\partial^2}{\partial \varphi^2} \right] \Phi_1(r, \varphi) = 0 \quad (2.365)$$

Furthermore Lu [89] finds sets of solution for Bessel beams and X-waves as follows:

For Bessel beams:

$$\Phi_{B_n}(\vec{r}, t) = \Phi_{B_n}(r, \varphi, z - c_1 t) = e^{in\varphi} J_n(\alpha r) e^{i(\beta z - \omega t)} \quad \text{for } n = 0, 1, 2, \dots \quad (2.366)$$

where

B_n = n th-order Bessel beam

α = scaling parameter

$J_n(\dots)$ = the n th-order Bessel function of first kind

$c_1 = \omega/\beta$ = the phase velocity wave

For X-waves:

$$\begin{aligned} \Phi_{X_n}(\vec{r}, t) &= \Phi_{X_n}(r, \varphi, z - c_1 t) \\ &= e^{in\varphi} \int_0^\infty B(k) J_n(kr \sin \zeta) e^{-k[a_0 - i \cos \zeta (z - c_1 t)]} dk \quad \text{for } n = 0, 1, 2, \dots \end{aligned} \quad (2.367)$$

where

X_n = the subscript means n th-order X-wave

$c_1 = c/\cos \zeta \geq c$ = both the phase and group velocity of wave

$|\zeta| < \pi/2$ = the Axicon angle of X-wave

a_0 = a positive free parameter that determines the decaying speed of the high frequency of the device (acoustic transducer or electromagnetic antenna) that produces the wave

Compare Eq. (2.367) with Eq. (2.366). It is easy to see the similarity and it is easy to see the similarity and difference between a Bessel beam and an X-wave. X-waves are multiple-frequency waves while Bessel beams have a single frequency. However, both waves have the same limited diffraction property, that is, they are propagation invariant. Because of multiple frequencies, X-waves can be localized in both transverse space and time to form a tight wave packet. They can propagate in the free space or isotropic/homogeneous media without spreading or dispersion [89, 90].

References

1. https://en.wikipedia.org/wiki/Standing_wave
2. <https://en.wikipedia.org/wiki/Seiche>
3. G.H. Darwin, *The Tides and Kindred Phenomena in the Solar System* (John Murray, London, 1898), pp. 21–31
4. Tsunamis are normally associated with earthquakes, but landslides, volcanic eruptions and meteorite impacts all have the potential to generate a tsunami
5. J. Proudman, *Dynamical Oceanography* (Methuen, London, 1953). §117 (p. 225). OCLC 223124129
6. J.R. Merian, *Ueber die Bewegung tropfbarer Flüssigkeiten in Gefässen [On the motion of drippable liquids in containers] (thesis) (in German)* (Schweighauser, Basel, 1828) OCLC 46229431
7. T. Pierce, “*Marine and coastal Services Abbreviations and Definitions*” (PDF) (*National Weather Service*, Office of Climate, Water, and Weather Services, July 5, 2006). Archived from *the original* (pdf) on May 17, 2008. Retrieved April 19, 2017
8. This behaves in a fashion similar to a tidal bore where incoming tides are funneled into a shallow, narrowing river via a broad bay. The funnel-like shape increases the height of the tide above normal, and the flood appears as a relatively rapid increase in the water level
9. https://en.wikipedia.org/wiki/MOSE_Project
10. J.R. Reitz, F.J. Milford, R.W. Christy, *Foundations of Electromagnetic Theory*, 3rd edn. (Addison–Wesley Publishing Company, Boston, MA, 1979)
11. J.D. Jackson, *Classical Electrodynamics*, 3rd edn. (Wiley, Hoboken, NJ, 1990), pp. 27–29
12. O.L. Brill, B. Goodman, *Am J Physiol* **35**, 832 (1967). for a detailed discussion of casualty in the Coulomb gauge
13. K. Meyl, *Scalar Waves*, INDEL GmbH, Verlagsabteilung, http://www.k-meyl.de/xt_shop/index.php?cat=c3_Books-in-English.html. ISBN 2.9802542.4-0
14. <http://www.cheniery.org/books/part1/teslaweapons.htm>
15. <http://www.cheniery.org/images/people/moray%20pics.htm>
16. http://www.prahlad.org/pub/bearden/Columbia_attack.htm
17. <http://www.cheniery.org/books/excalibur/moray.htm>
18. D. Griffiths, *Introduction to electrodynamics*, 3rd edn. (Prentice Hall, Upper Saddle River, NJ, 1999)
19. H.E. Ensle, *The Electromagnetic Universe*, 2nd edn. (2013)

20. B. Zohuri, *Plasma Physics and Controlled Thermonuclear Reactions Drive Fusion Energy*, 1st edn. (Springer, Cham, 2016)
21. B. Zohuri, *Dimensional Analysis and Self-Similarity Methods for Engineers and Scientists*, 1st edn. (Springer, Cham, 2015)
22. J.D. Jackson, *Classical Electrodynamics*, 2nd edn. (Wiley, New York, 1975), pp. 681–790
23. Y. Aharonov, D. Bohm, Significance of electromagnetic potentials in the quantum theory. *Phys. Rev.* **115**, 485–491 (1959)
24. M.A. Steane, *Relativity Made Relativity Easy* (Oxford Publishing Company, Oxford, 2012)
25. N. Tesla, *My Inventions, V. The Magnifying Transmitter*, *Electrical Experimenter*, (June 1919), p. 112. Other articles can be found in Reference [26] below.
26. T.E. Bearden, *Solutions to Tesla's Secrets and the Soviet Tesla Weapons* (Tesla Book Company, Millbrae, CA, 1981)
27. C.N. Yang, R.L. Mills, Conservation of isotopic spin and isotopic gauge invariance. *Phys. Rev.* **96**, 191–195 (1954)
28. J.Y. Dea, Instantaneous Interactions, in *Proc 1986 ITS*
29. S.J. Gates Jr., in *Mathematica Analysis of Physical System*, ed. by R. Nickkens (Van Nostrand Reinhold, New York, 1985)
30. L.D. Landau, E.N. Lifshitz, *Quantum Mechanics Non-Relativistic Theory* (Addison-Wesley, Boston, MA, 1958)
31. D. Forster, *Hydrodynamic Fluctuations, Broken Symmetry, and Correlation Functions* (W. A. Benjamin, Inc., Reading, MA, 1975)
32. K.H. Panofsky, M. Phillips, *Classical Electricity and Magnetism*, 2nd ed. (Dover, Mineola, 1656)
33. R.C. Gelinias, *Cruel-Free Vector Potential Effects in Simply Connected Space* (Casner and Gelinias Co., Inc., International Tesla Society, Inc., 1985), pp. 4–43
34. J.Y. Dea, Scalar Fields: their prediction from classical electromagnetism and interpretation from quantum mechanics, in *The Proceeding of the Tesla Centennial Symposium, an IEEE Centennial Activity*, Colorado College, Colorado Springs, Colorado, Aug. 9–11 (New York, NY, 1984), pp. 94–98
35. E.T. Whittaker, One the partial differential equations of mathematical physics. *Math. Ann.* **57**, 332–355 (1903)
36. E.T. Whittaker (1903 and 1904), *ibid.*, for the original basis of Scalar interferometry and its creation of my kind of Electromagnetic field, potential, and wave in the interference zone
37. See M.W. Evans, P.K. Anastasovski, T.E. Bearden et al., On Whittaker's Representation of Electromagnetic Entity in Vacuo, Part V: The production of Transverse Field and Energy by Scalar Interferometry, *J. New Energy (JNE)* **4**(3), 76 (Winter 1999), for mathematical proof of scalar interferometry. There are several other AIAS papers in the same issue of *JNE*, dealing with interferometry and with the implications of the Whittaker papers
38. This is a claim by T.E. Bearden and his book of *Fer De Lance, A Briefing on Soviet Scalar Electromagnetic Weapons* and not this author, so it is up to reader how they are taking this claim. "As an example, the U.S.S. Skylark surface companion of the Thresher, was beset by mysterious "jamming" of multiple types of EM systems in multiple bands. So bad was it, that it required more than an hour to get an emergency message to Naval Headquarters that the Thresher was in serious difficulty. Later, as the scalar interferometry field away, all the EM systems aboard the Skylark resumed normal functioning. The Skylark was in fact in a "splatter zone" of the underwater interference zone around the Thresher
39. R.G. Chambers, *Phys. Rev. Lett.* **5**, 3 (1960)
40. W. Tai Tsun, C.N. Yang, Concept of nonintegrable phase factors and global formulation of gauge fields. *Phys. Rev. D* **12**, 3845–3857 (1975)
41. R.P. Feynman, R.B. Leighton, M. Sands, *The Feynman Lectures on Physics, Volume II*, Section 15-5, pp. 15-8 to 15-14
42. J.D. Jackson, *Classical Electrodynamics*, vol 223, 2nd edn. (Wiley, Hoboken, NJ, 1975)

43. P.A. Kossey et al., Artificial Ionospheric Mirrors (AIM), in *Ionospheric Modification and Its Potential to Enhance or Degrade the Performance of Military Systems* (AGARD Conference Proceedings 485, October 1990), 17A-1
44. A. Robinson, J. Holland, *Quantum Wave Theory—A Model of Unity in Nature* (2011)
45. C. Vuille, Schrodinger's equation and general relativity. *J. Math. Phys.* **41**(8), 5256–5261 (New York, NY, 2000)
46. E.T. Whittaker, An expression of the electromagnetic field due to electrons by means of two scalar potential functions. *Proc. Lond. Math. Soc.* **1**, 367–372 (1904)
47. H.A. Lorentz, A. Einstein, H. Minkowski, H. Weyl, *The Principle of Relativity: A Collection of Original Memoirs on the Special and General Theory of Relativity* (Dover, New York, 1952)
48. L. Brillouin, A. Sommerfeld, *Wave Propagation and Group Velocity* (Academic Press, New York, 1960)
49. M. Born, E. Wolf, *Principles of Optics: Electromagnetic Theory of Propagation, Interference, and Diffraction of Light*, 7th edn. (Cambridge University Press, Cambridge, England, 1999)
50. L.D. Landau, E.M. Lifschitz, *Electrodynamics of Continuous Media*, 2nd edn. (Pergamon Press, Oxford, England, 1984)
51. L.J. Wang, A. Kuzmich, A. Dogariu, Gain-Assisted Superluminal Light Propagation. *Nature* **406**, 277–279 (2000)
52. W.A. Rodrigues, J.Y. Lu, On the existence of Undistorted Progressive Waves (UPWs) of arbitrary speeds in nature. *Found. Phys.* **27**, 435–508 (1997)
53. J.E. Maiorino, W.A. Rodrigues Jr. What is superluminal wave motion? *Sci. Tech. Mag.* **2** (Aug. 1999), <http://www.cptec.br/stm>.
54. <http://scienceworld.wolfram.com/physics/SmarandacheHypothesis.html>
55. R. Courant, D. Hilbert, *Methods of Mathematical Physics*, vol 2 (Wiley, New York, 1966), p. 760
56. H. Bateman, *Electrical and Optical Wave Motion* (Cambridge University Press, Cambridge, 1915)
57. A.O. Barut, G.D. Maccarrone, E. Recami, On the shape of tachyons, *Nuovo Cimento A* **71**, 509–533 (1982), and refs. therein; see also E. Recami and G. D. Maccarrone, *Lett. Nuovo Cim.* **28**, 151–157 (1980) and **37**, 345–352 (1983); P. Caldirola, G. D. Maccarrone, and E. Recami, *Lett. Nuovo Cim.* **29**, 241–250 (1980); G. D. Maccarrone, M. Pavsic, and E. Recami. *Nuovo Cim. B* **73**, 91–111 (1983)
58. E. Recami, M. Zamboni-Rached, C.A. Dartora, The X-shaped, localized field generated by a superluminal electric charge, LANL archives e-print physics/0210047. *Phys. Rev. E* **69**, 027602 (2004)
59. A.O. Barut, A. Grant, Quantum particle-like configurations of the electromagnetic field. *Found. Phys. Lett.* **3**, 303–310 (1990)
60. A.O. Barut, A.J. Bracken, Particle-like configurations of the electromagnetic field: an extension of de Broglie's ideas. *Found. Phys.* **22**, 1267–1285 (1992)
61. J.N. Brittingham, Focus wave modes in homogeneous Maxwell's equations: transverse electric mode. *J. Appl. Phys.* **54**, 1179–1189 (1983)
62. A. Sezginer, A general formulation of focus wave modes. *J. Appl. Phys.* **57**, 678–683 (1985)
63. In *Localized Waves*, ed. by H.E. Hernández-Figueroa, M. Zamboni-Rached, and E. Recami (John Wiley, New York, 2008), book of 386 p
64. E. Recami, Classical tachyons and possible applications, *Riv. Nuovo Cim.* **9**(6), 1–178 (1986), and refs. therein.
65. J.-Y. Lu, J.F. Greenleaf, Nondiffracting X-waves: exact solutions to free-space scalar wave equation and their finite aperture realizations. *IEEE Trans. Ultrason. Ferroelectr. Freq. Control* **39**, 19–31 (1992). and refs. therein.
66. J.-Y. Lu, J.F. Greenleaf, Experimental verification of nondiffracting X-waves. *IEEE Trans. Ultrason. Ferroelectr. Freq. Control* **39**, 441–446 (1992)
67. J.A. Stratton, *Electromagnetic Theory* (McGraw-Hill, New York, 1941), p. 356
68. R.W. Ziolkowski, I.M. Besieris, A.M. Shaarawi, *J. Phys. A Math. Gen.* **33**, 7227–7254 (2000)

69. G. Shan, Quantum superluminal communication does not result in casual loop, CERN preprint (1999a)
70. G. Shan, Quantum superluminal communication must exist, CERN preprint (1999b)
71. J.-Y. Lu, J.F. Greenleaf, E. Recami, Limited diffraction solutions to Maxwell (and Schrödinger) equations, LANL archives e-print physics/9610012, Report INFN/FM-96/01, Istituto Nazionale de Fisica Nucleare, Frascati, Italy Oct. 1996; E. Recami: On localized X-shaped superluminal solutions to Maxwell equations, *Physica A* **252**, 586–610 (1998), and refs. therein; see also R.W. Ziolkowski, I.M. Besieris, and A.M. Shaarawi, *J. Opt. Soc. Am. A* **10**, 75 (1993); *J. Phys. A Math. Gen.* **33**, 7227–7254 (2000)
72. R.W. Ziolkowski, I.M. Besieris, A.M. Shaarawi, Aperture realizations of exact solutions to homogeneous wave equations. *J. Opt. Soc. Am. A* **10**, 75–87 (1993)
73. A.M. Shaarawi, I.M. Besieris, On the superluminal propagation of X-shaped localized waves. *J. Phys. A* **33**, 7227–7254 (2000)
74. A.M. Shaarawi, I.M. Besieris, Relativistic causality and superluminal signaling using X-shaped localized waves. *J. Phys. A* **33**, 7255–7263 (2000). and refs. therein
75. M. Zamboni-Rached, E. Recami, H.E. Hernández-Figueroa, New localized superluminal solutions to the wave equations with finite total energies and arbitrary frequencies. *Eur. Phys. J. D* **21**, 217–228 (2002)
76. A.P.L. Barbero, H.E. Hernández, Figueroa, and E. Recami, On the propagation speed of evanescent modes, *Phys. Rev. E* **62**, 8628 (2000), and refs. therein; see also A.M. Shaarawi and I.M. Besieris, *Phys. Rev. E* **62**, 7415 (2000)
77. H.M. Brodowsky, W. Heitmann, G. Nimtz, *Phys. Lett. A* **222**, 125 (1996)
78. P. Saari, K. Reivelt, Evidence of X-shaped propagation-invariant localized light waves. *Phys. Rev. Lett.* **79**, 4135–4138 (1997)
79. P. Bowlan, H. Valtna-Lukner, et al., Measurement of the spatiotemporal electric field of ultrashort superluminal Bessel-X pulses. *Opt. Photonics News* **20**(12), 42 (December 2009)
80. A. Ciattoni, C. Conti, [Quantum electromagnetic X-waves](http://arxiv.org/abs/0704.0442). [arxiv.org 0704.0442 v1](http://arxiv.org/abs/0704.0442)
81. F.S. Crawford, *Waves* (Berkeley Physics Course Volume 3), Hardcover, 1st ed. (McGraw-Hill, 1968)
82. E. Recami, M. Zamboni-Rached. Non-diffracting waves, and frozen waves: an introduction, 121 pages online in *Geophysical Imaging with Localized Waves*, Sanya, China 2011 [UCSC, S. Cruz, Cal.], and refs, therein (2011). <http://es.ucsc.edu/~acti/sanya/SanyaRecamiTalk.pdf>. Accessed 27 April 2013
83. E. Recami, M. Zamboni-Rached, H.E. Hernandez-Figueroa, et al.. Method and Apparatus for Producing stationary (intense) wave fields of arbitrary shape. Patent, Application No. US-2011/0100880 2011
84. E. Recami, M. Zamboni-Rached, H.E. Hernández-Figueroa, *Localized Waves: a Historical and Scientific Introduction*. arXiv:0708.1655v2 [physics.gen-ph] 16 Aug 2007
85. A.C. Newell, J.V. Molone, *Nonlinear Optics* (Addison & Wesley, Redwood City, CA, 1992)
86. M. Zamboni-Rached, H.E. Hernández-Figueroa, E. Recami, Chirped optical X-shaped pulses in material media. *J. Opt. Soc. Am. A* **21**, 2455–2463 (2004)
87. J.-Y. Lu, J. Cheng, J. Wang, High frame rate imaging system for limited diffraction array beam imaging with square-wave aperture weightings. *IEEE Trans. Ultrason. Ferroelectr. Freq. Control* **53**(10), 1796–1812 (2006)
88. J.-Y. Lu, J.F. Greenleaf, Diffraction-limited beams and their applications for ultrasonic imaging and tissue characterization. *Proc. SPIE* **1733**, 92–119 (1992). ISBN: 0-8194-0906-5
89. J.Y. Lu, H. Zou, J.F. Greenleaf, Biomedical ultrasound beam forming. *Ultrasound Med. Biol.* **20**(5), 403–428 (1994)
90. J.Y. Lu, Limited-diffraction beams for high-frame-rate imaging, in *Non-Diffracting Waves*, eds. by H. E. Hernández-Figueroa and E. Recami, M. Zamboni-Rached (Wiley, Hoboken, NJ, 2008)

Chapter 3

Laser Beam Energy as Weapon



Laser technology is only 30 years old, but it is much diversified. There are already varieties of military applications, although there are many limitations restricting the use of lasers. Today, the armed forces in most countries routinely use a wide range of laser devices such as laser range finders and designators. In some countries, work is proceeding on more imaginative laser weapon concepts that will eventually fulfill realistic, yet very precise, military requirements. The design of a specific laser weapon is heavily influenced by the characteristics of the intended target. If the desired effect of the weapon is to neutralize aircraft, helicopters, or missiles by burning holes through them or tanks by putting many miniature cracks (crazing) in the glass vision blocks to make them appear to be frosted, a very-high-energy laser has to be used with a power output on the order of several megawatts (MW). Such a laser would be a true anti-material weapon. However, if the target is a sensitive electro-optical system or some other type of sensor system, which has to be jammed or destroyed by a laser operating in a countermeasure mode, the choice will be a low-energy laser operating within the frequency bandwidth of the target sensor. This use of a laser can also be considered anti-material. If the target is a soldier, there is one part of his body that is extremely sensitive to laser radiation—his eyes. It is sufficient to use a low-energy laser operating in the visible or near-infrared (near-IR) part of the spectrum to damage the soldier's eyes and, in effect, cause blindness. If the laser is to cause burn injuries to the soldier's skin or to set fire to his uniform, a high-energy laser is required. In either case, if the purpose of the laser is to blind or burn the soldier, it will obviously be antipersonnel.

3.1 Introduction

Even before the laser was invented, science fiction writers told of incredible weapons and machines that emitted a bright saber of light, a death ray that disintegrated everything in its path. Even today, science fiction movies and books place high

emphasis on weapons that use light instead of bullets. The laser beam is popularly thought of as a very powerful death ray which can be fired from a handheld laser gun to vaporize soldiers, demolish building, and burn through target armors. In reality, the laser is a suitable tool for many military applications and can be turned into a deadly weapon but there are definitely limitations to what a laser can do. The laser really is a ray weapon, and its light rays can damage some targets in a way that appeals to the most vivid imagination. It is important to take these somewhat speculative factors into consideration when studying the psychological effects of the use of laser weapons on the battlefield. Otherwise, it will not be possible to get a complete and realistic picture of what using a laser really means to the combatants.

3.2 Possible Targets

A discussion of laser weapon applications outlining what laser weapons can really do must start with the destination of the laser beam—the target. The desired effect on the target ultimately decides what is needed from the laser. To a large extent, the interaction between the laser beam that is selected and the target also determines which cost-effective weapons are developed, produced, and deployed into battlefield.

The sensitivity of the target to laser light determines whether a low-energy or high-energy laser is required. If the target is sufficiently sensitive to low levels of energy within a comparatively broad band of the spectrum, a cheap and cost-effective laser weapon can be designed and mass-produced. If high energy is required, the possibility of designing a usable and affordable laser weapon decreases drastically.

3.3 Energy Level at the Target

One of the basic questions facing the laser weapon designer is what energy level must be absorbed by the target in order to get the desired result. The absorbed energy (E) is some fraction (A) of the product of the power density or intensity (I) present in the laser beam and the emission duration (t). E is measured in energy units, joules (J), or watt seconds per area, usually expressed in square centimeters, I in power units, watts (W) per square centimeter, and time in seconds in the following equation:

$$E = A(I \times t) \quad (3.1)$$

This means that if the emission duration is required to be short, as it would be in the engagement of multiple targets, the power density has to be as high as possible. The power density is calculated as the beam power divided by the size of the

“beamed” area, which means that a high beam power and a small surface area will give a high power density. How much of the laser power will finally be absorbed by the target in the affected surface area will determine what destructive effect will be achieved. The laser power goes from the laser to the target, suffers transmission losses in the optical system and the atmosphere, and has a further loss when some of the power is reflected from the target surface. The absorbed power is normally no more than 20–60% of the original emitted laser power.

One parameter that is useful in determining the effectiveness of a Gaussian laser beam is the beam irradiance at the target. For a beam with output power P_0 and cross-sectional A at the target, the peak irradiance I_p at the target is

$$I_p = \frac{P_0 \tau}{A} \quad (3.2)$$

where τ is the atmospheric transmittance.

The effectiveness of a laser beam in causing mechanical damage is, thus, dependent on beam power, pulse duration, wavelength, air pressure, the material, and the finish of the target surface. For example, a painted area has considerably increased energy absorption when compared to an unpainted aluminum plate. The absorption varies widely between different materials and at different wavelengths. The absorption of a ruby laser at 694 nm is 11% for aluminum, 35% for light-colored human skin, and 20% for white paint. The corresponding figures for a CO₂ laser at 10,600 nm are 1.9, 95, and 90%. This also indicates that one way to counter a HEL weapon is to choose a very reflective material for the target surface. On the other hand, longer wavelengths emitted by the laser can reduce the effects of highly reflective materials and increase the absorption. Every factor in this very difficult pattern combines to determine the degree of target destruction as well as the final energy level that will be needed to produce the desired effect.

It is obvious that the level of energy required to destroy a target varies considerably depending on the circumstances. Therefore, it is not surprising that the required energy-level figures quoted in the open literature also show rather large variations. In spite of this, some numbers may be given which indicate the general range of energy levels.

An aircraft, helicopter, or missile could be hit with a HEL weapon in many different ways that in the end would nullify it. Fuel tanks could be ruptured, or the fuel itself could be caused to explode. Windshields could be shattered, and parts of the control surfaces such as elevators or rudders could be destroyed or disturbed enough to make it impossible to continue fighting. The rotor head of a helicopter or the wing of an airplane or a missile could be made to fail, resulting in a crash. Sensors, radars, and other navigation aids could be destroyed; if this destruction occurs during a sensitive and crucial moment in the last phase of an attack, it could result in a crash or an aborted mission. Also, in some situations, a HEL weapon could even explode the ammunition carried by an airborne attacker.

To punch through the metal skin of an airplane requires about 700 joules per square centimeter, although it should be noted that a hole burned in the skin of an

airplane may not be sufficient to destroy it in the air or even to make it crash. A more realistic energy level to disable an aircraft may be five to ten times higher, which means that a successful HEL weapon will have to be able to deliver at least 5000–10,000 joules per square centimeter on the target.

Optical sensors and radomes (plastic radar domes) are much easier to damage; no more than 10 joules per square centimeter needs to be delivered directly on the target. Furthermore, if the laser wavelength is within the sensitive wavelength region of the sensor in question, the energy needed could be extremely low. If the HEL weapon is used as an antipersonnel weapon, that is, as a long-range flamethrower, the energy necessary to burn exposed skin is merely 15 joules per square centimeter, and damage to the cornea, the clear window into the eye, requires only 1 joule per square centimeter.

3.4 Absorption and Scattering

The earth's atmosphere is acting like an absorbing medium. Absorption occurs when a photon of radiation is absorbed by a gaseous molecule of the atmosphere that converts the photon into the molecule's kinetic energy. Hence, absorption is a way and procedure by which the atmosphere is heated, and it is a strong function of laser or radiation of wavelength. For example, propagation of radiation essentially gets eliminated at a wavelength below 0.2 μm due to absorption by O^2 and O^3 , while there is very little absorption at the visible wavelengths (0.4–0.7 μm).

Scattering of electromagnetic waves in the visible and IR wavelengths occurs when the radiation propagates through certain air molecules and particles. Light scattering is strongly wavelength dependent, but there is no loss of energy like in absorption. The physical size of the scatters determines the type of scattering.

- *Rayleigh Scattering*—This is named after Lord Rayleigh caused by air molecules and haze that are small in comparison with the wavelength λ of the radiation (see Fig. 4.x below). Rayleigh scattering, also called *molecular scattering*, applies only to very clear atmosphere. The scattering coefficient is proportional to λ^{-4} , a relation known as the *Rayleigh law*. For these small air molecules, scattering is eligible at wavelengths greater than roughly 3 μm . At wavelengths below 1 μm , Rayleigh scattering produces the blue color of the sky as a consequence that blue light is scattered much more than other visible wavelengths (Fig. 3.1).

Fig. 3.1 Rayleigh scattering

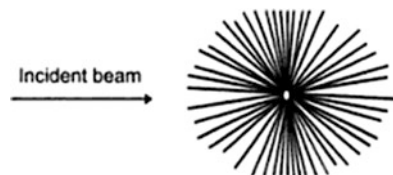
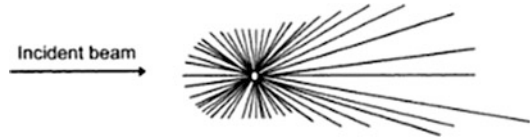


Fig. 3.2 Mie scattering



- *Mie Scattering* (named after Gustav Mie)—This is scattering by particles comparable in size to the radiation wavelength (also called *aerosol scattering*). Unlike Rayleigh scattering, scattering by particles comparable in size to or greater than the radiation wavelength is concentrated in the forward direction (see Fig. 3.2). Scattering losses decrease rapidly with increasing wavelength, eventually approaching the Rayleigh scattering case. Mie scattering is the reason why sunset appears red.

A term that is sometimes used to describe atmospheric “visibility” is the visual range, which corresponds to the range at which radiation at $0.55\ \mu\text{m}$ is attenuated to 0.02 times its transmitted level. Rayleigh scattering by molecules implies a visual range of approximately 340 km (or 213 miles).

Absorption and scattering are often grouped together under the topic of *extinction*, defined as the reduction or attenuation in the amount of radiation passing through the atmosphere. The *transmittance* (also called *atmospheric transmission*) of laser radiation that has propagated a distance L is related to extinction as described by Beer’s law, which can be written as

$$\tau = \exp[-\alpha(\lambda)L] \quad \text{unit less} \quad (3.3)$$

where $\alpha(\lambda)$ is the extinction coefficient¹⁸ and the product $\alpha(\lambda)L$ is called the *optical depth*. The extinction coefficient is composed of two parts:

$$\alpha(\lambda) = A_a + S_a \quad [\text{m}^{-1}] \quad (3.4)$$

where A_a is the absorption coefficient and S_a is the scattering coefficient. Absorption and scattering are deterministic effects that are fairly well known.

Software packages like LOWTRAN, FASCODE, MODTRAN, HITRAN, and PCLNWIN (most of these codes are available from Galaxy Advanced Engineering) are commonly used by both government and private industry to predict transmittance (attenuation) effects as a function of wavelength λ , based on a variety of conditions—meteorological range, latitude (tropical, mid, arctic), altitude, etc. A typical output from MODTRAN for rural aerosols with meteorological range of 23 km is shown in Fig. 3.3 as a function of wavelength over 1–10 μm .

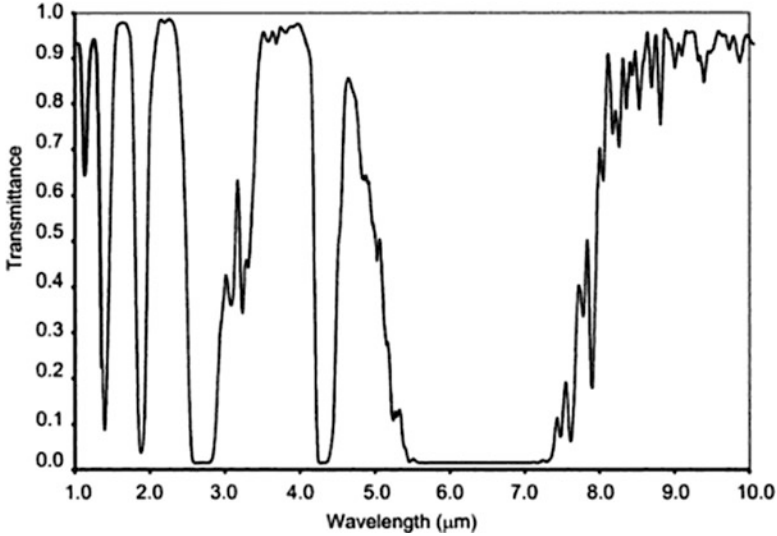


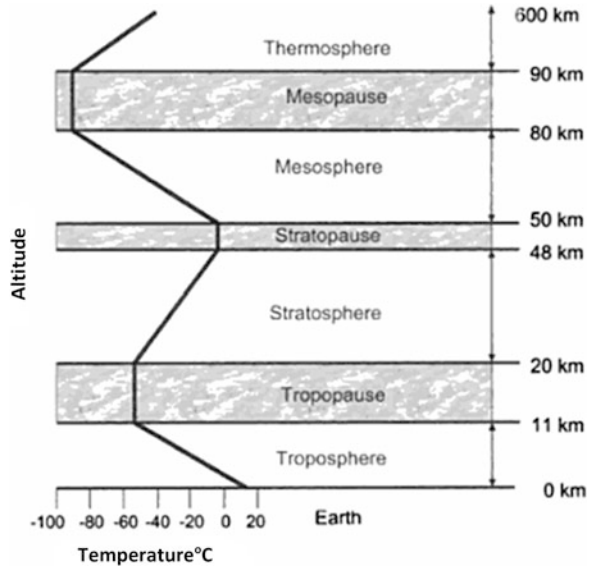
Fig. 3.3 Typical atmospheric transmittance for a horizontal 1 km path. Height above ground is 3 m with no rain or clouds

3.5 Atmospheric Structure with Altitude

The atmosphere is a gaseous envelope that surrounds the earth and extends to several 100 km above the surface. Over 98% of the atmosphere by volume is comprised of the elements nitrogen and oxygen. The major constituents of the atmosphere are water vapor, carbon dioxide, nitrous oxide, carbon monoxide, and ozone. Based mostly on temperature variations, the earth's atmosphere is divided into four primary layers (Fig. 3.4):

- *Troposphere*—extends up to 11 km and contains roughly 75% of the earth's atmospheric mass. Maximum air temperature occurs near the surface of the earth but decreases with altitude to -55°C . The *tropopause* is an isothermal layer extending 9 km above the troposphere where air temperature remains constant at -55°C . The tropopause and troposphere together are known as the *lower atmosphere*.
- *Stratosphere*—layer above the tropopause, which extends from 20 km up to 48 km altitude. The air temperature is roughly constant in the very lowest part of the stratosphere but then increases with altitude because the ozone gas in this layer absorbs ultraviolet sunlight, thereby creating heat energy. The ozone layer, which protects life from harmful ultraviolet radiation, is concentrated between 10 and 50 km. Separating the stratosphere from the mesosphere is the stratopause, another isothermal layer at approximately -3°C .
- *Mesosphere*—It extends from the stratopause to roughly 80 km. Temperature here generally decreases at a constant rate down to -90°C , which is the coldest

Fig. 3.4 Diagram depicting various atmospheric layers and air temperature



temperature in the atmosphere. The *mesopause* is the third isothermal layer, separating the mesosphere; along with the stratopause and mesopause, it constitutes what is commonly called the *middle atmosphere*.

- *Thermosphere*—This extends from the mesopause to roughly 600 km. Air temperature in the thermosphere increases quite strongly above 90 km due to the sun’s energy. Most of the *ionosphere* and the *exosphere* are included in the thermosphere. The ionosphere starts around 70 or 80 km up to an indefinite height (~1000 km) and is so named because it is sufficiently ionized by solar ultraviolet radiation that the concentration of free electrons in this layer affects the propagation of radio waves.

3.6 The Major Laser Weapon Concepts

There is generally more than one laser weapon alternative for each proposed laser weapon mission on the battlefield. It is quite possible to vary the laser properties and energy level, the tracking system, and the fire control equipment according to the military requirements for each specific mission. Environmental influences will also have a very strong impact on the final choice of laser weapon applications. For example, hydrogen fluoride (HF) laser is not the best choice for long-range use within the atmosphere, because its wavelength is strongly absorbed by the atmosphere. Every laser weapon that is designed to operate within the atmosphere over any great range, whether ground-based laser (GBL), sea-based laser (SBL), or

airborne-based laser (ABL), must use wavelengths at which the atmosphere absorption and scattering are as small as possible [1].

To be effective, the wavelength of a laser weapon must be short, at least in the visible band, but preferably in the ultraviolet or X-ray band. The greatest difficulty in designing short-wavelength lasers is power—the shorter the wavelength, the more energy that is required. Optical (visible or ultraviolet) lasers work by heating the skin of the target. The beam must remain at the same spot for several seconds until the skin is hot enough to do internal damage to the target. This is tough because the typical ballistic missile travels in excess of 6 miles per second. Imagine focusing on the same 2' or 3' spot over a distance of 50,000 ft and you have an idea how accurate such a laser weapon must be.

In addition to the problems of accuracy, laser weapons of any power tend to be monstrous and there are many technical obstacles that the designer should overcome. The SBL is using relay mirrors to direct the beam to the target. ABL lasers are using turbine-powered chemical jets and they are placed aboard aircraft, but the wavelength of the light is long—6–10 μm —far in the infrared region. This makes laser relatively inefficient at destroying their targets unless certain atmospheric and environmental conditions are met for target engagements.

X-ray lasers, still wrapped in secrecy, emit an extremely high-powered beam that can literally destroy a missile in mid-flight. X-rays can't be deflected by mirrors, however, which means that the weapon must be easily aimed and in a direct line of sight to the target. Fortunately, X-ray lasers can be built small, expert say, making them suitable for space-based operation. The biggest disadvantage to X-ray lasers is that they use an internal nuclear explosion to work, so they are essentially one shot device.

A relative newcomer to this laser weapon scene is the free-electron laser, which is being developed at the several national laboratories and universities. The free-electron laser (FEL) uses a stream of electrons that is made to emit photons of light after being oscillated by giant electromagnetic. Free-electron lasers (FELs) have been built and they do work. However, if put into production, an actual antiballistic missile FEL would take up a huge field such as football field or more. Obviously, such a device would be useful only as a stationary ground-based laser (GBL) weapon with its present technology [2].

Laser weapons may be used within an army's air defense against aircraft, helicopters, and missiles. The desired effect on the target may be either to burn holes or destroy key structures, to blind or trick the sensors, or blind the crews temporarily or permanently. The high-energy air defense laser may use all three effects at the same time if the target is within the reach of the main effects of the laser. At longer distances, only the anti-sensor and anti-eye capability will be possible. The low-energy air defense laser will use enough energy to be effective against sensors and eyes. It is also possible to field a laser with the main purpose of blinding or flash blinding the crews. Flash blinding will be most effective in the dark when the eye is dark adapted and much more sensitive to overload by bright flashes [1].

3.7 Small-Scale Weapons Using Lab-Type Lasers

So far part of this report has covered high-energy weapons, designed to counter major military conflicts and attack. Laser guns in the movies are often handheld devices, or at most small enough to prop on a vehicle. Lasers powerful enough to inflict damage, but small enough to be carried, have developed, but they are not used in any current military application. It's relatively easy, for example, to build a handheld ruby laser that puts out bursts of large amounts of light energy. When focused to a point, the light from a ruby laser can cut through paper, cloth, skin, or even thin metal.

Ruby crystals are poor conductors of heat, so ruby lasers emit only short pulses of light to allow the crystal to cool between firings. Nd:YAG lasers operate in a similar fashion as ruby lasers, but they can produce a continuous beam. Making a handheld Nd:YAG laser is no easy feat, however. The Nd:YAG crystal must be optically pumped by another high-powered laser or by an extremely bright-flash lamp or light source. Though the power output of an Nd:YAG laser is extremely high, considering the current state of the art, a handheld model is impractical. However, such a weapon could be built as a "laser canon," transported on an armored vehicle or on a towed trailer [3].

CO² lasers are often used in industry as cutting tools. This type of laser is known for its efficiency—30% or more compared to the 1–2% of most gas and crystal lasers. A pistol-sized CO² laser would probably be difficult to design and manufacture because the CO² gas mixture (which includes helium and nitrogen) must be constantly circulated through the tube. What's more, the laser requires a hefty electrical power supply. Still, such a weapon could be built in an enclosure about the same size as a personal rocket launcher. These are designed to be slung over a shoulder and fired when standing in an upright position [3].

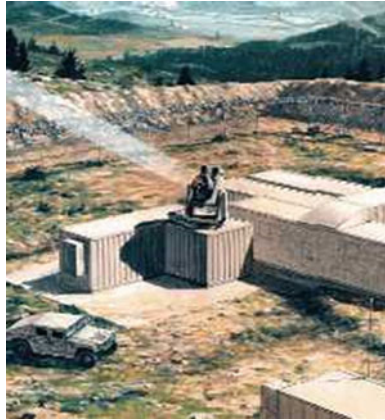
3.8 High-Energy Lasers as Weapons

An air defense HEL weapon designed to shoot down airplanes, helicopters, and missiles successfully must have the ability to keep a very powerful beam at one point on the target for a long enough time to deliver at least 5000 joules per square centimeter. This requires a laser in the megawatt range. If the shot is to be successful, it must be directed to a certain part of the target that is limited in size and very sensitive and then kept there until the desired effect is reached. Thus, the laser beam must track and follow a target if any great length of time is needed to achieve the desired effect.

Many parts of an aircraft or helicopter are highly resistant to a HEL weapon, but there are still enough thin-skin parts and sensitive areas to produce a devastating effect or destruction if hit precisely. On the other hand, it is obvious that at battlefield ranges even an extremely high-energy laser weapon cannot penetrate the heavy

armor on a tank or other armored vehicles and thus a HEL weapon is of no use for destroying resistant ground targets in the battlefield. However, sensors, optics, and related devices are still valid targets wherever they appear on the battlefield, even in a tank.

3.9 High-Energy Laser (HEL) Safety Program



As high-energy lasers move from the safe confines of the laboratory into the outdoor domain, new problems arise in dealing with laser safety. The Tri-Service Laser Bioeffects program at Brooks AFB will be examining the safety aspects of the new technologies and weapon systems to be employed in the future. Several new high-energy laser systems are now scheduled for deployment in the immediate future.

The Tactical High-Energy Laser (THEL), will be a ground-mobile system which will use a chemical laser to destroy low-flying threats. Currently under development in a cooperative program with Israel, the THEL conducted test-firing in FY1998, and continues several test phases at White Sands Missile Range today.

The Airborne Laser (ABL), with its megawatt-class laser systems, will engage tactical ballistic missiles during boost phase at altitudes over 40,000 ft. Its lasers will be test-fired in FY 2003, with Engineering and Manufacturing Development scheduled to begin soon after that. The high-power chemical oxygen iodine laser will have nominal eye-safe distances in the order of thousands of miles and will produce reflection patterns off targets that also have the potential for causing eye damage at very large distances (see Fig. 3.5).

Combining these laser characteristics with the planned usage of these weapon systems involving moving targets and possibly moving sources results in a complex series of laser safety calculations to allow safe testing and usage of high-energy lasers outdoors. The Air Force Research Laboratory, Optical Radiation Branch, is developing new tools and techniques for calculating laser hazard areas which include



Fig. 3.5 ABL on a refueling mission over California, December 2002

computer modeling of the interaction of high-energy lasers and moving targets, and the use of probabilistic methods to augment deterministic calculations.



One of the Missile Defense Agency's highest priority programs involves putting a weapon-class laser aboard a modified Boeing 747-400 series freighter aircraft and using that laser to destroy ballistic missiles shortly after launch. The program is called the Airborne Laser, and its development could forever change the way that nations wage war.

3.9.1 Airborne Laser (YAL-1A)

Destroying ballistic missiles is a complicated process, one that is confounded even more by the revolutionary use of a directed energy device as a weapon rather than as a targeting or range-finding apparatus. To be successful, ABL must:

- Be housed aboard a stable platform that can stay aloft for hours on end above weather systems whose clouds could refract its laser beams and nullify its effectiveness
- Be equipped with sensors able to locate a ballistic missile shortly after launch and hold the track long enough for other system elements to swing into operation

- Be implemented with a sophisticated computer system capable of keeping track of dozens of missiles and prioritizing them so that the most threatening is targeted first
- Have a highly developed optical system capable of measuring the amount of thermal disturbance between the aircraft and the target, and then be capable of directing a beam of energy that self-compensates for the clear-air obstacles
- Possess the ability to focus the killer beam on a rapidly rising target, which may be traveling at a speed of Mach 6 or more, and then keep the shaft of energy in place long enough to burn a hole in the missile's metal skin
- And lastly be provided with a laser powerful enough to prove lethal at a distance of hundreds of kilometers

Some of those requirements have already been tested:

- The first ABL aircraft—YAL-1A—made its virgin flight over western Kansas on July 18, 2002, staying aloft for 1 h and 22 min before returning to the Boeing modification facility in Wichita. Between then and the time it transitioned to its new temporary home at Edwards Air Force Base, California., in December, YAL-1A made an additional 13 flights logging more than 60 flight hours.
- As part of a Missile Defense Agency test over the Pacific Ocean in December 2002, ABL's infrared trackers successfully detected a Minuteman booster rocket as soon as it broke the clouds, holding a lock until the rocket's engines burned out 500 km downrange.
- Its battle management (computer) system was flight tested in late summer and early fall of 2002 to verify internal crew communications and the V/UHF radios, plus the data acquisition system and high-definition VHS.
- The six infrared search and track sensors were successfully flight tested.
- The first COIL module was installed on YAL-1A tested at 118% of anticipated power during a shakedown run at TRW's facility in San Juan Capistrano, Calif., in January 2002. Shortly afterwards, it was disassembled and shipped to Edwards Air Force Base.



First Flight

In December 2002, YAL-1A was pulled into a hangar at Edwards' Birk Flight Test Facility where it will be grounded while the lasers and optical components can be tested and installed.

The goal of the Missile Defense Agency, which has overall management responsibility for the program, and the Airborne Laser System Program Office at Kirtland Air Force Base, NM, is to have YAL-1A ready to shoot down a threat-representative

ballistic missile by December 2004. Currently, the missile is scheduled to be launched from Vandenberg Air Force Base, California, with the shoot down to take place over the Pacific.

Construction and testing of YAL-1A (prototype attack laser, model 1A), the first aircraft in a proposed fleet of so-far undetermined size, are the results of an effort by MDA, the program office, the Air Force, and three major contractors—Boeing, Lockheed Martin, and Northrop Grumman Space Technologies (formerly TRW). In addition, the US Air Force's Aeronautical Systems Center, headquartered at Wright-Patterson Air Force Base, Ohio, has provided office personnel. The Air Combat Command, headquartered at Langley Air Force Base, Va., will assume control over the plane once it is declared operational and transferred back to the Air Force.

The ABL program office was formed in 1993. Three years later, in November 1996, the Air Force awarded a \$1.1 billion contract to the Boeing Defense Group of Seattle, Washington D.C.; TRW Space and Electronics Group of Redondo Beach, California; and Lockheed Martin Missiles and Space of Sunnyvale, California.

Boeing built the aircraft in Everett, Washington D.C., and modified it in Wichita. The company also developed the hardware/software used in the battle management system and is managing integration of the main components. TRW built the megawatt-class COIL laser that produces the knockout punch to ballistic missiles, and Lockheed Martin is responsible for the optical system.

Another key organization is the Air Force Research Laboratory's Directed Energy Directorate, also at Kirtland Air Force Base, NM, where the COIL was invented in 1977. For a quarter of a century, the Laboratory has been conducting research into a myriad of technologies needed to make a laser-carrying aircraft a reality. Besides the COIL, the Laboratory also developed the technologies that will increase the distance laser light can travel through the atmosphere to destroy attacking missiles.

The Aircraft—The Air Force bought a 747-400F straight off the Boeing Commercial Aircraft assembly line and flew it to Wichita, Kansas, in January 2000. Boeing workers virtually rebuilt the aircraft, installing miles of wiring, grafting huge sheets of titanium to the plane's underbelly to protect the exterior from the heat of the laser exhaust, and, most importantly, adding a 12,000-pound bulbous turret on the front of the aircraft to house the 1.5 m telescope through which the laser beams will be fired. Company officials said that it was the largest military modification to a commercial aircraft that Boeing had ever attempted.

Acquisition, Tracking, and Pointing—In addition to a powerful laser, an airborne laser system must also be able to find and hit its targets. Numerous tests have been conducted at the White Sands Missile Range in southern New Mexico, both with lab-type instruments and with the actual aircraft, to demonstrate the system's ability to identify and follow a potential target.

The Lasers—Central to this system is the COIL. As a laser that generates its energy through chemical reaction, it has advantages over solid-state lasers, most

notably in the amount of energy it can produce. COIL energy is produced by chemical reaction when oxygen and iodine molecules are mixed. A tremendous additional advantage is that the laser propagates at 1.315 μm in the infrared (invisible) spectrum. This wavelength travels easily through the atmosphere and has greater brightness—or destructive potential—on the target. There are three other important lasers aboard the aircraft: the Active Ranger System, which provides preliminary tracking data; the Track Illuminator Laser, which produces more refined data; and the Beacon Illuminator Laser, which measures the amount of atmospheric disturbance.



Systems Integration Laboratory (foreground)
Ground Pressure Recovery Assembly (background)

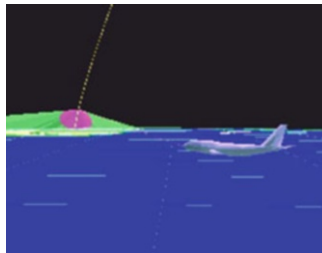
Correcting for Atmospheric Turbulence—The ability to find and track a boosting missile would be meaningless without a corresponding ability to lock onto and destroy the intended target. Since air, like water, is made up of many layers, scientists needed to find a way to compensate for these disturbances in the atmosphere in order to focus a high-energy beam on the target and hold the beam in place long enough for it to complete the destruction process. The system that will be installed on YAL-1A is the result of more than 15 years of research conducted by scientists at the Laboratory's Directed Energy Directorate and the Massachusetts Institute of Technology's Lincoln Laboratory. Working out of astronomical facilities at the Starfire Optical Range in the southeastern corner of Kirtland Air Force Base, researchers made revolutionary breakthroughs using lasers, computers, and deformable optics.

The ABL Integrated Test Force—It is actually a complex of buildings located at the historic Birk Flight Test Facility at Edwards Air Force Base, California. The gem of the ITF is the System Integration Laboratory (SIL), an 18,000 square foot building housing a surplus 747-fuselage test stand that will serve as a laser template for the ABL aircraft. The six modules that compose the COIL component initially will be tested in the SIL. Once those tests have been completed, the modules will be disassembled, and then reassembled on YAL-1A. Other resources in the ITF complex include a ground pressure recovery assembly (GPRA), which will enable simulation of ABL's anticipated cruising height, and a mixing area for basic hydrogen peroxide, a vital ingredient to the main laser's chemical reaction process.



History—Almost 20 years ago, the Air Force Research Laboratory and its predecessor units completed a project that showed the potential for an airborne laser. A KC-135A tanker airplane (a military version of the Boeing 707) was modified and equipped with a gas dynamic laser. This aircraft shot down a low-flying drone and five air-to-air missiles, proving that the concept was possible. Later tests also were conducted at White Sands Missile Range aimed at finding out how effective a laser would be. For these tests, the nation’s most powerful laser, the Mid-Infrared Advanced Chemical Laser, was used. In every case, scale models of typical targets were easily destroyed.

The System—Computer simulations indicate that an airborne laser would be very effective under battle conditions. Currently, the program will provide the United States with its only near-term boost-phase missile defense, that is, the ability to find and destroy a missile between the time it is launched, and its booster rockets burn out.



The Laser Range Safety Tool (LRST) is being developed to permit range safety officers to properly assess hazards and configure test scenarios such that these new weapon systems can be tested in a safe manner. For any given scenario, the tool assists in the evaluation of reflection patterns resulting from targeting various types of moving targets and predicts hazard zones and appropriate “keep-out” areas. The tool is based on the ANSI Z136.1 standard for eye safety calculations along with new bioeffects data for the specific wavelengths associated with the new high-powered laser systems. Moreover, new risk assessment techniques using probabilities associated with the various aspects of exposure and injury will provide more realistic predictions for use by the range safety officers, as well as the operational users.

3.9.2 Tactical High-Energy Laser for Air Defense

The US Army Space and Strategic Defense Command are working on a new active defense weapon system concept to combat the threat to our forces from so-called dumb munitions. The command's mobile Tactical High-Energy Laser or THEL weapon system will provide an innovative solution for the acquisition and close-in engagement problems associated with these threats not offered by existing systems and give the air defense commander an option that he does not currently have. It will significantly enhance the force protection for combat forces and theater-level assets for the Force XXI Army.

For the past several years, SSDC has been pursuing this concept that could provide new air and missile defense capability in force protection missions. Numerous Department of Defense high-energy laser development programs over the last 20 years have proven and demonstrated the laser beam generation and beam pointing technologies for the THEL concept. Force XXI advancements in the area of real-time situational awareness now make it possible to capitalize on the attributes of a THEL in operational scenarios.

A THEL will be able to rapidly fire for close-in engagements where timelines are very short, and cost only a few thousand dollars per kill or less with a deep magazine to counter saturation attacks. Not only can THELs destroy, but they can also degrade, disrupt, or damage to enhance operational flexibility and effectiveness against a wide variety of air threats. This system can, therefore, operate as an effective new weapon node in the short- to medium-range air defense architecture.

The effectiveness of high-energy lasers against short-range rockets was tested and demonstrated in the "Nautilus" program, an outgrowth of Project Strong Safety, in collaboration with Israel. The program was conducted primarily at SSDC's High Energy Laser Systems Test Facility or HELSTF at White Sands Missile Range, NM, and utilized a fraction of the power of the HELSTF Mid-Infrared Advanced Chemical Laser (MIRACL) to emulate the THEL weapon concept performance.

The MIRACL is a megawatt-class deuterium fluoride chemical laser that has been operational at HELSTF since the early 1980s. After a series of static and dynamic tests, the program successfully destroyed a short-range rocket in flight on February 9, 1996. This success triggered the next development in the SSDC THEL effort.

In April 1996, then Prime Minister of Israel, Shimon Peres, met President Clinton and Secretary of Defense William Perry. During the meeting, the United States made a commitment to assist Israel in the development of a THEL Advanced Concept Technology Demonstrator by the end of 1997, based on the success of the Nautilus program, to defeat the threat posed by Katyusha and other short-range rockets against the cities in northern Israel.

In July 1996, a contract was awarded by SSDC to TRW, Inc., of Redondo Beach, California, for the design, development, and fabrication of a THEL demonstrator, which will be a transportable, tactical sized deuterium fluoride chemical laser. Approximately 18 months will be required to design and build the system, followed by 12–18 months of testing.

If successful, the demonstrator may pave the way for future development of a THEL for use in US peacekeeping/contingency operations. The US Army Air Defense Artillery School in Fort Bliss, Texas, already officially designated as the proponent for THEL by the Training and Doctrine Command, is planning to develop a mission need statement and operational concept that could lead to an operational requirement for a THEL system.

Evolving high-energy laser, beam control, and digital battlefield information technologies promise to combine into a highly effective force protection THEL weapon system for the Force XXI Army.

Prepared September 1996 by John J. Wachs, Weapons Directorate, MDSTC, SSDC High-Energy Lasers Weapons.

3.10 Lasers for Air Defense

In its 1984 directed energy plan, SDIO planned to develop an acquisition, tracking, pointing, and fire control (ATPAWs) subsystem for directed energy weapons by fiscal year 1990 for \$1298 million. Through fiscal year 1993, SDIO allocated \$1634 million to this program, accomplishing some but not all of the program objectives. SDIO estimated that it will cost \$180 million and take 3 years to resolve the majority of the remaining technical issues. For another \$100 million, the ATP technology could be demonstrated in space.

All directed energy weapons need an ATP/FC system. In general terms, the system must quickly engage a large number of targets by placing a directed energy beam on the aim point of each target. These time and accuracy constraints dictate a rapid succession of handovers from one sensor to another. Each successive sensor in the system has a smaller field of view and greater accuracy.

The system locks on to the infrared signature of a missile (acquisition); calculates the flight path of the missile (tracking); calculates an aim point on the missile and directs the beam to the aim point (pointing); and assesses the results and selects the next target (fire control). Depending on the mission of the directed energy system, the ATP/FC system must perform these functions when ballistic missiles are in their boost, post-boost, and/or midcourse phases of flight.

The basic goal of the program was to resolve the technical issues sufficiently to support a space test of a directed energy weapon by 1990. The overall technology performance objectives in the 1984 plan were as follows:

- Reduce the effect on the accuracy of pointing and tracking devices of vibrations caused by operation of the spacecraft and laser to less than 4 in. on the target.
- Develop the capability to rapidly retarget the laser beam from one target to another in less than 2 s.
- Develop the capability to track targets at ranges of 2600 to 3100 miles at an accuracy of about 4 in.

- Develop fire control computer software to handle more than 100 targets at a rate of more than one target per second. The fire control functions are missile plume to missile hard body handover, tracking of multiple targets, target identification, aim point selection, and damage assessment.

The plan specified that \$1298 million would be required from fiscal years 1986 through 1990 to develop the system components and to fly space experiments to resolve integration and space operation issues. Experiments would permit the space test of a directed energy weapon in 1990.

SDIO met the plan's objectives for pointing and tracking technology and rapid retargeting technology for directed energy weapons. It did not meet the objectives for developing long-range fine tracking and fire control software. While not meeting all objectives, SDIO believes that it has met the basic program goal of resolving technical issues sufficiently to support a space test of directed energy technology. Through fiscal year 1993, SDIO spent about \$1684 million developing ATP/FC technologies. This amount is about \$286 million more than SDIO estimated was needed to accomplish the objectives. A majority of the funding was spent on a series of space- and ground-based experiments. All major space tracking experiments were canceled before completion due to a lack of funding. However, two space pointing experiments were completed.

At a cost of about \$262 million, SDIO reported that it completed the Relay Mirror Experiment and the Low Power Atmospheric Compensation Experiment, which were focused on resolving issues related to the ground-based laser program. Each was placed in a separate orbit by one Delta booster in 1990. The Relay Mirror Experiment successfully demonstrated high-pointing accuracy, laser beam stability, and long-duration beam relays. The Low Power Atmospheric Compensation Experiment successfully demonstrated low-power technology to compensate for laser beam distortions, which occur when beams go through the atmosphere from ground to space.

SDIO had spent about \$684 million from fiscal years 1985 through 1991 planning, designing, and fabricating hardware for four ATP/FC space experiments that were canceled before completion for the following reasons:

- Talon Gold was intended to demonstrate precision tracking and pointing in space for targeting satellites and boosters. After spending about \$26 million on Talon Gold, SDIO canceled the experiment because the cost estimates for integration and launch had increased an additional \$600 million.
- Pathfinder was started in September 1986 and was canceled in 1987 because it was too expensive. SDIO had spent about \$40 million on this experiment, which was to address plume phenomenology using a sensor array on the space shuttle.
- The Starlab space experiment was intended to demonstrate precision tracking and would have used the space shuttle to accomplish the experiment. After spending about \$603 million developing Starlab, SDIO canceled this experiment in part because the Challenger accident led to nearly a 3-year delay in the launch date, greatly increasing the overall cost. This coupled with changing priorities in the

directed energy program led to changes in requirements and increased costs, which made the experiment too expensive to complete.

- Altair, which was canceled after SDIO had spent about \$16 million in development costs, was intended to demonstrate the same types of technologies as Starlab and was planned to use some of the hardware developed for Starlab. An SDIO official estimated that it would have cost \$330 million to complete Altair.

SDIO replaced the Altair space experiment with a nonspace ATP/FC experiment called High Altitude Balloon Experiment. This experiment was intended to achieve most of the same objectives as Altair but at a much lower estimated cost of \$76 million. Balloons were used to carry AW/FC devices to an altitude of about 30 km where these devices will be used to acquire and track missiles in the boost phase. SDIO's program manager for ATP/FC expected this experiment to yield from 80% to 90% of the data that would have been obtained from a space experiment.

SDIO designed and constructed a rapid retargeting/precision pointing [R2P2] simulator that emulated the dynamics of a large spacecraft (e.g., motion and vibration). Using this facility, SDIO developed and tested techniques for ensuring the stability, accuracy, and precision of a simulated directed energy weapon's pointing device under rapid retargeting situations. This project demonstrated, within the limits of a ground laboratory, that ATP/FC techniques should work in space at the levels established in the original program plan. SDIO will have spent about \$42 million on this project from fiscal years 1986 through 1993.

Two other projects also demonstrated ATP/FC techniques. The Space Active Vibration Isolation project developed and tested ATP/FC techniques for negating the effects of spacecraft and weapon vibrations on the pointing device. This project produced hardware and technology that have improved the pointing stability of directed energy devices to below the program goal of less than 100 nanoradians, or about 4 in. from a distance of 1000 km. This project was followed by the Space Integrated Controls Experiment, which improved the pointing stability even further. SDIO spent about \$37 million on these two projects from fiscal years 1986 through 1993.

As of 1993 SDIO estimated that it would cost \$180 million and take three more years to resolve the vast majority of the ATP/FC technical issues and perform integrated ATP experiments against real targets from the High Altitude Balloon Experiment platform. This would substantially complete the objectives of the 1984 plan. An additional \$100 million would be needed to demonstrate operation in space, assuming that it would be done as part of another directed energy space experiment such as Star LITE, the experiment planned for the chemical laser. The major technical issues to be resolved from 1993 through 1996 included long-range fine tracking, fire control, integrated ATP/FC, and additional concept development.

For long-range fine tracking, the solid-state laser radar source program produced two laser illuminators. They still need to be tested in realistic target environments to determine their effectiveness in changing conditions and against a wide variety of targets. In addition, their capabilities must also be developed to support aim point selection and maintenance and damage assessment.

Fire control decision software had been demonstrated in computer simulations, but its practicality and robustness had yet to be tested in an integrated field operation. Each of the individual fire control decision algorithms needs to be tested with several sets of scene conditions with real data. Functional integration with sensors and autonomous operation must also be demonstrated. SDIO plans to test the operation of the software on the High Altitude Balloon Experiment platform against boosting targets at the White Sands Missile Test Range.

3.10.1 Target Acquisition for Combat Operations

This section discusses target acquisition, tracking, and combat operation by direct energy weaponry systems.

3.10.2 Overview

The goals of this sub-thrust can best be described in three major categories:

1. The measurement of atmospheric parameters on space and timescales required to support Air Force and directed energy weapon system and its missions in Global Reach-Global Power
2. The prediction of the future evolution of the atmosphere from a few hours to a few days
3. The assessment of weather impact on Air Force and directed energy weapon systems and operations.

3.10.3 Description

Theater Specification for Dominant Maneuvers sub-thrust conducts R&D programs to better understand the physical and dynamic processes of the lower atmosphere in order to design, develop, test, and transition remote sensing instrumentation, retrieval algorithms, and models in support of air and space war fighters.

Real-Time Measurements of Atmospheric Parameters from Satellites: The measurement goal emphasizes the application and interpretation of satellite sensor data, but also includes in situ sensor development as part of the program. Measurement emphasis is on the 3-dimensional determination of cloud cover at the highest spatial and temporal resolution to develop the models to support global surveillance and tactical warfare.

Atmospheric Optical Turbulence Measurements and Modeling: The technical objective is to specify and predict the atmospheric optical turbulence degradation to ground-, air-, and space-based laser systems. Optical turbulence is highly variable

from site to site, season to season, and day to day; however, as yet there are no good predictive models. In a program initiated in FY96, supported by the Airborne Laser (ABL) SPO, Phillips Lab is obtaining optical turbulence data in theaters of interest to the SPO.

Tactical Remote Sensing: The technical objective is to provide from aircraft and satellite platforms remote sensing of battlefield gasses and emissions. The PL/GPOR Lidar remote sensing program is set up to measure several atmospheric boundary layer parameters in high spatial resolution, including wind profiles, aerosol content, and size distribution, as well as the detection of trace elements, both natural and man-made. Current assets include the following:

- 10.6 μm CO_2 Doppler range-resolved wind profiler, dual-tunable 9–11 μm CO_2 Doppler range-resolved wind profiler, and DIAL system to obtain range-resolved water vapor and trace gas profiles
- 1.574 μm portable, environmental, eye-safe Lidar (or Ladar) for range-resolved aerosol and cloud profiles in addition to cloud depolarization features

New assets soon to be on hand include a coherent, tunable UV DIAL system for water vapor and ozone detection, a mechanical turbulence Lidar or Ladar for wind shear detection, and a refractive turbulence remote sensor to measure turbulence along a path.

The Theater Forecast for Precision Engagements FTA develops tailored weather products to support combat mission planning and execution worldwide.

Prediction of clouds and severe weather: The prediction goal emphasizes the data fusion of satellite and indigenous data sources in the battlefield where data denial may be a factor. The resulting analysis fields will then be tested in theater-scale prediction models on time and space scales appropriate to tactical weapon delivery.

Virtual weather: The goal of this program is to produce computer simulations of the atmosphere, with high physical fidelity, valid as a function of location, season, time of day, and geometry. In order to address these requirements, simulation models must be developed that produce 3-dimensional structure—the major shortfall of current capability. Initial efforts involve improving the physical reality of current cloud simulation models. Other projects include development of rain, fog, wind, humidity, lightning, and turbulence models. A strong emphasis is placed on physically correct visualization and generation of radiometrically correct atmospheric scenes.

Weather Impact Decision Aids (WIDA): The WIDA program is developing software technology for operationally predicting the impact of weather on the performance of airborne electro-optical navigation and weapon targeting systems. The program presently has four major ongoing and/or planned components: (1) Night Vision Goggle Operations Weather Software (NOWS), which will predict the impact of weather on night-vision goggle detection range for AFSOC and ACC; (2) IR Target Scene Software (IRTSS), which is developing software that will determine the impact of weather on air-to-ground target scenes in the infrared, and produce an IR scene visualization for transition to the Air Force Mission Support System (AFMSS); (3) Weather Automated Mission Planning Software (WAMPS), a

new start in FY97 to develop software to automatically incorporate weather impacts on airborne EO systems during theater mission planning in Theater Battle Management Core Systems (TBMCS); and (4) Target Acquisition Weather Software (TAWS), a new start in FY97, will provide a major upgrade to the current operational Electro-Optical Tactical Decision Aid (EOTDA) used by Air Force Weather (AFW) support personnel to provide weapon lock-on and acquisition ranges for EO weapon systems used by ACC.

1. User Impact:

None

2. User Impact:

Concept/technology

3. Images:

None

4. Related Initiatives:

- Target Acquisition for Combat Operations (see Sect. 5.1).
- Target Background Discrimination for Surveillance (see Sect. 5.2).

5. Related Requirements:

None

6. Related Categories:

3.10.3.1 Optical Surveillance Effects and Battle Space Operations

The importance of maintaining a reduced nuclear force and the emerging conventional ballistic force as a combat and cost-effective weapon is recognized by Air Force Space Command (AFSPC) mission area plans and Space and Missile Systems Command (SMSC) development plan as having the technology needs in advanced guidance technologies and astrodynamics.

- The goals of advanced guidance are the following:
 - Global Positioning System (GPS) Range Standardization/Safety Technology
 - Development of new miniature systems to lower range costs 30% by replacing radar systems and enhance safety with greater accuracy and reliability by FY01
 - GPS accuracy enhancements
 - To increase cost-effectiveness, missile navigation, and testing accuracy with improved GPS/INS coupling by FY98

- Development of precision fiber optic gyroscope (PFOG) with low loss integrated optics and fiber couplers and flexure mass accelerometer (FMA) with open-loop, two back-to-back microwave resonant cavities by FY99.
 - Decrease reliance on high-cost, high-precision inertial measurement systems with micromechanical updates on accelerometers and gyros by FY01
 - To fly the Missile Technology Demonstration III (MTD III) during FY01 to gain data on multiple penetrator warheads delivered on an ICBM
 - To develop anti-jam antennas
 - To integrate plasma physics with design
 - To develop and test materials for antenna windows
- The goals of astrodynamics are to:
 - Improve differential correction (DC) accuracy 90%
 - Improve propagation accuracy at the end of the prediction period by 90%
 - Demo integrated performance of high-accuracy lasers and astrodynamics algorithms to precisely locate and illuminate spacecraft
 - Demo next-generation initial orbit determination, DC, and propagation for space surveillance
 - Show deficiencies in current operational DC and propagation which could be eliminated
 - Demonstrate capability to maintain independent high-accuracy catalog of selected satellites (20–30 objects)

3.11 Target-Background Discrimination for Surveillance

The following sections will apply for this purpose.

3.11.1 Overview

Space-based surveillance, tracking, and interceptor systems must accurately and reliably discriminate target IR and optical signatures from the atmospheric and celestial IR and optical emissions against which the targets are viewed. When sensor specifications are optimized against realistic, accurate simulations of the atmospheric and celestial emissions in the sensor's field of view, then operational performance is significantly enhanced, and system over-design is minimized, thereby making DOD space-based systems much more affordable. The sub-thrust goals are to develop and demonstrate integrated background clutter mitigation technologies for SBIRS-High and -Low and next-generation hyper-spectral surveillance and threat warning systems, and to integrate clutter suppression technologies into hardware simulators to provide high-resolution spectral and spatial scene data of atmosphere, cloud, terrain, and celestial background clutter to support system designs.

This sub-thrust:

1. Defines the impact of optical and infrared backgrounds on surveillance and threat warning, theater and national missile defense, and intelligence, surveillance, and reconnaissance systems
2. Measures atmospheric and celestial infrared, ultraviolet, and visible backgrounds using satellite and rocket-borne sensors
3. Models atmospheric and celestial optical and infrared backgrounds for the full range of operational conditions and system design trade space
4. Provides real-world background scenes, global background statistics, and reliable background scene models to support systems engineering trade studies
5. Measures and models in-flight infrared signatures of aircraft and missiles
6. Distributes and provides online access to background phenomenology data
7. Defines optical and infrared background requirements for surveillance systems and battle space simulations

3.11.2 Description

This sub-thrust defines the impact of optical and infrared backgrounds on surveillance and threat warning, theater and national missile defense, and intelligence, surveillance, and reconnaissance systems and measures atmospheric and celestial infrared, ultraviolet, and visible backgrounds using satellite and rocket-borne sensors. The two main project areas of this sub-thrust are backgrounds and targets phenomenology and background clutter mitigation.

The goals of the backgrounds and target future technical architecture (FTA) are to provide high-resolution spectral and spatial scene data of atmospheric, cloud, terrain, and celestial background clutter to support SBIRS designs; provide high-throughput data processing, analysis, and distribution of background phenomenology data for SBIRS, BMDO, and other DoD programs; measure in-flight infrared signatures of aircraft and missiles; and develop models capable of predicting the infrared characteristics of all aircraft, particularly in the design and development stages. A major task under this FTA is to construct infrared atmospheric and celestial background scenes from the superb data measured by the MSX satellite and atmospheric scenes from the highly successful MSTI-3 satellite mission. The combined data set will be used to upgrade models for design of the new SBIRS surveillance system.

The goals of the background clutter mitigation FTA are to (1) characterize and predict atmosphere, cloud, and terrain infrared background clutter for full range of SBIRS operational conditions and system design trade space and (2) assess the impact of background clutter on SBIRS performance and mission capabilities. Spatial and temporal structure in atmospheric, cloud, and terrain backgrounds produces clutter against which infrared and optical sensor systems must detect and track theater ballistic missiles, cruise missiles, and aircraft threats as well as perform technical intelligence missions.

Under this program, tasks are being performed to:

1. Provide background clutter codes to extrapolate measured background data to the full SBIRS design trade space and all SBIRS operational conditions
2. Provide background model uncertainty bounds
3. Assess and upgrade background clutter codes for SBIRS using MSX and MSTI-3 data
4. Develop dynamic, statistical background clutter models to support adaptive hyper-spectral imaging
5. Provide expert user interface for code applications

1. User Impact:

None

2. User Impact:

Concept/technology

3. Images:

None

4. Related Initiatives:

- (a) Space-Based Infrared System—Low Earth Orbit (SBIRS-Low).

The Space-Based Infrared System (SBIRS) is in response to the US military forces increasing the need for accurate and timely warning of tactical missile attack. SBIRS will replace the current Defense Support Program (DSP) designed to meet US infrared space-based surveillance and warning needs through the next two to three decades. SBIRS improves support to theater CINCs, US deployed forces, and allies by providing detailed information in the four mission areas of missile warning, missile defense, technical intelligence, and battle space characterization. SBIRS will provide significant performance enhancements over DSP by improving quality and timeliness of missile warning data. SBIRS should enhance information superiority and support the Joint Vision 2010 operational concepts of full-dimensional protection and precision engagement, by providing this data directly to theater commanders in a timely, survivable manner, thus enabling US forces' immediate reaction to threat.

The SBIRS space segment includes a high and low component. The high component comprises six satellites: four in geosynchronous (GEO) earth orbit and two hosted payloads in highly elliptical orbit (HEO). The low component includes approximately 24 low earth orbit (LEO) satellites. The SBIRS high component will meet a subset of the operational requirements, including all key threshold requirements. The SBIRS low component will provide a unique, precision, mid-course-tracking capability critical for effective ballistic-missile defense, as well as enhanced capability in support of other SBIRS missions. SBIRS High, complemented by SBIRS Low satellites, will meet all of its operational requirements.

The SBIRS ground segment includes a Continental US (CONUS)-based Mission Control Station (MCS), a MCS backup (MCSB), a survivable MCS (SMCS), overseas relay ground stations, Multi-Mission Mobile Processors (M3P), and associated communication links. The SBIRS ground segment will be delivered incrementally. The first increment, scheduled to be operational in FY99, consolidates DSP and Attack and Launch Early Reporting to theater ground stations into a single CONUS ground station, and will operate with DSP satellite data. The second increment, scheduled for FY02, will provide the necessary ground segment functions required for the new high-altitude SBIRS satellites and the residual DSP satellites. Included in the second increment will be mobile terminals capable of fulfilling the Army Joint Tactical Ground Station in-theater and SBIRS strategic processing requirements. A third increment, which will be operational in FY03, will add the necessary ground segment functions for the first LEO satellite scheduled to be deployed in FY04.

Background Information:

SBIRS was initiated in 1995 as a replacement for the Follow-on Early Warning System acquisition, which was canceled due to cost and requirement problems. Since SBIRS satellites need to be completed before the last DSP satellite is launched, it was placed on an accelerated schedule and selected as a lead program for acquisition reform. Much of the traditional required documentation was reduced or consolidated into a Single Acquisition Management Plan, and emphasis was placed on direct involvement through Integrated Product Teams (IPTs) rather than traditional documentation reviews.

The SBIRS High component entered the EMD phase following a Milestone II DAB review in October 1996. This decision was supported by an OA conducted by AFOTEC and reviewed by DOT&E.

The first phase of IOT&E will be conducted in 1999 to verify performance of the Increment 1 ground station. Due to the critical role SBIRS plays in Integrated Tactical Warning and Attack Assessment (ITW/AA) of attack on the CONUS, DOT&E has become involved in this program early. DOT&E works closely with AFOTEC, the program office, and all users to ensure that the acquisition strategy fosters an operationally effective and suitable system while maintaining cost-effectiveness. DOT&E has supported SBIRS acquisition reform through heavy involvement in IPTs, early involvement in combined developmental and operational tests, and consolidation of developmental and operational test plans into a single Integrated T&E Plan.

The SBIRS test program includes a combination of OAs, combined DT/OT testing, and dedicated IOT&E. These OT&E events will progress in a building-block manner beginning with analyses, modeling, and validated simulation and ending with Hardware-in-the-Loop (HWIL) test beds and field tests. Modeling, simulation, and test beds will be used to assess those areas in which field testing cannot be conducted, such as actual missile attacks and operation in nuclear environments. SBIRS operational effectiveness and

suitability will be assessed on the basis of IOT&Es of each of the three major increments, which will include fixed and mobile assets.

Test and Evaluation Activity:

In 1998, DOT&E approved an initial TEMP that defined the top-level test strategy and mapped it into the overall acquisition strategy. DOT&E also continued its oversight of the following areas (each of which could impact schedule, cost, and system performance):

- Progress towards Increment 1 IOT&E
- HWIL test bed definition and dynamic effect modeling for Increment 2
- Risk reduction efforts for Increment 3
- Testability of SBIRS/NMD requirements for Increment 3

Progress towards Increment 1 IOT&E was assessed by an AFOTEC (OA) that addressed four areas: (1) major issues potentially affecting effectiveness and suitability; (2) programmatic voids; (3) testability of user requirements; and (4) ability of the program to support operational testing. DOT&E has specific program concerns about SBIRS Increment 1: (1) immature ground system software and delays in requirements and performance verification; (2) delays in procuring high-reliability communications links from the overseas ground stations to the Mission Control Station; and (3) adequate hardware for crew training. The Program Office is addressing many of these findings through specific risk reduction efforts to ensure readiness to enter IOT&E for the Increment 1 ground system in April 1999. There are still testability concerns involving the difficulty of testing SBIRS/NMD operational requirements within an acceptable confidence limit.

Test and Evaluation Assessment:

Year 2000 (Y2K) testing for SBIRS is well underway, and there are no anticipated problems with the system. Due to extensive use of commercial software and close cooperation between the contractor team and the Air Force, an adequate verification program is in place. Final Y2K testing will be complete prior to the start of IOT&E for the Increment 1 ground station in April 1999.

The major near-term challenge for the SBIRS program is to ensure a seamless transfer of operations from the current DSP ground stations to the new SBIRS Increment 1 MCS. This demanding task is complicated by the compressed timeline and issues associated with shared use facilities at the overseas relay ground stations. Additionally, there have been significant delays in validating software performance of the Increment 1 Ground System. Other near-term challenges for the SBIRS program include the adequacy of test bed design and the scope of models and simulations needed to validate the stressing requirements for the SBIRS High satellites and MCS Increment 2 and the significant technical risks associated with accelerated deployment of the low component by FY04. The demanding SBIRS High requirements are a significant improvement over DSP's demonstrated performance and require

extensive testing to validate assure the system's performance. For HWIL test beds, continued attention must be given to ensure that the test beds are adequate to support OT&E, including the need to portray dynamic backgrounds that accurately portray the earth's background as seen from space.

DOT&E's assessment is that the SBIRS compressed schedule to achieve "On Line in '99" remains at high risk, and delays in software integration and testing pose an increased risk in a "zero margin" schedule leading to Increment 1 IOT&E scheduled for April 1999. The primary challenge for Increment 1 is the verification of software performance and reliability. There have been significant delays in verifying software performance and reliability, as well as delays in hardware installation at the remote ground stations. While this type of problem is not unusual, many system interfacing with the SBIRS MCS are 1970s' legacy reporting systems, whose interfaces may not be adequately documented. Delays in starting testing of these interfaces put an inordinate amount of pressure on first opportunity success. The "never fail" nature of ITW/AA systems requires extensive "online" testing to validate reliable Increment 1 operations and a period of parallel operations prior to declaration of IOC. Any significant delays to IOT&E would lead to "ripple effect" delays in the Increment 1 IOC date, and further delay the IOC dates for subsequent ground system increments. Also, there is concern that the SBIRS Increment 1 ground system includes voids in areas of fault detection and isolation, operator training, and manpower.

SBIRS Increment 2 (both space and ground elements) remains on schedule but faces continued challenges in the areas of simulation and test bed development. For Increment 2, progress has been made in identifying real-world, dynamic effects in the short and medium wavelengths detected by the greatly improved SBIRS High sensors. The operational impact of these effects must be quantified and the SBIRS High sensor design shown to be robust enough to handle these natural phenomena. Resolution of these issues can be best accomplished by incorporation of adequate testing processes into the baseline sensor ground testing program. Until this testing is completed, the capabilities of the SBIRS sensor and signal processing to operate in the space environment remain a major concern.

Continuing significant technical problems with the SBIRS Low PDRR satellites demonstrate the wisdom of an extensive PDRR test phase before entering EMD to start construction of operational SBIRS Low satellites. The current schedule of events is very compressed and does not allow full evaluation of the PDRR satellites' performance. The current baseline SBIRS Low schedule requires successful completion of many difficult activities proceeding in parallel towards a successful FY04 first launch, thus violating recommendations outlined in the recently completed Welch Report on missile defense systems. Any additional delays in the PDRR competing contractor programs will require starting EMD prior to completion of PDRR to meet the congressional goal of an FY04 first launch. DOT&E is concerned that the baseline schedule, which includes the Flight Demonstrations System

and the Low Altitude Demonstrations System, will be delayed, presenting very few opportunities to collect “real-world” performance data on contractor designs to assess their ability to meet draft performance requirements. This period of evaluation of PDRR results is critical since “lessons learned” from PDRR test activities form the foundation for the government and contractor teams to perform Cost As an Independent Value satellite design trades. Any significant problems encountered during the PDRR phase (given the compressed schedule) may lead to premature launching of inadequately designed and tested satellites to maintain the FY04 initial deployment date.

To support Milestone II decisions, DOT&E has worked closely with AFOTEC, the program office, and the user community, to ensure that the acquisition strategy throughout the acquisition cycle fosters an operationally effective and suitable system while maintaining cost-effectiveness. This early involvement included active membership in IPTs, fostering combined developmental and operational tests, early validation of software maturity, and consolidation of developmental and operational test plans into a single Integrated T&E Plan.

5. Related Requirements:

None

6. Related Categories:

(a) Contributing sensors:

These sensors provide observation data on satellites to USSPACECOM on a contributing basis but are not directly under the operational control of USSPACECOM. Both mechanical radars and electro-optical systems are included in this category.

(b) Satellite operations:

The DoD procures, operates, and maintains a myriad of satellite systems to support national and tactical communications, missile warning, nuclear detonation detection, navigation, weather, and environmental monitoring. DoD’s satellite operations include the Defense Satellite Communications System (DSCS), Milstar, Fleet SATCOM System (FLTSATCOM), UHF Follow-on (UFO) System, the Defense Support Program (DSP), the Nuclear Detonation Detection System (NUDET), the Global Positioning System (GPS, also referred to as POSNAVTIME or position, navigation, and time), and the Defense Meteorological Satellite Program (DMSP) systems.

(c) Space-based warning system:

This category addresses space systems and sensors that have a surveillance and warning mission, which are operational, in development, or being studied.

(d) DoD space surveillance programs:

A constant and vigilant surveillance of potentially hostile military threats is critical in preserving the operational effectiveness of our armed forces around the world. Naval Space Command manages two distinct surveillance efforts

in support of Fleet and Fleet Marine Forces: tracking satellites in orbit and monitoring over-the-horizon threats from sea and air forces.

Over one million satellite detections, or observations, are collected by this surveillance network each month. Data gathered is transmitted to a computer center at Naval Space Command headquarters in Dahlgren, where it is used to constantly update a database of spacecraft orbital elements. This information is reported to Fleet and Fleet Marine Forces to alert them when particular satellites of interest are overhead. The command also maintains a catalog of all earth-orbiting satellites and supports USSPACECOM as part of the nation's worldwide Space Surveillance Network.

References

1. N.S. Kopeika, *A System Engineering Approach to Imaging* (SPIE. Optical Engineering Press, Bellingham, 1990)
2. H. Weichel, *Laser Beam Propagation in the Atmosphere* (SPIE. Optical Engineering Press, Bellingham, 1990)
3. L.C. Andrews, R.L. Phillips, *Laser Beam Propagation through Random Media*, 2nd edn. (SPIE Press, Bellingham, 2005)

Chapter 4

High-Power Microwave Energy as Weapon



High-power electromagnetic pulse generation techniques and high-power microwave technology have matured to the point where practical e-bombs (electromagnetic bombs) are becoming technically feasible, with new applications in both strategic and tactical information warfare. The development of conventional e-bomb devices allows their use in nonnuclear confrontations. This chapter discusses aspects of the technology base and weapon delivery techniques and proposes a doctrinal foundation for the use of such devices in warhead and bomb applications.¹ Brief biography of Dr. Carlo Kopp is presented in footnote at the end of this chapter.²

4.1 Introduction

High-power microwave (HPM) [1, 2] sources have been under investigation for several years as potential weapons for a variety of combat, sabotage, and terrorist applications. Due to classification restrictions, details of this work are relatively

¹<http://ncoic.com/empbomb/apjemp.htm>

²Carlo Kopp Born in Perth, Western Australia, the author graduated with first-class honors in electrical engineering in 1984, from the University of Western Australia. In 1996 he completed an MSc in Computer Science and is currently working on a PhD in the same discipline, at Monash University in Melbourne, Australia. He has over a decade of diverse industry experience, including the design of high-speed communications equipment, optical fiber receivers and transmitters, communications equipment including embedded code, Unix computer workstation motherboards, graphics adaptors, and chassis. More recently, he has consulted in Unix systems programming, performance engineering, and system administration. Actively publishing as a defense analyst in Australia's leading aviation trade journal, *Australian Aviation*, since 1980, he has become a locally recognized authority on the application of modern military technology to operations and strategy. His work on electronic combat doctrine, electromagnetic weapons doctrine, laser remote sensing, and signature reduction has been published by the Royal Australian Air Force's Air Power Studies Centre since 1992, and he has previously contributed to *CADRE Air Chronicles*.

unknown outside the military community and its contractors. A key point to recognize is the insidious nature of HPM. Due to the gigahertz-band frequencies (4–20 GHz) involved, HPM has the capability not only to penetrate radio front ends, but also for the most minute shielding penetrations throughout the equipment. At sufficiently high levels, as discussed, the potential exists for significant damage to devices and circuits. For these reasons, HPM should be of interest to the broad spectrum of EMC practitioners.

Electromagnetic pulse (EMP) and high-powered microwave (HMP) [1] weapons offer a significant capability against electronic equipment susceptible to damage by transient power surges. This weapon generates a very short, intense energy pulse producing a transient surge of thousands of volts that kills semiconductor devices. The conventional EMP and HMP weapons can disable non-shielded electronic devices including practically any modern electronic device within the effective range of the weapon.

Weapon of electrical mass destruction is based on high-power electromagnetic pulse (EMP) [3] generation techniques and high-power microwave technology.

Weapons that direct energy instead of matter on targets have undergone extensive research in the last two decades. They have two potential advantages over existing weapon systems. First, they use a power supply rather than a magazine of explosive munitions; this “deep magazine” is unlikely to be expended in battle. Second, they attack at the speed of light, 160,000 times faster than a bullet, thus making avoidance of the incoming bolt impossible and negating the advantage of increasingly swift tactical missiles.

Directed energy weapons (DEW) generally fall into three categories:

1. High-power lasers
2. Microwave or radio-frequency (RF) energy weapons
3. Charged particle beam weapons

High-power microwave (HPM) [1, 2] has an advantage over the other DEWs in that microwave does not face a serious propagation issue. Particle beams and lasers have difficulties in propagating through the atmosphere (thermal blooming in case of the laser), and electron beams cannot propagate in space. Moreover, both are pinpoint weapons with small spot sizes requiring precise pointing to hit the target. Antenna-directed microwave, on the other hand, spreads through diffraction and has spot size large enough to accommodate some lack of precision in pointing and tracking. Lasers and particle beams are also much less electrically efficient, more complex, and therefore costlier.

The electromagnetic bomb or e-bomb is another form of a weapon of mass destruction. The e-bomb takes advantage of how we rely so heavily on electricity. It is designed to not just disable but also destroy electronic devices by sending out an electromagnetic pulse or an EMP. An EMP is a burst of electromagnetic radiation from an explosion; the resulting electric and magnetic fields merge with electronic systems to produce catastrophic currents and voltage surges. An EMP is a form of electromagnetic induction as this is the production of voltage. If an e-bomb were to explode it alters the magnetic flux lines of the earth meaning that the North will not

be as affected but the East, South, and West will experience the blast if you will. This would mean thousands of volts of electromagnetic energy from the highest positives to the highest negative polarities transferred via air and powerlines. This is an important weapon to have in a war as it can take out your opponent's form of communication.

4.2 High-Power Microwave

The prosecution of a successful information warfare (IW) campaign against an industrialized or a postindustrial opponent will require a suitable set of tools. As demonstrated in the Desert Storm air campaign, air power has proven to be a most effective means of inhibiting the functions of an opponent's vital information processing infrastructure. This is because air power allows concurrent or parallel engagement of a large number of targets over geographically significant areas.

While Desert Storm demonstrated that the application of air power was the most practical means of crushing an opponent's information processing and transmission nodes, the need physically to destroy these with guided munitions absorbed a substantial proportion of available air assets in the early phase of the air campaign. Indeed, the aircraft capable of delivery of laser-guided bombs were largely occupied with this very target set during the first nights of the air battle.

The efficient execution of an IW campaign against a modern industrial or postindustrial opponent will require the use of specialized tools designed to destroy information systems. Electromagnetic bombs built for this purpose can provide, where delivered by suitable means, a very effective tool for this purpose.

4.3 E-Bomb

An e-bomb (electromagnetic bomb) is a weapon that uses an intense electromagnetic field to create a brief pulse of energy that affects electronic circuitry without harming humans or buildings. At low levels, the pulse temporarily disables electronics systems; midrange levels corrupt computer data. Very high levels completely destroy electronic circuitry, thus disabling any type of machine that uses electricity, including computers, radios, and ignition systems in vehicles. Although not directly lethal, an e-bomb would devastate any target that relies upon electricity: a category encompassing any potential military target and most civilian areas of the world as well. According to a CBS News report, the United States deployed an experimental e-bomb on March 24, 2003, to knock out Iraqi satellite television and disrupt the broadcast of propaganda.

In the United States, most e-bomb research has been carried out at the Air Force Research Laboratory at Kirtland Air Force Base in New Mexico, where researchers have been exploring the use of high-power microwaves (HPM). Although the

devices themselves may be relatively uncomplicated to manufacture (Popular Mechanics illustrated a simple design in September 2001), their usage poses a number of problems. To create an effective e-bomb, developers must not only generate an extremely high-powered pulse of energy but also find a way to control both the energy—which can behave in unpredictable ways—and the heat generated as its by-product. Furthermore, for nonnuclear e-bombs, the range is limited. According to most defense analysts' speculations, devices in development are likely to affect an area of only a few hundred yards.

The concept behind the e-bomb arose from nuclear weaponry research in the 1950s. When the US military tested hydrogen bombs over the Pacific Ocean, streetlights were blown out hundreds of miles away and radio equipment was affected as far as away as Australia. Although at the time these effects were considered incidental, since that time researchers have sought a means of focusing that energy.

4.4 The Electromagnetic Pulse Effect (EMP)

The electromagnetic pulse (EMP) effect was first observed during the early testing of high-altitude airburst nuclear weapons. The effect is characterized by the production of a very short (hundreds of nanoseconds) but intense electromagnetic pulse, which propagates away from its source with ever-diminishing intensity, governed by the theory of electromagnetism. The electromagnetic pulse is in effect an electromagnetic shock wave.

This pulse of energy produces a powerful electromagnetic field, particularly within the vicinity of the weapon burst. The field can be sufficiently strong to produce short-lived transient voltages of thousands of volts (i.e., kilovolts) on exposed electrical conductors, such as wires, or conductive tracks on printed circuit boards, where exposed.

It is this aspect of the EMP effect, which is of military significance, as it can result in irreversible damage to a wide range of electrical and electronic equipment, particularly computers and radio or radar receivers. Subject to the electromagnetic hardness of the electronics, a measure of the equipment's resilience to this effect, and the intensity of the field produced by the weapon, the equipment can be irreversibly damaged or in effect electrically destroyed. The damage inflicted is not unlike that experienced through exposure to close proximity lightning strikes, and may require complete replacement of the equipment, or at least substantial portions thereof.

Commercial computer equipment is particularly vulnerable to EMP effects, as it is largely built up of high-density metal oxide semiconductor (MOS) devices, which are very sensitive to exposure to high-voltage transients. What is significant about MOS devices is that very little energy is required to permanently wound or destroy them; any voltage typically in excess of tens of volts can produce an effect termed gate breakdown, which effectively destroys the device. Even if the pulse is not powerful enough to produce thermal damage, the power supply in the equipment

will readily supply enough energy to complete the destructive process. Wounded devices may still function, but their reliability will be seriously impaired [4, 5]. Shielding electronics by equipment chassis provides only limited protection, as any cables running in and out of the equipment will behave very much like antennae, in effect guiding the high-voltage transients into the equipment.

Computers used in data processing systems, communications systems, displays, industrial control applications including road and rail signaling, and those embedded in military equipment, such as signal processors, electronic flight controls, and digital engine control systems, are all potentially vulnerable to the EMP effect.

Other electronic devices and electrical equipment may also be destroyed by the EMP effect. Telecommunications equipment can be highly vulnerable, due to the presence of lengthy copper cables between devices. Receivers of all varieties are particularly sensitive to EMP, as the highly sensitive miniature high-frequency transistors and diodes in such equipment are easily destroyed by exposure to high-voltage electrical transients. Therefore, radar and electronic warfare equipment, satellite, microwave, UHF, VHF, HF, and low-band communications equipment and television equipment are all potentially vulnerable to the EMP effect.

It is significant that modern military platforms are densely packed with electronic equipment, and unless these platforms are well hardened an EMP device can substantially reduce their function or render them unusable.

4.5 The Technology Base for Conventional Electromagnetic Bombs

The technology base, which may be applied to the design of electromagnetic bombs, is both diverse, and in many areas quite mature. Key technologies, which are extant in the area, are explosively pumped flux compression generators (FCG), explosive or propellant-driven magnetohydrodynamic (MHD) generators, and a range of HPM devices, the foremost of which is the virtual cathode oscillator or vircator. A wide range of experimental designs have been tested in these technology areas, and a considerable volume of work has been published in unclassified literature. See Fig. 4.1.

This chapter reviews the basic principles and attributes of these technologies, in relation to bomb and warhead applications. It is stressed that this treatment is not exhaustive and is only intended to illustrate how the technology base can be adapted to an operationally deployable capability.

4.5.1 Explosively Pumped Flux Compression Generators

The explosively pumped flux compression generator (FCG) is the most mature technology applicable to bomb designs. The FCG was first demonstrated by

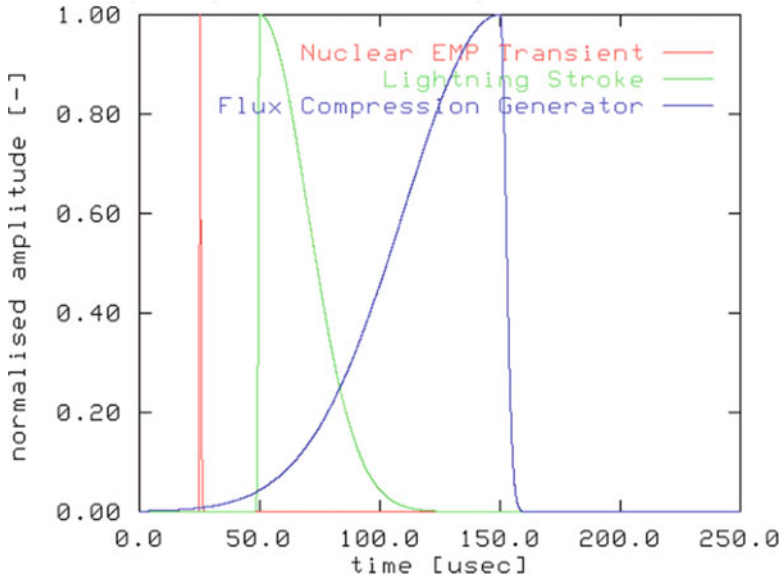


Fig. 4.1 Typical electromagnetic pulse shapes

Clarence Fowler at Los Alamos National Laboratories (LANL) in the late 1950s [6]. Since that time a wide range of FCG configurations have been built and tested, both in the United States and the USSR, and more recently CIS.

The FCG is a device capable of producing electrical energies of tens of megajoules in tens to hundreds of microseconds of time, in a relatively compact package. With peak power levels of the order of terawatts to tens of terawatts, FCGs may be used directly, or as one-shot pulse power supplies for microwave tubes. To place this in perspective, the current produced by a large FCG is between ten and thousand times greater than that produced by a typical lightning stroke [7].

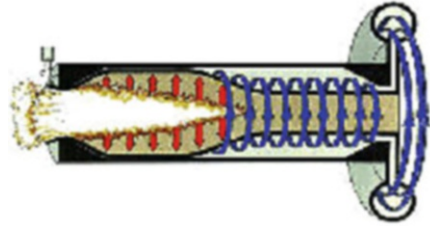
The central idea behind the construction of FCGs is that of using a fast explosive to rapidly compress a magnetic field, transferring much energy from the explosive into the magnetic field.

The initial magnetic field in the FCG prior to explosive initiation is produced by a start current. The start current is supplied by an external source, such as a high-voltage capacitor bank (Marx bank), a smaller FCG, or an MHD device. In principle, any device capable of producing a pulse of electrical current of the order of tens of kilo amperes to mega-amperes will be suitable.

A number of geometrical configurations for FCGs have been published (for examples see references) [8–10]. The most commonly used arrangement is that of the coaxial FCG. The coaxial arrangement is of particular interest in this context, as its essentially cylindrical form lends itself to packaging into munitions.

Magnetic flux compression generators (magnetocumulative generators (MCGs)) (Fig. 4.2) were independently invented by A. Sakharov in Russia and C.M. Fowler in the United States. They are the most powerful pulsed power devices ever built. Till

Fig. 4.2 Flux compression generator



the end of the Cold War, the applications of this technology were classified. Today it is possible to give international lectures on these devices and some of their applications:

1. C.M. Fowler, Los Alamos National Laboratories, USA
2. L. Altgilbers, US Army Space and Missile Defense Command, USA
3. Smith, University of Loughborough, UK

A flux compression generator (FCG) is basically a directed electromagnetic pulse (DEMP) gun. There are a number of uses for this technology but most of them are warfare related. See Fig. 4.3.

In a typical coaxial flux compression generator (FCG), a cylindrical copper tube forms the armature. This tube is filled with a fast high-energy explosive. A number of explosive types have been used, ranging from B- and C-type compositions to machined blocks of PBX-9501. The armature is surrounded by a helical coil of heavy wire, typically copper, which forms the FCG stator. The stator winding is in some designs split into segments, with wires bifurcating at the boundaries of the segments, to optimize the electromagnetic inductance of the armature coil.

The intense magnetic forces produced during the operation of the FCG could potentially cause the device to disintegrate prematurely if not dealt with. This is typically accomplished by the addition of a structural jacket of a nonmagnetic material. Materials such as concrete or fiberglass in an epoxy matrix have been used. In principle, any material with suitable electrical and mechanical properties could be used. In applications where weight is an issue, such as air-delivered bombs or missile warheads, a glass or Kevlar epoxy composite would be a viable candidate.

It is typical that the explosive is initiated when the start current peaks. This is usually accomplished with an explosive lens plane wave generator which produces a uniform plane wave burn (or detonation) front in the explosive. Once initiated, the front propagates through the explosive in the armature, distorting it into a conical shape (typically 12–14° of arc). Where the armature has expanded to the full diameter of the stator, it forms a short circuit between the ends of the stator coil, shorting and thus isolating the start current source and trapping the current within the device. The propagating short has the effect of compressing the magnetic field while reducing the inductance of the stator winding. The result is that such generators will produce a ramping current pulse, which peaks before the final disintegration of the device. Published results suggest ramp times of tens to hundreds of microseconds,

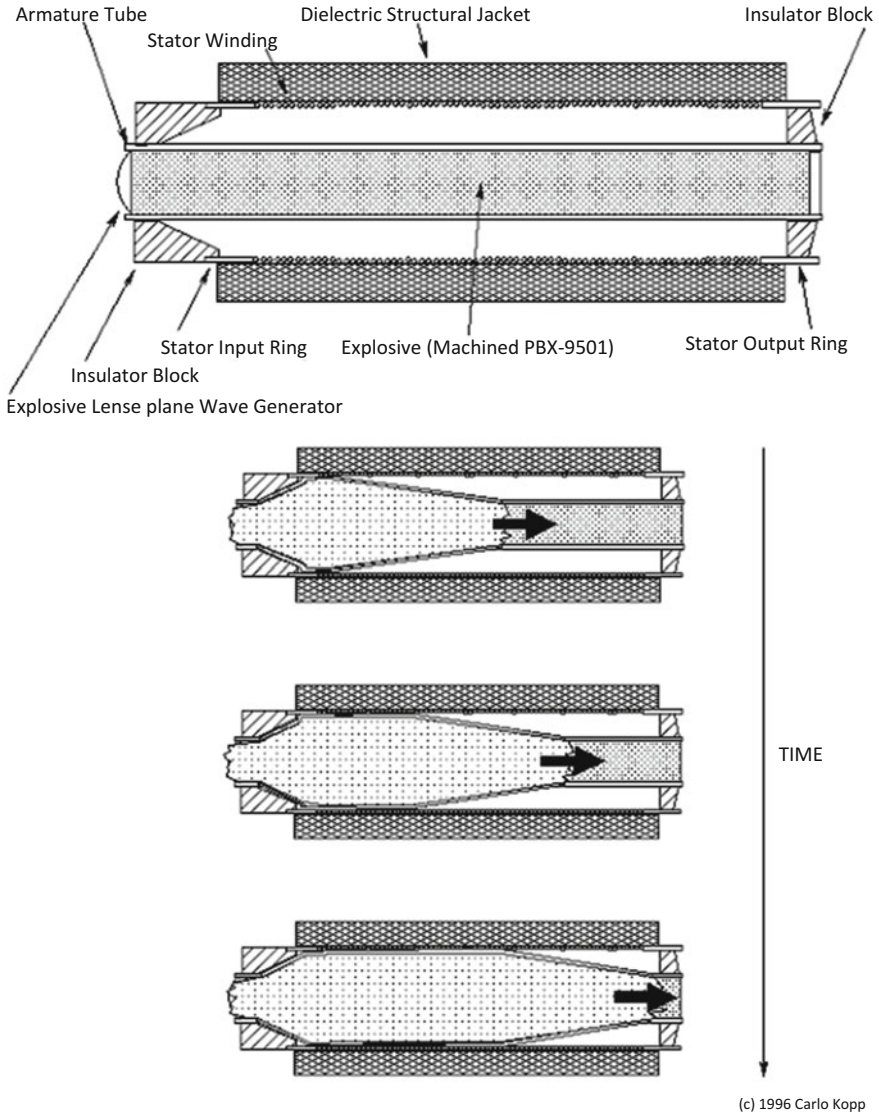


Fig. 4.3 Explosive pumped coaxial flux compression generator

specific to the characteristics of the device, for peak currents of tens of mega-amperes and peak energies of tens of megajoules.

The current multiplication (i.e., ratio of output current to start current) achieved varies with designs, but numbers as high as 60 have been demonstrated. In a munition application, where space and weight are at a premium, the smallest possible start current source is desirable. These applications can exploit cascading of FCGs, where a small FCG is used to prime a larger FCG with a start current.

Experiments conducted by LANL and AFRL have demonstrated the viability of this technique [8, 11].

The principal technical issues in adapting the FCG to weapon applications lie in packaging, supply of start current, and matching the device to the intended load. Interfacing to a load is simplified by the coaxial geometry of coaxial and conical FCG designs. Significantly, this geometry is convenient for weapon applications, where FCGs may be stacked axially with devices such as microwave victors. The demands of a load such as a victor, in terms of waveform shape and timing, can be satisfied by inserting pulse shaping networks, transformers, and explosive high-current switches.

4.5.2 Explosive and Propellant-Driven Magnetohydrodynamic (MHD) Generators

The design of explosive and propellant-driven magnetohydrodynamic generators is a much less mature art than that of FCG design. Technical issues such as the size and weight of magnetic field-generating devices required for the operation of MHD generators suggest that MHD devices will play a minor role in the near term. In the context of this chapter, their potential lies in areas such as start current generation for FCG devices.

The fundamental principle behind the design of MHD devices is that a conductor moving through a magnetic field will produce an electrical current transverse to the direction of the field and the conductor motion. In an explosive or propellant-driven MHD device, the conductor is a plasma of ionized explosive or propellant gas, which travels through the magnetic field. Current is collected by electrodes which are in contact with the plasma jet [12].

The electrical properties of the plasma are optimized by seeding the explosive or propellant with suitable additives, which ionize during the burn [12, 13]. Published experiments suggest that a typical arrangement uses a solid propellant gas generator, often using conventional ammunition propellant as a base. Cartridges of such propellant can be loaded much like artillery rounds, for multiple-shot operations.

4.5.3 High-Power Microwave Sources: The Vircator

While flux compression generators (FCGs) are potent technology base for the generation of large electrical power pulses, the output of the FCG is by its basic physics constrained to the frequency band below 1 MHz. Many target sets will be difficult to attack even with very high power levels at such frequencies; moreover, focusing the energy output from such a device will be problematic. An HPM device

overcomes both of the problems, as its output power may be tightly focused, and it has a much better ability to couple energy into many target types.

A wide range of HPM devices exist. Relativistic klystrons, magnetrons, slow-wave devices, reflex triodes, spark gap devices, and vircators are all examples of the available technology base [14, 15]. From the perspective of a bomb or warhead designer, the device of choice will be at this time the vircator, or in the nearer term a spark gap source. The vircator is of interest because it is a one-shot device capable of producing a very powerful single pulse of radiation, yet it is mechanically simple, small, and robust, and can operate over a relatively broad band of microwave frequencies.

The physics of the vircator tube are substantially more complex than those of the preceding devices. The fundamental idea behind the vircator is that of accelerating a high-current electron beam against a mesh (or foil) anode. Many electrons will pass through the anode, forming a bubble of space charge behind the anode. Under the proper conditions, this space charge region will oscillate at microwave frequencies. If the space charge region is placed into a resonant cavity which is appropriately tuned, very high peak powers may be achieved. Conventional microwave engineering techniques may then be used to extract microwave power from the resonant cavity. Because the frequency of oscillation is dependent upon the electron beam parameters, vircators may be tuned or chirped in frequency, where the microwave cavity will support appropriate modes. Power levels achieved in vircator experiments range from 170 kW to 40 GW over frequencies spanning the decimetric and centimetric bands [16].

The two most commonly described configurations for the vircator are the axial vircator (AV) (Fig. 4.4) and the transverse vircator (TV). The axial vircator is the simplest by design and has generally produced the best power output in experiments. It is typically built into a cylindrical waveguide structure. Power is most often extracted by transitioning the waveguide into a conical horn structure, which functions as an antenna. AVs typically oscillate in transverse magnetic (TM) modes. The

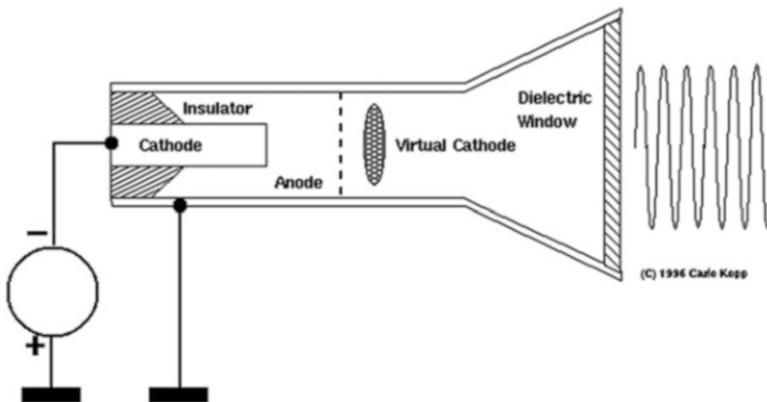


Fig. 4.4 Axial virtual cathode oscillator

transverse vircator injects cathode current from the side of the cavity and will typically oscillate in a transverse electric (TE) mode.

Technical issues in vircator design are output pulse duration, which is typically of the order of a microsecond and is limited by anode melting, stability of oscillation frequency often compromised by cavity mode hopping, conversion efficiency, and total power output. Coupling power efficiently from the vircator cavity in modes suitable for a chosen antenna type may also be an issue, given the high power levels involved and thus the potential for electrical breakdown in insulators.

4.6 The Lethality of Electromagnetic Warheads

The issue of electromagnetic weapon lethality is complex. Unlike the technology base for weapon construction, which has been widely published in the open literature, lethality-related issues have been published much less frequently.

While the calculation of electromagnetic field strengths achievable at a given radius for a given device design is a straightforward task, determining a kill probability for a given class of target under such conditions is not.

This is for good reasons. The first is that target types are very diverse in their electromagnetic hardness, or ability to resist damage. Equipment which has been intentionally shielded and hardened against electromagnetic attack will withstand orders of magnitude greater field strengths than standard commercially rated equipment. Moreover, various manufacturer's implementations of like types of equipment may vary significantly in hardness due to the idiosyncrasies of specific electrical designs, cabling schemes, and chassis/shielding designs used.

The second major problem area in determining lethality is that of coupling efficiency, which is a measure of how much power is transferred from the field produced by the weapon into the target. Only power coupled into the target can cause useful damage.

4.6.1 *Coupling Modes*

In assessing how power is coupled into targets, two principal coupling modes are recognized in the literature:

- Front door coupling occurs typically when power from an electromagnetic weapon is coupled into an antenna associated with radar or communications equipment. The antenna subsystem is designed to couple power in and out of the equipment, and thus provides an efficient path for the power flow from the electromagnetic weapon to enter the equipment and cause damage.
- Backdoor coupling occurs when the electromagnetic field from a weapon produces large transient currents (termed spikes, when produced by a low-frequency

weapon) or electrical standing waves (when produced by an HPM weapon) on fixed electrical wiring and cables interconnecting equipment or providing connections to mains power or the telephone network; see references [7, 17]. Equipment connected to exposed cables or wiring will experience either high-voltage transient spikes or standing waves which can damage power supplies and communications interfaces if these are not hardened. Moreover, should the transient penetrate into the equipment, damage can be done to other devices inside.

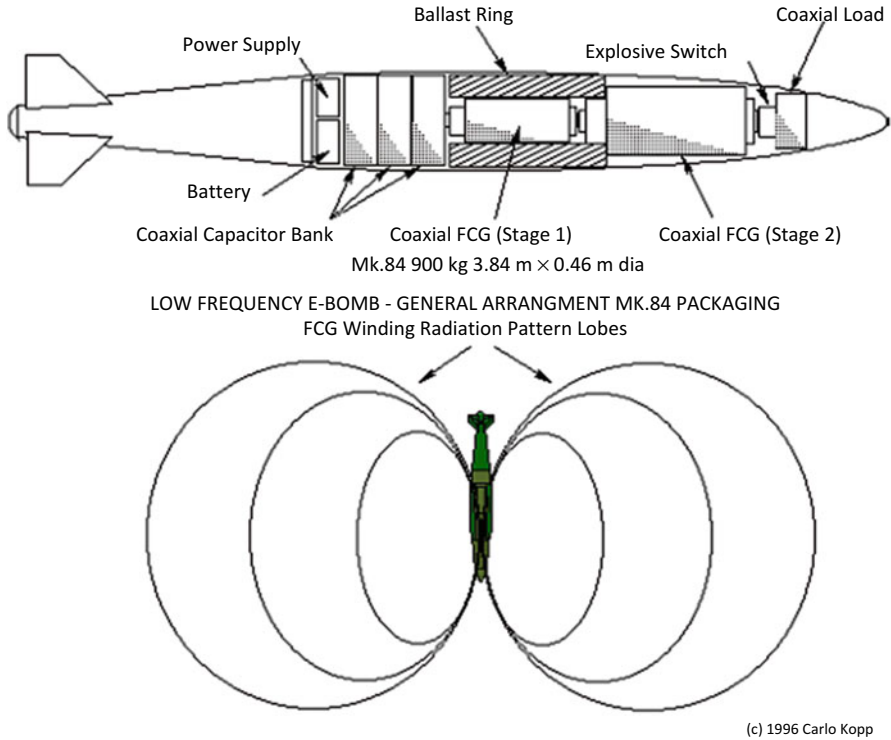
A low-frequency weapon will couple well into a typical wiring infrastructure, as most telephone lines, networking cables, and powerlines follow streets, building risers, and corridors. In most instances any particular cable run will comprise multiple linear segments joined at approximately right angles. Whatever the relative orientation of the weapon field, more than one linear segment of the cable run is likely to be oriented such that a good coupling efficiency can be achieved.

It is worth noting at this point the safe operating envelopes of some typical types of semiconductor devices. Manufacturer's guaranteed breakdown voltage ratings for silicon high-frequency bipolar transistors, widely used in communications equipment, typically vary between 15 V and 65 V. Gallium arsenide field effect transistors (FETs) are usually rated at about 10 V. High-density dynamic random access memories (DRAM), an essential part of any computer, are usually rated to 7 V against earth. Generic CMOS logic is rated between 7 V and 15 V, and microprocessors running off 3.3 V or 5 V power supplies are usually rated very closely to that voltage. While many modern devices are equipped with additional protection circuits at each pin, to sink electrostatic discharges, sustained or repeated application of a high voltage will often defeat these [18–20].

Communications interfaces and power supplies must typically meet electrical safety requirements imposed by regulators. Such interfaces are usually protected by isolation transformers with ratings from hundreds of volts to about 2–3 kV [21].

It is clearly evident that once the defense provided by a transformer, cable pulse arrestor, or shielding is breached, voltages even as low as 50 V can inflict substantial damage upon computer and communications equipment. The author has seen a number of equipment items (computers, consumer electronics) exposed to low-frequency high-voltage spikes (near-lightning strikes, electrical power transients), and in every instance the damage was extensive, often requiring replacement of most semiconductors in the equipment (see footnote 2).

HPM weapons operating in the centimetric and millimetric bands however offer an additional coupling mechanism to backdoor coupling. This is the ability to directly couple into equipment through ventilation holes, gaps between panels, and poorly shielded interfaces. Under these conditions, any aperture into the equipment behaves much like a slot in a microwave cavity, allowing microwave radiation to directly excite or enter the cavity. The microwave radiation will form a spatial standing wave pattern within the equipment. Components situated within the antinodes within the standing wave pattern will be exposed to potentially high electromagnetic fields.



(c) 1996 Carlo Kopp

Fig. 4.5 Low-frequency e-bomb warhead (MK 48 form factor)

Because microwave weapons can couple more readily than low-frequency weapons and can in many instances bypass protection devices designed to stop low-frequency coupling, microwave weapons have the potential to be significantly more lethal than low-frequency weapons. See Fig. 4.5.

What research has been done in this area illustrates the difficulty in producing workable models for predicting equipment vulnerability. It does however provide a solid basis for shielding strategies and hardening of equipment.

The diversity of likely target types and the unknown geometrical layout and electrical characteristics of the wiring and cabling infrastructure surrounding a target make the exact prediction of lethality impossible.

A general approach for dealing with wiring- and cabling-related backdoor coupling is to determine a known lethal voltage level, and then use this to find the required field strength to generate this voltage. Once the field strength is known, the lethal radius for a given weapon configuration can be calculated.

A trivial example is that of a 10 GW 5 GHz HPM device illuminating a footprint of 400–500 m diameter, from a distance of several hundred meters (Fig. 4.6).

This will result in field strengths of several kilovolts per meter within the device footprint, in turn capable of producing voltages of hundreds of volts to kilovolts on

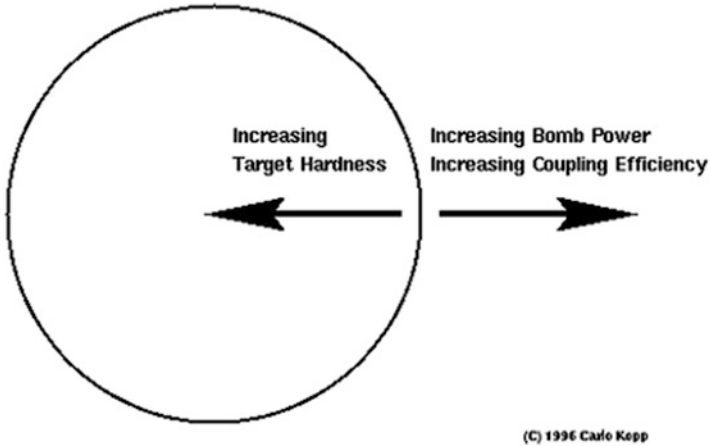


Fig. 4.6 E-bomb lethal radius

exposed wires or cables [17, 22]. This suggests lethal radii of the order of hundreds of meters, subject to weapon performance and target set electrical hardness.

4.6.2 Maximizing Electromagnetic Bomb Lethality

To maximize the lethality of an electromagnetic bomb it is necessary to maximize the power coupled into the target set.

The first step in maximizing bomb lethality is to maximize the peak power and duration of the radiation of the weapon. For a given bomb size, this is accomplished by using the most powerful flux compression generator (and vircator in a HPM bomb) which will fit the weapon size, and by maximizing the efficiency of internal power transfers in the weapon. Energy which is not emitted is energy wasted at the expense of lethality.

The second step is to maximize the coupling efficiency into the target set. A good strategy for dealing with a complex and diverse target set is to exploit every coupling opportunity available within the bandwidth of the weapon.

A low-frequency bomb built around an FCG will require a large antenna to provide good coupling of power from the weapon into the surrounding environment. While weapons built this way are inherently wide band, as most of the power produced lies in the frequency band below 1 MHz, compact antennas are not an option. One possible scheme is for a bomb approaching its programmed firing altitude to deploy five linear antenna elements. These are produced by firing off cable spools, which unwind several hundred meters of cable. Four radial antenna elements form a “virtual” earth plane around the bomb, while an axial antenna element is used to radiate the power from the FCG. The choice of element lengths would need to be carefully matched to the frequency characteristics of the weapon,

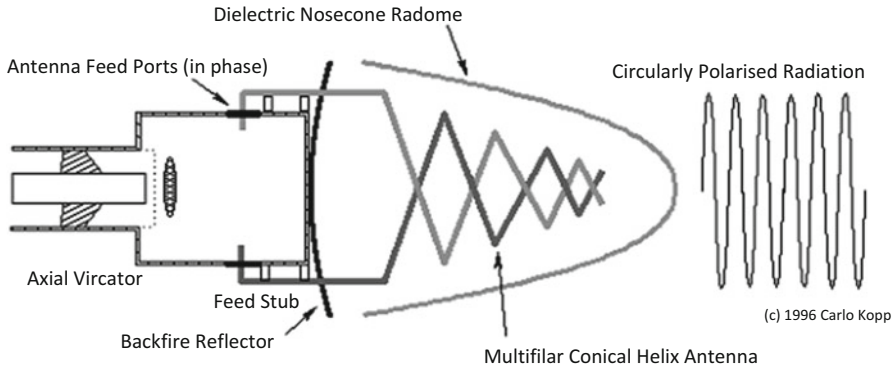


Fig. 4.7 HPM e-bomb warhead (MK 84 form factor)

to produce the desired field strength. A high-power coupling pulse transformer is used to match the low-impedance flux compression generator (FCG) output to the much higher impedance of the antenna and ensure that the current pulse does not vaporize the cable prematurely.

Other alternatives are possible. One is to simply guide the bomb very close to the target and rely upon the near field produced by the FCG winding, which is in effect of a loop antenna of very small diameter relative to the wavelength. While coupling efficiency is inherently poor, the use of a guided bomb would allow the warhead to be positioned accurately within meters of a target. An area worth further investigation in this context is the use of low-frequency bombs to damage or destroy magnetic tape libraries, as the near fields in the vicinity of a flux generator are of the order of magnitude of the coercivity of most modern magnetic materials.

Microwave bombs have a broader range of coupling modes and, given the small wavelength in comparison with bomb dimensions, can be readily focused against targets with a compact antenna assembly. Assuming that the antenna provides the required weapon footprint, there are at least two mechanisms, which can be employed to further maximize lethality. See Fig. 4.7.

The first is sweeping the frequency or chirping the vircator. This can improve coupling efficiency in comparison with a single-frequency weapon, by enabling the radiation to couple into apertures and resonances over a range of frequencies. In this fashion, a larger number of coupling opportunities are exploited.

The second mechanism, which can be exploited to improve coupling, is the polarization of the weapon's emission. If we assume that the orientations of possible coupling apertures and resonances in the target set are random in relation to the weapon's antenna orientation, a linearly polarized emission will only exploit half of the opportunities available. A circularly polarized emission will exploit all coupling opportunities.

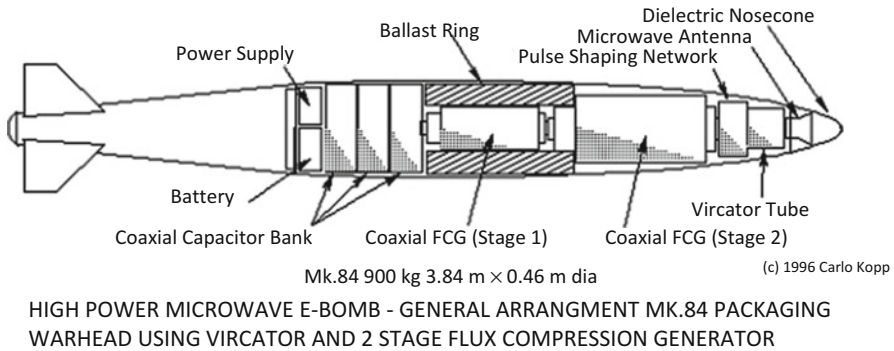


Fig. 4.8 Example of vircator/antenna assembly

The practical constraint is that it may be difficult to produce an efficient high-power circularly polarized antenna design, which is compact and performs over a wide band. Some work therefore needs to be done on tapered helix or conical spiral-type antennas capable of handling high power levels, and a suitable interface to a vircator with multiple extraction ports must be devised. A possible implementation is depicted in Fig. 4.8. In this arrangement, power is coupled from the tube by stubs, which directly feed a multi-filer conical helix antenna. An implementation of this scheme would need to address the specific requirements of bandwidth, beam width, and efficiency of coupling from the tube while delivering circularly polarized radiation.

Another aspect of electromagnetic bomb lethality is its detonation altitude, and by varying the detonation altitude a trade-off may be achieved between the size of the lethal footprint and the intensity of the electromagnetic field in that footprint. This provides the option of sacrificing weapon coverage to achieve kills against targets of greater electromagnetic hardness, for a given bomb size (Figs. 4.9 and 4.10). This is not unlike the use of airburst explosive devices.

4.7 Targeting Electromagnetic Bombs

The task of identifying targets for attack with electromagnetic bombs can be complex. Certain categories of target will be very easy to identify and engage. Buildings housing government offices and thus computer equipment, production facilities, military bases, and known radar sites and communications nodes are all targets, which can be readily identified through conventional photographic, satellite, imaging radar, electronic reconnaissance, and humint operations. These targets are typically geographically fixed and thus may be attacked providing that the aircraft

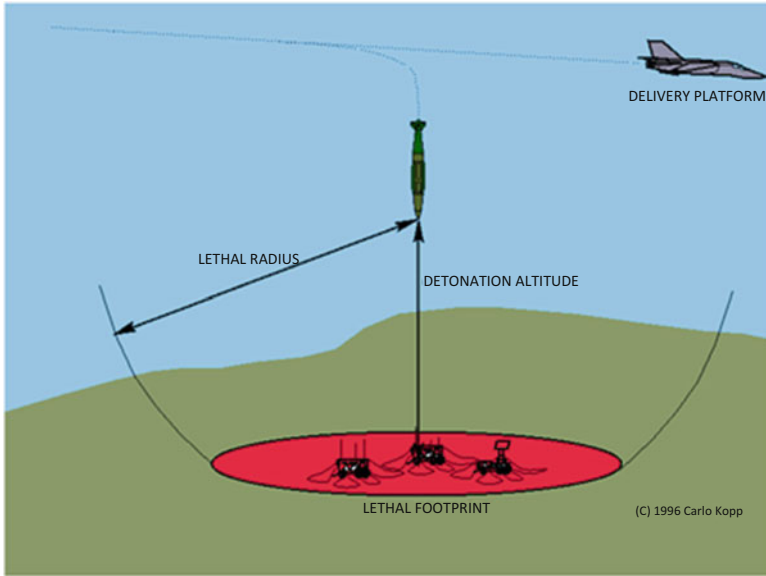


Fig. 4.9 Lethal footprint of low-frequency e-bomb in relation to altitude

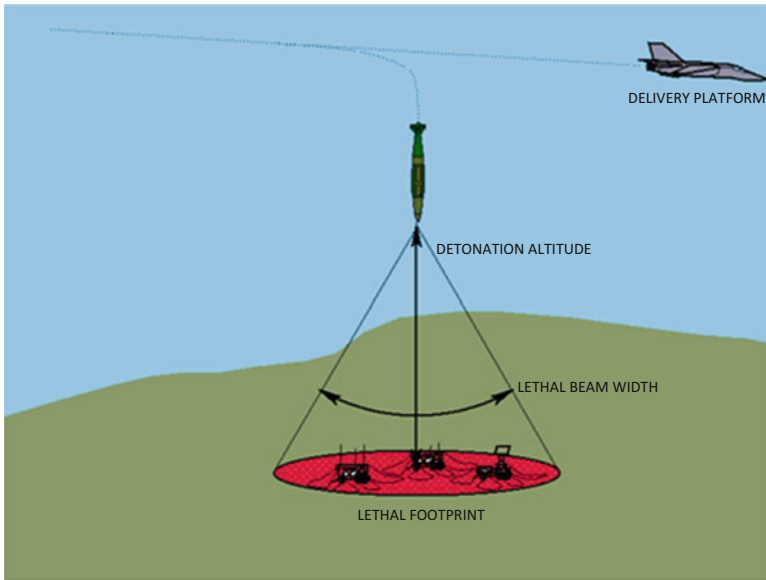


Fig. 4.10 Lethal footprint of an HPM e-bomb in relation to altitude

can penetrate to weapon release range. With the accuracy inherent in GPS/inertially guided weapons, the electromagnetic bomb can be programmed to detonate at the optimal position to inflict a maximum of electrical damage.

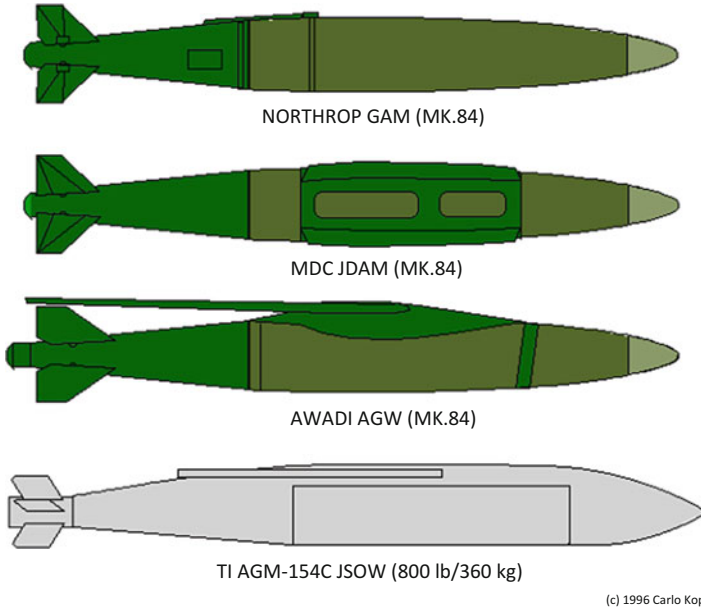
Mobile and camouflaged targets, which radiate overtly, can also be readily engaged. Mobile and relocatable air defense equipment, mobile communications nodes, and naval vessels are all good examples of this category of target. While radiating, their positions can be precisely tracked with suitable electronic support measures (ESM) and emitter locating systems (ELS) carried either by the launch platform or by a remote surveillance platform. In the latter instance target, coordinates can be continuously data linked to the launch platform. As most such targets move relatively slowly, they are unlikely to escape the footprint of the electromagnetic bomb during the weapon's flight time.

Mobile or hidden targets which do not overtly radiate may present a problem, particularly should conventional means of targeting be employed. A technical solution to this problem does however exist, for many types of target. This solution is the detection and tracking of unintentional emission (UE) [23]. UE has attracted most attention in the context of TEMPEST surveillance, where transient emanations leaking out from equipment due to poor shielding can be detected and, in many instances, demodulated to recover useful intelligence. Termed Van Eck radiation [24], such emissions can only be suppressed by rigorous shielding and emission control techniques, such as are employed in TEMPEST rated equipment.

While the demodulation of UE can be a technically difficult task to perform well, in the context of targeting electromagnetic bombs this problem does not arise. To target such an emitter for attack requires only the ability to identify the type of emission and thus target type, and to isolate its position with sufficient accuracy to deliver the bomb. Because the emissions from computer monitors, peripherals, processor equipment, switch mode power supplies, electrical motors, internal combustion engine ignition systems, variable duty cycle electrical power controllers (thyristor or triac based), superheterodyne receiver local oscillators, and computer networking cables are all distinct in their frequencies and modulations, a suitable emitter locating system can be designed to detect, identify, and track such sources of emission, Fig. 4.11.

A good precedent for this targeting paradigm exists. During the SEA (Vietnam) conflict, the US Air Force (USAF) operated a number of night interdiction gunships, which used direction-finding receivers to track the emissions from vehicle ignition systems. Once a truck was identified and tracked, the gunship would engage it [2].

Because UE occurs at relatively low power levels, the use of this detection method prior to the outbreak of hostilities can be difficult, as it may be necessary to overfly hostile territory to find signals of usable intensity [3]. The use of stealthy reconnaissance aircraft or long-range, stealthy unmanned aerial vehicles (UAV) may be required. The latter also raises the possibility of autonomous electromagnetic warhead armed expendable UAVs, fitted with appropriate homing receivers. These would be programmed to loiter in a target area until a suitable emitter is detected, upon which the UAV would home in and expend itself against the target.



(c) 1996 Carlo Kopp

Fig. 4.11 GPS-guided bomb/glide bomb kits

4.8 The Delivery of Conventional Electromagnetic Bombs

As with explosive warheads, electromagnetic warheads will occupy a volume of physical space and will also have some given mass (weight) determined by the density of the internal hardware. Like explosive warheads, electromagnetic warheads may be fitted to a range of delivery vehicles.

Known existing applications [4] involve fitting an electromagnetic warhead to a cruise missile airframe. The choice of a cruise missile airframe will restrict the weight of the weapon to about 340 kg (750 lb), although some sacrifice in airframe fuel capacity could see this size increased. A limitation in all such applications is the need to carry an electrical energy storage device, e.g., a battery, to provide the current used to charge the capacitors used to prime the FCG prior to its discharge. Therefore, the available payload capacity will be split between the electrical storage and the weapon itself.

In wholly autonomous weapons such as cruise missiles, the size of the priming current source and its battery may well impose important limitations on weapon capability. Air-delivered bombs, which have a flight time between tens of seconds to minutes, could be built to exploit the launch aircraft's power systems. In such a bomb design, the bomb's capacitor bank can be charged by the launch aircraft en route to target, and after release a much smaller onboard power supply could be used to maintain the charge in the priming source prior to weapon initiation.

An electromagnetic bomb delivered by a conventional aircraft [6] can offer a much better ratio of electromagnetic device mass to total bomb mass, as most of the bomb mass can be dedicated to the electromagnetic device installation itself. It follows therefore that for a given technology an electromagnetic bomb of identical mass to a electromagnetic warhead equipped missile can have a much greater lethality, assuming equal accuracy of delivery and technologically similar electromagnetic device design.

A missile-borne electromagnetic warhead installation will comprise the electromagnetic device, an electrical energy converter, and an onboard storage device such as a battery. As the weapon is pumped, the battery is drained. The electromagnetic device will be detonated by the missile's onboard fusing system. In a cruise missile, this will be tied to the navigation system; in an anti-shiping missile the radar seeker; and in an air-to-air missile the proximity fusing system. The warhead fraction (i.e., ratio of total payload (warhead) mass to launch mass of the weapon) will be between 15% and 30% [7].

An electromagnetic bomb warhead will comprise an electromagnetic device, an electrical energy converter, and an energy storage device to pump and sustain the electromagnetic device charge after separation from the delivery platform. Fusing could be provided by a radar altimeter fuse to airburst the bomb, a barometric fuse, or in GPS/inertially guided bombs, the navigation system. The warhead fraction could be as high as 85%, with most of the usable mass occupied by the electromagnetic device and its supporting hardware.

Due to the potentially large lethal radius of an electromagnetic device, compared to an explosive device of similar mass, standoff delivery would be prudent. While this is an inherent characteristic of weapons such as cruise missiles, potential applications of these devices to glide bombs, anti-shiping missiles, and air-to-air missiles would dictate fire and forget guidance of the appropriate variety, to allow the launching aircraft to gain adequate separation of several miles before warhead detonation.

The recent advent of GPS satellite navigation guidance kits for conventional bombs and glide bombs has provided the optimal means for cheaply delivering such weapons. While GPS-guided weapons without differential GPS enhancements may lack the pinpoint accuracy of laser or television-guided munitions, they are still quite accurate (circular error probable (CEP)/(40 ft)) and importantly cheap, autonomous all-weather weapons, Fig. 4.12.

The USAF has recently deployed the Northrop GAM (GPS-Aided Munitions) on the B-2 bomber [25] and will by the end of the decade deploy the GPS/inertially guided GBU-29/30 JDAM (Joint Direct Attack Munitions) [26] and the AGM-154 JSOW (Joint Stand Off Weapon) [27] glide bomb. Other countries are also developing this technology, the Australian BAeA AGW (Agile Glide Weapon) glide bomb achieving a glide range of about 140 km (75 nmi) when launched from altitude [28].

The importance of glide bombs as delivery means for HPM warheads is threefold. Firstly, the glide bomb can be released from outside effective radius of target air defenses, therefore minimizing the risk to the launch aircraft. Secondly, the large

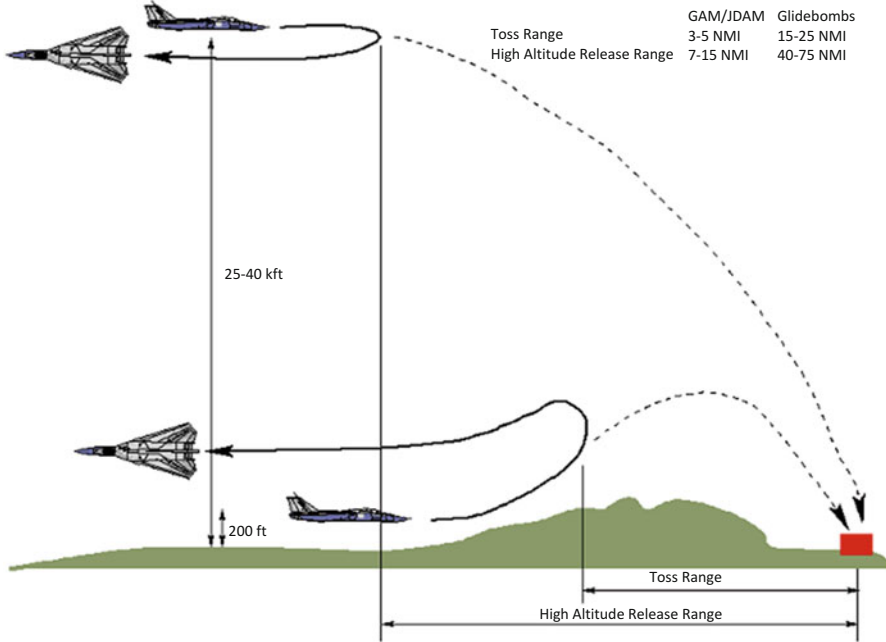


Fig. 4.12 Delivery profiles for GPS/inertial guided weapons

standoff range means that the aircraft can remain well clear of the bomb’s effects. Finally, the bomb’s autopilot may be programmed to shape the terminal trajectory of the weapon, such that a target may be engaged from the most suitable altitude and aspect.

A major advantage of using electromagnetic bombs is that they may be delivered by any tactical aircraft with a nav-attack system capable of delivering GPS-guided munitions. As we can expect GPS-guided munitions to become the standard weapon in use by Western air forces by the end of this decade, every aircraft capable of delivering standard guided munitions also becomes a potential delivery vehicle for an electromagnetic bomb. Should weapon ballistic properties be identical to the standard weapon, no software changes to the aircraft would be required.

Because of the simplicity of electromagnetic bombs in comparison with weapons such as anti-radiation missiles (ARM), it is not unreasonable to expect that these should be both cheaper to manufacture and easier to support in the field, thus allowing for more substantial weapon stocks. In turn, this makes saturation attacks a much more viable proposition.

In this context, it is worth noting that the USAF’s possession of the JDAM capable of F-117A and B-2A will provide the capability to deliver e-bombs against arbitrary high-value targets with virtual impunity. The ability of a B-2A to deliver up to 16 GAM/JDAM fitted e-bomb warheads with a 20 ft. class circular error probable (CEP) would allow a small number of such aircraft to deliver a decisive blow against

key strategic, air defense, and theater targets. A strike and electronic combat-capable derivative of the F-22 would also be a viable delivery platform for an e-bomb/JDAM. With its superb radius, low signature, and supersonic cruise capability an RFB-22 could attack air defense sites, command control communications and intelligence (C³I) sites, airbases, and strategic targets with e-bombs, achieving a significant shock effect. A good case may be argued for the whole F-22 build to be JDAM/e-bomb capable, as this would allow the USAF to apply the maximum concentration of force against arbitrary air and surface targets during the opening phase of an air campaign. See Fig. 4.12.

4.9 Defense Against Electromagnetic Bombs

The most effective defense against electromagnetic bombs is to prevent their delivery by destroying the launch platform or delivery vehicle, as is the case with nuclear weapons. This however may not always be possible, and therefore systems, which can be expected to suffer exposure to the electromagnetic weapon effects, must be electromagnetically hardened.

The most effective method is to wholly contain the equipment in an electrically conductive enclosure, termed as a Faraday cage, which prevents the electromagnetic field from gaining access to the protected equipment. However, most such equipment must communicate with and be fed with power from the outside world, and this can provide entry points via which electrical transients may enter the enclosure and effect damage. While optical fibers address this requirement for transferring data in and out, electrical power feeds remain an ongoing vulnerability. See Fig. 4.13.

Where an electrically conductive channel must enter the enclosure, electromagnetic arresting devices must be fitted. A range of devices exist; however, care must be taken in determining their parameters to ensure that they can deal with the rise time and strength of electrical transients produced by electromagnetic devices. Reports from the United States [8] indicate that hardening measures attuned to the behavior of nuclear EMP bombs do not perform well when dealing with some conventional microwave electromagnetic device designs.

It is significant that hardening of systems must be carried out at a system level, as electromagnetic damage to any single element of a complex system could inhibit the function of the whole system. Hardening new build equipment and systems will add a substantial cost burden. Older equipment and systems may be impossible to harden properly and may require complete replacement. In simple terms, hardening by design is significantly easier than attempting to harden existing equipment.

An interesting aspect of electrical damage to targets is the possibility of wounding semiconductor devices, thereby causing equipment to suffer repetitive intermittent faults rather than complete failures. Such faults would tie down considerable maintenance resources while also diminishing the confidence of the operators in the equipment's reliability. Intermittent faults may not be possible to repair economically, thereby causing equipment in this state to be removed from service

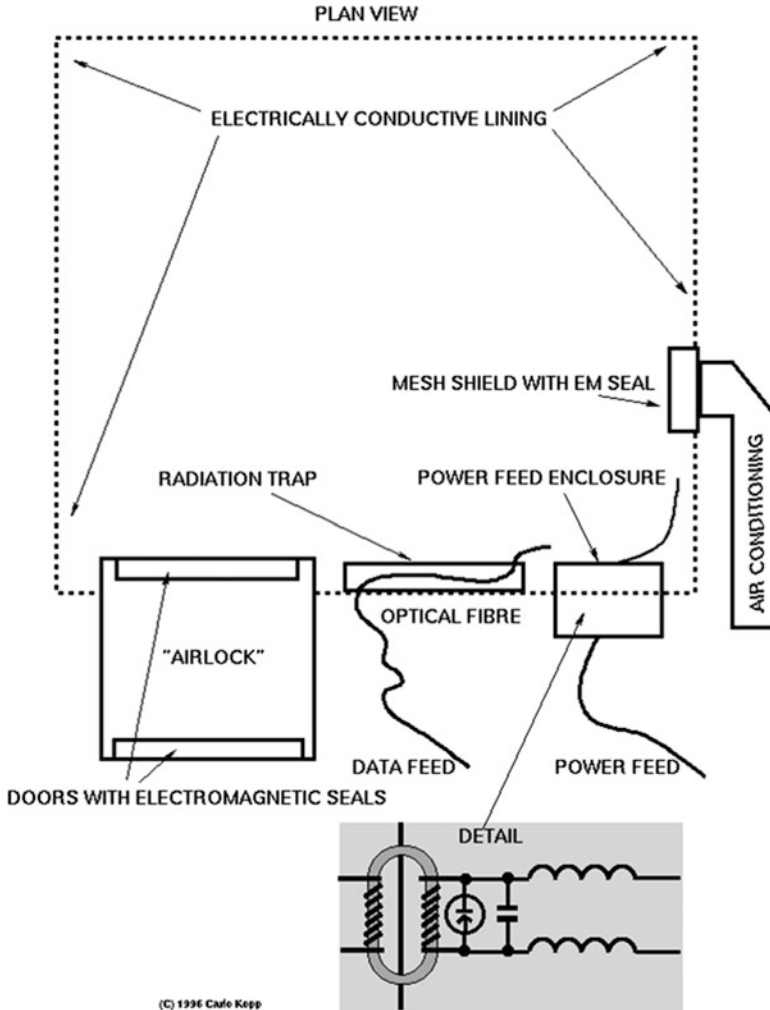


Fig. 4.13 Computer room hardened against EM attack

permanently, with considerable loss in maintenance hours during damage diagnosis. This factor must also be considered when assessing the hardness of equipment against electromagnetic attack, as partial or incomplete hardening may in this fashion cause more difficulties than it would solve. Indeed, shielding which is incomplete may resonate when excited by radiation and thus contribute to damage inflicted upon the equipment contained within it.

Other than hardening against attack, facilities, which are concealed, should not radiate readily detectable emissions. Where radio-frequency communications must be used, low probability of intercept (i.e., spread spectrum) techniques should be

employed exclusively to preclude the use of site emissions for electromagnetic targeting purposes [29]. Appropriate suppression of UE is also mandatory.

Communications networks for voice, data, and services should employ topologies with sufficient redundancy and failover mechanisms to allow operation with multiple nodes and links inoperative. This will deny a user of electromagnetic bombs the option of disabling large portions if not the whole of the network by taking down one or more key nodes or links with a single or small number of attacks.

4.10 Limitations of Electromagnetic Bombs

The limitations of electromagnetic weapons are determined by weapon implementation and means of delivery. Weapon implementation will determine the electromagnetic field strength achievable at a given radius, and its spectral distribution. Means of delivery will constrain the accuracy with which the weapon can be positioned in relation to the intended target. Both constrain lethality.

In the context of targeting military equipment, it must be noted that thermionic technology (i.e., vacuum tube equipment) is substantially more resilient to the electromagnetic weapon effects than solid state (i.e., transistor) technology. Therefore, a weapon optimized to destroy solid-state computers and receivers may cause little or no damage to a thermionic technology device, for instance early 1960s' Soviet military equipment. Therefore, a hard electrical kill may not be achieved against such targets unless a suitable weapon is used.

This underscores another limitation of electromagnetic weapons, which is the difficulty in kill assessment. Radiating targets such as radars or communications equipment may continue to radiate after an attack even though their receivers and data processing systems have been damaged or destroyed. This means that equipment which has been successfully attacked may still appear to operate. Conversely, an opponent may shut down an emitter if attack is imminent and the absence of emissions means that the success or failure of the attack may not be immediately apparent.

Assessing whether an attack on a non-radiating emitter has been successful is more problematic. A good case can be made for developing tools specifically for the purpose of analyzing unintended emissions, not only for targeting purposes, but also for kill assessment.

An important factor in assessing the lethal coverage of an electromagnetic weapon is atmospheric propagation. While the relationship between electromagnetic field strength and distance from the weapon is one of an inverse square law in free space, the decay in lethal effect with increasing distance within the atmosphere will be greater due to quantum physical absorption effects [30]. This is particularly so at higher frequencies and significant absorption peaks due to water vapor and oxygen existing at frequencies above 20 GHz. These will therefore contain the effect of high-power microwave (HPM) weapons to shorter radii than are ideally achievable in the K and L frequency bands.

Means of delivery will limit the lethality of an electromagnetic bomb by introducing limits to the weapon's size and the accuracy of its delivery. Should the delivery error be of the order of the weapon's lethal radius for a given detonation altitude, lethality will be significantly diminished. This is of particular importance when assessing the lethality of unguided electromagnetic bombs, as delivery errors will be more substantial than those experienced with guided weapons such as global positioning satellite (GPS)-guided bombs.

Therefore, accuracy of delivery and achievable lethal radius must be considered against the allowable collateral damage for the chosen target. Where collateral electrical damage is a consideration, accuracy of delivery and lethal radius are key parameters. An inaccurately delivered weapon of large lethal radius may be unusable against a target should the likely collateral electrical damage be beyond acceptable limits. This can be a major issue for users constrained by treaty provisions on collateral damage [31].

4.11 The Proliferation of Electromagnetic Bombs

At the time of writing, the United States (US) and the Commonwealth of Independent States (CIS) are the only two nations with the established technology base and the depth of specific experience to design weapons based upon this technology. However, the relative simplicity of the FCG and the vircator suggests that any nation with even a 1940s' technology base, once in possession of engineering drawings and specifications for such weapons, could manufacture them.

As an example, the fabrication of an effective flux compression generator (FCG) can be accomplished with basic electrical materials, common plastic explosives such as C-4 or Semtex, and readily available machine tools such as lathes and suitable mandrels for forming coils. Disregarding the overheads of design, which do not apply in this context, a two-stage FCG could be fabricated for a cost as low as \$1000–2000, at Western labor rates [8]. This cost could be even lower in a Third World or newly industrialized economy.

While the relative simplicity and thus low cost of such weapons can be considered of benefit to First World nations intending to build viable war stocks or maintain production in wartime, the possibility of less developed nations' mass producing such weapons is alarming. The dependence of modern economies upon their information technology infrastructure makes them highly vulnerable to attack with such weapons, providing that these can be delivered to their targets.

Of major concern is the vulnerability resulting from increasing use of communications and data communications schemes based upon copper cable media. If the copper medium were to be replaced en masse with optical fiber in order to achieve higher bandwidths, the communications infrastructure would become significantly more robust against electromagnetic attack as a result. However, the current trend is to exploit existing distribution media such as cable TV and telephone wiring to provide multiple megabit/s data distribution (e.g., cable modems, ADSL/HDSL/

VDSL) to premises. Moreover, the gradual replacement of coaxial Ethernet networking with 10-Base-T twisted pair equipment has further increased the vulnerability of wiring systems inside buildings. It is not unreasonable to assume that the data and service communications infrastructure in the West will remain a “soft” electromagnetic target in the near future.

At this time no counter-proliferation regimes exist. Should treaties be agreed to limit the proliferation of electromagnetic weapons, they would be virtually impossible to enforce given the common availability of suitable materials and tools.

With the former CIS suffering significant economic difficulties, the possibility of CIS-designed microwave and pulse power technology leaking out to Third World nations or terrorist organizations should not be discounted. The threat of electromagnetic bomb proliferation is very real.

4.12 A Doctrine for the Use of Conventional Electromagnetic Bombs

A fundamental tenet of IW is that complex organizational systems such as governments, industries, and military forces cannot function without the flow of information through their structures. Information flows within these structures in several directions, under typical conditions of function. A trivial model for this function would see commands and directives flowing outward from a central decision-making element, with information about the state of the system flowing in the opposite direction. Real systems are substantially more complex.

This is of military significance because stopping this flow of information will severely debilitate the function of any such system. Stopping the outward flow of information produces paralysis, as commands cannot reach the elements, which are to execute them. Stopping the inward flow of information isolates the decision-making element from reality, and thus severely inhibits its capacity to make rational decisions, which are sensitive to the currency of information at hand.

The recent evolution of strategic (air) warfare indicates a growing trend towards targeting strategies, which exploit this most fundamental vulnerability of any large and organized system [32]. The Desert Storm air war of 1991 is a good instance, with a substantial effort expended against such targets. Indeed, the model used for modern strategic air attack places leadership and its supporting communications in the position of highest targeting priority [33]. No less importantly, modern electronic combat concentrates upon the disruption and destruction of communications and information gathering sensors used to support military operations. Again, the Desert Storm air war provides a good illustration of the application of this method.

A strategy which stresses attack upon the information processing and communications elements of the systems which it is targeting offers a very high payoff, as it will introduce an increasing level of paralysis and disorientation within its target. Electromagnetic bombs are a powerful tool in the implementation of such a strategy.

4.12.1 Electronic Combat Operations Using Electromagnetic Bombs

The central objective of electronic combat (EC) operations is the command of the electromagnetic spectrum, achieved by soft and hard kill means against the opponent's electronic assets. The underlying objective of commanding the electromagnetic spectrum is to interrupt or substantially reduce the flow of information through the opponent's air defense system, air operations environment, and between functional elements of weapon systems.

In this context the ability of electromagnetic bombs to achieve kills against a wide range of target types allows their general application to the task of inflicting attrition upon an opponent's electronic assets, be they specialized air defense assets or more general command-control-communications (C³) and other military assets.

Electromagnetic bombs can be a means of both soft and hard electrical kill, subject to the lethality of the weapon and the hardness of its target. A hard electrical kill by means of an electromagnetic device will be achieved in those instances where such severe electrical damage is achieved against a target to require the replacement of most if not all of its internal electronics.

Electronic combat operations using electromagnetic devices involve the use of these to attack radar, C³, and air defense weapon systems. These should always be attacked initially with an electromagnetic weapon to achieve soft or hard electrical kills, followed up by attack with conventional munitions to preclude possible repair of disabled assets at a later time. As with conventional SEAD operations, the greatest payoff will be achieved by using electromagnetic weapons against systems of strategic importance first, followed in turn by those of operational and tactical importance [34].

In comparison with an anti-radiation missile (ARM)—a missile that homes on the emissions from a threat radar—the established and specialized tool in the conduct of Suppression of Enemy Air Defenses (SEAD) operations, an electromagnetic bomb can achieve kills against multiple targets of diverse types within its lethal footprint. In this respect, an electromagnetic device may be described as a weapon of electrical mass destruction (WEMD). Therefore, electromagnetic weapons are a significant force multiplier in electronic combat operations.

A conventional electronic combat campaign, or intensive electronic combat operations, will initially concentrate on saturating the opponent's electronic defenses, denying information, and inflicting maximum attrition upon electronic assets. The force multiplication offered by electromagnetic weapons vastly reduces the number of air assets required to inflict substantial attrition, and, where proper electronic reconnaissance has been carried out beforehand, also reduces the need for specialized assets such as ARM firing aircraft equipped with costly emitter locating systems.

The massed application of electromagnetic bombs in the opening phase of an electronic battle will allow much faster attainment of command of the

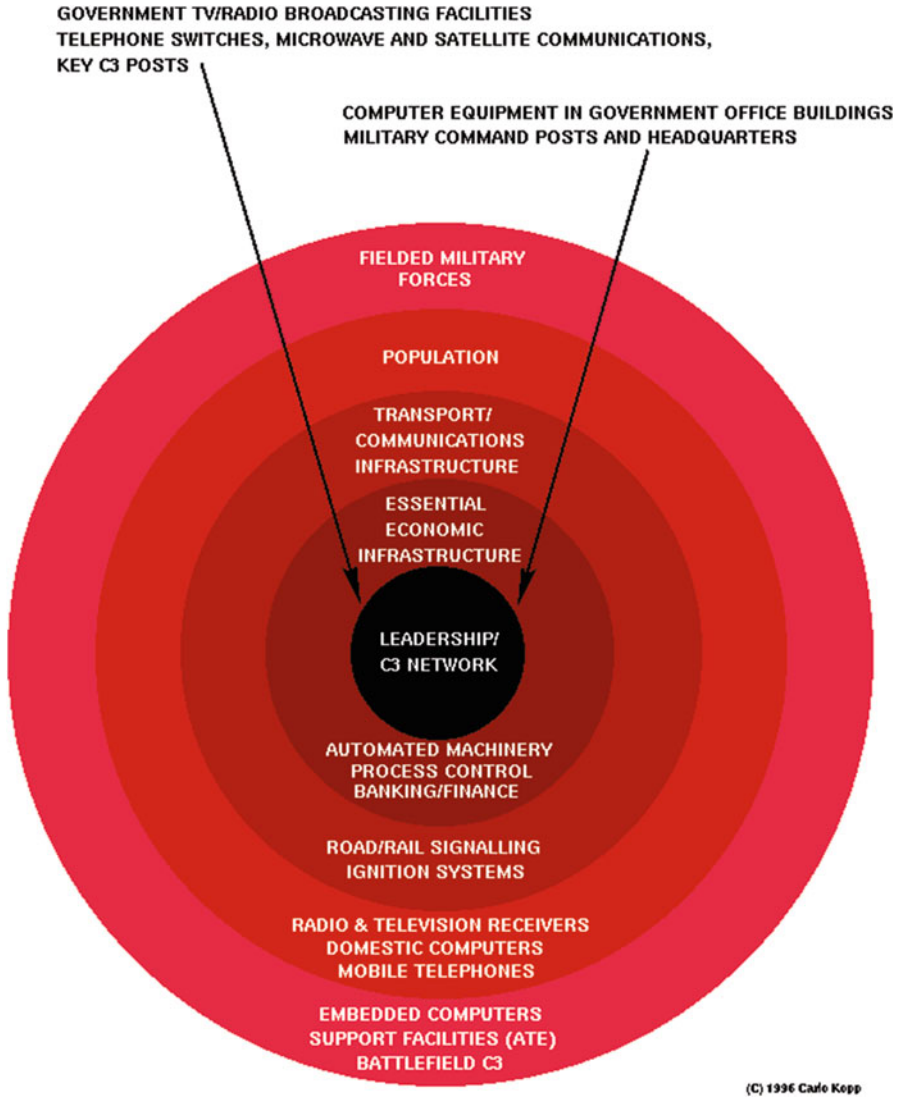


Fig. 4.14 Warden’s “Five Rings” strategic air attack model in the context of electromagnetically vulnerable target Sts

electromagnetic spectrum, as it will inflict attrition upon electronic assets at a much faster rate than possible with conventional means, Fig. 4.14.

While the immaturity of conventional electromagnetic weapons precludes an exact analysis of the scale of force multiplication achievable, it is evident that a single aircraft carrying an electromagnetic bomb capable of concurrently disabling a SAM site with its co-located acquisition radar and supporting radar-directed anti-

aircraft artillery (AAA) weapons will have the potency of the several ARM firing and support jamming aircraft required to accomplish the same result by conventional means. This and the ability of multirole tactical aircraft to perform this task allows for a much greater concentration of force in the opening phase of the battle, for a given force size.

In summary, the massed application of electromagnetic weapons to electronic combat operations will provide for a much faster rate of attrition against hostile electronic assets, achievable with a significantly reduced number of specialized and multirole air assets [12]. This will allow even a modestly sized force to apply overwhelming pressure in the initial phase of an electronic battle, and therefore achieve command of the electromagnetic spectrum in a significantly shorter time than by conventional means.

4.12.2 Strategic Air Attack Operations Using Electromagnetic Bombs

The modern approach to strategic air warfare reflects in many respects aspects of the IW model, in that much effort is expended in disabling an opponent's fundamental information processing infrastructure. Since we however are yet to see a systematic IW doctrine which has been tested in combat, this chapter approaches the subject from a more conservative viewpoint and uses established strategic doctrine.

Modern strategic air attack theory is based upon Warden's Five Rings model [33], which identifies five centers of gravity in a nation's war fighting capability. In descending order of importance, these are the nation's leadership and supporting C³ system, its essential economic infrastructure, its transportation network, its population, and its fielded military forces.

Electromagnetic weapons may be productively used against all elements in this model and provide a particularly high payoff when applied against a highly industrialized and geographically concentrated opponent. Of particular importance in the context of strategic air attack is that while electromagnetic weapons are lethal to electronics, they have little if any effect on humans. This is a characteristic which is not shared with established conventional and nuclear weapons.

This selectivity in lethal effect makes electromagnetic weapons far more readily applicable to a strategic air attack campaign and reduces the internal political pressure which is experienced by the leadership of any democracy which must commit to warfare. An opponent may be rendered militarily, politically, and economically ineffective with little if any loss in human life.

The innermost ring in the Warden model essentially comprises government bureaucracies and civilian and military C³ systems. In any modern nation these are heavily dependent upon the use of computer equipment and communications equipment. What is of key importance at this time is an ongoing change in the structure of computing facilities used in such applications, as these are becoming increasingly

decentralized. A modern office environment relies upon a large number of small computers, networked to interchange information, in which respect it differs from the traditional model of using a small number of powerful central machines.

This decentralization and networking of information technology systems produce a major vulnerability to electromagnetic attack. Whereas a small number of larger computers could be defended against electromagnetic attack by the use of electromagnetic hardened computer rooms, a large distributed network cannot. Moreover, unless optical fiber networking is used, the networking cables are themselves a medium via which electromagnetic effects can be efficiently propagated throughout the network, to destroy machines. While the use of distributed computer networks reduces vulnerability to attack by conventional munitions, it increases vulnerability to attack by electromagnetic weapons.

Selective targeting of government buildings with electromagnetic weapons will result in a substantial reduction in a government's ability to handle and process information. The damage inflicted upon information records may be permanent, should inappropriate backup strategies have been used to protect stored data. It is reasonable to expect that most data stored on machines which are affected will perish with the host machine or become extremely difficult to recover from damaged storage devices.

The cost of hardening existing computer networks is prohibitive, as is the cost of replacement with hardened equipment. While the use of hardened equipment for critical tasks would provide some measure of resilience, the required discipline in the handling of information required to implement such a scheme renders its utility outside of military organizations questionable. Therefore, the use of electromagnetic weapons against government facilities offers an exceptionally high payoff.

Other targets which fall into the innermost ring may also be profitably attacked. Satellite link and importantly control facilities are vital means of communication as well as the primary interface to military and commercial reconnaissance satellites. Television and radio broadcasting stations, one of the most powerful tools of any government, are also vulnerable to electromagnetic attack due to the very high concentration of electronic equipment in such sites. Telephone exchanges, particularly later generation digital switching systems, are also highly vulnerable to appropriate electromagnetic attack.

In summary the use of electromagnetic weapons against leadership and C³ targets is highly profitable, in that a modest number of weapons appropriately used can introduce the sought state of strategic paralysis, without the substantial costs incurred by the use of conventional munitions to achieve the same effect.

Essential economic infrastructure is also vulnerable to electromagnetic attack. The finance industry and stock markets are almost wholly dependent upon computers and their supporting communications. Manufacturing, chemical, petroleum product industries, and metallurgical industries rely heavily upon automation which is almost universally implemented with electronic programmable logic controller (PLC) systems or digital computers. Furthermore, most sensors and telemetry devices used are electrical or electronic.

Attacking such economic targets with electromagnetic weapons will halt operations for the time required to either repair the destroyed equipment or reconfigure for manual operation. Some production processes however require automated operation, either because hazardous conditions prevent human intervention or because the complexity of the control process required cannot be carried out by a human operator in real time. A good instance is larger chemical, petrochemical, and oil/gas production facilities. Destroying automated control facilities will therefore result in substantial loss of production, causing shortages of these vital materials.

Manufacturing industries which rely heavily upon robotic and semiautomatic machinery, such as the electronics, computer, and electrical industry, precision machine industry, and aerospace industries, are all key assets in supporting a military capability. They are all highly vulnerable to electromagnetic attack. While material processing industries may in some instances be capable of functioning with manual process control, the manufacturing industries are almost wholly dependent upon their automated machines to achieve any useful production output.

Historical experience³ suggests that manufacturing industries are highly resilient to air attack as production machinery is inherently mechanically robust and thus a very high blast overpressure is required to destroy it. The proliferation of electronic and computer-controlled machinery has produced a major vulnerability, for which historical precedent does not exist. Therefore, it will be necessary to reevaluate this orthodoxy in targeting strategy.

The finance industry and stock markets are a special case in this context, as the destruction of their electronic infrastructure can yield, unlike manufacturing industries, much faster economic dislocation. This can in turn produce large systemic effects across a whole economy, including elements which are not vulnerable to direct electromagnetic attack. This may be of particular relevance when dealing with an opponent which does not have a large and thus vulnerable manufacturing economy. Nations which rely on agriculture, mining, or trade for a large proportion of their gross domestic product are prime candidates for electromagnetic attack on their finance industry and stock markets. Since the latter are usually geographically concentrated and typically electromagnetically “soft” targets, they are highly vulnerable.

In summary there is a large payoff in striking at economic essentials with electromagnetic weapons, particularly in the opening phase of a strategic air attack campaign, as economic activity may be halted or reduced with modest expenditure of the attacker’s resources. An important caveat is that centers of gravity within the target economy must be properly identified and prioritized for strikes to ensure that maximum effect is achieved as quickly as possible.

³The classical argument here is centered upon Allied experience in bombing Germany during WW2, where even repeated raids on industrial targets were unable to wholly stop production, and in many instances only served to reduce the rate of increase in production. What must not be overlooked is that both the accuracy and lethality of weapons in this period bore little comparison to what is available today, and automation of production facilities was almost nonexistent.

Transport infrastructure is the third ring in the Warden model, and also offers some useful opportunities for the application of electromagnetic weapons. Unlike the innermost rings, the concentration of electronic and computer equipment is typically much lower, and therefore considerable care must be taken in the selection of targets.

Railway and road signaling systems, where automated, are most vulnerable to electromagnetic attack on their control centers. This could be used to produce traffic congestion by preventing the proper scheduling of rail traffic, and disabling road traffic signaling, although the latter may not yield particularly useful results.

Significantly, most modern automobiles and trucks use electronic ignition systems which are known to be vulnerable to electromagnetic weapon effects, although opportunities to find such concentrations so as to allow the profitable use of an electromagnetic bomb may be scarce.

The population of the target nation is the fourth ring in the Warden model, and its morale is the object of attack. The morale of the population will be affected significantly by the quality and quantity of the government propaganda it is subjected to, as will it be affected by living conditions.

Using electromagnetic weapons against urban areas provides the opportunity to prevent government propaganda from reaching the population via means of mass media, through the damaging or destruction of all television and radio receivers within the footprint of the weapon. Whether this is necessary, given that broadcast facilities may have already been destroyed, is open to discussion. Arguably it may be counterproductive, as it will prevent the target population from being subjected to friendly means of psychological warfare such as propaganda broadcasts.

The use of electromagnetic weapons against a target population is therefore an area which requires careful consideration in the context of the overall IW campaign strategy. If useful objectives can be achieved by isolating the population from government propaganda, then the population is a valid target for electromagnetic attack. Forces constrained by treaty obligations will have to reconcile this against the applicable regulations relating to denial of services to noncombatants [31].

The outermost and last ring in the Warden model is the fielded military forces. These are by all means a target vulnerable to electromagnetic attack, and C^3 nodes, fixed support bases, as well as deployed forces should be attacked with electromagnetic devices. Fixed support bases which carry out depot-level maintenance on military equipment offer a substantial payoff, as the concentration of computers in both automatic test equipment and administrative and logistic support functions offers a good return per expended weapon.

Any site where more complex military equipment is concentrated should be attacked with electromagnetic weapons to render the equipment unserviceable and hence reduce the fighting capability, and where possible also mobility of the targeted force. As discussed earlier in the context of electronic combat, the ability of an electromagnetic weapon to achieve hard electrical kills against any non-hardened targets within its lethal footprint suggests that some target sites may only require electromagnetic attack to render them both undefended and nonoperational. Whether

to expend conventional munitions on targets in this state would depend on the immediate military situation.

In summary the use of electromagnetic weapons in strategic air attack campaign offers a potentially high payoff, particularly when applied to leadership, C³, and vital economic targets, all of which may be deprived of much of their function for substantial periods of time. The massed application of electromagnetic weapons in the opening phase of the campaign would introduce paralysis within the government, deprived of much of its information processing infrastructure, as well as paralysis in most vital industries. This would greatly reduce the capability of the target nation to conduct military operations of any substantial intensity.

Because conventional electromagnetic weapons produce negligible collateral damage, in comparison with conventional explosive munitions, they allow the conduct of an effective and high-tempo campaign without the loss of life which is typical of conventional campaigns. This will make the option of a strategic bombing campaign more attractive to a Western democracy, where mass media coverage of the results of conventional strategic strike operations will adversely affect domestic civilian morale.

The long-term effects of a sustained and concentrated strategic bombing campaign using a combination of conventional and electromagnetic weapons will be important. The cost of computer and communications infrastructure is substantial, and its massed destruction would be a major economic burden for any industrialized nation. In addition, it is likely that poor protection of stored data will add to further economic losses, as much data will be lost with the destroyed machines.

From the perspective of conducting an IW campaign, this method of attack achieves many of the central objectives sought. Importantly, the massed application of electromagnetic weapons would inflict attrition on an opponent's information processing infrastructure very rapidly, and this would arguably add a further psychological dimension to the potency of the attack. Unlike the classical IW model of Gibsonian CyberWar, in which the opponent can arguably isolate his infrastructure from hostile penetration, parallel or hyperwar-style massed attack with electromagnetic bombs will be extremely difficult to defend against.

4.12.3 Offensive Counter Air (OCA) Operations Using Electromagnetic Bombs

Electromagnetic bombs may be usefully applied to offensive counter air (OCA) operations. Modern aircraft are densely packed with electronics, and unless properly hardened are highly vulnerable targets for electromagnetic weapons.

The cost of the onboard electronics represents a substantial fraction of the total cost of a modern military aircraft, and therefore stock levels of spares will in most instances be limited to what is deemed necessary to cover operational usage at some

nominal sortie rate. Therefore, electromagnetic damage could render aircraft unusable for substantial periods of time.

Attacking airfields with electromagnetic weapons will disable communications, air traffic control facilities, navigational aids, and operational support equipment, if these items are not suitably electromagnetic hardened. Conventional blast-hardening measures will not be effective, as electrical power and fixed communications cabling will carry electromagnetic induced transients into most buildings. Hardened aircraft shelters may provide some measure of protection due to electrically conductive reinforcement embedded in the concrete, but conventional revetments will not.

Therefore, OCA operations against airfields and aircraft on the ground should include the use of electromagnetic weapons as they offer the potential to substantially reduce hostile sortie rates.

4.12.4 Maritime Air Operations Using Electromagnetic Bombs

As with modern military aircraft, naval surface combatants are fitted with a substantial volume of electronic equipment, performing similar functions in detecting and engaging targets and warning of attack. As such they are vulnerable to electromagnetic attack, if not suitably hardened. Should they be hardened, volumetric, weight, and cost penalties will be incurred.

Conventional methods for attacking surface combatants involve the use of saturation attacks by anti-ship missiles or coordinated attacks using a combination of ARMs and anti-ship missiles. The latter instance is where disabling the target electronically by stripping its antennae precedes lethal attack with specialized anti-ship weapons.

An electromagnetic warhead detonated within lethal radius of a surface combatant will render its air defense system inoperable, as well as damaging other electronic equipment such as electronic countermeasures, electronic support measures, and communications. This leaves the vessel undefended until these systems can be restored, which may or may not be possible on the high seas. Therefore, launching an electromagnetic glide bomb on to a surface combatant, and then reducing it with laser- or television-guided weapons, is an alternate strategy for dealing with such targets.

4.12.5 Battlefield Air Interdiction Operations Using Electromagnetic Bombs

Modern land warfare doctrine emphasizes mobility, and maneuver warfare methods are typical for contemporary land warfare. Coordination and control are essential to

the successful conduct of maneuver operations, and this provides another opportunity to apply electromagnetic weapons. Communications and command sites are key elements in the structure of such a land army, and these concentrate communications and computer equipment. Therefore, they should be attacked with electromagnetic weapons, to disrupt the command and control of land operations.

Should concentrations of armored vehicles be found, these are also profitable targets for electromagnetic attack, as their communications and fire control systems may be substantially damaged or disabled as a result. A useful tactic would be initial attack with electromagnetic weapons to create a maximum of confusion, followed by attack with conventional weapons to take advantage of the immediate situation.

4.12.6 Defensive Counter Air, Air Defense Operation, and Electromagnetic Warhead

Providing that compact electromagnetic warheads can be built with useful lethality performance, a number of other potential applications become viable. One is to equip an air-air missile (AAM) with such a warhead. A weapon with data link midcourse guidance, such as the AIM-120, could be used to break up inbound raids by causing soft or hard electrical kills in a formation (raid) of hostile aircraft. Should this be achieved, the defending fighter will have the advantage in any following engagement as the hostile aircraft may not be fully mission capable. Loss of air intercept or navigation attack radar, EW equipment, mission computers, digital engine controls, communications, and electronic flight controls, where fitted, could render the victim aircraft defenseless against attack with conventional missiles. This is part of the task of defensive counter air (DCA) and defense operations utilizing the electromagnetic warheads.

This paradigm may also be applied to air defense operations using area defense SAMs. Large SAMs such as the MIM-104 Patriot, RIM-66E/M and RIM-67A Standard, 5V55/48N6 (SA-10), and 9M82/9M83 (SA-12) could accommodate an electromagnetic warhead comparable in size to a bomb warhead. A SAM site subjected to jamming by inbound bombers could launch a first round under data link control with an electromagnetic warhead to disable the bombers, and then follow with conventional rounds against targets which may not be able to defend themselves electronically. This has obvious implications for the electromagnetic hardness of combat aircraft systems.

4.12.7 A Strategy of Graduated Response

The introduction of nonnuclear electromagnetic bombs into the arsenal of a modern air force considerably broadens the options for conducting strategic campaigns.

Clearly such weapons are potent force multipliers in conducting a conventional war, particularly when applied to electronic combat, OCA, and strategic air attack operations.

The massed use of such weapons would provide a decisive advantage to any nation with the capability to effectively target and deliver them. The qualitative advantage in capability so gained would provide a significant advantage even against a much stronger opponent not in the possession of this capability.

Electromagnetic weapons however open up less conventional alternatives for the conduct of a strategic campaign, which derive from their ability to inflict significant material damage without inflicting visible collateral damage and loss of life. Western governments have been traditionally reluctant to commit to strategic campaigns, as the expectation of a lengthy and costly battle, with mass media coverage of its highly visible results, will quickly produce domestic political pressure to cease the conflict.

An alternative is a strategy of graduated response (SGR). In this strategy, an opponent who threatens escalation to a full-scale war is preemptively attacked with electromagnetic weapons, to gain command of the electromagnetic spectrum and command of the air. Selective attacks with electromagnetic weapons may then be applied against chosen strategic targets, to force concession. Should these fail to produce results, more targets may be disabled by electromagnetic attack. Escalation would be sustained and graduated, to produce steadily increasing pressure to concede the dispute. Air and sea blockade are complementary means via which pressure may be applied.

Because electromagnetic weapons can cause damage on a large scale very quickly, the rate at which damage can be inflicted can be very rapid, in which respect such a campaign will differ from the conventional, where the rate at which damage is inflicted is limited by the usable sortie rate of strategic air attack-capable assets.⁴

Should blockade and the total disabling of vital economic assets fail to yield results, these may then be systematically reduced by conventional weapons, to further escalate the pressure. Finally, a full-scale conventional strategic air attack campaign would follow, to wholly destroy the hostile nation's war fighting capability.

Another situation where electromagnetic bombs may find useful application is in dealing with governments which actively implement a policy of state-sponsored terrorism or info-terrorism, or alternately choose to conduct a sustained low-intensity land warfare campaign. Again, the strategy of graduated response, using

⁴This constraint primarily results from limitations in numbers. Strategic air attack requires precision delivery of substantial payloads and is thus most effectively performed with specialized bomber assets, such as the B-52, B-1, B-2, F-111, F-15E, F-117A, Tornado, or Su-24. These are typically more maintenance intensive than less complex multirole fighters, and this will become a constraint to the sortie rate achievable with a finite number of aircraft, assuming the availability of aircrew. While multirole fighters may be applied to strategic air attack, their typically lesser payload radius performance and lesser accuracy will reduce their effectiveness. In the doctrinal context, this can be directly related to existing USAF aerospace doctrine [35], in several areas.

electromagnetic bombs in the initial phases, would place the government under significant pressure to concede.

Importantly, high-value targets such as R&D and production sites for weapons of mass destruction (nuclear, biological, chemical) and many vital economic sites, such as petrochemical production facilities, are critically dependent upon high-technology electronic equipment. The proliferation of WMD into developing nations has been greatly assisted by the availability of high-quality test and measurement equipment commercially available from First World nations, as well as modern electronic process control equipment. Selectively destroying such equipment can not only paralyze R&D effort, but also significantly impair revenue-generating production effort. A Middle Eastern nation sponsoring terrorism will use oil revenue to support such activity. Crippling its primary source of revenue without widespread environmental pollution may be an effective and politically acceptable punitive measure.

As a punitive weapon electromagnetic device is attractive for dealing with belligerent governments. Substantial economic, military, and political damage may be inflicted with a modest commitment of resources by their users, and without politically damaging loss of life.

4.13 Conclusions

Electromagnetic bombs are weapons of electrical mass destruction with applications across a broad spectrum of targets, spanning both the strategic and tactical. As such their use offers a very high payoff in attacking the fundamental information processing and communication facilities of a target system. The massed application of these weapons will produce substantial paralysis in any target system, thus providing a decisive advantage in the conduct of electronic combat, offensive counter air, and strategic air attack.

Because e-bombs can cause hard electrical kills over larger areas than conventional explosive weapons of similar mass, they offer substantial economies in force size for a given level of inflicted damage and are thus a potent force multiplier for appropriate target sets.

The nonlethal nature of electromagnetic weapons makes their use far less politically damaging than that of conventional munitions, and therefore broadens the range of military options available.

This chapter has included a discussion of the technical, operational, and targeting aspects of using such weapons, as no historical experience exists as yet upon which to build a doctrinal model. The immaturity of this weapon technology limits the scope of this discussion, and many potential areas of application have intentionally not been discussed. The ongoing technological evolution of this family of weapons will clarify the relationship between weapon size and lethality, thus producing further applications and areas for study.

E-bombs can be an affordable force multiplier for military forces which are under post-Cold War pressures to reduce force sizes, increasing both their combat potential

and political utility in resolving disputes. Given the potentially high payoff deriving from the use of these devices, it is incumbent upon such military forces to appreciate both the offensive and defensive implications of this technology. It is also incumbent upon governments and private industry to consider the implications of the proliferation of this technology and take measures to safeguard their vital assets from possible future attack. Those who choose not to may become losers in any future wars.

Acknowledgements Thanks to Dr. D.H. Steven for his insightful comment on microwave coupling and propagation, and to Professor C.S. Wallace, Dr. Ronald Pose, and Dr. Peter Leigh-Jones for their most helpful critique of the drafts. Thanks also to the RAAF Air Power Studies Centre and its then Director, Group Captain Gary Waters, for encouraging the author to investigate this subject in 1993. Some material in this paper is derived from RAAF APSC Working Paper, “A Doctrine for the Use of Electromagnetic Pulse Bombs,” published in 1993 [36], and is posted with permission.

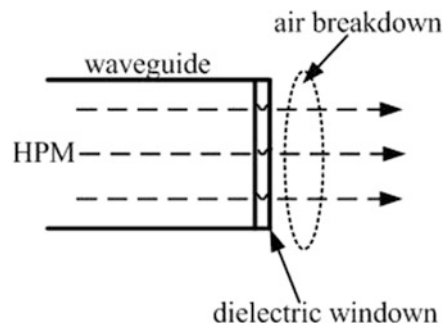
An earlier version of this chapter was presented at InfoWarCon V and first published in “Information Warfare—Cyberterrorism: Protecting Your Personal Security In the Electronic Age,” 1996, Thunder’s Mouth Press, 632 Broadway 7th FL, New York, NY, ISBN: 1-56025-132-8, <http://www.infowar.com>, posted with permission.

Breakdown in Air Produced by High-Power Microwaves

As a comment by the author of this book (i.e., Zohuri), readers should pay attention to very important drawback of high-power microwave when gets transmitted through the air and that is the phenomena of “breakdown in air” [5] and for more details readers should refer to the Appendix A of this book.

The air breakdown driven by the high-power microwave radiated from the circular waveguide is investigated using the 2-D fluid model. We focus on the case of the air pressure higher than 100 torr, and therefore neglect the electron diffusion loss to the wall in the fluid model. A proper numerical scheme for the finite-difference time-domain method is developed to solve the fluid model. See Fig. 4.15.

Fig. 4.15 Schematic of high-power microwave (HPM)



The results show that the air breakdown mainly occurs near the dielectric window due to the high electric field, and the generated nonuniform plasma causes significant attenuation in the radiated field. The wave reflection by the air plasma, far larger than the plasma absorption, attenuates the transmitted power significantly at low pressures, while at high pressures the plasma absorption plays a major role in the transmitted power loss. The accuracy of the fluid model is validated by comparing with the reported experimental results [1].

The high-power microwave (HPM) has important applications in many fields, such as heating and current drive of plasmas in tokamaks, radio-frequency acceleration in high-energy linear colliders, and radar and communication systems as well as directed energy weapons [2]. If the amplitude of the HPM is higher than the air breakdown threshold, then the HPM radiation and propagation are strongly affected due to the space-time-dependent plasma generated in the air breakdown. Therefore, it is very important to study and understand the air breakdown driven by the HPM.

A lot of work, both theoretically and experimentally, has been done to study the air breakdown driven by the HPM. It was found that the generated plasma in the air breakdown resulted in significant attenuation in the tail of the HPM pulse [3]. The empirical expressions for the ionization and collision frequency are employed in [4] to estimate the breakdown threshold and time. The fluid model with the effective diffusion coefficient is proposed in [4] to reproduce well the plasma structure observed experimentally in.

References

1. E. Schamiloglu, High power microwave sources and applications. IEEE MTT-S Int. Microw. Symp. Dig. **2**, 1001–1004 (2004)
2. P. Zhao, J. Feng, C. Liao, Breakdown in air produced by high power microwaves. IEEE Trans. Plasma. Sci. **42**, 6 (2014)
3. J.H. Yee, R.A. Alvarez, D.J. Mayhall, D.P. Byrne, J. Degroot, Theory of intense electromagnetic pulse propagation through the atmosphere. Phys. Fluids **29**(4), 1238–1244 (1986)
4. M. Löfgren, D. Anderson, M. Lisak, L. Lundgren, Breakdown induced distortion of high power microwave pulses in air. Phys. Fluids B Plasma Phys. **3**(12), 3528–3531 (1991)
5. J.P. Boeuf, B. Chaudhury, G.Q. Zhu, Theory and modeling of self-organization and propagation of filamentary plasma arrays in microwave breakdown at atmospheric pressure. Phys. Rev. Lett. **104**(1), 015002 (Jan. 2010)
6. C.M. Fowler, W.B. Garn, R.S. Caird, Production of very high magnetic fields by implosion. J. Appl. Phys. **31**(3), 588–594 (1960)
7. The EMP - A Triangular Impulse, 2.29, *A Handbook Series on Electromagnetic Interference and Compatibility* (Don White Consultants, Maryland, 1978)
8. R.E. Reinovsky, P.S. Levi, J.M. Welby, *An Economical, 2 Stage Flux Compression Generator System, Digest of Technical Papers, 5th IEEE Pulsed Power Conference* (IEEE, New York, 1985), p. 216
9. R.S. Caird et al., *Tests of an Explosive Driven Coaxial Generator, Digest of Technical Papers, 5th IEEE Pulsed Power Conference*, vol 220 (IEEE, New York, 1985)
10. C.M. Fowler, R.S. Caird, *The Mark IX Generator, Digest of Technical Papers, Seventh IEEE Pulsed Power Conference, 475* (IEEE, New York, 1989)

11. High Energy Microwave Laboratory, *Fact Sheet, USAF AFMC* (Phillips Laboratory, Kirtland AFB, 1994)
12. B.A. Fanthome, *MHD Pulsed Power Generation, Digest of Technical Papers, 7th IEEE Pulsed Power Conference* (IEEE, New York, 1989), p. 483
13. J. Flanagan, *High-Performance MHD Solid Gas Generator*, Naval Research Lab, Patent Application 4269637 (1981)
14. V.L. Granatstein, I. Alexeff, *High Power Microwave Sources* (Artech House, Boston, London, 1987)
15. R.F. Heoberling, M.V. Fazio, Advances in virtual cathode microwave sources. *IEEE Trans. Electromagn. Compat.* **34**(3), 252 (1992)
16. L.E. Thode, *Virtual-Cathode Microwave Device Research: Experiment and Simulation, Chapter 14 in High Power Microwave Sources* (1987)
17. C.D. Taylor, C.W. Harrison, On the coupling of microwave radiation to wire structures. *IEEE Trans. Electromagn. Compat.* **34**(3), 183 (1992)
18. Motorola RF, *Device Data* (Motorola Semiconductor Products Inc, Arizona, 1983)
19. Micron DRAM, *Data Book* (Micron Technology Inc, Idaho, 1992)
20. *CMOS Databook*, (National Semiconductor Corporation, Santa Clara, 1978)
21. NPI Local Area Network Products, *SMD Transformers* (Nano Pulse Industries, Brea, 1993)
22. J.D. Kraus, *Antennas*, 2nd edn. (McGraw-Hill, New York, 1988)
23. D. Herskowitz, The other SIGINT/ELINT. *J. Electron. Def.* (1996)
24. W. Van Eck, Electromagnetic radiation from video display units: An eavesdropping risk. *Comp. Sec.*, 269 (1985)
25. *B-2 Precision Weapons, unclassified briefing*, (Northrop-Grumman Corporation, 1995), unpublished material
26. Joint Direct Attack Munition (JDAM), *Unclassified Briefing* (McDonnell Douglas Corporation, 1995), Unpublished material
27. R. Pergler, *Joint Standoff Weapon System (JSOW), unclassified briefing* (Texas Instruments, Inc, Dallas, 1994). unpublished material
28. C. Kopp, *Australia's Kerkanya Based Agile Gliding Weapon* (Australian Aviation, Aerospace Publications, Canberra, 1996), p. 28
29. R.C. Dixon, *Spread Spectrum Systems* (John Wiley and Sons, New York, 1984)
30. See International Countermeasures Handbook, 14th Edition, p. 104
31. RAAF, DI(AF) AAP1003, *Ch. 8 The Law of Aerial Targeting, Operations Law for RAAF Commanders*, 1st edn. (RAAF APSC, Canberra, 1994)
32. G. Waters, *Gulf Lesson One*. Chapter 16 of this reference provides a good discussion of both the rationale and implementation of this strategy
33. J.A. Warden III, Col USAF, air theory for the twenty-first century, chapter 4, in *Battlefield of the Future, 21st Century Warfare Issues*, ed. by B. R. Schneider, L. E. Grinter, (Air University Press, Maxwell AFB, Alabama, 1995)
34. C. Kopp, *Command of the Electromagnetic Spectrum - An Electronic Combat Doctrine for the RAAF, Working Paper No. 8, Air Power Studies Centre* (Royal Australian Air Force, Canberra, 1992)
35. AFM1-1, *Basic Aerospace Doctrine of the United States Air Force*, Air Force Manual 1-1, vol. 1, March 1992
36. C. Kopp, *A Doctrine for the Use of Electromagnetic Pulse Bombs, Working Paper No. 15* (Air Power Studies Centre, Royal Australian Air Force, Canberra, 1993)

Chapter 5

Particle Beam Energy as Weapon



It is not that the generals and admirals are incompetent, but that the task has passed beyond their competence. Their limitations are due not to a congenital stupidity—as a disillusioned public is so apt to assume—but to the growth of science.

Dr. Richard M. Roberds (http://markfoster.net/struc/particle_beam_weapon.pdf).

5.1 Introduction

Considerable debate has been stirred by President Reagan's recent suggestion that the United States embark on a program that would use advanced-technology weaponry to produce an effective defense against Soviet ICBMS. On the one hand, critics argue that the idea of a defensive system that would neutralize the ICBM threat is naive and, at best, would require large expenditures in the development of a very-“high-risk” technology. Furthermore, they suggest that even if such a system could be developed, it would be too costly and would also be vulnerable to simple and cheap countermeasures. On the other hand, others argue that we *must* continue to explore such high-technology options until they have been either proved scientifically unachievable or developed into effective systems. If it were possible to build and effectively deploy such weapons, the payoff in terms of national security would be tremendous. In addition, certainly, if this weaponry is achievable, it must be the United States, not the Soviet Union, that first develops it.

The advanced technology that has raised the possibility of defeating an ICBM attack is referred to collectively as directed energy weapons, which gain their unprecedented lethality from several fundamental characteristics. Among their more important features are their ability to fire their “bullets” at or near the speed of light (186,000 miles a second), which would effectively freeze even high-speed targets in their motion; their ability to redirect their fire towards multiple targets very rapidly; their very long range (thousands of kilometers in space); and their ability to

transmit lethal doses of energy in seconds or even a fraction of a second. No conventional ammunition is required; only fuel for the power generator is needed.

There are three principal forms of directed energy weapons: the directed microwave energy weapon, the high-energy laser, and the particle beam. Only the last two types have received substantial government support.

Much has been written on the high-energy laser (HEL), and this category of directed energy weapon appears to be well understood by members of the defense community. Laser weapons have been under active development for 20 years and easily constitute the most advanced of the directed energy devices.

In contrast, the particle beam weapon (PBW) has been the “sleeping” among directed energy weapons until very recently. Enshrouded in secrecy, it began as a project sponsored by the Advanced Research Projects Agency (now called Defense Advanced Research Projects Agency better known as (DARPA)) as early as 1958, 2 years before the first scientific laser demonstration in 1960. Code-named Seesaw, the project was designed to study the possible use of particle beams for ballistic missile defense. Today while its development lags that of the high-energy laser, the particle beam weapon is viewed by some military technicians as the follow-on weapon to the laser, because of its higher potential lethality.

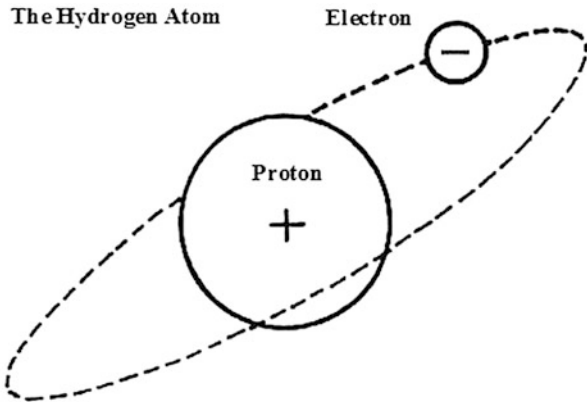
The successful development of a particle beam weapon would require significant technology gains across several difficult areas. However, even though the technical understanding to support the full-scale development of a PBW will not be available for several years, the technology issues that pace its development are not difficult to understand. The purpose of this chapter is to provide a basis for understanding the fundamental technology connected with particle beam weapon, with the hope of assisting DOD leaders and other members of the defense community in making sound decision about the development and possible deployment of PBWs in the days ahead.

5.2 What Is a Particle Beam Weapon?

The characteristic that distinguishes the particle beam weapon from other directed energy weapons is the form of energy it propagates. While there are several operating concepts for particle beam weapons, all such devices generate their destructive power by accelerating sufficient quantities of subatomic particles or atoms to velocities near the speed of light and focusing these particles into a very-high-energy beam. The total energy within the beam is the aggregate energy of the rapidly moving particles, each particle having kinetic energy due to its own mass and motion.

Currently, the particles being used to form the beam are electrons, protons, or hydrogen atoms. Each of these particles can be illustrated through a schematic of the hydrogen atom, the smallest and simplest of all atoms (see Fig. 5.1). The nucleus of the hydrogen atom is a proton, which weighs some 2000 times as much as the electron that orbits the single-proton nucleus. Each proton has an electric charge of a

Fig. 5.1 The hydrogen atom



positive one, while each electron carries a charge of a negative one. In the case of hydrogen, the single electron and proton combine to form a neutrally charged atom.

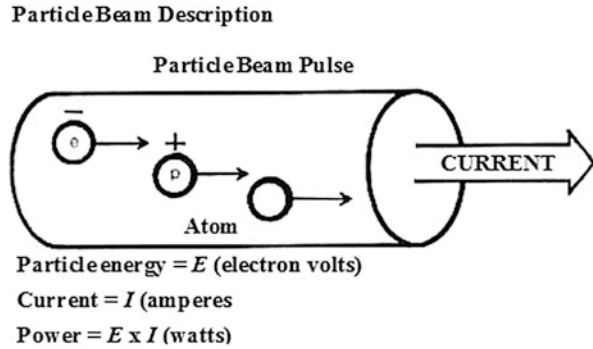
In Fig. 5.1, the hydrogen atom consists of a proton or positive charge, orbited by an electron of equal but opposite or negative charge. Together, they form a neutrally charged atom, which can serve as the “bullet” of a particle beam weapon in space. Also, the proton and the electron themselves are both viable candidates as the ammunition for an endoatmospheric weapon.

The particle beam itself is analogous to a natural phenomenon with which we are all familiar—the lightning bolt. The analogy is so close that particle beam pulses are referred to as “bolts.” The particles in a lightning bolt are electrons (an electric current) flowing from a negatively charged cloud to a positively charged cloud or section of the earth. While the electric field in lightning that accelerates the electrons is typically 500,000 volts per meter, these electron velocities are still less than that desired in a particle beam weapon. But the number of electrons (electric current) in the lightning bolt is nominally much greater. In any case, the phenomenon and its destructive results are very much the same.

Neither the proton nor the electron shows any conclusive advantage over the other in their use as the appropriate “ammunition” of a PBW. The determining factor of whether to use electrons or protons so far has been simply the specific particle *accelerator* concept planned for use in a beam weapon. Some accelerating schemes call for the acceleration of electrons, while others use protons.

The use of a hydrogen atom beam, however, is not based on the choice of a particular acceleration scheme. Because it is neutrally charged, the hydrogen atom has been selected specifically as the likely particle to be used in the initial space weapon. Neutral atoms would not be susceptible to bending by the earth’s magnetic field as would a charged-particle beam. Neither would the beam tend to spread due to the mutually repulsive force between particles of like-charge in the beam. (In the atmosphere, a charged-particle beam will neutralize itself by colliding with air molecules, effectively creating enough ions of the opposite charge to neutralize the beam.)

Fig. 5.2 Particle beam descriptors



The mechanism by which a particle beam destroys a target is a depositing of beam energy into the material of the target, which might be any material object. As the particles of the beam collide with the atoms, protons, and electrons of the material composing the target, the energy of the particles in the beam is passed on to the atoms of the target much as if a cue ball breaks apart a racked group of billiard balls. The result is that the target is heated rapidly to very high temperatures—which are exactly the effect that one observes in an explosion. Thus, a particle beam of sufficient energy can destroy a target by exploding it (although that is not the only means of destruction).

In describing a particle beam, it is conventional to speak of the energy of the beam (in electron volts), the beam current (in amperes), and the power of the beam (in watts) (see Fig. 5.2). The specific meaning of these terms as they pertain to a particle beam is derived from the close analogy between a particle beam and an electric current.

In Fig. 5.2 as it is illustrated, a particle beam consists of a stream of electrons, protons, or neutral atoms flowing with a real or imagined electric current. The particle energies are expressed in electron volts, while the current is stated in amperes. The product of the two yields the power of the beam in watts.

5.3 Particle Beam Description

The electron volt is a unit of measure for energy. It is the kinetic energy of an electron that has been accelerated by 1 V of electric potential. Nominally, all the particles in a beam will have been accelerated to the same velocity, or energy, so it is possible to characterize the energy of a particle beam in terms of the energy of a typical particle of the beam, usually millions of electron volts (MeV). Hence, a 20 MeV particle beam would be a beam of particles, each with a nominal energy of 20 million electron volts.

A measure of the number of particles in the beam (beam intensity) may be made from the magnitude of the electric current (amperes) in the beam. To be able to

assign a current to the beam, it is necessary to assume that each particle has an amount of electric charge equivalent to an electron (even if it is a neutral atom). This assumption enables an electric current to be ascribed to the particle beam, and an indication of the number of particles in the beam is inferred by the current magnitude expressed in amperes.

The power of a particle beam is the rate at which it transports its energy, which is also an indication of the rate at which it can deposit energy into a target. Again, the analogy with an electric circuit serves us well. The power developed in an electric circuit is the mathematical product of the voltage (E) and the current (I); its unit of measure is the watt. Since the unit of energy for a particle in a beam is the electron volt (E), and the beam has an electric current (I) ascribed to it, the power of the particle beam in watts is simply the energy in electron volts multiplied by the beam current in amperes.

5.4 Types of Particle Beam Weapons

There are two broad types of particle beam weapons: the charged-particle beam weapon and the neutral-particle beam weapon. The charged-particle variety would be developed for use within the atmosphere (endoatmospheric) and has a set of technological characteristics that are entirely different from the neutral-particle beam weapon that would be used in space (exoatmospheric). Primarily, the extremely high power and precisely defined beam characteristics required for a particle beam to propagate through the atmosphere distinguish an endoatmospheric device from a beam weapon designed to operate in space. The development of a power supply and particle accelerator with sufficient power and appropriately shaped pulses for endoatmospheric weapons depends on very-“high-risk” technology and is likely years away.¹

The technological problems associated with exoatmospheric weapons are considerable also, but they are not as difficult as those associated with endoatmospheric weapons. Here, the greatest challenge is in the area of directing the beam: the weapon must be able to focus its energy to strike a target that may be thousands of kilometers away. There are two aspects to this challenge. First, the weapon must create a high-intensity, neutral beam with negligible divergence as it leaves the accelerator. Second, the weapon must have a system for aiming its beam at the target. This system must be able to detect pointing errors in a beam (which is itself very difficult to detect because of its lack of an electric charge) and, when necessary, redirect a missed “shot” towards the target.

¹The major technological problems of the endoatmospheric weapon are twofold: to understand and demonstrate the propagation of the particle beam through the air and to create an electrical pulsed power source capable of generating billions of watts of power in extremely short, repetitive pulses.

Particle Beam Weapon System : Areas of Development

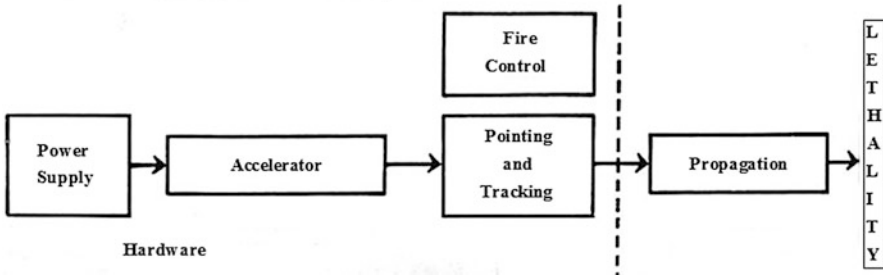


Fig. 5.3 Particle beam weapon system areas of development

Because of these two different sets of demands, the endo- and exoatmospheric devices represent two different types of weapon systems in appearance and operation. Nevertheless, there are certain fundamental areas of development that are common to both types of PBWS.

5.5 Development Areas for PBWs

The realization of an effective particle beam weapon (PBW) depends upon technology developments in five areas. Three of these concern hardware developments, while two others are related to advances in the understanding of beam weapon phenomena (see Fig. 5.3).

Based on Fig. 5.3, any particle beam weapon system may be broken into five major areas. Three of these areas are hardware related, and two concern the understanding of the associated phenomena. The current Department of Defense (DOD) particle beam program aims to develop each area sufficiently to determine the feasibility of a particle beam weapon.

5.6 Lethality of Particle Beam Weapon

One of the phenomenological aspects under study is lethality. Lethality refers to the general effectiveness of a weapon in engaging and destroying a target. There is no doubt that a particle beam is capable of destroying a military target. However, knowledge is needed of the precise effect that a particle beam would have when it impinges upon various-type targets composed of different materials and components. The problem is made more difficult from the fact that the particle beam can vary according to particle type, particle energy, and beam power. To gain such an understanding, beam/target interaction is the subject of continuing technological investigations and studies.

In assessing the unique value of a particle beam as a potential weapon system, it is important to consider six characteristics that would give the beam weapon a high degree of lethality.

Beam velocity. The particles “fired” by a PBW will travel at nearly the speed of light (186,000 miles per second). The advantage of such a high-velocity beam is that computing the aim point for a moving target is greatly simplified. The effect of this extremely high velocity is essentially to fix a target, even if the target attempts evasive action. For example, if the weapon were required to shoot at a reentry vehicle (RV) some 50 km distant and traveling at the high speed of 20,000 ft per second, the RV would travel only about 5 ft from the time the weapon fired until it was struck by the beam. This aspect of PBWs makes feasible the task of “shooting a bullet with a bullet,” as the ABM targeting problem is sometimes characterized.

Beam dwell time. Beam dwell time refers to the time that a beam remains fixed on a target. In an endoatmospheric weapon, the power of the beam would be sufficient to destroy the target instantaneously (in millionths of a second) upon impact, and no beam dwell time would be required. In space, where the required power of the beam is considerably less, some very short beam dwell time may be necessary.²

Rapid aim capability. The particle beam may be redirected very rapidly from one target to another by means of a magnetic field. This field would itself be generated by an electric current. Varying the current would change the magnetic field intensity, which would deflect the charged particles in the desired direction. Within certain limits, no physical motion of the weapon would be required as it engages enemy targets. This capability to very rapidly aim and redirect the beam would enhance significantly the weapon’s capability to engage multiple targets.

Beam penetration. The subatomic particles that constitute a beam have great penetrating power. Thus, interaction with the target is not restricted to surface effects, as it is with a laser. When impinging upon a target, a laser creates a blow-off of target material that tends to enshroud the target and shield it from the laser beam. Such beam/target interaction problems would not exist for the particle beam with its penetrating nature. Particle beams would be quite effective in damaging internal components or might even explode a target by transferring a massive amount of energy into it (the catastrophic kill mechanism). Furthermore, there would be no realistic means of defending a target against the beam; target hardening through shielding or material selection would be impractical or ineffective.

²For a different reason, all high-energy lasers (with the exception of the envisioned X-ray laser) require beam dwell time also. A laser needs such time to burn through the surface of the target. The question of how a beam of neutral atoms might be accelerated in a conventional RF linac may arise in the mind of the perceptive reader. A present approach is to attach an extra electron to a hydrogen atom, accelerate the charged atom in conventional fashion, and then strip off the extra electron by passing the beam through a tenuous gas as it exits the accelerator. This stripping causes the beam to spread slightly and must be controlled if the divergence specifications of a space weapon are to be met.

Ancillary kill mechanisms. In addition to the direct kill mechanism of the beam, ancillary kill mechanisms would be available. Within the atmosphere, a secondary cone of radiation symmetrical about the beam would be created by the beam particles as they collide with the atoms of the air. This cone would be comprised of practically every type of ionizing radiation known (i.e., X-rays, neutrons, alpha and beta particles). A tertiary effect from the beam would be the generation of an electromagnetic pulse (EMP) by the electric current pulse of the beam. This EMP would be very disruptive to any electronic components of a target. Thus, even if the main beam missed, the radiation cone and accompanying EMP could kill a target. While the EMP and the radiation cone would not be present in an exoatmospheric use of the weapon, there are other possible options in space that are not available in the atmosphere. Many intriguing possibilities come to mind. For example, using lower levels of beam power, the particle beam could expose photographic film in any satellite carrying photographic equipment, or it could damage sensitive electronic components in a satellite.

All-weather capability. Another advantage of a particle beam over the high-energy laser in an endoatmospheric application would be an all-weather capability. While such weather effects as clouds, fog, and rain can thwart a laser completely, these atmospheric phenomena would have little effect on the penetrating power of a particle beam weapon.

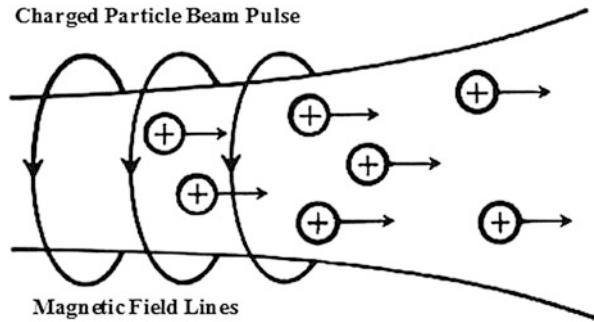
5.7 Propagation of the Beam

The successful development of a PBW depends on the ability of the beam to propagate directly and accurately to the target. As we ponder its similarity to lightning, we might consider the jagged, irregular path of a lightning bolt as it darts unpredictably through the sky. Such indeterminacy would never do for the particle beam of a weapon, which must have an extremely precise path of propagation as it traverses the kilometers to the enemy vehicle. This aspect, in fact, may be the Achilles' heel of the endoatmospheric weapon. However, the space weapon, which at this time is envisaged to be a neutral stream of hydrogen atoms, would not suffer from the beam instability problems that may possibly plague a beam of charged particles traveling through the air.

Another problem of propagation is possible beam spreading. An increase in beam diameter would result in a decrease of the energy density (intensity) of the beam as it travels towards the target. Over short ranges, a slight beam divergence can be tolerated, but the very long ranges that would be required of the space weapon place a tremendous restriction on the amount of beam divergence that is acceptable.

Use of a neutral beam in space would ensure that the beam would not spread due to mutual repulsion of the beam particles. Divergence would come strictly from that imparted by the accelerator. In the atmosphere, however, even if the beam particles were neutral, air molecules would strip the surrounding electrons quickly from the

Fig. 5.4 Charged-particle beam pulse



beam's neutral atoms, turning the beam into a charged-particle beam. The charged particles within the beam would then tend to repel one another, producing undesirable beam divergence. But as the beam propagates through the air, it would also strip electrons from the surrounding air molecules, creating a region of charged particles (ions) intermingling with the beam. The result of this phenomenon is to neutralize the overall charge of the beam, thereby reducing the undesired effect of mutual repulsion among the charged particles in the beam that is a cause of beam spreading. Another force that tends to prevent beam spreading is a surrounding magnetic field, created by the current of the charged particle beam. This field wraps itself around the beam and produces a conduit that inhibits beam divergence (see Fig. 5.4).

As it can be observed in Fig. 5.4, a charged-particle beam (CPM) will tend naturally to spread apart, due to the mutually repulsive forces between the like-charged particles constituting the beam. The electric current created by the moving field will tend to bind the beam together. However, unless there is some neutralization of the charge, the mutually repulsive force will always be the stronger force and the beam will blow itself apart.

The propagation of a charged-particle beam through the atmosphere is, in fact, the pacing issue for the endoatmospheric weapon. It has been theoretically calculated that specific threshold values of the beam parameters (beam current, particle energy, beam pulse length, etc.) are required for a beam to propagate through air with reliability. While the values of these parameters are classified, no particle beam accelerator is currently capable of creating a beam with the required parameters.

Two crucially important experimental programs are exploring the phenomena of atmospheric beam propagation. The first program, underway at the Lawrence Livermore National Laboratory, involves experiments with an accelerator called the Advanced Test Accelerator (ATA), the construction of which was completed in the fall of 1982. The second program, a joint Air Force/Sandia National Laboratories program, similarly is aimed at investigating beam propagation through the use of a radial-pulse-line accelerator (RADLAC). Continuation of the US program to explore the development of an endoatmospheric weapon will depend on a positive prognosis from these two experimental studies of atmospheric beam propagation.

5.8 Fire Control/Pointing and Tracking Technology

The fire control/pointing and tracking system of a PBW must acquire and track the target, point the weapon at the target, fire the beam at the proper time, and assess target damage. If the beam misses the target, the system must sense the error, repoint the weapon, and fire again. Much of the technology for this part of the weapon is not unique to a particle beam weapon (PBW), and its development has benefited considerably from the high-energy laser (HEL) weapon program, which has involved study of this problem for several years. Moreover, recent advances in radar technology and electro-optics, combined with projected developments in next-generation computers, portend a heretofore-unimagined capability in this area of technology.

This is not to say that serious development problems do not remain in the area of the fire control system. Many of the pointing and tracking problems will be entirely unique to a particle beam weapon and cannot be solved by a transfer of technology from the laser program. Nevertheless, none of these problems is such that they will demand exploration of basic issues in physics and the advancement of the state of the art, as will some other aspects of the beam weapon's development.

5.9 Accelerator Technology

The accelerator is the part of the weapon system that creates the high-energy particle beam. It is composed of a source of ions (electrons, protons, or charged atoms), a device for injecting the particles into the accelerating section, and the accelerating section itself. The accelerating section of all conventional linear accelerators is made up of a series of segments (modules) that sequentially apply an accelerating electric field to the charged particles. While the voltage in each segment may be relatively low, the repeated application of an accelerating voltage by the large number of modules ultimately produces very high particle energies.

The first subatomic particle accelerators were constructed in the 1930s for scientific investigations in the field of elementary particle physics. The accelerators used for the first-generation PBW system will be embellished variations of the present-day, linear accelerators (LinAcs), such as the two-mile-long Stanford Linear Accelerator Center (SLAC), which is a state-of-the-art device capable of producing electrons with an energy of 30 GeV (30 billion electron volts).

The SLAC represents a class of accelerators known as radio-frequency (RF) linear accelerators. The great majority of linacs in operation today are RF linacs. Although such devices can accelerate particles to energies high enough for use as a weapon, they are limited severely in their current-carrying capability and would not be candidates for the endoatmospheric weapon system, since beam power is a product of current and voltage.

The space weapon, however, does not call for the tremendously high beam power required for the endoatmospheric weapon. Its accelerator could be based on the design of a state-of-the-art RF linac [1]. The major demand for a space weapon is to create a high-intensity (high “brightness”) beam of neutral atoms with very precise collimation as it exits the accelerator. It is in this area of divergence that the greatest technical problems exist. If the beam were to diverge from a pencil point to only the diameter of a penny after 12 miles of travel, this would represent a divergence of one part in a million (1 m for each 1000 km traveled). A divergence much greater than this would not be acceptable for a space weapon that is to have a range of thousands of kilometers.

A second type of linear accelerator is called the induction linac. The world’s first induction linac, the Astron I accelerator, was built at the Lawrence Livermore Laboratory in 1963. It was designed to produce high-electron-beam currents that could be used in a magnetic confinement scheme for controlled thermonuclear fusion. The Advanced Test Accelerator is an art induction linac that grew out of this early accelerator technology. The ATA is designed to generate a 50 MeV beam with 10,000 amperes of current in pulses of 50 ns (50 billionths of a second) duration.³

The fundamental principle of operation (applying successively high voltage across a series of accelerating segments) is the same for both the RF and induction linacs. However, the mechanism for generating the electric voltage within the segments of the two types of linacs is quite different. Compared to the RF linac, the induction linac does not impart as much instability to the beam when a modest current limit is exceeded. Therefore, of the two types of accelerators, the induction linac is the more likely candidate for an endoatmospheric beam weapon (which will require very high beam currents).

In examining the Air Force charged-particle beam technology program, we find that its main thrust is the exploration of nonconventional acceleration techniques (neither RF nor induction linacs), with two main purposes in mind. The first is to develop a means of producing a particle beam with parameters closely resembling those that would be required for successful propagation through the atmosphere, so that beam propagation can be studied in depth and propagation theory refined. To date, a RADLAC I accelerator that has been developed has produced a 10 MeV beam of electrons with a 30,000-ampere current [2]. A more powerful RADLAC II is under construction.

The second purpose is to develop an accelerator with higher accelerating fields that would permit the building of a shorter device. The nominal accelerating gradient in conventional accelerators is about 5–10 MeV per meter of accelerator length. Thus, to produce a 1 GeV beam, a linear accelerator would need to be 100–500 m in length—far too long and cumbersome, particularly if the device were to be carried

³Private communication, Lieutenant Colonel James H. Head, High-Energy Physics Technology Program Manager, Air Force Weapons Laboratory, 6 February 1984.

aboard an aircraft. The Air Force hopes to build a device eventually that will generate a very powerful particle beam with an accelerator of more reasonable length.

5.10 Power Supply Technology

Possibly the most difficult technical problem in developing an atmospheric particle beam weapon is the development of its electrical power supply. To operate an endoatmospheric PBW requires that a tremendous amount of electrical energy be supplied over very short periods of time. Since power is energy divided by time, large amounts of energy over short spans of time translate into extremely high power levels. Building a power supply to produce high power in short bursts involves a very advanced field of technology known as pulsed power technology.

Basically, a pulsed power device can be divided into three component areas: the primary power source that provides electrical energy over the full operating time of the weapon (prime power source), the intermediate storage of the electrical energy as it is generated (energy storage), and the “conditioning” of the electrical power bursts or pulses of suitable intensity and duration (pulse-forming network) to fire the weapon. Each of these three areas represents a technological challenge.

Any electricity-producing device, such as a battery or generator, is a primary power source. The requirement of the particle beam weapon, however, is for a prime power source that can produce millions to billions of watts of electrical power yet be as lightweight and compact as possible. A conventional power station could provide the needed power levels, but it would be neither small nor lightweight. There is also a need for mobility in many of the envisaged applications; a power station would not meet this requirement. Some typical prime power candidates are advanced-technology batteries, turbine-powered generators, or an advanced magnetohydrodynamic (MHD) generator using superconducting circuitry. Whatever the primary source might be, a sizable advance in the present power-generating state of the art will be required, particularly for the endoatmospheric weapon.

Once electrical energy is generated for the weapon, it will likely have to be stored in some fashion. A typical storage method involves charging a series of large capacitors (often called a capacitor bank). Other more exotic methods are possible, e.g., spinning a huge mechanical flywheel or simply storing the energy in the form of a high-energy explosive that is released in a contained explosion. Actually, there are numerous schemes for storing and releasing the required energy; their advantages and disadvantages depend on their particular application (i.e., the type of accelerator that is used and whether the weapon is endo- or exoatmospheric).

The pulse-forming network would be designed to release the stored energy in the desired form. In the atmospheric weapon, a single shot or “bolt” would most likely be comprised of a very-short-duration pulse, repeated thousands of times per second. Hopefully, the prime power source would be able to generate energy at least at the

same rate as energy was dispatched. If not, the weapon would be required to remain quiescent while its generator rebuilt a charge for another series of bolts.

The development of a particle beam weapon by the United States is a logical follow-on to the current high-energy laser development program. The weapon's potential lethality against high-speed, multiple targets, coupled with its capacity for selective destruction, would make the PBW particularly suitable for the space defense role. While some of the technological and operational issues to be resolved appear formidable at this time, it is far too early to discount the eventual operational effectiveness of such a weapon. Several scientists have argued that the PBW cannot be built or effectively deployed, creating or exacerbating doubts in other individuals. Yet those so concerned might do well to recall that in 1949 Vannevar Bush—a highly respected national leader with a Ph.D. in electrical engineering who had served as head of the US Office of Scientific Research and Development during World War II—argued that technical problems made the development of an effective ICBM virtually impossible without astronomical costs. Nine years later, in 1958, the United States had its first operational ICBM, the Atlas.

The PBW offers a possibility for defending effectively against a launched ICBM, and even a glimmer of hope towards this end is worthy of pursuit. Should the United States terminate its exploration of particle beam technology, we would be opening the door for the Soviets to proceed at their own pace towards building such a weapon. We can ill afford technological surprise in an area as crucial as beam weapons.

The current pace of the US program in PBW development is both logical and orderly. Funding levels remain relatively low, as DARPA and the three services continue to focus on the pacing technologies that must be understood if such a weapon is to be built. Since the potential payoff of such activity is tremendous, it seems imperative that the United States continue to pursue the development of PBWs at least at the present level of funding.

References

1. B.M. Schwarzschild, ATA: 10-kA pulses of 50 MeV electrons. *Phys. Today*. 20 (1982)
2. V. Bush, *Modern arms and free men: a discussion of the role of science in preserving democracy* (Simon and Schuster, New York, 1949), pp. 84–87

Chapter 6

Scalar Wave Energy as Weapon



There is a wide confusion on what are “scalar waves” in serious and less serious literature on electrical engineering. In this chapter we explain that this type of waves are longitudinal waves of potentials. It is shown that a longitudinal wave is a combination of a vector potential with a scalar potential. There is a full analog to acoustic waves. Transmitters and receivers for longitudinal electromagnetic waves are discussed. Scalar wave was found and used at first by Nikola Tesla in his wireless energy transmission experiment. The scalar wave is the extension of Maxwell equation part that we can call it more complete electromagnetic (MCE) equation as described in this chapter.

6.1 Introduction

It is the purpose of this chapter to discuss a new unified field theory based on the work of Tesla. This unified field and particle theory explains quantum and classical physics, mass, gravitation, constant speed of light, neutrinos, wave, and particles, all can be explained by vortices [1], white to discuss on these unique, various recent inventions and their possible modes of operation, but to convince those listening of their value for hopefully directing a future program geared towards the rigorous clarification and certification, of the specific role the electroscalar domain might play in shaping a future, consistent, classical, electrodynamics. Also, by extension to perhaps shed light on current theory conceptual and mathematical inconsistencies do exist, in the present interpretation of relativistic quantum mechanics. In this regard, it is anticipated that by incorporating this more expansive electrodynamic model, the source of the extant problems with gauge invariance in quantum electrodynamics and the subsequent unavoidable divergences in energy/charge might be identified and ameliorated.

Not only does the electroscalar domain have the potential to address such lofty theoretical questions surrounding fundamental physics, but also another aim in this chapter is to show that the protocol necessary for generating these field effects may not be present only in exotic conditions involving large field strengths and specific frequencies involving expensive infrastructure such as the Large Hadron Collider (LHC), but as recent discoveries suggest may be present in the physical manipulation of ordinary everyday objects. We will also see that nature has been and may be engaged in the process of using scalar longitudinal waves (SLW) in many ways as yet unsuspected and undetected by humanity. Some of these modalities of scalar wave generation we will investigate will include the following: chemical bond breaking, particularly as a precursor to seismic events (illuminating the study and development of earthquake early warning system), solar events (related to eclipses), and sunspot activity and how it impacts the earth's magnetosphere. Moreover, this overview of the unique aspects of the electroscalar domain will suggest that many of the currently unexplained anomalies such as over-unity power observed in various energy devices, and exotic energy effects associated with low-energy nuclear reactions (LENR), may find some basis in fact.

In regards, to the latter “cold fusion or LENR fusion-type scenarios”, the electroscalar wave might be the actual agent needed to reduce the nuclear Coulomb barrier, thus providing the long-sought-out viable theoretical explanation of this phenomenon. Longitudinal electrodynamic forces in exploding wires, etc. may actually be due to the operation of electroscalar waves at the subatomic levels of nature. For instance, the extraordinary energies produced by Ken Shoulder's charge clusters (i.e., particles of like-charge repel each other—that is one of the laws describing the interaction between single subatomic particles) may also possibly be due to electroscalar mechanisms. Moreover, these observations, spanning as they do cross many cross-disciplines of science, beg the question as to the possible universality of the SLW—that the concept of the longitudinal electroscalar wave, not present in current electrodynamics, may represent a general, key, overarching principle, leading to new paradigms in other science besides physics. This idea will also be explored in the talk, showing the possible connection of scalar-longitudinal (also known as, electroscalar) wave dynamics to biophysical systems. Admittedly, we're proposing quite an ambitious agenda in reaching for these goals, but I think you will see that recent innovations will have proven equal to the task of supporting this quest.

6.2 Transverse and Longitudinal Wave Descriptions

As you know from classical physics point of view, typically there are three kinds of waves and wave equations that we can talk about (i.e., soliton wave is an exceptional case and should be addressed separately).

These three types are listed as:

1. Mechanical waves (i.e., wave on string)
2. Electromagnetic waves (i.e., \vec{E} and \vec{B} fields from Maxwell's equation to deduce the wave equations, where these waves carry energy from one place to another)
3. Quantum mechanical waves (i.e., using Schrödinger equations to study particle movement)

The second one is the subject of our interest, in terms of two types of waves involved in electromagnetic wave and they are:

- (a) Transverse waves
- (b) Longitudinal pressure waves (LPWs), also known as scalar longitudinal waves (SLWs)

From the above two waves, the scalar longitudinal wave (SLW) is the matter of interest in directed energy weapons (DEW) [2]; this is why, and first, we briefly describe the SLWs and their advantages for DEW purpose as well as communication within a nonhomogeneous media such as seawater with different electrical primitivity ϵ and magnetic permeability μ at different layers of ocean depth. See Chap. 4 of this book.

A wave is defined as a disturbance which travels through a particular medium. The medium is a material through which a wave travels from one to another location. Take the example of a slinky wave which can be stretched from one end to other end and then becomes in static condition. This static condition is called its neutral condition or equilibrium state.

In the slinky coil, the particles are moved up and down and then come into their equilibrium state. This generates disturbance in coil which is moved from one to another end. This is the movement of slinky pulse. **This is a single disturbance in medium from one to another location. If it is done continuously and in a periodical manner, then it is called a wave.** These are also called energy transport medium. They are found in different shapes, and show different behaviors and characteristic properties. On this basis, these are classified mainly in two types that are longitudinal, transverse, and surface waves. Here we are discussing the longitudinal waves, properties, and its examples. The movement of wave is parallel to the medium of particles in these waves.

6.2.1 Transverse Waves

For transverse waves the displacement of the medium is perpendicular to the direction of propagation of the wave. A ripple on a pond and a wave on a string are easily visualized transverse waves. See Fig. 6.1.

Transverse waves cannot propagate in a gas or a liquid because there is no mechanism for driving motion perpendicular to the propagation of the wave. In

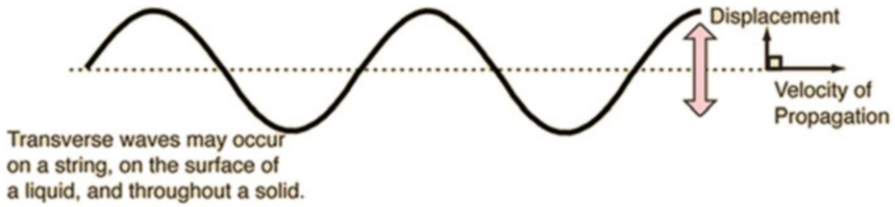


Fig. 6.1 Depiction of a transverse wave



Fig. 6.2 Depiction of a longitudinal wave

summary, it is a wave in which the oscillation is perpendicular to the direction of wave propagation. Electromagnetic waves [and secondary-waves (or S-waves or shear waves sometimes called an elastic S-waves) in general] are transverse waves.

6.2.2 Longitudinal Waves

In longitudinal waves the displacement of the medium is parallel to the propagation of the wave. A wave which is "slinky" is a good visualization. Sound waves in air are longitudinal waves. See Fig. 6.2.

In summary, it is a wave in which the oscillation is opposite to the direction of wave propagation. Sound waves [and primary-waves or (P-waves) in general] are longitudinal waves. On the other hand, a wave motion in which the particles of the medium oscillate about their mean positions in the direction of propagation of the wave is called longitudinal wave.

However, if we use our wand to expand the subject of longitudinal wave (LW), before we go deeper into the subject of scalar longitudinal wave (SLW), for longitudinal wave the vibration of the particles of the medium is in the direction of wave propagation. A longitudinal wave proceeds in the form of compression and rarefaction which is the stretch and compression in the same direction as the wave moves. For a longitudinal wave at places of compression the pressure and density tend to be maximum, while at places where rarefaction takes place the pressure and density are minimum. In gases only, longitudinal wave can propagate. Longitudinal waves are known as compression waves.

A longitudinal wave travels through a medium in the form of compressions or condensations C and rarefaction R . A compression is a region of the medium in which particles are compressed, i.e., particles come closer, i.e., distance between the particles becomes less than the normal distance between them. Thus, there is temporary decrease in volume and as a consequence increase in density of the medium in the region of compression. A rarefaction is a region of the medium in which particles are rarefied, i.e., particles get farther apart than what they normally are. Thus, there is temporary increase in volume and a consequent decrease in density of the medium in the region of rarefaction.

The distance between the centers of two consecutive rarefaction and two consecutive compressions is called wavelength. Examples of longitudinal waves are sound waves, tsunami waves, earthquake P-waves, ultrasounds, vibrations in gas, and oscillations in spring, internal water waves, and waves in slink.

1. Longitudinal Waves

The various examples of sound wave are:

- (a) Sound wave
- (b) Earthquake P-wave
- (c) Tsunami wave
- (d) Waves in a slink
- (e) Glass vibrations
- (f) Internal water waves
- (g) Ultrasound
- (h) Spring oscillations

2. Sound Waves

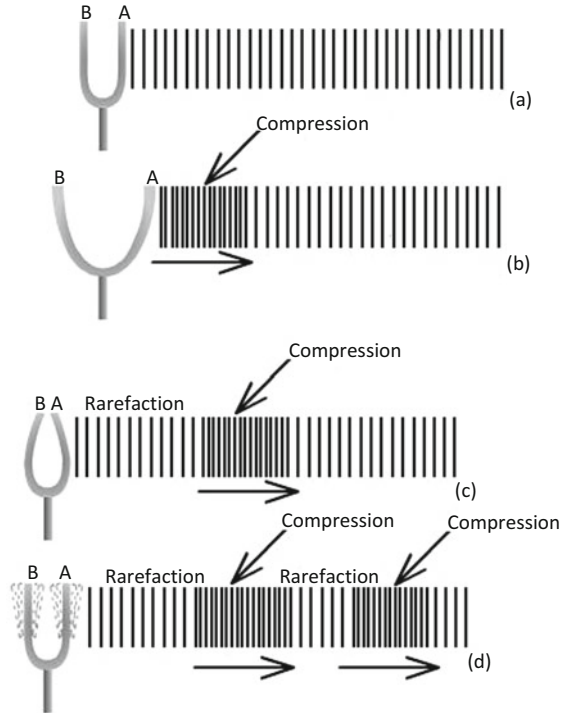
Now the question is that **are sound waves longitudinal?** The answer is **yes**, sound wave travels as longitudinal wave in nature. Sound wave behaves as a transverse wave in solids. Through gases, plasma, and liquid the sound travels as longitudinal wave. Through solids it can be transmitted as transverse as well as longitudinal wave.

Material medium is mandatory for the propagation of the sound waves. Sound waves are mostly longitudinal in common nature. Speed of sound in air at N.T.P. (normal standard and pressure) is 332 m/s. Vibrations of air column above the surface of water in the tube of a resonance apparatus are longitudinal. Vibrations of air column in organ pipes are longitudinal. Sound is audible only between 20 Hz and 20 KHz. Sound waves cannot be polarized.

Vibrations of air column in organ pipes are longitudinal. Vibrations of air columns above the surface of water in the tube of a resonance apparatus are longitudinal.

(a) Propagation of sound waves in air

Sound waves are classified as longitudinal waves. Let us now see how sound waves propagate. Take a tuning fork, vibrate it, and concentrate on the motion of one of its prongs, say prong A. The normal position of the tuning fork and the initial condition of air particles are shown in Fig. 6.3a. As the prong

Fig. 6.3 Tuning fork

A moves towards right, it compresses air particles near it, forming a compression as shown in Fig. 6.3b. Due to vibrating air layers, this compression moves forward as a disturbance.

As the prong A moves back to its original position, the pressure on its right decreases, thereby forming a rarefaction. This rarefaction moves forward like compression as a disturbance. As the tuning fork goes on vibrating, waves consisting of alternate compressions and rarefactions spread in air as shown in Fig. 6.3c, d. The direction of motion of the sound waves is same as that of air particles; hence they are classified as longitudinal waves. The longitudinal waves travel in the form of compressions and rarefactions.

The main parts of the sound wave are as follows:

The main parts of sound wave are listed below with their descriptions:

- **Amplitude:** The maximum displacement of a vibrating particle of the medium from the mean position. A shows amplitude in $y = A \sin(\omega t)$. The maximum height of the wave is called its amplitude. If the sound is more then the amplitude is more.
- **Frequency:** Number of vibrations made per second by the particles and is denoted by f which is given as $f = 1/T$ and its unit: Hz. We can also get the expression for angular frequency.

- **Pitch:** It is that characteristic of sound with the help of which we can distinguish between a SHRILL note and a note that is grave. When a sound is shriller it is said to be of higher pitch and is found to be of greater frequency, as $\omega = 2\pi f$. On the other hand, a grave sound is said to be of low pitch and is of low frequency. Hence pitch of a sound depends upon its frequency. It should be made clear that pitch is not the frequency but changes with frequency.
- **Wavelength:** The distance between two consecutive particles in the same phase or the distance traveled by the wave in one periodic time and denoted by λ .
- **Sound wave:** It is a longitudinal wave with regions of compression and rarefactions. The increase of pressure above its normal value may be written as

$$\sum p = \sum p_0 \sin \omega \left(t - \frac{c}{v} \right) \quad (6.1)$$

where

$\sum p$ = increase in pressure at x position at time t

$\sum p_0$ = maximum increase in pressure

$\omega = 2\pi f$ where f is frequency

If $\sum p$ and $\sum p_0$ are replaced by P and P_0 , then Eq. (6.1) has the following form as

$$P = P_0 \sin \omega \left(t - \frac{c}{v} \right) \quad (6.2)$$

(b) Sound intensity

Loudness of sound is related to the intensity of sound. The sound's intensity at any point may be defined as the amount of sound energy passing per unit time per unit area around that point in a perpendicular direction. It is a physical quantity. It is measured in Wm^{-2} in S.I.

The sound wave falling on the eardrum of the observer produces the sensation of hearing. The sound's sensation which enables us to differentiate between a loud and a faint sound is called **loudness** and we can designate by the symbol of L . It depends on the intensity of the sound I and the sensitivity of the ear of the observer at that place. The lowest intensity of sound that can be perceived by the human ear is called **threshold of hearing** and it is denoted by I_0 . The mathematical relation between intensity and loudness is

$$L = \log \frac{I}{I_0} \quad (6.3)$$

The intensity of sound depends on

- Amplitude of vibrations of the source
- Surface area of the vibrating source
- Distance of the source from the observer
- Density of the medium in which sound travels from the source
- Presence of other surrounding bodies
- Motion of the medium

(c) Sound reflection

When a sound wave gets reflected from a rigid boundary, the particles at the boundary are unable to vibrate. Hence the generation of reflected wave takes place which interferes with the oncoming wave to produce zero displacement at the rigid boundary. At the points where there is zero displacement, the variation in pressure is maximum. This shows that the phase of wave has been reversed but the nature of sound wave does not change, i.e., on reflection the compression is reflected back as compression and rarefaction as rarefaction. Let the incident wave be represented by the given equation:

$$Y = a \sin (\omega t - kx) \quad (6.4)$$

Then Eq. (6.4) of reflected wave takes the form

$$Y = a \sin (\omega t + kx + \pi) = -a \sin (\omega t + kx) \quad (6.5)$$

Here in both Eqs. (6.4) and (6.5) the symbol of a is basically designation of the amplitude of reflected wave.

A sound wave is also reflected if it encounters a rarer medium or free boundary or low-pressure region. A common example is traveling of a sound wave in a narrow open tube. On reaching an open end, the wave gets reflected. So, the force exerted on the particles there due to outside air is quite small and hence the particles vibrate with increasing amplitude. Due to this the pressure there tends to remain at the average value. This means that there is no alteration in the phase of the wave, but the ultimate nature of the wave has been altered; that is, on the reflection of the wave the compression is reflected as rarefaction and vice versa.

The amplitude of the reflected wave would be a' this time and Eq. (6.4) becomes

$$y = a' \sin (\omega t + kx) \quad (6.6)$$

3. Wave Interface

When listening to a single sine wave, amplitude is directly related to loudness and frequency is directly related to pitch. When there are two or more simultaneously sounding sine waves the wave interference takes place.

There are basically two types of wave interface:

- (a) **Constructive interference**
- (b) **Destructive interference**

4. Decibel

A smaller and practical unit of loudness is decibel (dB) and is defined as follows:

$$1 \text{ Decibel} = \frac{1}{10} \text{ bel} \quad (6.7)$$

In decibels, the loudness of a sound of intensity I is given by

$$L = 10 \log \left(\frac{I}{I_0} \right) \quad (6.8)$$

5. Timber

Timber can be called as the property which distinguishes two sounds and makes them different from each other even when they have the same frequency. For example, when we play violin and guitar on the same note and same loudness the sound is still different. It is also denoted as tone color.

6. S-Waves

An S-wave is a wave in an elastic medium in which the **restoring force** is provided by **shear**. S-waves are divergence-less:

$$\nabla \cdot \vec{u} = 0 \quad (6.9)$$

where \vec{u} is the displacement of the wave, and comes in two polarizations:

- (a) SV (vertical)
- (b) SH (horizontal)

The speed of an S-wave is given by

$$v_s = \sqrt{\frac{\mu}{\rho}} \quad (6.10)$$

where μ is the shear modulus and ρ is the density.

7. P-Waves

Primary-waves are also called P-waves. These are compressional waves. They are longitudinal in nature. These are a type of pressure waves. The speed of P-waves is greater than other waves. These are called the primary waves as they are the first to arrive during the earthquake. This is because of large velocity. The propagation of these waves knows no bounds and hence can travel through any type of material, including fluids.

P-waves, that is also called pressure waves, are longitudinal waves; that is, the oscillation occurs in the same direction (and opposite) as the direction of wave propagation. The restoring force for P-waves is provided by the medium's bulk modulus. In an elastic medium with rigidity or shear modulus being zero ($\mu = 0$), a harmonic plane wave has the form

$$S(z, t) = S_0 \cos(kz - \omega t + \phi) \quad (6.11)$$

where S_0 is the amplitude of displacement, k is the wave number, z is the distance along the axis of propagation, ω is the angular frequency, t is the time, and ϕ is a phase offset. From the definition of bulk modulus (K), we can write

$$K = -V \frac{dP}{dV} \quad (6.12)$$

where V is the volume and dP/dV is the derivative of pressure with respect to volume.

The bulk modulus gives the change in volume of a solid substance as the pressure on it is changed; then we can write

$$\begin{aligned} K &\equiv -V \left(\frac{dP}{dV} \right) \\ &\equiv \rho \left(\frac{\partial P}{\partial \rho} \right) \end{aligned} \quad (6.13)$$

Consider a wave front with surface area A , and then the change in pressure of the wave is given by the following relationship as

$$\begin{aligned} dP &= -K \frac{dV}{V} = -K \frac{A[S(z + \Delta z) - S(z)]}{A\Delta z} \\ &= -K \frac{S(z + \Delta z) - S(z)}{\Delta z} = -K \frac{\partial S}{\partial z} \end{aligned} \quad (6.14)$$

where ρ is the density. The bulk modulus has units of pressure.

6.2.3 Pressure Waves and More Details

As we did mention above the pressure waves present the behavior and concept of longitudinal waves; thus many of the important concepts and techniques used to analyze transverse waves on a string as part of mechanical wave components can also be applied to longitudinal pressure waves.

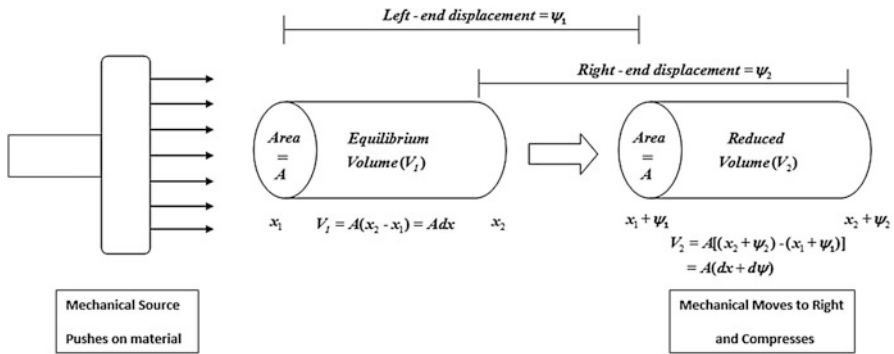


Fig. 6.4 Displacement and compression of a segment of materials

You can see an illustration of how a pressure wave works in Fig. 6.4. As the mechanical wave source moves through the medium, it pushes on a nearby segment of the material, and that segment moves away from the source and is compressed (that is, the same amount of mass is squeezed into a smaller volume, so the density of the segment increases). That segment of increased density exerts pressure on adjacent segments, and in this way a pulse (if the source gives a single push) or a harmonic wave (if the source oscillates back and forth) is generated by the source and propagates through the material.

The “disturbance” of such waves involves three things: the longitudinal displacement of material, changes in the density of the material, and variation of the pressure within the material. So, pressure waves could also be called “density waves” or even “longitudinal displacement waves,” and when you see graphs of the wave disturbance in physics and engineering textbooks, you should make sure that you understand which of these quantities is being plotted as the “displacement” of the wave.

As you can see in Fig. 6.4, we’re still considering one-dimensional wave motion (that is, the wave propagates only along the x -axis). But pressure waves exist in a three-dimensional medium, so instead of considering the linear mass density μ (as we did for the string in the previous section), in this case it’s the volumetric mass density ρ that will provide the inertial characteristic of the medium. But just as we restricted the string motion to small angles and considered only the transverse component of the displacement, in this case we’ll assume that the pressure and density variations are small relative to the equilibrium values and consider only longitudinal displacement (so the material is compressed or rarefied only by changes in the segment length in the x -direction).

The most straightforward route to finding the wave equation for this type of wave is very similar to the approach used for transverse waves on a string, which means you can use Newton’s second law to relate the acceleration of a segment of the material to the sum of the forces acting on that segment. To do that, start by defining the pressure (P) at any location in terms of the equilibrium pressure (ρ_0) and the incremental change in pressure produced by the wave (dP):

$$P = P_0 + dP \quad (6.15)$$

Likewise, the density (ρ) at any location can be written in terms of the equilibrium density (ρ_0) and the incremental change in density produced by the wave ($d\rho$):

$$\rho = \rho_0 + d\rho \quad (6.16)$$

Before relating these quantities to the acceleration of material in the medium using Newton's second law, it is worthwhile to familiarize yourself with the terminology and equations of volume compressibility. As you might imagine, when external pressure is applied to a segment of material, how much the volume (and thus the density) of that material changes depends on the nature of the material. To compress a volume of air by 1% requires a pressure increase of about 1000 Pa (pascals, or N/m^2) but to compress a volume of steel by 1% requires a pressure increase of more than 1 billion Pa. The compressibility of a substance is the inverse of its "bulk modulus" (usually written as K or B , with units of pascals), which relates an incremental change in pressure (dP) to the fractional change in density ($d\rho$) of the material:

$$K \equiv \frac{dP}{d\rho/\rho_0} \quad (6.17)$$

or

$$dP = K \frac{d\rho}{\rho_0} \quad (6.18)$$

With this relationship in hand, you are ready to consider Newton's second law for the segment of material being displaced and compressed (or rarefied) by the wave. To do that, consider the pressure from the surrounding material acting on the left and on the right sides of the segment, as shown in Fig. 6.5.

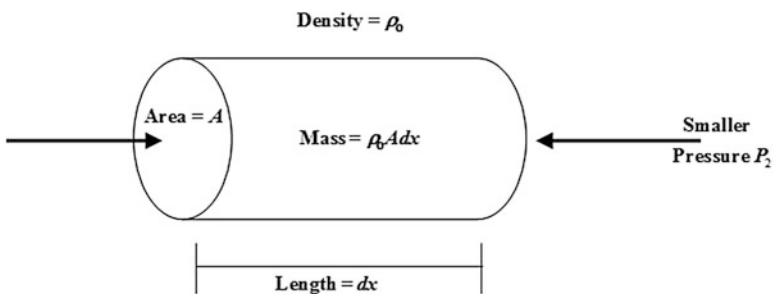


Fig. 6.5 Pressure on a segment of material

Notice that the pressure (P_1) on the left end of the segment is pushing in the positive x -direction and the pressure on the right end of the segment is pushing in the negative x -direction. Setting the sum of the x -direction forces equal to the acceleration in the x -direction gives

$$\sum F_x = P_1A - P_2A = ma_x \quad (6.19)$$

where m is the mass of the segment. If the cross-sectional area of the segment is A and the length of the segment is dx , the volume of the segment is $A dx$, and the mass of the segment is this volume times the equilibrium density of the material:

$$m = \rho_0 A dx \quad (6.20)$$

Notice also that the pressure on the right end of the segment is smaller than the pressure on the left end, since the source is pushing on the left end, which means that the acceleration at this instant will be towards the right. Using the symbol ψ to represent the displacement of the material due to the wave, the acceleration in the x -direction can be written as

$$a_x = \frac{\partial^2 \psi}{\partial t^2} \quad (6.21)$$

Substituting these expressions for m and a_x into Newton's second law Eq. (6.19) gives

$$\sum F_x = P_1A - P_2A = \rho_0 A dx \frac{\partial^2 \psi}{\partial t^2} \quad (6.22)$$

Writing the pressure P_1 at the left end as $P_0 + dP_1$ and the pressure P_2 at the right end as $P_0 + dP_2$ means that

$$\begin{aligned} P_1A - P_2A &= (P_0 + dP_1)A - (P_0 + dP_2)A \\ &= (dP_1 - dP_2)A \end{aligned} \quad (6.23)$$

But the change in dP (that is, the change in the overpressure (or under-pressure) produced by the wave) over the distance dx can be written as

$$\text{Change in overpressure} = dP_2 - dP_1 = \frac{\partial(dP)}{\partial x} dx \quad (6.24)$$

which means

$$-\frac{\partial(dP)}{\partial x} dx A = \rho_0 A dx \frac{\partial^2 \psi}{\partial t^2} \quad (6.25)$$

or

$$\rho_0 \frac{\partial^2 \psi}{\partial t^2} = - \frac{\partial(dP)}{\partial x} \quad (6.26)$$

But $dP = d\rho K/\rho_0$, so

$$\rho_0 \frac{\partial^2 \psi}{\partial t^2} = - \frac{\partial \left[\left(\frac{K}{\rho_0} \right) d\rho \right]}{\partial x} \quad (6.27)$$

The next step is to relate the change in density ($d\rho$) to the displacements of the left and right ends of the segment (ψ_1 and ψ_2). To do that, note that the mass of the segment is the same before and after the segment is compressed. That mass is the segment's density times its volume ($m = \rho V$) and the volume of the segment can be seen in Fig. 6.4 to be $V_1 = A dx$ before compression and $V_2 = A(dx + d\psi)$ after compression. Thus

$$\begin{aligned} \rho_0 V_1 &= (\rho_0 + d\rho) V_2 \\ \rho_0 (A dx) &= (\rho_0 + d\rho) A (dx + d\psi) \end{aligned} \quad (6.28)$$

The change in displacement ($d\psi$) over distance dx can be written as

$$d\psi = \frac{\partial \psi}{\partial x} dx \quad (6.29)$$

so

$$\begin{aligned} \rho_0 (A dx) &= (\rho_0 + d\rho) A \left(dx + \frac{\partial \psi}{\partial x} dx \right) \\ \rho_0 &= (\rho_0 + d\rho) \left(1 + \frac{\partial \psi}{\partial x} \right) \\ &= \rho_0 + d\rho + \rho_0 \left(\frac{\partial \psi}{\partial x} \right) + d\rho \left(\frac{\partial \psi}{\partial x} \right) \end{aligned} \quad (6.30)$$

Since we are restricting our consideration to the cases, in which the density change ($d\rho$) produced by the wave is small relative to the equilibrium density (ρ_0), the term $d\rho(\partial\psi/\partial x)$ must be small compared with the term $\rho_0(\partial\psi/\partial x)$. Thus to a reasonable approximation we can write

$$d\rho = -\rho_0 \frac{\partial \psi}{\partial x} \quad (6.31)$$

which we can insert into Eq. (6.27), giving the following:

$$\begin{aligned} \rho_0 \left(\frac{\partial^2 \psi}{\partial t^2} \right) &= - \frac{\partial \left\{ \left(\frac{K}{\rho_0} \right) \left[-\rho_0 \left(\frac{\partial \psi}{\partial x} \right) \right] \right\}}{\partial x} \\ &= \frac{\partial \left[K \left(\frac{\partial \psi}{\partial x} \right) \right]}{\partial x} \end{aligned} \quad (6.32)$$

Rearranging makes this into an equation with a familiar form of wave equation in one-dimensional:

$$\rho_0 \frac{\partial^2 \psi}{\partial t^2} = K \frac{\partial^2 \psi}{\partial x^2} \quad (6.33)$$

or

$$\frac{\partial^2 \psi}{\partial x^2} = \left(\frac{\rho_0}{K} \right) \frac{\partial^2 \psi}{\partial t^2} \quad (6.34)$$

As in the case of transverse waves on a string, you can determine the phase speed of a pressure wave by comparing the multiplicative term in the classical wave equation of Eq. (6.35) below, with that in Eq. (6.34):

$$\frac{\partial^2 \psi}{\partial x^2} = \frac{1}{v^2} \frac{\partial^2 \psi}{\partial t^2} \quad (6.35)$$

Setting these factors equal to one another gives the result of

$$\frac{1}{v^2} = \frac{\rho_0}{K} \quad (6.36)$$

or

$$v = \sqrt{\frac{K}{\rho_0}} \quad (6.37)$$

As expected, the phase speed of the pressure wave depends both on the elastic (K) and on the inertial (ρ_0) properties of the medium. Specifically, the higher the bulk modulus of the material (that is, the stiffer the material), the faster the components of the wave will propagate (since K is in the numerator), and the higher the density of the medium, the slower those components will move (since ρ_0 is in the denominator).

6.2.4 *What Are Scalar Longitudinal Waves*

Scalar longitudinal waves (SLW) are, conceived as longitudinal waves, as are sound waves. Unlike the transversal waves of electromagnetism, which move up and down perpendicularly to the direction of propagation, longitudinal waves vibrate in line with the direction of propagation. Transversal waves can be observed in water ripples: the ripples move up and down as the overall waves move outward, such that there are two actions, one moving up and down, and the other propagating in a specific direction outward.

Technically speaking, scalar waves have magnitude but no direction, since they are imagined to be the result of two electromagnetic waves that are 180° out of phase with one another, which leads to both signals being canceled out. This results in a kind of “pressure wave.”

Mathematical physicist James Clerk Maxwell, in his original mathematical equations concerning electromagnetism, established the theoretical existence of scalar waves. After his death, however, later physicists assumed that these equations were meaningless, since scalar waves had not been empirically observed and they were not repeatedly verified among the scientific community at large.

Vibrational or subtle energetic research, however, has helped advance our understanding of scalar waves. One important discovery states that there are many different types of scalar waves, not just those of the electromagnetic variety. For example, there are vital scalar waves (corresponding with the vital or “Qi” body), emotional scalar waves, mental scalar waves, causal scalar waves, and so forth. In essence, as far as we are aware, all “subtle” energies are made up of various types of scalar waves.

Qi Body Qi can be interpreted as the “life energy” or “life force,” which flows within us. Sometimes, it is known as the “vital energy” of the body. In traditional Chinese medicine (TCM) theory, qi is the vital substance constituting the human body. It also refers to the physiological functions of organs and meridians.

Some general properties of scalar waves (of the beneficial kind) include the following:

- Travel faster than the speed of light
- Seem to transcend space and time
- Cause the molecular structure of water to become coherently reordered
- Positively increase immune function in mammals
- Are involved in the formation process in nature

See more details of SLW applications in the next section below.

6.2.5 *Scalar Longitudinal Wave Applications*

The possibility of developing a means of establishing a communication through a nonhomogeneous means is looking very promising via utilization of more complete electrodynamic (MCE) theory [3]. This theory reveals the scalar longitudinal wave (SLW), which is created by a **gradient-driven** current, has **no** magnetic field, and thus is **not** constrained by the skin effect. The SLW is slightly attenuated by nonlinearities in the electrical conductivity as a function of electrical field magnitude. The SLW does not interfere with classical transverse electromagnetic (TEM) transmission or vice versa. By contrast, TEM waves are severely attenuated in conductive media due to magnetically driven eddy currents that arise from the skin effect. Consequently, only very-low- and ultralow-frequency TEM waves can be successfully used for long-distance underwater communications. The SLW also has immediate implications for the efficient redesign and optimization of existing TEM-based electronic technologies, because both TEM and SLW are created simultaneously with present electronic technologies.

The goal of application of SLW-based ≥ 150 kb/s digital data propagation over distances of many kilometers to address strategic, tactical, surveillance, and undersea warfare missions of the organization such as Navy. With this goal in mind, the optimization of SLW underwater-antenna design will be guided by development of a first-principle SLW simulator from the MCE theory, since all existing simulators model only circulating current-based TEM waves. A proof-of-principle demonstration of the prototype antenna through freshwater will be conducted in-house, followed by controlled tests at typical government underwater test range(s). These tests would include characterization of wave attenuation versus frequency, modulation bandwidth, and beamwidth control. The deliverable will be an initial prototype for SLW communications over tactical distances or more, followed by a field-deployable prototype, as dictated by Navy performance needs.

The unique properties of the scalar longitudinal wave lead to more sophisticated application areas, with implications for ocean surveillance systems, underwater imaging, energy production, power transmission, transportation, guidance, and national security. This disruptive technology has the potential to transform communications, as well as electrodynamic applications in general.

As far as low-energy nuclear reaction (LENR) is concerned, it is certain that most of us have heard of scalar electrodynamic. However, we probably have many questions about this electrodynamic phenomenon. Since it has been up to now mostly shrouded in mystery, we may even wonder whether it exists at all. And if it exists, do we need exotic conditions to produce and use it, or will it require a drastic transformation in our current understanding of classical electrodynamic, or how much of an impact will it have on future modes of power generation and conversion, whether has applications in weaponry, medical, or Low energy fusion driven as source of energy (D + D reaction as it was mentioned above)?

There is also a possibility of applying such scalar electrodynamics wave (SEW) in applications such as developing and demonstrating of an all-electronic (AE) engine that replaces electromechanical (EM) engines for vehicle propulsion.

As far as other applications of scalar longitudinal wave are concerned few can be listed here as well, and they are as follows:

6.2.5.1 Medical Application of Scalar Longitudinal Waves

Not all scalar waves, or subtle energies, are beneficial to living systems. Electromagnetism of the **60 Hz AC** variety, for example, emanates a secondary longitudinal/scalar wave that is typically detrimental to living systems.

However, to utilize the SLW as an application in biofield technology effectively, we need to cancel the detrimental aspect of wave scale and transmit it into a beneficial wave; therefore this innovative approach qualifies the medical application of SLW, where we can approach that biomedical folks to suggest such invention and ask for funding there as well. Last three bullet points are of vital interest in biofield approach application of SLW.

6.2.5.2 Bona Fide Application of SLW for Low-Temperature Fusion Energy

In case of low-temperature fusion interaction of $D + D$, by lowering nuclear potential barrier for the purpose of “cold fusion” for lack of better word, we know that in low-energy heavy-ion fusion, the term “Coulomb barrier” commonly refers to the barrier formed by the repulsive “Coulomb” and the attractive “nuclear” (nucleus-nucleus) interactions in a central (S-wave) collision. This barrier is frequently called fusion barrier (for light and medium mass heavy-ion systems) or capture barrier (heavy systems). In general, there is a centrifugal component to such a barrier (noncentral collisions). Experimenters may use the term “Coulomb barrier” to the nominal value of the “Coulomb barrier distribution” when either coupled-channel effects operate or (at least) a collision partner is deformed as the barrier features depend on orientation. To my knowledge, the terminology “transfer barrier” has not been used much. In my view, it could be applied to the transfer of charged particles/clusters.

There is a vast literature on the methods for calculating Coulomb barriers. For instance, the double-folding method is broadly used in the low-energy nuclear physics community. Based on this technique, there is a potential called “Sao-Paulo potential” because it has been developed by theorists in Sao Paulo city in Brazil.

The Coulomb barrier is calculated theoretically by adding the nuclear and Coulomb contributions of the interaction potential. For fusion, there are other contributions coming from the different degrees of freedom such as the angular momentum (centrifugal potential), and the vibrational and rotational states in both interacting nuclei in addition to the transfer contribution.

This is an area in which we may or could approach DOE or NRC with some RFP, in particular Idaho National Laboratory (INL).

6.2.5.3 Weapon Application of SLW as Directed Energy Weapons

The scalar beam weapons were originally invented in 1904 by Nicola Tesla, an American immigrant from Yugoslavia (1856 or 1857–1943). Since he died in 1943, many nations have secretly developed his beam weapons, which now further refined are so powerful that just by satellite one can make a nuclear-like destruction; earthquake; hurricane; tidal wave; and instant freezing—killing every living thing instantly over many miles. It can also cause intense heat like a burning fireball over a wide area; induce hypnotic mind control over a whole population; or even read anyone on the planet's mind by remote. Due to the nature of behaving as a pressure wave and carrying tremendous energy, SLW can remove something right out of its place in time and space faster than the speed of light, without any detectable warning by crossing two or more beams with each other. Moreover, any target can be aimed at even right through to the opposite side of the earth. If either of the major scalar weapon armed countries, e.g., the United States or Russia, were to fire a nuclear missile to attack each other this may possibly not even reach the target, because the missile could be destroyed with scalar technology before it even left its place or origin. The knowledge via radio waves that it was about to be fired could be eavesdropped and the target could be destroyed in the bunker, fired at from space by satellite.

Above 60 Hz Ac frequency, this wave can be very detrimental in nature. A scalar beam can be sent from a transmitter to the target, coupled with another sent from another transmitter, and as they cross an explosion can be made. This interference grid method could enable scalar beams to explode the missile before launch, as well as en route with knowing the right coordinates. If the target does manage to launch, what are known as Tesla globes or Tesla hemispheric shields can be sent to envelop a missile or aircraft. These are made of luminous plasma, which emanates physically from crossed scalar beams and can be created in any size, even over 100 miles across. Initially detected and tracked as it moves on the scalar interference grid, a continuous electromagnetic pulse (EMP) Tesla plasma globe could kill the electronics of the target. More intensely hot Tesla “fireball” globes could vaporize the missile. Tesla globes could also activate a missile's nuclear warhead en route by creating a violent low-order nuclear explosion. Various parts of the flying debris can be subjected to smaller and more intense Tesla globes where the energy density to destroy is more powerful than the larger globe first encountered. This can be done in pulse mode with any remaining debris given maximum continuous heating to vaporize metals and materials. If anything still rains down on Russia or the United States, either could have already made a Tesla shield over the targeted area to block it from entering the airspace.

Other useful aspect of SLW in military application: There is a community in the United States that believes the scalar waves are realizable in its nature of

mathematical approach. In recent conference sponsored by the Institute of Electrical and Electronics Engineers (IEEE), these were openly discussed and a proceeding on the conference exists. The conference was dedicated to Nicola Tesla and his work, and the papers presented claimed that some of Tesla's work used scalar wave concepts. Thus, there is an implied "Tesla connection" in all of this. As it was stated above, these are unconventional waves that are not necessarily a contradiction to Maxwell's equations as some have suggested but might represent an extension to Maxwell's understanding at the time. If realizable, the scalar longitudinal waves (SLWs) could represent a new form of wave propagation that could penetrate seawater (knowing the permeability, permittivity of salt water, and consequently skin depth), resulting in a new method of submarine communications and possibly a new form of technology for anti-submarine warfare (ASW). This technology also helps folks in Naval Special Warfare (NSW) Community such as Navy Seals to be able to communicate with each other even in a murky water condition.

Here are some mathematical notations and physics involved with this aspect of scalar longitudinal waves:

1. The scalar wave, as it is understood, is not an electromagnetic (EM) wave. An electromagnetic wave has both electric (\vec{E}) fields and magnetic (\vec{B}) fields and power flow in EM waves is by means of the Poynting vector, as Eq. (6.1) written below:

$$\vec{S} = \vec{E} \times \vec{B} \quad \text{W/m}^2 \quad (6.38)$$

The energy per second crossing a unit area whose normal is pointed in direction of \vec{S} is the energy in the electromagnetic wave.

A scalar wave has no time varying \vec{B} field. In some cases, it also has no \vec{E} field. Thus, it has no energy propagated in the EM wave form. It must be realized however that any vector could be added that may be integrated to zero over a closed surface and Poynting theorem still applies. Thus, there is some ambiguity in even stating the relationship that is given by Eq. (6.38), and that is the total EM energy flow.

2. The scalar wave could be accompanied by a vector potential \vec{A} , and yet \vec{E} and \vec{B} remain zero in the far field.

From EM theory, we can write as follows:

$$\begin{cases} \vec{E} = -\vec{\nabla} \phi - \frac{1}{c} \frac{\partial \vec{A}}{\partial t} \\ \vec{B} = \vec{\nabla} \times \vec{A} \end{cases} \quad (6.39)$$

In this case ϕ is the scalar (electric) potential and \vec{A} is the (magnetic) vector potential. The Maxwell's equations then predict the following mathematical relation as

$$\nabla^2 \phi - \frac{1}{c^2} \frac{\partial^2 \phi}{\partial t^2} = 0 \quad (\text{Scalar Potential Waves}) \quad (6.40)$$

$$\nabla^2 \vec{A} - \frac{1}{c^2} \frac{\partial^2 \vec{A}}{\partial t^2} = 0 \quad (\text{Vector Potential Waves}) \quad (6.41)$$

A solution appears to exist for the special case of $\vec{E} = 0$, $\vec{B} = 0$, and $\nabla \times \vec{A} = 0$, for a new wave satisfying the following relations:

$$\begin{cases} \vec{A} = \nabla S \\ \phi = -\frac{1}{c} \frac{\partial S}{\partial t} \end{cases} \quad (6.42)$$

s then stratifies the following relationship:

$$\nabla^2 S - \frac{1}{c^2} \frac{\partial^2 S}{\partial t^2} = 0 \quad (6.43)$$

Note that quantity c is a representation of speed of light.

Mathematically s is a “potential” with a wave equation, one that suggests propagation of this wave even through $\vec{E} = \vec{B} = 0$ and the Poynting theorem indicates no electromagnetic (EM) power flow.

- From bolt point paragraph 2 above, there is the suggestion of a solution to Maxwell’s equations involving a scalar wave with potential s that can propagate without Poynting vector EM power flow. However, the question arises as to where the energy is drawn from to sustain such a flow of energy. Some suggesting a vector that integrates to zero over a closed surface might be added in the theory, as suggested in paragraph or bolt point 1 above. Another is the possibility of drawing energy from the vacuum, assuming that net energy could be drawn from “free space.” Quantum electrodynamics allows random energy in free space but conventional electromagnetic (EM) theory has not allowed this to date. Random energy in free space that is built of force fields that sum to zero is a possible approach. If so, these might be a source of energy to drive the s waves drawn from “free space.” A number of engineers/scientists in the community suggested as stated in early statement within this write-up that, if realizable, the scalar wave could represent a new form of wave propagation that could penetrate seawater or be used as a new approach for directed energy weapons (DEWs).

This author suggests considering another scenario where we may need to look at equations of more complete electromagnetic theory (MCE) and new predictions of producing energy that way; thus we generate scalar longitudinal wave (SLW), where the Lagrangian density equation for MCE can be defined as

$$\mathcal{L} = -\frac{\epsilon c^2}{4} F_{\mu\nu} F^{\mu\nu} + J_\mu A^\mu - \frac{\gamma \epsilon c^2}{2} (\partial_\mu A^\mu)^2 - \frac{\epsilon c^2 k^2}{2} (A_\mu A^\mu) \quad (6.44)$$

where Lagrangian density equation is written in terms of the potentials \vec{A} and ϕ as follows:

The proof of equation was given in Chap. 5 of this book. See Eq. (5.126).

$$\begin{aligned} \mathcal{L}_{EM} = \frac{\epsilon c^2}{2} \left[\frac{1}{c^2} \left(\nabla \vec{\phi} + \frac{\partial \vec{A}}{\partial t} \right)^2 - (\nabla \times \vec{A})^2 \right] \\ - \rho \vec{\phi} + \vec{J} \cdot \vec{A} - \frac{\epsilon c^2}{2} \left(\underbrace{\frac{1}{c^2} \frac{\partial \vec{\phi}}{\partial t} + \nabla \cdot \vec{A}}_c \right)^2 \end{aligned} \quad (6.45)$$

This is the area where there are a lot of speculations among scientists, around the community of electromagnetic and utilization of scalar wave as a weapon application, and you find a lot of good as well as nonsense approaches in the Internet, by different folks.

The present approach uses several approaches:

1. One is acoustic signals that travel slowly (1500 m/s in seawater).
2. A second is blue-green laser light that has a typical range of 270 m, and is readily scattered by seawater particulates.
3. A third is high-frequency radio waves that are limited to a range of 7–10 m in seawater at high frequencies.
4. A fourth is extremely low-frequency radio signals that are of long range (world-wide) but transmit only a few characters per second for one-way, bell-ring calls to individual submarines.

The new feature of this proposed work is the use of a novel electrodynamic wave that has no magnetic field, and thus is not so severely constrained by the high conductivity of seawater, as regular radio waves are. We have demonstrated the low loss property of this novel (scalar longitudinal) wave experimentally by sending a video signal through two millimeters of solid copper at 8 GHz.

If one has a background in physics or electrical engineering you know that unquestionably our knowledge of the properties and dynamics of electromagnetic systems is believed to be the most solid and firmly established in all classical physics. By its extension, the application of quantum electrodynamics, describing accurately the interaction of light and matter at the subatomic realms, has resulted in the most successful theoretical scientific theory to date, agreeing with corresponding experimental findings to astounding levels of precision. Accordingly, these developments have led to the belief among physicists that the theory of classical electrodynamics is complete and that it is essentially a closed subject.

However, at least as far back to the era of Nikola Tesla, there have been continual rumblings of discontent stemming from occasional physical evidence from both laboratory experimental protocols and knowledge obtained from observation of natural phenomena such as the dynamics of atmospheric electricity to suggest that in extreme situations involving the production of high energies at specific frequencies, there might be some cracks exposed in the supposed impenetrable monolithic fortress of classical/quantum electrodynamics, implying possible key missing theoretical and physical elements. Unfortunately, some of these experimental phenomena have been difficult to replicate and produce on-demand. Moreover, some have been shown to apparently violate some of the established principles underlying classical thermodynamics. On top of that, many of those courageous individuals promoting the study of this phenomenon have couched their understanding of the limited reliable experimental evidence available from these sources, in language unfamiliar to the legion of mainstream technical specialists in electrodynamics, preventing clear communication of these ideas. Also, the various sources that have sought to convey this information have at times delivered contradictory statements.

It is therefore no wonder that for many decades, such exotic claims have been disregarded, ignored, and summarily discounted by mainstream physics. However, due to important developments over the past 2 years, there has been a welcome resurgence of research in this area, bringing back renewed interest towards the certification of the existence of these formerly rejected anomalous energy phenomena. Consequently, this renaissance of the serious enterprise in searching for specific weaknesses that currently plague a fuller understanding of electrodynamics has propelled the proponents of this research to more systematically outline in a clearer fashion the possible properties of these dynamics, how inclusion could change our current understanding of electricity and magnetic, as well as implications for potential, vast, practical ramifications to the disciplines of physics, engineering, and energy generation.

It is the purpose of this book and particularly this chapter to report on these unique, various recent inventions and their possible modes of operation, but also to convince those listening of their value for hopefully directing a future program geared towards the rigorous clarification and certification, of the specific role the electroscalar domain might play in shaping a future, consistent, classical, electrodynamics—also by extension to perhaps shed light on current thorny conceptual and mathematical inconsistencies that do exist, in the present interpretation of relativistic quantum mechanics. In this regard, it is anticipated that by incorporating this more expansive electrodynamic model, the source of the extant problems with gauge invariance in quantum electrodynamics and the subsequent unavoidable divergences in energy/charge might be identified and ameliorated.

Not only does the electroscalar domain have the potential to address such lofty theoretical questions surrounding fundamental physics, but also another aim of this chapter is to show that the protocol necessary for generating these field effects may not be present only in exotic conditions involving large field strengths and specific frequencies involving expensive infrastructure such as the large Hadron Collider (LHC), but as recent discoveries suggest may be present in the physical manipulation

of ordinary everyday objects. We will also see that nature has been and may be engaged in the process of using scalar longitudinal waves (SLW) in many ways as yet unsuspected and undetected by humanity. Some of these modalities of scalar wave generation we will investigate will include the following: chemical bond breaking, particularly as a precursor to seismic events (illuminating the study and development of earthquake early warning system), solar events (related to eclipses), and sunspot activity and how it impacts the earth's magnetosphere. Moreover, this overview of the unique aspects of the electroscalar domain will suggest that many of the currently unexplained anomalies such as over-unity power observed in various energy devices, and exotic energy effects associated with low energy nuclear reactions (LENR), may find some basis in fact.

As we did mention at the beginning of this chapter, under Sect. 6.0, in regards to the latter “cold fusion”-type scenarios, the electroscalar wave might be the actual agent needed to reduce the nuclear Coulomb barrier, thus providing the long-sought-after viable theoretical explanation of this phenomenon [4]. Longitudinal electrodynamic forces in exploding wires, etc. may actually be due to the operation of electroscalar waves at the subatomic levels of nature. For instance, the extraordinary energies produced by Ken Shoulder's charge clusters may also possibly be due to electroscalar mechanisms. Moreover, these observations, spanning as they do cross many cross-disciplines of science, beg the question as to the possible universality of the SLW—that the concept of the longitudinal electroscalar wave, not present in current electrodynamics, may represent a general, key, overarching principle, leading to new paradigms in other science besides physics. This idea will also be explored in the talk, showing the possible connection of scalar longitudinal (also known as electroscalar) wave dynamics to biophysical systems. Admittedly, we're proposing quite an ambitious agenda in reaching for these goals, but I think you will see that recent innovations will have proven equal to the task of supporting this quest.

Insight into the incompleteness of classical electrodynamics can begin with the Helmholtz theorem, which states that any sufficiently smooth three-dimensional vector field can be uniquely decomposed into two parts. By extension, a generalized theorem exists, certified through the recent scholarly work of physicist-mathematician Dale Woodside [5] (see Eq. (6.44) above as well) for unique decomposition of a sufficiently smooth Minkowski four-vector field (three spatial dimensions, plus time) into four-irrotational and four-solenoidal parts, together with the tangential and normal components on the bounding surface. With this background, the theoretical existence of the electroscalar wave can be attributed to failure to include certain terms in the standard, general, four-dimensional, electromagnetic, Lagrangian density that are related to the four-irrotational parts of the vector field. Here, ϵ is electrical permittivity—not necessarily of the vacuum. Specifically, the electroscalar field becomes incorporated in the structure of electrodynamics, when we let Eq. (6.44) above for $\gamma = 1$, and $k = (2\pi m c/h) = 0$. As we can see in this representation as it is written for Eq. (6.44), it is the presence of the third term that describes these new features.

We can see more clearly how this term arises by writing the Lagrangian density in terms of the standard electromagnetic scalar (ϕ) (see Eq. 6.45 above) and magnetic vector potentials (A), without the electroscalar representation included. This equation has zero divergence of the potentials (formally called solenoidal), consistent with classical electromagnetics, as we see here. The second class of four-vector fields has zero curl of the potentials (irrotational vector field), which will emerge once we add this scalar factor. Here we see that it is represented by the last term, which is usually zero in standard classical electromagnetics. The expression in the parentheses, when set equal to zero, describes what is known as the Lorentz condition, which makes the scalar potential and the vector potential in their usual form, mathematically *dependent* on each other. Accordingly, the usual electromagnetic theory then specifies that the potentials may be chosen arbitrarily, based on the specific, so-called, gauge that is chosen for this purpose. However, the MCE theory allows for a nonzero value for this scalar-valued expression, essentially making the potentials *independent* of each other, where this new scalar-valued component (C in Eq. 6.45 that we may call it *Lagrangian density*) is a dynamic function of space and time. It is from this new idea of independence of the potentials which the scalar value (C) is derived, and from which the unique properties and dynamics of the scalar longitudinal electrodynamic (SLW) wave arise.

To put all these in perspective, a more complete electrodynamic model may be derived from this last equation of the Lagrangian density. The Lagrangian expression is important in physics, since invariance of the Lagrangian under any transformation gives rise to a conserved quantity. Now, as is well known, conservation of charge current is a fundamental principle of physics and nature. Conventionally, in classical electrodynamics charged matter creates an \vec{E} field. Motion of charged matter creates a magnetic \vec{B} field from an electrical current which in turn influences the \vec{B} and \vec{E} fields.

Before we continue further, let us write the following equations as

$$\vec{E} = -\nabla\phi - \frac{\partial \vec{A}}{\partial t} \quad \text{Relativistic Covariance} \quad (6.46)$$

$$\vec{B} = \nabla \times \vec{A} \quad \begin{array}{l} \text{Classical fields } (\vec{B} \text{ and } \vec{E}) \\ \text{in terms of usual classical} \\ \text{potentials } (\vec{A} \text{ and } \phi) \end{array} \quad (6.47)$$

$$C = \frac{1}{c^2} \frac{\partial \phi}{\partial t} + \nabla \cdot \vec{A} \quad \text{Classical wave equation for } \vec{A}, \vec{B} \quad (6.48)$$

$$\nabla \times \vec{B} - \frac{1}{c^2} \frac{\partial \vec{E}}{\partial t} - \nabla C = \mu \vec{J} \quad \vec{E} \text{ and } \phi \text{ without the use of a gauge} \quad (6.49)$$

$$\nabla \cdot \vec{E} + \frac{\partial C}{\partial t} = \frac{\rho}{\epsilon} \quad \text{Condition (the MCE theory produces}$$

cancellation of $\partial C/\partial t$ and $-\nabla C$ in the

$$\text{classical wave equation for } \vec{\phi} \text{ and } \vec{A}, \quad (6.50)$$

thus eliminating the need for a gauge condition)

These effects can be modeled by Maxwell's equations. Now, exactly how and to what degree do these equations change when the new scalar-valued C field is incorporated. Those of you who are knowledgeable of Maxwellian theory will notice that the two homogeneous Maxwell's equations—representing Faraday's law and $\nabla \cdot \vec{B}$ (standard Gauss law equation for divergence-less magnetic field)—are both unchanged from the classical model. Notice that the last three equations incorporate this new scalar component which is labeled C . This formulation as defined by Eq. (6.48) creates a somewhat revised version of Maxwell's equations, with one new term $-\nabla C$ in Gauss law (Eq. 6.50), where ρ is the charge density, and one new term $(\partial C/\partial t)$ in Ampere's law (Eq. 6.49), where J is the current density. We see that these new equations lead to some important conditions. First, relativistic covariance is preserved. Second, unchanged are the classical fields \vec{E} and \vec{B} in terms of the usual classical potentials (\vec{A} and $\vec{\phi}$). We have the same classical wave equations for \vec{A} , $\vec{\phi}$, \vec{E} , and \vec{B} *without* the use of a gauge condition (and its attendant incompleteness) since the MCE theory shows cancellation of $\partial C/\partial t$ and $-\nabla C$, the classical wave equations for $\vec{\phi}$ and \vec{A} ; and a scalar longitudinal wave (SLW) is revealed, composed of the scalar and longitudinal electric fields.

A wave equation for C is revealed by use of the time derivative of Eq. (6.50), added to divergence of Eq. (6.49). Now, as is known, matching conditions at the interface between two different media are required to solve Maxwell's equations. The divergence theorem on Eq. (6.51) below will yield interface matching in the normal component (" \hat{n} ") of $\nabla C/\mu$ as shown in Eq. (6.15):

$$\frac{\partial^2 C}{\partial c^2 t^2} - \nabla^2 C = \square^2 C = \mu \left(\frac{\partial \rho}{\partial t} + \nabla \cdot \vec{J} \right) \quad (6.51)$$

$$\left(\frac{\nabla C}{\mu} \right)_{1n} = \left(\frac{\nabla C}{\mu} \right)_{1n} \quad (6.52)$$

$$C = C_0 \exp[j(kr - \omega t)]/r \quad (6.53)$$

Note: The above sets of Eqs. (6.51) and (6.52) present wave equation for scalar factor C matching condition in normal component of $\nabla C/\mu$; spherically symmetric wave solution for C ; and the operator $\square^2 = \frac{\partial^2}{\partial c^2 t^2} - \nabla^2$, and it is called d'Alembert operator.

The subscripts in Eq. (6.15) denote $\nabla C/\mu$ in medium 1 or medium 2, respectively, and (μ) is magnetic permeability—again not necessarily that of the vacuum. In this regard, with the vector potential (\vec{A}) and scalar potential ($\vec{\phi}$) now stipulated as independent of each other, it is the surface charge density at the interface which produces a discontinuity in the gradient of the scalar potential, rather than the standard discontinuity in the normal component of \vec{E} (see Hively) [3].

Notice also from Eq. (6.51) that the source for the scalar factor C implies a violation of charge conservation (RHS (right-hand side) nonzero), a situation which we noted cannot exist in macroscopic nature. Nevertheless, this will be compatible with standard Maxwellian theory if this violation occurs at very short time scales, such as occur in subatomic interactions. Now, interestingly, with the stipulation of charge conservation on large time scales, giving zero on RHS of Eq. (6.51), longitudinal wavelike solutions are produced with the lowest order form in a spherically symmetric geometry at a distance (r), $C = C_0 \exp [j(kr - \omega t)]/r$. Applying the boundary condition $C \rightarrow 0$ as $r \rightarrow \infty$ is thus trivially satisfied. The C wave therefore is a *pressure* wave, similar to that in acoustics and hydrodynamics. This is unique under the new MCE model since, although classical electrodynamics forbids a spherically symmetric *transverse* wave to exist, this constraint will be absent under MCE theory. Also, an unprecedented result is that these longitudinal C waves will have energy but no momentum. But this is not unlike charged-particle-antiparticle fluctuations which also have energy but no net momentum.

Now that we are here so far, the question of why this constraint prohibiting a spherically symmetric wave is lifted in MCE can be seen in the following sets of Eq. (6.54) as below for the wave equation for the vertical magnetic field:

$$\left\{ \begin{array}{l} \frac{1}{c^2} \frac{\partial^2 \vec{B}}{\partial t^2} - \nabla^2 \vec{B} = \mu_0 (\nabla \times \vec{J}) \\ \nabla \times \vec{J} = 0 \rightarrow J = \nabla k \\ \text{Gradient-Driven Current} \rightarrow \text{SLW} \end{array} \right. \quad (6.54)$$

The sets of Eq. (6.54) are established for wave equation for \vec{B} resulting gradient-driven current in more complete electrodynamic (MCE) for generating scalar longitudinal wave (SLW).

Notice again that the source of the magnetic field (right-hand side (RHS)) is a nonzero value of $\nabla \times \vec{J}$, which signifies solenoidal current density, as is the case in standard Maxwellian theory. When \vec{B} is zero, so is $\vec{\nabla} \times \vec{J}$. This is an important result. Then the current density is irrotational, which implies that $J = \nabla k$. Here κ is a scalar function of space and time. Thus, in contrast to closed current paths generated in ordinary Maxwell theory which result in classical waves that arise from a solenoidal current density ($\vec{\nabla} \times \vec{J} \neq 0$), J for the scalar longitudinal wave (SLW) is gradient driven and may be uniquely detectable. We also see from this result that a

zero value of the magnetic field is a necessary and sufficient condition for this gradient-driven current. Now, since in linearly conductive media the current density (\vec{J}) is directly proportional to the electric field intensity (\vec{E}) that produced it, where σ is the conductivity, this gradient-driven current will then produce a longitudinal \vec{E} field.

Based on so far calculations, we can establish wave equation for \vec{E} solution for longitudinal \vec{E} in MCE spherically symmetric wave solutions for \vec{E} and \vec{J} in *linearly conductive* media:

$$\frac{\partial^2 \vec{E}}{\partial c^2 t^2} - \nabla^2 \vec{E} = \left(\frac{\partial^2}{\partial c^2 t^2} - \nabla^2 \right) \vec{E} \equiv \square^2 \vec{E} = -\mu \frac{\partial \vec{J}}{\partial t} - \frac{\nabla \rho}{\epsilon} \quad (6.55)$$

$$E = E_r \hat{r} \exp[j(kr - \omega t)]/r \quad (6.56)$$

$$\vec{J} = \sigma \vec{E} \quad \rightarrow \quad \square^2 \vec{J} = 0 \quad (6.57)$$

We can also see this from examining the standard vectorial wave equation for the electric field. The wave equation for \vec{E} (Eq. 6.55) arises from the curl of Faraday's law, use of $\nabla \times \vec{B}$ from Ampere's law Eq. (6.49), and substitution of $\nabla \cdot \vec{E}$ from Eq. (6.50) with cancellation of the terms $\nabla(\partial C/\partial t) = (\partial/\partial t)\nabla C$. When the RHS of Eq. (6.50) is zero, the lowest order outgoing spherical wave is $E = E_r \hat{r} \exp[j(kr - \omega t)]/r$, where \hat{r} represents the unit vector in the radial direction and r represents the radial distance. The electrical field is also longitudinal. Substitution of $\vec{J} = \sigma \vec{E}$ into $\square^2 \vec{E} = 0$ results in $\square^2 \vec{J} = 0$, meaning that current density is also radial. The SLW equations for E and J are remarkable for several reasons. First, the vector SLW equations for \vec{E} and \vec{J} are fully captured in one wave equation for the scalar function (κ), $\square^2 \kappa = 0$. Second, these forms are like $\square^2 C = 0$. Third, these equations have zero on the RHS for propagation in conductive media. This arises since $\vec{B} = 0$ for the SLW, implying no back electromagnetic field from $\partial \vec{B} / \partial t$ in Faraday's law which in turn gives no circulating eddy currents. Experimentation has shown that the SLW is not subject to the skin effect in media with linear electric conductivity, and travels with minimum resistance in any conductive media.

This last fact affords some insight into another related ongoing conundrum in condensed matter physics—the mystery surrounding high-temperature superconductivity (HTS). As we know, the physical problem of high HTS is one of the major unsolved problems in theoretical condensed matter physics, in part, because the materials are somewhat complex, multilayered crystals.

Here the more complete electrodynamic (MCE) theory may provide an explanation on the basis of gradient-driven currents between (or among) the crystal layers. The new MCE Hamiltonian (Eq. 6.16) includes the SLW due to gradient-driven currents among the crystalline layers as an explanation for high temperature superconductivity (HTS).

The electrodynamic Hamiltonian for more complete electrodynamic (MCE) is written as

$$\mathcal{H}_{EM} = \left(\frac{\epsilon E^2}{2} + \frac{B^2}{2\mu} \right) + \left(\rho - \epsilon(\vec{\nabla} \cdot \vec{E}) \right) \vec{\phi} - \vec{J} \cdot \vec{A} + \frac{C^2}{2\mu} + \frac{C \vec{\nabla} \cdot \vec{A}}{\mu} \quad (6.58)$$

In conclusion we can build an antenna based on the above concept within laboratory environment and use a simulation software such as multi-physics COMSOL© or ANSYS computer code to model such antenna.

However, we believe that we have examined adequate analysis in this white paper to show the field of electrodynamics (classical and quantum), although considered to be totally understood, with any criticisms of incompleteness on the part of dissenters essentially taken as veritable heresy; nevertheless it needs re-evaluation in terms of apparent unfortunate sins of omission in the failure to include an electroscalar component. Anomalies previously not completely understood may get a boost of new understanding from the operation of electroscalar energy. We have seen in the three instances examined—the mechanism of generation of seismic precursor electrical signals due to the movement of the earth’s crust, ordinary peeling of adhesive tape, as well as irradiation by the special TESLAR chip, the common feature of the breaking of chemical bonds. In fact, we may ultimately find that any phenomena requiring the breaking of chemical bonds, in either inanimate or biological systems, may actually be scalar wave mediated.

Thus, we may discover that the scientific disciplines of chemistry or biochemistry may be more closely related to physics than is currently thought. Accordingly, the experimental and theoretical re-evaluation of even the simplest phenomena in this regard, such as tribo-electrification processes described above, is of the absolute essence for those researchers knowledgeable of the necessity for this reassessment of electromagnetics. As I said in my introduction, it may even turn out that the gradient-driven current and associated scalar longitudinal wave could be the umbrella concept under which many of the currently unexplained electrodynamic phenomena that are frequently under discussion in our conferences might find a satisfying explanation. The new scalar longitudinal wave patent itself—which is the centerpiece of this talk—is a primary example of the type of invention that probably would not have seen the light of day even 10 years ago. As I had previously mentioned, we are seeing more of this inspired breakthrough technology based on operating principles formerly viewed with rank skepticism boarding on haughty derision by mainstream science, now surfacing to provide an able challenge to the prevailing worldview by reproducible corroborating tests by independent sources. This revolution in the technological witness to the overhaul of current orthodoxy is definitely a harbinger

of the rapidly approaching time where many of the encrusted and equally ill-conceived still accepted paradigms of science, thought to underpin our sentient reality, will fall by the wayside. On a grander panoramic scale, our expanding knowledge gleaned from further examining the electroscalar wave concept, as applied to areas of investigation such as cold fusion research and over-unity power sources, will explicitly shape the future of society as well as science, especially concerning our openness to phenomena that challenge our current belief systems.

To the point, the incompleteness in our received understanding of the properties of electrodynamic systems can be attributed to the failure to properly incorporate what can be termed the electroscalar force in the structural edifice of electrodynamics. Unbeknownst to most specialists in the disciplines mentioned, over the last decade in technological circles of development, there has quietly but inexorably emerged bona fide physical evidence of the demonstration of the existence of scalar longitudinal wave dynamics in recent inventions and discoveries. As technology leads to new understanding, at this point we are certainly rapidly approaching a time in which these findings can no longer be pushed aside or ignored by orthodox physics, and physics must come to terms with their potential physical and philosophical impacts on our world society. By the time you read this book, this author thinks you might agree with the fact that we could be on the brink of a new era in science and technology, the likes of which this generation has never seen before. Despite what mainstream physics may claim, the study of electrodynamics is by no means a closed book. Further details are provided in the following sections of this chapter.

6.3 Description of $\vec{B}^{(3)}$ Field

During the investigation of the theory optically induced line shifts in nuclear magnetic resonance (NMR), people have come across the result that the antisymmetric part of the intensity tensor of light is directly proportional in free space to an entirely novel, phase-free, magnetic field of light, which was identified as $\vec{B}^{(3)}$ field, and which is defined in the following such as Eq. (6.59a–6.59c). The presence of $\vec{B}^{(3)}$ in free space shows that the usual, propagating, transverse waves of electromagnetic radiation are linked geometrically to the spin field $\vec{B}^{(3)}$, which indeed emerges directly from the fundamental, classical equation of motion of a single electron in a circularly polarized light beam [6]:

$$\vec{B}^{(1)} \times \vec{B}^{(2)} = iB^{(0)}\vec{B}^{(3)} \quad (6.59a)$$

$$\vec{B}^{(2)} \times \vec{B}^{(3)} = iB^{(0)}\vec{B}^{(1)*} \quad (6.59b)$$

$$\vec{B}^{(3)} \times \vec{B}^{(1)} = iB^{(0)}\vec{B}^{(2)*} \quad (6.59c)$$

Note that the symbol of (*) means conjugate form of the field, and super-scribe (1), (2), and (3) can be permuted to give the other two equations in Eq. (6.1); hence the fields $\vec{B}^{(1)}$, $\vec{B}^{(2)}$, and $\vec{B}^{(3)}$ are simply components of the magnetic flux density of *free space* electromagnetism in a circular, rather than in a Cartesian, basis. In the quantum field theory, the longitudinal component $\vec{B}^{(3)}$ becomes the fundamental photomagnetic of light, and operator defined by the following relationship as [7–12]

$$\widehat{B}^{(3)} = B^{(0)}\frac{\widehat{P}}{\hbar} \quad (6.60)$$

where \widehat{P} is the angular momentum operator of one photon. The existence of the longitudinal $\widehat{B}^{(3)}$ in free space is indicated experimentally by optically induced NMR shifts and by several well-known phenomena of magnetization by light, for example the inverse Faraday effects.

The core logic of Eqs. (6.59a–6.59c) asserts that there exists a novel cyclically symmetric field algebra in free space, implying that the usual transverse solutions of Maxwell's equations are tied to the longitudinal, nonzero, real, and physical magnetic flux density $\vec{B}^{(3)}$, which we name the spin field. This deduction changes fundamentally our current appreciation of electrodynamics and therefore the principles on which the old quantum theory was derived, for example the Planck law [13] and the light quantum hypothesis proposed in 1905 by Einstein. The belated recognition of $\vec{B}^{(3)}$ implies that there is a magnetic field in free space which is associated with the longitudinal space axis, z , which is labeled (3) in the circular basis. Conventionally, the radiation intensity distribution is calculated using only two, transverse, degrees of freedom, right and left circular, corresponding to (1) and (2) in the circular basis.

The $\vec{B}^{(3)}$ field of vacuum electromagnetism introduces a new paradigm of the field theory, summarized in the cyclically symmetric equations linking it to the usual transverse magnetic plane wave components $\vec{B}^{(1)} = \vec{B}^{(2)*}$ [3, 6, 14, 15].

The $\vec{B}^{(3)}$ field was first and obliquely inferred in January 1992 at Cornell University from a careful, re-examination of known magneto-optics phenomena [16, 17] which had previously been interpreted in orthodoxy through the conjugate product $\vec{E}^{(1)} \times \vec{E}^{(2)}$ of electric plane wave components $\vec{E}^{(1)} \times \vec{E}^{(2)*}$. In the intervening three and a half years its understanding has developed substantially into monographs and papers [3, 6, 14, 15] covering several fundamental aspects of field theory.

The $\vec{B}^{(3)}$ field produces magnetization in an electron plasma which is proportional to the square root of the power density dependence of the circularly polarized electromagnetic radiation, conclusive evidence for the presence of the phase-free $\vec{B}^{(3)}$ in the

vacuum. There are many experimental consequences of this finding, some of which are of practical utility, such as optical NMR. However, the most important theoretical consequence is that there exist longitudinal components in free space of electromagnetic radiation, a conclusion which is strikingly reminiscent of that obtained from the theory of finite photon mass. The two ideas are interwoven throughout the volume. The characteristic square root light intensity dependence of $\vec{B}^{(3)}$ dominates and is theoretically observable at low cyclotron frequencies when intense, circularly polarized electromagnetic radiation interacts with a single electron, or in practical terms an electron plasma or beam. The magnetization induced in such an electron ensemble by circularly polarized radiation is therefore expected to be proportional to the square root of the power density (i.e., the intensity in watts per square meter) of the radiation. This result emerges directly from the fundamental, classical, equation of motion of one electron in the beam, the relativistic Hamilton-Jacobi equation.

To establish the physical presence of $\vec{B}^{(3)}$ in the vacuum therefore requires the observation of this magnetization as a function of the beam's power density, a critically important experiment. Other possible experiments to detect $\vec{B}^{(3)}$, such as the optical equivalent of the Aharonov-Bohm effect, are suggested throughout the volume.

More details about the subject in this section can be found in the references that are mentioned in the count of this section and above and further details are beyond the scope of this book. Thus, we encourage the readers to refer themselves to those references from [3, 6–12, 14–17].

6.4 Scalar Wave Description

What is a “scalar wave” exactly? Scalar wave (SW) is just another name for a longitudinal wave (LW). The term “scalar” is sometimes used instead because the hypothetical source of these waves is thought to be a “scalar field” of some kind similar to the Higgs field for example.

In general, definition of longitudinal wave falls into the following description:

A wave motion in which the particles of the medium oscillate about their mean positions in the direction of propagation of the wave is called longitudinal wave.

For longitudinal wave the vibration of the particles of the medium is in the direction of wave propagation. A longitudinal wave proceeds in the form of compression and rarefaction which is the stretch and compression in the same direction as the wave moves. For a longitudinal wave at places of compression the pressure and density tend to be maximum, while at places where rarefaction takes place the pressure and density are minimum. In gases only longitudinal wave can propagate. Longitudinal waves are known as compression waves.

A longitudinal wave travels through a medium in the form of compressions or condensations C and rarefaction R . A compression is a region of the medium in

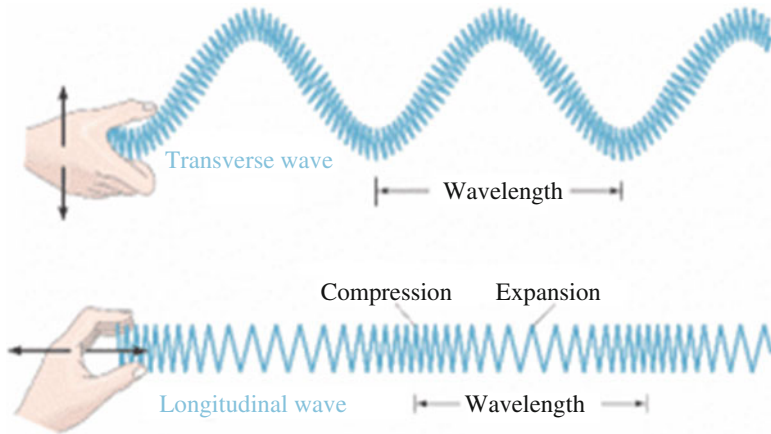


Fig. 6.6 Illustration of transverse wave and longitudinal wave

which particles are compressed, i.e., particles come closer, i.e., distance between the particles becomes less than the normal distance between them. Thus, there is temporary decrease in volume and as a consequence increase in density of the medium in the region of compression. A rarefaction is a region of the medium in which particles are rarefied, i.e., particles get farther apart than what they normally are. Thus, there is temporary increase in volume and a consequence decrease in density of the medium in the region of rarefaction. See Fig. 6.6.

There is nothing particularly controversial about longitudinal waves (LW) in general. They are a ubiquitous and well-acknowledged phenomenon in nature. Sound waves traveling through the atmosphere (or underwater) are longitudinal, as are plasma waves propagating through space (also known as Birkeland currents). Longitudinal waves moving through the earth's interior are known as "telluric currents." They can all be thought of as pressure waves of sorts.

SW/LW are quite different from "transverse" waves. You can observe transverse waves (TW) by plucking a guitar string or watching ripples on the surface of a pond. They oscillate (vibrate, move up and down, or side to side) perpendicular to their arrow of propagation (directional movement). Comparatively SW/LW oscillate in the same direction as their arrow of propagation. See Fig. 6.6.

In modern-day electrodynamics (both classical and quantum), electromagnetic waves (EMW) traveling in "free space" (such as photons in the "vacuum") are generally considered to be TW. But this was not always the case. When the preeminent mathematician James Clerk Maxwell first modeled and formalized his unified theory of electromagnetism in the late nineteenth century neither the EM SW/LW nor the EM TW had been experimentally proven, but he had postulated and calculated the existence of both.

After Heinrich Hertz demonstrated experimentally the existence of transverse radio waves in 1887, theoreticians (such as Heaviside, Gibbs, and others) went about

revising Maxwell's original equations (who was now deceased and could not object). They wrote out the SW/LW component from the original equations because they felt the mathematical framework and theory should be made to agree only with experiment. Obviously, the simplified equations worked—they helped make the AC/DC electrical age engineerable. But at what expense?

Then in 1889 Nikola Tesla, a prolific experimental physicist and inventor of alternative current (AC), threw a proverbial wrench in the works when he discovered experimental proof for the elusive electric scalar wave. This seemed to suggest that SW/LW, opposed to TW, could propagate as pure electric waves or as pure magnetic waves. Tesla also believed that these waves carried a hitherto-unknown form of excess energy he referred to as "radiant." This intriguing and unexpected result was said to have been verified by Lord Kelvin and others soon after.

However, instead of merging their experimental results into a unified proof for Maxwell's original equations, Tesla, Hertz, and others decided to bicker and squabble over who was more correct. In actuality they both derived correct results. But because humans (even "rational" scientists) are fallible and prone to fits of vanity and self-aggrandizement, each side insisted dogmatically that they were right, and the other side was wrong.

The issue was allegedly settled after the dawn of the twentieth century when:

- (a) The concept of the mechanical (passive/viscous) ether was purportedly disproven by Michelson-Morley and replaced by Einstein's relativistic space-time manifold.
- (b) Detection of SW/LWs proved much more difficult than initially thought (mostly due to the wave's subtle densities, fluctuating frequencies, and orthogonal directional flow). As a result, the truncation of Maxwell's equations was upheld.

SW/LW in free space however are quite real. Beside Tesla, empirical work carried out by electrical engineers such as Eric Dollard, Konstantin Meyl, Thomas Imlauer, and Jean-Louis Naudin (to name only some) have clearly demonstrated their existence experimentally. These waves seem able to exceed the speed of light, pass through EM shielding (also known as Faraday cages), and produce over-unity (more energy out than in) effects. They seem to propagate in a yet-unacknowledged counter-spatial dimension (also known as hyperspace, pre-space, false-vacuum, Aether, implicit order, etc.).

Because the concept of an all-pervasive material ether was discarded by most scientists, the thought of vortex-like electric and/or magnetic waves existing in free space, without the support of a viscous medium, was thought to be impossible. However later experiments carried out by Dayton Miller, Paul Sagnac, E.W. Silvertooth, and others have contradicted the findings of Michelson and Morley. More recently Italian mathematician-physicist Daniele Funaro, American physicist-systems theorist Paul LaViolette, and British physicist Harold Aspden have all conceived of (and mathematically formulated) models for a free space ether that is dynamic, fluctuating, and self-organizing, and allows for the formation and propagation of SW/LW.

With the appearance of experiments on nonclassical effects of electrodynamics, authors often speak of electromagnetic waves not being based on oscillations of electric and magnetic fields. For example, it is claimed that there is an effect of such waves on biological systems and the human body. Even medical devices are sold which are assumed to work on the principle of transmitting any kind of information via “waves,” which have a positive effect on human health. In all cases, the explanation of these effects is speculative, and even the transmission mechanism remains unclear because there is no sound theory on such waves, often subsumed under the notion “scalar waves.” We try to give a clear definition of certain types of waves which can serve to explain the observed effects [18].

Before analyzing the problem in more detail, we have to discern between “scalar waves,” which contain fractions of ordinary electric and magnetic fields and such waves which do not and therefore appear even more obscure. Often “scalar waves” are assumed to consist of longitudinal fields. In ordinary Maxwellian electrodynamics such fields do not exist, and electromagnetic radiation is said to be always transversal. In modern unified physics approaches like Einstein-Cartan-Evans theory [19, 20], however, it was shown that polarization directions of electromagnetic fields do exist in all directions of four-dimensional space. So, in the direction of transmission, an ordinary electromagnetic wave has a longitudinal magnetic component, the so-called $\vec{B}^{(3)}$ field of Evans [21]. (See Sect. 6 of this chapter for more details about $\vec{B}^{(3)}$ field.) The $\vec{B}^{(3)}$ field is detectable by the so-called inverse Faraday effect which is known experimentally since the 1960s [22]. Some experimental setups, for example the “magnifying transmitter” of Tesla [16, 17], make the claim to utilize these longitudinal components. They can be considered to consist of an extended resonance circuit where the capacitor plates have been displaced to the transmitter and receiver site each (see Fig. 6.7). In an ordinary capacitor (or cavity resonator), a very-high-frequent wave (GHz or THz range) leads to significant runtime effects of the signal so that the quasi-static electric field can be considered to be cut into pulses. These represent the near field of an electromagnetic wave and may be considered to

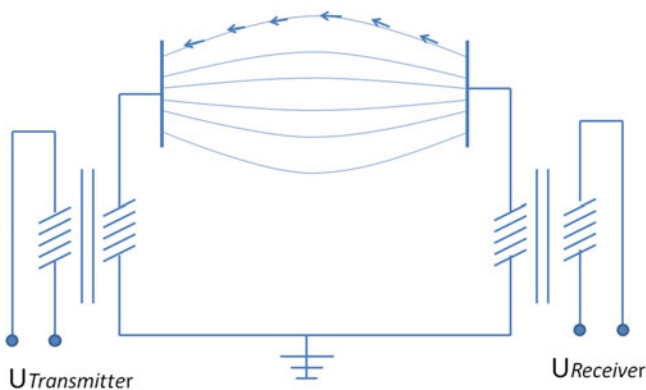


Fig. 6.7 Propagation of longitudinal electric wave according to Tesla

be longitudinal. For lower frequencies, the electric field between the capacitor plates remains quasi-static and therefore longitudinal too.

We do not want to go deeper into this subject here. Having given hints for the possible existence of longitudinal electric and magnetic fields, we leave this area and concentrate on mechanisms which allow transmission of signals even without any detectable electromagnetic fields.

Before we move on with more details of scalar wave we need to lay ground about the types of waves, where the scalar wave falls under that category; thus we need to have some idea about *transverse wave* and *longitudinal wave* and what their descriptions are. This is the subject that was discussed in previous section of this chapter quite extensively; however, we talk furthermore about the subject of longitudinal potential wave in the next section here.

6.5 Longitudinal Potential Waves

In the following we develop the theory of electromagnetic waves with vanishing field vectors. Such a field state is normally referred to as a “vacuum state” and was described in full relativistic detail in [22]. Vacuum states also play a role in the microscopic interaction with matter. Here we restrict consideration to ordinary electrodynamics to give engineers a chance to fully understand the subject. With \vec{E} and \vec{B} designating the classical electric and magnetic field vectors, a vacuum state is defined by

$$\vec{E} = 0 \quad (6.61)$$

$$\vec{B} = 0 \quad (6.62)$$

The only possibility to find electromagnetic effects then is by the potentials. These are defined as vector and scalar potentials to constitute the “force” fields \vec{E} and \vec{B} as

$$\vec{E} = -\nabla U - \dot{\vec{A}} \quad (6.63)$$

$$\vec{B} = \nabla \times \vec{A} \quad (6.64)$$

with electric scalar potential U and magnetic vector potential \vec{A} . The dot above the \vec{A} , in Eq. (6.63), denotes the time derivative. For the vacuum, conditions as stated in Eq. (6.61) and Eq. (6.62) will lead to the following sets of equations:

$$\nabla U = -\dot{\vec{A}} \quad (6.65)$$

$$\vec{\nabla} \times \vec{A} = 0 \quad (6.66)$$

From Eq. (6.66), it follows immediately that the vector potential is vortex free, representing a laminar flow. The gradient of the scalar potential is coupled to the time derivative of the vector potential, so both are not independent of one another. A general solution of these equations was derived in [22]. This is a wave solution where \vec{A} is in the direction of propagation, i.e., this is a longitudinal wave. Several wave forms are possible, which may even result in a propagation velocity different from the speed of light c . As a simple example we assume a sine-like behavior of vector potential \vec{A} as

$$\vec{A} = \vec{A}_0 \sin(\vec{k} \cdot \vec{x} - \omega t) \quad (6.67)$$

with direction of propagation \vec{k} (wave vector), space coordinate vector \vec{x} , and time frequency ω . Then it follows from Eq. (6.66) that

$$\nabla U = \vec{A}_0 \omega \cos(\vec{k} \cdot \vec{x} - \omega t) \quad (6.68)$$

This condition has to be met for any potential U . We make the approach as

$$U = U_0 \sin(\vec{k} \cdot \vec{x} - \omega t) \quad (6.69)$$

To find that

$$\nabla U = k U_0 \cos(\vec{k} \cdot \vec{x} - \omega t) \quad (6.70)$$

which, compared to Eq. (6.68), defines the constant \vec{A}_0 to be as

$$\vec{A}_0 = \vec{k} \left(\frac{U_0}{\omega} \right) \quad (6.71)$$

Obviously, the waves of \vec{A} and U have the same phase. Next, we consider the energy density of such a combined wave. This is in general given by

$$w = \frac{1}{2} \epsilon_0 \vec{E}^2 + \frac{1}{2\mu_0} \vec{B}^2 \quad (6.72)$$

From Eqs. (6.65) and (6.66), it is seen that the magnetic field disappears identically, but the electric field is a vanishing sum of two terms, which are different from zero.

These two terms evoke an energy density of space where the wave propagates. This cannot be obtained out of the force fields (these are zero) but must be computed from the constituting potentials. As discussed in the paper by (Eckardt and Lindstrom) [20], we have to write

$$w = \frac{1}{2} \epsilon_0 \left(\dot{\vec{A}}^2 + (\nabla U)^2 \right) \quad (6.73)$$

With Eqs. (6.67) and (6.69), it follows that

$$w = \epsilon_0 k^2 U_0^2 \cos^2(\vec{k} \cdot \vec{x} - \omega t) \quad (6.74)$$

This is an oscillating function, meaning that the energy density varies over space and time in phase with the propagation of the wave. All quantities are depicted in Fig. 6.8. Energy density is maximal where the potentials cross the zero axis.

There is a phase shift of 90° between both plots that can be observed in Fig. 6.8.

There is an analogy between longitudinal potential waves and acoustic waves. It is well known that acoustic waves in air or solids are mainly longitudinal too. The

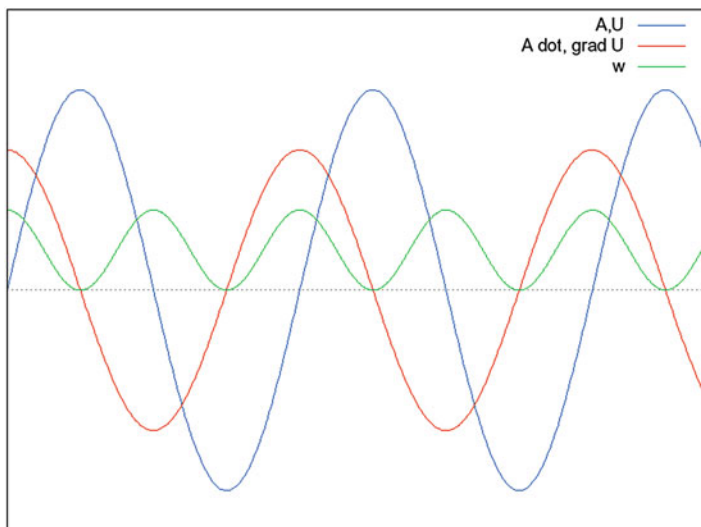


Fig. 6.8 Phases of potentials \vec{A} and U , and energy density w

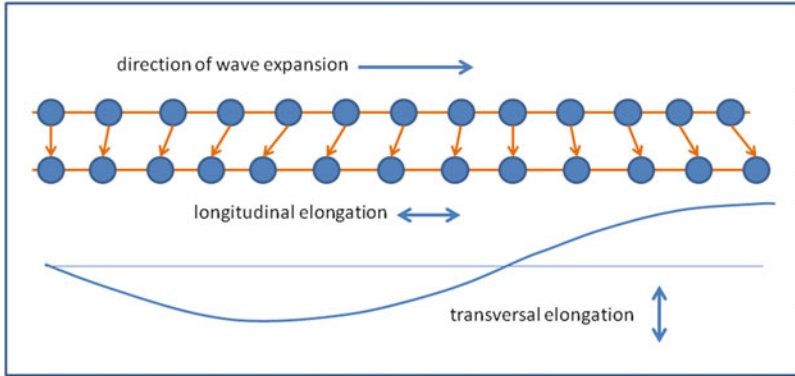


Fig. 6.9 Schematic representation of longitudinal and transversal waves

elongation of molecules is in direction of wave propagation as shown in Fig. 6.9. This is a variation in velocity. Therefore, the magnetic vector potential can be compared with a velocity field. The differences of elongation evoke a local pressure difference. Where the molecules are pressed together, the pressure is enhanced, and vice versa. From conservation of momentum, the force \vec{F} in a compressible fluid is given by

$$\vec{F} = \dot{\vec{u}} + \frac{\nabla p}{\rho} \tag{6.75}$$

In Eq. (6.75), the term \vec{u} is the velocity field, p is the pressure, and ρ is the density of the medium.

This is in full analogy to Eq. (6.63). In particular we see that in the electromagnetic case space-time must be “compressible”; otherwise there will be no gradient of the scalar potential. As a consequence, space itself must be compressible, leading us to the principles of general relativity.

6.6 Transmitters and Receiver for Longitudinal Waves

A sender for longitudinal potential waves has to be a device which avoids producing \vec{E} and \vec{B} fields but sends out oscillating potential waves. We discuss two propositions on how this can be achieved technically. In the first case, we use two ordinary transmitter antennas (with directional characteristic) with distance of half a wavelength (or an odd number of half-waves). This means that ordinary electromagnetic waves cancel out, assuming that the near field is not disturbing significantly. Since

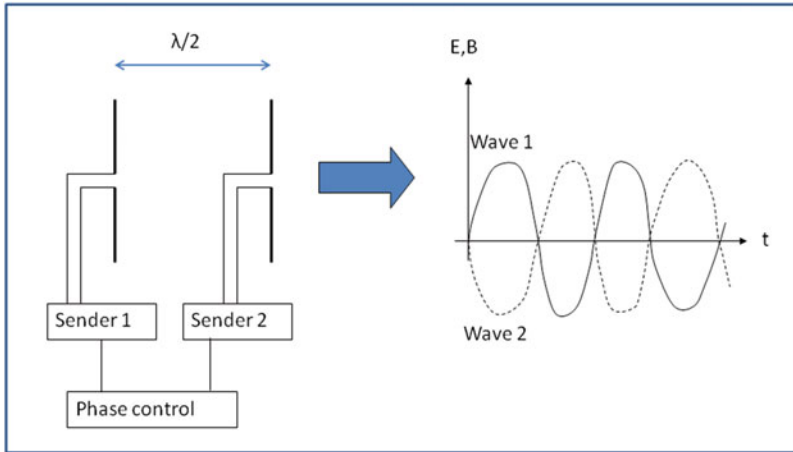


Fig. 6.10 Suggestion for a transmitter of longitudinal potential waves

the radiated energy cannot disappear, it must propagate in space and is transmitted in the form of potential waves. This is depicted in Fig. 6.10.

A more common example is a bifilar flat coil, for example from the patent of Tesla [23]; see Fig. 6.10, second drawing. The currents in opposite directions affect annihilation of the magnetic field component, while an electric part may remain due to the static field of the wires. See Fig. 6.11.

Construction of a receiver is not so straightforward. In principle no magnetic field can be retrieved directly from \vec{A} due to Eq. (6.66). The only way is to obtain an electrical signal by separating both contributing parts in Eq. (6.63) so that the equality [22] is out weighted and an effective electric field remains which can be detected by conventional devices. A very simple method would be to place two plates of a capacitor in distance of half a wavelength (or odd multiples of it). Then the voltage in space should have an effect on the charge carriers in the plates, leading to the same effect as if a voltage had been applied between the plates. The real voltage in the plates or the compensating current can be measured (Fig. 6.12). The “tension of space” operates directly on the charge carriers while no electric field is induced. The \vec{A} part is not contributing because the direction of the plates is perpendicular to it, i.e., no significant current can be induced.

Another possibility of a receiver is to use a screened box (Faraday cage). If the mechanism described for the capacitor plates is valid, the electrical voltage part of the wave creates charge effects which are compensated immediately due to the high conductivity of the material. As is well known, the interior of a Faraday cage is free of electric fields. The potential is constant because it is constant on the box surface. Therefore, only the magnetic part of the wave propagates in the interior where it can be detected by a conventional receiver; see Fig. 6.13.

Fig. 6.11 Tesla coils according to the patent [23]

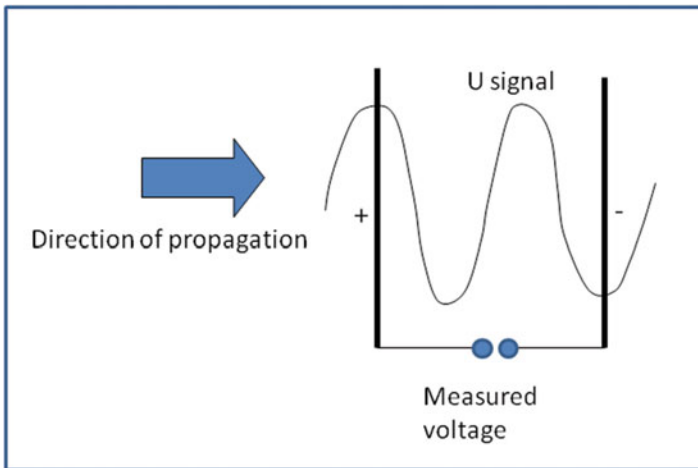
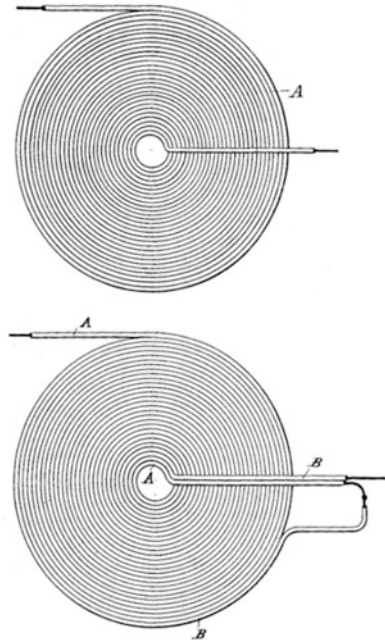


Fig. 6.12 Suggestion for a receiver of longitudinal potential waves (capacitor)

Another method of detection is using vector potential effects in crystalline solids. As is well known from solid-state physics, the vector potential produces excitations within the quantum mechanical electronic structure, provided that the frequency is near to the optical range. Crystal batteries work in this way. They can be

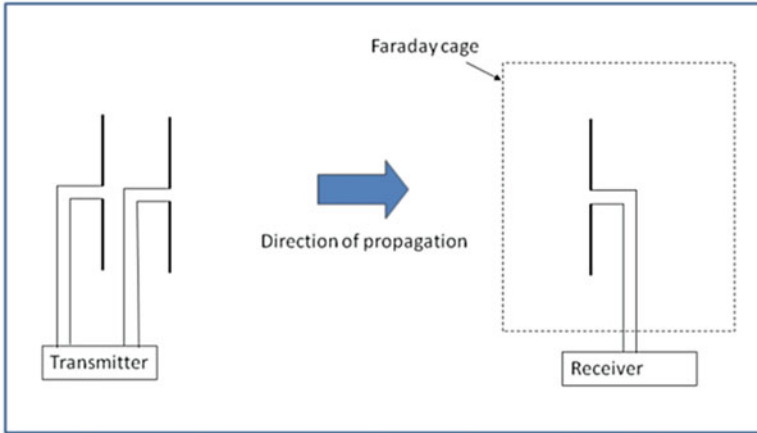


Fig. 6.13 Suggestion for a receiver of longitudinal potential waves (Faraday cage)

engineered through chemical vapor deposition of carbon. In the process you get strong lightweight crystalline shapes that can handle lots of heat and stress by high currents. For detecting longitudinal waves, the excitation of the electronic system has to be measured, for example by photoemission or other energetic processes in the crystal.

All these are suggestions for experiments with longitudinal waves. Additional experiments can be performed for testing the relation between wave vector k and frequency ω to check if this type of waves propagates with ordinary velocity of light c as

$$c = \frac{\omega}{k} \quad (6.76)$$

where k is defined from the wave length λ by the following relation:

$$k = \frac{2\pi}{\lambda} \quad (6.77)$$

As pointed out in the paper by Eckhardt [22], the speed of propagation depends on the form of the waves.

This can even be a nonlinear step function. The experimental setup of Fig. 6.11 can directly be used for finding the $\omega(\vec{k})$ relation because the wavelength and frequency are measured at the same time. There are rumors that Eric P. Dollard [24] found a propagation speed of longitudinal waves of $(\pi/2) \cdot c$, which is 1.5 times the speed of light, but there are no reliable experiments on this reported in the literature.

The ideas worked out in this write-up in this section may not be the only way how longitudinal waves can be explained and technically handled. As mentioned in the introduction, electrodynamics derived from a unified field theory (Evens et al.) [19] predicts effects of polarization in all space and time dimensions and may lead to a discovery of even richer and more interesting effects.

6.6.1 Scalar Communication System

The basic scalar communication system indicates that the communications antenna does not make any sense according to normal electromagnetic theory. The goal of a scalar antenna is to create powerful repulsion/attraction between two magnetic fields, to create large scalar bubbles/voids. This is done by using an antenna with two opposing electromagnetic coils that effectively cancel out as much of each other's magnetic field as possible. An ideal scalar antenna will emit no electromagnetic field (or as little as possible), since all power is being focused into the repulsion/attraction between the two opposing magnetic fields. Normal electromagnetic theory suggests that since such a device emits no measurable electromagnetic field, it is useless and will only heat up.

A scalar signal reception antenna similarly excludes normal electromagnetic waves and only measures changes in magnetic field attraction and repulsion. This will typically be a two-coil-powered antenna that sets up a static opposing or attracting magnetic field between the coils, and the coils are counter-wound so that any normal RF signal will be picked up by both coils and effectively cancel itself out.

It has been suggested that scalar fields do not follow the same rules as electromagnetic waves and can penetrate through materials that would normally slow or absorb electromagnetic waves. If true, a simple proving method is to design a scalar signal emitter and a scalar signal receiver and encasing each inside separate shielded and grounded metal box, known as Faraday cages. These boxes will absorb all normal electromagnetic energy and will prevent any regular non-scalar signal transmissions from passing from one box to the other.

Some people have suggested that organic life may make use of scalar energies in ways that we do not yet understand. Therefore, caution is recommended when experimenting with this fringe technology. However, keep in mind that if scalar fields do exist, we are likely already deeply immersed in an unseen field of scalar noise all the time, generated anywhere two magnetic fields oppose or attract. Common scalar field noise sources include AC electric cords and powerlines carrying high current, and electric motors which operate on the principle of powerful spinning regions of repulsion and attraction.

6.7 Scalar Wave Experiments

It can be shown that scalar waves, normally remaining unnoticed, are very interesting in practical use for information and energy technology for reason of their special attributes. The mathematical and physical derivations are supported by practical experiments. The demonstration will show:

1. The wireless transmission of electrical energy
2. The reaction of the receiver to the transmitter
3. Free energy with an over-unity effect of about 3
4. Transmission of scalar waves with 1.5 times the speed of light
5. The inefficiency of a Faraday cage to shield scalar waves

6.7.1 Tesla Radiation

Here is shown extraordinary science, five experiments, which are incompatible with textbook physics. Following short courses, that were given by Meyl [25], show the transmission of longitudinal electric waves.

It is a historical experiment, because already 100 years ago the famous experimental physicist Nikola Tesla has measured the same wave properties, as me. From him stems a patent concerning the wireless transmission of energy (1900) [26]. Since he also had to find out that at the receiver arrives more energy very much, than the transmitter takes up, he spoke of a “magnifying transmitter”.

By the effect back on the transmitter Tesla sees if he has found the resonance of the earth and that lies according to his measurement at 12 Hz. Since the Schumann resonance of a wave, which goes with the speed of light, however, lies at 7.8 Hz, Tesla comes to the conclusion that his wave has 1.5 times the speed of light c [27].

As founder of the diathermy Tesla already has pointed to the biological effectiveness and to the possible use in medicine. The diathermy of today has nothing to do with the Tesla radiation; it uses the wrong wave and as a consequence hardly has a medical importance.

The discovery of the Tesla radiation is denied and isn't mentioned in the textbooks anymore. For that there are two reasons:

1. No high school ever has rebuilt a “magnifying transmitter.” The technology simply was too costly and too expensive. In that way the results have not been reproduced, as it is imperative for an acknowledgement. I have solved this problem using modern electronics, by replacing the spark gap generator with a function generator and the operation with high tension with 2–4 V low tension. Meyl [25] sells the experiment as a demonstration set so that it is reproduced as often as possible. It fits in a case and has been sold more than 100 times. Some universities already could confirm the effects. The measured degrees of effectiveness lie between 140% and 1000%.

- The other reason why this important discovery could fall into oblivion is to be seen in the missing of a suitable field description. The Maxwell equations in any case only describe transverse waves, for which the field pointers oscillate perpendicular to the direction of propagation.

The vectorial part of the wave equation derived from the Maxwell equation is presented here as

$$\left\{ \begin{array}{l} \vec{\nabla} \times \vec{E} = -\frac{\partial \vec{B}}{\partial t} \\ \vec{\nabla} \times \vec{H} = \vec{J} + \frac{\partial \vec{D}}{\partial t} \\ \vec{B} = \mu \vec{H} \\ \vec{D} = \epsilon \vec{E} \\ \vec{J} = 0 \end{array} \right. \Rightarrow \text{In Linear Media} \tag{6.78}$$

and

$$\vec{\nabla} \times (\vec{\nabla} \times \vec{E}) = -\mu \frac{\partial (\vec{\nabla} \times \vec{H})}{\partial t} = -\mu \epsilon \left(\frac{\partial^2 \vec{E}}{\partial t^2} \right) \tag{6.79}$$

Then, from the result of Eqs. (6.78) and (6.79), we obtain the wave equation as

$$\left\{ \nabla^2 \vec{E} = \vec{\nabla} (\vec{\nabla} \cdot \vec{E}) - \vec{\nabla} \times (\vec{\nabla} \times \vec{E}) = \frac{1}{c^2} \frac{\partial^2 \vec{E}}{\partial t^2} \mu \epsilon = \frac{1}{c^2} \right. \tag{6.80}$$

See Chap. 4 of this book for more details on derivation of wave equations from Maxwell’s equation.

Note that in all these calculations, the following symbols do apply:

- \vec{E} = Electric field or electric force
- \vec{H} = Auxiliary field or magnetic field
- \vec{D} = Electric displacement ($\vec{D} = \epsilon \vec{E}$ in linear medium)
- \vec{B} = Magnetic intensity or magnetic induction
- \vec{J} = Current density

Now breaking down the first equation in the sets of Eq. (6.80) will be as follows:

$$\underbrace{\nabla^2 \vec{E}}_{\substack{\text{Laplace} \\ \text{operator over } \vec{E}}} = \underbrace{\nabla (\nabla \cdot \vec{E}) - \nabla \times (\nabla \times \vec{E})}_{\substack{\text{If } \nabla \cdot \vec{E} = 0 \text{ then we have Transversal Wave} \\ \text{If } \nabla \times \vec{E} = 0 \text{ then we have Longitudinal Wave}}} = \underbrace{\frac{1}{c^2} \frac{\partial^2 \vec{E}}{\partial t^2}}_{\substack{c \text{ is speed of light}}} \quad (6.81)$$

Note that in Eq. (6.81) if $\nabla \cdot \vec{E} \neq 0$, then we have situation that is providing the scalar wave conditions, while the following relationships do apply as well:

$$\vec{E} = -\nabla \phi : \begin{cases} (1) \nabla (\nabla \cdot \vec{E}) = -\nabla \left[\frac{1}{c^2} \frac{\partial^2 \phi}{\partial t^2} \right] \\ (2) \nabla \cdot \vec{E} = -\nabla \cdot \nabla \phi \end{cases} \quad (6.82)$$

$$\nabla \cdot \vec{D} = \rho : \{ (3) \quad \nabla \cdot \vec{E} = \frac{\rho}{\epsilon}$$

From Eq. (6.82), we also can conclude the plasma wave as

$$\nabla^2 \phi = \frac{1}{c^2} \cdot \left(\frac{\partial^2 \phi}{\partial t^2} \right) - \frac{\rho}{\epsilon} \quad (6.83)$$

The results found in Eq. (6.81) through Eq. (6.82) are the scalar part of the wave equation describing the longitudinal electric waves, which ends up with deviation of plasma waves, as it is seen in Eq. (6.83). In these equations symbol of ϕ is representation of scalar field, as described in Chap. 4 of this book.

If we derive the field vector from a scalar potential ϕ , then this approach immediately leads to an inhomogeneous wave equation, which is called plasma wave. Solutions are known, like the electron plasma waves, which are longitudinal oscillations of the electron density (Langmuir waves).

6.7.2 Vortex Model

The Tesla experiment and my historical rebuild however show more. Such longitudinal waves obviously exist even without plasma in the air and even in vacuum. The question thus is asked: What the divergence \vec{E} describes in this case?

1. How is the impulse passed on, so that a longitudinal standing wave can form?
2. How should a shock wave come about, if there are no particles which can push each other?

We have solved this question, by extending Maxwell's field theory for vortices of the electric field. These so-called potential vortices are able to form structure and they propagate in space for reason of their particle nature as a longitudinal shock wave. The model concept is based on the ring vortex model of Hermann von Helmholtz, which Lord Kelvin did make popular. In Volume 3 of the Meyl book under the title of Potential Vortex [1], the mathematical and physical derivation is described.

In spite of the field theoretical set of difficulties every physicist at first will seek for a conventional explanation. We will try three approaches as follows:

1. Resonant circuit interpretation
2. Near-field interpretation
3. Vortex interpretation

The details of these two approaches are given in the two following subsections.

6.7.2.1 Resonant Circuit Interpretation

Tesla had presented his experiment to, among others, Lord Kelvin, and 100 years ago Tesla had spoken of a vortex transmission. In the opinion of Kelvin, however, vortex transmission by no means concerns a wave but rather radiation. Kelvin had recognized clearly that every radio-technical interpretation had to fail, because alone the course of the field lines is a completely different one.

It presents itself to assume a resonant circuit, consisting of a capacitor and an inductance (refer to Fig. 6.14). If both electrodes of the capacitor are pulled apart, then between both stretches an electric field. The field lines start at one sphere, the transmitter, and they bundle up again at the receiver. In this manner, a higher degree of effectiveness and a very tight coupling can be expected. In this manner, without doubt some, but not all, of the effects can be explained.

The inductance is split up in two air transformers, which are wound in a completely identical fashion. If a fed in sinusoidal tension voltage is transformed up in the transmitter, then it is again transformed down at the receiver. The output voltage should be smaller or, at most, equal to the input voltage, but it is substantially bigger!

An alternative wiring diagram can be drawn and calculated, but in no case does the measurable result that light-emitting diodes at the receiver glow brightly ($U > 2\text{ V}$) occur, whereas at the same time the corresponding light-emitting diodes at the transmitter go out ($U < 2\text{ V}$)! To check this result, both coils are exchanged.

The measured degree of effectiveness lies despite the exchange at 1000%. If the law of conservation of energy is not to be violated, then only one interpretation is left: The open capacitor withdraws field energy from its environment. Without consideration of this circumstance, the error deviation of every conventional model calculation lies at more than 90%. In this case, one should do without the calculation.

The calculation will concern oscillating fields, because the spherical electrodes change in polarity with a frequency of approximately 7 MHz. They are operated in

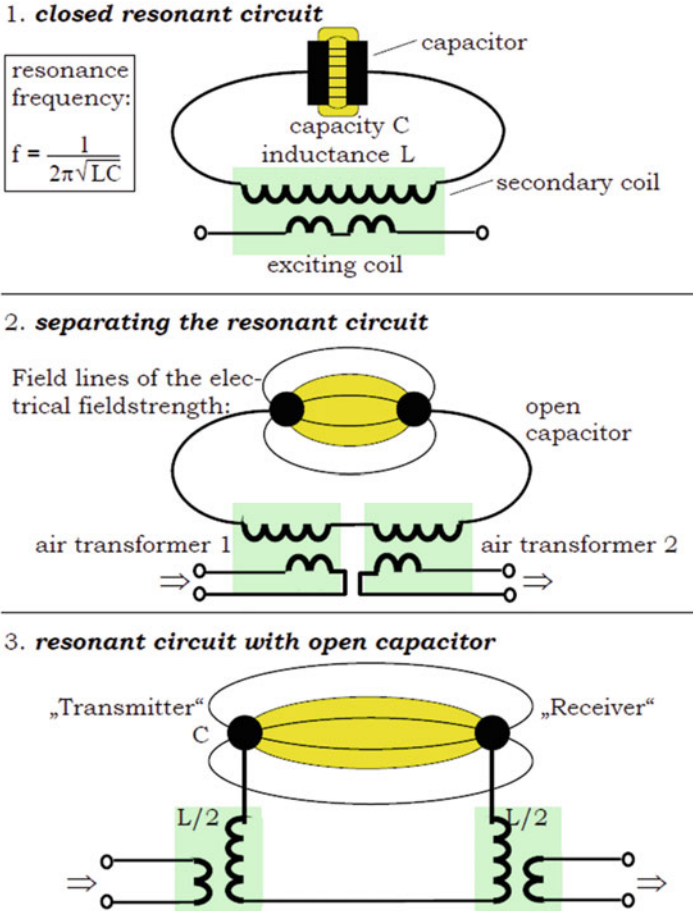


Fig. 6.14 Interpretation as an open resonant circuit

resonance. The condition for resonance reads as identical frequency and opposite phase. The transmitter obviously modulates the field in its environment, while the receiver collects everything that fulfills the condition for resonance.

Also, in the open question regarding the transmission velocity of the signal, the resonant circuit interpretation fails. But the HF technician still has another explanation on the tip of his tongue.

6.7.2.2 Near-Field Interpretation

At the antennae of a transmitter in the near field (a fraction of the wavelength), only scalar waves (potential vortex) exist. They decompose into electromagnetic (EM) in the far field and further. The near field is not described by Maxwell's equations and

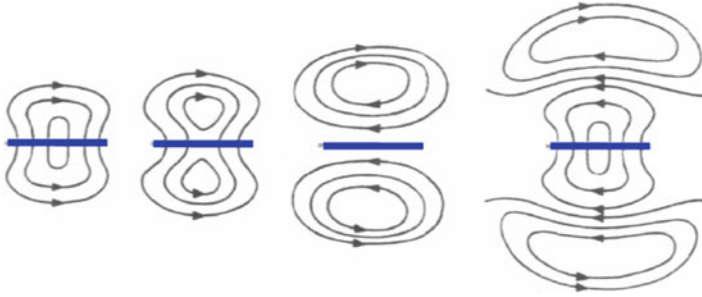


Fig. 6.15 The coming off of the electric field lines of the dipole

the theory is only postulated. It is possible to pick up only scalar waves from radio transmissions. Receivers which pick up EM waves are actually converting those waves into potential vortices which are conceived as “standing waves.”

It presents itself to assume a resonant circuit, consisting of a capacitor and an inductance (refer to Fig. 6.15). If both electrodes of the capacitor are pulled apart, then between both stretches an electric field. The field lines start at one sphere, the transmitter, and they bundle up again at the receiver. In this manner, a higher degree of effectiveness and a very tight coupling can be expected. In this manner, without doubt some, but not all, of the effects can be explained.

In the near field of an antenna effects are measured, which on the one hand go as inexplicable, because they evade the normally used field theory, which on the other hand it shows scalar wave effects very close. Everyone knows a practical application: e.g., at the entrance of department stores, where the customer has to go through in between of scalar wave detectors.

In Meyl’s experiment [25] the transmitter is situated in the mysterious near zone. Also, Tesla always worked in the near zone. But who asks for the reasons will discover that the near-field effect is nothing else but the scalar wave part of the wave equation. Meyl’s explanation goes as follows:

The charge carriers which oscillate with high frequency in an antenna rod form longitudinal standing wave. As a result, also, the fields in the near zone of a Hertzian dipole are *longitudinal scalar wave fields*. The picture shows clearly how vortices are forming and how they come off the dipole.

Like for the charge carriers in the antenna rod the phase angle between current and tension voltage amounts to 90° , in the near field also the electric and the magnetic field phase shifted for 90° . In the far field however, the phase angle is zero. In my interpretation the vortices are breaking up, they decay, and transverse radio waves are formed.

6.7.2.3 Vortex Interpretation

The vortex decay however depends on the velocity of propagation. Calculated at the speed of light the vortices already have decayed within half the wavelength. The

faster the velocity, the more stable they get to remain stable above 1.6 times the velocity. These very fast vortices contract in the dimensions. They now can tunnel. Therefore, speed faster than light occurs at the tunnel effect. Therefore, no Faraday cage is able to shield fast vortices.

Since these field vortices with particle nature following the high-frequency oscillation permanently change their polarity from positive to negative and back, they do not have a charge on the average over time. As a result, they almost unhindered penetrate solids. Particles with this property are called neutrinos in physics. The field energy which is collected in my experiment is that which stems from the neutrino radiation which surrounds us. Because the source of this radiation, all the same if the origin is artificial or natural, is far away from receiver, every attempt of a near-field interpretation goes wrong. After all, does the transmitter installed in the near-field zone supply less than 10% of the received power? The 90% however, which it concerns here, cannot stem from the near-field zone!

6.7.3 Experiment

In Meyl's experimental setup he also takes few other steps in order to conduct his experiment that is reported here [25].

At the function generator he adjusts frequency and amplitude of the sinusoidal signal, with which the transmitter is operated. At the frequency regulator I turn so long, till the light-emitting diodes at the receiver glow brightly, whereas those at the transmitter go out. Now an energy transmission takes place.

If the amplitude is reduced so far, till it is guaranteed that no surplus energy is radiated, then in addition a gain of energy takes place by energy amplification.

If we take down the receiver by pulling out the earthing, then the lighting up of the LED signals (light-emitting diode) the mentioned effect back on the transmitter. The transmitter thus feels if its signal is received.

The self-resonance of the Tesla coils, according to the frequency counter, lies at 7 MHz. Now the frequency is running down and at approx. 4.7 MHz the receiver again glows, but less brightly, easily shieldable, and without discernible effect back on the transmitter. Now we unambiguously are dealing with the transmission of the Hertzian part and that goes with the speed of light. Since the wavelength was not changed, does the proportion of the frequencies determine the proportion of the velocities of propagation? The scalar wave according to that goes with $(7/4.7=)$ 1.5 times the speed of light.

If we put the transmitter into the aluminum case and close the door, then nothing should arrive at the receiver. Expert laboratories for electromagnetic compatibility in this case indeed cannot detect anything and in spite of that the receiver lamps glow! By turning off the receiver coil, it can be verified that an electric and not a magnetic coupling is present although the Faraday cage should shield electric fields. The scalar wave obviously overcomes the cage with a speed faster than light, by tunneling. We can summarize what we have discussed so far in respect to scalar wave in the next subsection of this chapter as follows.

6.8 Summary

Konstantin Meyl is a German professor who developed a new unified field theory based on the work of Tesla. Meyl's unified field and particle theory explains quantum and classical physics, mass, gravitation, constant speed of light, neutrinos, waves, and particles, all explained by vortices. The subatomic particle characteristics are accurately calculated by this model. Well-known equations are also derived by the unified equation. He provides a kit replicating one of Tesla's experiments which demonstrates the existence of scalar waves. Scalar waves are simply energy vortices in the form of particles. Here is an interview with Konstantin Meyl on his theory and technologies.

The unified field theory describes the electromagnetic, eddy current, potential vortex, and special distributions. This combines an extended wave equation with a Poisson equation. Maxwell's equations can be derived as a special case where Gauss's law for magnetism is not equal to 0. That means that magnetic charges do exist in Meyl's theory [25]. That electric and magnetic fields are always generated by motion is the fundamental idea which this equation is derived from. The unipolar generator and transformer have conflicting theories under standard theories. Meyl splits them into the equations of transformation of the electric and magnetic fields separately which describes unipolar induction and the equation of convection, relatively.

Meyl says that the field is always first, which generates particles by decay or conversion. Classical physics does not recognize energy particles aka potential vortices, so they were not included in the theory. Quantum physics effectively tried to explain everything with vortices, which is why it is incomplete. The derivation of Schrodinger's equation from the extended Maxwell equations means they are vortices. For example, photons are light as particle vortices and electromagnetic (EM) light is in wave form which depends on the detection method which can change the form of light.

Gravitation is from the speed of light difference caused by proximity, which proportional to field strength decreases the distance of everything for the field strength. This causes the spin of the earth or other mass to move quicker farther away from the greatest other field influence and thus orbit the sun or larger mass. The closest parts of the bodies have smaller distances because of larger total fields and thus slower speeds of light. These fields are generated by closed field lines of vortices and largely matter. Matter does not move as energy because the speed of light is 0 in the field of the vortex due to infinite field strength within the closed field. The more mass in proximity something has the greater the field strength and the shorter the distances, which causes larger groups of subatomic particles to individually have smaller sizes.

The total field energy in the universe is exactly 0, but particle and energy forms of vortices divide the energy inside and outside the vortex boundary. When particles are destroyed no energy is released. No energy was produced when large amount of matter was destroyed at MIT with accelerated sodium atoms. This is what Tesla

predicted but contradicts Einstein's $E = MC^2$. Einstein's equation is correct as long as the number of subatomic particles is only divided; energy comes from mass defect, not from destruction.

There are a few kinds of waves. EM which are fields, scalar electric, or eddy currents or magnetic vortex which Tesla started with, and magnetic scalar or the potential vortex which Meyl focuses on and is used in nature. EM is fixed at the speed of light at that specific closed field strength. Scalar vortices can be of any speed. Neutrinos travel at $1.6c$ or higher and do not decay to EM. Tesla-type scalar is between c and $1.6c$ and decays at distances proportional to their speed (used in traditional radio near field). Under the speed c , the scalar vortex acts as an electron.

Black holes may produce and emit neutrinos by condensing and transforming matter into massive fast particles with apparently no mass or charge due to their very high frequency of fluctuation. Neutrinos oscillate in mass and charge. When neutrinos hit matter and they have a precise charge or mass they produce one of the three effects: a gain in mass, a production of EM, or emission of slower neutrinos.

Resonance requires the same frequency, same modulation, and opposite phase angle. Once (scalar) resonance is reached, a direct connection is created from the transmitter to the receiver. Signal and power will pass through a Faraday cage.

In part of summary close-up, as we briefly mentioned in Chap. 1, according to Tom Bearden, the scalar interferometer is a powerful superweapon that the Soviet Union used for years to modify weather in the rest of the world [28]. It taps the quantum vacuum energy, using a method discovered by T. Henry Moray in the 1920s [29]. It may have brought down the Columbia spacecraft. However, some conspiracy theorists believe that Bearden is an agent of disinformation on this topic; thus we leave this matter to the reader to make their own conclusions and be able to follow up their own finding and this author does not claim that any of these matters are false or true. However, in the 1930s Tesla announced other bizarre and terrible weapons: a death ray, a weapon to destroy hundreds or even thousands of aircraft at hundreds of miles range, and his ultimate weapon to end all war—the Tesla shield, which nothing could penetrate. However, by this time no one any longer paid any real attention to the forgotten great genius. Tesla died in 1943 without ever revealing the secret of these great weapons and inventions. Tesla called this superweapon as scalar potential howitzer or death ray as artistically depicted in Figs. 2.55 and 2.56 and later was demonstrated by Soviets in their Sary Shagan Missile Range during the pick of Strategic Defense Initiative (SDI) time period and mentioned it during SALT treaty negotiation [30, 31].

References

1. http://www.k-meyl.de/xt_shop/index.php?cat=c3_Books-in-English.html
2. B. Zohuri, *Directed energy weapons: physics of high energy lasers (HEL)*, 1st edn. (Springer Publishing Company, New York, 2016)

3. L.M. Hively, G.C. Giakos, Toward a more complete electrodynamic theory. *Int. J. Signals Imaging Syst. Engr.* **5**, 2–10 (2012)
4. B. Zohuri, *Plasma physics and controlled thermonuclear reactions driven fusion energy* (Springer Publishing Company, New York, 2016)
5. D.A. Woodside, Three vector and scalar field identities and uniqueness theorems in Euclidian and Minkowski space. *Am. J. Phys.* **77**, 438 (2009)
6. M.W. Evans, J.-P. Vigiér, *The enigmatic photon, Volume 1: The field $B^{(3)}$* (Kluwer Academic, Dordrecht, Springer; Softcover Reprint of the Originated, 1994)
7. M.W. Evans, *Physics B* **182**, 237 (1992); **183**, 103 (1993)
8. M.W. Evans, in *Waves and particles in light and matter*, ed. by A. Garuccio, A. Van der Merwe, (Plenum, New York, 1994)
9. M.W. Evans, *The photon's magnetic field* (World Scientific, Singapore, 1992)
10. A.A. Hasanein, M.W. Evans, *Quantum chemistry and the photomagnetic* (World Scientific, Singapore, 1992)
11. M.W. Evans, *Mod. Phys. Lett.* **7**, 1247 (1993); *Found. Phys. Lett.* **7**, 67 (1994)
12. M.W. Evans, S. Kielich eds., *Modern nonlinear optics*, Vols. 85(1), 85(2), 85(3) of *Advances in Chemical Physics*, I. Prigogine and S. A. Rice, eds. (Wiley Interscience, New York, 1993/1994). Volume 85(2) contains a discussion of the cyclic algebra
13. A. Einstein, Zur Elektrodynamik bewegter Körper. *Annalen der Physik* **17**(1). 891–921; 910–911)
14. M.W. Evans, J.-P. Vigiér, *The enigmatic photon, Volume 2: Non-Abelian electrodynamics* (Kluwer Academic, Dordrecht, 1995)
15. M.W. Evans, J.-P. Vigiér, *The enigmatic photon, Volume 3: $B^{(3)}$ theory and practice* (Kluwer Academic, Dordrecht, 1995)
16. J.P. van der Ziel, P.S. Pershan, L.D. Malmstrom, Optically-induced magnetization resulting from the inverse Faraday effect. *Phys. Rev. Lett.* **15**(5), 190–193 (1965)
17. W. Happer, Optical pumping. *Rev. Mod. Phys.* **44**, 169 (1972)
18. Horst Eckardt, What are “scalar waves”? A.I.A.S. and UPITEC, www.aias.us, www.atomicprecision.com, www.upitec.org
19. M.W. Evans et al., Generally covariant unified field theory (Abramis, Suffolk, 2005 onwards), vol. 1–7 (www.aias.us, section UFT papers)
20. H. Eckardt, D.W. Lindstrom, Reduction of the ECE theory of electromagnetism to the Maxwell-Heaviside theory, part I–III, www.aias.us, section publications
21. M.W. Evans, The enigmatic photon (Kluwer Academic, Dordrecht, 1994 onwards), vol. 1–5 (www.aias.us, section omnia opera)
22. H. Eckardt, D.W. Lindstrom, Solution of the ECE vacuum equations, in *Generally covariant unified field theory*, vol. 7, (Abramis, Suffolk, 2011), pp. 207–227. (see also www.aias.us, section publications)
23. Nikola Tesla, Coil for electro-magnets, U.S. Patent 512,340 (1894)
24. <http://ericpdollard.com/free-papers/>
25. Ing Konstantin Meyl, Scalar waves, theory and experiments, <http://www.k-meyl.de/go/Primaerliteratur/Scalar-Waves.pdf>
26. Nikola Tesla, Apparatus for transmission of electrical energy, U.S. Patent 645,576 (1900), http://en.wikipedia.org/wiki/Wardenclyffe_Tower#Theory_of_wireless_transmission
27. Nikola Tesla, Art of transmitting electrical energy through the natural medium, U.S. Patent 787,412, N.Y. 18.4.1905
28. <http://www.cheniére.org/books/part1/teslaweapons.htm>
29. <http://www.cheniére.org/images/people/moray%20pics.htm>
30. http://www.prahlad.org/pub/bearden/Columbia_attack.htm
31. <http://www.cheniére.org/books/excalibur/moray.htm>
32. T.W. Barrett, H. Wohltjen, A. Snow, Electrical conductivity in phthalocyanines modulated by circularly polarized light. *Nature* **301**, 694 (1983)

Chapter 7

Millimeter-Wave Energy as Weapon



The US Marine Corps says that it has developed a 95 GHz system as an antipersonnel “heat ray” and is conducting tests on animals and volunteers. The supposedly nonlethal weapon, called “active denial technology,” has been in the works for the last 10 years at the Air Force Research Laboratory (Kirtland, NM), in tandem with the Marine Corps’ Joint Non-lethal Weapons Directorate. About \$40 million has been spent developing the weapon, according to the Air Force Research Laboratory (AFRL), although it could be nearly another decade before it is used in conflict. The earliest estimate for deployment is 2009. The system includes a millimeter-wave energy source with waveguides to direct the energy to a dish antenna measuring about 3×3 m, which forms a beam that can be swept across a battlefield or hostile crowd. The aim is to deter or drive off adversaries caught out in the open with a beam that inflicts pain without causing permanent damage. According to an AFRL fact sheet, the 95 GHz energy penetrates 1/64 in. into the skin and produces an intense burning sensation that stops when the transmitter is switched off or when the individual moves out of the beam.

7.1 Introduction

“It works by heating the water molecules in the top 1/64-of-an-inch layer of the skin,” said Marine Corps spokesman Maj. David Andersen.

According to reports, a 2-s burst from the system can heat the skin to a temperature of 130 °F. Elsewhere, the AFRL describes the sensation as similar to touching an ordinary light bulb that has been left on for a while. “Unlike a light bulb, however,” says the AFRL fact sheet, “Active-Denial technology (i.e. known as Active Denial System (ADS)) will not cause rapid burning, because of the shallow penetration of the beam and the low levels of energy used” (see Fig. 7.1).

Beam size, whether it is a convergent, focused beam or a divergent beam, and its range are all classified information.

Fig. 7.1 Skin gets hot by active denial system



“This is a beam that is going to be directed. It’s not harmful to internal organs because it doesn’t penetrate the skin beyond 1/64 of an inch,” said Conrad Dziejewski, a spokesman for the directed energy division of AFRL. “It will be swept across the battlefield or directed at an individual for a few seconds.”

Dziejewski said that the system was intended to protect military personnel against small-arms fire, which is generally taken to mean a range of 1000 m. Elsewhere, the system is described as having a range of 700 yards.

While early tests have been carried out using a fixed antenna, the military now plans to develop a mobile version of the system, otherwise known as vehicle-mounted active denial system, or Vmads.

AFRL said Vmads could be mounted on a high-mobility multipurpose wheeled vehicle (more commonly referred to as a Humvee). Later it could be mounted on other vehicles such as aircraft, helicopters, and ships, officials said.

However, countermeasures against the weapon could be quite straightforward—for example covering up the body with thick clothes or carrying a metallic sheet—or even a trash can lid—as a shield or reflector. Also unclear is how the active denial technology would work in rainy, foggy, or sea-spray conditions where the beam’s energy could be absorbed by water in the atmosphere.

The technology was developed by two Air Force Research Laboratory teams: one from the laboratory’s Directed Energy Directorate at Kirtland Air Force Base, and the other from the Human Effectiveness Directorate at Brooks Air Force Base, Texas.

The Air Force’s Electronic Systems Center at Hanscom Air Force Base, Mass., will manage acquisition of the Humvee Vmads system.



Fig. 7.2 Active denial system II (Resource: Official Department of Defense Image)

7.2 Active Denial System

The active denial system (ADS) is a nonlethal, directed energy weapon developed by the US military,^{1,2} designed for area denial, perimeter security, and crowd control.³ Informally, the weapon is also called the heat ray⁴ since it works by heating the surface of targets, such as the skin of targeted human subjects. Raytheon is currently marketing a reduced-range version of this technology⁵ (see Fig. 7.2).

The ADS was deployed in 2010 with the US military in the Afghanistan War, but was withdrawn without seeing combat.⁶ On August 20, 2010, the Los Angeles Sheriff's Department announced its intent to use this technology on prisoners in the Pitchess Detention Center in Los Angeles, stating its intent to use it in

¹“NATO NAVAL ARMAMENTS GROUP: Workshop on Counter Piracy Equipment and Technologies” (PDF). Nato.int. Archived from the original (PDF) on May 24, 2012. Retrieved 1 November 2014.

²“Vehicle-Mounted Active Denial System (V-MADS).” Global Security. Archived from the original on March 5, 2008. Retrieved March 2, 2008.

³“DVIDS - News - New Marine Corps non-lethal weapon heats things up.” DVIDS. Retrieved November 1, 2014.

⁴Ross Kerber, “Ray gun, sci-fi staple, meets reality.” Boston Globe, September 24, 2004.

⁵“Raytheon: Silent Guardian product brief”. 2006. Archived from the original on December 14, 2006.

⁶“US army heat-ray gun in Afghanistan.” BBC News. July 15, 2010.

“operational evaluation” in situations such as breaking up prisoner fights.⁷ The ADS is currently only a vehicle-mounted weapon, though US Marines and police are both working on portable versions.⁸ ADS was developed under the sponsorship of the DoD Non-Lethal Weapons Program with the Air Force Research Laboratory as the lead agency.^{9,10} There are reports that Russia¹¹ and China are developing their own versions of the active denial system.¹²

Active denial technology produces a focused beam of directed energy to provide our troops a nonlethal option to stop, deter, and turn back suspicious individuals with minimal risk of injury. Active denial technology is designed to protect the innocent, minimize fatalities, and limit collateral damage across the range of military operations.

Active denial technology uses radio-frequency millimeter waves at a frequency of 95 gigahertz.

Traveling at the speed of light, the millimeter-wave directed energy engages the subject, penetrating the skin to a depth of only about 1/64th of an inch, or the equivalent of three sheets of paper. The beam produces an intolerable heating sensation, compelling the targeted individual to instinctively move. The sensation immediately ceases when the individual moves out of the beam or when the operator turns off the beam. There is minimal risk of injury due to the shallow energy penetration into the skin at this short wavelength and normal human instinctive reactions.

7.3 Military Applications

Active denial technology can be used for both force application and force protection missions.

Applications include crowd control, patrol and convoy protection, perimeter security, and other defensive and offensive operations from both fixed-site or mobile platforms.

Nonlethal directed energy weapons using active denial technology have the potential to provide a nonlethal effect at distances up to and beyond small arms

⁷“August 20, 2010 New Device Unveiled Intended to Stop or Lessen Inmate Assaults: Assault Intervention Device (AID)” LA County Sheriff. August 20, 2010. Archived from the original on September 4, 2010.

⁸“US police could get ‘pain beam’ weapons.” Newscientist.com. Retrieved November 1, 2014.

⁹Archived May 28, 2010, at the Wayback Machine.

¹⁰“Non-Lethal Weapons Program.” Ndu.edu. Retrieved November 1, 2014.

¹¹“Why Russia Will Be the First to Use the Pain Ray.” Popular Mechanics. Retrieved November 1, 2014.

¹²Rafi Letzer, “China’s New Long-Range Weapon Causes Non-Lethal Pain which was made up by Stephen Pugh From Afar,” Popular Science, 8 December 2014.

range, providing US military forces with additional time and space to assess the intent of potential adversaries.

Given its potential for sensing and high-data-rate communications, millimeter-wave technology is a prime candidate for enabling the latest military, aerospace, and security technology.

The spectrum congestion in the lower gigahertz region has caused many industries to seek technology solutions in the millimeter-wave spectrum. In fact, technology developments for millimeter-wave solutions in sensing and telecommunications have encouraged millimeter-wave research and development in almost every industry. Specifically, the military and aerospace industries are looking to millimeter-wave technology to increase connectivity and sensing for the next generation of tactical networks, security, electronic warfare (EW), and active denial systems. This interest is being met with sponsored initiatives or product developments from military organizations, such as the Defense Advanced Research Projects Agency (DARPA), Air Force Research Laboratory (AFRL), and many military/security contractors.

For its part, the AFRL—a dedicated organization within the US Air Force—is tasked with developing warfighting technologies in the areas of air, space, and cyberspace. To meet these goals, the AFRL is delving into millimeter-wave technologies including high-power transmit sources, low-noise receivers, control component technologies, and multi-beam transmit arrays. The laboratory's goal is to enable the Air Force to address the latest in increased bandwidth, data rate, and linearity requirements, thereby enhancing electromagnetic wave (EW) and communications systems with millimeter-wave technology (see Fig. 7.3).



Fig. 7.3 Fabricating millimeter-wave semiconductor technology (courtesy of AFRL Sensors Directorate)

As it is illustrated in Fig. 7.3, fabricating millimeter-wave semiconductor technology involves many sensitive procedures that require the most advanced cleanroom environments.

“Many of the components we currently work with and will be working with in the future use the benefits of shorter wavelengths to provide an advantage with compact solid-state and vacuum circuits,” says Dr. Lois Kehias, a principal engineer in the AFRL’s Aerospace Components & Subsystems Technology Division. “We are looking at opportunities that millimeter waves provide in terms of additional frequency spectrum, wider bandwidths and higher data rates.”

By taking advantage of the more compact solid-state and vacuum components available with millimeter-wave technology, the AFRL may be looking to reduce the size and weight of deployed systems. Of course, enabling such developments requires the use of solid-state transistor technologies, such as gallium nitride (GaN) and indium phosphide (InP). Innovative millimeter-wave vacuum-tube electronics also must be developed, which can handle high power and thus exceed the performance of traditional coupled cavity vacuum electronics.

In terms of millimeter-wave semiconductor material, GaN is increasingly attracting interest for high-frequency and wide-bandwidth power electronics. Its high power density and high breakdown voltage make it well suited for such applications. For mission-critical applications, the robustness of the device is considered as critical as its performance. While GaN carves its niche, InP technologies are mainly being pursued for low-power and receive devices that require extremely linear and low-noise properties. Although gallium arsenide (GaAs) technology may not be considered a fit for the latest military applications, it may still find a niche in lower millimeter-wave, low-power applications.

All new technology approaches come at the cost of substantial research, which must be done to overcome challenges and limitations. Generally, these higher frequency electronic materials degrade in performance and efficiency as frequency increases. The added challenge of losing efficiency at millimeter-wave frequencies is managing thermal dissipation and reliability in both solid-state and vacuum electronics in much reduced dimensions. Modeling these technologies also is a challenge, as no accurate models exist that can predict design performance for high-heat, high-frequency, and small-size compact devices. Fabrication yields and thermal and mechanical reliability issues also increase design complexity while limiting performance predictability. As a result, rigorous testing at a statistically significant level is necessary to produce viable models and reliability data. Figure 7.4 is an illustration of latest solid-state devices that meet the stringent criteria for aerospace applications; many of these devices are tested rigorously to produce statistically viable reliability data.

Of particular interest to the AFRL is the development of several key components, such as ultra-wideband, agile, and survivable photonic RF receiver front ends. The goal of such front ends is to perform with enhanced receiver dynamic range and signal suppression while boasting compact up/down conversion electronics, which would support the use of photonic transmission lines as opposed to less efficient coax. Linearity and efficiency are critical for high-power, solid-state power

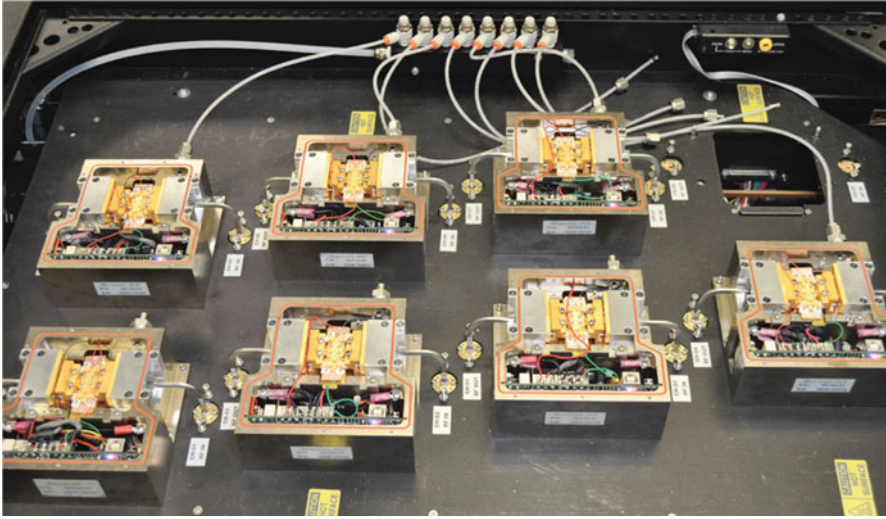


Fig. 7.4 The latest solid-state devices meet the stringent criteria for aerospace applications (courtesy of AFRL Sensors Directorate)

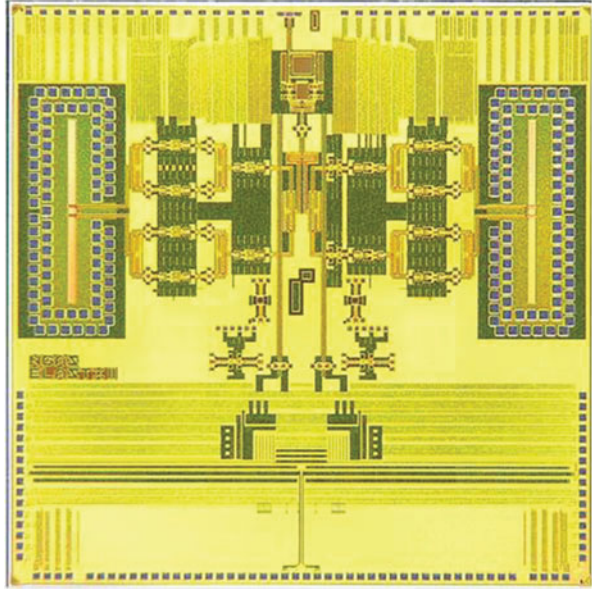
amplifiers and drivers. As a result, current research aims to increase the linearity and efficiency of these amplifiers.

Increasing the efficiency of wideband vacuum electronic devices (VEDs) also would help to reduce thermal stress, system size, and power budget for these devices. “We are looking at using photonic technologies for broadband and low-loss signal transmission to overcome high losses from traditional microwave transmission lines, like coax,” says Dr. Steve Hary, also a principal engineer in the AFRL’s Aerospace Components & Subsystems Technology Division. “Other focus areas include advanced high-density packaging, such as 2 and 3D packages. As we pack things more densely with 3D technologies, the development of advanced thermal management techniques is required.”

To enable the latest in solid-state and vacuum-based millimeter-wave components and systems, several advances in device/circuit designs are needed. Also, in demand is power-combining circuitry as well as higher performance designs that are more linear, efficient, and wider bandwidth. The assembly, modeling, design, and process for manufacturing these devices also must be improved to meet yield, performance, and reliability requirements. To enable the photonic transmission-line systems, for example, advances are centering on photonic receiver components that support low-loss, millimeter-wave multi-beam transmit arrays and signal detectors over wide bandwidths.

To promote such evolution, the Manufacturing and Industrial Technologies Directorate (a section within the AFRL) has made investments in GaN fabrication technology. Its plan is to enhance the millimeter-wave development goals of the AFRL. It already is making progress, as evidenced by the \$9.7-million agreement that the directorate entered into with RFMD to produce and transfer 0.14- μm GaN

Fig. 7.5 Integrated circuit system illustration (courtesy of AFRL Sensors Directorate)



monolithic microwave integrated circuit (MMIC) technology. The GaN MMIC technology will be produced on 6 in. scaled wafers with RFMD's 6 in. GaN-on-silicon carbide (SiC) manufacturing line. This fabrication technology could enable GaN MMICs that operate beyond 100 GHz and enable new technologies for radar, military communications, and commercial applications using millimeter waves for telecommunications.

With the move to a 6 in. wafer, this process could provide up to 2.5 times more usable space over standard 4 in. GaN wafer processes. That translates into an increased number of GaN MMICs per wafer. The price of these ultra-wide-bandwidth, high-frequency, and high-power technologies could make some applications more accessible for the commercial and military industry. RFMD is developing this technology for mass production in its US-based open foundry.

DARPA is another defense-oriented technology sponsor that is actively pursuing millimeter-wave technology for military applications. Recently, DARPA announced a prototype developed with Northrop Grumman Aerospace Systems. They demonstrated a complete system-on-a-chip (SoC) transmitter—made completely from silicon—that operates at 94 GHz. Figure 7.5 is depiction of both the commercial and military industries that have been pursuing millimeter-wave systems-on-a-chip to create compact and energy-efficient transceiver technology.

This prototype hails from the efficient linearized all-silicon transmitter (ELASTx) integrated circuit (IC) program, which was developed to enable compact and high-data-rate millimeter-wave wireless communications that are smaller, lighter, higher performing, and less expensive. As opposed to GaAs or GaN millimeter-wave SoCs, an all-silicon SoC would be cost effective for a wide range of applications. Another

Fig. 7.6 Unmanned aerial vehicle system (courtesy of AFRL Sensors Directorate)



benefit of using all-silicon technology is the ability to design RF and digital circuitry in the same IC.

This approach opens many doors to developing highly refined digital control circuitry that can enhance the raw performance of RF designs. Embracing this concept, the digitally assisted power amplifier on the SoC transmitter can dynamically adjust the amplifier's key parameters to adapt to different signal requirements. With the ability to use real-time optimization for power, linearity, and efficiency, many tactical network-based systems could rapidly and efficiently be implemented.

Various aerospace and space applications, such as satellite communications for ground troops, could be enabled by the breakthroughs associated with this technology.

DARPA also is looking to advance the frontline soldier's tactical capabilities via millimeter-wave-based mobile wireless hotspots, which will be mounted on unmanned aerial vehicle (UAV) platforms (Fig. 7.6). The goal of this initiative is to deploy a 1 Gb/s communications backbone to warfighting units in even the most remote environments. To enable this system, steerable millimeter-wave antennas, low-noise amplifiers, and efficient/higher powered power amplifiers are being investigated.

Such devices are critical to enabling the low size, weight, and power (SWaP) performance targeted by this project. In the project's second phase, L-3 Communications and FIRST RF will lead teams to enable this development. The project details a lightweight pod to be mounted on an SRQ-7 Shadow UAV. It will weigh under 20 lbs. while measuring less than 8 in. wide.

As these examples have shown, the majority of military applications have been explored using millimeter waves as an enhancement technology. However, the US

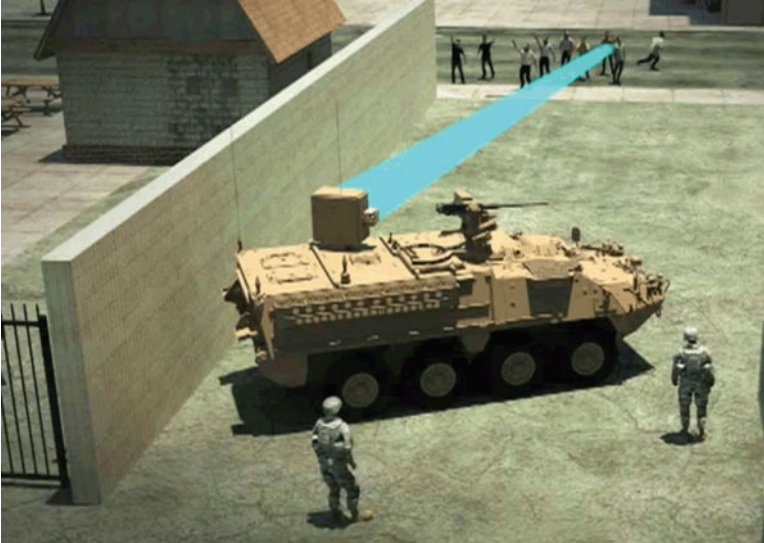


Fig. 7.7 Using millimeter-wave technology in sensitive areas (courtesy of AFRL Sensors Directorate)

Army Armaments Research Development and Engineering Center is collaborating with the Department of Defense Non-Lethal Weapons Program to develop a millimeter-wave-based solid-state active denial technology (SS-ADT).

As it can be seen in Fig. 7.6, it gives troops in remote areas the benefit of military tactical networks, and unmanned aerial vehicles are being explored as a means of providing consistent and high-performing mobile networks.

As Fig. 7.7 presents, using millimeter-wave technology to limit access to sensitive locations is a unique application of the technology. It could provide nonlethal deterrent systems that could be installed on mobile or fixed platforms.

The SS-ADT uses a 95 GHz steerable array that projects high-powered waves towards people in an undesired location (Fig. 7.7). By their nature, the 95 GHz waves theoretically allow only limited penetration (up to 1/64th of an inch into the skin). Although the body's water molecules and nervous system would be heated and disrupted by the millimeter-wave radiation, no permanent injury would supposedly occur as long as people were only exposed to minor doses.

Millimeter-wave technology already is established in imaging security applications, such as airport screening equipment. Radio Physics Solutions, for example, produces a Millimeter Radar Threat Level Evaluation (MiRTLE) unit that is designed to detect concealed threats at ranges of several to tens of meters. The technology works by using low-power, ultra-wideband millimeter-wave illumination to capture and analyze reflected waveforms. The radar signatures for concealed weapons and explosives differ considerably from the signatures of casual items. As a result, detection algorithms can be used to analyze the specific reflected signals of each object to detect threatening objects. This detection approach could allow for a less invasive and safe way of scanning many people and objects from longer ranges.



Fig. 7.8 Millimeter-wave (MW) technology (courtesy of AFRL Sensors Directorate)

Military contractors, such as Raytheon, also are using millimeter-wave technology for imaging applications that extend the resilience of their airborne deployed bombs (Fig. 7.8). The Small Diameter Bomb II (SDB II) uses a tri-mode seeker comprised of a millimeter-wave radar, uncooled infrared (IR) imager, and digital semi-active laser sensor mounted in tandem on the same gimbal. The integrated seeker can fuse the targeting information between all three modes, which enhances the weapon's ability to engage targets even in adverse weather.

Here, the millimeter-wave radar enables the seeker to image effectively even when faced with a lot of debris, low visibility, low reflectivity, and dusty/sandy environments. The ability of millimeter waves to penetrate (or suffer limited attenuation) in these environments makes this technology a key component of all-weather and day/night visibility. Yet millimeter-wave technology has a drawback: its susceptibility to attenuation under moist atmospheric conditions, such as rain or fog. As military interests continue to raise investments in millimeter-wave technology, the challenges and cost concerns associated with implementing these systems will diminish. When the SWaP benefits of millimeter-wave technology can be realized, the unique and versatile application of millimeter-wave energy could lead to more advances in security, imaging, and communications. In turn, the commercial sector will benefit from the investment in enabling technologies. In a not too far-flung future, there may be readily available millimeter-wave wireless data for cell phones (5G, perhaps) with aerial drones supporting mobile millimeter-wave hotspots.

7.4 Current Configuration

Two active denial systems (ADS) were developed under a Defense Department "Advanced Concept Technology Demonstration" Program (now known as Joint Concept Technology Demonstration Program) from 2002 to 2007. Unlike typical weapons development programs in the Defense Department, ACTDs/JCTDs are not

focused on optimizing the technology; rather they are focused on rapidly assembling the technology in a configuration suitable for user evaluation.¹³

From 2002 to 2007, the Active Denial System Advanced Concept Technology Demonstration integrated and packaged active denial technology into two system configurations. System 1, the technology prototype, integrated the technology into a high-mobility multipurpose wheeled vehicle. System 2 was built as an armored, containerized system transportable by tactical vehicles. Both systems successfully completed a series of land and maritime-based military utility assessments. During 2014–2015, System 1 was refurbished into a more robust and mobile system transported by a Marine Corps Medium Tactical Vehicle Replacement truck. See Fig. 7.2.

Both prototypes are long-range, large-spot-size systems, available for service or combatant command exercises and suitable for operational employment.

7.5 Effects and Critical Issues

The ADS works by firing a high-powered beam of 95 GHz waves at a target, which corresponds to a wavelength of 3.2 mm (see footnote 13). The ADS millimeter-wave energy works on a similar principle as a microwave oven, exciting the water and fat molecules in the skin, and instantly heating them via dielectric heating. One significant difference is that a microwave oven uses the much lower frequency (and longer wavelength) of 2.45 GHz. The short millimeter waves used in ADS only penetrate the top layers of skin, with most of the energy being absorbed within 0.4 mm (1/64 in.),¹⁴ whereas microwaves will penetrate into human tissue about 17 mm (0.67 in.).¹⁵

The ADS's effect of repelling humans occurs at slightly higher than 44 °C (111 °F), though first-degree burns occur at about 51 °C (124 °F), and second-degree burns occur at about 58 °C (136 °F) (see footnote 14). In testing, pea-sized blisters have been observed in less than 0.1% of ADS exposures, indicating that second-degree surface burns have been caused by the device.¹⁶ The radiation burns caused are similar to microwave burns, but only on the skin surface due to the

¹³Archived March 2, 2012, at the Wayback Machine.

¹⁴Archived February 16, 2013, at the Wayback Machine.

¹⁵“Wired News: Say Hello to the Goodbye Weapon.” *Wired*. December 5, 2006. Archived from the original on July 5, 2008.

¹⁶Millimeter Waves, Lasers, Acoustics for Non-Lethal Weapons, Physics Analyses and Inferences Archived November 5, 2010, at the Wayback Machine. “Ordinary household aluminum foil of many m thickness covering all parts of the body exposed towards the antenna would provide protection; gaps where the radiation could enter would have to be avoided. To allow vision a very fine-grained mesh in front of the face would be needed (holes markedly smaller than the wavelength of 3.2 mm; that is not bigger than, say, 0.1 mm).”

decreased penetration of shorter millimeter waves. The surface temperature of a target will continue to rise so long as the beam is applied, at a rate dictated by the target's material and distance from the transmitter, along with the beam's frequency and power level set by the operator. Most human test subjects reached their pain threshold within 3 s, and none could endure more than 5 s.¹⁷

A spokesman for the Air Force Research Laboratory described his experience as a test subject for the system:

For the first millisecond, it just felt like the skin was warming up. Then it got warmer and warmer and you felt like it was on fire. . . . As soon as you're away from that beam your skin returns to normal and there is no pain.

Like all focused energy, the beam will irradiate all matter in the targeted area, including everything beyond/behind it that is not shielded, with no possible discrimination between individuals, objects, or materials. Anyone incapable of leaving the target area (e.g., physically handicapped, infants, incapacitated, trapped) would continue to receive radiation until the operator turned off the beam. Reflective materials such as aluminum cooking foil should reflect this radiation and could be used to make clothing that would be protective against this radiation (see footnote 16).

Following approximately 10,000 test exposures of volunteers to ADS beams (see footnote 15), a Penn State Human Effects Advisory Panel (HEAP) concluded that ADS is a nonlethal weapon that has a high probability of effectiveness with a low probability of injury (see footnote 14):

- No significant effects for wearers of contact lenses or other eyewear (including night-vision goggles).
- Normal skin applications, such as cosmetics, have little effect on ADS's interaction with skin.
- No age-related differences in response to ADS exposures.
- No effect on the male reproduction system.
- Damage was the occurrence of pea-sized blisters in less than 0.1% of the exposures (6 of 10,000 exposures) (see footnote 15).

In April 2007, one airman in an ADS test was overdosed and received second-degree burns on both legs and was treated in a hospital for 2 ays (see footnotes 16 and 17). There was also one laboratory accident in 1999 that resulted in a small second-degree burn (see footnote 15).

As part of effects of millimeter wave (MW), we need to look at *Critical Issue* by "Determining Intent" of let say Pirate vs. Fisherman by raising the issue of the following:

- Are the existing warning zone capabilities effective enough to support emerging maritime counter piracy tactics, techniques, and procedures?

¹⁷Kris Osborn, "Airman injured in heat-beam test," Army Times, April 5, 2007.

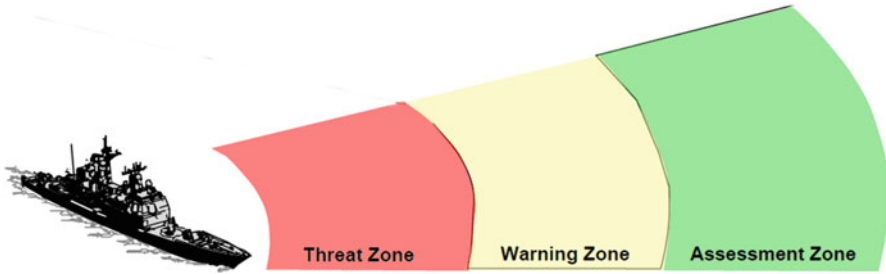


Fig. 7.9 Threat, warning, and assessment zone illustration

- Can active denial provide a significant mission capability to effectively control the next maritime piracy engagement situation?

This critical issue is illustrated artistically in Fig. 7.9 and leveraging technology to mitigate the next counter piracy situation.

7.5.1 *Human Effects*

Human effect testing on the large-scale version of active denial technology has included more than 13,000 exposures on volunteer subjects both in static demonstrations and in realistic operational assessments. Both laboratory research and full-scale test results demonstrated that there is only a 1/10th of 1% chance of injury from a System 1 or System 2 exposure. Research on the safety and effectiveness of 95 gigahertz millimeter-wave directed energy has been peer reviewed in numerous professional journals and independently reviewed by the Human Effects Advisory Panel.

7.5.2 *Possible Long-Term Effects*

Many possible long-term effects have been studied, with the conclusion that no long-term effects are likely at the exposure levels studied (see footnote 13). However, overexposures of either operators or targets may cause thermal injury. According to an official military assessment, “In the event of an overexposure to a power density sufficient to produce thermal injury, there is an extremely low probability that scars derived from such injury might later become cancerous. Proper wound management further decreases this probability, as well as the probability of hypertrophic scarring or keloid formation.”¹⁸

¹⁸Protocol # FWR 2003-03-31-H, Limited Military Utility Assessment of the Active Denial System (ADS)cached copy.

Cancer: A mouse cancer study was performed at two energy levels and exposures with a 94 GHz transmitter: a single 10 s, 1 W/cm² exposure, and repeated 10-s exposures over 2-week period at 333 mW/cm². At both energy levels, no increase in skin cancers was observed.¹⁹ No studies of higher energy levels or longer exposure times have been performed on millimeter-wave systems.

- Cornea damage: Tests on nonhuman primate eyes have observed no short-term or long-term damage as the blink reflex protects the eye from damage within 0.25 s [1].
- Birth defects: Millimeter waves only penetrate 0.4 mm (1/64 in.) into the skin, making direct damage to the testes or ovaries impossible.
- Blisters and scarring: Pea-sized blistering due to second-degree burns occurred in a very small minority (less than 0.1%) of tested exposures, which have a remote potential for scarring.

ADS operators would be exposed to more than the standard maximum permissible exposure (MPE) limits for RF energy, and military use requires an exception to these exposure limits.²⁰

7.6 Technogym Demonstration

Due to the novel nature of the active denial technology nonlethal effect, the Joint Non-Lethal Weapons Program has had a proactive strategy in raising the awareness of the benefits, safety, and effectiveness of this new technology. Several major broadcast and print media reporters have attended technology demonstrations, allowing for first-hand accounts on experiencing the effect of System 1 or 2. Active denial technology has been featured on CBS's *60 Minutes*, the Discovery Channel's *Future Weapons* program, and the History Channel's *Modern Marvels* program.

7.7 Emerging Technogym Configuration

While the Active Denial System Advanced Concept Technology Demonstration succeeded in demonstrating a large-scale version of active denial technology, a smaller-scale, more mobile version is also of military interest. Several efforts are underway to identify new millimeter-wave sources that will allow for reduced size, weight, and system cost with instant "turn-on" and "shoot-on-the-move" capabilities. See Fig. 7.10 for more details.

¹⁹Patrick A. Mason. "Lack of effect of 94 GHz radio frequency radiation exposure in an animal model of skin carcinogenesis." Carcin.oxfordjournals.org. Retrieved November 1, 2014.

²⁰"Non-Ionizing Radiation." Retrieved March 8, 2012.



Fig. 7.10 Conceptual next-generation ADT system

7.8 Active Denial System II

In 2011, the ADS was redesigned to make it smaller, more reliable, and able to be used on the move. ADS II is being designed to operate from moving aircraft, as well as moving ground vehicles. The redesign does not address problems in different environmental conditions.²¹

The Air Force Special Operations Command is experimenting with mounting an ADS of the AC-130 J Ghosthunter gunship to target threatening crowds or individuals on the ground. This is to give the gunship a nonlethal option, so the crew has more engagement options. Due to the increasing number of engagements in populated areas, the Air Force is aiming to have field a system within 5–10 years to have enough aircraft available with less lethal systems (see footnote 35). The aircraft will apparently use the ADS II version.²²

7.9 Concepts for Use

ADS was developed as a nonlethal weapon. According to Department of Defense policy, nonlethal weapons “are explicitly designed and primarily employed so as to incapacitate personnel or material, while minimizing fatalities, permanent injury to

²¹Death Ray Turns Warm And Fuzzy—Strategypage.com, October 3, 2012.

²²AC-130 J Gets A Ray Gun - Strategypage.com, 10 August 2015.

personnel, and undesired damage to property and the environment.”²³ ADS has applications for crowd control and perimeter defense, and filling “the gap between shouting and shooting.” Other crowd control methods—including pepper spray, tear gas, water cannons, slippery foam, and rubber bullets—carry implicit dangers of temporary or permanent injury or accidental death, and often leave residue or residual material. Combinations of acoustic and optical system platforms with ADS can be used to effectively communicate to, warn of escalation of force, introduce optical and auditory deterrents and step function the escalation of transmitted force from relatively benign to ultimately forced dispersal of a crowd, or to deny them from an area or access to an area. A group of people can theoretically be dispersed or induced to leave an area in a manner unlikely to damage personnel, noninvolved civilians (no stray bullets), or to nearby buildings or the environment.

Nonlethal weapons are intended to provide options to US troops, for example, “to stop suspicious vehicles without killing the drivers.”²⁴ Although the ADS millimeter-wave frequency does not affect a car’s electronic components, it can be used to deter a driver in an approaching vehicle.²⁵ In a broader strategic context, nonlethal weapons such as ADS have the potential to offer “precision, accuracy, and effective duration that can help save military and civilian lives, break the cycle of violence by offering a more graduated response, and even prevent violence from occurring if the opportunity for early or precautionary engagement arises.”²⁶

The Council on Foreign Relations noted that “wider integration of existing types of nonlethal weapons (NLW) into the U.S. Army and Marine Corps could have helped to reduce the damage done by widespread looting and sabotage after the cessation of major conflict in Iraq.”²⁷

In Afghanistan, the need to minimize civilian casualties has led to restrictive rules of engagement on the use of lethal force by US troops. A National Public Radio correspondent in Afghanistan “witnessed troops grappling with the dilemma of whether to shoot.”²⁸ Nonlethal weapons such as ADS provide an option for US forces in those situations.²⁹

²³“DoD Executive Agent for Non-Lethal Weapons (NLW), and NLW Policy” (PDF). Dtic.mil. Retrieved 1 November 2014.

²⁴Michael O’Hanlon. “Opinion: Troops need not shoot in Afghanistan.” Politico. Retrieved November 1, 2014.

²⁵Archived September 15, 2012, at the Wayback Machine.

²⁶Archived March 5, 2012, at the Wayback Machine.

²⁷Graham T. Allison. “Nonlethal Weapons and Capabilities.” Council on Foreign Relations. Retrieved November 1, 2014.

²⁸Archived October 27, 2011, at the Wayback Machine.

²⁹“Joint Non-Lethal Weapons Program Website – ADS.” Jnlwp.com. Archived from the original on September 30, 2007. Retrieved December 26, 2008.

7.10 Controversy

The effects of this radio frequency on humans have been studied by the military for years, and much, but not all, of the research has been published openly in peer-reviewed journals.³⁰

A news article criticized the sheer amount of time it is taking to field this system, citing the potential it had to avert a great deal of pain and suffering in volatile areas around the world.³¹

Although the effects are described as simply “unpleasant,” the device has the “potential for death.”³²

While it is claimed not to cause burns under “ordinary use,”^{33,34} it is also described as being similar to that of an incandescent light bulb being pressed against the skin (see footnote 31), which can cause severe burns in just a few seconds. The beam can be focused up to 700 meters away and is said to penetrate thick clothing although not walls.³⁵ At 95 GHz, the frequency is much higher than the 2.45 GHz of a microwave oven. This frequency was chosen because it penetrates less than 1/64 of an inch (0.4 mm), which—in most humans, except for eyelids and babies—avoids the second skin layer (the dermis) where critical structures are found such as nerve endings and blood vessels.

The early methodology of testing, in which volunteers were asked to remove glasses, contact lenses, and metallic objects that could cause hot spots, raised concerns as to whether the device would remain true to its purpose of nonlethal temporary incapacitation if used in the field where safety precautions would not be taken. However, these tests were early in the program and part of a thorough and methodical process to demonstrate the safety and effectiveness of the technology, which has now involved more than 600 volunteer subjects and some 10,200 exposures. As safety was demonstrated in each step of the process, restrictions were removed, and now, according to ADS proponents, there are no restrictions or precautions necessary for volunteers experiencing the effect. Long-term exposure to the beam may cause more serious damage, especially to sensitive tissues, such as those of the eyes. Two people have received second-degree burns after exposure to the

³⁰“Pentagon nixes ray gun weapon in Iraq” Archived February 2, 2009, at the Wayback Machine.. By Richard Lardner, Associated Press.

³¹Hambling, David (October 10, 2008). “Army Orders Pain Ray Trucks; New Report Shows ‘Potential for Death.’” *Wired*.

³²“Moody Airmen test new, nonlethal method of repelling enemy – Eric Schloeffel.” January 25, 2007. Archived from the original on December 13, 2007. Retrieved December 22, 2007.

³³Jump up to: a b Shachtman, Noah (April 6, 2007). “Pain Ray Injures Airman.” *Wired*. Archived from the original on February 2, 2009. Retrieved December 26, 2008.

³⁴Hooper, Duncan (January 25, 2007). “US unveils ‘heat gun’.” *The Daily Telegraph*. London. Retrieved April 23, 2010.

³⁵Active Denial System Factsheet. Joint non-lethal weapons program, 2007. Archived September 30, 2007, at the Wayback Machine.

device^{36,37,38,39,40,41} (the actual number of injuries, according to Ms. Stephanie Miller of AFRL/RDHR, is a total of eight—the two previously mentioned, and six others, who healed without medical intervention) [citation needed].

In addition, some claim that subjects who have body piercings, jewelry, or tattoos are likely to suffer serious skin damage. Tattooed people can become ill due to high amounts of toxic substances released from heated/melted tattoo pigment. Human effects testing on the large-scale version of ADS included more than 11,000 exposures on over 700 volunteers. Both laboratory research and full-scale test results demonstrated that there is only a 0.1% chance of injury from a System 1 or System 2 exposure.⁴²

Critics cite that, although the stated intent of the ADS is to be a nonlethal device designed to temporarily incapacitate, modifications or incorrect use by the operator could turn the ADS into a more damaging weapon that could violate international conventions on warfare (although at this time, ADS has gone through numerous treaty compliance reviews and legal reviews by AF/JAO, and in all cases complies with every treaty and law).⁴³

Some have focused on the lower threshold of use which may lead those who use them (especially civilian police) to become “trigger-happy,” especially in dealing with peaceful protesters. Others have focused on concerns that weapons whose operative principle is that of inflicting pain (though “nonlethal”) might be useful for such purposes as torture, as they leave no evidence of use, but undoubtedly have the capacity to inflict horrific pain on a restrained subject. According to Wired Magazine, the active denial system has been rejected for fielding in Iraq due to Pentagon fears that it would be regarded as an instrument of torture (see footnote 43).

³⁶Hearn, Kelly (August 19, 2005). “Rumsfeld’s Ray Gun.” AlterNet. Archived from the original on August 12, 2006. Retrieved August 15, 2006.

³⁷“PADS – Cold Stress.” Labor.state.ak.us. Archived from the original on February 2, 2009. Retrieved December 26, 2008.

³⁸https://www.jnlwp.com/misc/fact_sheets/ADT%20Fact%20Sheet%20Aug%2009%20FINAL.pdf. Retrieved September 23, 2009. Missing or empty |title = (help)[dead link]

³⁹Joint Non-Lethal Weapons Directorate Archived September 16, 2008, at the Wayback Machine. Source Documentation found in numerous press releases and Media Demo Days.

⁴⁰Weinberger, Sharon (August 30, 2007). “No Pain Ray for Iraq.” Wired. Archived from the original on December 10, 2008. Retrieved December 13, 2008.

⁴¹Hambling, David (May 8, 2009). “‘Pain ray’ first commercial sale looms.” Wired. Retrieved October 2, 2018.

⁴²“New ‘Laser’ Weapon Debuts in LA County Jail.” NBC Southern California. Retrieved November 1, 2014.

⁴³“Run away the ray-gun is coming: We test US army’s new secret weapon.” The Daily Mail. London. September 18, 2007.

Reference

1. S. Chalfin, J.A. D'Andrea, P.D. Comeau, M.E. Belt, D.J. Hatcher, Millimeter wave absorption in the nonhuman primate eye at 35 GHz and 94 GHz. *Health Phys.* **83**(1), 83–90 (2002)

Appendix A: Microwave Breakdown in Gases

A very large fraction of the work done in the field of gas discharge has been concerned with breakdown. Measurements of breakdown electric fields and voltages have been relatively reproducible and have thus provided a good method of checking the predictions of theory and establishment of Paschen's law accordingly. Electrical breakdown or dielectric breakdown is when current flows through an electrical insulator when the voltage applied across it exceeds the breakdown voltage. This results in the insulator becoming electrically conductive. Electrical breakdown may be a momentary event (as in an electrostatic discharge) or may lead to a continuous arc if protective devices fail to interrupt the current in a power circuit. Under sufficient electrical stress, electrical breakdown can occur within solids, liquids, gases, or vacuum. However, the specific breakdown mechanisms are different for each kind of dielectric medium.

A.1 Introduction

The problem of microwave breakdown near antennas at high altitudes could be considered in order to find out what is the limitation on transmission conditions [1].

Electrical breakdown is often associated with the failure of solid- or liquid-insulating materials used inside high-voltage transformers or capacitors in the electricity distribution grid, usually resulting in a short circuit or a blown fuse. Electrical breakdown can also occur across the insulators that suspend overhead powerlines, within underground power cables, or lines arcing to nearby branches of trees.

Airborne radar system may initiate electrical discharges in front of the antennas at high altitudes because, at ultrahigh frequencies, the electric field required to break down air at low pressures is, in general, much less than that required at atmospheric pressure. The processes which determine ultrahigh-frequency (UHF) breakdown

Fig. A.1 Electrical breakdown driving electric discharge



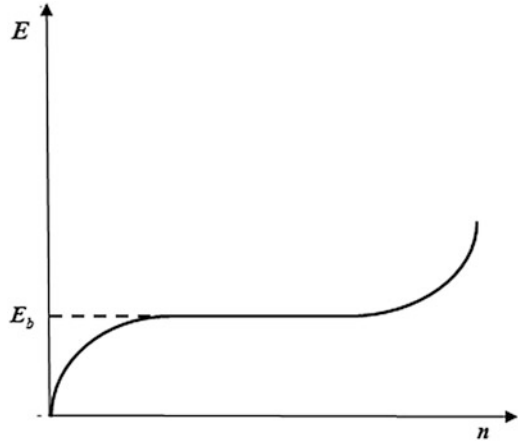
have been discovered and verified during the past decade. These have been applied to determining optimum transmission conditions for high-flying radar as an example.

Breakdown criteria take place when an electric field is applied to a gas, and then the free electrons move in the direction of the field, constituting a current. There is a small number of electrons present in any collection of gas because of ionization by cosmic rays or some other phenomenon, such as photoelectric effect. If the electric field is gradually increased from zero, the gas first appears to obey Ohm's law until the field becomes large enough to impart sufficient energy to some of the electrons to produce secondary electrons by collision. If the electric field is sufficiently great so that many secondary electrons are produced, there will come a point at which the gas will become highly conducting. For a very minute change in voltage or field near this value, the electron concentration and current will change by many orders of magnitude, and the gas will start to glow as it can be seen in Fig. A.1 [1].

Note that this criterion was defined by Townsend many years ago and a criterion, which enabled him to describe breakdown quantitatively. Although the description was designed for direct current discharges, the Townsend criterion has proved useful in considering discharges produced by electric fields of any frequency, including microwaves. In a gas discharge, electrons are being produced by ionization and being lost by diffusion, recombination, and other ways we need not consider at the moment. See Fig. A.2.

Dielectric breakdown is also important in the design of integrated circuits and other solid-state electronic devices. Insulating layers in such devices are designed to

Fig. A.2 Variation of electron concentration with electric field



withstand normal operating voltages, but higher voltage such as from static electricity may destroy these layers, rendering a device useless. The dielectric strength of capacitors limits how much energy can be stored and the safe working voltage for the device [2].

Breakdown mechanisms differ in solids, liquids, and gasses. Breakdown is influenced by electrode material, sharp curvature of conductor material (resulting in locally intensified electric fields), size of the gap between the electrodes, and density of the material in the gap (Fig. A.1).

In solid materials (such as in power cables) a long-time partial discharge typically precedes breakdown, degrading the insulators and metals nearest the voltage gap. Ultimately the partial discharge chars through a channel of carbonized material that conducts current across the gap.

Electrical breakdown occurs within a gas when the dielectric strength of the gas is exceeded. Regions of intense voltage gradients can cause nearby gas to partially ionize and begin conducting. This is done deliberately in low-pressure discharges such as in fluorescent lights. The voltage that leads to electrical breakdown of a gas is approximated by Paschen's law. See next section of this Appendix.

A.2 Paschen's Law

Paschen's law dates back to the nineteenth century, named after Friedrich Paschen, and is often referenced when in voltage breakdown calculations. For this effort you will find Friedrich Paschen in the Microwave Hall of Fame [3].

Paschen's law is an equation that gives the breakdown voltage, that is, the voltage necessary to start a discharge or electric arc, between two electrodes in a gas as a function of pressure and gap length [4, 5]. It is named after Friedrich Paschen who discovered it empirically in 1889 [6].

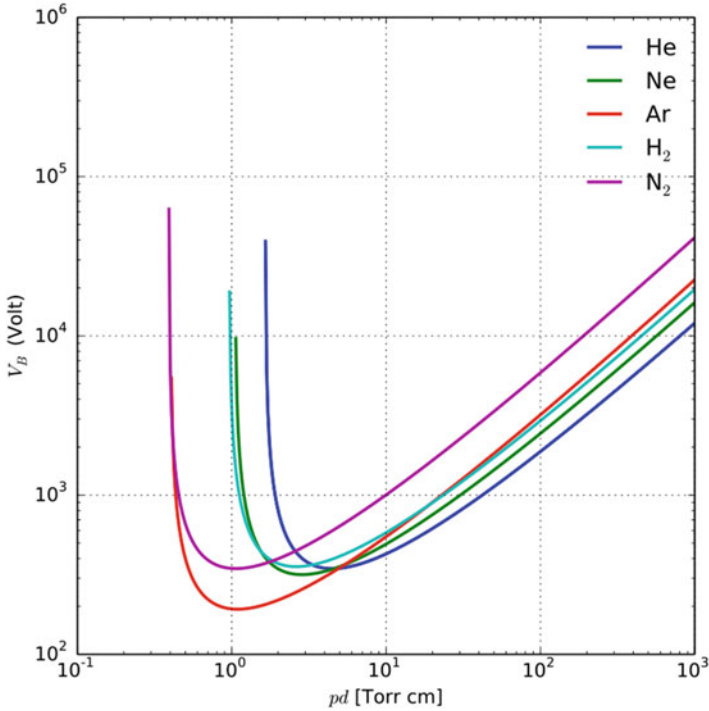


Fig. A.3 Paschen curves [7]

Paschen studied the breakdown voltage of various gases between parallel metal plates as the gas pressure and gap distance were varied:

- With a constant gap length, the voltage necessary to arc across the gap decreased as the pressure was reduced and then increased gradually, exceeding its original value.
- With a constant pressure, the voltage needed to cause an arc reduced as the gap size was reduced but only to a point. As the gap was reduced further, the voltage required to cause an arc began to rise and again exceeded its original value.

For a given gas, the voltage is a function only of the product of the pressure and gap length [4, 5]. The curve he found of voltage versus the pressure-gap length product (*right*) is called *Paschen’s curve*, Fig. A.3.

Figure A.3 is an illustration of Paschen curves obtained for helium, neon, argon, hydrogen, and nitrogen, using the expression for the breakdown voltage as a function of the parameters A and B that interpolate the first Townsend coefficient [7].

He found an equation that fit these curves, which is now called Paschen’s law, which is an empirical result as Eq. (A.1) [5]:

$$V_B = \frac{Bpd}{\ln(Apd) - \ln\left[\ln\left(1 + \frac{1}{\gamma_{se}}\right)\right]} \tag{Eq.A.1}$$

In this equation, V_B is the breakdown voltage in volts, p is the pressure in Pascals, d is the gap distance in meters, γ_{se} is the secondary electron emission coefficient, which is the number of secondary electrons produced per incident positive ion, A is the saturation ionization in the gas at a particular E/p (i.e., electron field/pressure), and B is related to the excitation and ionization energies.

The constants A and B are determined experimentally and found to be roughly constant over a restricted range of E/p for any given gas.

For example, air with an E/p in the range of 450–7500 V/(kPa·cm), $A = 112.50$ (kPa cm) $^{-1}$ and $B = 2737.50$ V/(kPa cm) [8].

The graph of this equation is the Paschen curve. By differentiating it with respect to and setting the derivative to zero, the minimal voltage can be found. This yields as illustrated in Eq. (A.2):

$$pd = \frac{e \cdot \ln \left(1 + \frac{1}{\gamma_{se}} \right)}{A} \quad (\text{A.2})$$

and predicts the occurrence of a minimal breakdown voltage for $pd = 7.5 \times 10^{-6}$ m·atm. This is 327 V in air at standard atmospheric pressure at a distance of 7.5 μm .

The composition of the gas determines both the minimal arc voltage and the distance at which it occurs. For argon, the minimal arc voltage is 137 V at a larger 12 μm . For sulfur dioxide (SO $_2$), the minimal arc voltage is 457 V at only 4.4 μm .

Note that in the above scenario for the atmosphere condition, we first consider the nature of the atmosphere from ground level to 500,000 ft. It is now generally agreed that the composition of the atmosphere is constant up to approximately 250,000 ft [9].

In this range, nitrogen and oxygen compose 99% of the total gases and their relative amounts do not change [1].

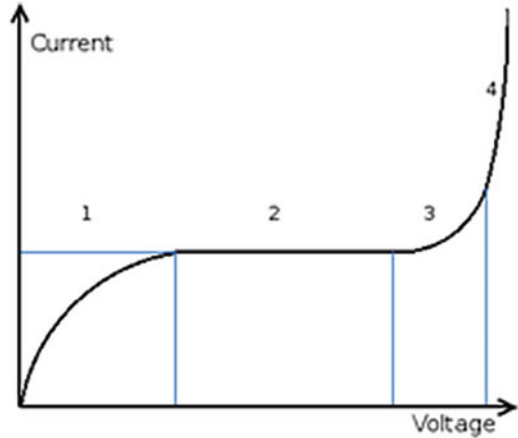
At higher pressures and gap lengths, the breakdown voltage is approximately *proportional* to the product of pressure and gap length, and the term Paschen's law is sometimes used to refer to this simpler relation [10]. However, this is only roughly true, over a limited range of the curve.

A.2.1 Voltage-Current Relation

Before gas breakdown, there is a nonlinear relation between voltage and current as shown in Fig. A.4. In region 1, there are free ions that can be accelerated by the field and induce a current. These will be saturated after a certain voltage and give a constant current, region 2. Regions 3 and 4 are caused by ion avalanche as explained by the Townsend discharge mechanism.

As we have mentioned in the previous Appendix A.2, Friedrich Paschen established the relation between the breakdown condition and breakdown voltage.

Fig. A.4 Voltage-current relation before breakdown



He derived a formula as written in Eq. (A.1) and that defines the breakdown voltage V_B for uniform field gaps as a function of gap length d and gap pressure p [11].

Paschen also derived a relation between the minimum value of pressure gap for which breakdown occurs with a minimum voltage as the following sets of equations [11]:

$$\begin{cases} (pd)_{\min} = \frac{2.718}{A} \ln \left(1 + \frac{1}{\gamma} \right) \\ (V_B) = 2.718 \frac{B}{A} \ln \left(1 + \frac{1}{\gamma} \right) \end{cases} \quad (\text{A.3})$$

where A and B are constants depending on the gas used and $\gamma = C_p/C_v$ is the gas adiabatic index with C_p and C_v being the gas specific heat at constant pressure and volume, respectively.

The high-voltage power system in general consists of a complex configuration of generators, long-distance transmission lines, and localized distribution networks with above- and below-ground conductors for delivering energy to users. Associated with this are a wide range of high-voltage components whose successful operation depends on the correct choice of the electrical insulation for the particular application and voltage level.

The condition of the insulating materials when new, and especially as they age, is a critical factor in determining the life of much equipment. The need for effective maintenance, including continuous insulation monitoring in many cases, is becoming an important requirement in the asset management of existing and planned power systems.

As the voltages and powers to be transmitted increased over the past 100 years the basic dielectrics greatly improved following extensive research by industry and in specialized high-voltage laboratories, where much of this work continues.

A.3 Atmospheric Breakdown Limit

When you design or operate an airborne transmitter with perhaps 1000 watts peak output power, it's time to think about atmospheric breakdown.

Power tubes are microwave circuits that employ high voltage; often it is the power supply that arcs, not the tube! To some extent breakdown is a function of frequency; as you go to higher frequencies breakdown voltage will decrease.

Things you can do to prevent arcing at high altitude:

- Turn off the high-voltage equipment (this is not always an option!). Do not forget to use bleeder circuits to discharge high-voltage capacitors.
- Eliminate sharp points, and maximize spacing between high-voltage conductors.
- Seal high-voltage components in pressurized containers.
- Pot high-voltage components. Typical potting materials are dielectrically loaded silicone goop. Potting a component will reduce your ability to troubleshoot it; it isn't easy to remove potting material!

When the "critical field" is exceeded, arcing occurs. Recall from that freshmen physics class you slept through what "field" means, its units are volts/meter, not volts, and it is "E" in an equation (for electric field), not V. At STP (standard temperature and pressure) for spherical electrodes, this happens at 3,300,000 volts/m. As you go up in altitude and air pressure drops, the critical field decreases. By the time you are at 50,000 ft, it might be 400,000 volts per meter.

Because power handling goes as voltage squared, your high-voltage design that works on the bench might be in a world of hurt when you fly it.

An approximate number for breakdown electric field is three million volts per meter, or 30,000 volts per centimeter, for a gap of 7 mm at 1 atmosphere. Quoting an exact value for breakdown in air is not possible unless you consider gap size, pressure, and humidity . . . even the geometry of the electrodes matters. Paschen's law applies to spherical electrodes (Figs. A.5 and A.6).

It is worth to mention that peak power handling in waveguide is subject to both heat (average power) and voltage breakdown (peak power) limitations.

Voltage breakdown in rectangular waveguide at sea-level air pressure can be predicted by the following approximated equation as

$$P_{br} = 600,000 \times a \times b \times (\text{Lambda}/\text{Lambda guide}) \text{ (Watts)} \quad (\text{A.4})$$

Lambda guide is a guide wavelength that is defined as the distance between two equal phase planes along the waveguide. The guide wavelength is a function of operating wavelength or frequency and the lower cutoff wavelength and is always longer than the wavelength would be in free space. Here is the equation for guide wavelength:

Fig. A.5 Paschen's law, breakdown voltage for 1 m separation in air

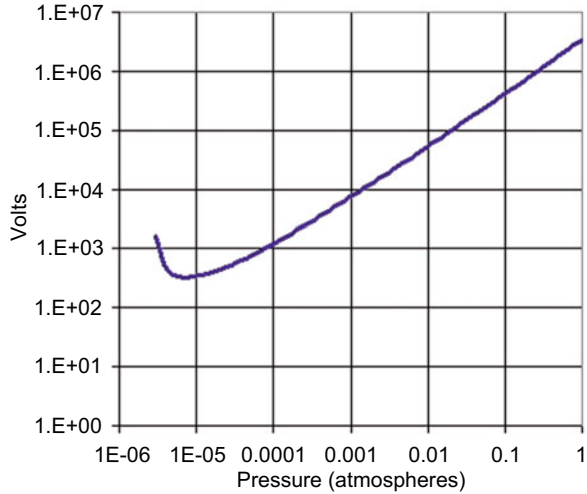
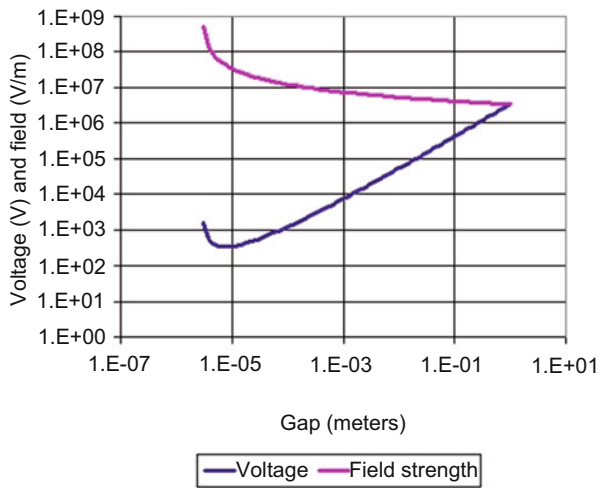


Fig. A.6 Paschen's law, breakdown voltage, and field at one atmosphere



$$\lambda_{\text{guide}} = \frac{\lambda_{\text{free space}}}{\sqrt{1 - \left(\frac{\lambda_{\text{free space}}}{\lambda_{\text{cutoff}}}\right)^2}} \tag{A.5}$$

$$\lambda_{\text{guide}} = \frac{c}{f} \times \frac{1}{\sqrt{1 - \left(\frac{c}{2a \cdot f}\right)^2}}$$

Guide wavelength is used when you design distributed structures in waveguide. For example, if you are making a PIN diode switch with two shunt diodes spaced 3/4 wavelength apart, use the 3/4 of a guide wavelength in your design.

The guide wavelength in waveguide is longer than wavelength in free space. This is not intuitive; it seems like the dielectric constant in waveguide must be less than unity for this to happen . . . don't think about this too hard you will get a headache.

Bear in your mind that arcing is caused when the electric field E exceeds a critical value which we will denote E_d for electric field at discharge. In air, the critical field is about 1,000,000 volts/m; in polytetrafluoroethylene (PTFE) (i.e., a long-chain molecule, one form of it is registered under the DuPont trademark "Teflon," Invented by Dr. Roy J. Plunkett of DuPont) it is raised to about 100,000,000. These numbers are approximate; there's no sense trying to be exact in calculating breakdown; just be sure that you avoid it by an order of magnitude or more and you will have little to worry about.

A.4 Phase Velocity and Group Velocity

Phase velocity is an almost useless piece of information you will find in waveguide mathematics. Here you multiply frequency time guide wavelength and come up with a number that exceeds the speed of light. See Eq. (A.6):

$$v_{\text{phase}} = \frac{c}{\sqrt{1 - \left(\frac{c}{2a \cdot f}\right)^2}} \quad (\text{A.6})$$

Be assured that the energy in your wave is not exceeding the speed of light, because it travels at what is called the *group velocity* of the waveguide as illustrated in Eq. (A.7) as

$$v = c \times \sqrt{1 - \left(\frac{c}{2a \cdot f}\right)^2} \quad (\text{A.7})$$

The group velocity is always less than the speed of light (Fig. A.7); we like to think of that this is because the EM wave is ping-ponging back and forth as it travels down the guide. Note that (group velocity) \times (phase velocity) = c^2 .

Group velocity in a waveguide is speed at which EM energy travels in the guide. Plotted below as a percentage of the speed of light (c), we see how group velocity varies across the band for WR-90 (X-band) waveguide. Note that the recommended operating band of WR-90 is from 8.2 to 12.4 GHz. At 8.2 GHz the signal is slowed to 60% of the free-space speed of light. At the lower cutoff (6.56 GHz), the wave is slowed to zero, and you can outrun it without breathing hard.

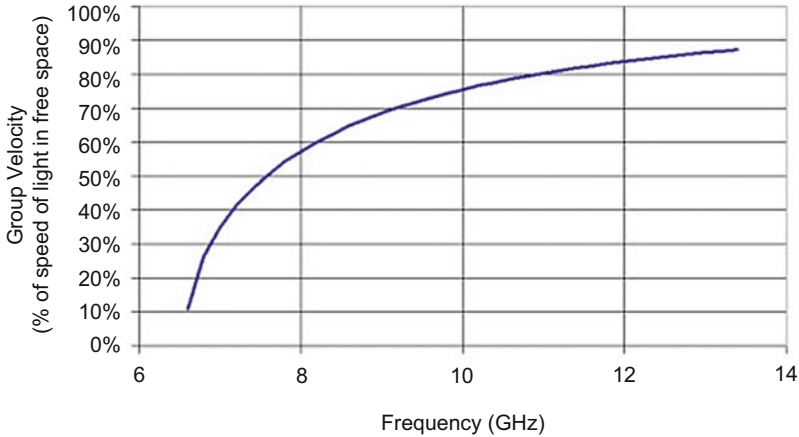


Fig. A.7 Group velocity as a function of frequency. WR-90 rectangular waveguide

A.5 Group Delay in Waveguide

Group delay is defined as the rate of change of transmission phase angle with respect to frequency. The units work out to time when the angle is in radians and frequency is in radians/time (seconds, nanosecond, picosecond, or whatever is convenient, depending on the length of the path). When group delay is extracted from S-parameters, unless the network is a perfect measurement of a perfect transmission line, there will be variations over frequency. But within a small amount of bandwidth, group delay is usually nearly constant. Thanks to Martin, for keeping us on our toes!

Martin further wishes to point out that group delay can actually be negative (in some rare occasions).

Group delay can be *construed* as a measurement of how long it takes a signal to traverse a network, or its *transit time*. It is proportional to the length of the network, and usually a weak function of frequency. In this sense, we at Microwaves101 show you how to use group delay to extract dielectric material properties.

In considering group delay, remember that in free space all electromagnetic signals travel at the speed of light, “c,” which is approximately 3×10^8 m per second.

You should know that the speed of light is exactly equal to $(1/\epsilon\mu)^{0.5}$, where ϵ is the permittivity of the medium, and μ is its permeability. While the one-nanosecond-per-foot rule works for free space, what about coax cables? The *group velocity* is reduced in coax by $1/\text{sqrt}(\epsilon_R)$. Most coax cables use 100% PTFE filling, which has a dielectric constant of about 2.2. This works out to a group delay of 1.45 ns for one foot of solid PTFE coax. Keep in mind that some flexible cables use PTFE that is partially filled with air; these cables provide group delay on the order of 1.3–1.4 ns per foot (Fig. A.8).

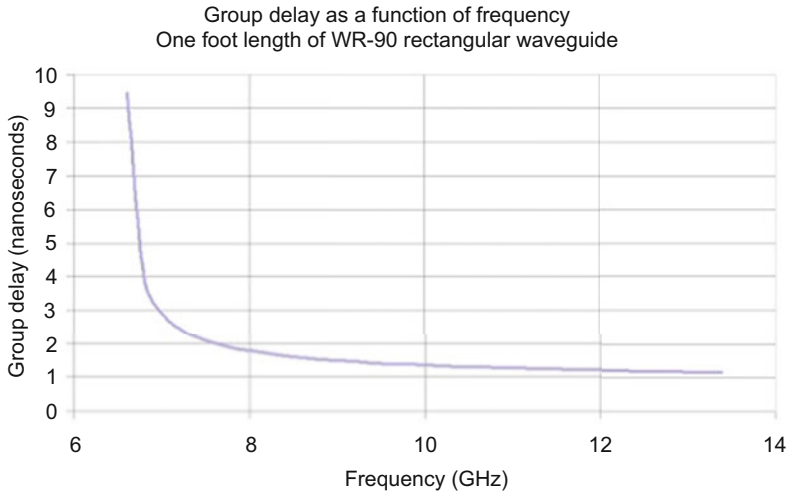


Fig. A.8 Group delay as a function of frequency

Now that we know the group velocity, we can calculate the group delay of any piece of waveguide, noting that time is distance divided by velocity as indicated in Eq. (A.8):

$$\text{Group delay} = \frac{\text{length}}{c \times \sqrt{1 - \left(\frac{c}{2a \cdot f}\right)^2}} \tag{A.8}$$

The group delay of rectangular waveguide components is a function of the frequency you are applying. Near the lower cutoff, the group delay gets longer and longer, as the EM wave ping-pongs down the guide and can easily be 10× the free-space group delay. But at the upper end of a waveguide’s band, the group delay approaches the free-space group delay, which follows the rule of thumb, approximately one foot per nanosecond, independent of frequency.

To compare with the 1 ns/foot rule of thumb, below is a plot of the group delay of one foot of WR-90 waveguide. At the upper end of the band you will see that very nearly the free-space group delay is achieved.

The problem of electromagnetic energy traveling at different speeds over frequency is commonly called dispersion. Soon we will have a page on this topic as well.

A.6 Peak Power Handling in Waveguide

As we said before and as described by Eq. (A.5), waveguide power handling is subject to both heat (average power) and voltage breakdown (peak power) limitations; consequently, to take a step back further in equation land, P_{br} may be written

as a function of the breakdown field strength (although we don't have an exact reference for where this came from, it can be presented in Eq. A.9):

$$P_{br} = 6.63 \times 10^{-4} \times a \times b[\text{Lambda}/\text{Lambda guide}] \times (E_{br})^2 (\text{Watts}) \quad (\text{A.9})$$

where E_{br} is in Volts/Cm, and a and b are in centimeters.

In this case you will notice that the E_{br} value that corresponds to 600,000 value in Eq. (A.1) is 30,000 volts/cm which represents a 7 mm gap at one atmosphere.

If you plug in the dimensions for WR-90, the power handling is in excess of 1 megawatt at band center where (Lambda/Lambda guide) is 0.75. Yikes!

For circular waveguide, the approximate power handling equation becomes

$$P_{br} = 450000d^2(\text{Lambda}/\text{Lambda guide})(\text{Watts}) \quad (\text{A.10})$$

where d is the diameter in centimeters.

These two last Eqs. (A.9) and (A.10) came from page 70 of Gershon Wheeler's excellent book, *Introduction to Microwaves*, circa 1963. Note that his information on the critical field for breakdown probably dated to WWII and more accurate numbers are now available. If knowing the exact power handling of a particular waveguide is important to you, you need to dive into this topic a little more than we have. Be sure to consider altitude effects on E_{br} .

Waveguide power handling can be increased by pressurizing or using certain inert gases which can withstand higher much electric fields, such as Freons.

A.7 Bleak Driving Future of High-Power Microwave

The propagation of high-power microwave pulses through the atmosphere has been a subject with considerable scientific interest [12–17]. This is because air breakdown produces ionization phenomena that can radically modify wave propagation. Ionization gives rise to a space-time-dependent plasma which attenuates the tail of the pulse but hardly affects the leading edge because of the finite time for the plasma to build up. A mechanism which is called “tail erosion” plays the primary role in limiting transmission of the pulse [12–14, 17]. Moreover, the nonlinear and nonlocal effects brought about by the space-time-dependent plasma also play important roles in determining the propagation characteristic of the pulses [16]. Therefore, any meaningful theoretical effort requires a self-consistent description of the propagation process. Consequently, an experimental effort could be more relevant and useful.

Basically, there are two fundamental issues to be addressed:

- One concerns the optimum pulse characteristics for maximum energy transfer through the atmosphere by the pulse.
- The second concern is maximizing the ionizations in the plasma trail following the pulse. In general, these two concerns are interrelated and must be considered together.

This is because in order to minimize the energy loss in the pulse before reaching the destination, one has to prevent the occurrence of excessive ionization in the background air. Otherwise, the over-dense plasma can cut off the propagation of the remaining part of the pulse and cause the tail of the pulse to be eroded via the reflection process. This process is believed to be far more severe in causing tail erosion than the normal process attributed to ionization and heating. Once this process occurs, the remaining pulse will become too narrow to ionize dense enough plasma whose nonlinear effect is thought to help in sufficient focusing to compensate for wave spreading beyond the Fresnel distance.

Electrical breakdown problems (EBPs) is a general problem of most high-power microwave tubes of both conventional and fast-wave type. It is a phenomenon related to the window material, its surface field strength, and electrical characteristics. Accumulation of radio-frequency (RF) losses in the ceramic material causes an increase in the surface electric field strength and thereby leads to electric breakdown.

Proper evacuation of the transmission line could avert such breakdown situations. However, care should be taken by arc detection and other electrical means to avoid breakdowns causing physical damage to the windows.

Furthermore, high-power microwave (HPM) in the form of long-wavelength radars achieved weapons-class power levels decades ago. However, reducing the size of the system to a size smaller than a warship has kept the technology at bay and off of the battlefield for many years, until recent technology of the active denial effect (ADE) was discovered and exploited.

Note that the active denial system (ADS) (Fig. A.9) is a nonlethal directed energy weapon (DEW) developed by the US military, and designed for area denial, perimeter security, and crowd control.



Fig. A.9 Active denial system 2 (source: Official Department of Defense Image)

Informally, the weapon is also called the *heat ray* [18] since it works by heating the surface of targets, such as the skin of targeted human subjects. Raytheon Corporation is currently marketing a reduced-range version of this technology [19]. The ADS was deployed in 2010 with the US military in the Afghanistan War, but was withdrawn without seeing combat.

Active denial technology produces a focused beam of directed energy to provide our troops a nonlethal option to stop, deter, and turn back suspicious individuals with minimal risk of injury. Active denial technology is designed to protect the innocent, minimize fatalities, and limit collateral damage across the range of military operations.

In summary, the powerful, ground-based radars fielded in the 1950s by both the United States and the Soviet Union of the time, first for air defense and later to detect incoming intercontinental ballistic missiles (ICBMs). Some of these radars produce electromagnetic energy in the microwave band range and are used today in applications that range from profiling atmospheric winds to tracking aircraft as well. A radar system today has *look-down/shoot-down* capability in most modern fighter aircraft built by different countries around the world, if it can detect, track, and guide a weapon to an air target moving below the horizon as seen by the radar or ground-based target as well. Early radars in the 1940s generated hundreds of kilowatts, and their power has increased through the recent years. In case of airborne radar system for example, in the late 1970s, the MIG-23 Russian-built fighter jet influenced ground-attack aircraft, the MIG-27, and entered service with the Russian military Air Force. See Fig. A.10.



Fig. A.10 Illustration of ground attack MIG-27 in landing mode

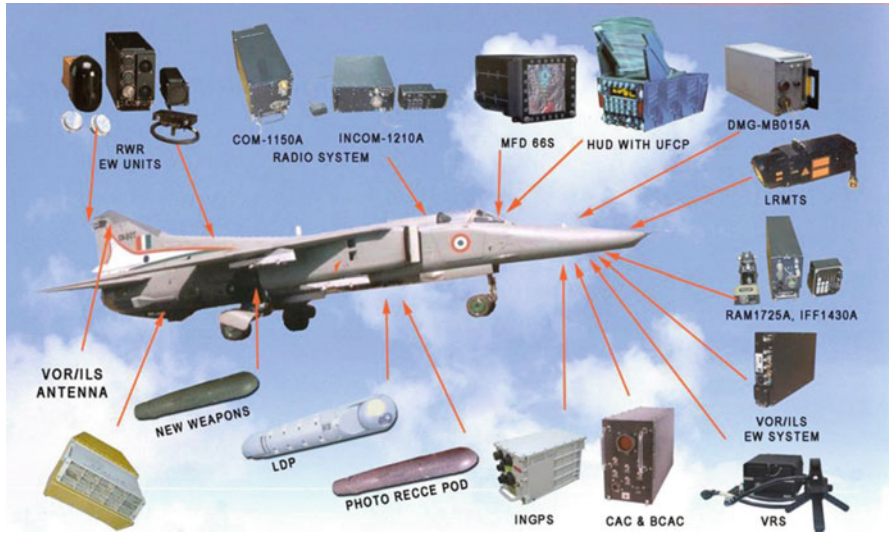


Fig. A.11 Holistic electronic configuration of MIG-27 aircraft

Faithful to the progressive trend in the military, it is a more powerful, yet not-necessarily-as-swift, fighter. The concept of variable geometry was not new to the Soviets and was conceived several years before and integrated into the design of the MiG-27 Flogger’s forerunner, and in Sukhoi’s Su-7. Its great advantages are found one, for the pilot, for whom is afforded smoother acceleration, and for the craft, which can lift within a smaller runway space and carry more cargo for greater distances. The MiG-27’s family ranges from its initial version to the K model and beyond, and its different models include features like fixed air engine intakes, and dual-position afterburners. The plane also contains modifications such as a guidance system for combat within inclement weather or at night, and an aft-position tracker. See Fig. A.11.

Other characteristics of the improved MiG-27 are, within its electronics system, an active countermeasure jammer, a laser rangefinder, an “identification-friend or foe” antenna, a tri-optical camera reconnaissance packages, Klein state-of-the-art signal transference, as well as numerous antennae and variable-frequency communications capabilities. The Flogger transports a variety of armament. 30-millimeter Gsh-6-30 guns may be used, as are the Atoll-D and R13M air-to-air missiles. Radio-guided surface-to-air weapons like the AS-7 Kerry are also employed. In the past, the plane was known to have carried tactical nuclear weapons, as well as the S-4240-millimeter and UB-32 or UB-16 57-millimeter rockets.

The capacity for dropping napalm, eight bombs weighing over 1000 pounds each, and firing flares is also possessed by the MiG-27. A six-barrel 23-millimeter rotating Gatling gun also resides under the craft’s body. The total of the weapons that can typically be carried on a combat mission with the plane is over 8000 pounds. While little is known about the Flogger’s performance within a war zone, it apparently is

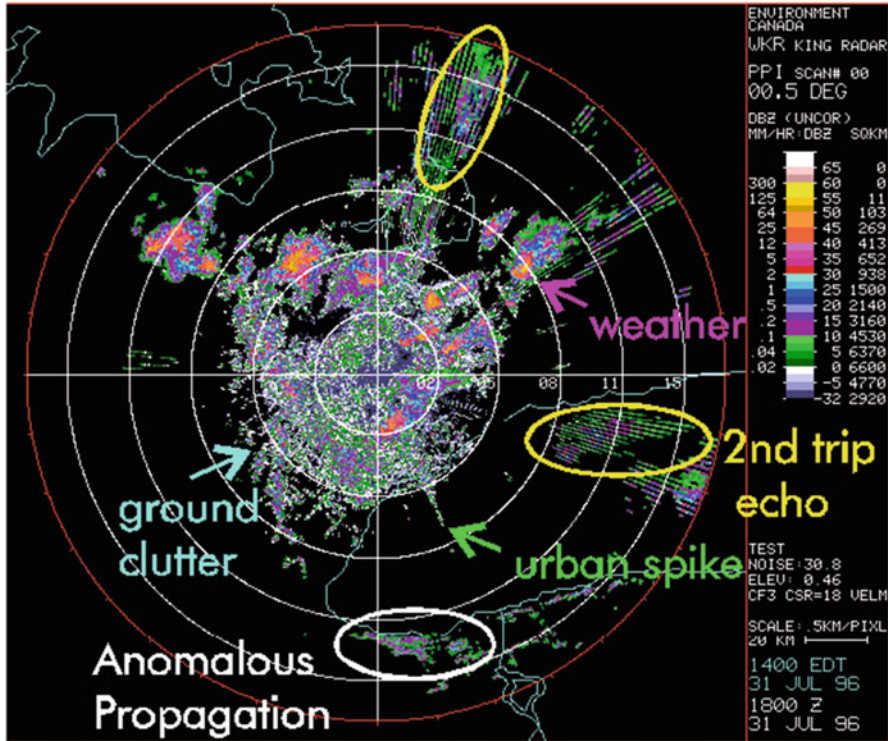


Fig. A.12 Different radar artifact cluttering the radar display

servicing its air force consumers well, as it continues to currently be produced in India as the Bahadur, or “Valiant.”

Furthermore, airborne intercept radar relying exclusively on time domain radar techniques is effectively blind any time the radar’s antenna is aimed near the earth’s surface. That is because pointing the radar at the ground produces a large reflection. That reflection and the ensuing “cluttered” display overwhelm human operators and computing systems such as ground clutter as illustrated in Fig. A.12.

Note: *Clutter* is a term used for unwanted echoes in electronic systems, particularly in reference to radars. Such echoes are typically returned from ground, sea, rain, animals/insects, chaff, and atmospheric turbulences, and can cause serious performance issues with radar systems.

The only way to prevent that problem for these kinds of radar is to not point the radar at the ground. This creates a zone of weakness near and below the horizon that is used to hide from the radar (terrain masking).

Also note that terrain masking is *nap-of-the-earth* which is a type of very-low-altitude flight course used by military aircraft to avoid enemy detection and attack in a high-threat environment.

Airborne radar clutter spectrum can be seen in Fig. A.13 here as well.

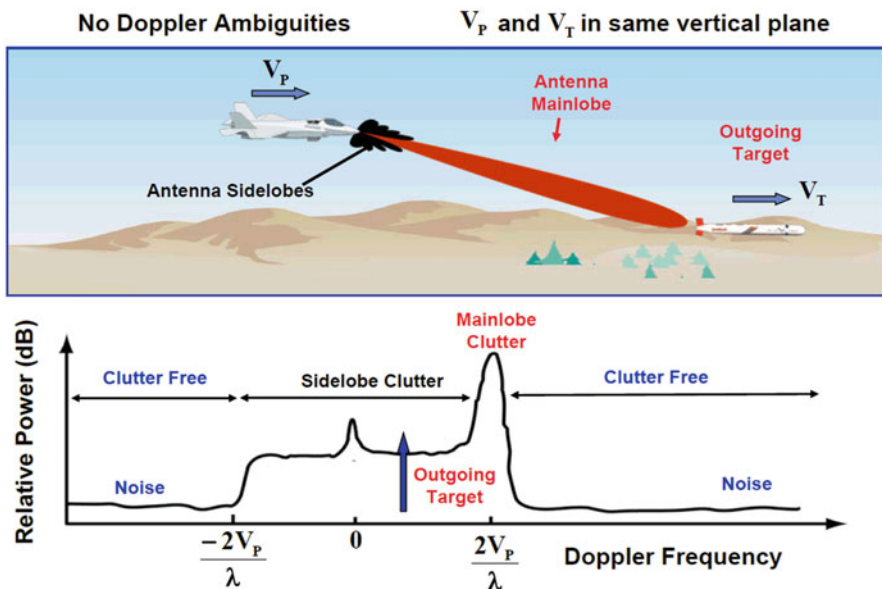


Fig. A.13 Airborne radar clutter spectrum

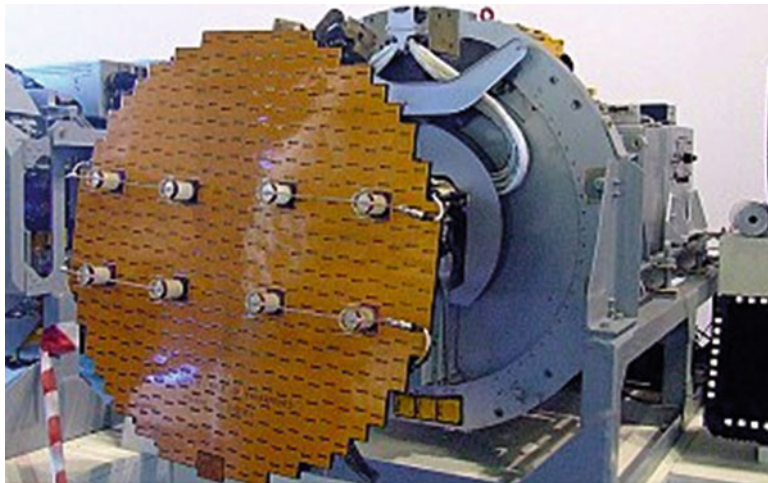


Fig. A.14 Airborne pulse-Doppler radar antenna

Frequency domain signal processing combined with time domain signal processing, as in pulse-Doppler radar, is a way to eliminate that vulnerability (Fig. A.14).

A *pulse-Doppler radar* is a radar system that determines the range to a target using pulse-timing techniques and uses the Doppler effect of the returned signal to

determine the target object's velocity. It combines the features of pulse radars and continuous-wave radars, which were formerly separate due to the complexity of the electronics.

Pulse-Doppler systems were first widely used on fighter aircraft starting in the 1960s. Earlier radars had used pulse timing in order to determine the range and the angle of the antenna (or similar means) to determine the bearing. However, this only worked when the radar antenna was not pointed down; in that case the reflection off the ground overwhelmed any returns from other objects. As the ground moves at the same speed but opposite direction of the aircraft, Doppler techniques allow the ground return to be filtered out, revealing aircraft and vehicles. This gives pulse-Doppler radars "look-down/shoot-down" capability. A secondary advantage in military radar is to reduce the transmitted power while achieving acceptable performance for improved safety of stealthy radar.

Pulse-Doppler techniques also find widespread use in meteorological radars, allowing the radar to determine wind speed from the velocity of any precipitation in the air. Pulse-Doppler radar is also the basis of synthetic aperture radar used in radar astronomy, remote sensing, and mapping. In air traffic control, they are used for discriminating aircraft from clutter. Besides the above conventional surveillance applications, pulse-Doppler radar has been successfully applied in healthcare, such as fall risk assessment and fall detection, for nursing or clinical purposes.

Look-down/shoot-down concepts can be described as follows:

1. Look Down:

Militaries require performance of airborne intercept radar under all aspects, including downwards. By using techniques to effectively remove clutter, human operators and computers can focus on targets of interest. This allows the radar system to "look down" for an airborne radar as shown in different military aircraft in Fig. A.15, and that eliminates the zone of weakness. Military air combat vehicles that lack this capability are blind to attack from below and along the line of the horizon [20].

2. Shoot Down:

Once the radar can "look down," it is subsequently desirable to "shoot down." Various weapon systems (including guns and missiles) are then employed against designated radar targets, relying on either the aircraft's radar employing the "look-down" capability as it is presented in semi-active radar homing (SARH) or the weapon's own active radar to resolve the indicated target as it is a technology used in active radar homing (ARH).

Note: *Semi-active radar homing (SARH)* is a common type of missile guidance system, perhaps the most common type for longer range air-to-air and surface-to-air missile systems. The name refers to the fact that the missile itself is only a passive detector of a radar signal—provided by an external ("off-board") source—as it reflects off the target (in contrast to active radar homing, which uses an active radar: transceiver). Semi-active missile systems use bistatic continuous-wave radar. See Fig. A.16.



Fig. A.15 Examples of airborne radar

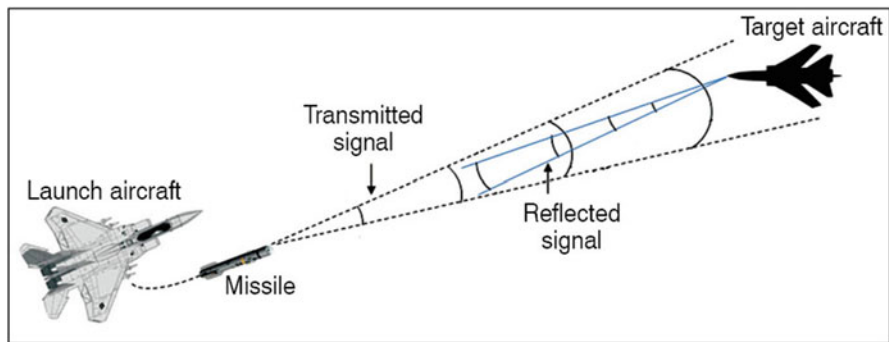


Fig. A.16 Semi-active radar homing guidance basic concept

The NATO brevity code for a semi-active radar homing missile launch is *Fox One*.

Bear in mind that a *transceiver* is a device comprising both a transmitter and a receiver that are combined and share common circuitry or a single housing. When no circuitry is common between transmit and receive functions, the device is a transmitter-receiver. The term originated in the early 1920s. Similar devices include transponders, transverters, and repeaters as illustrated in Fig. A.17, where in telecommunications a *repeater* is an electronic device that receives a signal and retransmits it. Repeaters are used to extend transmissions so that the

Fig. A.17 A radio repeater retransmits a radio signal

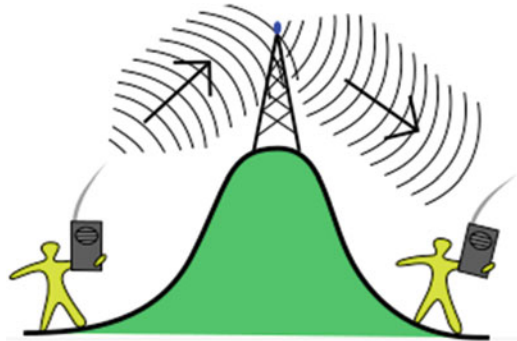


Fig. A.18 RBS-15F Anti-Ship Missile (on right) under the wing of a JAS 39 Gripen Fighter

signal can cover longer distances or be received on the other side of an obstruction.

Furthermore, *active radar homing (ARH)* is a missile guidance method in which a missile contains a radar transceiver (in contrast to semi-active radar homing, which uses only a receiver) and the electronics necessary for it to find and track its target autonomously. See Fig. A.18.

The NATO brevity code for an air-to-air active radar homing missile launch is *Fox Three*.

3. Concept:

The technical challenge encountered by airborne radar is discerning relatively small radar returns (e.g., other aircraft, targets) in the presence of large radar

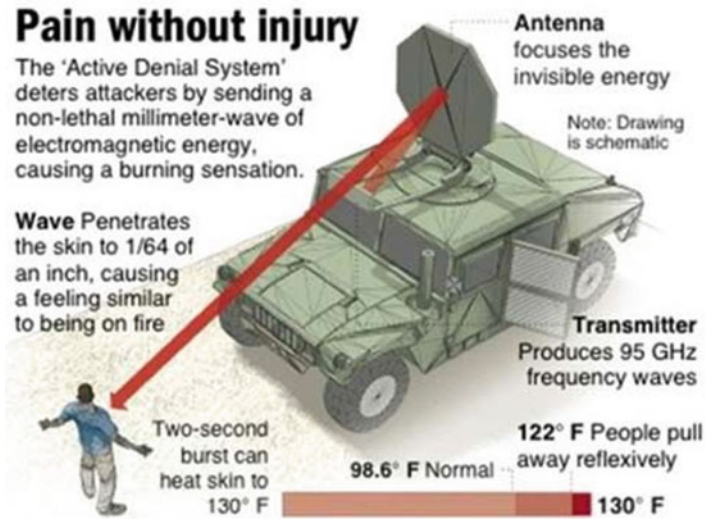


Fig. A.19 Illustration of LPADS driving pain without injury in humans

returns (e.g., terrain) when the radar is pointed at the ground, “looking down.” The ground strongly reflects the radar energy while the target relatively weakly reflects the radar energy, creating confusing clutter on the radar screen. It is difficult or impossible to separate the radar image of low-flying aircraft from the surrounding ground clutter.

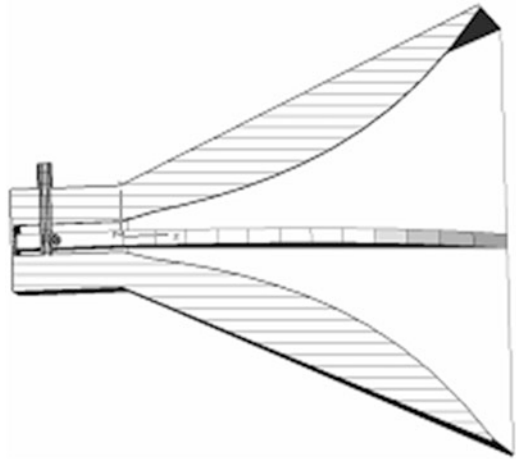
Look-down/shoot-down radars have been enhanced with electronic programs that process the radar image and search for moving objects, which are detected by looking for Doppler shifts in the radar return. See moving target indication. The radar removes all stationary objects (e.g., the ground and buildings) from the display and shows only moving objects. Since the radar is linked to the aircraft’s fire control system, it can provide targeting information to weapons once it has detected a moving object.

Look-down/shoot-down radars provide combat aircraft with the ability to engage targets flying below them. This is highly desirable, as it allows an aircraft to detect and attack targets while maintaining the tactically advantageous position conferred by superior altitude.

Now that we have built our knowledge around active denial system (ADS) and its related technology as well as radar system now we can get back to the subject and topic of this section and further explain why bleak is driving the high-power microwave (HPM). It is one thing to use a relatively low-power active denial system (LPADS) against humans as illustrated in Fig. A.19.

The system has been in development for years, including one abortive deployment to Afghanistan (it was never fired in anger). But in recent tests, the Marines and Army expanded the range of uses for the system, using it to repel boarders from

Fig. A.20 Based on the ultra-wideband ridged horn antenna



small boats—as might be done to stop Somali pirates from trying to board a civilian ship.

An official news story says this was “the first time the system fired from aboard a boat, performed vessel-to-vessel engagement and deterred human targets aboard hostile moving watercraft.”

The test used small boats that could threaten “the safety of military vessels and everyone on board.” The test demonstrated the active denial system’s ability to “keep hostile targets at bay without having to lethally engage them with machineguns or cannons.”

Let us continue with the subject of this section, i.e., fielding an ultra-power high-power microwave (UPHMP) system (Fig. A.20) against electronic equipment, as bulk of researchers’ efforts for years.

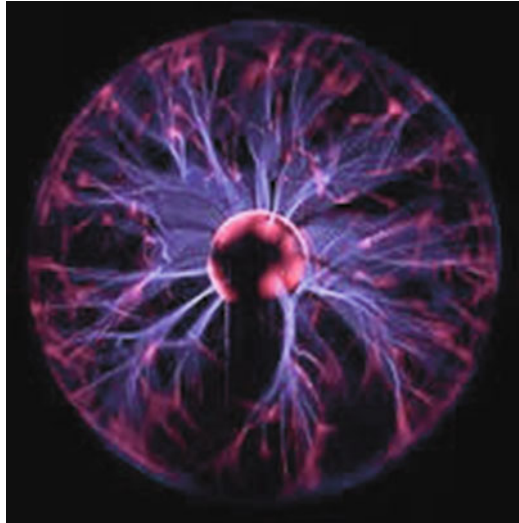
Really high-power HPM systems, the kind needed on a battlefield, are presently unfeasible.

A senior government official once said, “The smarter the weapon, the dumber HPM can make it.” There might be some truth to this statement and can turn to a fact that sometimes in future it comes to beam weapon application, but it takes enormous power to do that, and HPM has two things going against it as part of bleak factor.

First, at very high power levels, microwave energy creates a plasma in air that prevents the microwave from propagating. This is called the atmospheric breakdown limit as it was described in Appendix A.3 of this Appendix and as we stated many years ago Townsend defined a criterion, which enabled him to describe breakdown quantitatively.

The above condition can be simply explained by saying that, when the microwave energy is greater than the energy binding the air molecules together, the air molecules dissociate into a hot, gas-like state called a plasma that we know it forth state of matter or when gas is fully ionized into *ions* and *electrons* and this state which is

Fig. A.21 A plasma globe illustration



after solid, liquid, and gas and has no relation as well as nothing to do with plasma found in the blood as we know about it.

Most solid matters turn into a gas; when heated more, that liquid turns into gas; and when heated even more, electrons are stripped off the gas molecules and a hot, mushy state of matter called a plasma is formed at this state. See Fig. A.21.

Plasma is one of the four fundamental states of matter and was first described by chemist Irving Langmuir in the 1920s and makes up an ionized gas consisting of positive ions and free electrons in proportions resulting in more or less no overall electric charge, typically at low pressures (as in the upper atmosphere and in fluorescent lamps) or at very high temperatures as in stars and nuclear fusion reactors.

Figure A.21 illustrates some of the more complex plasma phenomena, including filamentation as it can be seen in Fig. A.22.

Lightning as an example of plasma present at earth's surface: Typically, lightning discharges 30 kiloamperes at up to 100 megavolts, and emits radio waves, light, X-, and even gamma rays. Plasma temperatures can approach 30,000 K and electron densities may exceed 10^{24} m^{-3} .

Lightning is a sudden electrostatic discharge that occurs typically during a thunderstorm. This discharge occurs between electrically charged regions of a cloud (called intra-cloud lightning or IC), between two clouds (CC lightning), or between a cloud and the ground (CG lightning).

The charged regions in the atmosphere temporarily equalize themselves through this discharge referred to as a *flash*. A lightning flash can also be a *strike* if it involves an object on the ground. Lightning creates light in the form of black body radiation from the very hot plasma created by the electron flow, and sound in the form of thunder. Lightning may be seen and not heard when it occurs at a distance too great for the sound to carry as far as the light from the strike or flash.



Fig. A.22 Sky lightning event

Plasma makes up over 99% of the universe and consists of the stuff that also makes up stars, solar wind, and interstellar gas as well as what is happening at the surface of the sun where fusion reaction is taking place between two isotopes of hydrogen (H) known as deuterium (D) and tritium (T).

The impact of the plasma on radio communication can also be observed, just as astronauts lose radio contact with ground control in Houston, Texas, when a plasma is created around their spaceship as it enters the earth atmosphere during reentry stage, and thus microwaves cannot transmit through earth atmospheric breakdown. Thus, consequently as a result of such breakdown, it is not good when your HPM weapon cannot propagate and it is like having a gun that cannot shoot a silver bullet not further than few feet. Although it looks pretty, it is not a practical situation.

Now there exists a second problem that is also driving the bleak of high-power microwave (HPM), and that is because the wavelength is tens of thousands of times longer than a laser's wavelength; HPM spreads out 10,000 times more than lasers in case of thermal blooming phenomena [21].

Figure A.23 shows diffraction pattern of red laser beam made on a plate after passing through a small circular aperture in another plate.

Remember the discussion of the diffraction from your basic college physics course (Fig. A.23), whereas a laser beam can shoot hundreds of kilometers, up to space and back, without spreading out that much [21], yet an HPM beam is not good for much more than a kilometer or so.

Although it takes relatively little microwave energy to kill electronic devices, it is tough if not impossible to get the microwaves beam to the target. However, HPM weapon is not much good until you can figure out how to get its microwaves close to a target without spreading out, no matter how powerful it is.

Fig. A.23 Diffraction pattern of red laser beam

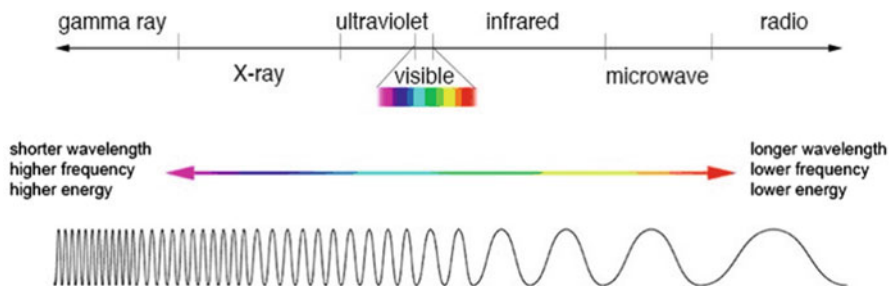
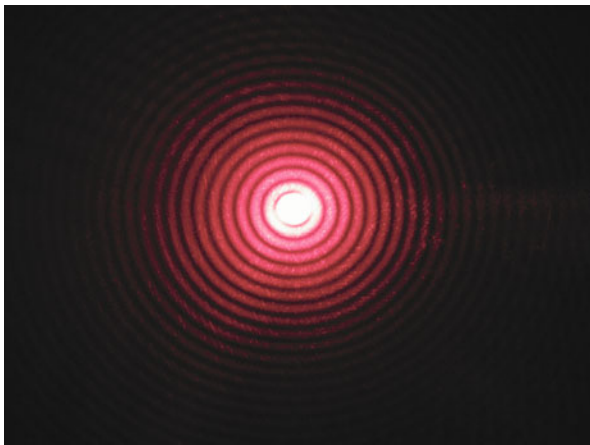


Fig. A.24 Electromagnetic spectrum sketch

Finally, the technology to shrink an HMP system to a size that can be reliably used on a battlefield is still decades away. The only attempt to exploit non-personnel uses of HPM is through a relatively new, very-high-risk program that many folks view as a last-ditch effort to overcome the bleak of HPM by implementing a new technology or new discovery such as ideas behind the longitudinal scalar wave (LSW) energy as was presented in Chap. 6 of this book as a new beam weapon.

In conclusion, a decade or so from now, high power microwave (HPM) weapons may be used on the battlefield of tomorrow to attack electronic targets almost at the speed of light; but until the problems of shrinking 30-foot-dimaterere antennas, miniaturizing megawatt power sources, and overcoming atmospheric breakdowns are solved, HPM will not be feasible as dawn of new beam weapon.

As it is sketched in Figs. A.24 and A.25, it seems that only millimeter waves, and with a limited range against humans in the form of active denial technology (ADT), appear plausible in the near future.

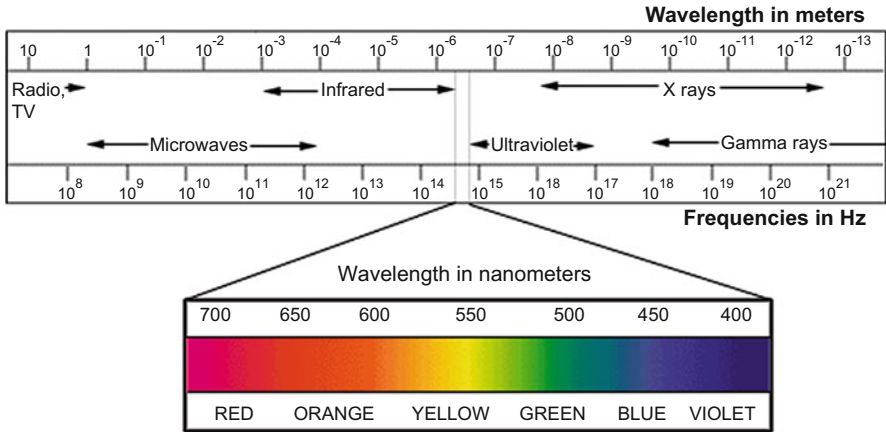


Fig. A.25 Log scale of electromagnetic spectrum

Figure A.25 illustrates a sketch of the electromagnetic spectrum, with wavelength increasing from left to right. As it can be observed lasers, on the left, have wavelengths 10,000 times smaller than microwaves, shown on the right.

Anyway history is full of surprises when it comes to the demand for new technologies.

References

1. A.D. MacDonald, *Microwave Breakdown in Gases* (Wiley Publisher, New York, 1966)
2. A. Belkin, A. Bezryadin, L. Hendren, A. Hubler, Recovery of alumina nanocapacitors after high voltage breakdown. *Sci. Rep.* **7**, 932 (2017)
3. <https://www.microwaves101.com/encyclopedias/microwave-hall-of-fame-part-i/paschen>
4. Paschen's Law. *Merriam-Webster Online Dictionary*. (Merriam-Webster, Inc., 2013). Accessed 9 June 2017
5. C.L. Wadhwa, *High Voltage Engineering*, 2nd edn. (New Age International, New Delhi, 2007), pp. 10–12. ISBN:978-8122418590
6. F. Paschen, Ueber die zum Funkenübergang in Luft, Wasserstoff und Kohlensäure bei verschiedenen Drucken erforderliche Potential differenz (on the potential difference required for spark initiation in air, hydrogen, and carbon dioxide at different pressures). *Ann. Phys.* **273**(5), 69–75 (1889)
7. M.A. Lieberman, A.J. Lichtenberg, *Principles of Plasma Discharges and Materials Processing*, 2nd edn. (Wiley-Interscience, Hoboken, NJ, 2005), p. 546. ISBN:978-0471005773
8. E. Husain, R. Nema, Analysis of Paschen curves for air, N₂ and SF₆ using the Townsend breakdown equation. *IEEE Trans. Electr. Insul.* **EI-17**(4), 350–353 (August 1982)
9. S.K. Paneth, *Rocket Exploration of the Upper Atmosphere* (Pergamon Press, London, 1954), p. 157
10. R.F. Graf, *Modern Dictionary of Electronics*, 7th edn. (Newnes, Oxford, 1999), p. 542. ISBN:978-0750698665
11. S. Ray, *An Introduction to High Voltage Engineering* (PHI Learning, Delhi, 2009), pp. 19–21. ISBN:978-8120324176
12. W.M. Bollen, C.L. Vee, A.W. Ali, M.J. Nagurney, M.E. Read, High-power microwave energy coupling to nitrogen during breakdown. *J. Appl. Phys.* **54**, 101–106 (1983)
13. J.H. Yee, R.A. Alvarez, D.J. Mayhall, N.K. Madsen, H.S. Cabayan, Dynamic characteristics of intense short microwave propagation in an atmosphere. *J. Radiat. Eff. Res. Eng.* **3**, 152–160 (1984)
14. B. Goldstein, C. Longmire, Microwave absorption and plasma heating due to microwave breakdown in the atmosphere. *J. Radiat. Eff. Res. Eng.* **3**, 1626–1628 (1984)
15. W. Woo, J.S. DeGroot, Microwave absorption and plasma heating due to microwave breakdown in the atmosphere. *Phys. Fluids* **27**, 475 (1984)
16. J.H. Yee, R.A. Alvarez, D.J. Mayhall, D.P. Byrne, J. DeGroot, Theory of intense electromagnetic pulse propagation through the atmosphere. *Phys. Fluids* **29**, 1238 (1986)
17. C.L. Vee, A.W. Ali, W.M. Bollen, Microwave coupling in a nitrogen-breakdown plasma. *J. Appl. Phys.* **54**, 1278–1283 (1983)

18. R. Kerber, Ray gun, sci-fi staple, meets reality. *Boston Globe*, 24 Sept 2004
19. Raytheon: Silent Guardian product brief. 2006. Archived from the original on 14 Dec 2006
20. *Radar Systems Engineering Lecture 14 Airborne Pulse Doppler Radar*. IEEE New Hampshire Section; University of New Hampshire
21. B. Zohuri, *Directed Energy Weapons: Physics of High Energy Lasers (HEL)*, 1st edn. (Springer Publishing Company, New York, NY, 2016)

Index

A

Active denial effect (ADE), 409
Active denial systems (ADS), 17, 377, 379, 387, 409, 417
Active radar homing (ARH), 414
Advanced Test Accelerator (ATA), 317
Agile Glide Weapon (AGW), 288
Aharonov and Bohm effect, 175
Aharonov-Bohm effect, 154, 158, 207, 354
Air Combat Command, 251
Air Force Research Laboratory (AFRL), 381
Air Force Space Command (AFSPC), 260
Air Force Weather (AFW), 260
Airborne based laser (ABL), 246
Airborne laser (ABL), 248, 259
All-electronic (AE), 340
Alternative current (AC), 356
Anti-aircraft artillery (AAA), 296
Anti-radiation missile (ARM), 289, 295
Anti-submarine warfare (ASW), 342
Artificial ionospheric mirror (AIM), 205
Atmospheric transmission, 243
Axial vircator (AV), 278
Axicon angle, 230

B

$B^{(3)}$ Field, 352
Ballistic Missile Defense (BMD), 46
Ballistic Missile Defense Organization (BMDO), 49
Bessel beam, 221
Biot-Savart law, 79, 144, 145, 149
Birkeland currents, 86

C

Canonical momentum, 152
Charge continuity equation, 146
Charge couple device (CCD), 197
Charge field, 136
Chemical oxygen Iodine laser (COIL), 39
Circular error probable (CEP), 288, 289
Classical electromagnetism, 151
Classical mechanics, 151
Classical wave equation, 58
Command-control-communications (C^3), 295
Commonwealth of Independent States (CIS), 293
Constrained propagation, 136
Continuity equation, 146
Coulomb barrier, 346
Coulomb gauge, 170, 172
Coulomb radiation, 82
Coulomb's Law, 79
Curl-free vector potential (CFVP), 172, 174, 176
Current density, 145

D

d' Alembert, 228
 d' Alembert operator, 348
Death ray, 239
Defense Advanced Research Projects Agency (DARPA), 310, 381
Defense Satellite Communications System (DSCS), 267
Defensive counter air (DCA), 303
Differential correction (DC), 261

Directed electromagnetic pulse (DEMP), 275
 Directed energy weapons (DEWs), 2–6, 409
 Durnin's beams, 223
 Dynamic random access memories (DRAM), 280

E

E-Bomb, 270
 Efficient linearized all-silicon transmitter (ELASTx), 384
 Einstein-Cartan-Evans theory, 357
 Electric displacement, 102
 Electrical breakdown problems (EBPs), 409
 Electrical primitivity, 325
 Electric-wave, 113
 Electromagnetic compatibility (EMC), 104
 Electromagnetic (EM) wave, 342, 370
 Electromagnetic field, 72
 Electromagnetic pulse (EMP), 12, 189, 270, 272, 316
 Electromagnetic waves (EMW), 86, 355, 381
 Electro-mechanical (EM), 340
 Electronic combat (EC), 295
 Electro-Optical Tactical Decision Aid (EOTDA), 260
 Electroscalar wave, 324
 Electrostatic scalar potential (ESP), 209
 Emitter locating systems (ELS), 286
 Energy continuity equation, 133
 Energy equations, 95
 Epilimnion layer, 70
 Euclidean space, 94
 Euler equation, 135
 Euler-Lagrange, 151
 Euler-Lagrange equations, 152
 Euler's formula, 63
 Extremely low frequency (ELF), 120

F

Faraday cage, 89, 362, 365, 372, 374
 Faraday's law, 348
 Field effect transistors (FETs), 280
 Field equations, 94, 95
 Finite aperture approximations (FAA), 218
 First-order partial differential equation, 78
 Flexure mass accelerometer (FMA), 261
 Flux compression generators (FCGs), 273, 275, 277, 283, 293
 Fourier transform spectroscopy, 197
 Four-irrotational, 346
 Four-solenoidal, 346
 Free-electron lasers (FELs), 246
 Future combat systems program, 19

G

Gallium nitride (GaN), 382
 Gauge invariance, 81
 Gauge transformation, 81
 Gaussian pulse, 230
 Generalized force, 152
 Geosynchronous (GEO), 263
 Global positioning satellite (GPS), 44, 293
 Global positioning system (GPS), 260
 Gradient-driven, 339
 Ground based laser (GBL), 245, 246
 Ground-based midcourse defense (GMD), 46, 52

H

Hamilton's canonical equation, 153
 Hamiltonian, 151
 Heisenberg, W., 116
 Hertz, H., 86, 119
 Hertzian dipole, 371
 Hertzian part, 372
 High energy laser (HEL), 17, 310, 318
 High frequency (HF), 205
 High Frequency Active Auroral Research Program (HAARP), 205
 High power microwave (HPM), 270, 271, 292, 307
 High temperature superconductivity (HTS), 351
 Highly elliptical orbit (HEO), 263
 High-power microwave (HPM), 417, 420
 Homogeneous scalar wave equation, 101
 Human effects advisory panel (HEAP), 389
 Hydrogen fluoride (HF), 245
 Hypolimnion layer, 70

I

Index of refraction, 75
 Indium phosphide (InP), 382
 Inhomogeneous scalar wave equation, 102
 Instantaneous Coulomb potential, 82
 Institute of electrical and electronics engineers (IEEE), 342
 Integrated circuit (IC), 384
 Inter-Continental Ballistic Missile (ICBM), 46
 Inverse Faraday effects, 353
 Ionospheric Research Instrument (IRI), 205
 Irritational current, 83

K

Kinetic energy weapons (KEWs), 4
 Kirtland Air Force Base, 271
 Klein-Gordon equation, 167

L

Ladar, 259
 Lagrangian, 151
 Lagrangian density, 347
 Lagrangian density equation, 343
 Langmuir waves, 102, 368
 Large Hadron Collider (LHC), 324, 345
 Laser Range Safety Tool (LRST), 253
 Laser-induced plasma channel (LIPC), 3, 7
 LED's signals, 372
 Lidar, 259
 Light amplification by the stimulated emission of radiation (LASER), 40
 Linear accelerators (LinAcs), 318
 Linearly conductive media, 350
 Localized waves (LW), 205, 219
 Long frequency (LW), 120
 Longitudinal current, 83
 Longitudinal oscillations, 368
 Longitudinal pressure waves (LPWs), 325
 Longitudinal propagation, 98
 Longitudinal scalar wave fields, 371
 Longitudinal scalar waves (LSW), 84, 194
 Longitudinal wave (LW), 86, 99, 326, 354, 358
 Longmuir oscillation, 102
 Lorentz condition, 81
 Lorentz Force, 154
 Lorentz transformation, 168
 Los Alamos National Laboratories (LANL), 274
 Low earth orbit (LEO), 263
 Low energy nuclear reactions (LENR), 324, 339, 346

M

Magnetic flux density, 353
 Magnetic permeability, 325
 Magnetic-wave, 113
 Magneto cumulative generators (MCGs), 274
 Magneto-hydrodynamic (MHD), 273
 Magnifying transmitter, 366
 Massachusetts Institute of Technology (MIT), 3
 Maxwell's equations, 78, 93
 Mechanical damage, 241
 Medium wave (MW), 120
 Merian's formula, 67
 Mesosphere, 244
 Metal oxide semiconductor (MOS), 272
 Mie scattering, 243
 Millikan, R., 119
 Millimeter Radar Threat Level Evaluation (MiRTLE), 386
 Millimeter wave (MW), 389

Minkowski space, 94
 Missile Defense Agency (MDA), 46
 Mission Control Station (MCS), 264
 Mitochondria, 90
 Möbius coil, 90
 Monochromatic waves, 73
 More complete electromagnetic (MCE), 339, 343, 348, 349, 351
 Multiple independently targetable reentry vehicle (MIRV), 29

N

NASA Jet Propulsion Laboratory (NASA-JPL), 201
 National Missile Defense (NMD), 48
 Nd:YAG lasers, 247
 Near-field, 111
 Night Vision Goggle Operations Weather Software (NOWS), 259
 Nikola Tesla, 345
 Non-diffracting wave (NDW), 225
 Non-linear X-wave (NLX), 224
 Nuclear Detonation Detection System (NUDET), 267
 Nuclear magnetic resonance (NMR), 352

O

Offensive counter air (OCA), 301

P

Particle beam weapons (PBWs), 3, 6, 314, 318
 Particle equation, 138
 Patriot advanced capability-3 (PAC-3), 53
 Patriot PAC-3, 49
 Pauli exclusion principle, 176
 Plasma wave, 368
 Polytetrafluoroethylene (PTFE), 405
 Potential vortex, 370
 Potential waves, 162
 Poynting theorem, 342
 Poynting vector, 133, 343
 Precision fiber optic gyroscope (PFOG), 261
 Principle of least action, 152
 Prithvi Air Defense (PAD), 51
 Programmable logic controller (PLC), 298

Q

Quantum-electro-dynamic (QED), 208
 Quantum electromagnetic (QE), 208

Quantum mechanics (QM), 151, 208
 Quantum wave, 212
 Quantum wave theory, 213

R

Radial-pulse-line accelerator (RADLAC), 317
 Radio-frequency (RF), 409
 Radomes (plastic radar domes), 242
 Rayleigh scattering, 242, 243
 Reentry vehicle (RV), 315
 Relativistic Hamilton-Jacobi equation, 354
 Restricted gauge transformation, 81

S

Scalar factor, 348
 Scalar field, 93, 98, 146, 151, 368
 Scalar longitudinal electrodynamic (SLW), 347
 Scalar longitudinal wave (SLW), 5, 324–326,
 338, 343, 348, 349
 Scalar magnetic field, 93
 Scalar potential, 79, 82, 155, 217
 Scalar waves (SW), 85, 99, 120, 126, 159, 194,
 344, 354, 357, 372
 Schrödinger equation, 170
 Scientific Consciousness Interface Operation
 (SCIO), 92
 Sea based laser (SBL), 245
 Semi-active radar homing (SARH), 414
 Shalimar Treaty, 218
 Short wave (SW), 120
 Silicon carbide (SiC), 384
 Size, weight, and power (SWaP), 385
 Solenoidal current, 83
 Solid-state active denial technology
 (SS-ADT), 386
 Soliton wave, 324
 Space and Missile Systems Command
 (SMSC), 260
 Special unitary (SU), 166
 Spherically symmetric wave solutions, 350
 Standing wave, 62, 91, 111, 121
 Stanford Linear Accelerator Center
 (SLAC), 318
 Stationary field theory, 95
 Stationary waves, 64
 Stephan–Boltzmann’s law, 1
 Strategic defense initiative (SDI), 10, 30, 374
 Strategy of graduated response (SGR), 304
 Stratosphere, 244
 Superluminal phenomenon, 218

Suppression of Enemy Air Defenses
 (SEAD), 295
 Symmetric wave solution, 348
 System-on-a-chip (SoC), 384

T

Tactical ballistic missiles (TBMs), 39
 Tactical high energy laser (THEL), 248
 Target acquisition, 258
 Telluric currents, 86, 355
 Tension of space, 362
 Terminal High Altitude Area Defense
 (THAAD), 34, 46, 52
 Theater Battle Management Core Systems
 (TBMCS), 260
 Thermal Blooming, 270
 Thermosphere, 245
 Threshold of hearing, 329
 Time-dependent Maxwell’s equations
 configuration, 79
 Transverse current, 83
 Transverse electric (TE), 205, 279
 Transverse electromagnetic (TEM), 339
 Transverse gauge, 82
 Transverse magnetic (TM), 278
 Transverse vircator (TV), 278
 Transverse wave (TW), 87, 355, 358
 Troposphere, 244
 Tunneling, 372

U

Ultra high frequency (UHF), 120, 205, 397
 Ultra-power high power microwave
 (UPHMP), 418
 Undistorted progressive waves (UPWs), 218
 Unified field, 323
 Unified field theory, 373
 Unintentional emission (UE), 286
 United States (US), 293
 United States Air Force (USAF), 286
 Unmanned aerial vehicle (UAV), 286, 385

V

Vacuum electronic devices (VEDs), 383
 Vacuum state, 358
 Vector potential, 79, 82, 155, 217, 359
 Very high frequency (VHF), 205
 Very large array (VLA), 202
 Very low frequency (VLF), 120

W

Wave equations, 98

Wave length, 364

Wave-packet, 62

Weapon of electrical mass destruction
(WEMD), 295

Weather Automated Mission Planning Software
(WAMPS), 259

Weather Impact Decision Aids
(WIDA), 259